Oxidative Medicine and Cellular Longevity

Interplay between ROS and Autophagy in Cancer and Aging: From Molecular Mechanisms to Novel Therapeutic Approaches

Lead Guest Editor: Marco Cordani
Guest Editors: Massimo Donadelli, Raffaele Strippoli, Alexandr V. Bazhin, and Miguel Sanchez-Alvarez

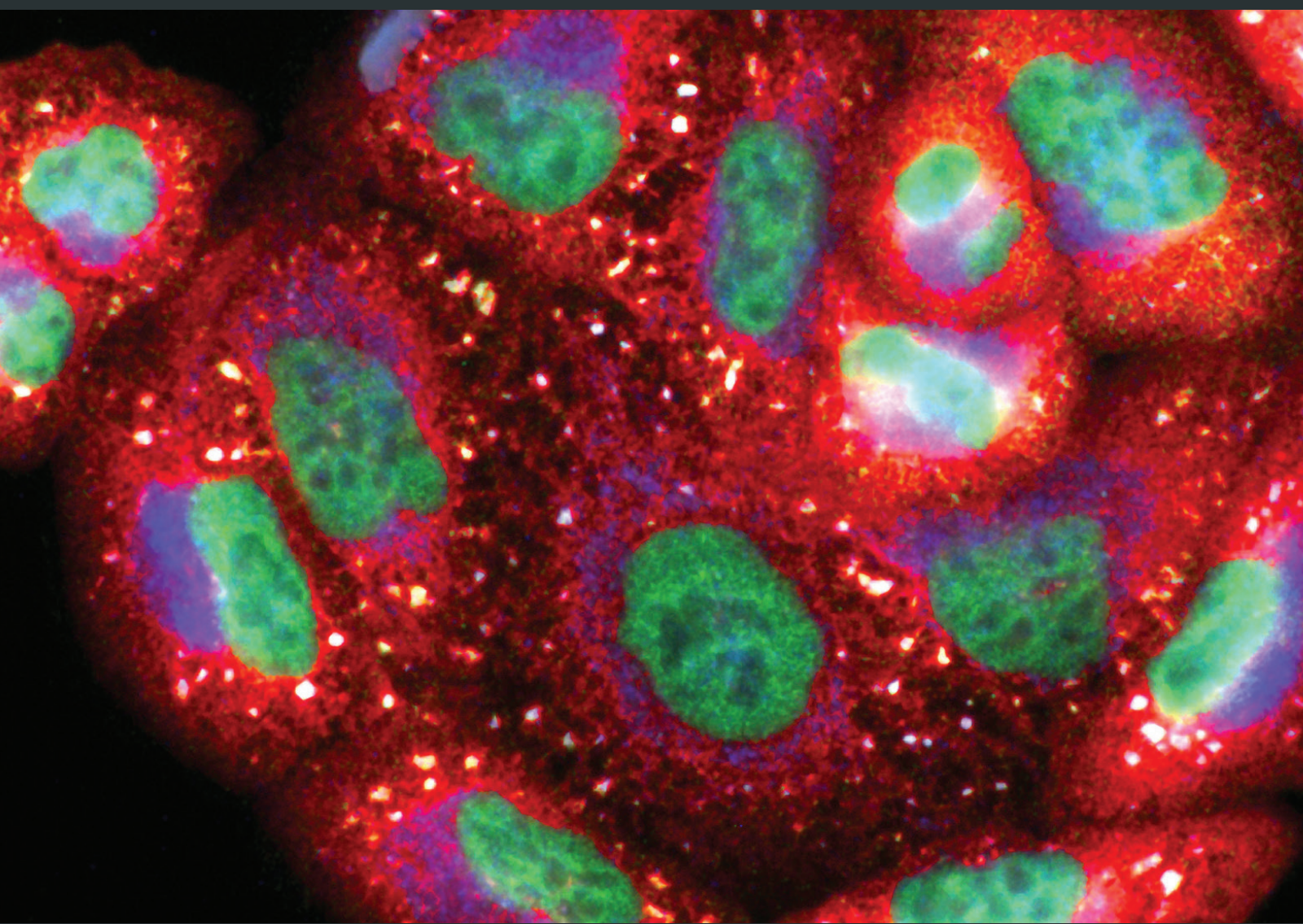

Interplay between ROS and Autophagy in Cancer and Aging: From Molecular Mechanisms to Novel Therapeutic Approaches

Oxidative Medicine and Cellular Longevity

Interplay between ROS and Autophagy in Cancer and Aging: From Molecular Mechanisms to Novel Therapeutic Approaches

Lead Guest Editor: Marco Cordani
Guest Editors: Massimo Donadelli, Raffaele Strippoli, Alexandr V. Bazhin, and Miguel Sanchez-Alvarez

Editorial Board

Contents

Hindawi
Oxidative Medicine and Cellular Longevity
Volume 2019, Article ID 8794612, 3 pages
https://doi.org/10.1155/2019/8794612

Editorial

Interplay between ROS and Autophagy in Cancer and Aging: From Molecular Mechanisms to Novel Therapeutic Approaches

Marco Cordani[1], **Massimo Donadelli**[2], **Raffaele Strippoli**[3,4], **Alexandr V. Bazhin**[5] and **Miguel Sánchez-Álvarez**[6]

[1]*Instituto Madrileño de Estudios Avanzados en Nanociencia (IMDEA Nanociencia), CNB-CSIC-IMDEA Nanociencia Associated Unit "Unidad de Nanobiotecnología", Madrid 28049, Spain*
[2]*Department of Neurosciences, Biomedicine and Movement Sciences, Section of Biochemistry, University of Verona, Verona, Italy*
[3]*Department of Molecular Medicine Sapienza, University of Rome, Rome, Italy*
[4]*Gene Expression Laboratory, National Institute for Infectious Diseases "Lazzaro Spallanzani" IRCCS, Rome, Italy*
[5]*Department of General, Visceral and Transplantation Surgery, Ludwig-Maximilians University, Munich, Germany*
[6]*Mechanoadaptation & Caveolae Biology Lab, Cell and Developmental Biology Area, Centro Nacional de Investigaciones Cardiovasculares (CNIC), Madrid 28029, Spain*

Correspondence should be addressed to Marco Cordani; marco.cordani@imdea.org

Received 27 June 2019; Accepted 27 June 2019; Published 4 August 2019

Aging and cancer are highly related biological phenomena. Cellular processes that underpin several malignant phenotypic traits, including DNA damage responses, oxidative stress, metabolic rewiring, and cellular senescence, also contribute to aging. Reactive oxygen species (ROS) play an essential role as intra- and extracellular messengers, orchestrating functional and metabolic states of the cell through the regulation of different signaling pathways [1, 2]. Importantly, ROS levels are persistently elevated in cancer cells as a result of their increased metabolic activity, mitochondrial dysfunction, and activation of oncogenes [3]. However, ROS are also powerful oxidizing agents, which can induce cell injury upon modification of lipids, proteins, or DNA, altering normal cell physiology and increasing the risk of DNA mutation and tumorigenesis. Autophagy is a key node for the regulation of ROS levels as well as for ROS-dependent cellular regulation. Autophagy comprises salvaging processes, commonly triggered by metabolic stress responses by which macromolecules and organelles are targeted by autophagic vesicles to lysosomes for degradation and recycling of their constituents [4]. Many studies revealed that alterations in ROS and autophagy are implicated in cancer biology and aging. However, while it is established that high levels of ROS and impaired autophagy drive aging in mammalian cells, their role in regulating cancer cell death or survival is highly contextual and dependent on the source of stress, tumor particularities, and its metabolic status [5]. Despite the fact that both ROS and autophagy can promote tumorigenesis and tumor progression, their exacerbation may induce cell death following a nonspecific injury or an excessive degradation of macromolecules and cellular organelles required for cellular processes. Interestingly, many oncogenic stimuli that induce ROS generation also trigger autophagy, including nutrient starvation, mitochondrial dysfunction, and hypoxia, suggesting the existence of the interplay between ROS and autophagy. Among the plethora of signaling pathways regulating this interplay, the mechanistic Target Of Rapamycin Complex 1 (mTORC1) and 5′AMP-activated protein kinase (AMPK) interpret multiple cues, including oxidative stress, to integrate them with the control of energy management, anabolism, and cell growth [6]. Conversely, these signaling systems regulate metabolism and growth which are in turn the major ROS sources themselves. Thus, the understanding of the molecular mechanisms

linking ROS and autophagy may acquire an exceptional significance to develop novel, tailored, preventive, and therapeutic strategies against cancer disease and aging processes.

In this special issue, we present seven research communications dedicated to the molecular mechanisms mediated by the crosstalk between ROS and autophagy involved in cancer development and progression and four review articles covering/providing a perspective of the state of the art on some of the current developments in this emerging field.

Melanoma is the most aggressive cancer with high mortality rate, especially when diagnosed late. Intriguingly, a number of studies support a key role of autophagy-related genes (ARGs) in melanoma onset. D. D'Arcangelo et al. demonstrated for the first time the expression levels of a large number of ARGs in several melanoma samples and identified three genes (BAG1, PEX3, and WIPI1) known to play a key role in autophagy, as novel relevant melanoma markers. Therefore, such molecules may represent valuable novel markers of melanoma onset and progression.

Different studies highlight the beneficial effects of exogenous preparations, such as plant-derived extracts to prevent cancer and aging through the regulation of the interplay between ROS and autophagy. Here, B. I. Fernandez-Gil et al. report novel molecular insights by which melatonin enhances the antitumor effects of irradiation and cisplatin on head and neck squamous cell carcinoma (HNSCC) cell lines. The authors show that melatonin induces intracellular ROS, whose accumulation plays a role in mitochondrion-mediated apoptosis and autophagy though upstream modulation. These findings indicate that melatonin, when combined with cisplatin and radiotherapy, is a potential adjuvant agent. In another study by Y. Lin et al., cucurbitacin B has been identified as a compound with antiaging activity in yeast *Saccharomyces cerevisiae* through regulating autophagy, ROS, antioxidant ability, and aging-related genes.

Resistance to tumor necrosis factor-related apoptosis-inducing ligand (TRAIL) in cancer cells is a huge obstacle to creating effective TRAIL-targeted clinical therapies. A study by L. Hu et al. shows that SNX-2112, an Hsp90 inhibitor, when combined with TRAIL treatment synergistically enhanced TRAIL-induced cytotoxicity in HeLa cells. They found that SNX-2112 downregulated antiapoptotic proteins, inhibited AKT/mTOR signaling, and induced autophagic cell death upon the activation of a ROS/JNK/p53 signaling axis. The findings reported by the authors may provide a novel strategy to overcome apoptosis resistance during cancer treatment.

Contrast-induced nephropathy (CIN) is a leading cause of hospital-acquired acute kidney injury (AKI), but its physiopathology and therapeutic targets remain poorly characterized. X. Gong et al. now report that this morbid condition courses with the impairment of mitochondria quality control and induction of CCL2/CCR2-mediated inflammation, pointing towards novel mechanisms by which tetramethylpyrazine (TMP) prevents CM-induced kidney injury.

M. Cordani et al. summarize the current knowledge on sestrins (SESNs), a family of stress surveillance proteins which play a key role in the integration of ROS control and autophagy regulation in cancer- and age-related disorders and may constitute an interesting source of novel therapeutic opportunities. Hepatocellular carcinoma (HCC) is an aggressive tumor with a very poor prognosis for which several environmental risk factors, particularly viral infections and alcohol abuse, have been shown to promote carcinogenesis via augmentation of oxidative stress and autophagy. F. Ciccarone et al. review in depth our current understanding of the interplay between ROS and autophagy in HCC and their links to risk factors, environmental stress conditions, and therapeutic treatments.

Mitophagy is an essential cellular process that involves the selective degradation of dysfunctional and/or damaged mitochondria by autophagy and is requested for mitochondrion turnover and for responding to novel energetic requirements. In another review article, E. Vernucci et al. discuss the dual role that mitophagy plays in cancer- and age-related pathologies, as a consequence of oxidative stress, focusing on mechanisms and molecular targets for its therapeutic control using nanoparticles. Poly(ADP-ribosyl)ation (PARylation) is a covalent and reversible posttranslational modification (PTM) of proteins mediated by poly(ADP-ribose) polymerases (PARPs) with functions in DNA repair, replication, genome integrity, cell cycle, and metabolism. J. M. Rodriguez-Vargas et al. review the current understanding of PARP1 activation and PARylation in response to starvation-induced autophagy.

Some DNA damage sensors, such as FOXO3a, ATM, ATR, and p53, are important autophagy regulators, and autophagy seems therefore to have a role in DNA damage response (DDR). The existence of a link between autophagy and DDR is corroborated by the evidence that alterations in autophagy lead to increased DNA damage, highlighting its fundamental role in the maintenance of genomic stability. In this regard, S. Galati et al. provide novel insights about the role of autophagy in cell response to genotoxic stress. They report that the modulation of autophagy is a successful approach to reduce toxicity or to enhance the activity of anticancer drugs.

Epithelial mesenchymal transition (EMT) is considered a driving force in tumor progression, and increasing evidence reveals that ROS are crucial players in EMT engagement. In this sense, Y. Sun et al. report that activating ferritinophagic flux, by a novel iron chelator, leads the enhancement in ROS production, highlighting its relevance as a driving force in EMT fate.

In summary, the broad coverage in this special issue provides several new perspectives on the biology of ROS and autophagy regulation with an emphasis on molecular aspects and novel therapeutic approaches and places the interplay between autophagy regulation and oxidative stress as a priority subject in biomedical research addressing aging and cancer biology.

Conflicts of Interest

The authors declare that there is no conflict of interest regarding the publication of this editorial.

Marco Cordani
Massimo Donadelli
Raffaele Strippoli
Alexandr V. Bazhin
Miguel Sánchez-Álvarez

References

[1] S. Lin, Y. Li, A. A. Zamyatnin Jr., J. Werner, and A. V. Bazhin, "Reactive oxygen species and colorectal cancer," *Journal of Cellular Physiology*, vol. 233, no. 7, pp. 5119–5132, 2018.

[2] B. D'Autréaux and M. B. Toledano, "ROS as signalling molecules: mechanisms that generate specificity in ROS homeostasis," *Nature Reviews Molecular Cell Biology*, vol. 8, no. 10, pp. 813–824, 2007.

[3] M. Schieber and N. S. Chandel, "ROS function in redox signaling and oxidative stress," *Current Biology*, vol. 24, no. 10, pp. R453–R462, 2014.

[4] N. Mizushima, "Physiological functions of autophagy," *Current Topics in Microbiology and Immunology*, vol. 335, pp. 71–84, 2009.

[5] Y. Kondo, T. Kanzawa, R. Sawaya, and S. Kondo, "The role of autophagy in cancer development and response to therapy," *Nature Reviews. Cancer*, vol. 5, no. 9, pp. 726–734, 2005.

[6] Y. Zhao, X. Hu, Y. Liu et al., "ROS signaling under metabolic stress: cross-talk between AMPK and AKT pathway," *Molecular Cancer*, vol. 16, no. 1, p. 79, 2017.

Hindawi
Oxidative Medicine and Cellular Longevity
Volume 2019, Article ID 5692958, 12 pages
https://doi.org/10.1155/2019/5692958

Research Article

Autophagy: A Player in response to Oxidative Stress and DNA Damage

Serena Galati,[1,2] **Christian Boni**,[3] **Maria Carla Gerra**,[4] **Mirca Lazzaretti**,[1,2] **and Annamaria Buschini**[1,2]

[1]*Centre for Molecular and Translational Oncology-COMT, University of Parma, Parma 43124, Italy*
[2]*Department of Chemistry, Life Sciences and Environmental Sustainability, University of Parma, Parma 43124, Italy*
[3]*Department of Medicine, General Pathology Section, University of Verona, Verona 37134, Italy*
[4]*Department of Health Science and Technology, University of Aalborg, Aalborg 9220, Denmark*

Correspondence should be addressed to Serena Galati; serena.galati@unipr.it

Received 22 February 2019; Revised 7 May 2019; Accepted 10 June 2019; Published 29 July 2019

Academic Editor: Alexandr V. Bazhin

Autophagy is a catabolic pathway activated in response to different cellular stressors, such as damaged organelles, accumulation of misfolded or unfolded proteins, ER stress, accumulation of reactive oxygen species, and DNA damage. Some DNA damage sensors like FOXO3a, ATM, ATR, and p53 are known to be important autophagy regulators, and autophagy seems therefore to have a role in DNA damage response (DDR). Recent studies have partly clarified the pathways that induce autophagy during DDR, but its precise role is still not well known. Previous studies have shown that autophagy alterations induce an increase in DNA damage and in the occurrence of tumor and neurodegenerative diseases, highlighting its fundamental role in the maintenance of genomic stability. During DDR, autophagy could act as a source of energy to maintain cell cycle arrest and to sustain DNA repair activities. In addition, autophagy seems to play a role in the degradation of components involved in the repair machinery. In this paper, molecules which are able to induce oxidative stress and/or DNA damage have been selected and their toxic and genotoxic effects on the U937 cell line have been assessed in the presence of the single compounds and in concurrence with an inhibitor (chloroquine) or an inducer (rapamycin) of autophagy. Our data seem to corroborate the fundamental role of this pathway in response to direct and indirect DNA-damaging agents. The inhibition of autophagy through chloroquine had no effect on the genotoxicity induced by the tested compounds, but it led to a high increase of cytotoxicity. The induction of autophagy, through cotreatment with rapamycin, reduced the genotoxic activity of the compounds. The present study confirms the cytoprotective role of autophagy during DDR; its inhibition can sensitize cancer cells to DNA-damaging agents. The modulation of this pathway could therefore be an innovative approach able to reduce the toxicity of many compounds and to enhance the activity of others, including anticancer drugs.

1. Introduction

Autophagy is a highly conserved catabolic pathway in eukaryotic cells, but its role is still controversial. What is certain is that it is necessary for cell survival and for the maintenance of homeostasis. In healthy cells, the pathway is activated at low basal levels, as a quality control pathway that eliminates long-lived or damaged proteins and organelles; it is also induced following different stressors to digest both intracellular and extracellular materials [1]. At the same time, under stress conditions, it can induce a programmed cell death, called "autophagy-dependent cell death" (ADCD) [2]. The autophagic pathway appears to be related to many biologic processes as aging, neurodegeneration, cardiovascular diseases, and cancer [3, 4].

Evidence shows autophagy activation also during the DNA damage response (DDR), through mTORC1 signaling [5–7]. Usually, damage to DNA induces several cellular processes; DDR enables cells either to eliminate or evade damage or to activate cell death pathways. Response to the DNA damage is mainly dependent on phosphorylation/dephosphorylation cascades driven by specific kinases as ATM (ataxia

telangiectasia-mutated kinase), ATR (ataxia telangiectasia-mutated and Rad3-related protein), and the complex Rad17-RFC/9-1-1 complex (Rad9, Rad1, and Hus1). The 9-1-1 complex through Rad17 detects single-strand breaks on DNA (ss-DNA) and induces the activation of specific checkpoint signaling pathways. ATM and ATR are two serine/-threonine kinases that control several processes as DNA replication, transcription, metabolic signaling, and DNA splicing. These kinases are able to counteract many proteins involved in cell cycle control (checkpoint kinases CHK1 and CHK2), cell survival (p53), genome surveillance (BRCA1), chromatin remodeling (HDAC1 and HDAC2), and regulation of DNA repair (FOXO3) [8]. It has been demonstrated that ATM has also a role in autophagy induction. As described by Stagni and collaborators, ATM activates the LKB1/AMPK/TSC2 signaling axis that culminates with the inhibition of the negative regulator mTOR complex 1 (mTORC1), resulting in autophagy induction through the activation of ULK1 (Unc-51-like autophagy activating kinase), which drives the nucleation and formation of the autophagosome membrane [9].

p53, a protein with a key role in genome stability and apoptosis induction, also seems to act as a regulator of the autophagic pathway. It can lead to autophagy during adverse growth conditions, keeping cells on a quiescent state. p53 also controls the switch from autophagy to apoptosis, through the regulation of the expression of autophagy (ULK and ATG family) and apoptosis- (Bcl2, PUMA, and Bax) related genes, depending on its activation signal. p53 phosphorylated on Ser15 induce p53/MDM2 dissociation, and free p53 inhibits Beclin1 and LC3, culminating in apoptosis activation and autophagy inhibition. In addition, p53 phosphorylated on Ser392 inhibits ULK1 directly, switching autophagy to apoptosis [10].

Alterations in autophagy have been shown to induce an increase in DNA damage and promote tumor and neurodegenerative disease occurrence, highlighting the importance of this pathway in maintenance of genomic stability [11]. Under DNA damage conditions, autophagy could act as a source of energy during cell cycle arrest and during repair mechanisms. On the other hand, autophagy seems to act also in degrading some components of repair machinery [12].

In the present study, in order to better understand the real role of autophagy in DNA damage response, we have evaluated the induction of autophagy in a histiocytic lymphoma cell line (U937) during the treatment with molecules which are able to induce DNA damage through different mechanisms of action (menadione, ethyl methanesulphonate (EMS), and bleomycin) or to induce a cell insult without affecting DNA integrity (bortezomib). U937 cells have the peculiarity to express many of the monocytic-like characteristics and were selected as a model cell line since autophagy plays an important role in acute leukemias [13], and in addition, this pathway seems to play a pivotal role in the growth and differentiation of this cell line [14]. Furthermore, the U937 cell line shows sensitivity to the drugs selected for this study [15–18].

Bleomycin is a radiomimetic antitumor antibiotic, widely used for the treatment of different cancers, namely, testicular cancer, lymphoma, lung cancer, cervical cancer, and cancers of the head and neck [19–21]. The best-known mechanism of action of this chemotherapeutic agent is the induction of DNA strand breaks, but bleomycin also seems to inhibit incorporation of thymidine into DNA strands. Bleomycin-mediated DNA degradation requires the presence of metal ions such as Fe^{2+} or Cu^{+} and molecular oxygen; the link between bleomycin and metal ions induces the formation of a pseudoenzyme that reacts with oxygen producing superoxide and hydroxide free radicals that cleave DNA. Bleomycin may also bind to specific sites in the DNA strand and induce breaks by extracting the hydrogen atom from the base, leading a Criegee-type rearrangement or the formation of an alkali-labile lesion, eventually resulting in DNA cleavage. This compound also mediates lipid peroxidation and oxidation of other cellular molecules [22]. BLM is able to induce ROS-mediated reticulum stress and autophagy in MCA205 (fibrosarcoma), B16F10 (melanoma) cell lines of C57BL/6 mice, and CT26 (colon carcinoma) cell line [23].

Ethyl methanesulphonate (EMS) is an alkylating agent with mutagenic, teratogenic, and carcinogenic properties [24]. It induces nucleotide substitution producing point mutations mainly. The principal base modification produced by EMS is the guanine alkylation to O^6-ethylguanine leading to the transition mutation G:C to A:T [25, 26]. Alkylating agents promote RhoB phosphorylation and sumoylation, inhibiting mTORC1 activity, through the translocation of tuberous sclerosis complex (TSC complex) to lysosomes and then initiating autophagy [27].

Menadione, also named vitamin K3, is an organic compound whose principal mechanism of action is the generation of reactive oxygen species [28, 29]. Treatment with this compound induces cell growth inhibition and apoptosis in cancer cells. Apoptosis is induced via the reactive oxygen species-dependent mitochondria-related pathway [30–32]; the reactive oxygen species cause changes in mitochondrial membrane permeability, leading to the activation of caspases [33] and bringing the depletion of intracellular antioxidants such as glutathione (GSH). The depletion of GSH activates the apoptotic pathway [34]. Furthermore, menadione induces protein arylation [35]. Menadione induces autophagy and ER stress in Hela cells. Autophagy triggered by menadione prevents ER stress and the mitochondrial pathway of apoptosis [36].

Bortezomib is the only molecule used in this work which is unable to induce DNA damage (Figure 1(b)). It is a proteasome inhibitor with antitumor activity against hematologic and nonhematologic malignancies [37]. Bortezomib could trigger autophagy enhancing the expression of autophagy-associated proteins LC3-II and Atg5–Atg12 complex and decreasing the expression of p62 in Hela and CaSki cells [38].

The toxic and genotoxic effects of the single compounds have been assessed on the U937 cell line, both alone and in combination with an inhibitor or an inducer of autophagy, chloroquine and rapamycin, respectively.

2. Materials and Methods

2.1. Chemicals. All chemicals were analytical grade, or they complied with the standards required for tissue culture

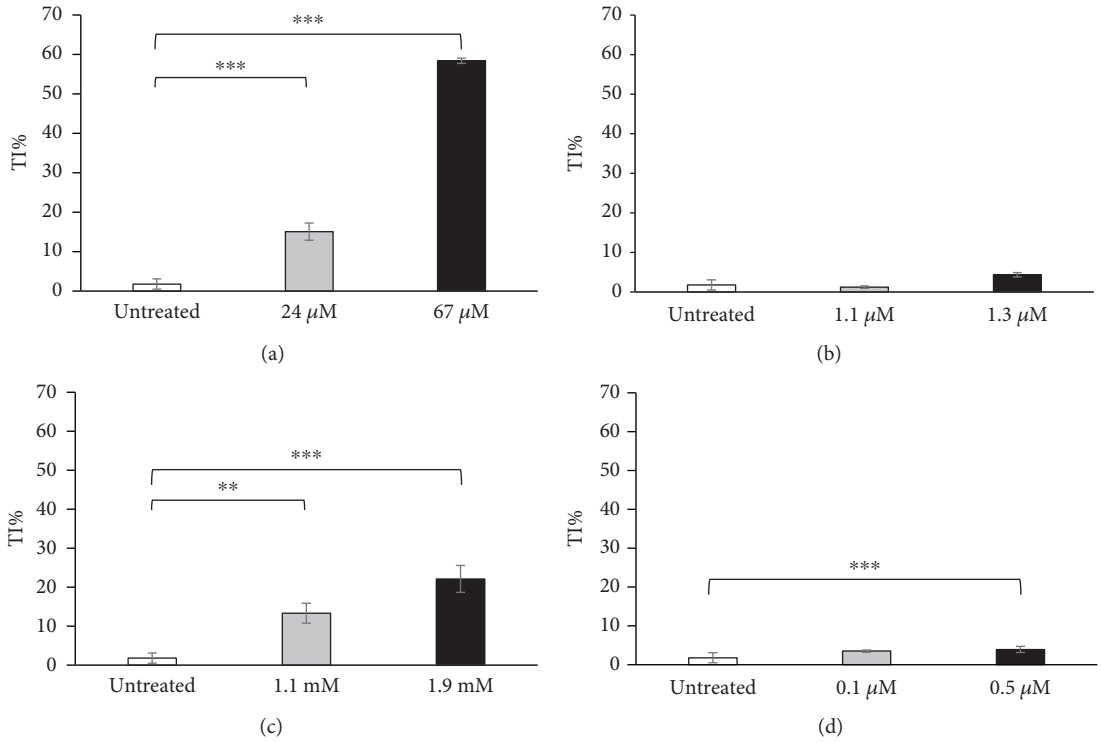

Figure 1: Genotoxicity evaluated through the comet assay in the U937 cell line after 24 h treatment with 24 and 67 μM bleomycin (a), 0.1 and 0.5 μM bortezomib (b), 1.1 and 1.9 mM ethyl methanesulphonate (c), and 1.1 and 1.3 μM menadione (d). Data are given in terms of percentage of DNA in the comet tail (tail intensity percentage: TI%). The error bars represent the standard deviation of two independent experiments. $^{*}p < 0.05$, $^{**}p < 0.01$, and $^{***}p < 0.001$.

experiments. Rapamycin, chloroquine, ethyl methanesulphonate, bortezomib, bleomycin, menadione, reagents for electrophoresis, normal melting point (1%) and low melting point (0.7%) agarose, dimethylsulfoxide, ethidium bromide, and general laboratory chemicals were from Sigma-Aldrich Company Limited (Milan, Italy). The cell culture medium and reagents were from BioWhittaker (Lonza, Milan, Italy).

2.2. Cell Lines. The U937 cells, a human histiocytic lymphoma, were obtained from American Type Culture Collection (Rockville, Maryland). They derived from malignant cells of a pleural effusion of a 37-year-old Caucasian male with diffuse histiocytic lymphoma. Nevertheless, they present the peculiarity to express many of the monocytic-like characteristics. The U937 cells were cultured in RPMI-1640 medium (Roswell Park Memorial Institute), supplemented with 10% (vol/vol) fetal bovine serum, 100 U/ml penicillin, 100 mg/ml streptomycin, and 2 mmol/l L-glutamine. Cells were maintained at 37°C in a humidified (95%) CO_2 (5%) incubator and subcultured twice a week.

2.3. Cell Proliferation. Cell proliferation was detected by the CellTiter 96® AQ_{ueous} One Solution Cell Proliferation Assay (MTS) (Promega Corporation, Madison, WI, USA) as described by Ferrarini et al. [39]. This test contains a tetrazolium compound (MTS, inner salt) and an electron-coupling reagent (phenazine ethosulfate). The MTS tetrazolium compound is bioreduced by cells into a colored formazan product that is soluble in the culture medium. This conversion is accomplished by NADPH or NADH produced by dehydrogenase enzymes in metabolically active cells. In order to determine cell viability, in the exponential phase of growth, the cells were seeded at 5×10^4/ml in ninety-six-well plates, in RPMI-1640 supplemented with 1% glutamine, 1% penicillin/streptomycin, and 5% fetal bovine serum. After seeding (24 h), U937 cells were treated, in quadruplicate, with increasing concentrations of the molecules and incubated for 24 h at 37°C in a humidified (95%) CO_2 (5%) incubator. The cytotoxicity assay was performed by adding 20 μl of the CellTiter 96® AQ_{ueous} One Solution Cell Proliferation Assay directly to culture wells, incubating for 4 h, and then recording the absorbance at 450 nm with a ninety-six-well plate reader (Multiskan EX; Thermo Electron Corporation, Vantaa, Finland).

The MTS assay was used to obtain a dose-effect curve for every compound, and according to Shoemaker [40], the concentrations able to inhibit the 10% (GI_{10}) and the 50% (GI_{50}) of the cell growth, the concentration that totally inhibits cell growth (TGI), and the 50% lethal concentration (LC_{50}) were extracted from concentration-response curves by linear interpolation.

2.4. Evaluation of the Genotoxicity of Molecules on Human Cells. To assess primary DNA damage, the alkaline version of the comet assay was performed with U937 cells as described by Buschini et al. [41]. Briefly, the cells were seeded at a concentration of 2×10^5 cell/ml in 24-well plates in 1 ml of RPMI-1640 (Roswell Park Memorial Institute), supplemented

with 1% glutamine, 1% penicillin/streptomycin, and 10% fetal bovine serum and then incubated at 37°C in a humidified (95%) CO_2 (5%) incubator. After 24 h, cells were treated, in duplicate, with the GI_{10} and GI_{50} of bleomycin, bortezomib, ethyl methanesulphonate, and menadione, calculated through the MTS assay. After 24 h of treatment, the determination of the cell number and viabilities was performed with the trypan blue exclusion method. DNA was stained with 75 μl ethidium bromide (10 μg/ml) before the examination at 400x magnification under a Leica DMLS fluorescence microscope (excitation filter BP 515-560 nm and barrier filter LP 580 nm), using an automatic image analysis system (Comet Assay IV, Perceptive Instruments Ltd., UK).

The total percentage of fluorescence in the tail (TI (tail intensity)) provided representative data on genotoxic effects. For each sample, coded and evaluated blind, 100 cells were analyzed and the median value of TI was calculated. At least two independent experiments were performed for each extract, and the mean of the median TI values was used for statistical analyses.

2.5. Autophagy Assessment. The formation of autophagic vesicles was assessed using a CYTO-ID Autophagy Detection Kit (Enzo Life Sciences, Farmingdale, NY), according to the manufacturer's instructions [42, 43]. This kit monitors autophagic flux in live cells using a novel dye that selectively labels autophagic vacuoles (preautophagosomes, autophagosomes, and autophagolysosomes). Rapamycin (0.1 μM), a known autophagy inducer, was used as a positive control and chloroquine (10 μM), an autophagy inhibitor, as a negative control. Autophagy analysis was performed by incubating cells with GI_{10} and GI_{50} of bleomycin, bortezomib, ethyl methanesulphonate, and menadione for 24 h at 37°C prior to treatment with the CYTO-ID Green Detection Reagent and analyzing fluorescence by flow cytometry using the NovoCyte Flow Cytometer (ACEA, Biosciences Inc.). For every condition, 20000 events were collected. In order to better evaluate the possible induction of autophagy with the different compounds, a cotreatment with the autophagy inhibitor (chloroquine), which is able to induce the accumulation of autophagosomes in the cytoplasm, was performed for every tested molecule.

Autophagic pathway activation has been also evaluated through a transfection protocol using a plasmid encoding the autophagosome marker LC3 fused with the fluorescent protein EGFP (pEGFP-LC3 human, Addgene). Transfection was performed using the Lipofectamine™ reagent (Invitrogen®), consisting of lipidic subunits that can form liposomes in an aqueous environment that entraps plasmid and drives it inside the cells. Transfection allows cells a constitutive LC3-EGFP fusion protein synthesis. Its nuclear and cytoplasmic distribution confers a uniform fluorescence to the cell; autophagy activation induces the formation of LC3-EGFP aggregates that determine the fluorescent signal amplification, conferring a punctuated morphology with the green spot in the cytoplasm exclusively (Figure 2).

For the assay execution, $2.5 * 10^3$ cells were seeded in 24-well plates in 1 ml of growth medium and then incubated at 37°C in a humidified (95%) CO_2 (5%) incubator. After 24 h, cells were transfected with the plasmid as described above according to the following protocol: 4 μg of plasmid was diluted in 200 μl of Opti-MEM (Invitrogen®) and at the same time, 5 μl of Lipofectamine™ is gently mixed with 200 μl Opti-MEM. After the first incubation for 5–10 min, the diluted plasmid solution and diluted Lipofectamine™ solution were gently mixed and incubated for 20 min to promote the formation of Lipofectamine™:plasmid complexes, 30 μl of solution containing the Lipofectamine™:plasmid complexes was added to each well, and cells were incubated at 37°C in a humidified (95%) CO_2 (5%) incubator for 24 h. At the end of transfection, cells were treated with the GI_{50} of the molecules for 24 h. After treatment, growth medium was removed; cells were washed twice with PBS, dropped on a glass slide, and then fixed in 400 μl of fixative solution for 30 min at RT; fixative solution was removed; cells were washed three times with PBS; and cover slips were mounted onto slides using the VECTASHIELD mounting medium with DAPI. For the visualization of LC3-EGFP aggregates, cells were examined through a fluorescent microscope using an oil immersion objective (63x magnification). For each sample, 200 transfected cells were analyzed; in autophagy-negative cells, LC3-EGFP exhibits a diffuse cytoplasmic signal; when autophagy is induced, LC3-EGFP chimeric proteins aggregate in autophagic vacuoles, leading to a punctuate cytoplasmic staining [44].

2.6. Autophagic Pathway Modulation. In order to investigate the role of autophagy in the cell response to the stress induction, cells were cotreated with the GI_{10} and the GI_{50} of the tested molecules and an autophagic inhibitor (chloroquine, 3 μM) or an activator (rapamycin, 0.1 μM). Variations in terms of cytotoxicity and genotoxicity were evaluated through the MTS assay (see Cell Proliferation) and comet assay (see Evaluation of the Genotoxicity of Molecules on Human Cells), respectively.

2.7. Statistical Evaluation. The data were analyzed using the statistical and graphical functions of SPSS 25 (SPSS Inc., Chicago, IL, USA). Differences were assessed using ANOVA, followed by Bonferroni's post hoc test as appropriate, for parameters normally distributed such as means of optical density values and of median TI values. Significance was accepted at the $p < 0.05$ level.

3. Results

3.1. Cell Proliferation. Cell proliferation, detected through the MTS assay, allowed us to calculate GI_{10}, GI_{50}, TGI, and LC_{50} from a dose-effect curve (Table 1). A lethal concentration has been identified only for menadione; this molecule seems to induce a high toxicity at very low concentrations. A concentration that could induce a growth inhibition over 50% has not been found for EMS, even in assaying really high concentrations; as reported in literature, this compound is a potent mutagen with a low cytotoxic activity [45]. For bortezomib and bleomycin, a total growth inhibition concentration was identified but the 50% lethal concentration was not reached at the assayed concentrations.

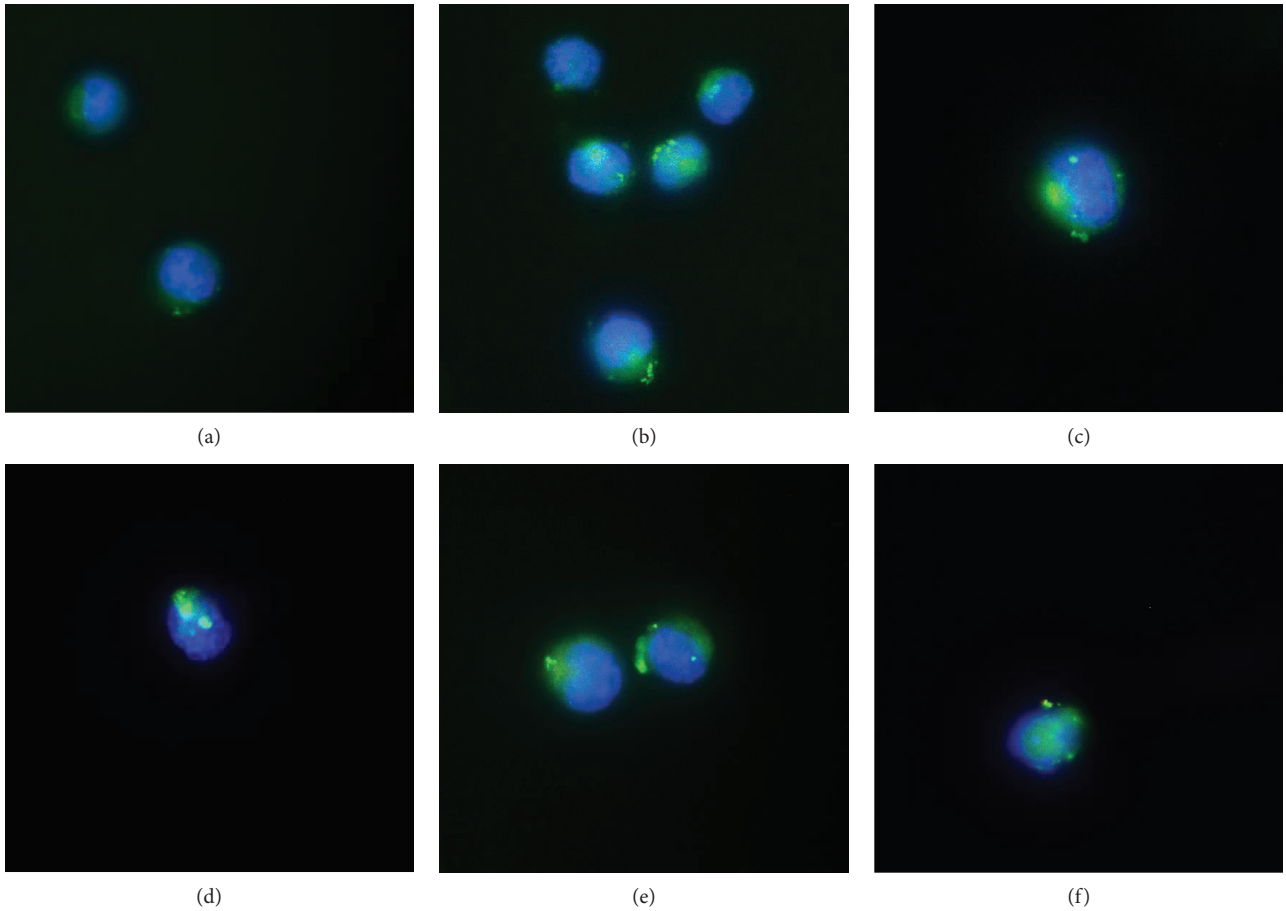

Figure 2: Autophagasome accumulation induction detected through a transfection protocol with the pEGFP-LC3 human plasmid in the untreated U937 cell line (a) after a 16 h treatment with 0.1 μM rapamycin (b) and after a 24 h treatment with 1.9 mM ethyl methanesulphonate (c), 67 μM bleomycin (d), 1.3 μM menadione (e), and 0.5 μM bortezomib (f).

Table 1: GI_{10} (10% growth inhibition), GI_{50} (50% growth inhibition), TGI (total growth inhibition), and LC_{50} (50% lethal concentration) extracted from the concentration-response curves by linear interpolation.

	Compound			
	Bleomycin	Bortezomib	EMS	Menadione
GI_{10}	24 μM	0.1 μM	1.2 mM	1.1 μM
GI_{50}	67 μM	0.5 μM	1.9 mM	1.3 μM
TGI	100 μM	2.4 μM	>2 mM	1.7 μM
LC_{50}	>100 μM	>10 μM	>2 mM	1.9 μM

3.2. DNA Damage Induction. The capability of the selected compounds to induce DNA damage after 24 h of treatment was evaluated through the alkaline version of the comet assay. The known genotoxic molecules (bleomycin, EMS, and menadione) showed an increase in tail intensity percentage in a dose-dependent manner (Figures 1(a), 1(c), and 1(d)). Bleomycin is the one that induced the higher DNA fragmentation, followed by EMS and lastly menadione. The relative low DNA damage observed after treatment with menadione is explained because the oxidative damage, the principal insult induced through treatment with this molecule, is one of the most rapidly repaired. Reactive oxygen species are a by-product of respiration, and cells remove them through antioxidant enzymes or scavengers such as glutathione and activating DNA repair mechanisms, like base excision repair. The damage measured is in a "dynamic steady state" [46]. As expected, no genotoxicity was observed after the treatment with bortezomib (Figure 1(b)).

3.3. Autophagic Pathway Induction. Induction of the autophagic pathway after treatment with the genotoxic drugs (bleomycin, EMS, and menadione) and the proteasome inhibitor (bortezomib) was revealed through a transfection assay; an increase in fluorescent dots was observed in U937 cells treated with all the assayed molecules and with the positive control rapamycin (Figure 2).

During the treatment with the tested molecules, the involvement of the autophagic pathway in cell response was also assessed through the CYTO-ID Autophagy Detection Kit. Also, in this case, all the tested compounds seemed to act as autophagic inducers in cells treated both with the GI_{50} (Figure 3) and with the GI_{10} (Figure S1, in Supplementary Materials).

The cotreatment of the single molecules with chloroquine induced an increase in the fluorescence signal, similar to that registered for cells cotreated with chloroquine

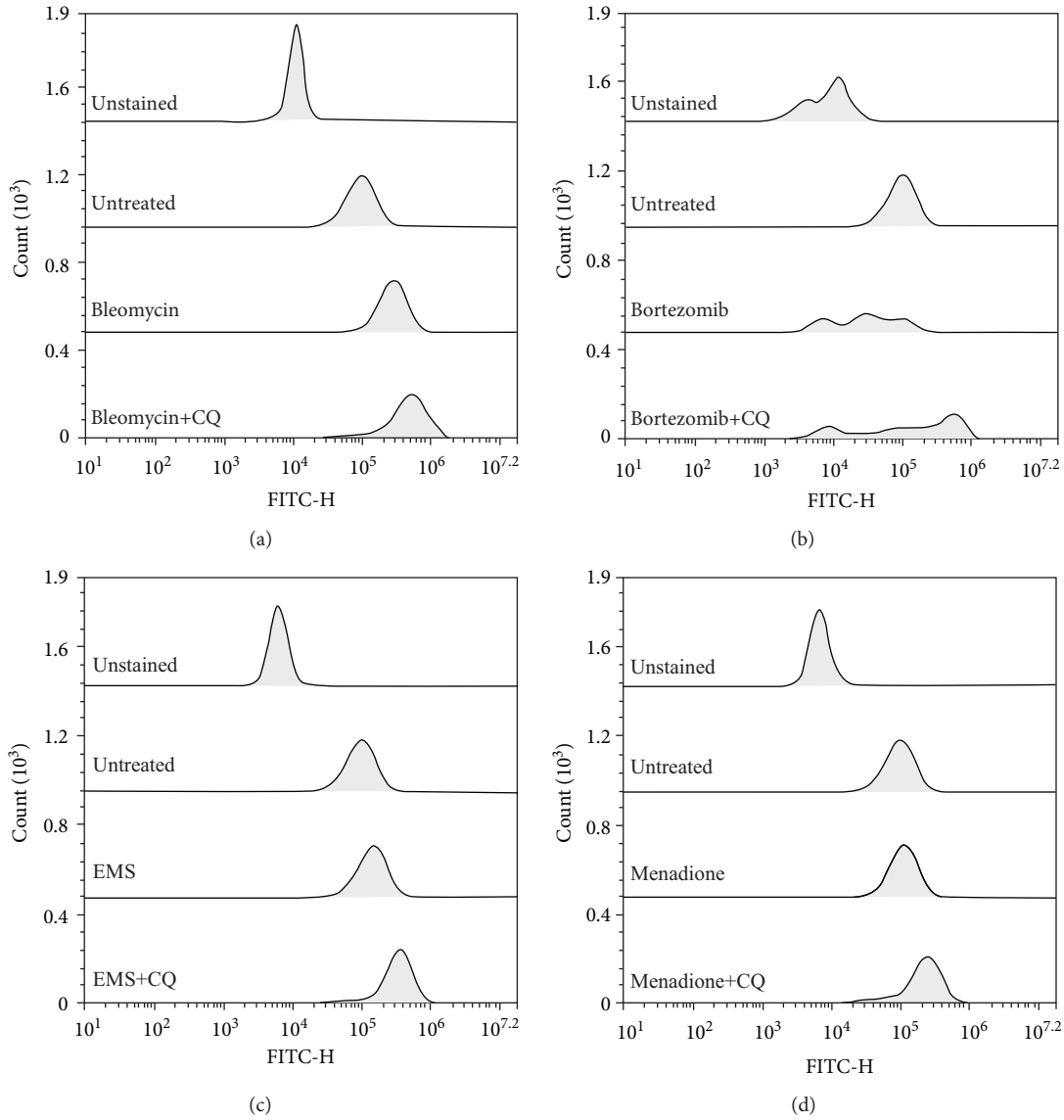

Figure 3: Autophagic pathway induction evaluated through flow cytometry in the U937 cell line after a 24 h treatment with 67 μM bleomycin (a), 0.5 μM bortezomib (b), 1.9 mM ethyl methanesulphonate (c), and 1.3 μM menadione (d). The accumulation of autophagic vesicles was induced through the treatment with the autophagy inhibitor, 10 μM chloroquine. 20000 events were collected for every tested condition through the NovoCyte Flow Cytometer (ACEA, Biosciences Inc.).

and rapamycin (Figure S2, in Supplementary Materials), meaning the accumulation of autophagosomes in the cytoplasm (Figure 3).

Autophagy is a highly expressed pathway under stress conditions, such as following treatment with cell-damaging drugs. It is fundamental to understand the role of this pathway in response to every compound, because of its dual mode of action. Autophagy can act to promote cell survival, acting as a protein or organelle quality control mechanism, or during extremely stress condition, to induce intracellular toxicity and cell death [19].

3.4. Autophagic Pathway Modulation. In order to better understand the role of the autophagic pathway during the DNA damage response, cotreatments with the GI_{50} of the selected molecules and chloroquine, as an autophagy inhibitor, or rapamycin, as an autophagy activator, were performed. Variations in terms of cytotoxicity and genotoxicity, compared to those observed after the treatment with the single compounds, were evaluated through the MTS assay and comet assay.

The inhibition of autophagy during the treatment with the DNA-damaging molecules induced variations in terms of cell proliferation in the U937 cell line. Specifically, we have observed a high cytotoxic effect in the case of cells treated with bleomycin and menadione (Figures 4(a) and 4(d)) and a cytostatic one in those treated with ethyl methanesulphonate (Figure 4(c)). The inhibition induced an increase in DNA fragmentation detected through the comet assay only in U937 cells treated with menadione (Figure 5(d)), maybe

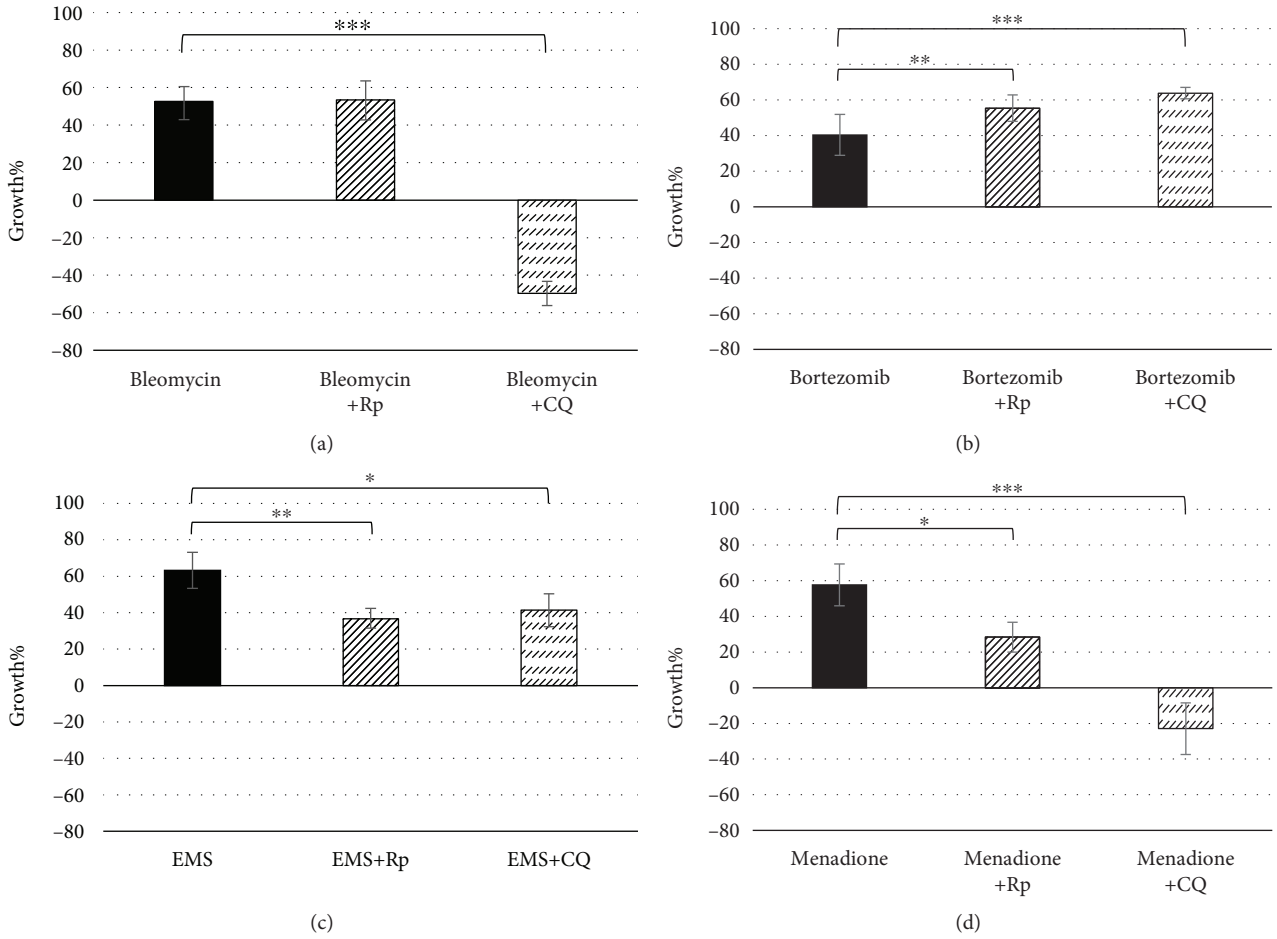

Figure 4: Cell proliferation evaluated through the MTS assay in the U937 cell line cotreated for 24 h with 0.1 μM rapamycin or 3 μM chloroquine and 67 μM bleomycin (a), 0.5 μM bortezomib (b), 1.9 mM ethyl methanesulphonate (c), and 1.3 μM menadione (d). Data are given in terms of growth percentage (Growth%). The error bars represent the standard deviation of four independent evaluations. $^{*}p < 0.05$, $^{**}p < 0.01$, and $^{***}p < 0.001$.

due to the activation of apoptosis as a consequence of autophagy inhibition or to the major disposal of reactive oxygen species. The cotreatment with the autophagy inducer, rapamycin, determined a cytostatic effect in cells treated with ethyl methanesulphonate and menadione (Figures 4(c) and 4(d)), but there were no variation in terms of cell proliferation in U937 treated with bleomycin (Figure 4(a)). Interestingly, a reduction of DNA damage was observed after the activation of the autophagy by all three DNA-damaging compounds (Figures 5(a), 5(c), and 5(d)), confirming an involvement of the autophagic pathway in the maintenance of the DNA integrity.

The alteration of the autophagic pathway during the treatment with the proteasome inhibitor, bortezomib, induced an increase of cell proliferation (Figure 4(b)). This confirms the fundamental role of autophagy in the maintenance of cell cycle arrest induced through the treatment with bortezomib. The increase in DNA damage observed after autophagy induction (Figure 5(b)) could be due to the triggering of apoptosis that sometimes occurs following autophagy activation [47].

4. Discussion and Conclusion

In recent years, the scientific community has focused its attention on the autophagic pathway because of its involvement both in cellular homeostasis and in human pathologies, such as neurodegeneration, cardiovascular diseases, and cancer. At first, this pathway was studied as an alternative pathway of cell death; subsequently, it was revaluated and associated with mechanisms of repair and cell survival. Recently, its role in DNA damage response is extensively investigated.

In this work, we have selected four different molecules which are able to induce different kinds of cellular damages; in particular, three of these (bleomycin, EMS, and menadione) are known to induce different DNA damages, and the last one (bortezomib) is a known chemotherapeutic agent, acting as an inhibitor of the proteasome. For each compound, we have selected the concentrations which are able to reduce by 10% (GI_{10}) and by 50% (GI_{50}) of the cell growth (Table 1). These concentrations have been used to investigate cellular response in terms of genotoxicity and autophagic response.

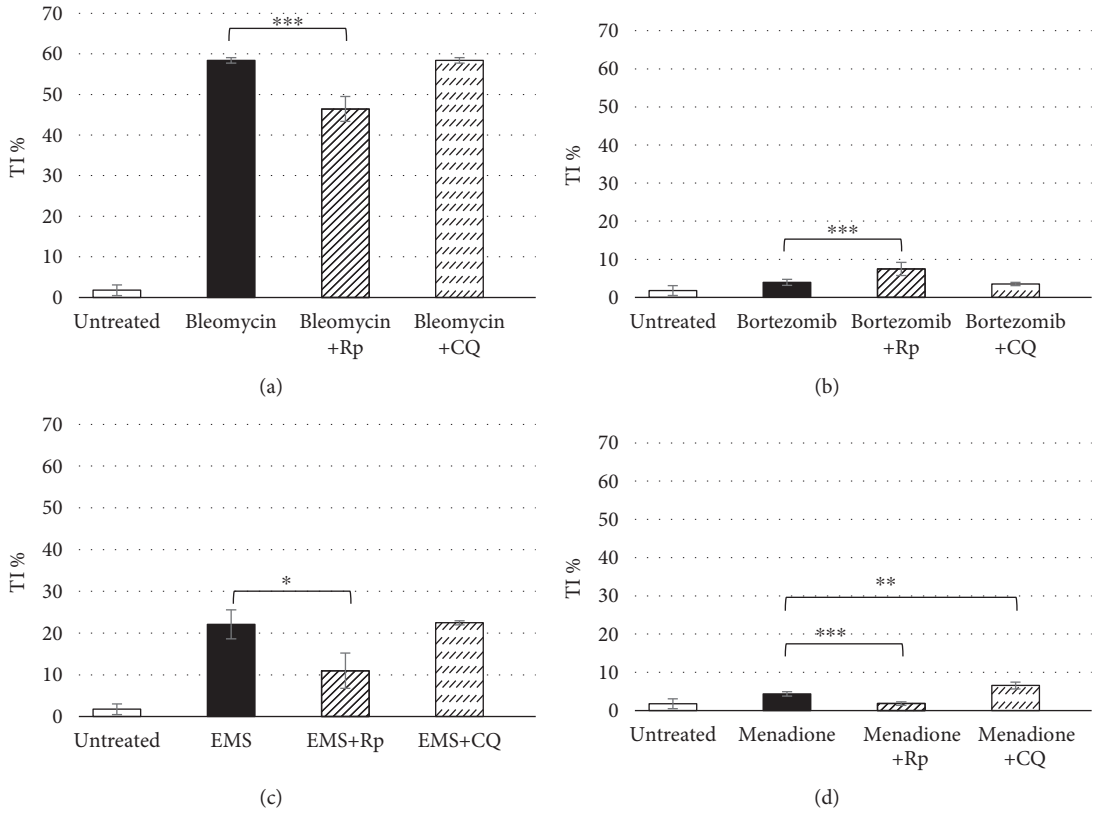

Figure 5: DNA damage evaluated through the comet assay in the U937 cell line cotreated for 24 h with 0.1 μM rapamycin or 3 μM chloroquine and 67 μM bleomycin (a), 0.5 μM bortezomib (b), 1.9 mM ethyl methanesulphonate (c), and 1.3 μM menadione (d). Data are given in terms of percentage of DNA in the comet tail (tail intensity percentage: TI%). The error bars represent the standard deviation of two independent experiments. $^{*}p < 0.05$, $^{**}p < 0.01$, and $^{***}p < 0.001$.

Through a preliminary comet assay, we have confirmed the induction of DNA damage after the treatment with bleomycin, EMS, and menadione, but not after the treatment with bortezomib, as expected (Figure 1). Activation of the autophagic pathway after treatments was revealed through different protocols: a transfection method using a plasmid encoding the autophagosome marker LC3 fused with the fluorescent protein EGFP (Figure 2) and a flow cytometric detection of the formation of autophagic vesicles through the CYTO-ID Autophagy Detection Kit (Figure 3).

Due to the great heterogeneity in the mechanisms of action of these four compounds, it has been indispensable to analyze each single molecule individually.

Bleomycin is a radiomimetic antibiotic with a complex mechanism of action including induction of DNA strand breaks and DNA oxidative damage. In our study, *in vitro* treatment of the U937 cell line with bleomycin induced, in addition to DNA damage (Figure 1(a)), a high level of autophagy, as shown in Figures 2(d) and 3(a); the cotreatment of the cells with bleomycin and chloroquine, the autophagy inhibitor, induced a high accumulation of autophagic vesicles (Figure 3(a)). The high level of autophagy might be explained in the light of the peculiar mechanism of action of bleomycin just described, such as the induction of oxidative stress and protein modification. The inhibition of autophagy through chloroquine during cell treatment with bleomycin induced a high reduction of cell viability (Figure 4(a)); this observation supports a prosurvival role for autophagy during the treatment with this molecule. The involvement of the autophagic pathway in the cell response to DNA damage is confirmed by the reduction of the fragmentation of DNA induced through bleomycin after the cotreatment with rapamycin, the autophagic inducer (Figure 5(a)). Autophagy seems to have a role in the protection of the cell after DNA clastogenic insult.

EMS is an alkylating agent inducing mainly gene mutation. Our data confirm the activation of the autophagic pathway in cells treated with this compound (Figures 2(c) and 3(c)). Autophagy modulation, through rapamycin or chloroquine, induced a reduction of cell proliferation (Figure 4(c)), confirming that autophagy is a finely controlled pathway. The capability of this molecule to induce alkylation, not only on DNA but also on proteins and cell structures, could be the principle responsible for autophagy induction. Autophagy could act as a cell scavenger, eliminating damaged and misfolded cellular components. Our data seem to confirm also its role in DNA damage response and repair; a reduction in DNA damage induced by EMS was observed after cotreatment with the autophagy inducer (Figure 5(c)), as already seen for bleomycin.

Menadione is a vitamin whose principal mechanism of action is the generation of ROS, resulting in DNA damage. This molecule was able to induce the autophagic pathway (Figures 2(e) and 3(d)). The inhibition of the autophagic

pathway led to an increase of cytotoxicity (Figure 4(d)) together with an increase in DNA fragmentation (Figure 5(d)), maybe due to a major bioavailability of the reactive oxygen species, and finally to the activation of cell death pathways as apoptosis. The cell cotreatment with menadione-rapamycin leads to a decrease in cell proliferation (Figure 4(d)), followed by a reduction of the DNA damage (Figure 5(d)), as seen for bleomycin and EMS too.

Bortezomib is a proteasome inhibitor and is the only molecule used in this work without genotoxic activity (Figure 1(b)). Bortezomib seems to act as an autophagy inducer (Figures 2(f) and 3(b)), as expected, because of the cross talk existing between the two intracellular degradation systems, the ubiquitin-proteasome system (UPS) and the autophagy [48]. Inhibition of the UPS leads to autophagy activation [49–51], and autophagy inhibition enhances UPS activity [52]. The contextual cell treatment with bortezomib and chloroquine or rapamycin induced an increase in cell proliferation (Figure 4(b)), maybe due to the loss of cell cycle arrest in the G2/M phase induced by bortezomib [53–55]. This could confirm the involvement of the autophagic pathway in the antimitogenic action of proteasome inhibitors [51]. No variations in terms of DNA damage were observed after cotreatment with chloroquine, but autophagy activation induced DNA fragmentation (Figure 5(b)). The appearance of fragmented DNA could be due to the activation of apoptosis. Usually, autophagy inhibits this cell death pathway, and apoptosis-associated caspase activation switches off the autophagic process, but it has been reported that sometimes the induction of autophagy facilitates the activation of apoptosis [47]. Proteins that have an essential role in autophagy may have proapoptotic activity; many intracellular signal pathways induced by stress regulate both autophagy and apoptosis, explaining the sequential activation of both processes. In the presence of high stress conditions such as ionizing radiation, chemotherapeutic agents, and inhibition of growth factor receptors or starvation, autophagy is rapidly induced as a mechanism to adapt to stress, and subsequently, it is followed by the activation of cell death pathways [56, 57]. In particular, during the treatment with bortezomib, the autophagosome formation activates caspase 8, and consequently, the activation of the effector caspase 3 is detectable [58]. Moreover, autophagy may deplete endogenous inhibitors of apoptosis [47]. Finally, the hyperactivation of autophagy could induce the elimination of fundamental proteins for the maintenance of genomic stability [59].

The data reported in this study show a different behavior of the autophagic pathway in the U937 cell line treated with DNA-damaging molecules versus those treated with bortezomib. In the first case, the inhibition of autophagy induces cytotoxicity, especially in cells treated with bleomycin and menadione, confirming the protective role of autophagy in response to external stressors, as reported in the literatures [60–62]. On the contrary, in cells treated with bortezomib, the inhibition of autophagy induces an increase in cell proliferation. The most interesting observations come from cells cotreated with the autophagy inducer rapamycin; a reduction in DNA damage induced by the single treatment has been observed in all the treatments with the three DNA-damaging molecules, associated with a reduction of cell proliferation only after treatment with EMS and menadione. Literature data show that autophagy has an important role in the prevention of DNA damage; autophagy-deficient cancer cells accumulate γ-H2aX foci and genome damage, leading to tumor progression [63]. The real role of autophagy in DNA integrity maintenance is still unclear, but it could play a vital role in the elimination of proteins, organelles, and damaged DNA or in the recovery of ATP, essential for cellular functions required to maintain genome integrity, such as mitosis, DNA replication, and repair [64–66]. Autophagy is able to limit cellular damage through the maintenance of energy homeostasis, oxidative stress reduction, and elimination of damaged proteins and organelles [67]. Deficient autophagy compromises the cell adaptation to metabolic stress, including insufficient ATP generation and accumulation of damaged mitochondria [68].

In conclusion, we have observed a similar behavior during the autophagy modulation in cells treated with the DNA-damaging molecules; the induction of autophagic pathway enables cells to partially recover the DNA damage. In the presence of molecules which are able to induce oxidative stress (i.e., bleomycin and menadione), the inhibition of autophagy induces high cytotoxicity. These data confirm the important role of autophagy in cell response to genotoxic stress. Modulation of autophagy appears to be a successful approach to reduce toxicity or to enhance the activity of different molecules, including anticancer drugs.

Data Availability

All the data used to support the findings of this study are included within the article.

Conflicts of Interest

The authors declare no conflict of interest.

Authors' Contributions

S.G. and A.B. designed the study and drafted and revised the manuscript. S.G. and C.B. performed cyto- and genotoxicity experiments. S.G., M.C.G., and M.L. performed autophagy assessments. A.B. supervised the entire study.

Acknowledgments

We thank Antonietta Cirasolo for her technical support.

Supplementary Materials

Supplementary materials integrate data described in the main document. In particular, Figure S1 of supplementary materials shows the induction of autophagy, evaluated through flow cytometry, in the U937 cell line treated for 24 h with the GI_{10} of the assayed compounds (i.e., 24 μM bleomycin, 0.1 μM bortezomib, 1.1 mM ethyl methanesulphonate, and 1.1 μM menadione). Figure S2 reports the flow cytometric analysis of cells treated with rapamycin (0.1 μM), chloroquine (10 μM), and rapamycin and chloroquine

together to detect the accumulation of autophagic vesicles in the cytoplasm. *(Supplementary Materials)*

References

[1] L. Murrow and J. Debnath, "Autophagy as a stress-response and quality-control mechanism: implications for cell injury and human disease," *Annual Review of Pathology: Mechanisms of Disease*, vol. 8, no. 1, pp. 105–137, 2013.

[2] S. Bialik, S. K. Dasari, and A. Kimchi, "Autophagy-dependent cell death – where, how and why a cell eats itself to death," *Journal of Cell Science*, vol. 131, no. 18, article jcs215152, 2018.

[3] B. Levine and D. J. Klionsky, "Development by self-digestion: molecular mechanisms and biological functions of autophagy," *Developmental Cell*, vol. 6, no. 4, pp. 463–477, 2004.

[4] P. H. Park, "Autophagy induction: a critical event for the modulation of cell death/survival and inflammatory responses by adipokines," *Archives of Pharmacal Research*, vol. 41, no. 11, pp. 1062–1073, 2018.

[5] C. H. Jung, S.-H. Ro, J. Cao, N. M. Otto, and D.-H. Kim, "mTOR regulation of autophagy," *FEBS Letters*, vol. 584, pp. 1287–1295, 2011.

[6] Y. Rabanal-Ruiz, E. G. Otten, and V. I. Korolchuk, "mTORC1 as the main gateway to autophagy," *Essays In Biochemistry*, vol. 61, no. 6, pp. 565–584, 2017.

[7] S. Martens, "A division of labor in mTORC1 signaling and autophagy," *Science Signaling*, vol. 11, no. 559, article eaav3530, 2018.

[8] P. Czarny, E. Pawlowska, J. Bialkowska-Warzecha, K. Kaarniranta, and J. Blasiak, "Autophagy in DNA damage response," *International Journal of Molecular Sciences*, vol. 16, no. 2, pp. 2641–2662, 2015.

[9] V. Stagni, C. Cirotti, and D. Barilà, "Ataxia-telangiectasia mutated kinase in the control of oxidative stress, mitochondria, and autophagy in cancer: a maestro with a large orchestra," *Frontiers in Oncology*, vol. 8, p. 73, 2018.

[10] F. M. Simabuco, M. G. Morale, I. C. B. Pavan, A. P. Morelli, F. R. Silva, and R. E. Tamura, "p53 and metabolism: from mechanism to therapeutics," *Oncotarget*, vol. 9, no. 34, pp. 23780–23823, 2018.

[11] H. Rodriguez-Rocha, A. Garcia-Garcia, M. I. Panayiotidis, and R. Franco, "DNA damage and autophagy," *Mutation Research/Fundamental and Molecular Mechanisms of Mutagenesis*, vol. 711, no. 1-2, pp. 158–166, 2011.

[12] T. Robert, F. Vanoli, I. Chiolo et al., "HDACs link the DNA damage response, processing of double-strand breaks and autophagy," *Nature*, vol. 471, no. 7336, pp. 74–79, 2011.

[13] C. Evangelisti, C. Evangelisti, F. Chiarini et al., "Autophagy in acute leukemias: A double-edged sword with important therapeutic implications," *Biochimica et Biophysica Acta (BBA) - Molecular Cell Research*, vol. 1853, no. 1, pp. 14–26, 2015.

[14] L. Chen, P. Guo, Y. Zhang, X. Li, P. Jia, and J. Tong, "Autophagy is an important event for low-dose cytarabine treatment in acute myeloid leukemia cells," *Leukemia Research*, vol. 60, pp. 44–52, 2017.

[15] M. P. Minisini, S. Kantengwa, and S. P. Barbara, "DNA damage and stress protein synthesis induced by oxidative stress proceed independently in the human premonocytic line U937," *Mutation Research/DNA Repair*, vol. 315, no. 2, pp. 169–179, 1994.

[16] A. Buschini, S. Pinelli, R. Alinovi et al., "Unravelling mechanisms behind the biological activity of bis(*S*-citronellalthiosemicarbazonato)nickel(II)," *Metallomics*, vol. 6, no. 4, pp. 783–792, 2014.

[17] C. Zani, F. Bisceglie, F. M. Restivo et al., "A battery of assays as an integrated approach to evaluate fungal and mycotoxin inhibition properties and cytotoxic/genotoxic side-effects for the prioritization in the screening of thiosemicarbazone derivatives," *Food and Chemical Toxicology*, vol. 105, pp. 498–505, 2017.

[18] J. Bozic, K. Bidovec, M. VizoviseK, I. Dolenc, and V. Stoka, "Menadione-induced apoptosis in U937 cells involves Bid cleavage and stefin B degradation," *Journal of Cellular Biochemistry*, vol. 120, no. 6, pp. 10662–10669, 2019.

[19] A. A. Alshatwi, V. S. Periasamy, J. Athinarayanan, and R. Elango, "Synergistic anticancer activity of dietary tea polyphenols and bleomycin hydrochloride in human cervical cancer cell: Caspase-dependent and independent apoptotic pathways," *Chemico-Biological Interactions*, vol. 247, pp. 1–10, 2016.

[20] M. Laprise-lachance, P. Lemieux, and J. P. Grégoire, "Risk of pulmonary toxicity of bleomycin and filgrastim," *Journal of Oncology Pharmacy Practice*, 2018.

[21] R. A. Watson, H. D. La Peña, M. T. Tsakok et al., "Development of a best-practice clinical guideline for the use of bleomycin in the treatment of germ cell tumours in the UK," *British Journal of Cancer*, vol. 119, no. 9, pp. 1044–1051, 2018.

[22] S. M. Hecht, "Bleomycin: new perspectives on the mechanism of action 1," *Journal of Natural Products*, vol. 63, no. 1, pp. 158–168, 2000.

[23] G. M. H. Bugaut, M. Bruchard, H. Berger et al., "Bleomycin exerts ambivalent antitumor immune effect by triggering both immunogenic cell death and proliferation of regulatory T cells," *PLoS One*, vol. 8, no. 6, article e65181, 2013.

[24] E. Gocke, H. Bürgin, L. Müller, and T. Pfister, "Literature review on the genotoxicity, reproductive toxicity, and carcinogenicity of ethyl methanesulfonate," *Toxicology Letters*, vol. 190, no. 3, pp. 254–265, 2009.

[25] G. A. Sega, "A review of the genetic effects of ethyl methanesulfonate," *Mutation Research*, vol. 134, no. 2-3, pp. 113–142, 1984.

[26] J. Cole and F. N. Richmond, "Comparative induction of gene mutations and chromosome damage by 1-methoxy-1,3,5-cycloheptatriene (MCHT), 2. Results using L5178Y mouse lymphoma cells to detect both gene and chromosome damage; validation with ionizing radiation, methyl methanesulphonate, ethyl methanesulphonate and benzo[*a*]pyrene," *Mutation Research/Fundamental and Molecular Mechanisms of Mutagenesis*, vol. 230, no. 1, pp. 81–91, 1990.

[27] M. Liu, T. Zeng, X. Zhang et al., "ATR/Chk1 signaling induces autophagy through sumoylated RhoB-mediated lysosomal translocation of TSC2 after DNA damage," *Nature Communications*, vol. 9, no. 1, article 4139, 2018.

[28] D. N. Criddle, S. Gillies, H. K. Baumgartner-Wilson et al., "Menadione-induced reactive oxygen species generation via redox cycling promotes apoptosis of murine pancreatic acinar cells," *Journal of Biological Chemistry*, vol. 281, no. 52, pp. 40485–40492, 2006.

[29] G. Loor, J. Kondapalli, J. M. Schriewer, N. S. Chandel, T. L. Vanden Hoek, and P. T. Schumacker, "Menadione triggers cell death through ROS-dependent mechanisms involving PARP activation without requiring apoptosis," *Free Radical Biology and Medicine*, vol. 49, no. 12, pp. 1925–1936, 2011.

[30] H. K. Baumgartner, J. V. Gerasimenko, C. Thorne et al., "Caspase-8-mediated apoptosis induced by oxidative stress is independent of the intrinsic pathway and dependent on cathepsins," *American Journal of Physiology-Gastrointestinal and Liver Physiology*, vol. 293, no. 1, pp. G296–G307, 2019.

[31] M. Ogawa, S. Nakai, A. Deguchi et al., "Vitamins K2, K3 and K5 exert antitumor effects on established colorectal cancer in mice by inducing apoptotic death of tumor cells," *International Journal of Oncology*, vol. 31, pp. 323–331, 2007.

[32] T. Akiyoshi, S. Matzno, and M. Sakai, "The potential of vitamin K_3 as an anticancer agent against breast cancer that acts via the mitochondria-related apoptotic pathway," *Cancer Chemotherapy and Pharmacology*, vol. 65, no. 1, pp. 143–150, 2009.

[33] J. S. Armstrong, "Mitochondria: a target for cancer therapy," *British Journal of Pharmacology*, vol. 147, no. 3, pp. 239–248, 2006.

[34] M. L. Circu and T. Y. Aw, "Glutathione and apoptosis," *Free Radical Research*, vol. 42, no. 8, pp. 689–706, 2008.

[35] H. L. Wiraswati, E. Hangen, and A. B. Sanz, "Apoptosis inducing factor (AIF) mediates lethal redox stress induced by menadione," *Oncotarget*, vol. 7, no. 47, pp. 76496–76507, 2016.

[36] C. Yu, X. Huang, Y. E. Xu et al., "Lysosome dysfunction enhances oxidative stress-induced apoptosis through ubiquitinated protein accumulation in Hela cells," *The Anatomical Record: Advances in Integrative Anatomy and Evolutionary Biology*, vol. 296, no. 1, pp. 31–39, 2013.

[37] R. Schwartz and T. Davidson, "Pharmacology, pharmacokinetics, and practical applications of bortezomib," *Oncology*, vol. 18, no. 14, 2004Supplement 11, 2004.

[38] Y. Zhang, C. Bai, D. Lu, and X. Wu, "Endoplasmic reticulum stress and autophagy participate in apoptosis induced by bortezomib in cervical cancer cells," *Biotechnology Letters*, vol. 38, no. 2, pp. 357–365, 2016.

[39] L. Ferrarini, N. Pellegrini, T. Mazzeo et al., "Anti-proliferative activity and chemoprotective effects towards DNA oxidative damage of fresh and cooked Brassicaceae," *The British Journal of Nutrition*, vol. 107, no. 9, pp. 1324–1332, 2012, Epub 2011 Nov 17.

[40] R. H. Shoemaker, "The NCI60 human tumour cell line anticancer drug screen," *Nature Reviews Cancer*, vol. 6, no. 10, pp. 813–823, 2006.

[41] A. Buschini, L. Ferrarini, S. Franzoni et al., "Genotoxicity revaluation of three commercial nitroheterocyclic drugs: nifurtimox, benznidazole, and metronidazole," *Journal of Parasitology Research*, vol. 2009, Article ID 463575, 11 pages, 2009.

[42] L. L.-Y. Chan, D. Shen, A. R. Wilkinson et al., "A novel image-based cytometry method for autophagy detection in living cells," *Autophagy*, vol. 8, no. 9, pp. 1371–1382, 2012.

[43] T. Kozako, P. Mellini, T. Ohsugi, A. Aikawa, Y. Uchida, and S. Honda, "Novel small molecule SIRT2 inhibitors induce cell death in leukemic cell lines," *BMC Cancer*, vol. 18, no. 1, p. 791, 2018.

[44] E. Tasdemir, L. Galluzzi, M. C. Maiuri et al., "Methods for assessing autophagy and autophagic cell death," *Methods in Molecular Biology*, vol. 445, pp. 29–76, 2008.

[45] S. M. Morris, L. J. Mcgarrity, O. E. Domon et al., "The role of programmed cell death in the toxicity of the mutagens, ethyl methanesulfonate and *N*-ethyl-*N*′-nitrosourea, in AHH-1 human lymphoblastoid cells," *Mutation Research/Fundamental and Molecular Mechanisms of Mutagenesis*, vol. 306, no. 1, pp. 19–34, 1994.

[46] A. Collins and V. Harrington, "Repair of oxidative DNA damage: assessing its contribution to cancer prevention," *Mutagenesis*, vol. 17, no. 6, pp. 489–493, 2002.

[47] G. Mariño, M. Niso-Santano, E. H. Baehrecke, and G. Kroemer, "Self-consumption: the interplay of autophagy and apoptosis," *Nature Reviews Molecular Cell Biology*, vol. 15, no. 2, pp. 81–94, 2014.

[48] B. Tang, J. Cai, L. Sun et al., "Proteasome inhibitors activate autophagy involving inhibition of PI3K-Akt-mTOR pathway as an anti-oxidation defense in human RPE cells," *PLoS One*, vol. 9, no. 7, article e103364, 2014.

[49] W. Ding, H. Ni, W. Gao et al., "Linking of autophagy to ubiquitin-proteasome system is important for the regulation of endoplasmic reticulum stress and cell viability," *The American Journal of Pathology*, vol. 171, no. 2, pp. 513–524, 2007.

[50] K. Zhu and D. J. Mcconkey, "Proteasome inhibitors activate autophagy as a cytoprotective response in human prostate cancer cells," *Oncogene*, vol. 29, no. 3, pp. 451–462, 2010.

[51] W. K. K. Wu, Y. C. Wu, L. Yu, Z. J. Li, J. J. Y. Sung, and C. H. Cho, "Induction of autophagy by proteasome inhibitor is associated with proliferative arrest in colon cancer cells," *Biochemical and Biophysical Research Communications*, vol. 374, no. 2, pp. 258–263, 2008.

[52] X. J. Wang, J. Yu, S. H. Wong et al., "A novel crosstalk between two major protein degradation systems: regulation of proteasomal activity by autophagy," *Autophagy*, vol. 9, no. 10, pp. 1500–1508, 2013.

[53] P. Bonvini, E. Zorzi, G. Basso, and A. Rosolen, "Bortezomib-mediated 26S proteasome inhibition causes cell-cycle arrest and induces apoptosis in CD-30^+ anaplastic large cell lymphoma," *Leukemia*, vol. 21, no. 4, pp. 838–842, 2007.

[54] G. Hutter, M. Rieken, A. Pastore et al., "The proteasome inhibitor bortezomib targets cell cycle and apoptosis and acts synergistically in a sequence-dependent way with chemotherapeutic agents in mantle cell lymphoma," *Annals of Hematology*, vol. 91, no. 6, pp. 847–856, 2012.

[55] N. Rastogi and D. P. Mishra, "Therapeutic targeting of cancer cell cycle using proteasome inhibitors," *Cell Division*, vol. 7, no. 1, p. 26, 2012.

[56] P. Boya, R. Gonza, N. Casares et al., "Inhibition of macroautophagy triggers apoptosis," *Molecular and Cellular Biology*, vol. 25, no. 3, pp. 1025–1040, 2005.

[57] H. Shen and P. Codogno, "Autophagic cell death: Loch Ness monster or endangered species?," *Autophagy*, vol. 7, no. 5, pp. 457–465, 2011.

[58] M. M. Young, Y. Takahashi, O. Khan et al., "Autophagosomal membrane serves as platform for intracellular death-inducing signaling complex (iDISC) -mediated caspase-8 activation and apoptosis," *The Journal of Biological Chemistry*, vol. 287, no. 15, pp. 12455–12468, 2012.

[59] G. Hewitt and V. I. Korolchuk, "Repair, reuse, recycle: the expanding role of autophagy in genome maintenance," *Trends in Cell Biology*, vol. 27, no. 5, pp. 340–351, 2017.

[60] Z. Wang, T. Du, X. Dong, Z. Li, G. Wu, and R. Zhang, "Autophagy inhibition facilitates erlotinib cytotoxicity in lung cancer cells through modulation of endoplasmic reticulum stress," *International Journal of Oncology*, vol. 48, no. 6, pp. 2558–2566, 2016.

[61] W. Guo, Y. Wang, Z. Wang, Y. Wang, and H. Zheng, "Inhibiting autophagy increases epirubicin's cytotoxicity in breast cancer cells," *Cancer Science*, vol. 107, no. 11, pp. 1610–1621, 2016.

[62] S. Aveic, M. Pantile, P. Polo, V. Sidarovich, and M. De Mariano, "Autophagy inhibition improves the cytotoxic effects of receptor tyrosine kinase inhibitors," *Cancer Cell International*, vol. 18, no. 1, p. 63, 2018.

[63] Y. Wang, N. Zhang, Y. Wang et al., "Autophagy regulates chromatin ubiquitination in DNA damage response through elimination of SQSTM1/p62," *Molecular Cell*, vol. 63, no. 1, pp. 34–48, 2016.

[64] A. T. Vessoni, E. C. Filippi-chiela, C. F. M. Menck, and G. Lenz, "Autophagy and genomic integrity," *Cell Death and Differentiation*, vol. 20, no. 11, pp. 1444–1454, 2013.

[65] W. Lin, N. Yuan, Z. Wang et al., "Autophagy confers DNA damage repair pathways to protect the hematopoietic system from nuclear radiation injury," *Scientific Reports*, vol. 5, no. 1, pp. 1–12, 2015.

[66] X. Song, M. Sophie, I. Mariana, and P. Hohensinner, "Autophagy deficient keratinocytes display increased DNA damage, senescence and aberrant lipid composition after oxidative stress in vitro and in vivo," *Redox Biology*, vol. 11, pp. 219–230, 2017.

[67] R. Mathew, C. M. Karp, B. Beaudoin et al., "Autophagy suppresses tumorigenesis through elimination of p62," *Cell*, vol. 137, no. 6, pp. 1062–1075, 2009.

[68] V. Karantza-wadsworth, S. Patel, O. Kravchuk et al., "Autophagy mitigates metabolic stress and genome damage in mammary tumorigenesis," *Genes & Development*, vol. 21, no. 13, pp. 1621–1635, 2007.

Hindawi
Oxidative Medicine and Cellular Longevity
Volume 2019, Article ID 8753413, 14 pages
https://doi.org/10.1155/2019/8753413

Research Article

Ferritinophagic Flux Activation in CT26 Cells Contributed to EMT Inhibition Induced by a Novel Iron Chelator, DpdtpA

Yanjie Sun,[1,2] Cuiping Li,[1] Jiankang Feng,[1] Yongli Li,[3] Xinbo Zhai,[2] Lei Zhang,[2] and Changzheng Li[1,2,4]

[1]*Department of Molecular Biology and Biochemistry, Xinxiang Medical University, Xinxiang, Henan 453003, China*
[2]*Experimental Teaching Center of Biology and Basic Medical Sciences, Sanquan College of Xinxiang Medical University, Xinxiang, Henan 453003, China*
[3]*Department of Histology and Embryology, Sanquan College of Xinxiang Medical University, Xinxiang, Henan 453003, China*
[4]*Laboratory of Molecular Medicine, Xinxiang Medical University, Xinxiang, Henan 453003, China*

Correspondence should be addressed to Changzheng Li; changzhenl@yahoo.com

Received 24 January 2019; Revised 7 April 2019; Accepted 8 May 2019; Published 20 June 2019

Guest Editor: Marco Cordani

Epithelial-mesenchymal transition (EMT) contributes to metastasis and drug resistance; inhibition of EMT may attenuate metastasis and drug resistance. It has been demonstrated that ferritinophagy involves the process of many diseases; however, the relationship between EMT and ferritinophagy was not fully established. Some iron chelators show the ability to inhibit EMT, but whether ferritinophagy plays a role in EMT is largely unknown. To this end, we investigated the effect of a novel iron chelator, DpdtpA (2,2′-di-pyridylketone dithiocarbamate propionic acid), on EMT in the CT26 cell line. The DpdtpA displayed excellent antitumor ($IC_{50} = 1.5 \pm 0.2\,\mu M$), leading to ROS production and apoptosis occurrence. Moreover, the ROS production correlated with ferritin degradation. The upregulation of LC3-II and NCOA4 from immunofluorescence and Western blotting analysis revealed that the occurrence of ferritinophagy contributed to ROS production. Furthermore, DpdtpA could induce an alteration both in morphology and in epithelial-mesenchymal markers, displaying significant EMT inhibition. The correlation analysis revealed that DpdtpA-induced ferritinophagy contributed to the EMT inhibition, implying that NCOA4 involved EMT process, which was firstly reported. To reinforce this concept, the ferritinophagic flux (NCOA4/ferritin) in either treated by TGF-β1 or combined with DpdtpA was determined. The results indicated that activating ferritinophagic flux would enhance ROS production which accordingly suppressed EMT or implementing the EMT suppression seemed to be through "fighting fire with fire" strategy. Taken together, our data demonstrated that ferritinophagic flux was a dominating driving force in EMT proceeding, and the new finding definitely will enrich our knowledge of ferritinophagy in EMT process.

1. Introduction

Epithelial-to-mesenchymal transition (EMT) is a cellular process allowing epithelial cells to undergo several biochemical alterations that permit a polarized epithelium switches to a highly invasive mesenchymal phenotype [1], accordingly suppression of epithelial markers; upregulation of mesenchymal markers occur [2, 3]. It has been demonstrated that the transforming growth factor (TGF), receptor tyrosine kinase (RTK), Wnt, Notch, hedgehog, hippo, cytokine, and nuclear receptor pathways have all been implicated in the onset of EMT [4, 5]. In addition, microRNAs (miRNAs), hypoxia, and the generated reactive oxygen species (ROS) can also induce EMT [6]. EMT is considered as a crucial event in cancer metastasis. During metastasis, the malignant cells spread from the primary tumor to distant site, which causes failure of vital organs, consequently leading to the death of patients. In addition, accompanied with metastasis, the cells acquire an ability to resist conventional treatments [7]. Therefore, insight into the cellular, molecular mechanism of EMT is required in order to develop new diagnostic and therapeutic strategies to prevent and treat metastases.

EMT is considered as a driving force in tumor progression, while compelling evidence reveals reactive oxygen

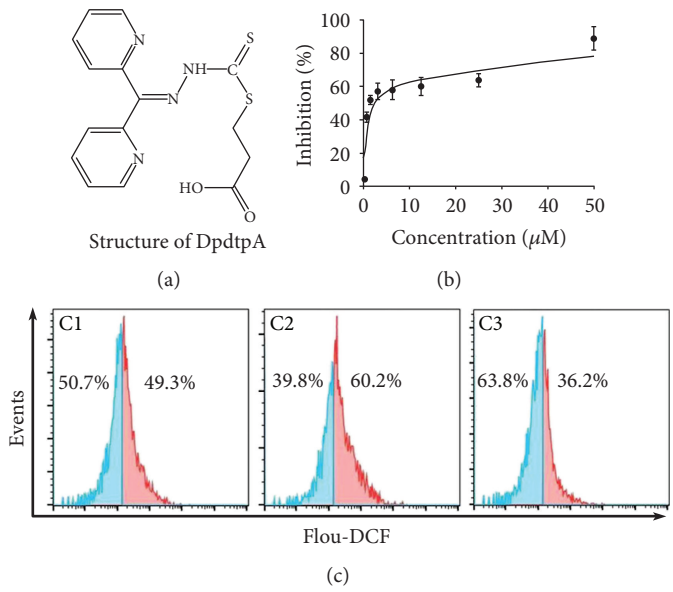

Figure 1: DpdtpA-induced growth inhibition involved ROS generation. (a) Structure of DpdtpA; (b) antiproliferative effect of DpdtpA on the CT26 cells; (c) DpdtpA induced ROS production: C1, 0.7% DMSO; C2, 0.78 μM DpdtpA; C3, 0.78 μM DpdtpA+NAC (1.5 mM). The data from MTT were from five measurements, and ROS assays were conducted twice.

species (ROS) as crucial conspirators in EMT engagement [8]. ROS are radicals, ions, or molecules that own a single unpaired electron in their outermost shell of electrons. They are constantly generated inside cells by a serial of dedicated enzyme complexes or as by-products of redox reactions, such as mitochondrial respiration [9–11]. ROS act as signaling molecules and are finely modulated and responsive to a wide array of environmental cues [10]. In addition, the degradation of iron-containing macromolecules (ferritin and mitochondrial components) or endocytosed erythrocytes (by macrophages) in lysosomes contributes large amounts of iron that can be reduced to Fe(II) in reducing lysosomal environment. Fe(II) either in lysosome or in labile iron pool (LIP) is known to catalyze Fenton reaction, yielding extremely reactive hydroxyl radicals [12]. As mentioned above, accumulating evidence shows that ROS are involved in EMT transition [13–17]; however, the functions of ROS in the processes of EMT remain unclear.

Since redox regulates epithelial-mesenchymal transition of tumor cell, scavenging ROS favors restoration of MET (mesenchymal-to-epithelial transition), which may efficiently slow dissemination of tumor cells [18, 19]. A lot of compounds either from natural products or artificially synthesized exhibit the ability in EMT reversion; different signal pathway was proposed [20–23]. Recently, iron depletion has been discovered to suppress tumor growth and EMT phenotypes via upregulation of the N-Myc downstream-regulated gene 2 (NDRG2) [24–27].

Labile iron pool (LIP) is regulated by ferritin, a highly conserved iron storage protein which is composed of two subunits, H-ferritin and L-ferritin, and the twelve pairs of subunits binding head to foot form the 24 subunit ferritin cages [28]. When the iron level in the cell is low, ferritin is degraded allowing the release of iron for use by the cell; therefore, ferritin plays an important role in cellular redox modulation. Iron chelator can induce ferritin degradation through ubiquitination or autophagy; the former occurs in proteasomes, latter in lysosomes. The worn-out proteins or organelle generally is degraded in lysosomes, and microtubule-associated protein light chain 3 (LC3) is involved in the proteolytic process. During autophagy, the cytosolic form of LC3 (LC3-I) conjugates to phosphatidylethanolamine to form LC3-phosphatidylethanolamine conjugate (LC3-II), which is recruited to autophagosomal membranes that engulf the damaged proteins. It has shown that when ferritin degrades in lysosome, nuclear receptor coactivator 4 (NCOA4) is required for ferritin delivery to autophagosome; the proteolytic process is termed ferritinophagy [29]. Currently, iron chelator, DFO and DpdtC, has been reported to own the ability in ferritinophagy induction [29, 30], but whether the iron chelator induced EMT reversion through ferritinophagy remains to be determined. In the present study, we firstly reported that activating ferritinophagic flux (NCOA4/ferritin) could inhibit EMT in the DpdtpA-treated CT26 cell, indicating that NCOA4 also involves in EMT process. Although the effect of autophagy on EMT is contradictory in different literature [31], and the role of ferritinophagy in EMT is not fully determined, therefore the results from this study will definitely enrich our knowledge in EMT transition.

2. Results

2.1. The Antiproliferative Action of the DpdtpA Was ROS Dependent. 2,2′-Di-pyridineketone hydrazone dithiocarbamate propionic acid (DpdtpA, Figure 1(a)) displayed significant proliferative inhibition against hepatoma carcinoma cell line in previous study, and its copper complex owned enhanced proliferative inhibition compared to DpdtpA;

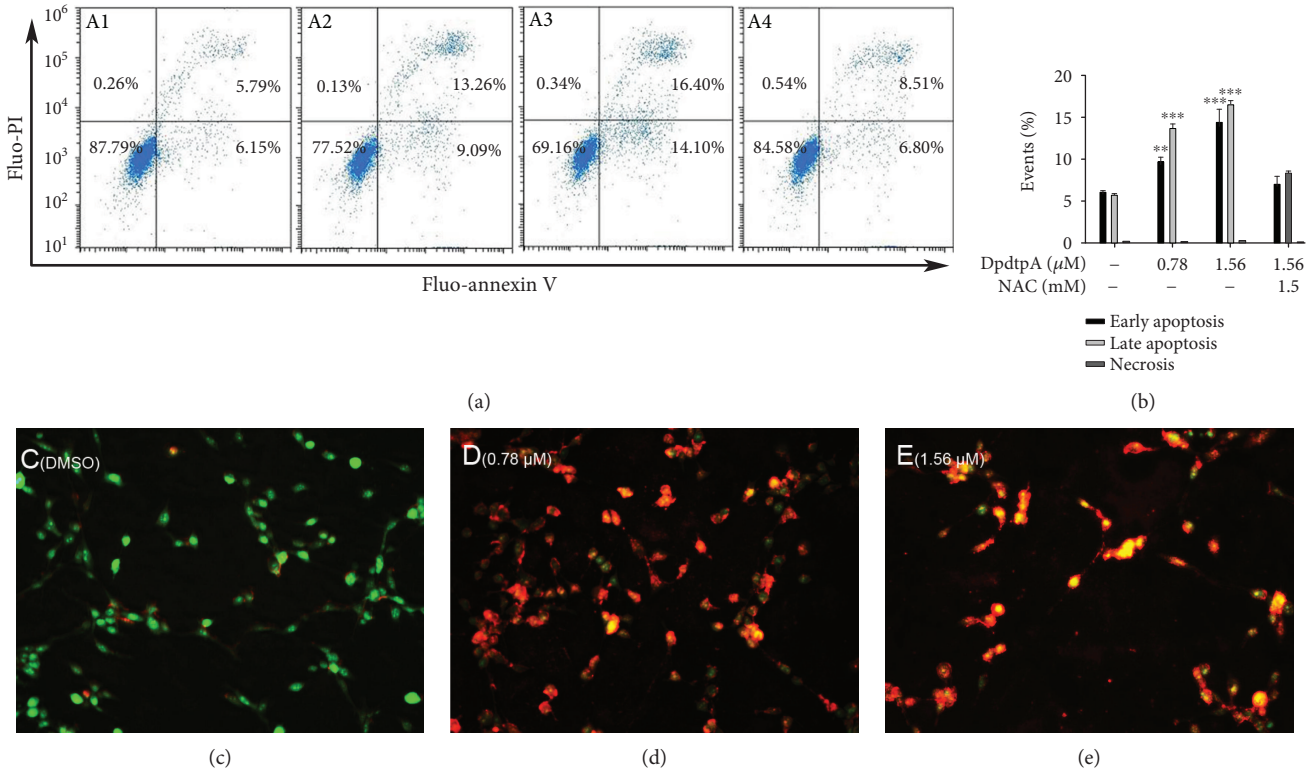

Figure 2: A DpdtpA induced apoptosis in the CT26 cell after 24 h posttreatment as detected by flow cytometry and EtBr/AO staining assay. Flow cytometry analysis: (A1) DMSO; (A2) 0.78 μM DpdtpA; (A3) 1.56 μM DpdtpA; (A4) 1.56 μM DpdtpA+NAC (1.5 mM). (b) Quantification analysis of apoptosis and necrosis induced by DpdtpA. The data were from two measurements. Microscopical analysis by EtBr/AO stains: (c) DMSO; (d) 0.78 μM DpdtpA; (e) 1.56 μM DpdtpA. Green, orange, and red fluorescence indicates live, apoptotic, and dead cells, respectively. Images were captured by fluorescence microscope (Nikon ECLIPSE TiE) at ×10 magnification. AO: acridine orange; EtBr: ethidium bromide. The measurements were performed thrice from different field of view (AO/EtBr stains); the quantification analysis of apoptosis by flow cytometry was from two measurements.

however, this did not correlate with ROS production [32]. To determine that whether the correlation between ROS production and growth inhibition was cell line dependent, we firstly evaluated the effect of DpdtpA on the proliferation of the CT26 cells. The dose-response curve is depicted in Figure 1(b). As expected, DpdtpA had significant growth inhibition for CT26 cells (IC_{50}: 1.5 ± 0.2 μM). Next, the cellular ROS level was measured by flow cytometry as described previously [33]. As shown in Figure 1(c), the populations in higher fluorescence intensities significantly increased by ~10% after the exposure of DpdtpA to the cells for 24 h, but the addition of NAC, a ROS scavenger, significantly decreased ROS production (~23%), hinting that the antiproliferative action involved ROS production. However, whether ROS production contributed to the growth inhibition needed to be further determined; thus, the growth inhibition in the presence of NAC was further assessed. As shown in Figure S1, the addition of NAC (0.15 mM) could attenuate the inhibitory ability of DpdtpA on the proliferation of the CT26 cell, indicating that ROS production played a role in the growth inhibition.

2.2. DpdtpA-Induced Growth Inhibition Involved Apoptosis. Since ROS production involved the growth inhibition induced by DpdtpA, the apoptosis might occur. To determine the correlation, the apoptotic populations at early and late stages were evaluated via flow cytometry after annexin V/propidium iodide (PI) staining, which measures externalization of phosphatidylserine on the cell surface of apoptotic cells specifically. Figure 2 showed that DpdtpA-induced early apoptosis and late apoptosis were in a concentration-dependent manner (Figure 2, A1-A3, from 11.94 to 30.5%, DpdtpA-induced early apoptosis and late apoptosis compared to control had statistical significance, $p < 0.05$ or 0.01); however, the apoptosis induction could be attenuated by addition of NAC (Figure 2, A4), indicating that ROS production played a role in the growth inhibition of DpdtpA. The quantification analysis of each group in apoptosis and necrosis is presented in Figure 2(b). In addition, detection of cell apoptosis using AO/EB is an additional method; thus, assay of apoptosis engagement via AO/EtBr stains was also conducted by the aid of fluorescence microscope [33, 34]. As shown in Figures 2(c)–2(e), live cells appeared uniformly green and had intact membrane, whereas early apoptotic cells and late apoptotic cells appeared as bright green and orange, respectively; necrotic cells appeared as red. Those supported that DpdtpA-induced growth inhibition involved apoptosis.

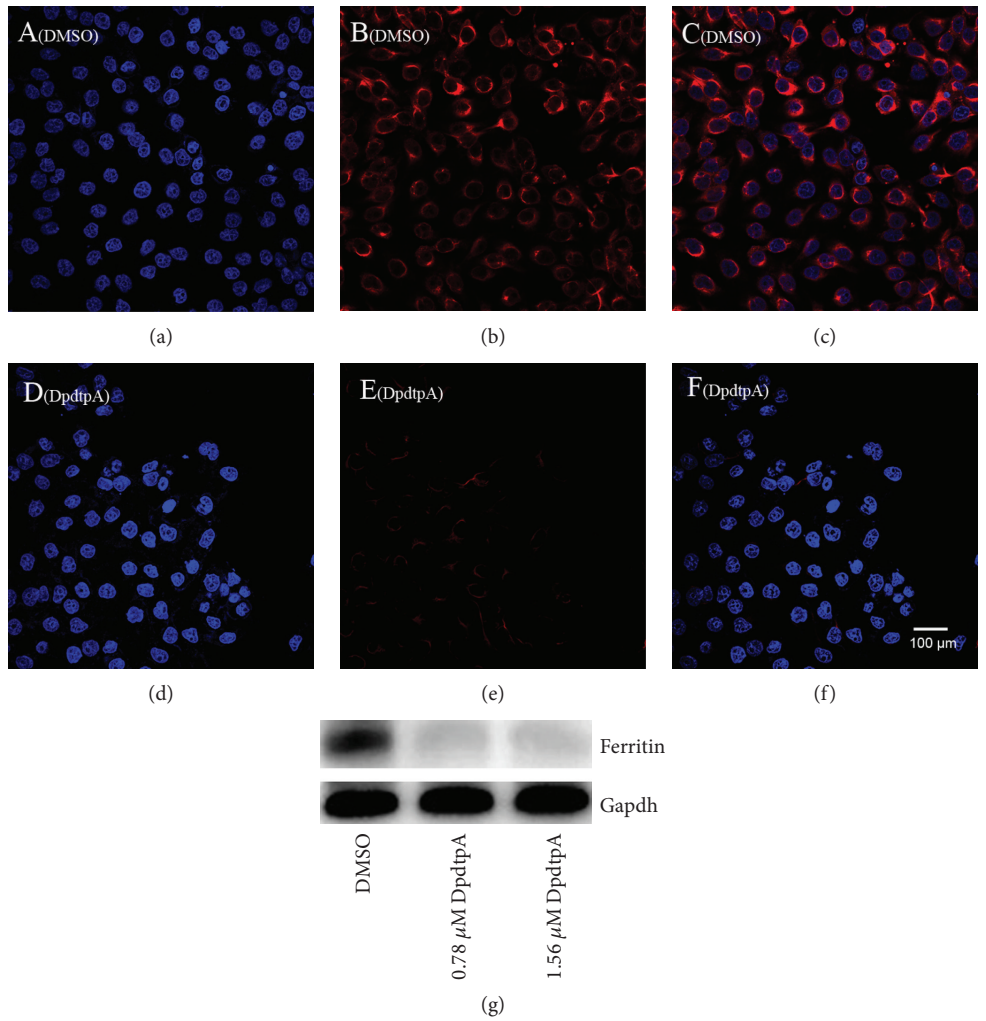

Figure 3: DpdtpA induced ferritin degradation. The nuclei stained by DAPI in blue, ferritin labeled in red. (a-c) Control group (DMSO): (a) nuclei in blue; (b) ferritin in red; (c) merge of nuclei and ferritin. (d-f) DpdtpA-treated CT26 cells: (d) nuclei in blue; (e) ferritin in red; (f) merge of nuclei and ferritin. The measurements were performed thrice. (g) Western blotting analysis. Scale bar: 100 μm.

2.3. DpdtpA Induced Ferritin Degradation. As described above, DpdtpA-induced growth inhibition involved ROS production; thus, the potential sites of ROS production were further explored. As well documented, ferritin degradation triggers Fenton reaction that is an important contributor in ROS production; therefore, the level of ferritin was determined; Figure 3(g) showed the status of ferritin based on Western blotting analysis. It was clear that DpdtpA indeed induced ferritin downregulation, which hinted that the ROS production may attribute to ferritin degradation. Similarly, the additional evidence from immunofluorescence analysis further supported ferritin downregulation after DpdtpA treatment as the red fluorescence of ferritin was significantly decreased (Figure 3(b)) compared to that of control (Figure 3(e)); those indicated that the growth inhibition induced by DpdtpA involved ferritin degradation that may contribute the ROS production.

2.4. DpdtpA Exposure Induced an Occurrence of Ferritinophagy. Next, we determined the site of ferritin degradation; it may occur in proteasomes. To this end, the levels of ferritin either in the condition of DpdtpA treatment alone or its combination with a proteasomes inhibitor, MG132, were determined. Beyond our expectation, the addition of MG132 did not attenuate the ferritin downregulation induced by DpdtpA (Figure S2), indicating that the ferritin degradation was not through the ubiquitination pathway. Thus, the proteolysis of ferritin in lysosomes could be further considered. To test the hypothesis, the changes of cellular ferritin and autophagic marker, LC3, were monitored via immunofluorescence technique. As shown in Figure 4, DpdtpA exposure resulted in upregulated LC3 (green in Figure 4(g)) and downregulated ferritin (red in Figure 4(f)) compared to control (Figures 4(b) and 4(c)), hinting that the ferritin degradation might be through autophagic proteolysis. To corroborate the above hint, the 3-MA, an inhibitor in the formation of autophagic vacuole, was added during the exposure of DpdtpA to the CT26 cells. As expected, the ferritin degradation was significantly attenuated (Figure 4(j)), and the level of ferritin and LC3 was restored to that of control (Figures 4(d) and 4(k)), further supporting that the downregulated ferritin was due

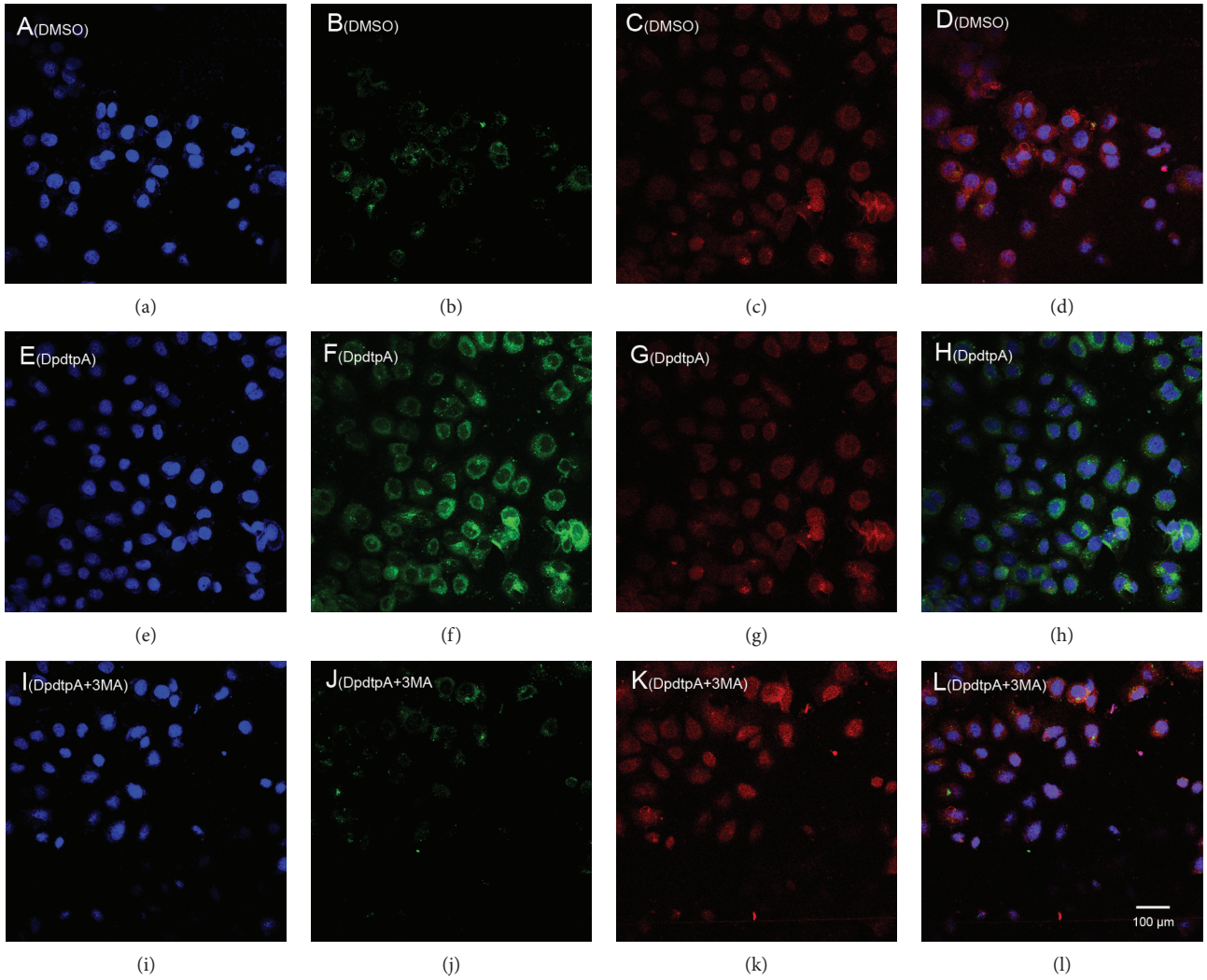

Figure 4: DpdtpA induced ferritin autophagy (ferritinophagy). The nuclei stained by DAPI in blue, ferritin labeled in red; LC3 labeled in green. (a-d) Control group: (a) nuclei in blue; (b) ferritin in red; (c) LC3 in green; (d) merge of ferritin with LC3. (e-h) DpdtpA-treated group: (e) nuclei in blue; (f) ferritin in red; (g) LC3 in green; (h) merge of ferritin with LC3. (i-l) DpdtpA combined with 3-MA group: (i) nuclei in blue; (j) ferritin in red; (k) LC3 in green; (l) merge of ferritin with LC3. The experiments were performed thrice. Scale bar: 100 μm.

to autophagic degradation. In addition, since ferritin degradation occurs through autophagy, the ferritinophagy may occur, which requires a specific carrier, NCOA4 for ferritin degradation; thus, cellular levels of NCOA4, ferritin, and autophagy-related proteins before and after DpdtpA exposure were determined by Western blotting. As shown in Figure 5, the ferritin was decreased with increased DpdtpA, but the autophagic markers (LC3-II, beclin) and NCOA4 were increased with increased DpdtpA; however, the addition of 3-MA or DFO as well as NAC could markedly attenuate those upregulated proteins. The quantitative comparisons of ferritin and NCOA4 are shown in Figure 5(b); moreover, similar analyses of LC3-II and beclin were performed in Figure S3. Those clearly indicated that DpdtpA indeed induced an occurrence of ferritinophagy, acting as other ferritinophagy-inducing agents [29, 30]. To further support ferritinophagy occurrence, the total iron content before and after DpdtpA exposure to the CT26 cells was determined by atomic absorbance spectrometry. As shown in Figure S4, DpdtpA treatment resulted in markedly decrease of iron abundance, in accordance with results from immunofluorescence and Western blotting analysis. Figure S5 showed that DpdtpA induced formation of massive autophagic vacuoles, which could be attenuated by 3-MA, or DFO as well as NAC, indicating that ferritin degradation correlated to autophagy that contributed to ROS production.

2.5. The DpdtpA Induced EMT Reversal. DpdtpA displayed significant growth inhibition for CT26 cells; the effect of it on cellular morphology was further determined. As shown in Figures 6(a)–6(c), the exposure of DpdtpA led to evident alteration in morphology, which encouraged us to consider whether it affected EMT transformation, favoring metastasis inhibition of cancers [35]. Thus, the molecular alterations in epithelial-mesenchymal markers were investigated before and after the exposure of DpdtpA to CT26 cells. The immunofluorescence is widely used to label an interested protein; to this end, CT26 cells were stained by fluorescence antibody

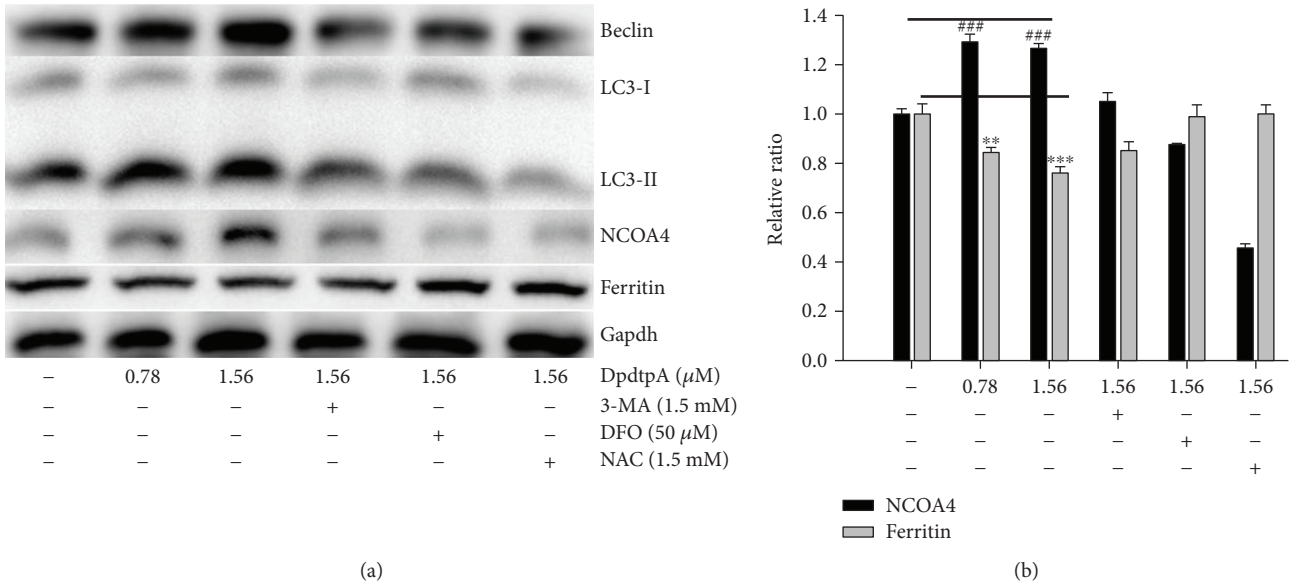

Figure 5: DpdtpA exposure resulted in alterations of ferritinophagy and autophagy proteins. (a) Western blotting analysis of autophagic and ferritinophagic proteins; (b) the quantitative comparisons of the proteins from (a). The quantification analysis of NCOA4 and ferritin was from two experiments. The condition was as indicated in the figure ($^{**}p < 0.05$; $^{***,\#\#\#}p < 0.01$).

after treatment of DpdtpA. As shown in Figure 6, the green fluorescence of E-cadherin was increased (Figures 6(f) and 6(j)), while the red fluorescence which represented vimentin was decreased (Figures 6(g) and 6(k)). The merged photographs (Figures 6(h) and 6(l)) clearly showed the alterations in E-cadherin and vimentin; the proportion of red fluorescence (vimentin) in Figure 6(h) was much higher than that in Figure 6(l), indicating that DpdtpA could inhibit the EMT. The supporting evidence from Western blotting also demonstrated that DpdtpA could downregulate mesenchymal marker, vimentin, and N-cadherin, contrarily upregulated epithelial marker, E-cadherin (Figure 6(d)), in accordance with that from immunofluorescence analysis, supporting the inhibitory effect of DpdtpA on EMT transformation.

2.6. DpdtpA Suppressed TGF-β1-Induced EMT through the Ferritinophagy Pathway. As mentioned above, DpdtpA could modulate expressions of epithelial-mesenchymal markers, owning the ability to suppress EMT. To validate the ability of DpdtpA, a model that was undergoing EMT needed to be created. TGF-β1 is the most powerful EMT inducer; thus, the CT26 cells were pretreated with TGF-β1 for 48 h, which resulted in obviously morphological alteration. As shown in Figure S6, the CT26 cells became more spindle-shaped, fibroblast-like cells, and these morphological characteristics were considered cells undergoing the EMT [36]. Next, we examined the effect of DpdtpA on EMT induced by TGF-β1. Immunofluorescence analysis revealed that TGF-β1 markedly reduced the level of E-cadherin in the CT26 cells (Figure 7(b)); however, the reduction in the E-cadherin level was markedly attenuated after DpdtpA treatment (compared Figure 7(b) with Figure 7(f)). As the E-cadherin increased, the upregulated vimentin was significantly suppressed by DpdtpA (Figures 7(c) and 7(g)); the merged photographs (Figures 7(d) and 7(h)) clearly showed the alterations of epithelial-mesenchymal transformation before and after treatment of DpdtpA, corroborating that DpdtpA was able to resist TGF-β1-induced EMT.

Next, we further questioned whether DpdtpA still induced ferritinophagy in the presence of TGF-β1. To this end, the levels of cellular NCOA4 and ferritin were determined by immunofluorescence. As shown in Figure 8, DpdtpA treatment markedly increased NCOA4 expression and attenuated ferritin expression, indicating that DpdtpA-suppressed TGF-β1-inhibited EMT involved ferritinophagy.

Since DpdtpA induced both EMT inhibition and ferritinophagy, we speculated there might be a correlation between the two events. Thus, we introduced a term, ferritinophagic flux, that was defined as the ratio of NCOA4/-ferritin and observed how ferritinophagic flux influences EMT status. As shown in Figure 9, TGF-β1 boosted EMT (upregulated vimentin and downregulated E-cadherin) through lowering ferritinophagic flux, contrarily DpdtpA inhibited EMT (upregulated E-cadherin, downregulated vimentin) through elevating ferritinophagic flux (Figure 9(a)). Therefore, the level of ferritinophagic flux was an important index for EMT status. To further support the hypothesis, a small interfering RNA was used to knock down the ferritinophagy-specific cargo, NCOA4, which resulted in downregulation of E-cadherin and upregulation of vimentin (Figure S7), suggesting that NCOA4 was involved in EMT transformation. To the best of our knowledge, the involvement of NCOA4 in EMT was first reported in the present study.

2.7. ROS Production in Lysosomes Led to Alteration of Permeability of Lysosomal Membrane of the CT26 Cell. As described in Section 2.1, the cellular ROS were increased when DpdtpA was exposed to the CT26 cells. It was

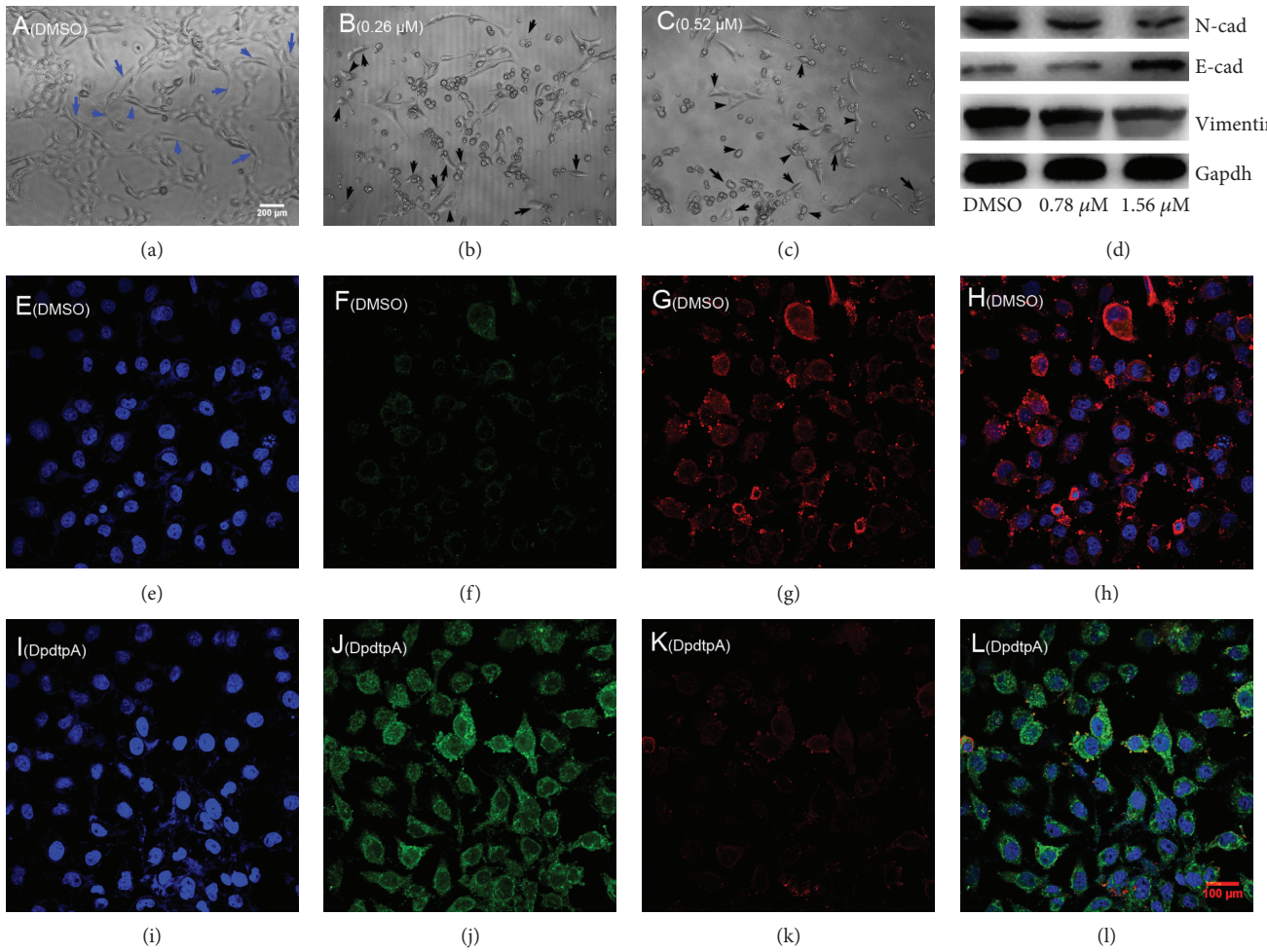

FIGURE 6: DpdtpA induced alteration in morphology correlated with EMT modulation. (a-c) Alteration in morphology treated by DpdtpA for 48 h at indicated concentration; the blue arrow: spindle-shaped cells, black arrow: retracted and rounded cells; (a) 0.7% DMSO; (b) 0.26 μM DpdtpA; (c) 0.52 μM DpdtpA; objective size: 20 × 10, scale bar: 200 μm. (d) Western blotting analysis. (e-l) Immunofluorescence analysis of epithelial-mesenchymal markers. (e-h) (0.7% DMSO): (e) nuclei in blue; (f) E-cadherin in green; (g) vimentin in red; (h) merge of nuclei, E-cadherin, and vimentin in the DMSO group. (i-l) DpdtpA-treated group: (i) nuclei in blue; (j) E-cadherin in green; (k) vimentin in red; (l) merge of nuclei, E-cadherin and vimentin in the DpdtpA-treated group. The measurements were performed thrice from different field of view. Objective size: 40 × 10 (fluorescence), scale bar: 100 μm.

conceivable that the intracellular ROS at least partially were generated from lysosomes due to occurrence of ferritinophagy that may trigger Fenton-like reaction [37]. To test the speculation, the lysosomal membrane of permeability (LMP) was determined as described previously [38]. As shown in Figure 10, the lysosomotropic dye, LysoTracker Red was accumulated in lysosomes in a concentration-dependent manner (Figures 10(a)–10(c)), but addition of 3-MA drastically attenuated the accumulation (Figure 10(e)), in consistent with results from observation of ferritinophagy. In addition, addition of NAC and DFO (iron chelator) also markedly decreased the accumulation of the dye (Figures 10(d) and 10(f)); the quantitative analysis is shown in Figure 10(g). Those indicated that ROS production indeed occurred in lysosomes (Figure 10). Owing to the change of LMP, the hydrolase in lysosome may be released. Therefore, a protease cathepsin in lysosome was determined. As shown in Figure 10(h), more cathepsin D was presented in cytoplasm during DpdtpA treatment, but the level of cathepsin D could be attenuated by 3-MA, NAC, and DFO, supporting that ferritinophagy triggered Fenton reaction was a critical contributor in ROS production. In addition, the data from flow cytometry revealed that the DpdtpA suppressed TGF-β1-induced EMT seemed to be through producing more ROS (Figure S8). To gain more evidence, the levels of EMT-related proteins were further determined in the absence or presence of NAC. As shown in Figure S9, the addition of NAC could attenuate the EMT inhibition induced by DpdtpA, supporting that the EMT inhibition seemed to be achieved through "fighting fire with fire" strategy.

3. Discussion

Cancer metastasis is responsible for approximately 90% of all cancer-related deaths. Certain patients may benefit from resection, though mostly transiently for lack of clinical marker for surgeon due to cancer metastasis [39]; therefore,

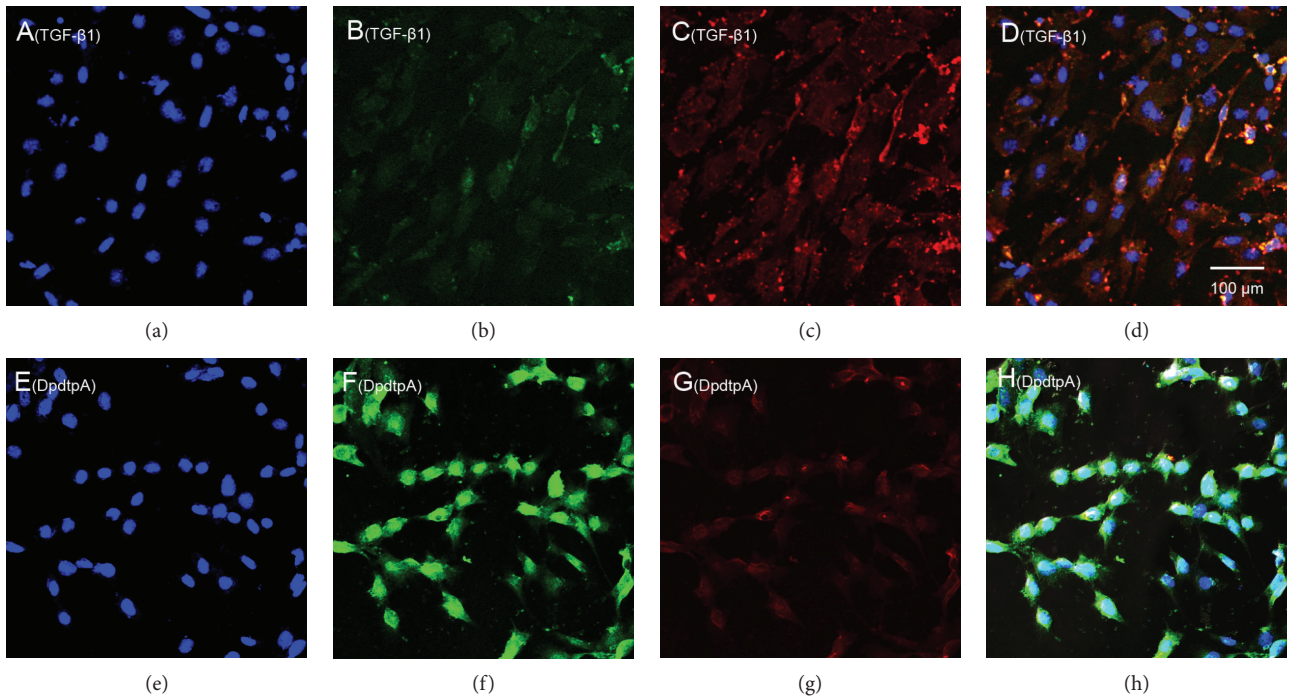

Figure 7: DpdtpA resisted TGF-β1-induced EMT. (a-d) (TGF-β1-treated group): (a) nuclei stained by DAPI in blue (DMSO); (b) E-cadherin in green; (c) vimentin in red; (d) merge of nuclei, E-cadherin, and vimentin. (e-h) (TGF-β1 treatment plus DpdtpA): (e) nuclei in blue; (f) E-cadherin in green; (g) vimentin in red; (h) merge of nuclei, E-cadherin, and vimentin. The measurements were performed thrice from different field of view. Objective size: 40×10, scale bar: 100 μm.

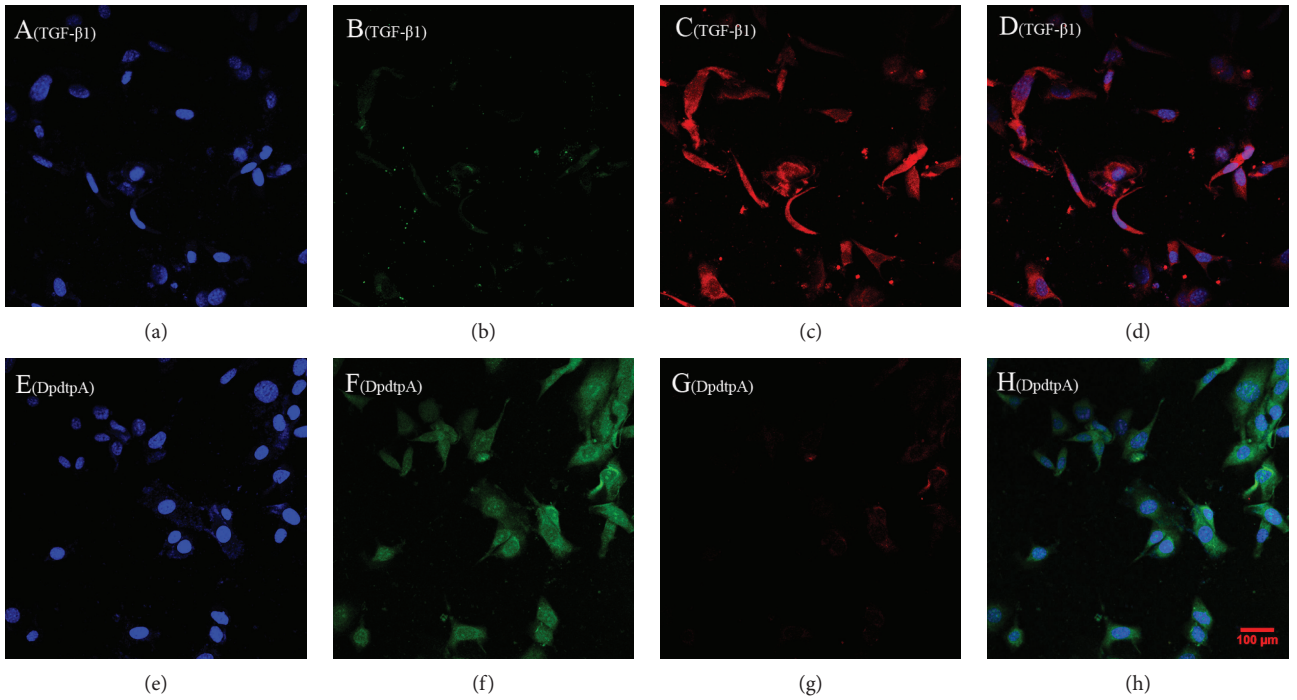

Figure 8: DpdtpA induced ferritinophagy in the presence of TGF-β1. The nuclei stained by DAPI in blue, NCOA4 in green, and ferritin in red. (a-d) (0.7% DMSO, TGF-β1 treatment only): (a) nuclei in blue; (b) NCOA4 in green; (c) ferritin in red; (d) merge of nuclei, ferritin, and NCOA4. (e)-(h) TGF-β1 combined with DpdtpA: (e) nuclei in blue; (f) NCOA4 in green; (g) ferritin in red; (h) merge of nuclei, ferritin, and NCOA4. Objective size: 40×10, scale bar: 100 μm. The measurements were performed thrice from different field of view.

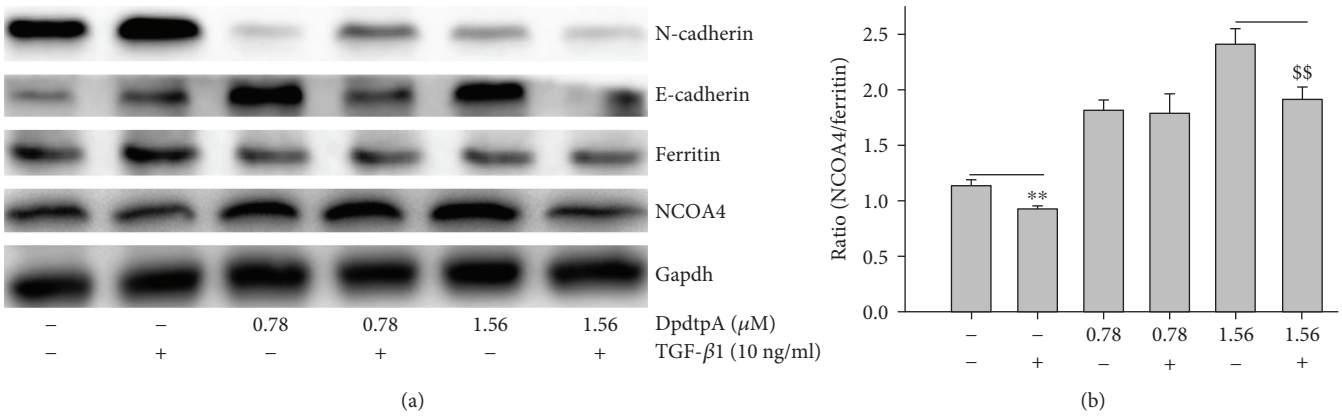

Figure 9: Ferritinophagic flux played an important role in EMT process. (a) The alterations in ferritinophagy and EMT-related proteins when either TGF-β1 or combined with DpdtpA treatment; (b) quantitative analysis of the ferritinophagic flux in the investigated condition. The quantification analysis of ferritinophagic flux was from three experiments ($^{**, \$\$}p < 0.05$; one-way ANOVA).

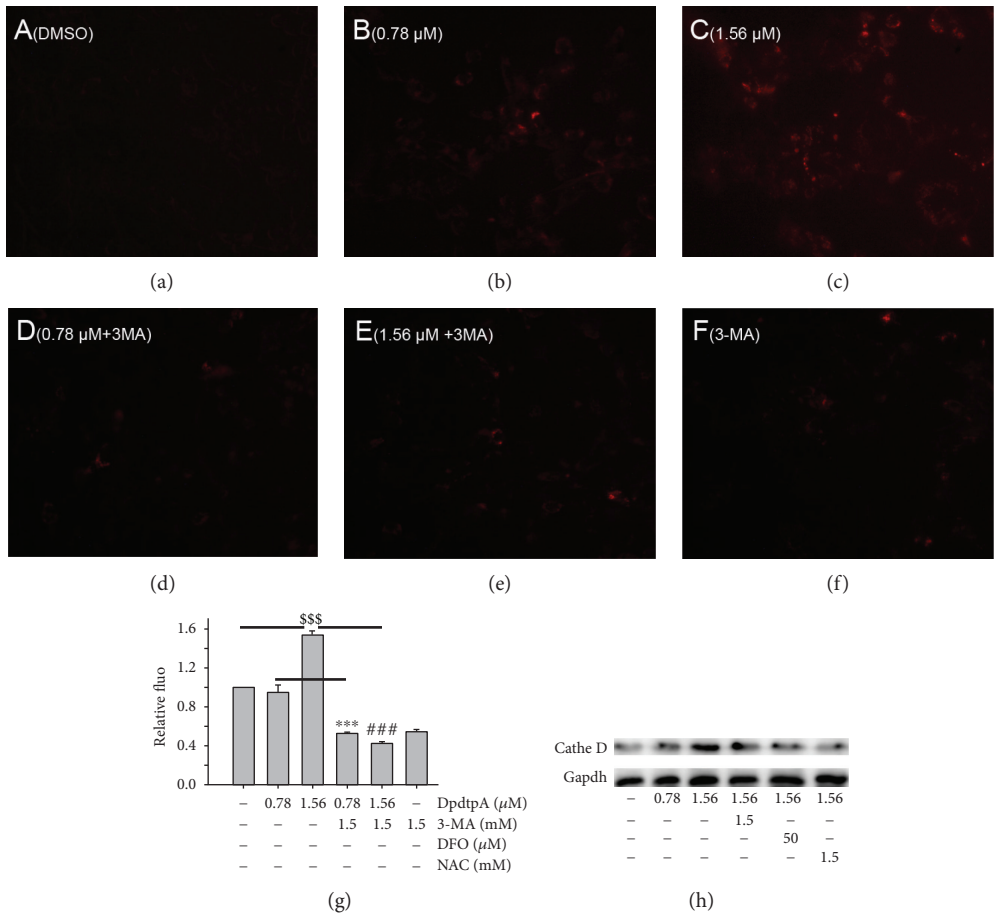

Figure 10: DpdtpA induced alteration in lysosomal membrane permeability and release of cathepsin D. (a) DMSO; (b) 0.78 μM DpdtpA; (c) 1.56 μM DpdtpA; (d) 0.78 μM DpdtpA+3-MA (5 mM); (e) 1.56 μM DpdtpA+3-MA (5 mM); (f) 3-MA (5 mM); (g) quantitative analysis of alteration in fluorescence after treated by either DpdtpA or combined with 3-MA; (h) DpdtpA induced cathepsin D release. The quantification analysis of intensity of red fluorescence was from three measurements. The Western blots were performed twice ($^{***, ###, \$\$\$}p < 0.01$).

effective means are needed to suppress invasion and metastasis. To this end, understanding the underlying details of metastasis in a molecular level is required. It has been demonstrated that epithelial-mesenchymal transition (EMT) involves metastatic process, and EMT is a key metastasis-promoting step in many cancers [40]; thus, inhibiting EMT

is an alternative option in cancer therapy. The occurrence of EMT results in cytoskeleton reorganization, loss of cell-cell adhesion molecules, and transformation to mesenchymal cell phenotype, which endows the cells with an invasive ability [41]; the alterations in abundance of E-cadherin, N-cadherin, and vimentin determine EMT status. A number of transcription factors are known to be involved in the regulation of EMT, such as ZEB 1 and ZEB 2, snail, slug, and twist [42]. In addition, growth factors and cytokines, ECM components, Wnt proteins, hypoxia, ROS, and mechanical stress trigger EMT [43]. Recently, the effect of ferritin heavy chain (FHC) on EMT has received widely attention. Karicheva et al. reported that oxidant-induced autophagy and ferritin degradation contributed to epithelial-mesenchymal transition through lysosomal iron in A549 cell line [16]. Zhang et al. revealed that FHC played a critical role in TGF-β1-induced EMT in AML-12 cells [44]. Aversa et al. showed that FHC silencing caused EMT in MCF-7 and H460 cell lines through the CXCR4/CXCL12 axis [45]. Meanwhile, those studies also demonstrated that ROS production stemmed from ferritin degradation (downregulation) had a role in EMT process. It is well documented that ferritin degradation may occur either in proteasomes through ubiquitination or in lysosomes via ferritinophagy; however, distinct route for its degradation (or regulation) in EMT process received lesser concern. Iron chelator induced ferritin degradation has been reported in several studies [27, 46]; some iron chelator can inhibit EMT [27], but whether NCOA4-mediated ferritinophagy engages EMT modulation remains unclear. In the present study, we presented a new insight into the role of ferritinophagic flux in EMT process. DpdtpA, a dithiocarbamate derivative, exhibited significant growth inhibition against the CT26 cells (Figure 1), which involved ROS-dependent apoptosis induction (Figure 2). To gain insight into the mechanism in ROS production, the level of ferritin before and after DpdtpA treatment was investigated, and a downregulation of ferritin both from immunofluorescence and Western blot was observed, hinting the ROS production might stem from ferritin degradation (Figure 3). To determine whether the ferritin degradation occurred in proteasomes, a proteasome inhibitor, MG132 was employed; as shown in Figure S2, the inhibitor did not attenuate ferritin decrease, indicating that DpdtpA-induced ferritin degradation was not through ubiquitination. Thus, lysosomal proteolysis could be considered. To support the hypothesis, the alterations in autophagic marker, LC3 and ferritinophagy-specific cargo, and NCOA4 were investigated; the data clearly showed that DpdtpA induced an occurrence of ferritinophagy as DpdtC acted (Figures 4 and 5) [30], hinting that ROS production may stem from lysosomal iron that triggered Fenton reaction. In addition, DpdtpA could also induce morphological change of the CT26 cells (Figure 6), which prompted us to consider that the DpdtpA might also affect EMT. To confirm the effect of DpdtpA on EMT, the levels of epithelial and mesenchymal marker after DpdtpA treatment were determined (Figure 6). As expected, the upregulated E-cadherin and downregulated vimentin clearly demonstrated that DpdtpA inhibited EMT. Furthermore, additional evidence from the EMT model induced by TGF-β1 validated the ability of DpdtpA [36], because the DpdtpA treatment resulted in an increase of E-cadherin and a decrease of vimentin (Figure 7), in accordance with other iron chelator acted [27].

It was interesting that the EMT inhibition was accompanied by upregulation of LC3 and NCOA4 and downregulation of ferritin (Figure 8), which hinted that there was a correlation between EMT and ferritin degradation. Thus, the term, ferritinophagic flux, was used to describe the correlation. As shown in Figure 9(b), TGF-β1 triggered EMT through attenuating ferritinophagic flux, but DpdtpA inhibited EMT through increasing ferritinophagic flux, indicating that ferritinophagic flux determined the status of EMT. To support the hypothesis, a small interfering RNA of NCOA4 was used to knockdown the ferritinophagy-specific cargo, which resulted in both downregulation of E-cadherin and upregulation of vimentin, supporting that NCOA4 was involved in EMT process. Our finding suggested that ferritinophagic flux was also a dominant driving force in EMT process, which firstly described that NCOA4 involved EMT transformation. Similar result was found in other cell lines (the results will be reported later). Currently, NCOA4 function differently depends on the cancer context, while robust evidence for the role of ferritinophagy in tumorigenesis is lacking [40]; here, we presented that NCOA4-mediated ferritinophagy contributed to EMT inhibition, which may enrich our knowledge for NCOA4 in tumor development.

Owing to occurrence of ferritinophagy, the abundance of lysosomal iron should be increased; oxidative stress and cell death may come up [47]. The consequence of ferritinophagy inevitably led to lysosomal destruction; Figure 10 showed that more LysoTracker Red dyes were accumulated in lysosomes after DpdtpA treatment, but this accumulation could be attenuated by addition of 3-MA, in accordance with the observation reported previously [30], indicating that the damage of lysosomal membrane (or integrity) was due to occurrence of ferritinophagy. It was imagined that the ferric iron liberated from digested ferritin would reduce further by the endosomal ferrireductase Steap3 in the acidified lysosome [48]; the resulting ferrous ion triggered Fenton reaction. To confirm that the lysosomal ROS production contributed to EMT transformation, the ROS production in either stimulating by TGF-β1 or combined with DpdtpA was investigated. TGF-β1 indeed induced rising of ROS in the CT26 cells, in accordance with reported previously [16]. It was more interesting that ROS production induced by DpdtpA exceeded that triggered by TGF-β1, seeming to support that DpdtpA induced EMT inhibition through a "fighting fire with fire" strategy (Figure S8, S9).

Taken together, DpdtpA-induced growth inhibition in the CT26 cells was ROS dependent. Mechanistic study revealed that DpdtpA was able to induce ferritinophagy that contributed to ROS production. Furthermore, DpdtpA was also able to inhibit EMT; the correlation analysis revealed that the ferritinophagic flux was a dominating factor in EMT process, attenuating the ferritinophagic flux resulted in EMT occurrence, while enhancing ferritinophagic flux favored to inhibit EMT (reversing EMT), indicating that NCOA4 played an important role in EMT process. In

addition, DpdtpA induced EMT inhibition through producing massive ROS that were due to occurrence of ferritinophagy. However, the effect of ferritinophagic flux on EMT in different cell lines *in vivo* and *in vitro* requires more studies in the future due to the diversity of iron chelators in structure and complex interactions with biological molecules.

4. Materials and Methods

4.1. Materials. All chemicals used were analytical reagents (AR) grade. 3-(4,5-Dimethylthiazol-2-yl)-2,5-diphenyltetrazolium bromide (MTT), monodansylcadaverine (MDC), 3-methyladenine (3-MA), chloroquine, dichlorofluorescein (H_2DCF-DA), desferoxamine (DFO), 4′,6-diamidino-2-phenylindole (DAPI), Roswell Park Memorial Institute (RPMI) 1640, and other chemicals were purchased from Sigma-Aldrich. Antibodies of vimentin (60330-1-lg, 10366-1-AP), LC3 (14600-1-AP), NCOA4 (E11-17114C), N-cadherin (22018-1-AP), and Gadph (E12-052) for Western blotting were obtained from Proteintech Group Inc. (Wuhan, China). Antibodies of E-cadherin (3195), ferritin (H chain, 3998S), secondary antibodies (fluorescence labeled for immunofluorescence, 8890S, 4412S), and cathepsin D were purchased from Cell Signaling Technology (USA). Ferritin antibody (SC-376594) for immunofluorescence was obtained from Santa Cruz Biotechnology (USA, Santa Cruz). NCOA4 antibody (HPA0512) for immunofluorescence was purchased from Atlas Antibody (Sweden). Secondary antibodies for Western blotting were obtained from EarthOx, LLC (San Francisco, USA).

4.2. Cytotoxicity Assay (MTT Assay). The stock solution of DpdtpA (10 mM) was prepared in 70% DMSO and diluted to the required concentration with 70% DMSO. The CT26 cells were cultured in RPMI 1640 medium supplemented with 10% fetal calf serum (FCS) and antibiotics. The cells in the exponential phase were collected and seeded equivalently into a 96-well plate; next, the varied DpdtpA (or in the presence of NAC) was added after the cells adhered. Following 48 h incubation at 37°C in a humidified atmosphere of 5% CO_2, 10 μl MTT solution (5 mg/ml) was added and further incubated for 4 h; next, 100 μl DMSO was added in each well to dissolve the formazan crystals after removing cell culture. The measurement of absorbance of the solution was performed on a microplate reader (MK3, Thermo Scientific) at 570 nm. Percent growth inhibition was defined as percent absorbance inhibition within appropriate absorbance in each cell line. The same assay was performed in triplet.

4.3. Flow Cytometric Analysis of Apoptosis and Cellular ROS. Cells were seeded into a 6-well plate and treated as described in the section of cytotoxicity assay. The cells were treated with different concentrations of the agent (0.78 and 1.56 μM DpdtpA) for 24 h. Then, the cell culture was removed, following PBS washing, trypsin digestion; finally, the annexin V and propidium iodide (a kit from Dojindo Laboratories, Kumamoto, Japan) were added as recommended by the company. The stained cells were subjected to flow cytometer analysis (Becton-Dickinson, USA). Similar to apoptosis assay, the CT26 cells were resuspended in H_2DCF-DA containing serum-free culture medium and incubated for 30 min. Next, after removing the H_2DCF-DA contained medium by centrifugation, washing with PBS, finally resuspended the cells in PBS. The intracellular ROS assay was performed on a flow cytometer (Becton-Dickinson, USA).

4.4. Immunofluorescence Analysis. The CT26 cells were first cultured in a 6-well plate with cover glass overnight. Following DpdtpA treatment for 24 h, cells were first fixed with 4% paraformaldehyde in PBS for 15 min at 37°C and then permeabilized with 0.2% triton-X-100 in PBS for 10 min. After blocking with 1% BSA in PBS for 30 min, the cells were incubated with either ferritin (H chain, Santa Cruz Biotechnology), or combined with LC3 (or NCOA4 (Atlas Antibodies)), or vimentin combined with E-cadherin (Cell Signaling Technology) primary antibody based on the protocol recommended by the company; at 4°C, the plate was shaken overnight. Next, removing the primary antibodies and washing with PBS, the cells were further incubated with fluorescence-labeled secondary antibody for 3 h at room temperature. After removing the secondary antibody, the cells were further counterstained with DAPI. Finally, a confocal laser scanning microscope (Nikon eclipse Ts2, Japan) was used to visualize the cells; the representative cells were selected and photographed.

4.5. Assay of Lysosomal Membrane Permeability (LMP). The alteration of LMP was assayed as previously described [30]. For detection of the acidic cellular, LysoTracker Red (Invitrogen, USA) was used, which emits bright red fluorescence in acidic vesicles, after treatment of the cells with the agent, LysoTracker Red (the concentration used as recommended), for a period of 30 min. Following PBS washing, the fluorescent micrographs were captured using an inverted fluorescence microscope (Nikon eclipse Ts2, Japan).

4.6. Western Blotting Analysis. The protocol for Western blotting was followed as described previously [30]; briefly, 1×10^7 CT26 cells that treated with or without DpdtpA were scraped in lysis buffer (50 mM Tris-HCl, pH 8.0, 150 mM NaCl, 1.0% NP-40, 10% glycerol, and protease inhibitors) on ice for 30 min., followed by centrifugation at 14,000 × g. The clear supernatant was stored at -80°C. Protein concentration was determined using a colorimetric Bio-Rad DC protein assay using the MK3 microplate reader at 570 nm. Proteins (30 μg) were separated on a 13~15% sodium dodecyl sulfate-polyacrylamide gel at 200 V for 3 h. The separated proteins were subsequently transferred onto a PVDF membrane at 60 V for 2 h. The membrane was washed with Tris-buffered saline (TBS) and then blocked for 2 h in TBS containing 0.1% Tween-20 and 5% nonfat skimmed milk. The membrane was incubated at 4°C overnight with the appropriate primary antibody. The membrane was then washed several times with TBST and subsequently incubated with the appropriate HRP-conjugated secondary antibody (1 : 2,000 in TBST) for 1 h at room temperature. Following washing with TBST, the protein bands were detected using a super sensitive ECL solution (Boster Biological Technology

Co. Ltd.) and visualized using a Syngene G:BOX imager (Cambridge, United Kingdom). Quantifications of protein band intensities and fluorescence intensity were performed using ImageJ software.

4.7. Statistical Analysis. Data were analyzed with Prism 5.0 (GraphPad Software Inc., USA). Comparisons were made using a one-way analysis of variance or a two-tailed t-test. Results are presented as the mean ± SEM. A p value < 0.05 was considered statistically significant.

Data Availability

The data used to support the findings of this study are included within the article.

Conflicts of Interest

The authors declare no conflict of interest.

Authors' Contributions

Yanjie Sun, Cuiping Li, and Jiankang Feng performed the experiments; they contributed equally to this work. Changzheng Li conceived and designed the experiments; Yongli Li, Xinbo Zhai, and Lei Zhang analyzed the data and generated figures. Changzheng Li prepared and wrote the paper.

Acknowledgments

The present study was supported by grants awarded by the Natural Science Foundation of China (No. 21571153), the Henan Provincial Department of Science and Technology (No. 152300410118), the Key Research Project Funding Program of Higher Educational Institutions of Henan Province (19A310021), and innovation team awarded by Sanquan College of Xinxiang Medical University (SQTD201703, SQTD201802).

Supplementary Materials

Figure S1: NAC attenuated DpdtpA-induced growth inhibition of the CT26 cell. The procedure was similar to that in the MTT assay section except 24 h incubation. The experimental condition was as indicated (∗∗' ## $p < 0.05$; one-way ANOVA). Figure S2: MG312 did not attenuate DpdtpA-induced ferritin degradation. The experiments were performed twice. Figure S3: quantification analyses of autophagy-related proteins. The results of quantification analysis of LC3-II and beclin were from two experiments ($^{**}p < 0.05$, $^{***}p < 0.01$ compared to DMSO; $^{\#\#\#}p < 0.01$ compared to 1.56 μM treated group). Figure S4: Alteration of iron abundance when the cells were subjected to DpdtpA treatment or combination with 3-MA ($^{***}p < 0.01$). Figure S5: MDC staining for determination of autophagosomes induced by DpdtpA. The condition was as indicated. Figure S6: TGF-β1 induced cellular alteration in morphology. (A) The treatment without TGF-β1 and (B) with TGF-β1. Figure S7: NCOA4 plays a role in EMT transformation. (A) Western blotting analyses of EMT-related and ferritinophagy proteins; (B) quantification analyses of E-cadherin, vimentin, ferritin, NCOA4, and ferritinophagic flux. The experiments were performed thrice ($^{**}p < 0.05$ and $^{***}p < 0.01$). Figure S8: ROS production induced by DpdtpA was a time-dependent manner. The condition was indicated in the figure. Figure S9: ROS scavenger attenuated the ability of DpdtpA in EMT reversal. (A) The alterations in EMT-related markers when the CT26 cells treated by DpdtpA in the absence or presence of NAC; (B) quantification analysis based on (A). The condition was indicated in the figure. The experiments were performed thrice ($^{***}p < 0.01$)." Also, please enclose "$^{***}p < 0.01$" in a math environment. *(Supplementary Materials)*

References

[1] P. Savagner, "Epithelial–Mesenchymal Transitions," *Current Topics in Developmental Biology*, vol. 112, pp. 273–300, 2015.

[2] J. H. Tsai, J. L. Donaher, D. A. Murphy, S. Chau, and J. Yang, "Spatiotemporal regulation of epithelial-mesenchymal transition is essential for squamous cell carcinoma metastasis," *Cancer Cell*, vol. 22, no. 6, pp. 725–736, 2012.

[3] S. Lamouille, J. Xu, and R. Derynck, "Molecular mechanisms of epithelial–mesenchymal transition," *Nature Reviews Molecular Cell Biology*, vol. 15, no. 3, pp. 178–196, 2014.

[4] A. Moustakas and C. H. Heldin, "Signaling networks guiding epithelial-mesenchymal transitions during embryogenesis and cancer progression," *Cancer Science*, vol. 98, no. 10, pp. 1512–1520, 2007.

[5] R. Derynck, B. P. Muthusamy, and K. Y. Saeteurn, "Signaling pathway cooperation in TGF-β-induced epithelial–mesenchymal transition," *Current Opinion in Cell Biology*, vol. 31, pp. 56–66, 2014.

[6] Z. Wang, Y. Li, and F. Sarkar, "Signaling mechanism(s) of reactive oxygen species in epithelial-mesenchymal transition reminiscent of cancer stem cells in tumor progression," *Current Stem Cell Research & Therapy*, vol. 5, no. 1, pp. 74–80, 2010.

[7] J. Massague, E. Batlle, and R. R. Gomis, "Understanding the molecular mechanisms driving metastasis," *Molecular Oncology*, vol. 11, no. 1, pp. 3-4, 2017.

[8] E. Giannoni, M. Parri, and P. Chiarugi, "EMT and oxidative stress: a bidirectional interplay affecting tumor malignancy," *Antioxidants & Redox Signaling*, vol. 16, no. 11, pp. 1248–1263, 2012.

[9] D. Han, E. Williams, and E. Cadenas, "Mitochondrial respiratory chain-dependent generation of superoxide anion and its release into the intermembrane space," *Biochemical Journal*, vol. 353, no. 2, pp. 411–416, 2001.

[10] Y. M. W. Janssen-Heininger, B. T. Mossman, N. H. Heintz et al., "Redox-based regulation of signal transduction: principles, pitfalls, and promises," *Free Radical Biology and Medicine*, vol. 45, no. 1, pp. 1–17, 2008.

[11] M. P. Murphy, "How mitochondria produce reactive oxygen species," *Biochemical Journal*, vol. 417, no. 1, pp. 1–13, 2009.

[12] A. Terman and T. Kurz, "Lysosomal iron, iron chelation, and cell death," *Antioxidants & Redox Signaling*, vol. 18, no. 8, pp. 888–898, 2013.

[13] Y. Dong, Z. Wu, M. He et al., "ADAM9 mediates the interleukin-6-induced epithelial-mesenchymal transition and metastasis through ROS production in hepatoma cells," *Cancer Letters*, vol. 421, no. 1, pp. 1–14, 2018.

[14] J. Jiang, K. Wang, Y. Chen, H. Chen, E. C. Nice, and C. Huang, "Redox regulation in tumor cell epithelial-mesenchymal transition: molecular basis and therapeutic strategy," *Signal Transduction and Targeted Therapy*, vol. 2, no. 1, 2017.

[15] A. Sioutas, L. Vainikka, M. Kentson et al., "Oxidant-induced autophagy and ferritin degradation contribute to epithelial-mesenchymal transition through lysosomal iron," *Journal of Inflammation Research*, vol. Volume 10, pp. 29–39, 2017.

[16] O. Karicheva, J. M. Rodriguez-Vargas, N. Wadier et al., "PARP3 controls TGFβ and ROS driven epithelial-to-mesenchymal transition and stemness by stimulating a TG2-Snail-E-cadherin axis," *Oncotarget*, vol. 7, no. 39, pp. 64109–64123, 2016.

[17] W. Li, Z. Jiang, X. Xiao et al., "Curcumin inhibits superoxide dismutase-induced epithelial-to-mesenchymal transition via the PI3K/Akt/NF-κB pathway in pancreatic cancer cells," *International Journal of Oncology*, vol. 52, pp. 1593–1602, 2018.

[18] J. P. Thiery and J. P. Sleeman, "Complex networks orchestrate epithelial-mesenchymal transitions," *Nature Reviews Molecular Cell Biology*, vol. 7, no. 2, pp. 131–142, 2006.

[19] K. Hara, C. Hamada, K. Wakabayashi et al., "Scavenging of reactive oxygen species by astaxanthin inhibits epithelial-mesenchymal transition in high glucose-stimulated mesothelial cells," *PLoS One*, vol. 12, no. 9, article e0184332, 2017.

[20] W. B. Zhu, Z. F. Zhao, and X. Zhou, "AMD3100 inhibits epithelial-mesenchymal transition, cell invasion, and metastasis in the liver and the lung through blocking the SDF-1α/CXCR4 signaling pathway in prostate cancer," *Journal of Cellular Physiology*, vol. 234, no. 7, pp. 11746–11759, 2019.

[21] C. Zhang and Y. Wang, "Metformin attenuates cells stemness and epithelial-mesenchymal transition in colorectal cancer cells by inhibiting the Wnt3a/β-catenin pathway," *Molecular Medicine Reports*, vol. 19, no. 2, pp. 1203–1209, 2019.

[22] T. J. Wu, B. Xu, G. H. Zhao, J. Luo, and C. Luo, "IL-37 suppresses migration and invasion of gallbladder cancer cells through inhibition of HIF-1α induced epithelial-mesenchymal transition," *European Review for Medical and Pharmacological Sciences*, vol. 22, no. 23, pp. 8179–8185, 2018.

[23] C. Ricca, A. Aillon, M. Viano, L. Bergandi, E. Aldieri, and F. Silvagno, "Vitamin D inhibits the epithelial-mesenchymal transition by a negative feedback regulation of TGF-β activity," *The Journal of Steroid Biochemistry and Molecular Biology*, vol. 187, pp. 97–105, 2019.

[24] S. Nishitani, K. Noma, T. Ohara et al., "Iron depletion-induced downregulation of N-cadherin expression inhibits invasive malignant phenotypes in human esophageal cancer," *International Journal of Oncology*, vol. 49, no. 4, pp. 1351–1359, 2016.

[25] D. J. Lane, T. M. Mills, N. H. Shafie et al., "Expanding horizons in iron chelation and the treatment of cancer: role of iron in the regulation of ER stress and the epithelial-mesenchymal transition," *Biochimica et Biophysica Acta*, vol. 1845, no. 2, pp. 166–181, 2014.

[26] J. Wang, D. Yin, C. Xie et al., "The iron chelator Dp44mT inhibits hepatocellular carcinoma metastasis via N-Myc downstream-regulated gene 2 (NDRG2)/gp130/STAT3 pathway," *Oncotarget*, vol. 5, no. 18, pp. 8478–8491, 2014.

[27] Z. Chen, D. Zhang, F. Yue, M. Zheng, Z. Kovacevic, and D. R. Richardson, "The iron chelators Dp44mT and DFO inhibit TGF-β-induced epithelial-mesenchymal transition via up-regulation of N-Myc downstream-regulated gene 1 (NDRG1)," *Journal of Biological Chemistry*, vol. 287, no. 21, pp. 17016–17028, 2012.

[28] M. C. Linder, H. R. Kakavandi, P. Miller, P. L. Wirth, and G. M. Nagel, "Dissociation of ferritins," *Archives of Biochemistry and Biophysics*, vol. 269, no. 2, pp. 485–496, 1989.

[29] J. D. Mancias, X. Wang, S. P. Gygi, J. W. Harper, and A. C. Kimmelman, "Quantitative proteomics identifies NCOA4 as the cargo receptor mediating ferritinophagy," *Nature*, vol. 509, no. 7498, pp. 105–109, 2014.

[30] T. Huang, Y. Sun, Y. Li et al., "Growth Inhibition of a Novel Iron Chelator, DpdtC, against Hepatoma Carcinoma Cell Lines Partly Attributed to Ferritinophagy-Mediated Lysosomal ROS Generation," *Oxidative Medicine and Cellular Longevity*, vol. 2018, Article ID 4928703, 13 pages, 2018.

[31] Z. Zhao, J. Zhao, J. Xue, X. Zhao, and P. Liu, "Autophagy inhibition promotes epithelial-mesenchymal transition through ROS/HO-1 pathway in ovarian cancer cells," *American Journal of Cancer Research*, vol. 6, no. 10, pp. 2162–2177, 2016.

[32] T. Wang, Y. Fu, T. Huang et al., "Copper ion attenuated the antiproliferative activity of di-2-pyridylhydrazone dithiocarbamate derivative; however, there was a lack of correlation between ROS generation and antiproliferative activity," *Molecules*, vol. 21, no. 8, p. 1088, 2016.

[33] K. Liu, P. C. Liu, R. Liu, and X. Wu, "Dual AO/EB staining to detect apoptosis in osteosarcoma cells compared with flow cytometry," *Medical Science Monitor Basic Research*, vol. 21, pp. 15–20, 2015.

[34] S. Kasibhatla, G. P. Amarante-Mendes, D. Finucane, T. Brunner, E. Bossy-Wetzel, and D. R. Green, "Acridine orange/ethidium bromide (AO/EB) staining to detect apoptosis," *Cold Spring Harbor Protocols*, vol. 2006, no. 21, pp. -pdb.prot4493–pdb.prot4493, 2006.

[35] N. Gavert and A. Ben-Ze'ev, "Epithelial-mesenchymal transition and the invasive potential of tumors," *Trends in Molecular Medicine*, vol. 14, no. 5, pp. 199–209, 2008.

[36] V. Ellenrieder, S. F. Hendler, W. Boeck et al., "Transforming growth factor beta1 treatment leads to an epithelial-mesenchymal transdifferentiation of pancreatic cancer cells requiring extracellular signal-regulated kinase 2 activation," *Cancer Research*, vol. 61, no. 10, pp. 4222–4228, 2001.

[37] N. K. Urbañski and A. Berêsewicz, "Generation of .OH initiated by interaction of Fe2+ and Cu+ with dioxygen; comparison with the Fenton chemistry," *Acta Biochimica Polonica*, vol. 47, no. 4, pp. 951–962, 2000.

[38] A. C. Gasparovic, M. Jaganjac, B. Mihaljevic, S. B. Sunjic, and N. Zarkovic, "Assays for the measurement of lipid peroxidation," *Methods in Molecular Biology*, vol. 965, pp. 283–296, 2013.

[39] D. Spano and M. Zollo, "Tumor microenvironment: a main actor in the metastasis process," *Clinical and Experimental Metastasis*, vol. 29, no. 4, pp. 381–395, 2012.

[40] J. Xu, R. Wang, Z. H. Xie et al., "Prostate cancer metastasis: Role of the host microenvironment in promoting epithelial to mesenchymal transition and increased bone and adrenal gland metastasis," *Prostate*, vol. 66, no. 15, pp. 1664–1673, 2006.

[41] Y. L. Li, T. T. Wang, Y. Sun et al., "p53-Mediated PI3K/AKT/mTOR Pathway Played a Role in PtoxDpt-Induced EMT Inhibition in Liver Cancer Cell Lines," *Oxidative Medicine and Cellular Longevity*, vol. 2019, Article ID 2531493, 15 pages, 2019.

[42] T. R. Samatov, A. G. Tonevitsky, and U. Schumacher, "Epithelial-mesenchymal transition: focus on metastatic cascade, alternative splicing, non-coding RNAs and modulating compounds," *Molecular Cancer*, vol. 12, no. 1, p. 107, 2013.

[43] K. Lee and C. M. Nelson, "New insights into the regulation of epithelial–mesenchymal transition and tissue fibrosis," *International Review of Cell and Molecular Biology*, vol. 294, pp. 171–221, 2012.

[44] K. H. Zhang, H. Y. Tian, X. Gao et al., "Ferritin heavy chain–mediated iron homeostasis and subsequent increased reactive oxygen species production are essential for epithelial-mesenchymal transition," *Cancer Research*, vol. 69, no. 13, pp. 5340–5348, 2009.

[45] I. Aversa, F. Zolea, C. Ieranò et al., "Epithelial-to-mesenchymal transition in FHC-silenced cells: the role of CXCR4/CXCL12 axis," *Journal of Experimental Clinical Cancer Research*, vol. 36, no. 1, p. 104, 2017.

[46] P. Liu, K. He, H. Song, Z. Ma, W. Yin, and L. X. Xu, "Deferoxamine-induced increase in the intracellular iron levels in highly aggressive breast cancer cells leads to increased cell migration by enhancing TNF-α-dependent NF-κB signaling and TGF-β signaling," *Journal of Inorganic Biochemistry*, vol. 160, pp. 40–48, 2016.

[47] N. Santana-Codina and J. Mancias, "The role of NCOA4-mediated ferritinophagy in health and disease," *Pharmaceuticals*, vol. 11, no. 4, p. 114, 2018.

[48] N. Bresgen and P. Eckl, "Oxidative stress and the homeodynamics of iron metabolism," *Biomolecules*, vol. 5, no. 2, pp. 808–847, 2015.

Hindawi
Oxidative Medicine and Cellular Longevity
Volume 2019, Article ID 2641712, 15 pages
https://doi.org/10.1155/2019/2641712

Review Article

PARP1 and Poly(ADP-ribosyl)ation Signaling during Autophagy in Response to Nutrient Deprivation

José Manuel Rodríguez-Vargas,[1] **Francisco Javier Oliver-Pozo**,[2] **and Françoise Dantzer**[1]

[1]*Poly(ADP-ribosyl)ation and Genome Integrity, Laboratoire d'Excellence Medalis, UMR 7242, CNRS/Université de Strasbourg, Institut de Recherche de L'Ecole de Biotechnologie de Strasbourg, 300 bld. S. Brant, CS10413, 67412 Illkirch, France*
[2]*Cellular Biology and Immunology, Instituto de Parasitología y Biomedicina López Neyra, CSIC/IPBLN, CIBERONC, Parque Tecnológico de Ciencias de la Salud de Granada, 17 Avenida del Conocimiento, 18016 Armilla, Spain*

Correspondence should be addressed to José Manuel Rodríguez-Vargas; jmrodriguez@unistra.fr

Received 18 February 2019; Revised 28 April 2019; Accepted 7 May 2019; Published 9 June 2019

Guest Editor: Marco Cordani

Autophagy is considered to be the primary degradative pathway that takes place in all eukaryotic cells. Morphologically, the autophagy pathway refers to a process by which cytoplasmic portions are delivered to double-membrane organelles, called autophagosomes, to fuse with lysosomes for bulk degradation. Autophagy, as a prosurvival mechanism, can be stimulated by different types of cellular stress such as nutrient deprivation, hypoxia, ROS, pH, DNA damage, or ER stress, promoting adaptation of the cell to the changing and hostile environment. The functional relevance of autophagy in many diseases such as cancer or neurodegenerative diseases remains controversial, preserving organelle function and detoxification and promoting cell growth, although in other contexts, autophagy could suppress cell expansion. Poly(ADP-ribosyl)ation (PARylation) is a covalent and reversible posttranslational modification (PTM) of proteins mediated by Poly(ADP-ribose) polymerases (PARPs) with well-described functions in DNA repair, replication, genome integrity, cell cycle, and metabolism. Herein, we review the current state of PARP1 activation and PARylation in starvation-induced autophagy.

1. Introduction

ADP-ribosylation is a posttranslational modification of proteins with a prominent function in the regulation of diverse biological processes such as, among others, chromatin dynamics, gene transcription, and cell response to DNA damage. Utilizing the oxidized form of NAD^+ as a substrate, Poly(ADP-ribose) polymerase (PARP) (17 members) catalyzes the covalent attachment of ADP-ribose units onto glutamate, aspartate, tyrosine, lysine, and serine residues of target proteins [1]. Based on their enzymatic activity, PARP enzymes are defined as either mono-ADP-ribose polymerases because they add a single ADP-ribose unit onto their targets (PARP3, vPARP, PARP6, tiPARP, PARP8, PARP10, PARP11 PARP12, PARP14, and PARP15) or Poly(ADP-)ribose polymerases when they create linear or branched Poly(ADP-ribose) chains (PAR chains) (PARP1, PARP2, PARP5a, and PARP5b). No enzymatic activity has been identified for PARP13 while mono-ADP-ribosylation of ubiquitin has been proposed for PARP9 in heterodimerization with the histone H3 ligase Dtx3L (see Table 1) [1, 2].

PARP1, the founding member of the family, has been long defined as a central DNA damage-responsive element required for the maintenance of genome integrity. In response to DNA strand interruptions inflicted by various genotoxic agents, PARP1 promotes an immediate and local production of Poly(ADP-ribose) chains needed for chromatin relaxation through the addition of negatively charged ADP-ribose units onto histones and necessary to coordinate the spatiotemporal assembly of PAR-binding proteins including DNA repair proteins, transcription factors, DNA- and RNA-binding proteins, and intrinsically disordered proteins [3]. As fundamentally important as PAR synthesis in stress response is the following degradation of the ADP-ribose chains by families of ADP-ribose hydrolases. While some enzymes preferentially degrade

Table 1: Nomenclature, enzymatic activity, and biological functions of PARP proteins.

PARP	Alternative names	Demonstrated activity	Cellular localization	Biological processes
PARP1	ARTD1	PARylation	(i) Nucleus	(i) DNA repair (ii) Genome integrity (iii) Transcription (iv) Replication (v) Cell cycle (vi) Metabolism and development (vii) Proteasome degradation (viii) Diseases: cancer, inflammation, and HIV
PARP2	ARTD2	PARylation	(i) Nucleus	(i) DNA repair (ii) Genome integrity (iii) Transcription (iv) Cell cycle (v) Metabolism (vi) Cancer/inflammation
PARP3	ARTD3	MARylation	(i) Nucleus	(i) DNA repair (ii) Genome integrity (iii) Cell cycle (iv) Development (v) Cancer
PARP4	ARTD4/VPARP	MARylation	(i) Nucleus (ii) Exosomes (iii) Cell membrane	(i) Vault biology (ii) Cancer
TNK1	ARTD5/PARP5A	PARylation	(i) Nucleus (ii) Telomeres (iii) Golgi (iv) Cytoplasm	(i) Mitotic spindle (ii) Telomere maintenance (iii) Metabolism
TNK2	ARTD6/PARP5B	PARylation	(i) Nucleus (ii) Telomeres (iii) Golgi (iv) Cytoplasm	(i) Inflammation (ii) Telomere maintenance? (iii) Metabolism
PARP6	ARTD17	Not determined	(i) Cytoplasm?	(i) Cell proliferation
PARP7	ARTD14/TIPARP	MARylation	(i) Nucleus? (ii) Cytoplasm?	(i) Transcription (ii) Antiviral effects (iii) Cytosolic RNA processing
PARP8	ARTD16	Not determined	(i) Not determined	(i) Unknown
PARP9	ARTD9/BAL1	Inactive/unknown	(i) Nucleus (ii) Cell membrane (iii) Cytoplasm?	(i) Cell migration (ii) Tumor formation
PARP10	ARTD10	MARylation	(i) Nucleus (ii) Cytoplasm	(i) Cell proliferation (ii) Transcription (iii) Cytosolic RNA processing
PARP11	ARTD11	Not determined	(i) Unknown	(i) Unknown
PARP12	ARTD12	MARylation	(i) Cytoplasm	(i) RNA processing
PARP13	ARTD13/ZAP/ZC3HAV1	Inactive/unknown	(i) Cytoplasm	(i) RNA processing
PARP14	ARTD8/BAL2	MARylation	(i) Nucleus (ii) Cell membrane	(i) Inflammation (ii) Transcription (iii) Metabolism (iv) Tumor formation (v) Nuclear RNA processing
PARP15	ARTD7/BAL3	MARylation	(i) Cytoplasm	(i) Cytosolic RNA processing (ii) Tumor formation
PARP16	ARTD15	MARylation	(i) Cell membrane (ii) ER	(i) Unfolded protein response (UPR)

Poly(ADP-ribose) chains (the macrodomain containing PARG endowed with exo- and endoglycohydrolase activities or ARH3), the removal of the last protein ADP-ribose bond is mediated by a panel of recently identified enzymes including ARH3, TARG1, macroD1, macroD2, NUDT16, or ENPP1 [4].

Owing to its decisive role in DNA repair, the inhibition of PARP1 has emerged as a prominent therapeutic option in cancer treatment, either to potentialize the cytotoxic action of chemotherapy or radiation therapy or to target repair-deficient tumors [5]. To date, three PARP inhibitors have been FDA approved for the treatment of ovarian or breast cancer, namely, Olaparib, Rucaparib, and Niraparib.

The last decades have helped to expand the knowledge on other members of the PARP family and the number of functions of PARP proteins in different cellular pathways. The effects of PARP1 activation (considered the major producer of Poly(ADP-ribose)), its autoPARylation, and PARylation of different targets (which is called transPARylation or heteroPARylation) are translated to cellular responses in several different ways.

Although the majority of functions mediated or regulated by PARPs are related to cellular stress response as DNA damage, it is well known that recent investigations have increased the number and importance of documented PARP-mediated functions and PARylation in noncellular stress situations (see Table 1). The great majority of PAR has a nuclear localization where it will act as a potent posttranslational modification of proteins related to maintenance of genome integrity, gene expression, or cell cycle. However, the cytoplasm has been described, including various organelles, as a large receptor of Poly(ADP-ribose) and single molecules of ADP-ribose. Moreover, PARylated proteins can be transferred to the cytosol, interfering in many different biochemical processes [6]. Noncovalent binding of free Poly(ADP-ribose) is considered a factor of high relevance in the function of the targeted protein. In conclusion, the consequences of PARylation, PAR signaling, or the biochemical interaction of PARP members with partner proteins affect many cellular events ranging from genome homeostasis to vital cellular functions such as cell proliferation, differentiation, metabolism, prosurvival pathways, and programmed cell death.

For some years, it has also become increasingly appreciated that PARP1-catalyzed Poly(ADP-ribosyl)ation regulates cell survival and stress adaptation programs, with among them, the well-conserved self-eating mechanism of cell survival termed autophagy. Herein, we concentrate on the most recent discoveries to encompass the different mechanisms by which PARP1 activity operates in autophagy during periods of nutrient deprivation.

2. PARP-Dependent Bioenergetic Changes: NAD^+ Catabolism and Downstream

PARP1 is considered the main guardian of the genome, able to synthesize up to 85%-90% of the PAR polymer that is needed to maintain cell homeostasis. While the contribution of PARP2 could be considered up to 10%-15%, contribution of other PARPs seems insignificant compared to the total Poly(ADP-ribose) pool. Biochemically, PARP1 constitutes the majority of NAD^+ catabolic activity in the cells, depleting NAD^+ to 20% of its normal levels within minutes upon DNA damages [7]. NAD^+ provides a direct link between the cellular redox status and the control of signaling events, since it is considered an oxidoreductase cofactor in cell physiology and acts as a substrate for a wide range of enzymes. NAD^+ could be considered to be metabolic fuel in high competence for three kinds of proteins: NAD^+-dependent protein deacetylases or Sirtuins, Poly(ADP-ribose) polymerases, and transcription factors. Depending on the metabolic context in which the cell is located, the competition for NAD^+ will be unbalanced towards one pathway or another. Generally, NAD^+ requirement in the case of PARPs, mainly DNA-dependent PARPs, is higher and is accompanied by a high amount of ATP to complete the synthesis and PARylation of various acceptors. Therefore, PARP overactivity will be triggered in a situation of ATP depletion and promotes a scenario that will compromise the cells. Glycolysis is probably the most immediate energy pathway compromised during PARP overactivation. NAD^+ is an important cofactor in metabolism; the reduction of NAD^+ to NADH is essential for the glyceraldehyde 3-phosphate (GAPDH) step of glycolysis and multiple steps in the tricarboxylic acid cycle (TCA). All those situations that could compromise glycolysis immediately impair the major source of ATP production in cells, used, for example, in the cycle to regenerate NAD^+, and the Krebs cycle. Since the major source to create secondary metabolites and antioxidant precursors is blocked, this creates a negative feedback loop that compromises cell survival [7, 8].

Inside the nucleus, we could focus on the high competence for NAD^+ in PARP1/SIRT1, cleaving NAD^+ to produce nicotinamide and ADP-ribosyl products and the enzymes related with Poly(ADP-ribose) recycling such as Poly(ADP-ribose) glycohydrolases (PARGs) and ADP-ribose hydrolase 3 (ARH3). SIRT1 is a NAD^+-dependent type III histone deacetylase member of the Sirtuin family. Sirtuin proteins catalyze the reaction of NAD^+ with acyl lysine groups to remove the acyl modification from substrate proteins, resulting in the final production of deacetylated lysine, nicotinamide, and $2'$-*O*-acetyl-ADP-ribose (*O*AADPr). This deacetylation integrates cellular NAD^+ metabolism into a large spectrum of cellular processes, such as cell metabolism, cell survival, cell cycle, apoptosis, DNA repair, and mitochondrial homeostasis [9, 10]. *O*AADPr is considered a second messenger linked with decreased ROS-mediated stress, gene silencing, and ion channel activation [10]. On the other hand, several studies report that PARPs and Poly(ADP-ribosyl)ation can modulate mitochondria from the nucleus through PAR translocation, depletion of NAD^+ pools, and epigenetic regulation of nuclear genes that are involved in mitochondrial DNA transcription or repair. Short PAR chains and single units of ADP-ribose (ADPr) can be produced from the coordinate actions of PARPs and PARG, which cleavage Poly(ADP-ribose) to free monomers of ADPr. Several data suggest that PARP1-induced loss of ATP requires PARG activity. Under specific scenarios of PARP1 hyperactivation, PARG-dependent production of the single unit of ADPr

can exit from the nucleus and interfere with ATP production in mitochondria, promoting nonenzymatic ADP-ribosylation of cell death proteins and metabolic cofactors [4, 6, 7].

Free units of ADPr and *O*AADPr have potential signaling functions in cytoplasm, suggesting mitochondrion-related enzymes as putative targets. The existence of enzymes capable of metabolizing these second messengers suggests that their cellular concentrations may be targeted in metabolism in several pathophysiological situations such as neurodegenerative diseases, acute brain injury, or cancer [4, 6]. Many enzymes target *O*ADDPr and Poly(ADP-ribose) preventing unnecessary effects in the nucleus and cytoplasm. *O*ADDPr is cleaved to ADPr by macroD1, macroD2, and ARH3 enzymes in the nucleus; moreover, in mitochondria, the interconnected activity of PARG/ARH3 degrades short Poy(ADP-ribose) chains to ADPr in the mitochondrial matrix, preventing the heteroPARylation of AIF (apoptosis-inducing factor), mitochondria collapse, and PARthanatos cell death [8].

In the last 30 years, a superfamily of enzymes has gained prominence in the field of Poly(ADP-ribosyl)ation and PAR-mediated biology. These ADPr hydrolases, called NUDIX hydrolases, are considered the major regulators of the intracellular levels of ADPr. The NUDIX superfamily is found in all classes of organisms among eukaryotes, bacteria, and viruses [11]. NUDIX hydrolases are basically pyrophosphohydrolases that act on substrates with the general structure NDP-X (nucleoside diphosphate linked to some moiety, X). Various cellular compounds include the canonical structure NDP-X and also contain oxidized and canonical nucleoside di- and triphosphates, nucleotide sugars, and alcohol, presenting potential toxic properties; so, originally, NUDIX enzymes were proposed to function in housecleaning controlling the availability of intermediates in metabolism [11]. NUDIX hydrolyze ADPr to adenosine monophosphate (AMP) and ribose 5-phosphate in an Mg^{2+}-dependent reaction (or a similar cofactor, e.g., Zn^{2+}), thereby limiting free ADPr accumulation. In human cells, members of the NUDIX family often exhibit substrate selectivity for specific nucleotide derivatives; NUDT9, an ADPr pyrophosphatase, is highly specific for the mitochondrial ADPr pool, while NADT5, an ADP-sugar pyrophosphatase, only has preference for cytosolic ADPr and other ADP-sugar conjugates; both enzymes catalyze the production of AMP [12, 13]. Recent studies have also demonstrated that NUDIX are potential metabolizing enzymes of the byproduct of Sirtuin activity, *O*ADDPr, producing AMP and *O*-acetylated-ribose-5-phosphate [11]. These studies allowed describing an active crosstalk between mitochondrial PARG/ARH3 Poly(ADP-ribose) metabolisms and subsequently altering the levels of GTP and ATP.

Mitochondrial AMP phosphorylation by adenylate kinase 3 (AK3) and low NAD^+ levels causes depletion in mitochondrial GTP, compromising mitochondrial fusion. On the other hand, high levels of AMP also increase AMP : ADP ratios, which lead to the activation of AMPk kinases. AMPk phosphorylates the mitochondrial fusion factor or MFF inducing Drp1 translocation from cytosol to mitochondria causing constriction and fission. The final situation results in excessively fragmented mitochondria and eventually leads to mitophagy [14]. Additionally, better understanding of mitochondrial profiles of Poly(ADP-ribosyl)ation and mono(ADP-ribosyl)ation and the complexities of AMPk in relation to mitochondrial dynamics should be taken up in future studies. The crosstalk between nuclear DNA-dependent NAD^+, energy collapse dependent of PARP1 overactivation, and AMPk activity in response to the proautophagy stimulus will be analyzed in other sections of this review.

PARP1 and SIRT1 compete for a limited nuclear pool of NAD^+, and of course, each activity could guide the other one, leading to diverse consequences for cells. Different *in vivo* studies have demonstrated the metabolic crosstalk in important models of differentiation, neurogenesis, inflammation, and cancer. PARP inhibitors increase intracellular NAD^+ levels, promoting specific nuclear deacetylase activity of SIRT1 but not affecting other SIRTs located in cytoplasm or mitochondria; however, the negative correlation was only found under physiological conditions in specific scenarios such as muscle differentiation [15]. In the case of PARP2, new data reflects no evident competence for NAD^+ with SIRT1 and shRNA-mediated depletion of PARP2 produces little effect on NAD^+ balance; however, there is a demonstrated physical interaction between both proteins. *Parp2*$^{-/-}$ mice exhibit elevated SIRT1 expression with decreased acetylation of SIRT1 targets FOXO1 and PGC-1α which are transcriptional regulators of mitochondrial bioenergetics due to the fact that 63% of mitochondrial localized proteins contain lysine acetylation sites [16]. Indeed, PARP2 deletion in mice produces increased mitochondrial biogenesis in upregulation genes involved in mitochondrial respiration, antioxidant precursor activity, and lipid oxidation such as tpn1, SDH, UCP2, or MCAD [16]. Thus, any consideration of selective PARP2 inhibition in tumor cells and during metabolic unbalance will require better understanding of the exact mechanism of PARP2-dependent metabolic regulation.

DNA-dependent PARPs can be considered transcriptional modulators of several metabolic pathways. PARP1 and PARP2 could be considered important precursors of the activity of different transcription factors that modulate mitochondrial oxidative phosphorylation and lipid oxidation such as PPARγ, FOXO1 by direct PARylation of them, and their cofactors or modulators, consuming high amounts of NAD^+ and ATP [17]. However, the mechanism whereby PARPs and PARylation transcriptionally mediate metabolic transcription factors remains an unexplored field.

3. Cell Death Modulation by PARP1 during Energy Stress

Over the course of the years, different groups have demonstrated that the influence of PARP activity goes beyond the nucleus and directly impacts NAD^+ metabolism, energy pathways, and oxidative metabolism. Many studies have concluded that in a scenario of energy depletion guided by oxidative stress, PARPs potentiate cell survival or cell death

pathways [4, 18]. Reversible PARylation is a pleiotropic regulator of various cellular functions, but uncontrolled PARP activation may also lead to cell death. Moreover, noncovalent PARylation or MARylation (PTM by monomers of ADP-ribose) could be considered as an effective cytosolic posttranslational modification of diverse MAPk kinases and mitochondrial cell death factors, protecting cells from acute DNA damage and stress conditions [18].

Attending the origin of DNA damages, the intensity and "durability" of these damages, and the activation levels of PARP1, we can define several destinations of the cells. When DNA damage is minimal, the recruitment of PARP1 to sites of DNA lesions activates the DNA damage response consuming a controlled amount of NAD^+ and ATP. Depending on the type of lesion encountered, signaling mediated by molecules such as p53 and ATM or ATR promote cell cycle arrest, buying time for DNA repair enzymes to work [18, 19]. In this context, the energy expenditure and NAD^+ required can be so great that the cells would enter almost immediately cell death or cellular "suicidal" pathways mediated by PARylation because even though the DNA damage is repaired, the collateral damage to the cellular energy machinery is too great (see Figure 1).

To link PARP1 (potent consumer of ATP and NAD^+) energy collapse (oxidative phosphorylation to create ATP) and oxidative stress (collapse of mitochondrial ETC), several groups propose a theory in the form of a feedback loop: oxidative conditions lead to DNA damage, triggering PARP1 overactivation that promotes more energy collapse by over-PARylation and noncovalent MARylation that finally guide the cells to die. The suicidal over-PARylation disrupts the mitochondrial energy mechanisms, impairing the antioxidant capacity of the Krebs cycle and favoring the liberation of proapoptotic mitochondrial factors [20].

PAR-mediated cell death pathways can be subdivided into two subcategories, depending on the Poly(ADP-ribose) synthesis levels associated with the process (see Figure 1): (1) Low PAR synthesis cell death: PARP1 and "suicidal" proteases. Apoptosis is a nonreversible cell death pathway characterized by activation of caspases, membrane depolarization, exportation of mitochondrial death precursors, and nuclear disintegration. Apoptosis involves a biochemical expense which irreversibly leads to cell death. PARP1 is a preferred substrate for several "suicidal" proteases (caspases, calpains, cathepsins, granzymes, and matrix metalloproteinases (MMPs)). The proteolytic action of these proteases on PARP1 produces several specific cleavage fragments with different molecular weights. Each fragment could be associated with specific stress situations inside the cells or cell death programs [21]. When DNA damage is irreparable or the signaling by PARP1 does not lead to an optimal repair, cells enter irreversibly in cell death by apoptosis. In the initial steps of apoptosis, caspases 3 and 7 cleave the DNA-binding domain from the catalytic domain of PARP1 resulting in the inactivation of PARP1 and blocking the ATP competition between PARPs and caspases [21]. (2) Overactivation of PARP1 and cell death: PARthanatos and necroptosis. In response to intense and sustained damage, a large amount of Poly(ADP-ribose) is synthesized. The overactivation of PARP1 collapses the cellular energetic machinery and triggers necrosis, translated in proinflammatory conditions in the tissues. An indeterminate amount of Poly(ADP-ribose) could be exported to the cytosol and enter the mitochondria, promoting PARylation on AIF proteins (apoptosis-inducing factor). PARylated-AIF enzymes translocate from the mitochondrion to the nucleus, triggering chromatin condensation and DNA fragmentation into large fragments (~50 kb) which irreversibly leads to cell death called PARthanatos [22]. Actually, new studies have demonstrated in DNA double-strand break-dependent energy depletion models that the bioenergetic changes are adaptively regulated during PARthanatos, especially under macroautophagy deficiency [23].

For decades, necrosis has been considered a passive and unregulated process, linked in many cases to overactivation of PARP1 that leads the cell to a scenario of energy collapse, oxidative chaos, and alteration of biomembranes. Current studies have revealed several models of cell death with characteristics of necrosis but are certainly regulated by various proteins. A clear example is necroptosis mediated by RIP1 in response to TNFα death ligand released during inflammatory conditions. Upon binding to TNFR1, TRADD, TRAFs, RIP1, and cIAPs, proteins are recruited to form complex I blocking apoptosis and leading to expression of proinflammatory cytokines. In this model, the overactivation of PARP1 is considered a central element causing depletion of NAD^+/ATP, releasing cathepsins and favoring AIF translocation. Furthermore, RIP1 protein has been proposed as a clear acceptor of PAR chains. However, there are many unanswered questions about whether necroptosis will be considered or not such as a programmed cell death mechanism [24, 25]. Autophagy is considered a housekeeping mechanism to recycle long-lived protein, aberrant organelles, and unfolded proteins and blocking intracellular pathogen invasion. Autophagy is generally thought of as a survival mechanism, although its deregulation has been linked to nonapoptotic cell death. The goal of necroptosis is to eliminate unnecessary or abnormal cells from the body under stress situations, metabolic diseases, or other pathological scenarios. Thus, a controlled recycling of damaged organelles in response to energy deletion under PARP overcativation palliate inflammatory response in tissues controlling the levels of necroptosis and PARthanatos [25]. The idea of autophagy as a mechanism for maintaining energy homeostasis under a context of activation of PARP proteins will be taken up in different sections of this review.

4. Autophagy in Mammalian Cells: Concept, Types, and Functions

Macroautophagy (referred to simply as "autophagy") is an evolutionary ancient homeostatic "self-eating" pathway that has been highly conserved among eukaryotic cells. Autophagy is a catabolic lysosomal-associated process that targets intracellular components, from small portions of the cytosol, macromolecules, and unwanted organelles to chaperone-associated cargoes. Morphologically, this pathway is characterized by active membrane trafficking through formation

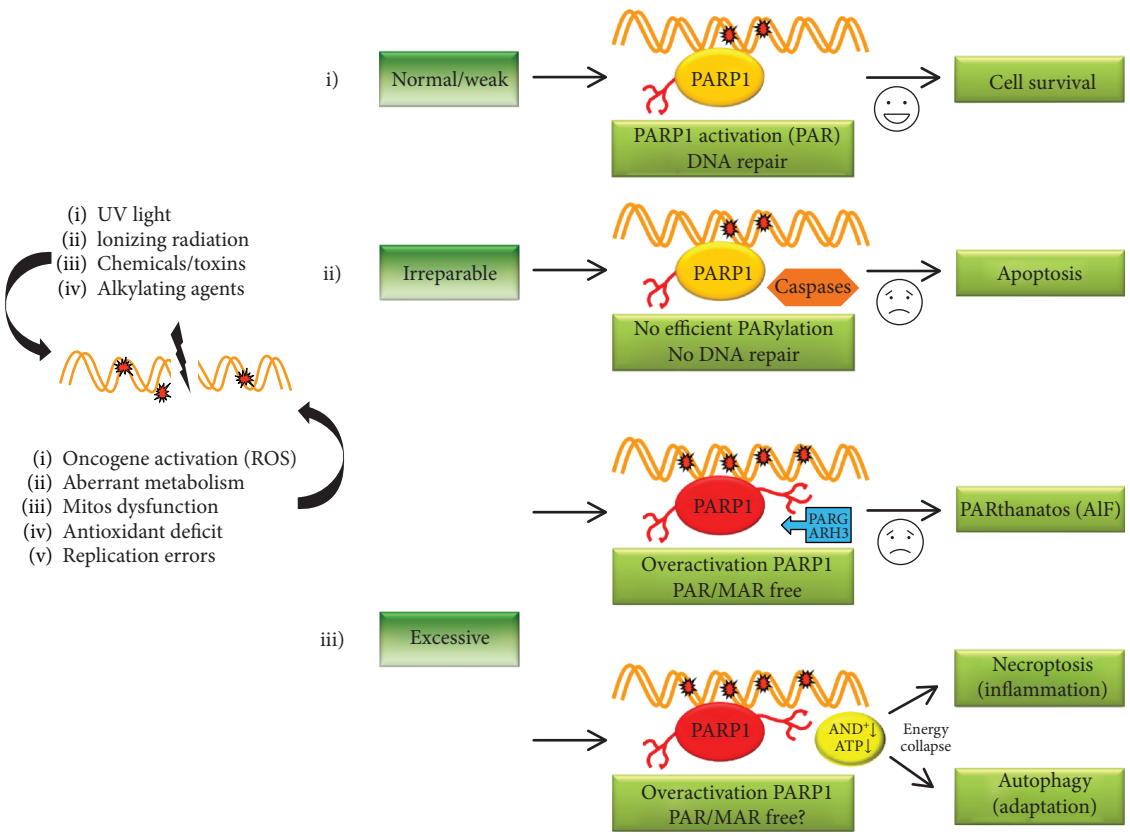

Figure 1: The intensity of the stimulus that induces DNA damage and the degree of activation of PARP1 determines the fate of a cell toward survival or death. *Destination 1*. When a slight damage occurs in DNA by endogenous or exogenous agents, PARP1 recognizes these damage points; PARylates itself, histones, and structural chromatin-related proteins; and finally promotes recruitment of DNA repair enzymes. If the DNA is repaired successfully, cells will survive. The effect on nuclear NAD^+/ATP never leads to energy collapse. *Destination 2*. Multiple intense damage that despite the activity of PARP1 never will be repaired successfully. The cell enters in irreversible apoptosis, effector caspases 3 and 7 degrade PARP1 as the main competitor for the ATP, and the "eat-me" signal will appear on the cell surface. *Destination 3*. Excessive DNA damages, though not necessarily lethal, produce a phenomenon of overactivation of PARP1 and over-PARylation in nucleus. The energy consequences are lethal for cells, and the nuclear pool of NAD^+/ATP will be seriously affected. Poly(ADP-ribose) glycohydrolases and ADP-ribose hydrolases mediate a rapid turnover and recycling of the bulk of PAR modification on nuclear PARylated proteins, autoPARylated PARPs, and free chains of ADP-ribose. The free monomers and little PAR chains are exported to cytosol to induce mitochondrial AIF translocation to nucleus. Finally, cell will die in a non-caspase-dependent process or PARthanatos. Overactivation of PARP1 consumes both NAD^+ and ATP in nucleus triggering a high imbalance in the total pool of energy in the cells. This total energy collapse alters the functions of the main energy organelles such as mitochondria, ribosomes, or endosomes, favoring a total energy imbalance. At the same time, the presence of PAR chains and free ADP-ribose monomers in the cytosol modifies enzymes such as RIP1, triggering necroptosis. *As an alternative* to death by necroptosis, autophagy appears as an adaptive pathway to try to alleviate the energy crisis and prevent cell death arising. The nature of the stimulus and its durability will determine recycling of damage organelles, misfolded proteins, or lipid aggregates. PARylation could be considered a highly dynamic posttranslational modification of several proteins forming the autophagosome core or targeting intracellular components to be degraded. At the same time, cells are given an alternative source of energy until the damage is repaired or the stress situation ceases.

of a unique double-membrane structure, called autophagosome, where engulfed cytosolic structures are delivered to the lysosome for bulk degradation [26, 27]. Autophagy plays a housekeeping role in the turnover of long-lived proteins, disposal of damaged organelles, and clearance of aggregate-prone proteins. The main objective is the adaptation and survival of the cell to the changing environment and finally to maintain the normal growth cellular fate [28]. Considering the origin of the subcellular material to be removed, we will refer to "basal" autophagy, which describes a nonstop removal of specific cargo, including unfolded or aggregated proteins, lipid droplets, or whole organelles. Thus, macroautophagy is the most selective autophagy pathway and is characterized by the formation of double-membrane intracellular phagosomes. "Stress-induced autophagy" normally is induced by nutrient deprivation or hypoxia and depends on the availability of autophagomes; however, deprivation of nutrients, oxygen, or growth factors does not exclude the activation of selective autophagy towards a specific cellular substrate with the ultimate goal of obtaining energy and basic components (amino acids, nucleosides, or lipids) used in cell maintenance and survival [29, 30].

Macroautophagy is interconnected with different pathways which regulate nutrient uptake, cell growth, and cell

death programs. At the tissue level, autophagy should be considered an active player in physiological processes such as brain development, lineage differentiation, tissue architecture, and regulation of energy homeostasis of important organs (liver, brain, or heart).

It is widely demonstrated that extracellular proteins are degraded in the lysosomes by phagocytosis, pinocytosis, or endocytosis; however, intracellular unfolded or long-lived proteins could be degraded and recycled into amino acids by macroautophagy (proteins are engulfed in autophagosomes and degraded after fusion with lysosomes), microautophagy (soluble cytosolic proteins are directly internalized through the membrane of the lysosomes), and chaperone-mediated autophagy (CMA) (chaperone-dependent selection of proteins that are then targeted to lysosomes and directly translocated across the lysosome membrane for degradation) to maintain ATP levels compatible with cell survival. Different types of ordered organelle-selective autophagy pathways have been described and characterized as new macroautophagy examples, and in all of them, the active flux of biomembranes to engulf portions of cytosol is the main morphological characteristic. Many groups have described endothelial reticulum or ER-phagy, mitophagy (mitochondria), and ribophagy (ribosomes). Recent studies have determined selective autophagosome formation, engulfing lipid droplets (lipophagy) or toxic protein aggregates (aggrephagy) [28, 31].

The consequences of defects in autophagy for diseases are apparent, with growing evidence linking the mutation or loss of function of key autophagy genes to cancer, neuropathies, heart disease, autoimmune diseases, and inflammation. In cancer biology and tumor progression, it remains controversial when considering autophagy as beneficial or harmful for tumor cells and consequently for the growth and expansion of the tumor. Autophagy may act as a tumor-suppressive pathway, promoting cell cycle arrest or limiting necrosis and inflammation, or as a prooncogenic pathway, favoring cell survival in the presence of stressful conditions [29, 32]. The impact that autophagy causes in growth, development, and expansion of a tumor can be summarized as follows: tumor-initiating events (oncogene activation, impaired DNA repair pathways, or high metabolic defaults) promote cell proliferation, but also apoptosis, which limits tumor growth. Tumor growth is initially limited by the absence of a blood supply which can trigger autophagy-mediated survival in the most metabolically stressed tumor regions, commonly the hypoxic and starved center [33]. The eventual recruitment of a blood supply prevents hypoxia, provides glucose and amino acids, and reduces metabolic stress. In tumors enriched by cells with defects in both apoptosis and autophagy, necrotic cell death is stimulated in metabolically stressed tumor regions and this necrosis is associated with the activation of an inflammatory response, DNA damage, and tumor progression. Thus, autophagy will play a dual role, promoting survival, and adaptation to try to survive or in the opposite case could be used as a "Trojan Horse" of these cancer cells, inhibiting angiogenesis, promoting more selective apoptosis, and favoring the "eat-me" signals [33].

In other diseases such as neuropathies (Huntington's, Alzheimer's, and Parkinson's diseases) and ischemic heart disease, autophagy is more widely accepted as beneficial given its role in eliminating toxins, aberrant structures, and promoting cell viability. Most neurodegenerative disorders are characterized by the accumulation of misfolded proteins that coalesce into "inclusions" and become visible under the light microscope in the brains and spinal cords of affected patients. The high sensitivity of mature neurons to misfolded protein stress is well known, impairing the right neuronal functions, promoting neuron cell death and neurodegenerative disorders. *In vivo* animal models of neuropathies have demonstrated that basal levels of autophagy are required for the continued health and normal function of neurons [34, 35]. Autophagy plays a key role in cardiomyocyte growth and satisfactory heart activity. Autophagy may antagonize ventricular hypertrophy by increasing protein degradation, which decreases tissue mass in ischemic mouse models. However, the rate of protective autophagy declines with age, demonstrating an eventual autophagy/aging crosstalk.

5. Molecular Machinery of Autophagosome Formation

In mammalian cells, autophagy sequestration features important membrane traffic and begins with the active formation of omegasome structures on the rough endoplasmic reticulum called phagophores. Phagophores expand into double-membrane autophagosomes while surrounding a portion of the cytoplasm. Autophagosomes may fuse with endosomes (product of endocytosis from the external microenvironment) considering itself heterophagy (the cell is able to internalize and degrade the material that originates from outside of the cell). The newborn organelles are called amphisomes. The final destination of autophagosomes or amphisomes is to fuse with several lysosomes, which supply acid hydrolases. In this new cellular compartment or autolysosome, the engulfed cargo will be recycled into macromolecules which are released in the cytosol (see Figure 2(a)).

One of the elusive fields of autophagy is deciphering the molecular details of autophagosome biogenesis. In many cases, the sequestration step is the most complex part of autophagy because the cytoplasm must be segregated, often in a direct or specific manner, and moved from the intracellular space into the vacuole or lysosome lumen. Initiation of double-membrane phagophores requires a specific cascade of proteins, kinases, and E-like ligases to allow the recruitment, formation, and sequestration of intracellular portions.

The journey into the molecular realm of autophagy began with the identification of a set of evolutionary conserved genes termed autophagy- (ATG-) related genes. Independent genetic screens in yeast model systems have identified 38 ATG genes which are involved in various subtypes of macroautophagy, including starvation-induced autophagy, the cytoplasm-to-vacuole targeting (Cvt) pathway, and pexophagy. Many of the genes have known orthologues in other eukaryotes [36, 37].

In yeast, approximately 20 Atg proteins are considered essential in the initial steps of phagophore formation and closuring of autophagosomes. These proteins have been classified into five functional groups based on identified protein-

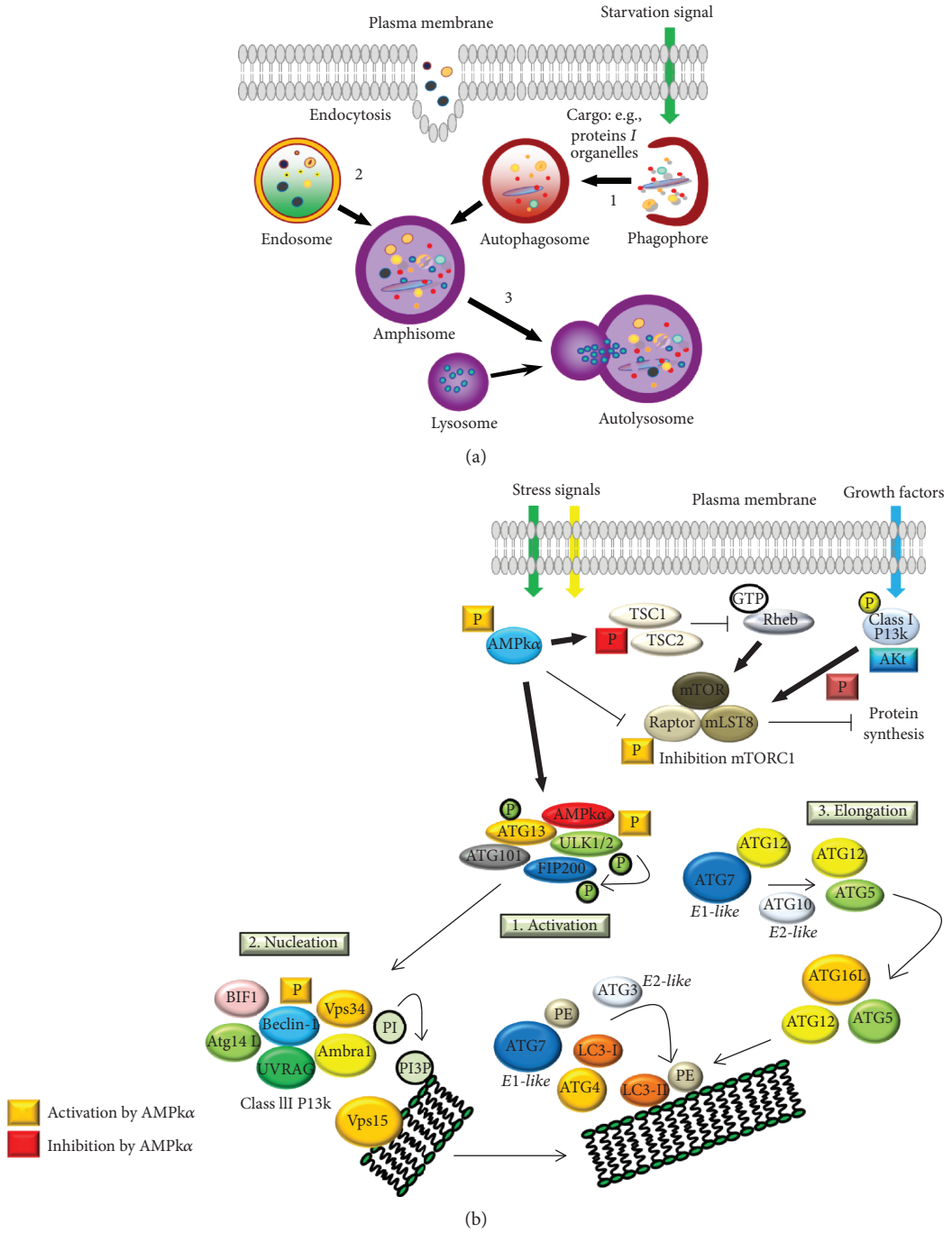

Figure 2: Autophagy steps. (a) Membrane traffic associated to autophagosome formation. During autophagy, sequestration begins with the formation of a phagophore that expands into a double-membrane autophagosome. (1) Stages of nucleation and elongation: the autophagic charge will be engulfed by a double-lipid membrane called phagophore; the phagophore suffers elongation and closure to form an autophagosome. (2) This autophagosome may, or not, fuse with an endosome to form an amphisome. (3) Finally, the amphisome will fuse with lysosomes to form an autolysosome; in this step, acid hydrolases degrade the content of the autolysosome. Finally, the content may be recycled through permeases that efflux the content to the cytosol. (b) Vesicle induction and phagosome creation. In response to stress signals (starvation, hypoxia, and growth factor depletion), AMPk is activated and mTORC1 is inhibited, leading the stimulation of the ULK1 core (activation). ULK1 kinase will phosphorylate Beclin-1 leading to VPS34 activation and the initiation of phagophore formation (nucleation). ATG5-ATG12 conjugation involves ATG7 and ATG10 promoting an "E-like ligase" reaction of ATG12-ATG5-ATG16L influencing on the phospholipidic elongation of the double membranes. The complex ATG12-ATG5-ATG16L acts like an E3-function towards the LC3-PE assembly (LC3-II isoform) (elongation). Autophagosome maturations also involve fusion with lysosomes, degradation and recycling of nutrients and metabolites, and recycling of LC3-I isoform. This membrane trafficking maintains the same molecular events in nonselective and organelle-specific autophagy (mitophagy, ribophagy, and selective formation of amphisomes).

protein interaction: Atg1 kinase complex, autophagy-specific class III phosphatidylinositol 3-kinase or PI(3)K complex, Atg9-Atg2/Atg18 complex, Atg12 conjugation complex, and Atg8 conjugation system. Extensive research has demonstrated functional interactions between them in the core of newborn autophagosomes [38]. In mammalian cells, the number is higher, including an intricate number of 400 members from different families. Classically, an integrated view of mammalian autophagy establishes several steps in the final double-membrane vesicle formation and engulfment of the cargo [39, 40]. In this review, we focus on the phagophore formation step, briefly describing the discovery and functions of the key players sensing stress situations and promoting the biochemical organization of double-membrane engulfing proteins, organelles, or portions of the cytosol. The implication of the PARylation process in the regulation of the initial stages of autophagy is analyzed in detail below.

6. Vesicle Induction: Phagophore Formation—Regulation by AMPk and mTORC1

Autophagy disassembles unnecessary or dysfunctional components, resulting in a highly modulated catabolic pathway in response to several physiological cell stresses and pathological situations. The delicate balance between external energy and nutrient supply and internal production and consumption is a demanding task in the cells. There are two interconnected proteins with the autophagy core-regulating signaling network: AMPk and mTORC1. Both proteins have the capacity to sense ATP and nutrient availability, modulating the activity of the main ATG1 functional orthologue in autophagosome closuring, called ULK1 (unc-51-like autophagy-activating kinase 1), in mammals.

AMP-activated protein kinase (AMPk) is a highly conserved kinase considered to be the major energy sensor in eukaryotic cells (sensing increases in intracellular AMP/ATP and ADP/ATP ratios). AMPk is a serine/threonine kinase that negatively regulates several enzymes of the lipid metabolism and activates different catabolic processes in eukaryotic cells such as glucose uptake and metabolism, increasing ATP generation pathways and decreasing ATP consumption pathways. The balance of ATP synthesis/consumption allows the maintenance of energy homeostasis, makes the energy distribution into growth fates adequate, and triggers several adaptive cellular programs during stressful situations. Structurally, AMPk is a trimeric protein which presents three differentiated domains: a catalytic subunit (α) and two regulatory subunits (β and γ). Different groups have determined the crystal structure of several holoenzymes of AMPk [41, 42]. The α subunit is encoded by two isoforms, while the regulatory subunits present three isoforms in which expression and combination into the AMPk structure are dependent on the cell type. The most widely expressed isoforms of AMPk are AMPkα1, AMPkβ1, and AMPkγ1; however, other isoforms are more restricted to specific tissues [42]. Under nutrient deprivation, hypoxia, DNA damage, or mitochondrial failure, the AMP/ADP : ATP ratio is sensed by LKB1 (liver kinase B1) which promotes the regulatory phosphorylation of Thr172 on the AMPkα subunit. Under this context, AMPk triggers catabolic processes in order to restore the ATP levels through the breakdown of different macromolecules [41, 42].

The mammalian target of Rapamycin (mTOR) is the major nutrient sensor and a central regulator of growth and metabolism in the cell, involved with processes including angiogenesis, autophagy, and protein metabolism. mTOR is a ubiquitously conserved serine/threonine kinase which represents the molecular core component of two multisubunit complexes, mTORC1 and mTORC2. mTORC1 senses the availability of amino acids, oxygen, and growth factors in basal and stressed conditions, promoting cell growth and anabolic pathways. On the other hand, mTORC2 is considered mainly as a regulator of the organization and rearrangement of the cytoskeleton [43]. Structural differences between mTORC1 and mTORC2 determine the sensitivity to Rapamycin. mTORC1 basically is formed by three subunits, mTOR kinase (the functional unit), RAPTOR (a regulatory protein sensitive to inhibition by Rapamycin), and mLST8 (mammalian lethal with Sec13 protein 8). The biochemical regulation of the mTORC1 activity is highly dependent on the tumor suppressor TSC2, an upstream component of the mTORC1 complex. TSC2 contains a GTPase domain that inactivates the small Ras-like GTPase Rheb, which has been shown to associate and activate the mTORC1 complex. Loss of TSC2 (and TSC1) leads to overactivation of mTORC1, triggering translation (by $p70^{S6k}$ and 4E-BP1 regulation), cell cycle, and cell growth (see Figure 2(b)). mTORC2 exhibits the mTOR kinase and mLTS8 subunits and also DEPTOR (DEP domain-containing mTOR-interacting protein), and in this complex, RAPTOR is replaced by RICTOR (Rapamycin insensitive companion of mTOR) which is not sensitive to Rapamycin. Under energy and growth factor availability, mTORC2 controls cellular metabolism and cytoskeleton dynamics (by Akt/GSk3β activation).

In terms of autophagy regulation, AMPk is considered the major positive regulator of autophagy (catabolism) while mTORC1 is considered the major negative regulator of phagophore induction (anabolism). Under a proautophagic scenario in the cells such as amino acid starvation or energy depletion, binding of AMP or ADP to the γ subunit of AMPk promotes Thr172 phosphorylation by LKB1 in the α subunit and full activation of AMPk kinase. Recent studies suggest that AMPk may also be a redox-sensing protein. Reactive oxygen species (ROS) are naturally produced by many metabolic reactions, notably by the production of ATP in the mitochondria, and the strict control of their levels is important for cellular homeostasis. ROS can indirectly activate AMPk through increases in AMP or by post translational modifications of the α subunit of AMPk [44]. AMPk potently promotes autophagy inhibiting mTORC1 through phosphorylation of TSC2 and indirectly blocks GTPase Rheb-positive regulation on mTOC1 activity. In this context, protein synthesis and several anabolic pathways are inhibited; in a second step, AMPk binds the inactive autophagy core ULK1 complex (formed by ULK1 kinase, ATG13 regulator, ATG101/FIP200 which is a key component of the

autophagy initiation process) and it phosphorylates the component ULK1/2 kinase. As a consequence of a cascade of autophosphorylations between ULK1/2 and ATG101/-FIP200, ULK1 stimulates autophagy initiation.

The ULK1/2 complex translocates to the phagophore localization, where it activates the class III phosphatidylinositol 3-kinase (class III PI3k) complex composed of VPS34 (vacuolar protein sorting 34 or PI3k enzyme), Beclin-1, VPS15, and ATG14 proteins. The kinase activity of ULK1/2 enhances the VPS34 activity by direct phosphorylation on Beclin-1. Class III PI3k activity is inhibited when Beclin-1 is bound to Bcl-2 [45] but is stimulated upon UVRAG recruitment to the complex [46]. Interestingly, Ambra1 also directly binds Beclin-1 to regulate the stability of Beclin-1/PI3k complex formation, competing under specific proautophagic condition with Ambra1 to stabilize the complex [46]. These events lead to autophagosome formation following the extension and closure of the mature autophagosomes (see Figure 2(b)). AMPk presumably suppresses nonessential vesicle trafficking in favor of membrane trafficking into the autophagy pathway during nutrient starvation in a VPS15/VPS34 class III phosphatidylinositol 3-kinase or PI (3) kinase-dependent manner [42, 47].

Following the nucleation step, other Atg proteins are recruited to the membrane of the preautophagosomes to promote the elongation and expansion of these newborn organelles. Elongation membranes require Atg3, Atg4, Atg7, Atg10, and an Atg5-Atg12-Atg16L complex to conjugate phosphatidylethanolamine (PE) to the microtubule-associated protein 1 light chain 3- (LC3-) I to form LC3-II [48]. The lipidated isoform LC3-II translocates from cytoplasm to the membrane of the preautophagosomes. Once the autophagosomes are closed, engulfing organelles, proteins, lipid droplets, or pathogens, a large majority of Atg proteins are released from the surface of autophagosomes to begin a new round of nucleation and membrane elongation. Currently, there is controversy about the amount of isoform LC3-II that is released and recycled from mature autophagosomes, given that a percentage of LC3-II is exposed on the inner side of the membranes and therefore would be subject to the action of lysosomal acid hydrolases [49].

7. DNA Damage Response and Autophagy: A Survival Association

In response to DNA damage induced by ROS (or reactive nitrogen species (RNS)), cells activate a high number of pathways in order to repair and maintain genome integrity and mediate survival pathways. Several kinds of proteins are implicated in DNA damage responses (DDRs) which are considered sensors (recognize and signal the damage), mediators, and effectors (repair the damage). Mediators and effectors are molecules that transduce nuclear signals to the cytosol where several processes are activated in order to better face adverse conditions. During DDRs, two events must be controlled in order to promote adaptation and survival: cell cycle checkpoints are activated to block proliferation and allow repair, and cell death pathways must be "kept on alert" in case of any unrepaired or excessive DNA damage.

ROS have been repeatedly reported as early inducers of autophagy due to their ability to produce oxidation of proteins, alteration of biological membranes, and DNA damage. The DNA lesions induced by ROS are involved in mutations, cancer, and many other diseases. PARPs are pivotal guardians in maintaining the integrity of the genome and triggering diverse kinds of metabolic strategies to escape from these adverse conditions. Currently, there are several groups that have demonstrated an active connection between the events that lead to DNA repair and the induction of autophagy. Accumulating evidence suggests that autophagy can be activated by DNA damage. ATM, a DNA damage-activated kinase, has been described as an important link between the DNA damage response (DDR) and the induction of autophagy. ATM binds to double-strand breaks (DSBs) in conjunction with the MRN complex and undergoes autophosphorylation and activation. In turn, ATM activates various downstream effector proteins, including Chk2 and Chk1 involved in cell cycle control or the tumor suppressor p53 which regulates cell survival versus death and HDAC1 and HDAC2 which are responsible for chromatin remodeling [50]. In response to DNA damage by mitochondrial ROS, external toxins, or irradiation, ATM is autophosphorylated within a MRN multiprotein complex that binds DSBs. Activated ATM initiates a pathway that results in activation of AMPk and its target TSC2 which functions as an inhibitor of mTORC1, promoting ULK1-dependent autophagosome formation. In addition, ATM directly phosphorylates and stabilizes p53 which transcriptionally regulates various regulators of the autophagic pathway including AMPk (energy sensor and autophagy activator) in colon cancer cells and during spermatogenesis, DAPK1 (death-associated protein kinase 1 or regulator of cell death and autophagy), and PTEN (phosphatase and tumor suppressor) in hepatocarcinoma cells and other cancer cell lines [51–53].

Recent studies have shown that treatment of certain types of tumor cells with genotoxic agents activate AMPk in a nucleus-independent way. Etoposide activates specifically the isoform AMPkα1 and not the α2 isoform, primarily within nucleus. AMPkα1 activation is independent of ATM signaling during etoposide-dependent DDRs. In this model, etoposide increased the intracellular Ca^{+2} levels and leads the activation of CaMkk2 kinase. AMPkα1 protected tumor cells against etoposide by limiting entry into the S-phase [54]. Considering the high energy cost and NAD^{+} involved during nuclear overactivation of PARP1 in response to DNA damage, regardless of whether the stimulus has a proautophagic character or not, we must explain that in most DDR models and autophagy described in normal and tumor cells, the activation of PARP1 has triggered a highly regulated process of autophagy aimed at survival. Therefore, it is obvious to think that treatment combined with PARP inhibitors inside a context of compromised autophagy could be considered as an interesting and novel antitumor therapy.

Several studies propose a role of PARP1 in the regulation of autophagy in response to DNA damage. Different models

of MEF 3T3 *KO* for PARP1 and in combination with PARP inhibitors (PARPi) (PJ34, DPQ, or Olaparib) were used by different groups to describe controlled overactivation of PARP1 and highly modulated prosurvival autophagy in response to alkylating and intercalating agents or ionizing radiation. Doxorubicin treatment leads to overactivation of PARP1, followed by ATP and NAD^+ depletion that trigger the nontoxic accumulation of autophagosomes in a model of MEF $parp1^{+/+}$ cells. An effective *KO* model for PARP1 (MEF $parp1^{-/-}$) or the treatment of MEF $parp1^{+/+}$ with PARPi increased the sensitivity of the cells to Doxorubicin, promoting high and uncontrolled levels of cell death. On the other hand, pharmacological or genetic inhibition of autophagy in a PARP1 KO model resulted in increased necrosis, suggesting a PARP1-mediated protective role of autophagy in response to chemotherapy [55]. A study in $Bax^{-/-}$ $Bak^{-/-}$ double knockout MEFs has elucidated the signaling pathway and biological function of autophagy induced by MNNG, a commonly used DNA-alkylating agent. In response to MNNG, double *KO* MEFs activated PARP1, reducing intracellular ATP levels and triggering the AMPk pathway and mTORC1 suppression. As a result, there was an accumulation of autophagosomes and cells showed Poly(ADP-ribose) profiles and persistent resistance for a long time of treatment. Suppression of the AMPk pathway blocked MNNG-induced autophagy and enhanced cell death [56]. Finally, other studies obtained the same conclusions in a nasopharyngeal carcinoma model exploring overactivation of PARP1, PARylation-dependent energy depletion and upregulation of the AMPk and ULK1 pathways in CNE-2 carcinoma cells upon ionizing radiation [57].

Many genotoxic agents activate AMPk kinase. Depending on the type of agent that induces DNA damage, the downstream cell response mediated by AMPk will be different. In tumor biology, the DNA-dependent AMPk activation could be considered protumorigenic promoting cell viability/survival or antitumorigenic cells would be more vulnerable to genotoxic stress. All these studies have demonstrated that autophagy should be considered as an important target in cancer during the induction of DNA damage, and consequently, new strategies based on the concept of synthetic lethality of PARPi must be explored.

8. ROS-Induced DNA Damage Leads to PARP1-Mediated AMPk Activation during Starvation-Induced Autophagy

Cancer cells require a continuous source of nutrients and oxygen, which is supplied through the growth of new blood vessels, providing the tumor with nutrients and evacuating metabolic wastes. At the cellular level, the exchange of nutrients, oxygen, and growth factors with the intracellular medium is a crucial process given that the absence of nutrients (starvation) or the deficiency of oxygen (hypoxia) can induce metabolic stress, oxidation of biomolecules, DNA damage, and PARP1 activation, situations in which cells activate autophagy as an adaptation and survival pathway. In this context, one initial signal during starvation-induced autophagy involves the activation PARP1 and the posttranslational modification by Poly(ADP-ribosyl)ation of several autophagy machinery proteins, favoring the autophagosome closure.

A large amount of evidence has demonstrated that starvation-induced autophagy is delayed in the absence of PARP1 in different models of normal and tumoral cells. Chemical inhibitors of autophagy as 3-methyl adenine (3-MA) (inhibitor of class III PI3k) or siRNA-based knockdown of ATG7 (nucleation of autophagosomes) completely prevented autophagy in $parp1^{-/-}$ 3T3 MEFs under starvation conditions. These data demonstrated that the absence of PARP1 synergizes with 3-MA or genetic knockdown to suppress autophagy during starvation. On the other hand, chemical inhibition of Poly(ADP-ribosyl)ation with several PARPi or specific silencing by siRNA of PARP1 reduced the percentage of $parp1^{+/+}$ 3T3 MEFs showing impaired membrane trafficking and LC3 translocation during autophagosome formation. The importance of controlled Poly(ADP-ribose) accumulation, due to PARP1 overactivation, in the initial steps of starvation-induced autophagy has been demonstrated [58]. Concomitant elimination of Poly(ADP-ribose) glycohydrolase (PARG) (enzyme degrading Poly(ADP-ribose) and ATG proteins1 (as ATG7, ULK1, or ATG5) has demonstrated that PAR accumulation after nutrient deprivation does not compromise cell viability; thus, the increased levels of autophagy are not ascribed to a cellular attempt to detoxify the excess of the PAR polymer in autophagosomes. There may be a mechanism of fine-tuning in the induction of PARylation-mediated autophagy [58, 59].

The origin of PARP1 activation during starvation focuses on the mitochondrial production and nuclear translocation of ROS. Under these oxidative conditions, DNA damage is recognized by PARP1, leading to PAR synthesis and triggering the initiation of autophagy. Although PARP1 knockout cells also produce ROS during starvation, this production does not lead to massive DNA damage and PARP1 activation. Consequently, these cells display an impaired starvation-induced autophagy [58] (see Figure 3(a)).

How is PARP1 able to modulate the cytosolic assembly of autophagosomes? Most classical studies have characterized DNA-dependent PARPs as genome integrity maintenance enzymes enclosing their activity in the nucleus and highly fixed in DNA functions. However, different groups are demonstrating that the influence of PARP activity goes beyond the nucleus and directly impacts the main cellular metabolic pathways, anabolism and catabolism. In general, PARPs modulate NAD^+ metabolism, energy pathways, and oxidative metabolism so we could conclude that inside a scenario of energy depletion guided by oxidative stress, PARPs potentiate cell scape or cell death pathways. Reversible PARylation is a pleiotropic regulator of various cellular functions but uncontrolled PARP activation may also lead to cell death. Moreover, noncovalent PARylation or MARylation could be considered as an effective cytosolic posttranslational modification of diverse MAPk kinases and mitochondrial cell death factors. To link PARP1 (potent consumer of ATP and NAD^+) energy collapse (oxidative phosphorylation to create

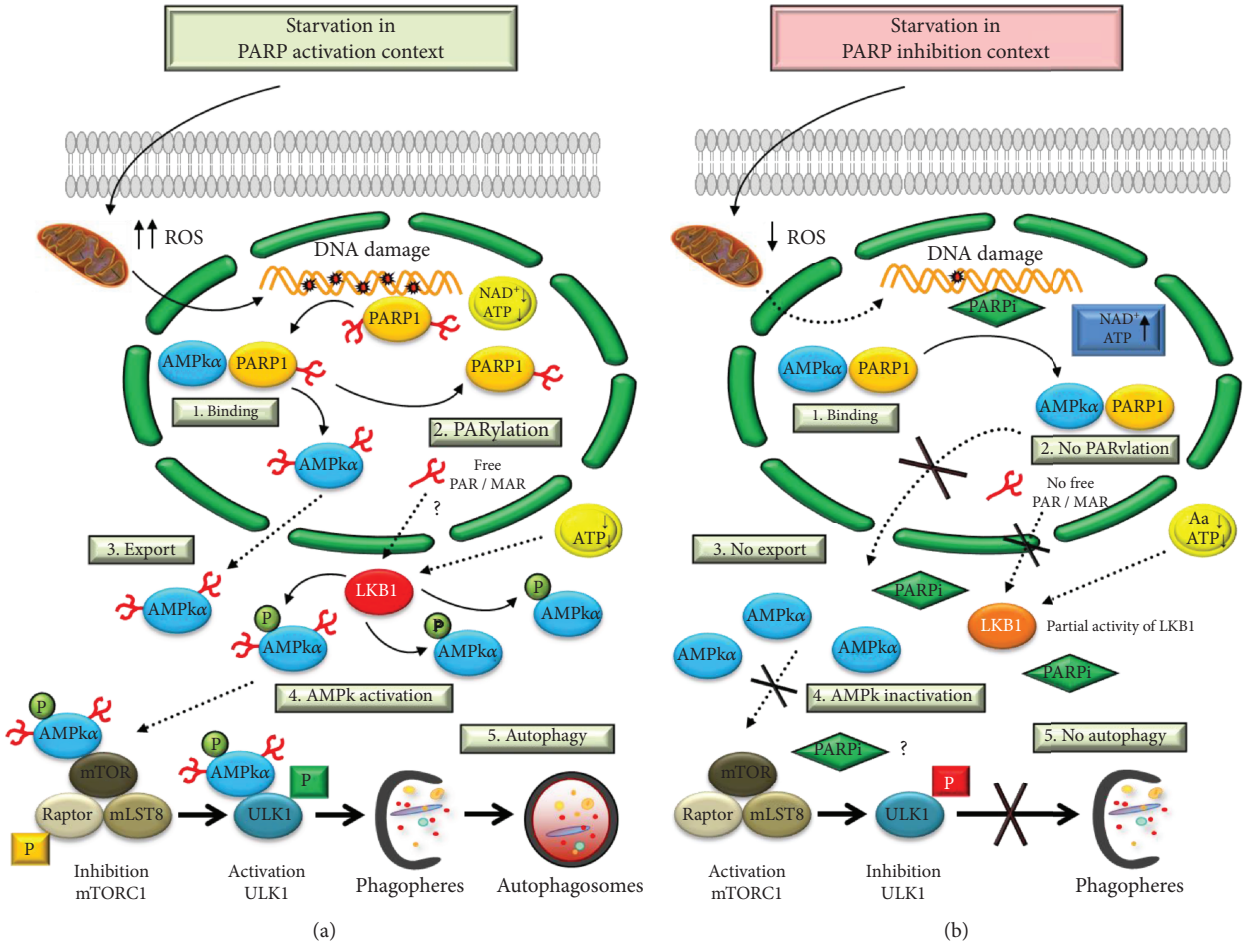

Figure 3: (a) PARylation regulates autophagy through AMPKα activation. PARP1 forms a complex with AMPKα in nucleus (1). During the starvation-induced autophagy, ROS production induces DNA damage and overactivation of PARP1. Auto-PARylated PARP1 is able to modify by PARylation in the AMPKα1 subunit (2). The complex is disrupted and PAR-AMPKα is exported to cytosol (3). The presence of PAR-AMPK and the continuous absence of amino acids and ATP depletion favor total activation of AMPKα population by LKB1, inhibition of mTORC1, interaction PAR-phospho-AMPK/ULK1, and autophagosome formation (4). LKB1 activity is presumably modified in a PARylation-dependent manner. (b) Starvation-induced ROS production was abrogated during the treatment with PARP inhibitors. Following AMPKα1/PARP1 interaction (1), the AMPKα1 subunit is not PARylated and the nuclear export of AMPK is inhibited (2 and 3). In spite of nutrient and energy depletion, AMPKα is inhibited; mTORC1 is partially activated and interacts with ULK1 favoring its inhibition (4). Finally, the autophagosomes production will be delayed.

ATP) and oxidative stress (collapse of mitochondrial ETC), several groups propose a theory in the form of a feedback loop: oxidative conditions lead to DNA damage and trigger PARP1 overactivation that intensifies energy collapse by over-PARylation that finally guides the cells to die. The suicidal over-PARylation disrupts mitochondrial energy mechanisms, impairing the antioxidant capacity of the Krebs cycle and favoring the liberation of proapoptotic mitochondrial factors [20]. Autophagy must be considered a scape pathway restoring ATP levels and blocking or delaying cell death.

DNA damage derived from starvation-induced ROS triggers an important depletion in intracellular ATP levels by overactivation of PARP1. The role of PARP1 in starvation-induced autophagy is related to its ability to sense DNA damage and deplete energy stores after its overactivation. This energy collapse is sensed by LKB1, promoting AMPk activation and mTORC1 inhibition. Knockout cells or cells with inefficient PARP1 activity show a potent downregulation on specific phospho-Thr172 AMPkα by LKB1. In consequence, the mTORC1 targets $p70^{S6k}$ and 4E-BP1 maintain their phosphorylation inhibiting autophagosome formation [58]. However, in this model, it is not possible to exclude the possibility of a perturbation in Ca^{2+}/calcium-/calmodulin-dependent kinase kinase 2 (CaMKK2) flux after PARP1 ablation upstream of the mitochondria leading to altered ATP synthesis and AMPk activation [60].

A nuclear population of the α isoform of AMPk has been described to interact with PARP1 [35]. The modification of AMPkα by Poly(ADP-ribose) and the mutual interaction between PARP1 and AMPkα function as a multifaceted molecular switch to optimize the initiation of autophagy. In Figure 3, we summarize two demonstrated scenarios: (I) starvation in a PARP1 activation context: a well-defined, non-PARylated AMPkα population has been described in the nucleus in functional interaction with PARP1 in

nonstarved cells. During nutrient deprivation, ROS exported from mitochondria induce DNA damage and PARP1 recognizes this damage; in order to promote DNA repair, PARP1 is over activated, consuming ATP and NAD^+ as substrates to synthetize Poly(ADP-ribose). The energy depletion could be sensed by LKB1 kinases to initiate autophagosome formation. PARylation of AMPkα at the AMPkα/PARP1 complex is a key event in initiating autophagy. AMPkα is transiently PARylated, disrupting the complex with PARP1 and being exported from the nucleus to the cytosol. PARylated cytosolic AMPkα triggers the total activation by LKB1 of the cytosolic AMPkα pool. Finally, the total pool of active AMPkα inhibits the mTORC1 complex and activates the autophagy core ULK1 complex, favoring the nucleation and elongation of phagophores around cytosol portions in order to be degraded and recycled into amino acids and other essential biomolecules (see Figure 3(a)).

The specific Poly(ADP-ribosyl)ation of the α subunit is needed to undergo AMPkα nuclear export. Abolishing the active nuclear translocation of PARylated AMPkα or the genetically engineered mutation on putative PARyaltion sites blocks efficiently the nuclear export compromising the autophagosomes formation [59]. The interaction between PARP1 and AMPkα has been described for DNA damage-dependent PARP1 activation while PARP1 has been reported to be a target of AMPkα [61]. During proinflammatory situations, PARP1 is able to modulate the expression of Bcl-6 through its binding at Bcl-6 intron 1. Phosphorylation of PARP1 at serine 177 (Ser-177) by AMPk kinase promotes dissociation from Bcl-6 intron 1, increases Bcl-6 expression, and inhibits expression of inflammatory mediators, demonstrating an anti-inflammatory crosstalk linking AMPk and PARP1 activity [61].

To evaluate the possibility of a mutual interaction between AMPkα and PARP1 leading to PARP1 phosphorylation, starved cells treated with the AMPk kinase inhibitor compound C showed decreased PARylation of AMPkα, suggesting that full AMPk activity was needed for PARP1 activation during nutrient deprivation [59]. (II) Starvation in a PARP1 inhibition context: PARP1-deficient cells display a reduced production of ROS, even at very early time points following starvation [58]. This finding is consistent with previous results showing reduced ROS production in lymphocytes challenged with exogenous oxidative stress and treated with PARP inhibitors [62]. PARP1 knockout cells or cells treated with a PARP inhibitor show sharply reduced DNA damage levels, and the machinery to repair DNA damage is not as efficient as in PARP1 wild-type cells, resulting in a residual level of damage after long times of starvation of which the final consequence is compromised autophagy and prominent apoptosis cell death [58].

In PARP1-inactivated cells, the absence of efficient PARylation retains the stability of the PARP1/AMPkα complex and AMPkα is not transported from the nucleus to the cytosol during starvation. The final consequence is an inefficient activation of the cytosolic AMPkα pool, partially maintaining the activity of mTORC1 and seriously compromising the activation of ULK1 and the initiation of phagophores [59] (see Figure 3(b)).

The crucial role of neonatal autophagy was clearly demonstrated by targeted inactivation of the autophagy-related genes ATG5 and ATG7. Mice deficient in ATG5/ATG7 were apparently normal in birth, except for a slightly lower body weight than control or wild-type (approximately 10% in ATG5-null and 18% in ATG7-null mice). Moreover, ATG7-null animals presented deficiency in the liver causing hepatomegaly and hepatic cell swelling. The curve of survival of neonates demontrated that the null animals showed serious difficulties to growth and survive, indicating the important role of the proteins that regulate the formation of autophagosomes during embryonic development [63]. It is described that phenotypically, PARP1 knockout mice had the average litter size smaller than wild-type mice (approximately 20%). Several *in vivo* observations in starved neonates of PARP1 mutant mice showed decreased frequency of hepatic multimembrane lipid droplets, presumably autophagosomes engulfing mitochondria and cytosol portions, implying a physiological role of PARP1 in starvation-induced autophagy [58].

In conclusion, the nucleus and the functional interaction between PARP1 and AMPkα are initial and essential sensors of the metabolic alterations derived from perturbations in the nutritional extracellular status, not necessarily related with the alterations in genomic integrity.

9. Concluding Remarks

One of the most remarkable findings in our study is the need for the AMPkα nuclear export to perform its cytosolic function during the initial steps of starvation-induced autophagy, but how PARylated AMPkα coming out of the nucleus "hits" cytosolic AMPkα remains to be clarified. Nuclear sensors, including PARP1, detect perturbations in nuclear and genetic homeostasis to activate a mechanism to repair and, in case of failure, promote different types of cell death for the benefit of the organism homeostasis. Considering different studies, we could conclude that DNA lesions are potential activators of nonselective autophagy mechanisms. In this way, we have enough evidence to affirm that PARP1 and PARylation play a key role in autophagy, beyond the nuclear activation of PARP1.

This model has been demonstrated in normal and cancer cells, so efficient treatment with drugs on cancer cells opens a new, interesting, and novel field with PARP inhibitors and molecules targeting prosurvival pathways under physiological stimuli such as starvation, hypoxia, growth factor deprivation, etcetera.

Conflicts of Interest

The authors declare no conflicts of interest.

Acknowledgments

Authors would like to acknowledge all the people and foundations that have contributed to the development of all the projects cited in this review, the Spanish Foundation Ramón Areces (Madrid, Spain) and the Spanish National

Research Council (CSIC). We apologize to investigators and laboratories whose research could not be included in this paper due to space limitations. This work is supported by grants from Université de Strasbourg—Institute for Advance Studies (USIAS program/Unistra)—and Centre National de la Recherche Scientifique.

References

[1] S. Vyas, I. Matic, L. Uchima et al., "Family-wide analysis of poly(ADP-ribose) polymerase activity," *Nature Communications*, vol. 5, no. 1, article 4426, 2014.

[2] C.-S. Yang, K. Jividen, A. Spencer et al., "Ubiquitin modification by the E3 ligase/ADP-ribosyltransferases Dtx3L/Parp9," *Molecular Cell*, vol. 66, no. 4, pp. 503–516.e5, 2017.

[3] R. Gupte, Z. Liu, and W. L. Kraus, "PARPs and ADP-ribosylation: recent advances linking molecular functions to biological outcomes," *Genes & Development*, vol. 31, no. 2, pp. 101–126, 2017.

[4] H. Qi, B. D. Price, and T. A. Day, "Multiple roles for mono- and poly (ADP-ribose) in regulating stress responses," *Trends Genet*, vol. 35, no. 2, pp. 159–172, 2019.

[5] K. Y. Lin and W. L. Kraus, "PARP inhibitors for cancer therapy," *Cell*, vol. 169, no. 2, p. 183, 2017.

[6] J. Krietsch, M. Rouleau, É. Pic et al., "Reprogramming cellular events by poly(ADP-ribose)-binding proteins," *Molecular Aspects of Medicine*, vol. 34, no. 6, pp. 1066–1087, 2013.

[7] R. H. Houtkooper, C. Cantó, R. J. Wanders, and J. Auwerx, "The secret life of NAD^+: an old metabolite controlling new metabolic signaling pathways," *Endocrine Reviews*, vol. 31, no. 2, pp. 194–223, 2010.

[8] B. A. Gibson and W. L. Kraus, "New insights into the molecular and cellular functions of poly (ADP-ribose) and PARPs," *Nature Reviews Molecular Cell Biology*, vol. 13, no. 7, pp. 411–424, 2012.

[9] A. Luna, M. I. Aladjem, and K. W. Kohn, "SIRT1/PARP1 crosstalk: connecting DNA damage and metabolism," *Genome Integrity*, vol. 4, no. 1, p. 6, 2013.

[10] N. Zhang and A. A. Sauve, "Regulatory effects of NAD^+ metabolic pathways on sirtuin activity," *Progress in Molecular Biology and Translational Science*, vol. 154, pp. 71–104, 2018.

[11] A. G. McLennan, "The Nudix hydrolases superfamily," *Cellular and Molecular Life Sciences*, vol. 63, no. 2, pp. 123–143, 2006.

[12] A.-L. Perraud, B. Shen, C. A. Dunn et al., "NUDT9, a member of the Nudix hydrolases, is an evolutionary conserved mitochondrial ADP-ribose pyrophosphatase," *Journal of Biological Chemistry*, vol. 278, no. 3, pp. 1794–1801, 2003.

[13] M. Zha, Q. Guo, Y. Zhang et al., "Molecular mechanism of ADP-ribose hydrolysis by human NUDT5 from structural and kinetic studies," *Journal of Molecular Biology*, vol. 379, no. 3, pp. 568–578, 2008.

[14] C. Wang and R. Youle, "Cell biology: form follows function for mitochondria," *Nature*, vol. 530, no. 7590, pp. 288-289, 2016.

[15] P. Bai, C. Cantó, H. Oudart et al., "PARP-1 inhibition increases mitochondrial metabolism through SIRT1 activation," *Cell Metabolism*, vol. 13, no. 4, pp. 461–468, 2011.

[16] P. Bai, C. Canto, A. Brunyánszki et al., "PARP-2 regulates SIRT1 expression and whole-body energy expenditure," *Cell Metabolism*, vol. 13, no. 4, pp. 450–460, 2011.

[17] J.-i. Sakamaki, H. Daitoku, K. Yoshimochi, M. Miwa, and A. Fukamizu, "Regulation of FOXO1-mediated transcription and cell proliferation by PARP1," *Biochemical and Biophysical Research Communications*, vol. 382, no. 3, pp. 497–502, 2009.

[18] H. Schuhwerk, C. Bruhn, K. Siniuk et al., "Kinetics of poly(ADP-ribosyl)ation, but not PARP1 itself, determines the cell fate in response to DNA damage *in vitro* and *in vivo*," *Nucleic Acids Research*, vol. 45, no. 19, pp. 11174–11192, 2017.

[19] R. Aguilar-Quesada, J. Muñoz-Gámez, D. Martín-Oliva et al., "Interaction between ATM and PARP1 in response to DNA damage and sensitization of ATM deficient cells through PARP Inhibition," *BMC Molecular Biology*, vol. 8, no. 1, p. 29, 2007.

[20] L. Virag, A. Robaszkiewicz, J. M. Rodríguez-Vargas, and F. J. Oliver, "Poly(ADP-ribose) signaling in cell death," *Molecular Aspects of Medicine*, vol. 34, no. 6, pp. 1153–1167, 2013.

[21] M. Redza-Dutordoir and D. A. Averill-Bates, "Activation of apoptosis signaling pathways by reactive oxygen species," *Biochimica et Biophysica Acta (BBA) - Molecular Cell Research*, vol. 1863, no. 12, pp. 2977–2992, 2016.

[22] E. Daugas, S. A. Susin, N. Zamzami et al., "Mitochondrio-nuclear translocation of AIF in apoptosis and necrosis," *The FASEB Journal*, vol. 14, no. 5, pp. 729–739, 2000.

[23] C.-T. Huang, D.-Y. Huang, C.-J. Hu, D. Wu, and W.-W. Lin, "Energy adaptive response during parthanatos is enhanced by PD98059 and involves mitochondrial function but not autophagy induction," *Biochimica et Biophysica Acta (BBA) - Molecular Cell Research*, vol. 1843, no. 3, pp. 531–543, 2014.

[24] L. Galluzzi, I. Vitale, J. M. Abrams et al., "Molecular definitions of cell death subroutines: recommendations of the Nomenclature Committee on Cell Death 2012," *Cell Death and Differentiation*, vol. 19, no. 1, pp. 107–120, 2012.

[25] T. Wang, Y. Jin, W. Yang et al., "Necroptosis in cancer: an angel or a demon?," *Tumor Biology*, vol. 39, no. 6, pp. 1–11, 2017.

[26] Y. Feng, D. He, Z. Yao, and D. J. Klionsky, "The machinery of macroautophagy," *Cell Research*, vol. 24, no. 1, pp. 24–41, 2014.

[27] Z. Yang and D. J. Klionsky, "Mammalian autophagy: core molecular machinery and signaling regulation," *Current Opinion in Cell Biology*, vol. 22, no. 2, pp. 124–131, 2010.

[28] Z. Yin, C. Pascual, and D. Klionsky, "Autophagy: machinery and regulation," *Microbial Cell*, vol. 3, no. 12, pp. 588–596, 2016.

[29] M. Marinkovic, M. Sprung, M. Buljubasic, and I. Novak, "Autophagy modulation in cancer: current knowledge on action and therapy," *Oxidative Medicine and Cellular Longevity*, vol. 2018, Article ID 8023821, 18 pages, 2018.

[30] I. Cotzomi-Ortega, P. Aguilar-Alonso, J. Reyes-Leyva, and P. Maycotte, "Autophagy and its role in protein secretion: implications for cancer therapy," *Mediators of Inflammation*, vol. 2018, Article ID 4231591, 17 pages, 2018.

[31] G. Kroemer, G. Marino, and B. Levine, "Autophagy and the integrated stress response," *Molecular Cell*, vol. 40, no. 2, pp. 280–293, 2010.

[32] S. K. Bhutia, S. Mukhopadhyay, N. Sinha et al., "Autophagy: cancer's friend or foe?," in *Advances in Cancer Research*, vol. 118, pp. 61–95, 2013.

[33] E. White, "The role of autophagy in cancer," *The Journal of Clinical Investigation*, vol. 125, no. 1, pp. 42–46, 2015.

[34] M. A. Rahman and H. Rhim, "Therapeutic implication of autophagy in neurodegenerative diseases," *BMB Reports*, vol. 50, no. 7, pp. 345–354, 2017.

[35] F. M. Menzies, A. Fleming, A. Caricasole et al., "Autophagy and neurodegeneration: pathogenic mechanisms and therapeutic opportunities," *Neuron*, vol. 93, no. 5, pp. 1015–1034, 2017.

[36] D. Glick, S. Barth, and K. F. Macleod, "Autophagy: cellular and molecular mechanism," *The Journal of Pathology*, vol. 221, no. 1, pp. 3–12, 2010.

[37] M. Mauthe and F. Reggiori, "ATG proteins: are we always looking at autophagy?," *Autophagy*, vol. 12, no. 12, pp. 2502-2503, 2016.

[38] L. H. Chew and C. K. Yip, "Structural biology of the macroautophagy machinery," *Frontiers in Biology*, vol. 9, no. 1, pp. 18–34, 2014.

[39] M. Mehrpour, A. Esclatine, I. Beau, and P. Codogno, "Overview of macroautophagy regulation in mammalian cells," *Cell Research*, vol. 20, no. 7, pp. 748–762, 2010.

[40] K. Abounit, T. M. Scarabelli, and R. B. McCauley, "Autophagy in mammalian cells," *World Journal of Biological Chemistry*, vol. 3, no. 1, pp. 1–6, 2012.

[41] L. Chen, F. J. Xin, J. Wang et al., "Conserved regulatory elements in AMPk," *Nature*, vol. 498, no. 7453, pp. E8–E10, 2013.

[42] D. Garcia and R. J. Shaw, "AMPK: mechanisms of cellular energy sensing and restoration of metabolic balance," *Molecular Cell*, vol. 66, no. 6, pp. 789–800, 2017.

[43] F. Boutouja, C. M. Stiehm, and H. W. Platta, "mTOR: a cellular regulator interface in health and disease," *Cells*, vol. 8, no. 1, pp. 18–23, 2019.

[44] S. A. Hawley, F. A. Ross, C. Chevtzoff et al., "Use of cells expressing γ subunit variants to identify diverse mechanisms of AMPK activation," *Cell Metabolism*, vol. 11, no. 6, pp. 554–565, 2010.

[45] S. Pattingre, A. Tassa, X. Qu et al., "Bcl-2 antiapoptotic proteins inhibit Beclin1-dependent autophagy," *Cell*, vol. 122, no. 6, pp. 927–939, 2005.

[46] C. Liang, P. Feng, B. Ku et al., "Autophagic and tumor suppressor activity of a novel Beclin1-binding protein UVRAG," *Nature Cell Biology*, vol. 8, no. 7, pp. 688–698, 2006.

[47] J. Kim, Y. C. Kim, C. Fang et al., "Differential regulation of distinct Vps34 complexes by AMPK in nutrient stress and autophagy," *Cell Metabolism*, vol. 152, no. 1-2, pp. 290–303, 2013.

[48] N. Fujita, T. Itoh, H. Omori, M. Fukuda, T. Noda, and T. Yoshimori, "The Atg16L complex specifies the sites of LC3 lipidation for membrane biogenesis in autophagy," *Molecular Biology of the Cell*, vol. 19, no. 5, pp. 2092–2100, 2008.

[49] S. R. Yoshii and N. Mizushima, "Monitoring and measuring autophagy," *International Journal of Molecular Sciences*, vol. 18, no. 9, pp. 1865–1878, 2017.

[50] A. Maréchal and L. Zou, "DNA damage sensing by the ATM and ATR kinases," *Cold Spring Harbor Perspectives in Biology*, vol. 5, no. 9, pp. a012716–a012716, 2013.

[51] Y. Niu, W. Sun, J.-J. Lu et al., "PTEN activation by DNA damage induces protective autophagy in response to cucurbitacin B in hepatocellular carcinoma cells," *Oxidative Medicine and Cellular Longevity*, vol. 2016, Article ID 4313204, 15 pages, 2016.

[52] R. Li, X. Luo, Y. Zhu et al., "ATM signals to AMPK to promote autophagy and positively regulate DNA damage in response to cadmium-induced ROS in mouse spermatocytes," *Environmental Pollution*, vol. 231, Part2, pp. 1560–1568, 2017.

[53] A. Eisenberg-Lerner and A. Kimchi, "PKD is a kinase of Vps34 that mediates ROS-induced autophagy downstream of DAPk," *Cell Death & Differentiation*, vol. 19, no. 5, pp. 788–797, 2012.

[54] D. Vara-Ciruelos, M. Dandapani, A. Gray, E. O. Egbani, A. M. Evans, and D. G. Hardie, "Genotoxic damage activates the AMPK-α1 isoform in the nucleus via Ca^{2+}/CaMKK2 signaling to enhance tumor cell survival," *Molecular Cancer Research*, vol. 16, no. 2, pp. 345–357, 2018.

[55] J. A. Muñoz-Gámez, J. M. Rodríguez-Vargas, R. Quiles-Pérez et al., "PARP-1 is involved in autophagy induced by DNA damage," *Autophagy*, vol. 5, no. 1, pp. 61–74, 2009.

[56] J. Zhou, S. Ng, Q. Huang et al., "AMPK mediates a pro-survival autophagy downstream of PARP-1 activation in response to DNA alkylating agents," *FEBS Letters*, vol. 587, no. 2, pp. 170–177, 2013.

[57] Z. T. CHEN, W. ZHAO, S. QU et al., "PARP-1 promotes autophagy via the AMPK/mTOR pathway in CNE-2 human nasopharyngeal carcinoma cells following ionizing radiation, while inhibition of autophagy contributes to the radiation sensitization of CNE-2 cells," *Molecular Medicine Reports*, vol. 12, no. 2, pp. 1868–1876, 2015.

[58] J. M. Rodríguez-Vargas, M. J. Ruiz-Magaña, C. Ruiz-Ruiz et al., "ROS-induced DNA damage and PARP-1 are required for optimal induction of starvation-induced autophagy," *Cell Research*, vol. 22, no. 7, pp. 1181–1198, 2012.

[59] J. M. Rodríguez-Vargas, M. I. Rodríguez, J. Majuelos-Melguizo et al., "Autophagy requires poly (adp-ribosyl) ation-dependent AMPK nuclear export," *Cell Death & Differentiation*, vol. 23, no. 12, pp. 2007–2018, 2016.

[60] C. Cárdenas, R. A. Miller, I. Smith et al., "Essential regulation of cell bioenergetics by constitutive InsP3 receptor Ca^{2+} transfer to mitochondria," *Cell*, vol. 142, no. 2, pp. 270–283, 2010.

[61] B. Gongol, T. Marin, I. C. Peng et al., "AMPkα2 exerts its anti-inflammatory effects through PARP1 and Bcl-6," *Proceedings of the National Academy of Sciences of USA*, vol. 110, no. 8, pp. 3161–3166, 2013.

[62] L. Virág, A. L. Salzman, and C. Szabó, "Poly(ADP-ribose) synthetase activation mediates mitochondrial injury during oxidant-induced cell death," *Journal of Immunology*, vol. 161, no. 7, pp. 3753–3759, 1998.

[63] M. Komatsu, S. Waguri, T. Ueno et al., "Impairment of starvation-induced and constitutive autophagy in Atg7-deficient mice," *The Journal of Cell Biology*, vol. 169, no. 3, pp. 425–434, 2005.

Hindawi
Oxidative Medicine and Cellular Longevity
Volume 2019, Article ID 4517091, 15 pages
https://doi.org/10.1155/2019/4517091

Research Article

Cucurbitacin B Exerts Antiaging Effects in Yeast by Regulating Autophagy and Oxidative Stress

Yanfei Lin,[1] Yuki Kotakeyama,[2] Jing Li,[1] Yanjun Pan,[1] Akira Matsuura,[3] Yoshikazu Ohya,[2] Minoru Yoshida,[4,5] Lan Xiang,[1] and Jianhua Qi[1]

[1]*College of Pharmaceutical Sciences, Zhejiang University, 866 Yu Hang Tang Road, Hangzhou, China*
[2]*Departments of Integrated Biosciences, Graduate School of Frontier Sciences, University of Tokyo, 5-1-5 Kashiwanoha, Kashiwa, Chiba 277-8562, Japan*
[3]*Department of Biology, Graduate School of Science, Chiba University, Chiba 263-8522, Japan*
[4]*Chemical Genomics Research Group, RIKEN Center for Sustainable Resource Science, 2-1 Hirosawa, Wako, Saitama 351-0198, Japan*
[5]*Department of Biotechnology and Collaborative Research Institute for Innovative Microbiology, The University of Tokyo, Yayoi 1-1-1, Bunkyo-ku, Tokyo 113-8657, Japan*

Correspondence should be addressed to Lan Xiang; lxiang@zju.edu.cn and Jianhua Qi; qijianhua@zju.edu.cn

Received 30 January 2019; Revised 27 March 2019; Accepted 23 April 2019; Published 2 June 2019

Guest Editor: Marco Cordani

The budding yeast *Saccharomyces cerevisiae* has been used as a model organism for the basic mechanism of aging, which provides useful assay systems for measuring both replicative and chronological lifespans. In the course of our screening program for substances that extend replicative lifespan, cucurbitacin B (CuB) was found as a hit compound from a compound library, which contains cerebrosides, phenols, sesquiterpenoid, triterpenoids, and sterols isolated from natural products by our research group. Importantly, it prolonged not only the replicative lifespan but also the chronological lifespan in yeast. CuB increased *ATG32* gene expression, suggesting that CuB induces autophagy. Indeed, the GFP signal generated from the cleavage of GFP-Atg8, which is a signature of autophagy, was increased upon CuB treatment. On the other hand, CuB failed to increase the chronological lifespans when either *ATG2* or *ATG32*, essential autophagy genes, was deleted, indicating that the lifespan extension by CuB depends on autophagy induction. Furthermore, CuB significantly increased superoxide dismutase (Sod) activity and the survival rate of yeast under oxidative stress, while it decreased the amount of reactive oxygen species (ROS) and malondialdehyde (MDA) production, indicating that CuB has activity to antagonize oxidative stress. Additionally, CuB did not affect replicative lifespans of *sod1*, *sod2*, *uth1*, and *skn7* mutants with the K6001 background, indicating that aging-related genes including *SOD1*, *SOD2*, *UTH1*, and *SKN7* participate in the antiaging effect of CuB. These results suggest that CuB exerts antiaging activity by regulating autophagy, ROS, antioxidative ability, and aging-related genes. Finally, we discuss the possible intracellular targets of CuB based on the phenotypic comparison between the CuB and global gene deletion databases.

1. Introduction

Yeast has the replicative lifespan and chronological lifespan. The replicative lifespan measures the number of daughters of a single mother cell, which can asexually produce prior to senescence. The chronological lifespan is defined as the length of time a yeast cell can survive in the nondividing G0 state [1]. Both of them are regulated by many environmental and genetic factors [2]. In our study, we used K6001 yeast as an aging model, which is a mutant yeast strain derived from W303. A unique character of K6001, in which only mother cells can produce daughter cells in glucose medium, but not in galactose medium [3], can be used for measuring replicative lifespan. Under the guidance of K6001 replicative lifespan assay, we have isolated several compounds with antiaging activity from natural products [4, 5].

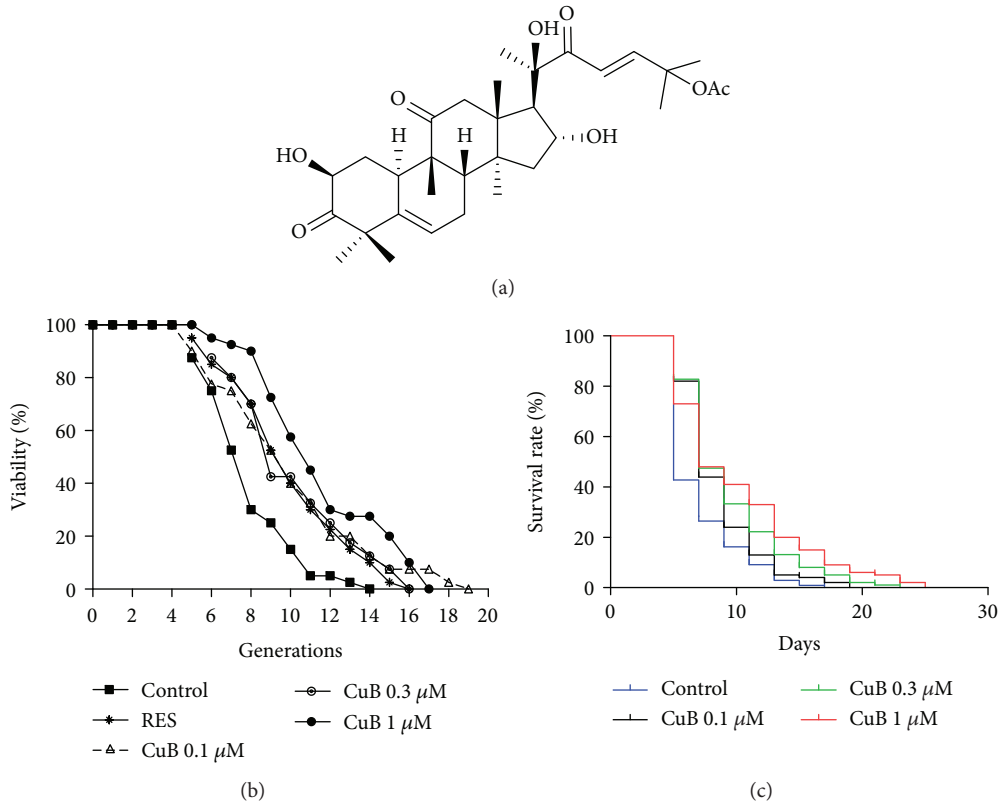

Figure 1: Chemical structure and antiaging activity of cucurbitacin B (CuB). (a) Chemical structure of CuB. (b) Effect of CuB on the replicative lifespan of K6001 yeast. RES (10 μM) was used as the positive control. (c) Effect of CuB on the chronological lifespan of YOM36 yeast.

Autophagy is a highly conserved pathway in organisms from yeast to human, which involves degradation of damaged organelles and proteins and circulation of amino acids and other metabolites [6]. It regulates the genomic integrity via suppression of cell division in yeast under starvation [7]. Besides, decreased autophagy leads to down-regulation of proteostasis, which is one of the hallmarks for aging. Dysfunction or decreased expression of autophagy genes leads to shorter lifespan in yeast and fruit fly. Conversely, enhanced autophagy promotes the longevity in aging models and protects against aging and age-related disorders [8]. Specially, the lifespan-extending effects of rapamycin in *C. elegans*, fruit fly, and mice are abolished by knocking out or knocking down of *ATG* genes [9]. In addition, caloric restriction and resveratrol (RES) induced autophagy dependent on Sir2 function in yeast and *C. elegans*, and the deleted and silenced *ATG* genes avoid the antiaging effect of caloric restriction, RES, and overexpression of *SIR2* [10]. Therefore, autophagy has a close link to aging.

Oxidative stress is another cause of aging. Free radicals produced through aerobic metabolism accumulate over time and accelerate aging [11]. In yeast, the accumulation of ROS promotes replicative and chronological aging. The upregulation of antioxidant removes excess ROS and maintains redox balance, eventually delaying the progression of aging in yeast [12]. In our previous studies, we showed that antioxidative activity plays an important role in the antiaging effects of cholesterol and parishin [4, 5].

CuB has been shown as a promising compound for anticancer treatment in recent years, and it also shows antioxidative and anti-inflammatory activities [13, 14]. The regulation of STAT3 and Raf/MEK/ERK signaling pathways by CuB is likely to be involved in its antitumor activity such as induction of apoptosis in tumor cells [15]. Moreover, CuB was found to induce autophagy in cells [16]. In the present study, we identified CuB as a compound with antiaging activity in yeast, resulting from our screening for antiaging compounds from a compound library using yeast replicative and chronological lifespan assays. Here, we report a unique activity of CuB, which exerts antiaging effects in yeast through regulating autophagy and oxidative stress.

2. Materials and Methods

2.1. CuB, Yeast Strains, and Medium. CuB was isolated from *Pedicellus melo* in accordance with a methodology that was previously used by our group. The chemical structure of CuB (Figure 1(a)) was identified by comparing HR ESI-MS, ^{1}H NMR, and ^{13}C NMR data with reported data [17]. ^{1}H NMR (500 MHz, acetone-d_6): δ 0.91 (3H, s), 1.02 (3H, s), 1.11 (1H, q, J = 13.0 Hz), 1.28 (3H, s), 1.32 (3H, s), 1.39 (3H, s), 1.40 (1H, m), 1.44 (3H, s), 1.51 (3H, s), 1.55 (3H, s), 1.84 (1H, m), 1.96 (3H, s), 1.97 (2H, m), 2.11 (1H, m), 2.40 (1H, dd, J = 5.5, 19.0 Hz), 2.51 (1H, d, J = 14.5 Hz), 2.66 (1H, d, J = 6.5 Hz), 3.02 (1H, d, J = 12.5 Hz), 3.40 (1H, d, J = 14.5 Hz), 4.45 (1H, m), 4.51 (1H, s), 4.56

Table 1: Yeast strains used in the present study.

Strains	Genotype	Source
K6001	*MATa*, *ade2-1*, *trp1-1*, *can1-100*, *leu2-3,112*, *his3-11,15*, *GAL*, *psi+*, *ho*::HO::*CDC6* (at HO), *cdc6*::*hisG*, *ura3*::*URA3 GAL-ubiR-CDC6* (at *URA3*)	Gifted by Professor Michael Breitenbach
Δ*uth1* of K6001, Δ*skn7* of K6001, Δ*sod1* of K6001, Δ*sod2* of K6001, Δ*atg2* of K6001, Δ*atg32* of K6001	Replace the *UTH1* gene, *SKN7* gene, *SOD1* gene, *SOD2* gene, *ATG2* gene, and *ATG32* gene in K6001 with kanamycin gene, respectively	Constructed by Professor Akira Matsuura
BY4741	*MATa*, *his3Δ1*, *leu2Δ0*, *met15Δ0*, *ura3Δ0*	Gifted by Professor Akira Matsuura
YOM36	Prototrophic derivative of BY4742 (*MATα*, *his3Δ1*, *leu2Δ0*, *lys2Δ0*, *ura3Δ0*)	Gifted by Professor Akira Matsuura
Δ*atg2* of YOM36, Δ*atg32* of YOM36	Replace the *ATG2* gene and *ATG32* gene in YOM36 with kanamycin gene, respectively	Constructed by Professor Akira Matsuura
YOM38 containing plasmid pR316-GFP-ATG8	Prototrophic derivative of BY4742 (*MATα*, *his3Δ1*, *leu2Δ0*, *lys2Δ0*) containing plasmid pR316-GFP-ATG8	Constructed by Professor Akira Matsuura
YO2458	*MATa, his3Δ1, leu2Δ0, met15Δ0, ura3Δ0, YOR202w::KanMX4*	Provided by Professor Yoshikazu Ohya

(1H, m), 5.82 (1H, d, $J = 3.0$ Hz), 6.81 (1H, d, $J = 16.0$ Hz), and 6.98 (1H, d, $J = 16.0$ Hz); ^{13}C NMR (125 MHz, acetone-d_6): δ 19.2, 20.2, 20.6, 21.8, 22.0, 24.7, 25.1, 26.4, 27.1, 29.9, 34.2, 37.1, 43.6, 46.6, 49.0, 49.1, 49.4, 51.1, 51.4, 59.1, 71.4, 72.3, 79.6, 80.1, 120.8, 122.3, 142.0, 151.0, 170.3, 203.5, 212.7, and 213.7; and high-resolution ESI-TOF-MS m/z 581.3085, calcd for $C_{32}H_{46}NaO_8$ $(M+Na)^+$ 581.3090. All the yeast strains used in the present study are listed in Table 1.

2.2. Replicative and Chronological Lifespan Assays. The replicative lifespan assay was performed following a previously described methodology [5]. In brief, the K6001 strain was inoculated in galactose medium and cultured for 24–28 h in a shaking incubator at 160 rpm and 28°C. After washing with phosphate-buffered saline (PBS) for three times, approximately 4000 cells were spread onto glucose agar plates (2% glucose, 2% hipolypeptone, 1% yeast extract, and 2% agar) supplemented with 0, 0.1, 0.3, or 1 μM CuB or 10 μM RES. Afterward, the yeast cells were cultured at 28°C for 2 days. Forty microcolonies from each group were observed under microscopy, and the number of daughter cells in each microcolony was counted. The replicative lifespan assays of K6001 mutants (Δ*uth1*, Δ*skn7*, Δ*sod1*, Δ*sod2*, Δ*atg2*, and Δ*atg32* of K6001) were conducted similarly to those of the wild-type K6001. RES was procured from J&K Scientific Ltd. (Beijing, China) and was used as positive control.

The chronological lifespan assay was conducted in accordance with a previous methodology [18]. Briefly, YOM36 yeast cells were cultured in synthetic defined (SD) medium (0.17% yeast nitrogen base without amino acids and ammonium sulfate (BD Difco), 0.5% ammonium sulfate, and 0.2% glucose) for 24 h and then inoculated into the SD medium containing 0, 0.1, 0.3, or 1 μM CuB with the initial OD600 value of 0.01. Cultures were grown in a shaker at 180 rpm and 30°C. Growth kinetics was recorded by measuring the OD600 value every 2 or 4 h until the stationary phase was reached. In addition, the survival rate was measured by counting colony-forming units (CFUs) every 2 days. The CFUs on day 3 was denoted as 100% survival.

2.3. Real-Time Polymerase Chain Reaction Analysis. Wild-type BY4741 were incubated with the negative control or 1 μM CuB in glucose medium overnight. RNA was extracted through a hot phenol method. cDNA was synthesized through the reverse transcription method using the HiFi-MMLV cDNA Kit (CoWin Biotech, Beijing, China) and 5 μg of RNA. Real-time polymerase chain reaction (RT-PCR) was performed in reference to a previous study [5] by using CFX96 Touch (Bio-Rad, Hercules, USA) and SYBR Premix Ex Taq (Takara, Otsu, Japan). The thermal cycling parameters were as follows: for *ATG2* and *ATG32*, 40 cycles, 94°C for 15 s, 51.6°C for 15 s, and 68°C for 20 s. The primers used for RT-PCR are as follows: for *ATG2*, sense 5′-GCT CCT GTC AGA TCG TTT AT-3′ and antisense 5′-TTC AGA CTC CTT CCC AAA TG-3′; for *ATG32*, sense 5′-ACC GTC TCA TCC CTT TAA AC-3′ and antisense 5′-CTT CCT CAA AAG CCT CAT CT-3′; and for *TUB1*, sense 5′-CCA AGG GCT ATT TAC GTG GA-3′ and antisense 5′-GGT GTA ATG GCC TCT TGC AT-3′. The $2^{-\Delta\Delta Ct}$ method was used to analyze relative gene expression data. The mRNA levels of *ATG2* and *ATG32* were normalized to those of *TUB1*.

2.4. GFP–ATG8 of Yeast Analyzed with Fluorescent Microscopy. YOM38 yeast cells containing pR316-GFP-ATG8 or YOM36 yeast cells were cultured in the SD medium with the initial OD600 value of 0.1 and treated with 0, 0.1, 0.3, or 1 μM CuB or 300 μM RES for 22 h. Subsequently, yeast cells were stained with 20 μg/mL DAPI in dark for 10 min and washed with the PBS for three times. Yeast

cells were observed using a two-photon confocal fluorescence microscope (Olympus FV1000BX-51, Tokyo, Japan) or fluorescent microscope (Leica DMI3000 B, Wetzlar, Germany). Pictures were acquired using image acquisition and analysis software.

2.5. Western Blot Analysis. YOM38 yeast cells containing the pR316-GFP-ATG8 plasmid were cultured as described in the previous section. At first, yeast cells were incubated with 300 μM RES or CuB at doses of 0, 0.1, 0.3, or 1 μM, and the yeast cells were collected at the specified time point and washed three times with PBS. After that, the samples were ultrasonicated for five times (1 min for each time), freeze-thawed for five times, and sonicated for five times again. The cell lysates were centrifuged, and the protein concentrations of the supernatant were measured with BCA Protein Assay Kit (CoWin Biotech, Beijing, China). Approximately 20 μg protein was separated with SDS-PAGE and transferred to PVDF membranes. The membranes were incubated with primary antibodies followed by secondary antibodies. Antigens were visualized using ECL Western Blot Kit (CoWin Biotech, Beijing, China). The primary antibodies used are as follows: anti-GFP antibody (Medical & Biological Laboratories, Nagoya, Japan) and anti-β-actin antibody (CoWin Biotech, Beijing, China). The secondary antibodies used are as follows: horseradish peroxidase-linked anti-rabbit and anti-mouse IgGs (CoWin Biotech, Beijing, China).

2.6. Antioxidative Assay. BY4741 yeast cells with the initial OD600 value of 0.1 were cultured in liquid glucose medium and treated with 0, 0.1, 0.3, or 1 μM CuB or 10 μM RES for 24 h. Afterward, 5 μL of yeast culture in each group with the same OD600 value was dropped onto glucose agar plates containing 9 mM H_2O_2. After 3 days, the growth of yeast was observed and photographed. Besides, further spots of 1/10, 1/100, and 1/1000 dilutions in each group were also dropped onto glucose agar plates containing 9 mM H_2O_2, and the growth was observed after 5 days.

Another method was performed to quantify the effect of CuB on the oxidative stress response of yeast. Similar to that in the former method, BY4741 yeast cells were treated with 0, 0.1, 0.3, or 1 μM CuB or 10 μM RES. 200 yeast cells from each group were spread onto glucose agar plates supplemented with or without 5 mM H_2O_2. The growth of yeast was observed after 2 days, and the number of microcolonies in each plate was counted. The survival rate was calculated as the ratio of the number of microcolonies in the presence of 5 mM H_2O_2 divided by the number of microcolonies in the absence of 5 mM H_2O_2.

2.7. ROS, MDA, and Sod Enzyme Assays. CuB- or RES-treated BY4741 yeast cells were cultured for 23 h in liquid glucose medium at 28°C. DCFH-DA (2′,7′-dichlorodihydrofluorescein diacetate, 1 μL, 10 mM) was added to 1 mL of the cells. The mixture was then incubated at 28°C in the dark with shaking for 1 h. The cells were quickly washed with PBS thrice in the dark, and the DCF (2′,7′-dichlorofluorescein) fluorescence intensity of 1×10^7 cells was recorded using the SpectraMax M3 multimode microplate reader (Molecular Devices Corporation, California, USA) under the excitation wavelength of 488 nm and emission wavelength of 525 nm.

BY4741 yeast cells were treated with CuB or RES in liquid glucose medium for 24 or 48 h at 28°C with the initial OD of 0.1. Yeast cells were collected through centrifugation and five cycles of ultrasonication (1 min for each time). Then, the cells were frozen for 5 min in liquid nitrogen, subsequently thawed for 2 min in a 37°C water bath, and sonicated for five cycles. The cell lysates were centrifuged, and the supernatant was removed for MDA quantification. MDA levels were quantified by using the MDA assay kit (Nanjing Jiancheng Bioengineering Institute, Nanjing, China) following the manufacturer's instructions.

BY4741 yeast cells were treated in a manner similar to that in MDA assay. Briefly, cells were treated with CuB or RES in the liquid glucose medium for 24 or 48 h at 28°C. Then, yeast cells were collected and subjected to five 1 min cycles of ultrasonication. Subsequently, the total super oxide dismutase (T-Sod) and Sod1 enzyme activities of the supernatant were tested using SOD Assay Kits (A001-1, A001-2) (Nanjing Jiancheng Bioengineering Institute, Nanjing, China) following the manufacturer's instructions.

2.8. Growth Curves of Yeast Cells with CuB. To test growth inhibition in liquid culture, the YPD medium containing 0, 1.56, 6.25, 25, or 50 μM CuB was used. Cultures of Y02458, *his3*Δ of BY4741 (*MATa*, *his3Δ1*, *leu2Δ0*, *met15Δ0*, *ura3Δ0*, and *YOR202w::KanMX4*) were treated with CuB and grown at 25°C for 25 h. Optical density from 0 to 25 hours was measured at 10 min intervals using an absorption spectrometer at 660 nm. The assay was repeated at least 2 times.

2.9. High-Dimensional Phenotypic Analysis. High-dimensional phenotypic analysis was conducted in accordance with a previous report [19]. Yeast cells were cultured in YPD medium with or without CuB, and cells in the logarithmic phase were fixed with 3.7% formaldehyde. Yeast cells, nuclear DNA, and actin were stained with 20 mg/mL fluorescein isothiocyanate-Con A, 4,6-diamidino-2-phenylindole, and rhodamine phalloidin, respectively. Morphological changes were observed through fluorescence microscopy. CalMorph was used to characterize each yeast cell through the quantification of 501 morphological parameters.

2.10. Fitness. To estimate fitness, we employed a previously published dataset of logarithmic strain growth rate coefficients for haploid nonessential gene deletion mutants grown on a basal medium (LSC basal) [20]. We used the p value calculated as the significance of lower fitness from the wild type of each strain based on one tail of the estimated probability distribution [20, 21] and calculated FDR as described previously [21].

2.11. Data Processing. Coefficient of variation values were highly dependent on the mean values in a nonlinear manner [22] and therefore were not suited for normalization. Instead, we defined noise values as the residuals between observed and predicted values, as described previously [21, 23].

2.12. Detection of Specific Morphologically Abnormal Mutants. The probability distribution of the wild-type replicates for each trait of the 501 parameters was estimated using maximum likelihood estimation with one of four probability density functions (gamma, beta, Gaussian, and beta-binomial distribution), as described previously [24]. We calculated the p value of every nonessential deletion mutant as morphological abnormality from the wild type for each trait (two-sided one-sample test) and identified the lowest p value among 501 traits as the "specific morphological abnormality," as described previously [21]. Maximum likelihood estimation and calculation of the p value were performed using the gamlss function in R software's (http://www.r-project.org) gamlss package [25]. The FDR, a rate of type I errors in the rejected null hypothesis due to multiple comparisons, was calculated using the qvalue R function in the qvalue package [26]. We plotted specific morphologically abnormal mutants as circles filled with green.

2.13. Plot of Single-Gene Deletion Strains with Increased Lifespan. To plot single-gene deletion strains with increased lifespan, we employed a previously published dataset of replicative lifespan for nonessential gene deletion mutants [27].

2.14. Statistical Analysis. All statistical analyses were performed using GraphPad Prism 5 (GraphPad Software Inc.). Survival analysis was used for chronological lifespan assay. Analysis of variance was used to determine the significant differences among groups in all experiments, followed by two-tailed multiple t-tests with Bonferroni correction. A p value of less than 0.05 was considered statistically significant.

3. Results

3.1. CuB Has Significant Antiaging Effects. We have previously isolated a number of antiaging substances, such as cholesterol and parishin, from natural products on the basis of the K6001 lifespan assay [4, 5]. In the present study, we again used the K6001 lifespan assay to screen for antiaging compounds from a compound library and identified the active compound CuB (Figure 1(a)) as a potential antiaging compound. Subsequently, we performed chronological lifespan assay to confirm antiaging effects of CuB. As shown in Figure 1(b) and Table 2, the average replicative lifespan of each treatment group was as follows: 6.95 ± 0.34 generations for the control group, 9.03 ± 0.47 generations for the group treated with 10 μM RES, 8.90 ± 0.55 generations for the group treated with 0.1 μM CuB, 8.95 ± 0.51 generations for the group treated with 0.3 μM CuB, and 9.60 ± 0.49 generations for the group treated with 1 μM CuB. These results indicate that treatment with 0.1, 0.3, and 1 μM CuB significantly prolongs the replicative lifespan of K6001 ($p < 0.05$, $p < 0.05$, and $p < 0.01$, respectively). As shown in Figure 1(c), CuB increased the survival rate of yeast ($p < 0.001$, $p < 0.001$, and $p < 0.001$, respectively). CuB significantly increased the days at which viability is equal to 0 of yeast from 15 ± 1.15 days to 17 ± 1.15, 21 ± 1.15, and 23.67 ± 0.67 days, respectively. These results suggest that CuB has significant antiaging effects on yeast cells.

3.2. CuB Regulates Autophagy in Yeast. Autophagy is a degenerative process that degrades cellular components for recycling into amino acids and other metabolites. It has essential roles in cell growth, differentiation, development, and aging [8]. Hence, we investigated the effect of CuB on autophagy. *ATG2* and *ATG32* are two of the most important genes that mediate autophagy in yeast; we first explored *ATG2* and *ATG32* gene expression in CuB-treated yeast. As shown in Figure 2(a), CuB significantly enhanced *ATG32* gene expression but did not significantly affect *ATG2* gene expression.

Furthermore, we constructed *atg2* and *atg32* mutants with K6001 background to do replicative lifespan assay. The changes of the lifespan are shown in Figures 2(b) and 2(c) and Table 2. The significant decrease in replicative lifespan of *atg2* and *atg32* mutants was not observed compared with that of K6001. After the treatment of CuB, the replicative lifespan of *atg2* and *atg32* mutants was also not affected. These results suggested that Atg2 and Atg32 did not take an important role in the replicative lifespan of yeast. However, they were required in the replicative lifespan extension of CuB.

To test whether CuB induces autophagy, we used the YOM38 strain, which expresses GFP-Atg8 at a physiological level and monitored the level of GFP upon treatment with CuB under fluorescent microscopy. The fluorescent images are displayed in Figure 2(d), and the statistic result is shown in Figure 2(e). CuB significantly enhanced the percentage of cells with green fluorescence at a dose of 0.3 μM as does RES. In order to investigate whether the GFP signal came from autophagy or autofluorescence of yeast, the YOM36 yeast strain was also treated with RES or CuB. As shown in Figure 2(d), YOM36 expressed no green fluorescence. Besides, western blot analysis showed generation of free GFP, which is released into the vacuole during the autophagy flux. CuB increased the amount of released GFP in yeast in a time course manner, and 0.3 μM CuB significantly increased the amount of free GFP (Figures 2(f) and 2(g)). These results confirm that CuB induces autophagy.

Furthermore, we performed chronological lifespan measurements using *atg2* and *atg32* mutants derived from a phototrophic derivative of BY4741 (YOM36) (Figure 2(h)). The results showed that the survival rate of *atg2* and *atg32* mutants significantly decreased ($p < 0.05$, $p < 0.01$) compared to YOM36 yeast strain. In addition, CuB at 1 μM increased the survival rate of YOM36 yeast during the whole assay ($p < 0.001$), but failed to prolong the chronological lifespans of *atg2* and *atg32* mutants. The days at which viability is equal to 0 of *atg2* and *atg32* mutants were 14 ± 1 and 16 ± 1 days, respectively, and were shorter than those of the wild-type yeast (17 ± 0 days). In addition, CuB extended the days at which viability is equal to 0 of the wild-type yeast from 17 ± 0 days to 19 ± 2 days. However, the days at which viability is equal to 0 of the *atg2* and *atg32* mutants in CuB-treated groups were 13 ± 2 and 16 ± 1 days, respectively, indicating that CuB failed to prolong the chronological

Table 2: Replicative lifespan of K6001 and its mutants.

Figures	Yeast strains	Treatment (μM)	Replicative lifespan (generations)
Figure 1(b)	K6001	Control	6.95 ± 0.34
		RES-10	9.03 ± 0.47*
		CuB-0.1	8.90 ± 0.55*
		CuB-0.3	8.95 ± 0.51*
		CuB-1.0	9.60±0.49**
Figures 2(b) and 2(c)	K6001	Control	7.05 ± 0.35
		RES-10	9.05 ± 0.55*
		CuB-1.0	9.65±0.61**
	atg2 mutant of K6001	Control	6.95 ± 0.43
		RES-10	7.30 ± 0.40
		CuB-1.0	7.18 ± 0.45
	atg32 mutant of K6001	Control	6.73 ± 0.42
		RES-10	7.40 ± 0.44
		CuB-1.0	7.10 ± 0.47
Figure 4	K6001	Control	6.95 ± 0.34
		RES-10	9.03 ± 0.47*
		CuB-1.0	9.60±0.49**
	sod1 mutant of K6001	Control	6.93 ± 0.43
		RES-10	7.73 ± 0.39
		CuB-1.0	7.45 ± 0.46
	sod2 mutant of K6001	Control	7.35 ± 0.37
		RES-10	6.85 ± 0.47
		CuB-1.0	7.10 ± 0.33
	uth1 mutant of K6001	Control	9.95 ± 0.63
		RES-10	9.30 ± 0.59
		CuB-1.0	9.90 ± 0.69
	skn7 mutant of K6001	Control	8.43 ± 0.58
		RES-10	9.13 ± 0.52
		CuB-1.0	9.30 ± 0.60

Replicative lifespan was shown as average ± SEM; * and ** represent significant differences compared to the corresponding control groups ($p < 0.05$, $p < 0.01$.).

lifespans of *atg2* and *atg32* mutants. These results indicate that CuB exerts its activity through regulating autophagy, which requires *ATG2* and *ATG32*.

3.3. CuB Improves the Survival Rate of Yeast under Oxidative Conditions. Oxidative stress is a major factor of aging and age-related diseases, and high levels of oxidative stress result in DNA damage, lipid peroxidation, and protein oxidation [28]. Therefore, we performed antioxidative experiments to determine whether antioxidative activity is involved in the antiaging effect of CuB. We used two methods to investigate the effect of CuB on the growth of yeast with 5 μL culture or 1/10, 1/100, and 1/1000 dilutions of each group under oxidative stress at 9 mM H_2O_2. The growth of yeast in both conditions (Figure 3(a)) was significantly improved, respectively. We also examined the survival rate of yeast under oxidative stress and found that the survival rate was 38.09% ± 1.39 in the control group, 42.19% ± 0.87 in the RES group, 47.74% ± 2.03 in the 0.1 μM CuB group ($p < 0.01$), 53.73% ± 0.73 in the 0.3 μM CuB group ($p < 0.001$), and 55.01% ± 1.35 in the 1 μM CuB group ($p < 0.001$) (Figure 3(b)). These results indicate that the regulation of antioxidative activity has an important role in the antiaging effect of CuB.

3.4. CuB Decreases ROS Accumulation and MDA Production and Increases Sod Activity. ROS are by-products of aerobic respiration and various metabolic processes. They cause secondary reactions, such as lipid peroxidation and protein oxidation [29]. MDA, a biomarker of lipid peroxidation in

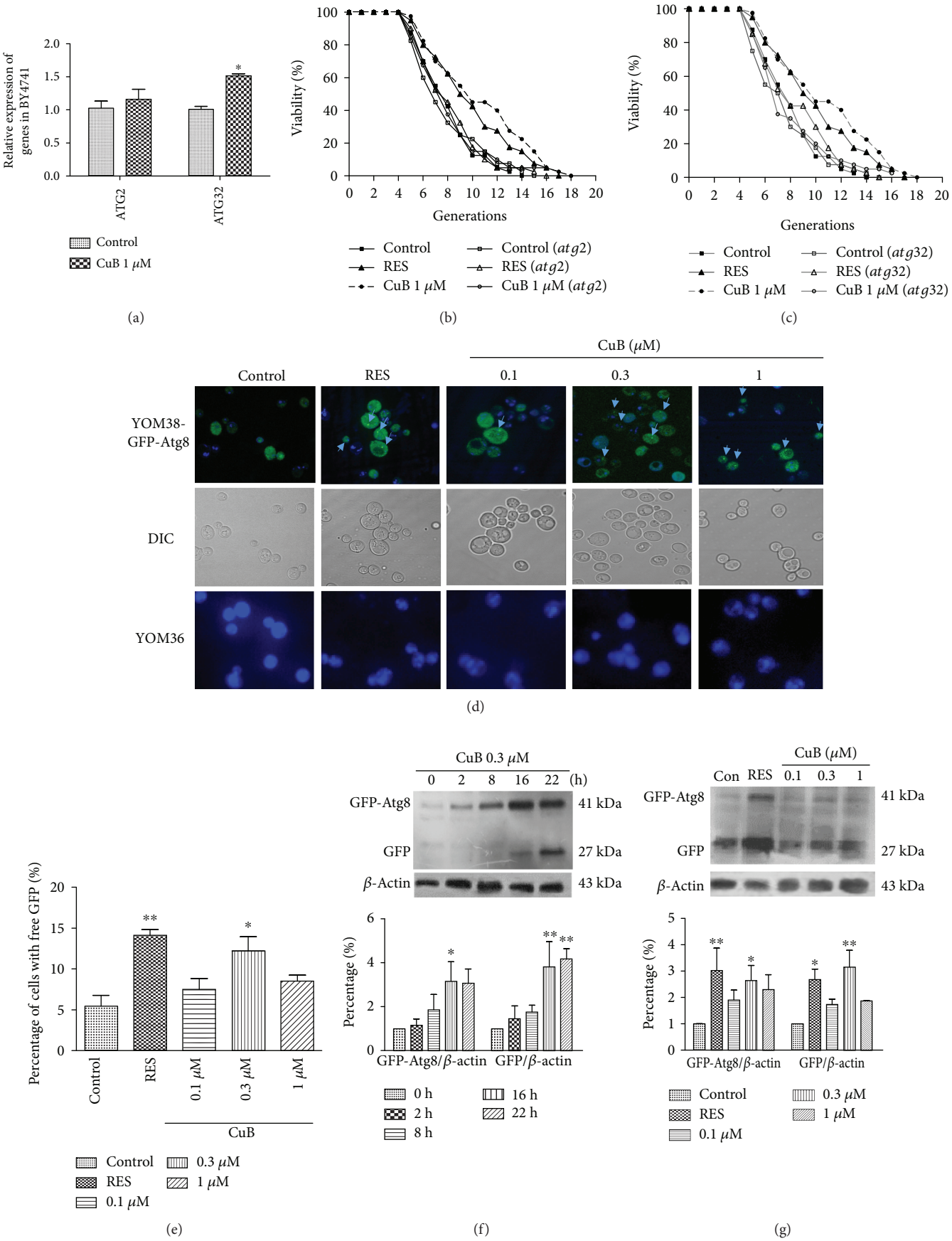

Figure 2: Continued.

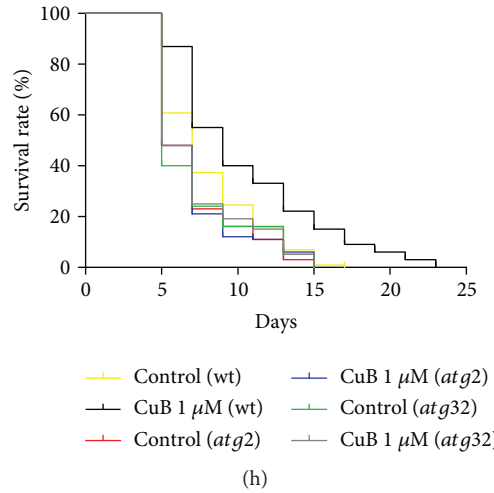

Figure 2: Effect of CuB on autophagy in yeast. (a) Effect of CuB on *ATG2* and *ATG32* gene expression after 12 h of treatment. (b, c) Effect of CuB on the replicative lifespan of K6001 and *atg2* (b) and *atg32* (c) mutants with K6001 background. (d) Fluorescent images of YOM38 yeast contained plasmid pR316-GFP-ATG8 and YOM36 yeast after treatment of RES or different doses of CuB in the SD medium and DAPI staining observed with a two-photon confocal fluorescent microscope. The upper line and middle line showed merged and DIC images of YOM38 yeast cells containing plasmid pR316-GFP-ATG8, respectively. The line below showed fluorescent images of YOM36. (e) Effect of CuB on the percentage of YOM38 cells containing plasmid pR316-GFP-ATG8 with free GFP. Three pictures containing more than 60 cells in each group were used for statistical analysis. (f) Western blot analysis of GFP-Atg8 and free GFP in yeast after shifting to the SD medium containing 0.3 μM CuB for different times. (g) Western blot analysis of GFP-Atg8 and free GFP in yeast after treatment with RES or CuB for 22 h in the SD medium. (h) Effect of CuB on the chronological lifespan of wild-type YOM36 and *atg2* and *atg32* mutants with YOM36 background. $*$ and $**$ indicate significant difference between treatment groups and the corresponding control group ($p < 0.05$, $p < 0.01$).

living cells, has cytotoxic effects [30]. Thus, we tested the change in ROS accumulation and MDA levels in CuB-treated yeast. ROS accumulation in yeast notably decreased after 48 h of incubation with 0.1, 0.3, and 1 μM CuB (Figure 3(c)). Similarly, significant decreases were observed in MDA production by yeast. MDA production decreased after 24 h of incubation with 0.3 μM CuB and 48 h of incubation with 0.1, 0.3, and 1 μM CuB (Figure 3(d)). These results suggested that CuB could significantly inhibit the production of ROS and MDA in yeast.

Sod is a component of antioxidative defense systems that can scavenge ROS and other free radicals in cells. Yeast has two kinds of Sod, Sod1 and Sod2. Sod1 is a stable Sod that localizes in the cytoplasm, and mitochondrial Sod2 is more sensitive to environmental factors. Therefore, we evaluated total-Sod and Sod1 activity in yeast incubated with CuB for 24 or 48 h. As shown in Figures 3(e) and 3(f), T-Sod and Sod1 enzyme activity significantly improved after 24 and 48 h of treatment with 0.3 and 1 μM CuB. Besides, Sod1 activity also improved after 24 h of treatment with 0.1 μM CuB. The results show that CuB can significantly decrease ROS and MDA levels and increase T-Sod and Sod1 enzyme activity in yeast at 0.3 and 1 μM CuB. These results suggest that CuB exerts its antiaging effect by regulating antioxidative activity.

3.5. CuB Does Not Affect the Replicative Lifespans of the Sod1, Sod2, Uth1, and Skn7 Mutants of K6001 Yeast. The results shown in Figure 3 suggest that antioxidative activity is involved in the antiaging activity of CuB and that *SOD1* and *SOD2* participate in oxidative stress responses. Therefore, we used *sod1* and *sod2* mutants with the K6001 background to investigate the involvement of *SOD1* and *SOD2* genes in the antiaging effect of CuB. As shown in Figures 4(a) and 4(b) and Table 2, the average replicative lifespan of the wild-type K6001 yeast was 6.95 ± 0.34 generations under the control treatment, 9.03 ± 0.47 generations under the RES treatment, and 9.60 ± 0.49 generations under the 1 μM CuB treatment. The average replicative lifespan of the *sod1* mutant was 6.93 ± 0.43 generations under the control treatment, 7.73 ± 0.39 generations under the RES treatment, and 7.45 ± 0.46 generations under the 1 μM CuB treatment. The average replicative lifespan of the *sod2* mutant was 7.35 ± 0.37 generations under the control treatment, 6.85 ± 0.47 generations under the RES treatment, and 7.10 ± 0.33 generations under the 1 μM CuB treatment. These results show that the replicative lifespans of the *sod1* and *sod2* mutants are unaffected by RES or CuB treatment.

UTH1 is an aging gene that is involved in the regulation of programmed cell death in yeast [31]. Skn7 is the transcriptional activator of *UTH1* and is associated with protection against oxidative stress [32]. In our previous study, *UTH1* gene expression in *skn7* mutant was significantly decreased [33]. To explore whether *UTH1* and *SKN7* genes are involved in the lifespan-extending effect of CuB, we measured the replicative lifespans of *uth1* and *skn7* mutants after CuB treatment. The average replicative lifespan of the *uth1*

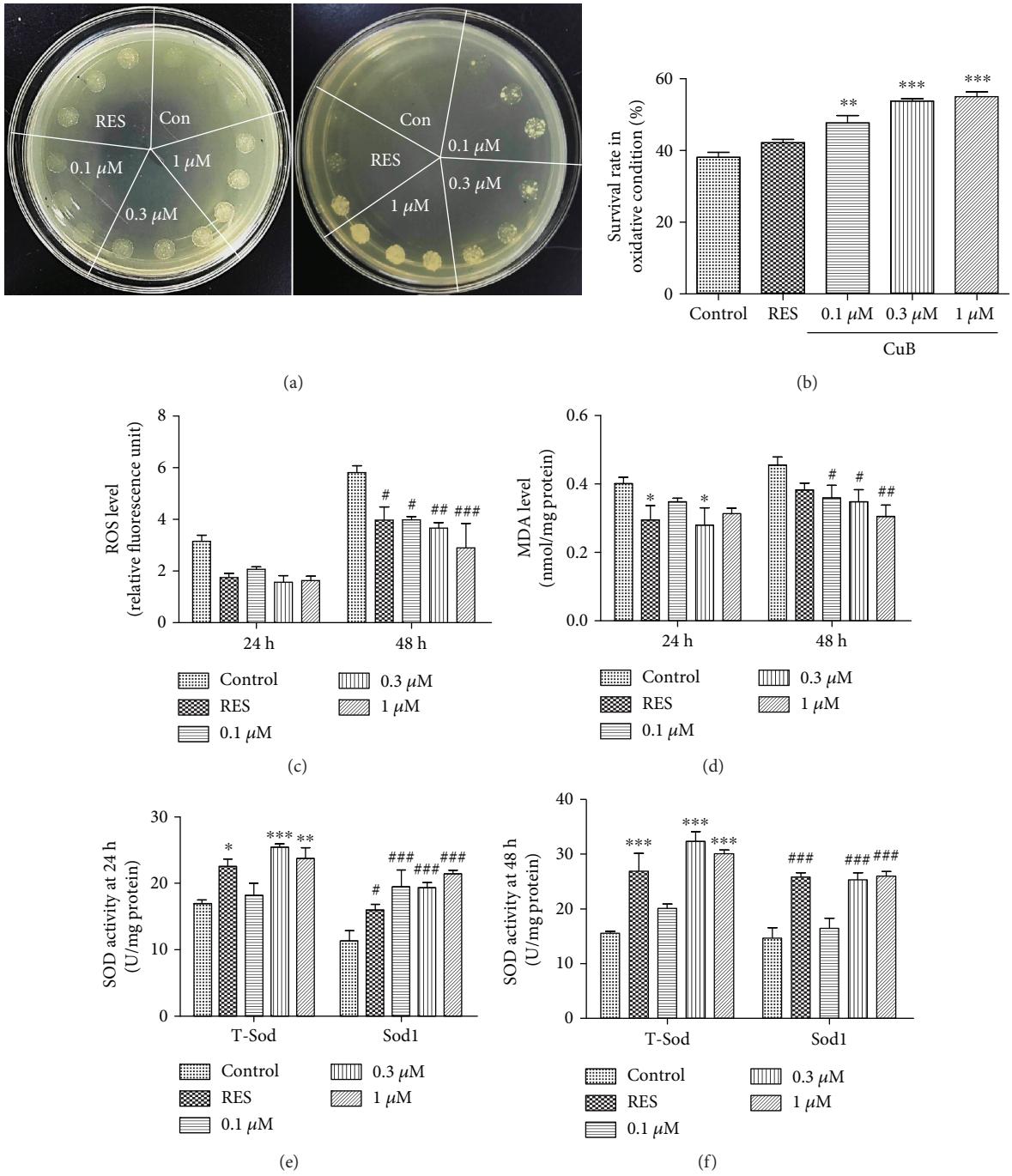

Figure 3: Effect of CuB on oxidative stress in yeast. (a) Effect of CuB on yeast growth with 5 μL yeast culture and 1/10, 1/100, and 1/1000 dilutions under oxidative conditions simulated with 9 mM H_2O_2. (b) Effect of CuB on the survival rate of yeast under oxidative conditions simulated with 5 mM H_2O_2. ** and *** represent significant differences compared to the control group ($p < 0.01$ and $p < 0.001$, respectively). (c, d, e, f) Effect of CuB on ROS level, MDA accumulation, T-Sod, and Sod1 enzyme activity at 24 or 48 h. *, **, *** and #, ##, ### indicate significant differences from the corresponding control ($p < 0.05$, $p < 0.01$, and $p < 0.001$, respectively).

mutant was 9.95 ± 0.63 generations under the control treatment, 9.30 ± 0.59 generations under the RES treatment, and 9.90 ± 0.69 generations under the 1 μM CuB treatment (Figure 4(c) and Table 2). The average replicative lifespan of the *skn7* mutant was 8.43 ± 0.58 generations under the control treatment, 9.13 ± 0.52 generations under the RES treatment, and 9.30 ± 0.60 generations under the 1 μM CuB treatment (Figure 4(d) and Table 2). The replicative lifespans of the two mutants after CuB treatment did not significantly change. As the average replicative lifespan of the wild-type K6001 yeast was 6.95 ± 0.34 generations under the control treatment, the replicative lifespan of the *uth1* mutant was

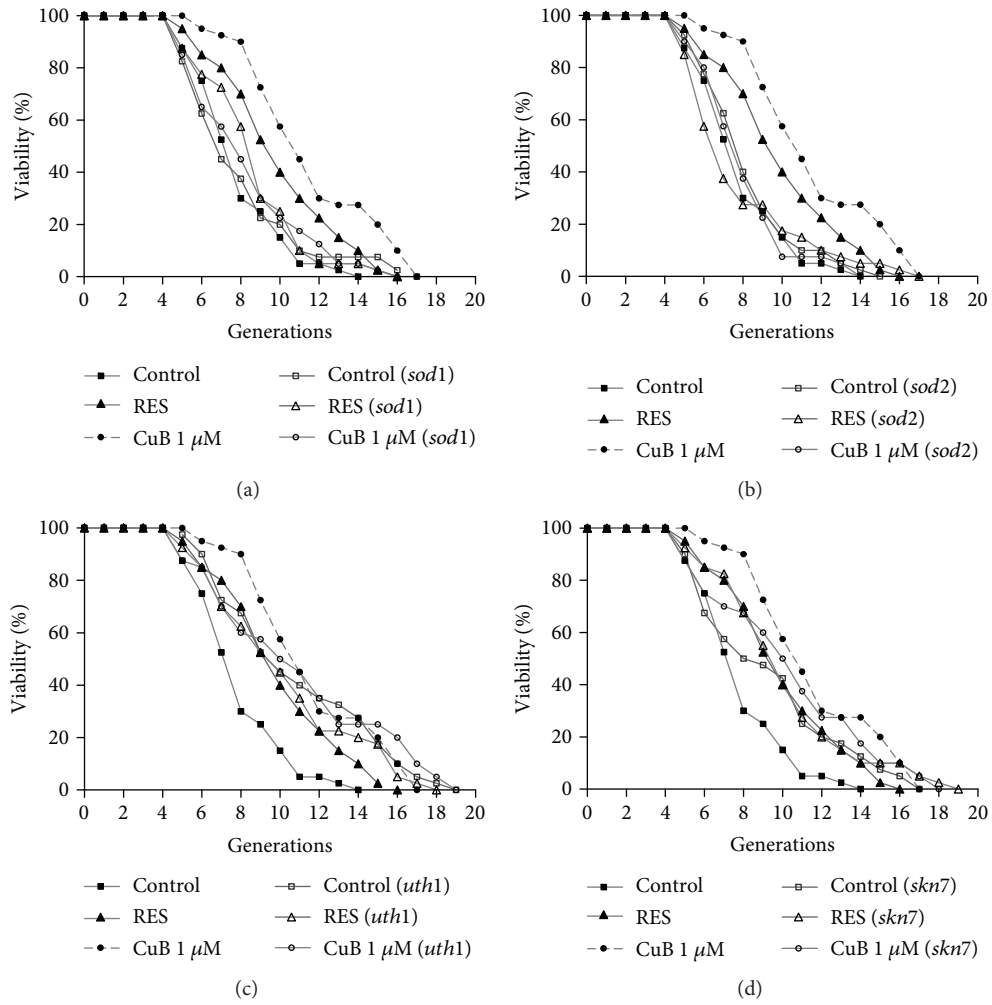

Figure 4: Effect of CuB on the replicative lifespans of *sod1* (a), *sod2* (b), *uth1* (c), and *skn7* (d) mutants with K6001 background. The procedure for the replicative lifespan assay was the same as that for the K6001 lifespan assay.

longer than that of the wild-type K6001. This result was consistent with other reports that deletion of *UTH1* increased yeast lifespan [34, 35]. These results indicate that *SOD1*, *SOD2*, *UTH1*, and *SKN7* are involved in the antiaging activity of CuB.

3.6. CuB Does Not Affect the Growth Nor Morphology of Yeast Cells. Many active compounds have been investigated in yeast with growth assay and morphological examination to understand their bioactivity. This is because both cell growth and morphology reflect numerous essential cellular processes, such as DNA replication, transcription, translation, vesicular transport, organelle assembly, and cell cycle regulation. Compared with the cells treated with solvent only (1% EtOH), treatment with 1.56 μM to 50 μM CuB failed to inhibit cell growth (Figure 5(a)). Since treatment with 0.1, 0.3, or 1 μM CuB prolongs lifespan, cell growth is less affected by this drug. Examination of yeast morphology after fluorescent staining of the cell wall, actin, and nuclear DNA revealed that treatment with 10 μM CuB did not cause obvious cell morphological changes (Figure 5(b)). After the fluorescent image pictures were quantified with a high-throughput, processing system CalMorph [19], we also statistically analyzed dose-dependent morphological changes with the Jonckheere-Terpstra test [36]. None of the 501 morphological parameters measured by CalMorph exhibited significant dose-dependent changes with FDR of 5%, confirming that CuB-treated cells did not change morphology significantly. These results suggested that CuB neither inhibits cell growth nor affects yeast morphology.

3.7. Potential CuB Targets. Characterization of nonessential gene deletion mutants in terms of cell growth and morphology can be used to classify genes into four groups: genes not responsible for growth and morphology (group I, 1137 genes), genes only important for morphology (group II, 2294 genes), genes required for both growth and morphology (group III, 997 genes), and genes only required for growth (group IV, 203 genes) (Figure 5(c)) [21]. We attempted to use this information for prediction of the drug target by assuming that inhibition of the gene product by the drug

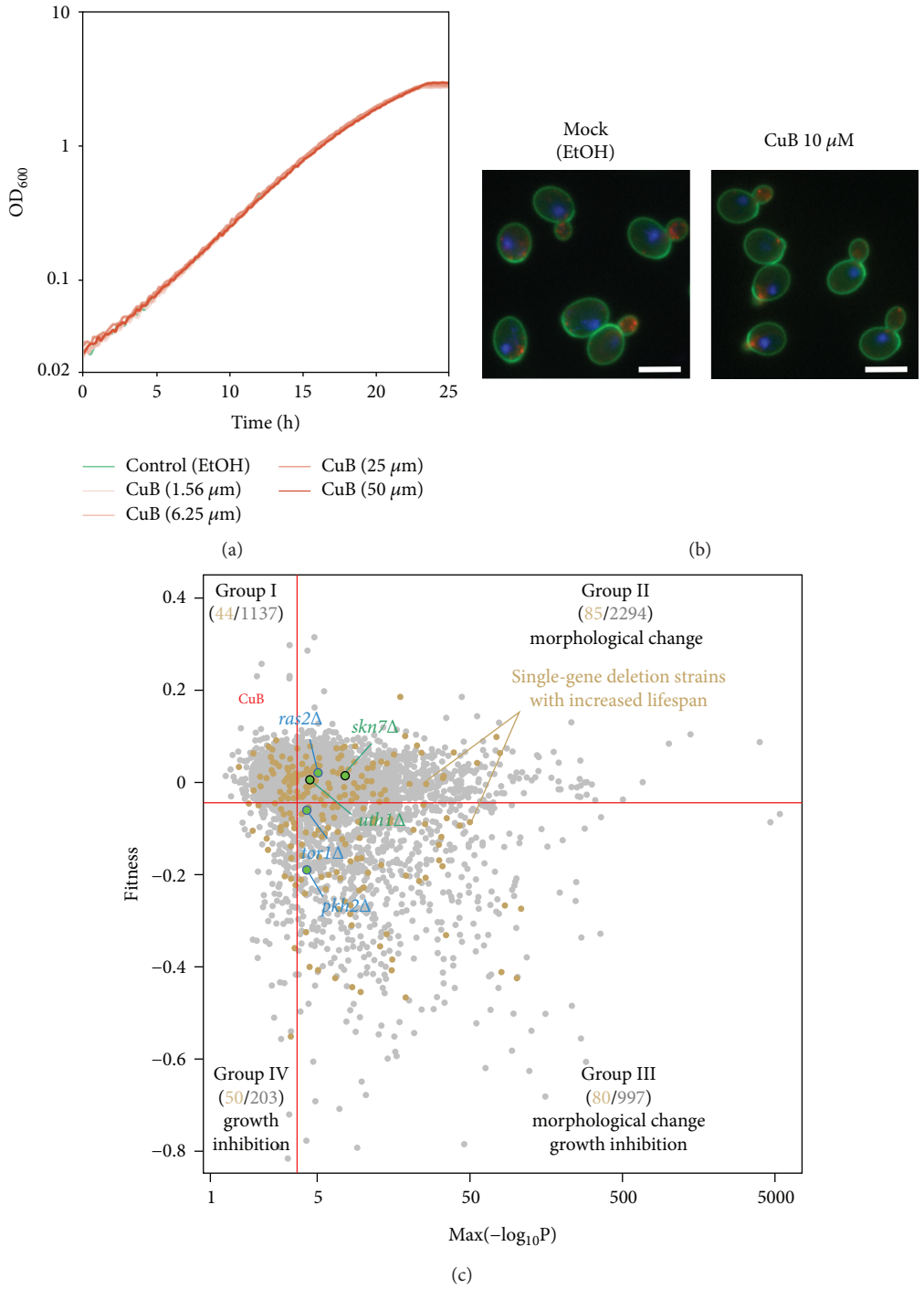

Figure 5: CuB neither inhibits cell growth nor causes morphological changes. (a) The growth curve of *Saccharomyces cerevisiae* in the presence and absence of CuB was plotted. The assay was repeated at least twice. (b) Images of cells treated with control (1% EtOH) or CuB (10 μM). The fluorescent dyes fluorescein isothiocyanate-Con A, 4,6-diamidino-2-phenylindole, and rhodamine-phalloidin were used to stain the cell wall, nuclear DNA, and actin, respectively. Scale bar, 5 μm. (c) Scatter plot of mutants with nonessential gene deletions in terms of specific morphological abnormality (x-axis) and growth rate (y-axis). The horizontal and vertical red lines indicate the false discovery rate of 0.01 for growth rate and morphology, respectively. The number shown in each area indicates the number of mutants categorized on the basis of cell growth and morphology (single-gene deletion strains with increased lifespan/mutants categorized on the basis of cell growth and/or morphology).

is equivalent to the functional defect by gene deletion. Since CuB neither affects growth nor morphology, CuB likely inhibits the gene function belonging to group I (Figure 5(c)). Our genetic evidence suggested that the aging-related genes, *UTH1* and *SKN7*, participate in antiaging effect of CuB. However, its interaction is likely indirect,

Table 3: The targets list of CuB predicted by CalMorph.

ORF	Gene	Description
YBL052C	SAS3	Something about silencing
YBR007C	DSF2	Deletion suppressor of mptfive/puffive mutation
YBR034C	HMT1	HnRNP methyl transferase
YBR042C	CST26	Chromosome stability
YDL093W	PMT5	Protein O-mannosyl transferase
YDL095W	PMT1	Protein O-mannosyl transferase
YDR006C	SOK1	Suppressor of kinase
YDR099W	BMH2	Brain modulosignalin homolog
YDR110W	FOB1	Fork blocking less
YDR313C	PIB1	Phosphatidylinositol(3)-phosphate binding
YDR486C	VPS60	Vacuolar protein sorting
YEL020C	PXP1	Peroxisomal protein
YER164W	CHD1	Chromatin organization modifier helicase and DNA-binding domains
YFR015C	GSY1	Glycogen synthase
YFR040W	SAP155	Sit4-associated protein
YGL006W	PMC1	Plasma membrane calcium
YGL079W	KXD1	KxDL homolog
YGL200C	EMP24	Endomembrane protein
YGR254W	ENO1	Enolase
YHL002W	HSE1	Has symptoms of class E mutants; resembles Hbp, STAM, and EAST
YIL002C	INP51	Inositol polyphosphate 5-phosphatase
YJL013C	MAD3	Mitotic arrest-deficient
YJL098W	SAP185	Sit4-associated protein
YKL098W	MTC2	Maintenance of telomere capping
YLR176C	RFX1	Regulatory factor X
YMR058W	FET3	Ferrous transport
YMR126C	DLT1	Defect at low temperature
YMR127C	SAS2	Something about silencing
YMR221C	FMP42	Found in mitochondrial proteome
YMR251W	GTO3	Glutathione transferase omega-like
YMR251W-A	HOR7	Hyperosmolarity-responsive
YNL142W	MEP2	Mourning's ends part II
YOL071W	SDH5	Succinate dehydrogenase
YOR311C	DGK1	Diacylglycerol kinase
YPR111W	DBF20	Dumbbell forming
YPL177C	CUP9	Homeodomain-containing transcriptional repressor
YBR054W	YRO2	Protein with a putative role in response to acid stress
YBR238C	YBR238C	Mitochondrial membrane protein
YIL089W	YIL089W	Protein of unknown function found in the ER and vacuole lumen
YCR101C	YCR101C	Putative protein of unknown function
YNL034W	YNL034W	Putative protein of unknown function
YDL172C	YDL172C	Dubious open reading frame
YDR048C	YDR048C	Dubious open reading frame
YGL165C	YGL165C	Dubious open reading frame

because *UTH1* and *SKN7* belong to group II (Figure 5(c)). We also plotted gene deletion mutants with increased lifespan in Figure 5(c) [27]. Because group I contains 44 aging-related genes, we propose that CuB could target one of these 44 genes listed in Table 3. However, it cannot be excluded that the inhibition of the target by CuB is only partial, and that other genes, including essential ones, could be the main target of the drug.

4. Discussion

In China, CuB has been used to treat hepatitis for many years [37]. CuB also has potent anticancer, antioxidative, and anti-inflammatory activities [13, 14]. In the present study, we performed replicative lifespan assays to screen for antiaging substances from compounds library and used chronological lifespan assay to confirm the activity. We identified CuB as a potential antiaging compound. The chronological and replicative lifespan results shown in Figures 1(b) and 1(c) imply that CuB exerts significant antiaging effects in a dose-dependent manner.

We previously applied the replicative lifespan assay to evaluate the antiaging activities of other compounds. However, we found that this assay exhibits deficiencies that may affect the accuracy of its results. For example, random selection and subjective factors affect the quantification of daughter cells in the replicative lifespan assay. Therefore, to increase the accuracy of the bioassay results in the present study, we utilized the chronological lifespan assay to evaluate the antiaging activity of CuB. Yeasts have replicative and chronological lifespans. Replicative aging in yeast resembles the aging of mitotic cells in higher organisms, and chronological aging is similar to the aging of nondividing cells in higher eukaryotes [38]. The results of replicative and chronological lifespan assays suggest that CuB affects both the replicative and chronological lifespans of yeast.

In the present study, we focused on autophagy, oxidative stress, and longevity-related genes to investigate the mechanism of action of CuB. Autophagy levels decrease with age, and autophagy activation ameliorates age-related symptoms and has potential functions against aging [8]. Autophagy-related (*ATG*) or vacuolar protein-sorting genes encode some of the proteins that mediate autophagy [6]. Autophagy consists of nonselective and selective autophagy. Atg2 participates both nonselective and selective pathways of autophagy, including macroautophagy and pexophagy [39]; Atg32 is only essential for mitophagy [40]. Thus, we analyzed *ATG2* and *ATG32* expressions and performed replicative lifespan assays with *atg2* and *atg32* mutants with K6001 background and K6001 yeast and chronological lifespan assays with *atg2* and *atg32* mutants and YOM36 yeast to investigate the effect of autophagy on the antiaging activity of CuB. The results of gene expression, replicative lifespan, and chronological lifespan shown in Figures 2(a)–2(c) and 2(h) suggest that *ATG2* and *ATG32* genes have essential roles in the antiaging activity of CuB. Besides, enhanced mitophagy contributes to the extension of longevity by CuB.

Atg8 is an important component for autophagic machinery and participates in the whole process of autophagy, and it is a biomarker of autophagy in yeast [41]. Therefore, we investigated the effect of CuB on autophagy through detection of Atg8 with GFP-ATG8 fluorescent imaging and western blot analysis. Because RES can induce autophagy at 100 μM in mammalian cultured cells [10], we used it as a positive control in experiments for detection of autophagy in the present study. The changes of GFP in yeast in Figures 2(d) and 2(e) and western blot results in Figures 2(f) and 2(g) suggest that CuB significantly induces the autophagy of yeast.

We also investigated the effect of antioxidative activity on the antiaging function of CuB. The changes in the survival rate and Sod, ROS, and MDA levels of yeast shown in Figure 3 demonstrate that CuB exerts its antiaging effect in yeast by regulating antioxidative activity.

Longevity-related and aging-related genes have important roles in the regulation of aging and longevity. *UTH1* is a yeast aging gene and takes part in oxidative stress [42]. *SKN7* is the transcriptional activator of *UTH1* and is related with protection against oxidative stress [32]. *SOD1* and *SOD2* genes encode Sod1 and Sod2 enzymes, respectively, which are important for redox homeostasis in cells. The replicative lifespan assay results of yeast mutants are shown in Figure 4 and Table 2 and reveal that *UTH1*, *SKN7*, *SOD1*, and *SOD2* genes are required in the lifespan-extension activity of CuB. In addition, the replicative lifespan of the *uth1* mutant is longer than that of the wild type. This result is consistent with the result of a previous study [35].

To predict the target of CuB, we used CalMorph to analyze the morphological changes exhibited by CuB-treated yeast cells. CalMorph is the image-processing software that has been used to analyze the morphology of 4718 nonessential gene mutants in more than 200 yeast strains. It can effectively identify compound targets [19]. The growth curve and morphological changes of cells treated with CuB are shown in Figure 5 and provide an important clue for the identity of the target genes of CuB. CuB does not cause growth inhibition nor cell morphological changes, and therefore, it could target one of the genes that are not involved in cell growth or morphology. After plotting mutations with long lifespan, we would pinpoint the possible targets of CuB among the 44 genes (Table 3). The results shown in Figure 5(c) suggest that CuB does not directly inhibit the genes mentioned in this study and that CuB might extend the lifespan of yeast by inhibiting upstream of aging-related genes mentioned in this study or by even activating some genes, such as *SIR2*, *SOD1*, and *SOD2*. If CuB activates some genes; activation of the CuB target would not cause growth inhibition or cell morphological changes. In this sense, the possible targets of CuB are not associated with cell growth or cell morphology. Nevertheless, additional efforts are needed to definitively identify the targets of CuB.

5. Conclusions

Overall, we found that CuB significantly prolongs the replicative and chronological lifespans of yeast in a dose-dependent manner. CuB exerts its antiaging effect by regulating autophagy and antioxidative activity. Moreover, the target identification of CuB suggests that 44 proteins that are not associated with cell growth or morphology are potential targets of CuB. However, the specific target of CuB requires further study, such as bioassay on these 44 proteins. Furthermore, given that CuB is already used to treat hepatitis cases in China, it may be developed as an antiaging drug.

Data Availability

All the figures and table used to support the findings of this study are included within the article.

Conflicts of Interest

The authors declare that there are no conflicts of interest regarding the publication of this paper.

Acknowledgments

This work was financially supported by the National Key R&D Program of China (Grant No. 2017YFE0117200), and the National Natural Science Foundation of China (Grant Nos. 21661140001, 21877098, and 21572204). We greatly thank Michael Breitenbach (Salzburg University, Austria) for gifts of the K6001 yeast strain.

Supplementary Materials

Supplementary Fig. 1. The western blot analysis of GFP-ATG8 and free GFP of yeast after administrating CuB at different times and doses. Each experiment was independently repeated three times. *(Supplementary Materials)*

References

[1] M. A. Deprez, E. Eskes, J. Winderickx, and T. Wilms, "The TORC1-Sch9 pathway as a crucial mediator of chronological lifespan in the yeast *Saccharomyces cerevisiae*," *FEMS Yeast Research*, vol. 18, no. 5, article foy048, 2018.

[2] M. Polymenis and B. K. Kennedy, "Chronological and replicative lifespan in yeast: do they meet in the middle?," *Cell Cycle*, vol. 11, no. 19, pp. 3531-3532, 2012.

[3] S. Jarolim, J. Millen, G. Heeren, P. Laun, D. Goldfarb, and M. Breitenbach, "A novel assay for replicative lifespan in *Saccharomyces cerevisiae*," *FEMS Yeast Research*, vol. 5, no. 2, pp. 169–177, 2004.

[4] Y. Sun, Y. Lin, X. Cao, L. Xiang, and J. Qi, "Sterols from Mytilidae show anti-aging and neuroprotective effects via anti-oxidative activity," *International Journal of Molecular Sciences*, vol. 15, no. 12, pp. 21660–21673, 2014.

[5] Y. Lin, Y. Sun, Y. Weng, A. Matsuura, L. Xiang, and J. Qi, "Parishin from *Gastrodia elata* extends the lifespan of yeast via regulation of Sir2/Uth1/TOR signaling pathway," *Oxidative Medicine and Cellular Longevity*, vol. 2016, Article ID 4074690, 11 pages, 2016.

[6] J. K. Tyler and J. E. Johnson, "The role of autophagy in the regulation of yeast life span," *Annals of the New York Academy of Sciences*, vol. 1418, no. 1, pp. 31–43, 2018.

[7] A. Matsui, Y. Kamada, and A. Matsuura, "The role of autophagy in genome stability through suppression of abnormal mitosis under starvation," *PLOS Genetics*, vol. 9, no. 1, article e1003245, 2013.

[8] D. C. Rubinsztein, G. Mariño, and G. Kroemer, "Autophagy and aging," *Cell*, vol. 146, no. 5, pp. 682–695, 2011.

[9] I. Bjedov, J. M. Toivonen, F. Kerr et al., "Mechanisms of life span extension by rapamycin in the fruit fly *Drosophila melanogaster*," *Cell Metabolism*, vol. 11, no. 1, pp. 35–46, 2010.

[10] E. Morselli, G. Mariño, M. V. Bennetzen et al., "Spermidine and resveratrol induce autophagy by distinct pathways converging on the acetylproteome," *Journal of Cell Biology*, vol. 192, no. 4, pp. 615–629, 2011.

[11] D. Harman, "Aging: a theory based on free radical and radiation chemistry," *Journal of Gerontology*, vol. 11, no. 3, pp. 298–300, 1956.

[12] G. Farrugia and R. Balzan, "Oxidative stress and programmed cell death in yeast," *Frontiers in Oncology*, vol. 2, p. 64, 2012.

[13] Y. Cai, X. Fang, C. He et al., "Cucurbitacins: a systematic review of the phytochemistry and anticancer activity," *The American Journal of Chinese Medicine*, vol. 43, no. 7, pp. 1331–1350, 2015.

[14] T. Tannin-Spitz, M. Bergman, and S. Grossman, "Cucurbitacin glucosides: Antioxidant and free-radical scavenging activities," *Biochemical and Biophysical Research Communications*, vol. 364, no. 1, pp. 181–186, 2007.

[15] K. T. Chan, K. Li, S. L. Liu, K. H. Chu, M. Toh, and W. D. Xie, "Cucurbitacin B inhibits STAT3 and the RAF/MEK/ERK pathway in leukemia cell line K562," *Cancer Letters*, vol. 289, no. 1, pp. 46–52, 2010.

[16] T. Zhang, Y. Li, K. A. Park et al., "Cucurbitacin induces autophagy through mitochondrial ROS production which counteracts to limit caspase-dependent apoptosis," *Autophagy*, vol. 8, no. 4, pp. 559–576, 2012.

[17] P. L. Wu, F. W. Lin, T. S. Wu, C. S. Kuoh, K. H. Lee, and S. J. Lee, "Cytotoxic and anti-HIV principles from the rhizomes of *Begonia nantoensis*," *Chemical and Pharmaceutical Bulletin*, vol. 52, no. 3, pp. 345–349, 2004.

[18] Y. Maruyama, T. Ito, H. Kodama, and A. Matsuura, "Availability of amino acids extends chronological lifespan by suppressing hyper-acidification of the environment in *Saccharomyces cerevisiae*," *PLoS One*, vol. 11, no. 3, article e0151894, 2016.

[19] Y. Ohya, J. Sese, M. Yukawa et al., "High-dimensional and large-scale phenotyping of yeast mutants," *Proceedings of the National Academy of Sciences of the United States of America*, vol. 102, no. 52, pp. 19015–19020, 2005.

[20] J. Warringer, E. Ericson, L. Fernandez, O. Nerman, and A. Blomberg, "High-resolution yeast phenomics resolves different physiological features in the saline response," *Proceedings of the National Academy of Sciences of the United States of America*, vol. 100, no. 26, pp. 15724–15729, 2003.

[21] G. Suzuki, Y. Wang, K. Kubo, E. Hirata, S. Ohnuki, and Y. Ohya, "Global study of holistic morphological effectors in the budding yeast *Saccharomyces cerevisiae*," *BMC Genomics*, vol. 19, no. 1, p. 149, 2018.

[22] S. F. Levy and M. L. Siegal, "Network hubs buffer environmental variation in *Saccharomyces cerevisiae*," *PLoS Biology*, vol. 6, no. 11, article e264, 2008.

[23] G. Yvert, S. Ohnuki, S. Nogami et al., "Single-cell phenomics reveals intra-species variation of phenotypic noise in yeast," *BMC Systems Biology*, vol. 7, no. 1, p. 54, 2013.

[24] M. Yang, S. Ohnuki, and Y. Ohya, "Unveiling nonessential gene deletions that confer significant morphological phenotypes beyond natural yeast strains," *BMC Genomics*, vol. 15, no. 1, p. 932, 2014.

[25] D. M. Stasinopoulos and R. A. Rigby, "Generalized additive models for location scale and shape (GAMLSS) in R," *Journal of Statistical Software*, vol. 23, no. 7, 2007.

[26] J. D. Storey, "A direct approach to false discovery rates," *Journal of the Royal Statistical Society: Series B*, vol. 64, no. 3, pp. 479–498, 2002.

[27] M. A. McCormick, J. R. Delaney, M. Tsuchiya et al., "A comprehensive analysis of replicative lifespan in 4,698 single-gene deletion strains uncovers conserved mechanisms of aging," *Cell Metabolism*, vol. 22, no. 5, pp. 895–906, 2015.

[28] P. X. Shaw, G. Werstuck, and Y. Chen, "Oxidative stress and aging diseases," *Oxidative Medicine and Cellular Longevity*, vol. 2014, Article ID 569146, 2 pages, 2014.

[29] H. Cui, Y. Kong, and H. Zhang, "Oxidative stress, mitochondrial dysfunction, and aging," *Journal of Signal Transduction*, vol. 2012, Article ID 646354, 13 pages, 2012.

[30] S. Gaweł, M. Wardas, E. Niedworok, and P. Wardas, "Malondialdehyde (MDA) as a lipid peroxidation marker," *Wiadomosci Lekarskie*, vol. 57, no. 9-10, pp. 453–455, 2004.

[31] J. J. Ritch, S. M. Davidson, J. J. Sheehan, and N. O. P. Austriaco, "The *Saccharomyces* SUN gene, *UTH1*, is involved in cell wall biogenesis," *FEMS Yeast Research*, vol. 10, no. 2, pp. 168–176, 2010.

[32] J. S. Fassler and A. H. West, "Fungal skn7 stress responses and their relationship to virulence," *Eukaryotic Cell*, vol. 10, no. 2, pp. 156–167, 2011.

[33] K. Sun, L. Xiang, S. Ishihara, A. Matsuura, Y. Sakagami, and J. Qi, "Anti-aging effects of hesperidin on *Saccharomyces cerevisiae via* inhibition of reactive oxygen species and *UTH1* gene expression," *Bioscience Biotechnology and Biochemistry*, vol. 76, no. 4, pp. 640–645, 2012.

[34] N. R. Austriaco Jr., "Review: to bud until death: the genetics of ageing in the yeast, *Saccharomyces*," *Yeast*, vol. 12, no. 7, pp. 623–630, 1996.

[35] B. K. Kennedy, N. R. Austriaco Jr., J. Zhang, and L. Guarente, "Mutation in the silencing gene *SIR4* can delay aging in *S. cerevisiae*," *Cell*, vol. 80, no. 3, pp. 485–496, 1995.

[36] A. R. Jonckheere, "A test of significance for the relation between *m* rankings and *k* ranked categories," *British Journal of Statistical Psychology*, vol. 7, no. 2, pp. 93–100, 1954.

[37] Z. Wang, W. Zhu, M. Gao et al., "Simultaneous determination of cucurbitacin B and cucurbitacin E in rat plasma by UHPLC-MS/MS: a pharmacokinetics study after oral administration of cucurbitacin tablets," *Journal of Chromatography B Analytical Technologies in the Biomedical and Life Sciences*, vol. 1065-1066, pp. 63–69, 2017.

[38] V. D. Longo, G. S. Shadel, M. Kaeberlein, and B. Kennedy, "Replicative and chronological aging in *Saccharomyces cerevisiae*," *Cell Metabolism*, vol. 16, no. 1, pp. 18–31, 2012.

[39] C. W. Wang, J. Kim, W. P. Huang et al., "Apg2 is a novel protein required for the cytoplasm to vacuole targeting, autophagy, and pexophagy pathways," *Journal of Biological Chemistry*, vol. 276, no. 32, pp. 30442–30451, 2001.

[40] T. Kanki, K. Wang, Y. Cao, M. Baba, and D. J. Klionsky, "Atg32 is a mitochondrial protein that confers selectivity during mitophagy," *Developmental Cell*, vol. 17, no. 1, pp. 98–109, 2009.

[41] N. Amar, G. Lustig, Y. Ichimura, Y. Ohsumi, and Z. Elazar, "Two newly identified sites in the ubiquitin-like protein Atg8 are essential for autophagy," *EMBO reports*, vol. 7, no. 6, pp. 635–642, 2006.

[42] P. D. S. Bandara, J. A. Flattery-O'Brien, C. M. Grant, and I. W. Dawes, "Involvement of the *Saccharomyces cerevisiae UTH1* gene in the oxidative-stress response," *Current Genetics*, vol. 34, no. 4, pp. 259–268, 1998.

Hindawi
Oxidative Medicine and Cellular Longevity
Volume 2019, Article ID 7096912, 12 pages
https://doi.org/10.1155/2019/7096912

Research Article

Tetramethylpyrazine Prevents Contrast-Induced Nephropathy via Modulating Tubular Cell Mitophagy and Suppressing Mitochondrial Fragmentation, CCL2/CCR2-Mediated Inflammation, and Intestinal Injury

Xuezhong Gong,[1,2] **Yiru Duan**,[1] **Junli Zheng**,[1] **Zi Ye**,[1] **and Tom K. Hei**[2]

[1]*Department of Nephrology, Shanghai Municipal Hospital of Traditional Chinese Medicine, Shanghai University of Traditional Chinese Medicine, 274 Zhijiang Middle Road, Shanghai 200071, China*
[2]*Center for Radiological Research, Department of Radiation Oncology, College of Physician and Surgeons, Columbia University, 630 West 168th Street, NY 10032, USA*

Correspondence should be addressed to Xuezhong Gong; shnanshan@hotmail.com

Received 11 February 2019; Revised 26 March 2019; Accepted 7 April 2019; Published 16 May 2019

Guest Editor: Marco Cordani

Contrast-induced nephropathy (CIN) is a leading cause of hospital-acquired acute kidney injury (AKI), but detailed pathogenesis and effectual remedy remain elusive. Here, we tested the hypothesis that contrast media (CM) impaired mitochondrial quality control (MQC) in tubules, including mitochondrial fragmentation and mitophagy, induced systemic inflammation, and intestinal injury. Since we previously demonstrated that the natural antioxidant 2,3,5,6-tetramethylpyrazine (TMP) can be a protectant against CIN, we moreover investigated the involved renoprotective mechanisms of TMP. In a well-established CIN rat model, renal functions, urinary AKI biomarkers, and renal reactive oxygen species (ROS) production were measured. Mitochondrial damage and mitophagy were detected by transmission electron microscopy (TEM) and western blot. The abundance of Drp1 and Mfn2 by western blot and immunohistochemistry (IHC) was used to evaluate mitochondrial fragmentation. TUNEL staining, TEM, and the abundance of cleaved-caspase 3 and procaspase 9 were used to assay apoptosis. We demonstrated that increased mitophagy, mitochondrial fragmentation, ROS generation, autophagy, and apoptosis occurred in renal tubular cells. These phenomena were accompanied by renal dysfunction and an increased excretion of urinary AKI biomarkers. Meanwhile, CM exposure resulted in concurrent small intestinal injury and villous capillary endothelial apoptosis. The abundance of the inflammatory cytokines CCL2 and CCR2 markedly increased in the renal tubules of CIN rats, accompanied by increased concentrations of IL-6 and TNF-α in the kidneys and the serum. Interestingly, TMP efficiently prevented CM-induced kidney injury *in vivo* by reversing these pathological processes. Mechanistically, TMP inhibited the CM-induced activation of the CCL2/CCR2 pathway, ameliorated renal oxidative stress and aberrant mitochondrial dynamics, and modulated mitophagy in tubular cells. In summary, this study demonstrated novel pathological mechanisms of CIN, that is, impairing MQC, inducing CCL2/CCR2-mediated inflammation and small intestinal injury, and provided novel renoprotective mechanisms of TMP; thus, TMP may be a promising therapeutic agent for CIN.

1. Introduction

Contrast-induced nephropathy (CIN) has become the third most common cause of hospital-acquired renal failure, affecting as many as 25% of susceptible patients because of the increasing use of iodine contrast media (CM) after angiocardiography or radiological procedures in clinics [1]. However, the pathogenesis of CIN is still not fully understood, and as a result, there is still a lack of effective strategies for the prevention and mitigation of CIN [2]. Hence, there is an urgent need for novel therapeutic regimens for the clinical management of CIN.

Previous studies by our laboratory and other investigators have demonstrated that oxidative stress due to the

overproduction of free radicals induces the apoptosis of renal cells and represents an important pathogenic mechanism in CIN [3–5]. As highly dynamic organelles that undergo frequent movement (fission and fusion), mitochondria are the major source of cellular reactive oxygen species (ROS) as well as a major target of ROS-induced damage [6]. Dysfunctional mitochondria may exhibit fragmentation and membrane depolarization, and these events induce further ROS production [7]. Renal proximal tubular cells are rich in mitochondria, and thus, tubules are vulnerable to mitochondrial damage [8]. The process of removing damaged mitochondria through autophagy, which is termed mitophagy, has recently been proposed to be critical in ischemia and drug-induced tissue damage [6]. Furthermore, mitophagy and mitochondrial fragmentation are critical components of the intracellular mitochondrial quality control (MQC) machinery [9–11]. Thus, we speculated that although the roles of mitophagy induction and mitochondrial fragmentation in CIN remain unknown, mitophagy may be involved in the pathogenesis of CIN. Previous work from our laboratory has shown that autophagy requires the activity of the protein Drp1 [12, 13], which was used as a marker of autophagy in this study.

ROS and inflammation are tightly linked in both acute kidney injury (AKI) and chronic kidney disease [14–16]. Inflammation might play a crucial role in the pathogenesis of CIN, but the underlying molecular mechanisms remain largely unknown [17, 18]. As a member of the C-C chemokine family, CCL2, which is also known as MCP-1, is an important inflammatory mediator, and chemokine receptor 2 (CCR2) could act as its major specific receptor [19, 20]. Recent studies have indicated that CCL2/CCR2-mediated inflammation plays crucial roles in regulating tubular damage in both renal ischemia and reperfusion AKI as well as some experimental models of chronic tissue injury [20, 21]. However, the role of CCL2/CCR2 signaling in the pathogenesis of CIN has not yet been clarified and was therefore investigated in this study.

There is evidence from animal studies that AKI is a multisystem disease affecting the lung, heart, liver, and intestine [22–25]. However, to our knowledge, potential extrarenal complications in CIN have not been previously studied. Thus, another focus of the present study was to elucidate the link between CIN and intestinal injury using an *in vivo* model of CIN.

2,3,5,6-Tetramethylpyrazine (TMP) is an active ingredient of the Chinese herb *Ligusticum wallichii* Franch and has been found to function as a vasodilator, a free radical scavenger, and a suppressor of inflammation [26–28]. It is used in traditional Chinese medicine to protect the kidney from tubular damage caused by gentamicin, diabetes, and ischemia/reperfusion [14, 29, 30]. Our previous studies clearly highlighted that TMP might be a new potential therapeutic agent to prevent CIN by inhibiting p38 MAPK and FoxO1 pathways and could protect renal tubular cells against arsenite-induced nephrotoxicity by preventing mitochondrial dysfunction and autophagy [14, 31]. We thus further speculated that TMP might modulate MQC in tubules.

In the present study, we aimed to test the hypothesis that CM impaired MQC in tubules, including mitochondrial fragmentation and mitophagy; induced CCL2/CCR2-mediated systemic inflammation and intestinal injury; and investigated the involved renoprotective mechanisms of TMP against CIN.

2. Materials and Methods

2.1. Reagents. All chemicals were purchased from Sigma-Aldrich (St. Louis, MO, USA) unless otherwise stated. The CM iohexol (Omnipaque) was purchased from Amersham Health (Princeton, NJ, USA).

2.2. Animals. All studies involving animals were previously reviewed and approved by the Animal Welfare and Ethical Use Committee of the Shanghai Municipal Hospital of Traditional Chinese Medicine. Thirty-two adult 8–10-week-old male Sprague Dawley rats weighing 200-250 g were purchased from the Shanghai Laboratory Animal Research Center (certificate number: 2017-010). The rats were housed in an air-conditioned room at 23°C with a cycle of 12 h/12 h light/dark. Food and water were provided *ad libitum* except for the day of dehydration treatment.

2.3. Experimental Protocol and Drugs. A well-established rat model of CIN was used [3, 32–34]. Briefly, rats were randomly assigned into 4 groups of 8 animals each: controls (Con), rats injected with CM (CIN), rats treated with 150 mg/kg/d *N*-acetylcysteine (NAC) and injected with CM (CIN+NAC), and rats treated with 80 mg/kg/d TMP and injected with CM (CIN+TMP). TMP and NAC were injected intraperitoneally (ip) once daily for 4 consecutive days (days 1-4). The Con and CIN groups were administered with the same volume of saline. On day 3, all rats were kept without water for 24 h. On day 4, 20 min after injecting saline, NAC, or TMP, the CIN, CIN+NAC, and CIN+TMP groups were injected with N(G)-nitro-L-arginine methyl ester (10 mg/kg, ip). Then, after a further 15 and 30 min, respectively, they were injected with indomethacin (10 mg/kg, ip) and iohexol (1.5-2 g iodine/kg, ip). The Con group received an equivalent volume of saline by ip injection. On day 5, all rats were provided with regular chow and tap water in metabolic cages for 24 h.

Twenty-four-hour urine samples were collected in metabolic cages on days 1 (baseline) and 5 for the determination of urinary *N*-acetyl-β-glucosaminidase (UNAG) and urinary γ-glutamyl transpeptidase (UGGT). Baseline blood samples were taken under ether anesthesia from the tail vein for the measurement of serum creatinine (Scr), blood urea nitrogen (BUN), and plasma cystatin-C (CysC). At the end of day 5, blood samples were taken from the abdominal aorta under pentobarbital (50 mg/kg) anesthesia for the measurement of Scr, BUN, and CysC. Subsequently, the rats were euthanized, and the kidneys were collected for biochemical and morphological examinations.

3. Histopathological Examinations

3.1. Light Microscopy. Tissue samples from the left kidney were fixed in 10% formalin and prepared for examination

by light microscopy using either hematoxylin and eosin staining or immunohistochemistry (IHC).

IHC was performed as previously described [3, 14, 31]. Briefly, tissue sections (4 mm) were incubated for 1 h at room temperature with one of the following primary antibodies: anti-Drp1, Abcam (Cambridge, UK), 1 : 500; anti-Mfn2, Abcam, 1 : 500; anti-CCL2, Cell Signaling Technology, 1 : 1000; and anti-CCR2, Cell Signaling Technology, 1 : 1000. Immunodetection was performed using an appropriate biotinylated immunoglobulin and a horseradish peroxidase-labeled avidin kit (Zhongshan Golden Bridge Biotechnology, Beijing, China) with diaminobenzidine as the substrate. Finally, the slides were lightly counterstained with hematoxylin for 30 s. The positive signals were measured using a Motic Med 6.0 CMIAS image analysis system (Motic China Group, Xiamen, China). The staining intensity was measured in a double-blinded manner by two independent investigators and was calculated as the ratio of the stained areas over the total analyzed fields. Ten randomly chosen fields per section were analyzed.

3.2. Transmission Electron Microscopy (TEM). Right renal cortex samples were divided into pieces (2×2 mm) on ice, fixed in 2.5% (*v*/*v*) glutaraldehyde-polyoxymethylene solution for 6–8 h at 4°C, and then embedded in Epon® 812 resin. Ultrathin sections (60–70 nm) were stained with uranyl acetate and alkaline lead citrate and visualized under a JEM 100CX transmission electron microscope (JEOL Ltd., Tokyo, Japan) to perform ultrastructural analyses and evaluate autophagy as well as mitophagy. The number of autophagic vacuoles per tubular cell was counted.

3.3. Measurement of ROS Generation, IL-6, TNF-α, and Terminal Deoxynucleotidyl Transferase dUTP Nick End Labeling (TUNEL) Staining. The oxidation of 2′,7′-dichlorofluorescin diacetate (DCFDA, Jiancheng Research Institute, China) was used to detect intracellular ROS in whole kidney homogenates. Briefly, whole kidney homogenates were incubated with fresh DCFDA (10 μmol/L) for 30 min at 37°C. The absorbance of DCFDA fluorescence at 485 nm was measured against that at 525 nm as the reference wavelength. ROS production was expressed in arbitrary units corrected for protein concentration (AU/mg protein). The concentrations of IL-6 and TNF-α in supernatants from renal tissue homogenates and sera were assessed using enzyme-linked immunosorbent assay kits (Abcam, UK) in accordance with the manufacturer's instructions. All assays were performed in duplicate. For TUNEL staining, an *in situ* cell death detection kit (Roche Applied Science, Penzberg, Germany) was used according to the manufacturer's instructions. TUNEL-positive tubular cell numbers were counted randomly in 20 nonoverlapping cortical fields under 400x magnification.

3.4. Quantitative Polymerase Chain Reaction (qPCR). Renal cortexes were dissected and total RNA was extracted using TRIzol® reagent according to the manufacturer's instructions (Invitrogen, Carlsbad, CA). cDNA was synthesized using random primers and a high-capacity cDNA reverse transcription kit (Applied Biosystems, Foster City, CA). The following primers were used: *HO-1* F-TTAAGCTGGTGATGGCCTCC, R-GTGGGGCATAGACTGGGTTC; *NQO1* F-GTTTGCCTGGCTTGCTTTCA, R-ACAGCCGTGGCAGAACTATC; and *beta-actin* F-CTGTGTGGATTGGTGGCTCT, R-GCAGCTCAGTAACAGTCCGC. qPCR was performed on a 7500 real-time PCR system (Applied Biosystems).

3.5. Western Blot Analysis. Western blotting was performed as previously described [3, 5]. The primary antibodies used were as follows: anti-LC3B (Cell Signaling Technology, Danvers, MA), 1 : 1000; anti-beclin-1 (Cell Signaling Technology, Danvers, MA), 1 : 1000; anti-CCL2 (Abcam, UK), 1 : 1000; anti-CCR2 (Abcam, UK), 1 : 1000; anti-p62 (Abcam, UK), 1 : 1000; anti-Drp1 (Abcam, UK), 1 : 1000; anti-Mfn2 (Abcam, UK), 1 : 1000; anti-procaspase 9 (Cell Signaling Technology, Danvers, MA), 1 : 1000; anti-cleaved caspase 3 (Cell Signaling Technology, Danvers, MA), 1 : 1000; anti-histone (Cell Signaling Technology, Danvers, MA), 1 : 2000; and anti-GAPDH (Cell Signaling Technology, Danvers, MA), 1 : 5000. All experiments were performed at least three times (i.e., three separate protein preparations) under the same conditions.

3.6. Statistical Analysis. Results are expressed as means ± SD. One-way analysis of variance (ANOVA) with Tukey's post hoc multiple-comparison test was used to determine the significance of differences in multiple comparisons. Differences were considered significant if $p < 0.05$ and highly significant if $p < 0.01$.

4. Results

4.1. TMP Protected the Kidney from Damage in a Rat CIN Model. As shown in Figure 1, the levels of Scr, BUN, CysC, UNAG, and UGGT in the CIN group were markedly elevated compared with those in the Con group at day 5 ($p < 0.01$). Pretreatment with either TMP or NAC significantly suppressed the levels of Scr, BUN, CysC, UNAG, and UGGT in the CIN rats ($p < 0.01$) with similar activities (Figure 1).

Histologic analysis demonstrated a normal glomerulus structure in the Con animals (Figure 1(f)), while severe renal tubular interstitial injury was observed in the kidneys of the CIN-treated rats, including obvious vacuolar degeneration of tubular epithelial cells, loss of the tubular brush border, increased epithelial cell shedding, and necrosis of tubular epithelial cells (Figure 1(g)). These signs of tissue damage were markedly relieved by treatment with TMP and NAC (Figures 1(h) and 1(i), respectively).

4.2. TMP Modulated Renal Tubular Cell Autophagy, Mitophagy, and Apoptosis in the Kidneys of CIN Rats. We performed ultrastructural analyses to ascertain the presence of renal tubular programmed cell death (autophagy and apoptosis) as well as mitophagy in CIN rats using TEM. As shown in Figures 2(c) and 2(e), renal tubular autophagy in CIN kidneys after 24 h of CM injection was characterized by higher quantities of autophagosomes (indicated by yellow or red frames in Figures 2(c), 2(e), and 2(l)) and double or multiple membrane-encapsulated

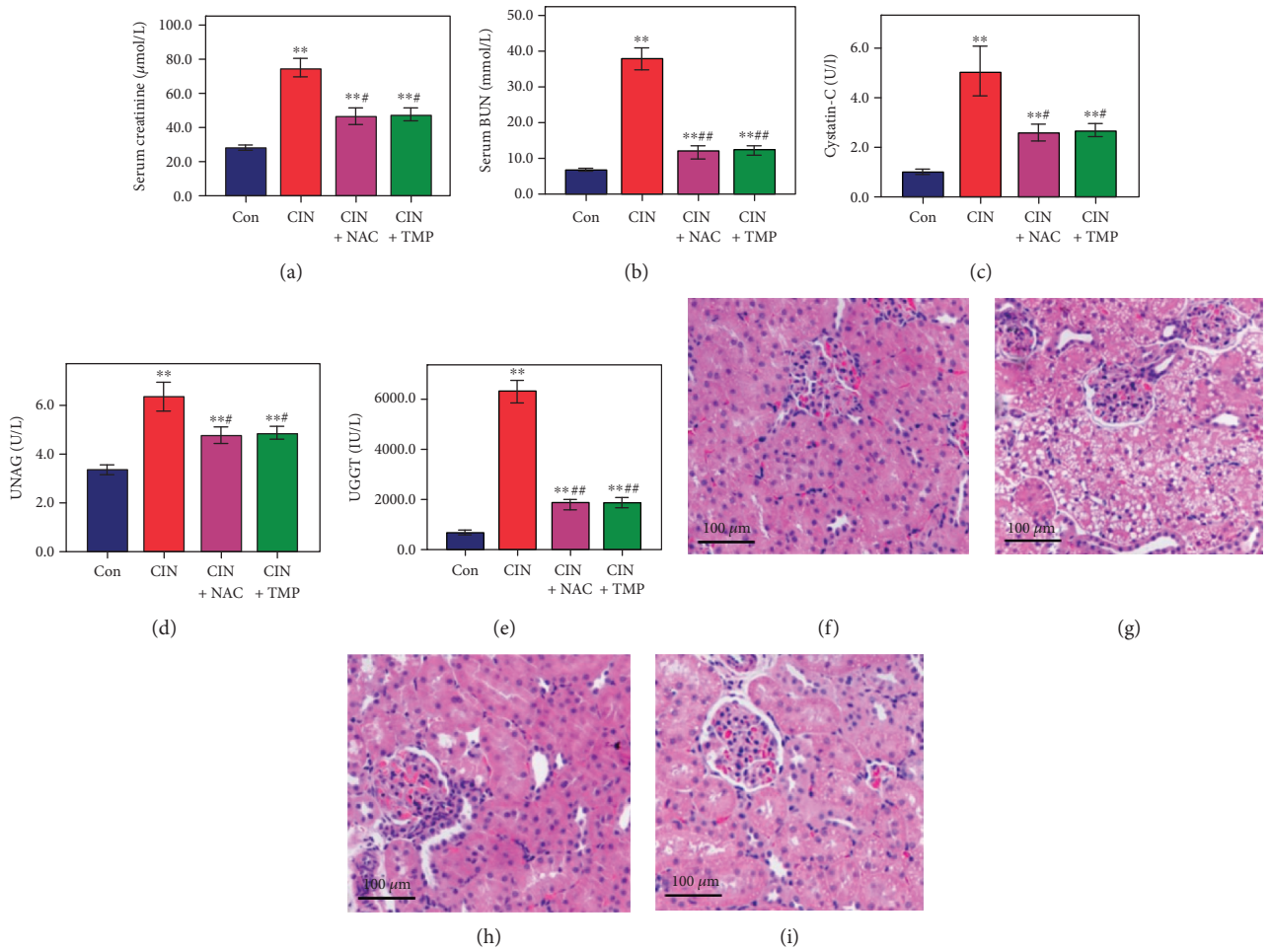

Figure 1: Tetramethylpyrazine (TMP) protected the kidney from damage in a rat contrast-induced nephropathy (CIN) model. The serum levels of creatinine (a), blood urea nitrogen (b), cystatin-C (c), urinary *N*-acetyl-β-glucosaminidase (d), and urinary γ-glutamyl transpeptidase (e) were examined using automated biochemistry assays. Photomicrographs (original magnification, ×200) illustrate hematoxylin and eosin staining of the kidney tissues from rats in the following groups: control (Con; (f)), CIN without treatment (CIN; (g)), CIN with *N*-acetyl cysteine treatment (CIN+NAC; (h)), and CIN with TMP treatment (CIN+TMP; (i)). Figures are representative of 5–8 rats from each group. Data are represented as means ± standard deviation (SD; $n = 5$). $^{**}p < 0.01$ versus Con and $^{\#\#}p < 0.01$ versus CIN.

components when compared to that in control kidneys. These results indicated that CM induced renal tubular cell autophagy in rats.

To verify the induction of renal tubular autophagy in CIN-treated rats, we examined the abundance of the autophagy-associated proteins LC3B and beclin-1 by western blotting. As shown in Figures 3(a) and 3(b), CM treatment significantly increased the conversion of LC3B-I to LC3B-II, resulting in a higher abundance of LC3B-II in CIN-treated rats than in controls. Similar findings were also obtained for the abundance of beclin-1 in CIN-treated rats (Figures 3(a) and 3(d)), while the opposite result was observed for the abundance of p62 (Figures 3(a) and 3(c)).

Meanwhile, renal tubular cells undergoing apoptosis were characterized by condensation of the nuclear chromatin and wrinkling of nuclear membranes (red frame in Figure 2(b)). In addition to TEM, renal tubular apoptosis was further confirmed by a marked increase in the proportion of TUNEL-positive tubular cells in the CIN group (Figures 3(e) and 3(f)). Consistent with our previous findings [14], the glomerulus appeared normal under TEM in CIN-treated kidneys (Figure 2(k)).

Our results indicated that CM might simultaneously induce autophagy and apoptosis in tubular epithelial cells. We next investigated whether CM exposure could also influence the selective degradation of mitochondria through mitophagy using higher magnification TEM, which is regarded as the best approach to provide direct evidence for mitophagy [6]. Concomitantly, as shown in Figure 2(c)–2(g), CM-induced mitophagy (indicated by red frames in the figures) was evident in renal tubular epithelial cells. We found that exposure to CM induced the autophagosomal encapsulation of mitochondria, which confirmed that CM induced mitophagy. Moreover, we observed both the early stage (autophagosome with engulfed mitochondria, Figures 2(c) and 2(d)) and the late stage (single-membrane autolysosomes with residual mitochondria, Figure 2(e)–2(g)) of mitophagy in CIN rats. These results provided strong evidence that CM-induced mitophagy is involved in the pathogenesis of CIN.

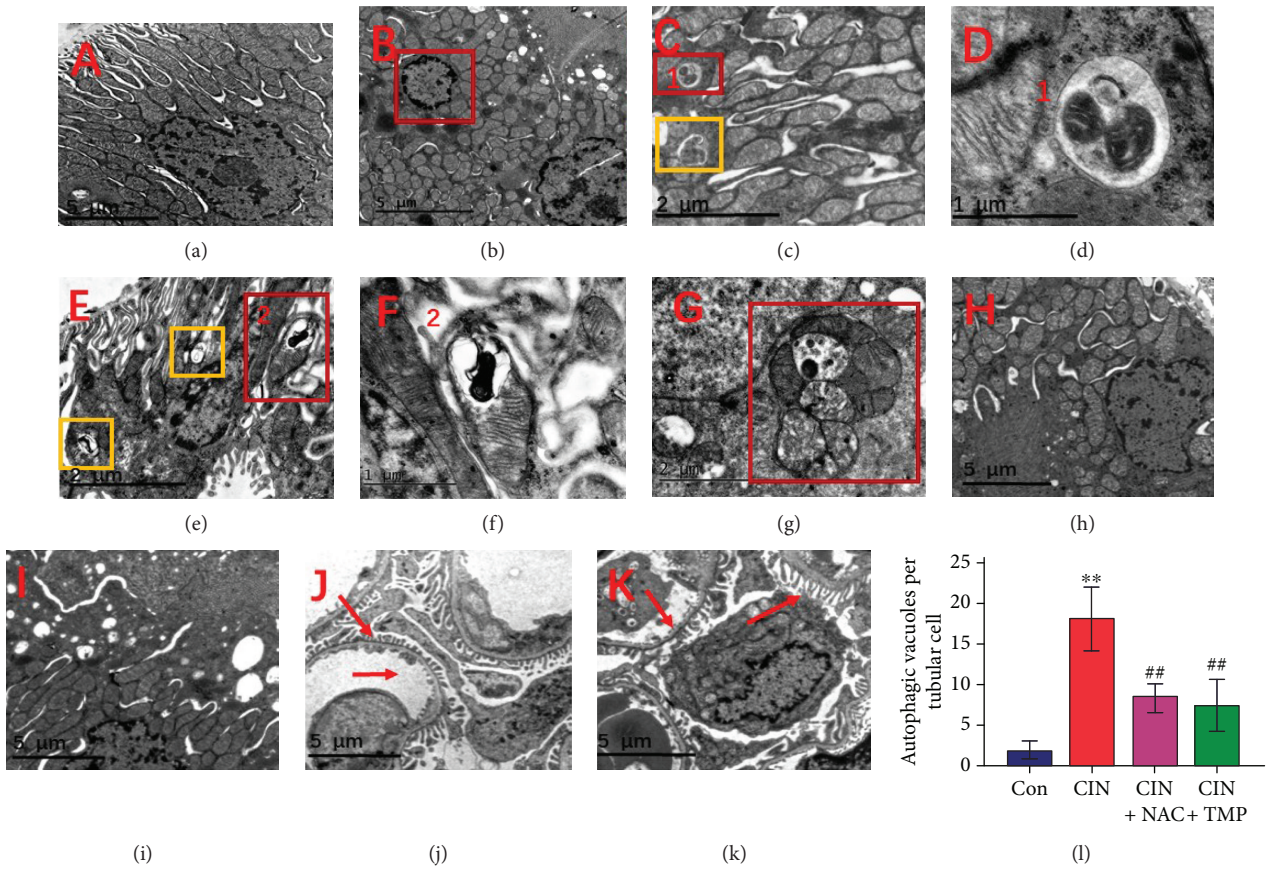

Figure 2: Tubular epithelial cell mitophagy and autophagy were increased in CIN rats and suppressed by TMP pretreatment. Transmission electron microscopy (TEM) images of the kidney in the Con (a), CIN (b–g), CIN+NAC (h), and CIN+TMP (i) rats. The red frame in (b) indicates renal tubular cells undergoing apoptosis in CIN rats as characterized by the condensation of nuclear chromatin. TEM of autophagosomes in CIN rats (orange frames in (c) and (e), indicative of autophagy) and mitochondria encapsulated in autophagosomes in CIN rats (red frames in (c), (e), and (g), indicative of mitophagy) (×9000). (d) Higher magnification TEM of (c) (×27000). (f) Higher magnification TEM of (e) (×27000). Red arrows indicate the normal glomerular basement membrane and podocytes in CON rats (j) and CIN rats (k) (×4200). (l) Quantification of the numbers of autophagic vacuoles in each tubular cell. $^{**}p < 0.01$ versus Con and $^{\#\#}p < 0.01$ versus CIN.

Interestingly, treatment with either TMP or NAC markedly reduced the quantity of autophagosomes and the degree of mitophagy (Figures 2(h) and 2(i)), the abundance of LC3B-II and beclin-1 (Figure 3(a)–3(c)), and the frequency of apoptotic cells detected by TUNEL staining (Figures 3 E3, E4 and 3(f)).

4.3. TMP Prevented Mitochondrial Fragmentation by Restoring the Alterations in Drp1 and Mfn2 Expression in CIN Rats. Mitochondria are highly dynamic organelles that undergo frequent fission and fusion. Drp1 and Mfn2 are representative profission and profusion proteins, respectively. The abundance of Drp1 and Mfn2 was evaluated using IHC at 24 h after treatment with CM. As shown in Figures 4(a), A2; 4(b), B2; 4(c); and 4(d), the abundance of Drp1 was remarkably upregulated in the tubules of CIN rats as compared to that of the Con group, while that of Mfn2 was downregulated. Both the TMP and NAC treatments significantly reduced the abundance of Drp1 and restored that of Mfn2 in the kidney as compared with that of the CIN group (Figure 4). Similar changes were demonstrated using western blotting (Figure 4(e)–4(g)). These results suggest that the modulation of MQC might play a role in the renoprotective effect of TMP against CM-induced kidney injury.

4.4. TMP Suppressed the Increase in the Abundance of CCL2/CCR2 in Tubular Epithelial Cells of CIN Kidneys. We examined the regulation of the CCL2/CCR2 expression by CM in the kidney of CIN rats. As shown in Figure 5(a)–5(c), the abundance of CCL2 and CCR2 was found to be elevated in the kidneys of CIN rats ($p < 0.01$ versus the Con group) by western blotting, while their abundance was suppressed by either TMP or NAC treatment ($p < 0.01$ versus the CIN group).

We next examined the localization of CCL2 and CCR2 in the kidney using immunohistochemistry. As shown in Figure 5, the abundance of both CCL2 (Figure 5(d), D2) and CCR2 (Figure 5(e), E2) was markedly higher in the renal tubules of CIN kidneys than in those of the control kidneys (Figures 5(f) and 5(g), respectively, $p < 0.01$). Furthermore, pretreatment with TMP (Figures 5(d), D4; 5(e), E4; 5(f); and 5(g)) or NAC (Figures 5(d), D3; 5(e), E3; 5(f); and

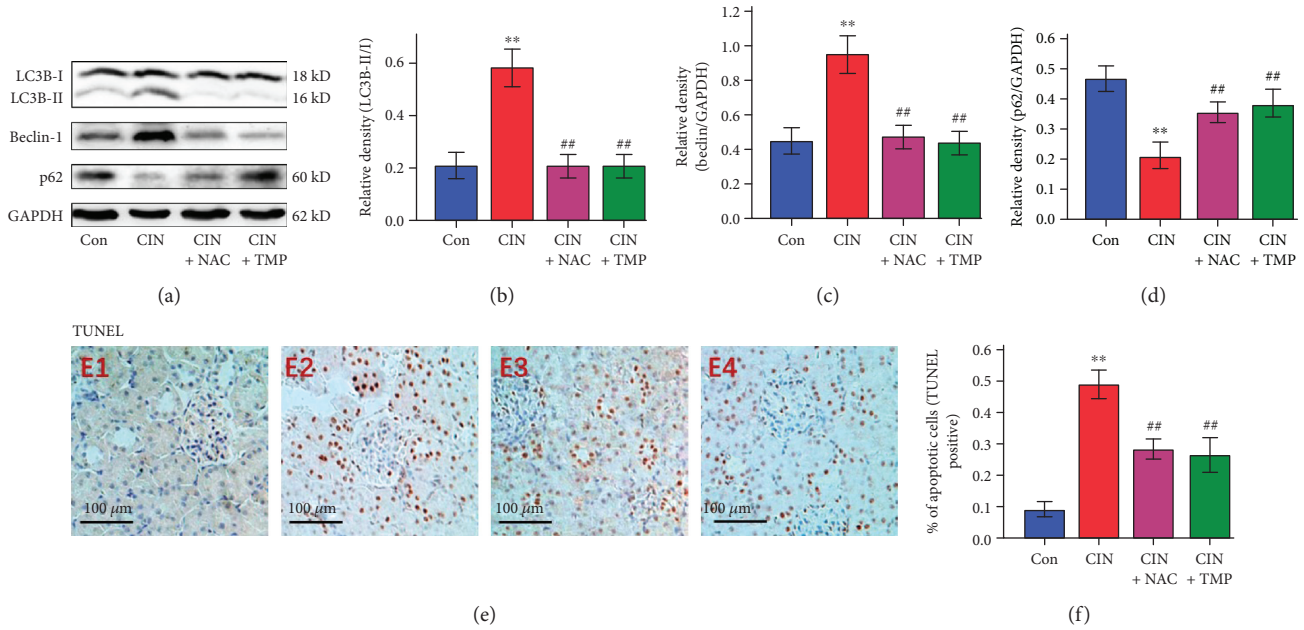

Figure 3: Analysis of LC3B, beclin-1, and p62 protein abundance and terminal deoxynucleotidyl transferase dUTP nick end labeling (TUNEL) staining. The autophagy-associated proteins LC3B and beclin-1 were detected by western blotting (a). The abundance of LC3B-II (b), beclin-1 (c), and p62 (d) was quantified by densitometry and normalized to that of LC3B-I or GAPDH, respectively. Renal tubular cell apoptosis was assessed by TUNEL (e) staining in Con (E1), CIN (E2), CIN+NAC (E3), and CIN+TMP (E4) rats. Semiquantitative analysis of TUNEL staining (f). Figures are representative of 5–8 rats from each group. Data are represented as means ± SD ($n = 5$). $^{**}p < 0.01$ versus Con and $^{\#\#}p < 0.01$ versus CIN.

5(g)) significantly decreased the abundance of CCL2 and CCR2 relative to its abundance in the CIN kidneys ($p < 0.01$).

4.5. TMP Suppressed Renal ROS Production and Reduced the Concentrations of IL-6 and TNF-α in the Serum and the Kidney. As shown in Figure 6(a), renal ROS production was increased by 2.1-fold in CIN rats as compared with controls. Conversely, pretreatment with either TMP or NAC notably decreased renal ROS production.

There were significant increases in the concentrations of IL-6 (5.1-fold; $p < 0.01$; Figure 6(b)) and TNF-α (5.5-fold; $p < 0.01$; Figure 6(c)) in the serum of CIN rats when compared with those of the controls. Furthermore, enzyme-linked immunosorbent assay analysis showed that CM significantly increased the concentrations of IL-6 and TNF-α in the CIN kidneys as compared with those in the control kidneys ($p < 0.01$; Figures 6(d) and 6(e)). Treatment with TMP or NAC significantly decreased the concentrations of IL-6 and TNF-α in both the serum and the kidneys of CIN rats ($p < 0.01$; Figure 6).

4.6. TMP Prevented Small Intestine Villous Capillary Endothelial Apoptosis and Inflammation after CIN. The underlying mechanism of AKI remains unclear. Recent studies have provided new mechanistic insights and proposed a potential connection between intestinal injury and AKI [24, 35]. Therefore, we next investigated the effects of CM exposure on the small intestine in rats and found obvious signs of intestinal injury, including the congestion of villous capillaries and the swelling and blunting of villi (Figure 7(a)–7(d)). Furthermore, apoptosis of the intestinal villous capillary endothelial cells was demonstrated by an increased abundance of cleaved caspase 3 in CIN rats as detected by IHC and western blotting (Figures 7(f), 7(i), 7(j), and 7(l)). Accordingly, the abundance of procaspase 9 in the intestine was found to be decreased in CIN rats, which further confirmed the occurrence of intestinal cell apoptosis (Figures 7(j) and 7(k)). Interestingly, pretreatment with either TMP or NAC attenuated the intestinal injury as compared with the CIN group (Figure 7).

5. Discussion

Despite the introduction of newer and safer CM options, risk stratification for the patient, and additional preventive methods, CIN has become a serious problem in clinical practice and represents the third leading cause of hospital-acquired AKI [1]. At present, no specific drugs or strategies that effectively prevent CIN and could be widely used in clinical practice are available except for extracellular volume expansion [17, 36]. Thus, the development of potential drugs or strategies for CIN prevention and mitigation is badly needed. Our previous studies have shown that TMP has a beneficial effect on CIN by preventing p38 MAPK pathway-mediated renal tubular cell apoptosis under both *in vivo* and *in vitro* conditions [3]. The present data further indicated that the modulation of renal tubular cell autophagy and mitophagy also contributes to the renoprotective effects of TMP against CIN, including the prevention of mitochondrial fragmentation and renal tubular cell apoptosis. Additionally, we further investigated the roles of

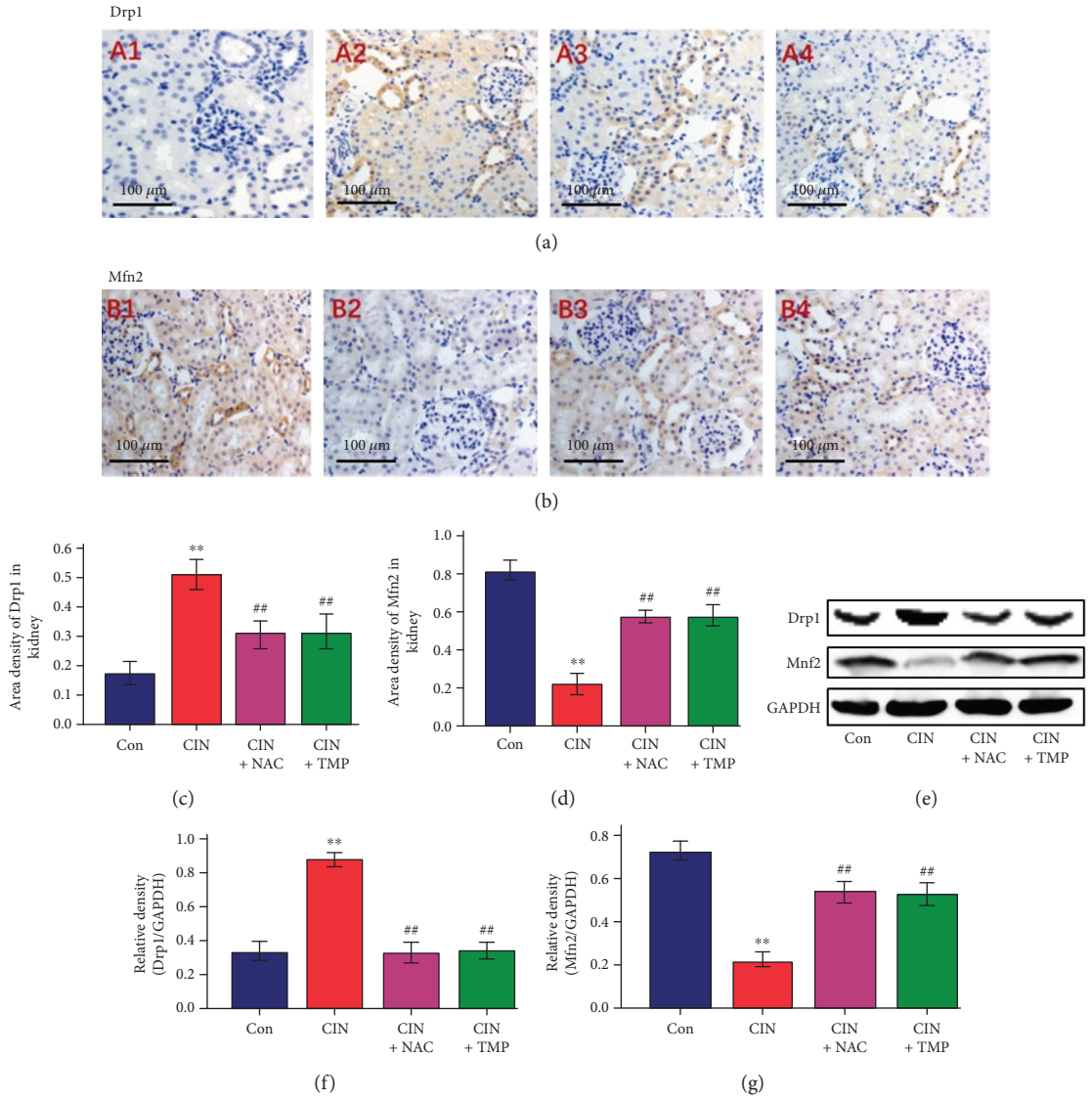

Figure 4: TMP restored mitochondrial dynamic-related protein expression in CIN rats. (a) Drp1 expression was assessed by immunohistochemistry (IHC) in the kidneys of Con (A1), CIN (A2), CIN+NAC (A3), and CIN+TMP (A4) rats (original magnification, ×200). (b) Evaluation of Mfn2 expression in the kidneys of Con (B1), CIN (B2), CIN+NAC (B3), and CIN+TMP (B4) rats by IHC (original magnification, ×200). Semiquantitative analysis of IHC staining for Drp1 (c) and Mfn2 (d). (e) Western blotting analyses of Drp1 and Mfn2 in the kidneys of rats. Relative densitometry analysis of the ratio of Drp1 (f) or Mfn2 (g) to GAPDH. Figures are representative of 5-8 rats from each group. Data are represented as means ± SD ($n = 5$). $^{**}p < 0.01$ versus Con and $^{\#\#}p < 0.01$ versus CIN.

the proinflammatory CCL2/CCR2 signal and CM-induced small intestinal injury in the pathogenesis of CIN. To our knowledge, this study is the first to demonstrate that renal tubular cell mitophagy, mitochondrial fragmentation, small intestinal injury, and the CCL2/CCR2 signal are critically involved in the pathogenesis of CIN.

TMP showed similar renoprotective effects to 150 mg/kg NAC in this study, including the prevention of histological changes in the kidneys of CIN rats and the induction of the decreases in the levels of urinary AKI biomarkers and Scr, BUN, and CysC. These results are highly consistent with our previous report [3]. As an important mechanism for mediating intracellular homeostasis, autophagy is now regarded as an adaptive response that can be specifically activated by stress or environmental changes [15, 37]. Although it remains controversial whether autophagy has a protective or destructive role in the CIN kidney, work by our laboratory and other investigators has suggested that autophagy contributes to maintaining renal tubule function and protecting against acute tubular injury [14, 37, 38]. The administration of CM resulted in an increase in the quantity of autophagosomes as well as significant elevations in the abundance of LC3B-II and beclin-1 and decreased p62 expression, which further supported that autophagy is involved in the pathological process of CIN and the TMP-dependent renoprotective effect against CIN. The antioxidant and anti-inflammatory functions of TMP as well as its abilities to regulate autophagy and apoptosis were consistent

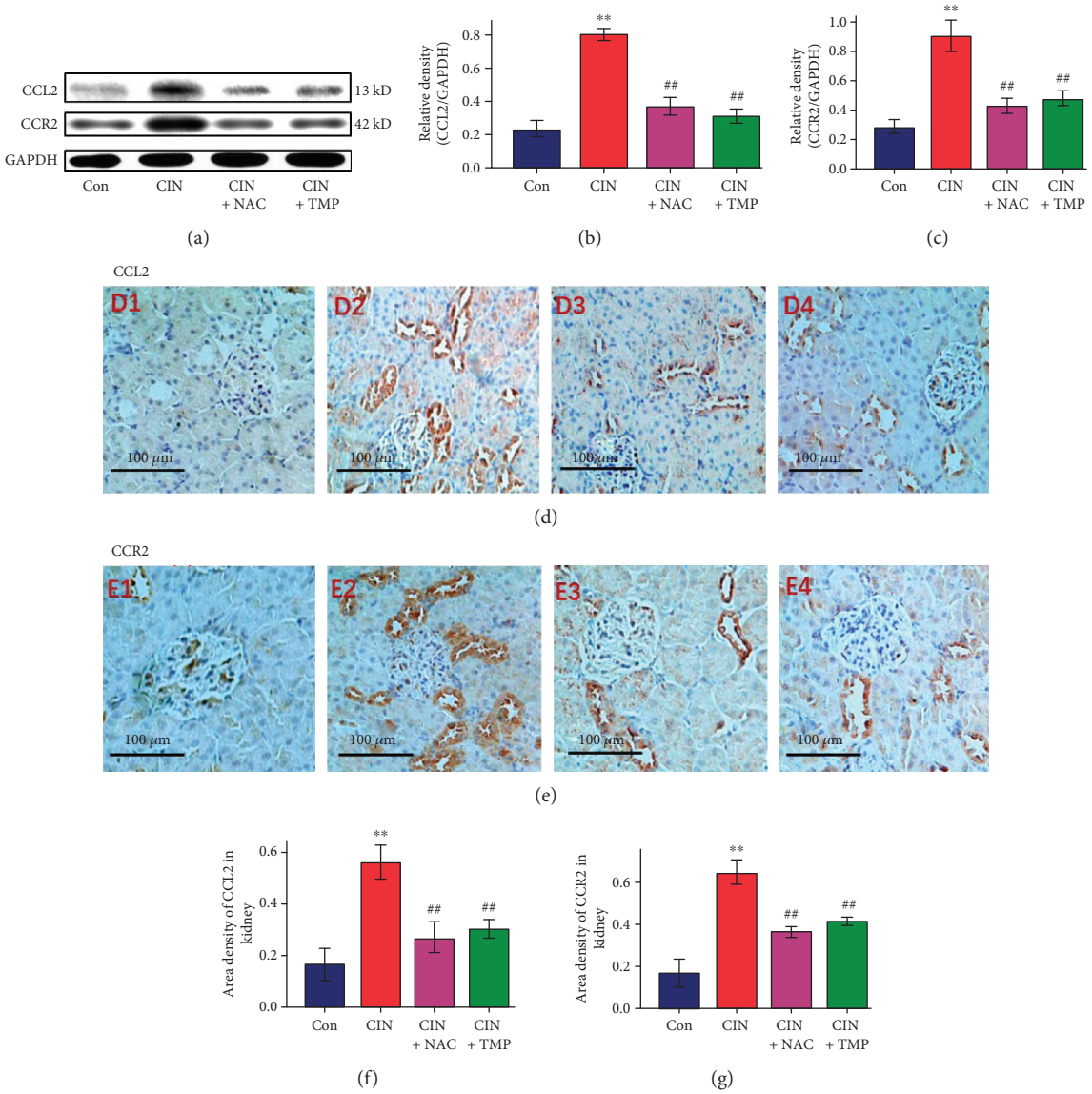

Figure 5: TMP suppressed the increase in the abundance of CCL2 and CCR2 in the tubular epithelial cells of the CIN kidneys. (a) Western blotting analyses of CCL2 and CCR2. Relative densitometry analysis of the ratio of CCL2 (b) or CCR2 (c) to GAPDH. (d) Photomicrographs (original magnification, ×200) illustrate CCL2 staining in the kidney tissues of Con (D1), CIN (D2), CIN+NAC (D3), and CIN+TMP (D4) rats. (e) Photomicrographs (original magnification, ×200) illustrate CCR2 staining in the kidney tissues of Con (E1), CIN (E2), CIN+NAC (E3), and CIN+TMP (E4) rats. Quantitative data for CCL2 (f) or CCR2 (g) staining are graphically presented. Figures are representative of 5–8 rats from each group. Data are represented as means ± SD ($n = 5$). $^{**}p < 0.01$ versus Con and $^{\#\#}p < 0.01$ versus CIN.

with our previous findings of arsenite-induced nephrotoxicity in HK2 cells [14, 31].

Damaged or dysfunctional mitochondria are regarded as toxic to cells. Therefore, the timely removal of these organelles is critical for the maintenance of cellular viability [6, 39]. Mitophagy, which is a highly selective mechanism for the degradation of mitochondria via autophagy, is critical for maintaining proper cellular functions [39]. There are very limited data on the significance of mitophagy in kidney diseases including CIN [6]. Currently, TEM is regarded as the best method for providing direct evidence of mitophagy. As shown in Figure 2, we demonstrated for the first time that mitophagy was significantly increased in CIN rats, including the early and late stages of mitophagy. These data clearly indicate that mitophagy participates in the pathological mechanism of CIN and might be critical for the maintenance of homeostasis in kidney cells. Notably, the observed increases in mitophagy and mitochondrial fragmentation were accompanied by enhanced renal oxidative stress, aggravated renal histological changes, significantly increased levels of urinary AKI biomarkers and Scr, and higher levels of apoptosis in tubular cells. Thus, these data suggest that oxidative stress and mitochondrial degradation by mitophagy are interrelated in CIN and provide support for the notion that ROS can act as an inducer of autophagy [17]. We thus speculated that mitophagy occurs in tubular cells as a response to the elevation of oxidative stress during the early phase after CM exposure; conversely, when oxidative stress

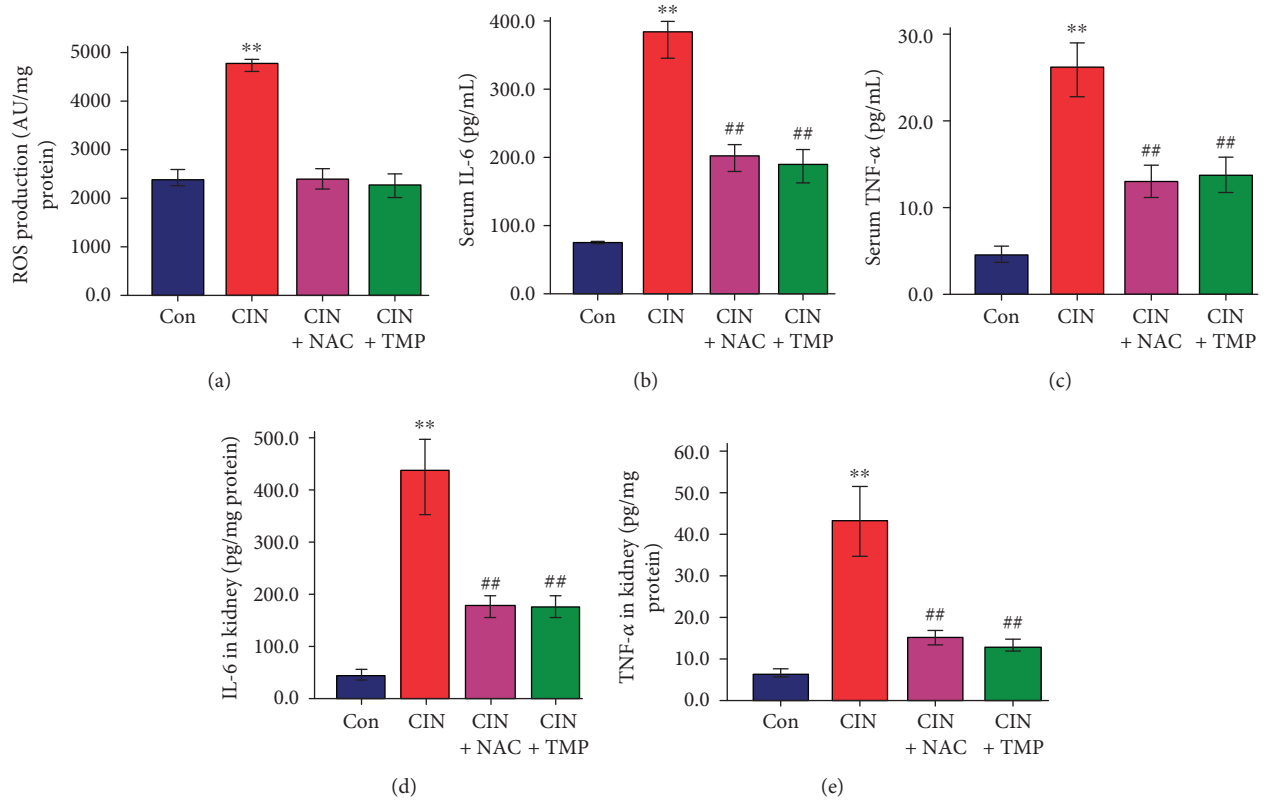

Figure 6: TMP attenuated renal reactive oxygen species production and suppressed contrast medium-induced IL-6 and TNF-α upregulation in the serum and kidney. (a) Renal reactive oxygen species production in rats as assessed by the 2′,7′-dichlorofluorescin diacetate method. Concentrations of IL-6 (b) and TNF-α (c) in the serum. Abundance of IL-6 (d) and TNF-α (e) in the kidney. Data are represented as means ± SD ($n = 5$). $^{**}p < 0.01$ versus Con and $^{\#\#}p < 0.01$ versus CIN.

is controlled, mitophagy and autophagy are suppressed. Based on the present data, TMP appeared to suppress renal ROS production and protect tubular cells against CM cytotoxicity via decreased mitophagy, autophagy, and apoptosis. There is increasing evidence to suggest that overproduction of mitochondrial ROS leads to an increase in mitochondrial fragmentation that results in tubular cell damage and apoptosis in diabetic kidney disease (DKD) [12]. Our present data are highly consistent with these findings in DKD. Our results are also consistent with those of other studies that have suggested that the activation of autophagy as a response to mitochondrial pathologies plays essential roles in maintaining renal tubule function and protecting against both acute and chronic kidney diseases [17, 40, 41].

Intracellular MQC includes biogenesis, fusion, fission, and mitophagy. Drp1 plays a key role in mitochondrial fission, whereas Mfn2 is required for mitochondrial fusion (38, 39). As shown in Figure 4, the abundance of Drp1 in CIN rats was significantly higher than that in the control group, while the abundance of Mfn2 was lower. Thus, our data revealed that CM exposure results in enhanced mitochondrial fission and fragmentation as well as mitophagy. Additionally, an abnormal mitochondrial morphology of tubular cells was observed within 24 h after CM exposure, suggesting that CM exposure induces changes in mitochondrial dynamics and intracellular MQC. This finding thus provides new evidence to support the concept that cells can segregate and eliminate dysfunctional mitochondria via intracellular MQC processes. Interestingly, in our study, TMP prevented CM-induced mitochondrial fission and fragmentation. Thus, our present data indicate for the first time that regulating the intracellular MQC of tubular epithelial cells might be a novel mechanism for the renoprotective effects of TMP.

The relationship between inflammation and the pathogenesis of renal damage in CIN has not been fully defined. CCL2, which is a member of the C-C chemokine family, can be produced by many cell types in response to inflammatory stimuli [19, 20]. Previous reports [20] have indicated that renal tubular epithelial cells could act as the initial source of CCL2 in the development of chronic renal damage in a murine renovascular hypertension model. This further suggests a critical role of the inflammatory CCL2 signal in renal disease.

Our previous studies confirmed that the induction of apoptotic cell death in tubular epithelial cells via the p38 MAPK pathway by CM is an important pathogenic mechanism in CIN and that TMP could reverse CM-induced kidney damage by inhibiting the activation of p38 MAPK [3, 5]. Furthermore, p38 MAPK is an important proinflammatory signal regulator, and the p38 MAPK signal cascade is required for the production of various inflammatory cytokines including IFN-γ, TNF-α, IL-6, and CCL2 [40, 42]. Based on these data, we speculated that the activation of the

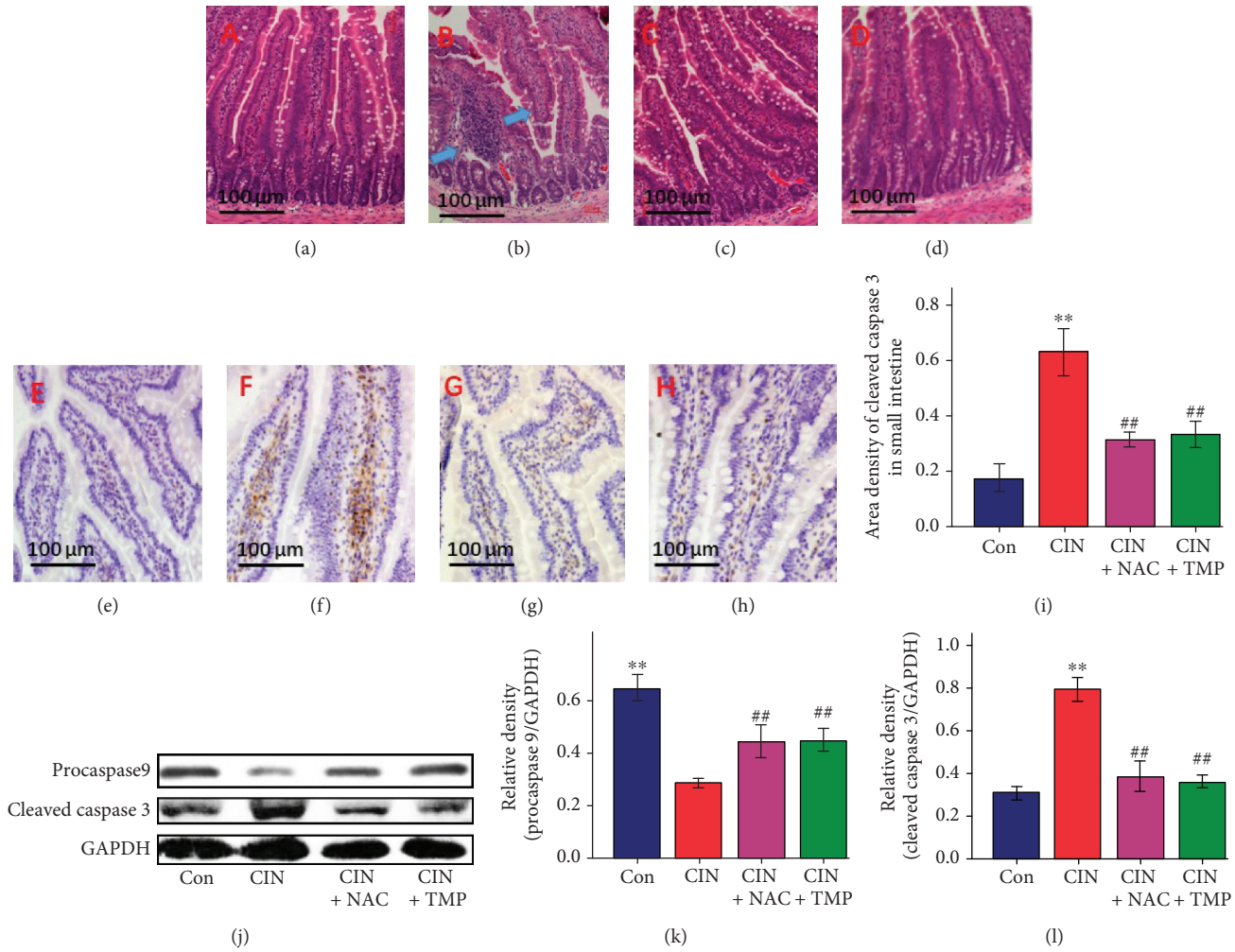

Figure 7: Effects of TMP on the induction of small intestinal villous capillary endothelial apoptosis and inflammation after CIN. Photomicrographs (original magnification, ×200) illustrate hematoxylin and eosin staining of the small intestinal tissues in Con (a), CIN (b), CIN+NAC (c), and CIN+TMP (d) rats (blue arrows indicate the congestion of villous capillaries and the swelling and blunting of villi). Photomicrographs (original magnification, ×200) illustrate cleaved caspase 3 staining in the small intestinal tissues of Con (e), CIN (f), CIN+NAC (g), and CIN+TMP (h) rats. (i) Quantitative data for cleaved caspase 3 staining are graphically presented. (j) Western blotting analyses of procaspase 9 and cleaved caspase 3. Relative densitometry analysis of the ratio of procaspase 9 (k) or cleaved caspase 3 (l) to GAPDH. Figures are representative of 5–8 rats from each group. Data are represented as means ± SD ($n = 5$). $^{**}p < 0.01$ versus Con and $^{\#\#}p < 0.01$ versus CIN.

p38 MAPK pathway after CM exposure could result in an increased production of CCL2 in the kidney. CCL2 activates chemotaxis by binding to specific receptors, and CCR2 is the primary receptor for CCL2 [19]. We thus detected the abundance of CCL2 and CCR2 in the kidneys of the CIN model rats and found that, consistent with our assumption, CM exposure substantially increased their abundance. These findings suggested that the CCL2/CCR2 pathway potentially has a pivotal role in the pathogenesis of CIN.

The abundance of IL-6 and TNF-α was substantially higher in the CIN kidneys than in the control kidneys, while pretreatment with either TMP or NAC reversed their upregulation, which further confirmed that inflammation plays a critical role in CIN. Furthermore, TMP and NAC exhibited renoprotective effects against CM-induced AKI by inhibiting the CCL2/CCR2 signal and the subsequent induction of cytokines.

Another novel finding of the current study is that CM exposure led to intestinal injury in addition to CIN and the characteristic lesions included small intestinal villous capillary endothelial apoptosis and inflammation. These findings confirmed again that AKI not only is a disease of the kidney but is also associated with systemic dysfunctions and has numerous complications [22–24]. Interestingly, TMP also showed efficacy in protecting the small intestine against the injuries induced by CM exposure. It is highly probable that its protective effects are closely linked to its antioxidant, anti-inflammatory, and antiapoptotic functions in this model. Our findings are consistent with the preliminary work by Tóth et al. [41], who reported that the intravenous administration of TMP might ameliorate intestinal ischemia-reperfusion injury in rats.

In conclusion, the present study demonstrated novel pathological mechanisms of CIN, including induction of

mitophagy, mitochondrial fragmentation, and small intestinal villous capillary endothelial apoptosis. Therefore, targeting damaged mitochondria by activating mitophagy and MQC might be a novel approach for treating CIN. Furthermore, TMP efficiently prevented CM-induced kidney injury *in vivo* by reversing these pathological processes. Mechanistically, TMP efficiently reversed the CM-induced activation of the CCL2/CCR2 pathway, ameliorated renal oxidative stress and aberrant mitochondrial dynamics, and modulated mitophagy in tubular cells. These data provide a novel mechanistic explanation for the renoprotective effects of TMP, and TMP may be a promising therapeutic agent for CIN.

Data Availability

The data used to support the findings of this study are included within the article.

Conflicts of Interest

The authors declare that they have no conflict of interest.

Acknowledgments

The authors would like to thank Professor Andong Qiu for the advice and helpful discussion. This work was supported by the National Natural Science Foundation of China Grants 81573936, 81873280, and 81373614 and sponsored by the Shanghai Pujiang Program (No. 15PJD036) and the Municipal Human Resources Development Program for Outstanding Leaders in Medical Disciplines in Shanghai (No. 2017BR020).

References

[1] I. Zealley, H. Wang, P. T. Donnan, and S. Bell, "Exposure to contrast media in the perioperative period confers no additional risk of acute kidney injury in surgical patients," *Nephrology Dialysis Transplantation*, vol. 33, no. 10, pp. 1751–1756, 2018.

[2] J. Silvain, L. S. Nguyen, V. Spagnoli et al., "Contrast-induced acute kidney injury and mortality in ST elevation myocardial infarction treated with primary percutaneous coronary intervention," *Heart*, vol. 104, no. 9, pp. 767–772, 2018.

[3] X. Gong, Q. Wang, X. Tang et al., "Tetramethylpyrazine prevents contrast-induced nephropathy by inhibiting p38 MAPK and FoxO1 signaling pathways," *American Journal of Nephrology*, vol. 37, no. 3, pp. 199–207, 2013.

[4] C. Quintavalle, M. Brenca, F. De Micco et al., "In vivo and in vitro assessment of pathways involved in contrast media-induced renal cells apoptosis," *Cell Death & Disease*, vol. 2, no. 5, p. e155, 2011.

[5] X. Gong, G. Celsi, K. Carlsson, S. Norgren, and M. Chen, "N-Acetylcysteine amide protects renal proximal tubular epithelial cells against iohexol-induced apoptosis by blocking p38 MAPK and iNOS signaling," *American Journal of Nephrology*, vol. 31, no. 2, pp. 178–188, 2010.

[6] C. Tang, L. He, J. Liu, and Z. Dong, "Mitophagy: basic mechanism and potential role in kidney diseases," *Kidney Diseases*, vol. 1, no. 1, pp. 71–79, 2015.

[7] L. Wiley, D. Ashok, C. Martin-Ruiz et al., "Reactive oxygen species production and mitochondrial dysfunction in white blood cells are not valid biomarkers of ageing in the very old," *PLoS One*, vol. 9, no. 3, article e91005, 2014.

[8] T. A. Schiffer and M. Friederich-Persson, "Mitochondrial reactive oxygen species and kidney hypoxia in the development of diabetic nephropathy," *Frontiers in Physiology*, vol. 8, 2017.

[9] T. Yang, X. M. Zhang, L. Tarnawski et al., "Dietary nitrate attenuates renal ischemia-reperfusion injuries by modulation of immune responses and reduction of oxidative stress," *Redox Biology*, vol. 13, pp. 320–330, 2017.

[10] Y. Kiriyama and H. Nochi, "Intra- and intercellular quality control mechanisms of mitochondria," *Cells*, vol. 7, no. 1, p. 1, 2018.

[11] D. Wang, J. Chen, X. Liu et al., "A Chinese herbal formula, Jian-Pi-Yi-Shen decoction, improves muscle atrophy via regulating mitochondrial quality control process in 5/6 nephrectomised rats," *Scientific Reports*, vol. 7, no. 1, p. 9253, 2017.

[12] J. Wu, B. Zhang, Y. R. Wuu, M. M. Davidson, and T. K. Hei, "Targeted cytoplasmic irradiation and autophagy," *Mutation Research/Fundamental and Molecular Mechanisms of Mutagenesis*, vol. 806, pp. 88–97, 2017.

[13] B. Zhang, M. M. Davidson, H. Zhou, C. Wang, W. F. Walker, and T. K. Hei, "Cytoplasmic irradiation results in mitochondrial dysfunction and DRP1-dependent mitochondrial fission," *Cancer Research*, vol. 73, no. 22, pp. 6700–6710, 2013.

[14] X. Gong, V. N. Ivanov, M. M. Davidson, and T. K. Hei, "Tetramethylpyrazine (TMP) protects against sodium arsenite-induced nephrotoxicity by suppressing ROS production, mitochondrial dysfunction, pro-inflammatory signaling pathways and programed cell death," *Archives of Toxicology*, vol. 89, no. 7, pp. 1057–1070, 2015.

[15] L. He, Q. Wei, J. Liu et al., "AKI on CKD: heightened injury, suppressed repair, and the underlying mechanisms," *Kidney International*, vol. 92, no. 5, pp. 1071–1083, 2017.

[16] M. Nangaku, Y. Hirakawa, I. Mimura, R. Inagi, and T. Tanaka, "Epigenetic changes in the acute kidney injury-to-chronic kidney disease transition," *Nephron*, vol. 137, no. 4, pp. 256–259, 2017.

[17] Y. Yuan, H. Qiu, X. Hu et al., "Predictive value of inflammatory factors on contrast-induced acute kidney injury in patients who underwent an emergency percutaneous coronary intervention," *Clinical Cardiology*, vol. 40, no. 9, pp. 719–725, 2017.

[18] X. Tan, X. Zheng, Z. Huang, J. Lin, C. Xie, and Y. Lin, "Involvement of S100A8/a9-TLR4-NLRP3 inflammasome pathway in contrast-induced acute kidney injury," *Cellular Physiology and Biochemistry*, vol. 43, no. 1, pp. 209–222, 2017.

[19] B. Shen, J. Liu, F. Zhang et al., "CCR2 Positive Exosome Released by Mesenchymal Stem Cells Suppresses Macrophage Functions and Alleviates Ischemia/Reperfusion-Induced Renal Injury," *Stem Cells International*, vol. 2016, Article ID 1240301, 9 pages, 2016.

[20] S. Kashyap, G. M. Warner, S. P. Hartono et al., "Blockade of CCR2 reduces macrophage influx and development of chronic renal damage in murine renovascular hypertension," *American Journal of Physiology-Renal Physiology*, vol. 310, no. 5, pp. F372–F384, 2016.

[21] K. Ohno, A. Kuno, H. Murase et al., "Diabetes increases the susceptibility to acute kidney injury after myocardial infarction through augmented activation of renal Toll-like receptors

in rats," *American Journal of Physiology-Heart and Circulatory Physiology*, vol. 313, no. 6, pp. H1130–H1142, 2017.

[22] S. W. Park, S. W. C. Chen, M. Kim et al., "Cytokines induce small intestine and liver injury after renal ischemia or nephrectomy," *Laboratory Investigation*, vol. 91, no. 1, pp. 63–84, 2011.

[23] A. Andres-Hernando, C. Altmann, R. Bhargava et al., "Prolonged acute kidney injury exacerbates lung inflammation at 7 days post-acute kidney injury," *Physiological Reports*, vol. 2, no. 7, p. e12084, 2014.

[24] V. Andrade-Oliveira, M. T. Amano, M. Correa-Costa et al., "Gut bacteria products prevent AKI induced by ischemia-reperfusion," *Journal of the American Society of Nephrology*, vol. 26, no. 8, pp. 1877–1888, 2015.

[25] on behalf of the National Taiwan University Hospital Study Group on Acute Renal Failure (NSARF) and the Taiwan Consortium for Acute Kidney Injury and Renal Diseases (CAKs), C.-C. Shiao, P.-C. Wu et al., "Long-term remote organ consequences following acute kidney injury," *Critical Care*, vol. 19, no. 1, 2015.

[26] Y. Zhao, Y. Liu, and K. Chen, "Mechanisms and clinical application of tetramethylpyrazine (an interesting natural compound isolated from *Ligusticum wallichii*): current status and perspective," *Oxidative Medicine and Cellular Longevity*, vol. 2016, Article ID 2124638, 9 pages, 2016.

[27] T. Zhang, J. Gu, L. Wu et al., "Neuroprotective and axonal outgrowth-promoting effects of tetramethylpyrazine nitrone in chronic cerebral hypoperfusion rats and primary hippocampal neurons exposed to hypoxia," *Neuropharmacology*, vol. 118, pp. 137–147, 2017.

[28] M. Guo, Y. Liu, and D. Shi, "Cardiovascular actions and therapeutic potential of tetramethylpyrazine (active component isolated from *Rhizoma Chuanxiong*): roles and mechanisms," *BioMed Research International*, vol. 2016, Article ID 2430329, 9 pages, 2016.

[29] B. Zhang, C. Lu, M. Bai et al., "Tetramethylpyrazine identified by a network pharmacology approach ameliorates methotrexate-induced oxidative organ injury," *Journal of Ethnopharmacology*, vol. 175, pp. 638–647, 2015.

[30] B. Wang, Q. Ni, X. Wang, and L. Lin, "Meta-analysis of the clinical effect of ligustrazine on diabetic nephropathy," *The American Journal of Chinese Medicine*, vol. 40, no. 01, pp. 25–37, 2012.

[31] X. Gong, V. N. Ivanov, and T. K. Hei, "2,3,5,6-Tetramethylpyrazine (TMP) down-regulated arsenic-induced heme oxygenase-1 and ARS2 expression by inhibiting Nrf2, NF-κB, AP-1 and MAPK pathways in human proximal tubular cells," *Archives of Toxicology*, vol. 90, no. 9, pp. 2187–2200, 2016.

[32] Y. Agmon, H. Peleg, Z. Greenfeld, S. Rosen, and M. Brezis, "Nitric oxide and prostanoids protect the renal outer medulla from radiocontrast toxicity in the rat," *Journal of Clinical Investigation*, vol. 94, no. 3, pp. 1069–1075, 1994.

[33] Y. Yokomaku, T. Sugimoto, S. Kume et al., "Asialoerythropoietin prevents contrast-induced nephropathy," *Journal of the American Society of Nephrology*, vol. 19, no. 2, pp. 321–328, 2008.

[34] H. T. Lee, M. Jan, S. C. Bae et al., "A1 adenosine receptor knockout mice are protected against acute radiocontrast nephropathy in vivo," *American Journal of Physiology-Renal Physiology*, vol. 290, no. 6, pp. F1367–F1375, 2006.

[35] H. T. Lee, M. Kim, J. Y. Kim et al., "Critical role of interleukin-17a in murine intestinal ischemia-reperfusion injury," *American Journal of Physiology-Gastrointestinal and Liver Physiology*, vol. 304, no. 1, pp. G12–G25, 2013.

[36] N. Kiss and P. Hamar, "Histopathological evaluation of contrast-induced acute kidney injury rodent models," *BioMed Research International*, vol. 2016, Article ID 3763250, 15 pages, 2016.

[37] M. Jiang, Q. Wei, G. Dong, M. Komatsu, Y. Su, and Z. Dong, "Autophagy in proximal tubules protects against acute kidney injury," *Kidney International*, vol. 82, no. 12, pp. 1271–1283, 2012.

[38] G. P. Kaushal and S. V. Shah, "Autophagy in acute kidney injury," *Kidney International*, vol. 89, no. 4, pp. 779–791, 2016.

[39] J. J. Lemasters, "Variants of mitochondrial autophagy: types 1 and 2 mitophagy and micromitophagy (type 3)," *Redox Biology*, vol. 2, pp. 749–754, 2014.

[40] H. Cakmak, Y. Seval-Celik, S. Arlier et al., "p38 Mitogen-Activated Protein Kinase is Involved in the Pathogenesis of Endometriosis by Modulating Inflammation, but not Cell Survival," *Reproductive Sciences*, vol. 25, no. 4, pp. 587–597, 2017.

[41] S. Tóth Jr., T. Pekarova, J. Varga et al., "Intravenous administration of tetramethylpyrazine reduces intestinal ischemia-reperfusion injury in rats," *The American Journal of Chinese Medicine*, vol. 41, no. 04, pp. 817–829, 2013.

[42] M. B. Menon, J. Gropengiesser, J. Fischer et al., "$p38^{MAPK}$/MK2-dependent phosphorylation controls cytotoxic RIPK1 signalling in inflammation and infection," *Nature Cell Biology*, vol. 19, no. 10, pp. 1248–1259, 2017.

Hindawi
Oxidative Medicine and Cellular Longevity
Volume 2019, Article ID 6387357, 19 pages
https://doi.org/10.1155/2019/6387357

Review Article

Mitophagy and Oxidative Stress in Cancer and Aging: Focus on Sirtuins and Nanomaterials

Enza Vernucci,[1] **Carlo Tomino**,[2] **Francesca Molinari**,[3] **Dolores Limongi**,[4] **Michele Aventaggiato**,[5] **Luigi Sansone**,[6] **Marco Tafani**,[7] **and Matteo A. Russo**[6,8]

[1]*Department of Cardiovascular, Nephrologic, Anesthesiologic and Geriatric Sciences, Sapienza University of Rome, Viale Regina Elena 324, 00161 Rome, Italy*
[2]*IRCCS San Raffaele, Scientific Direction, Via Val Cannuta 247, 00166 Rome, Italy*
[3]*Department of Experimental Medicine, Sapienza University of Rome, Viale Regina Elena 324, 00161 Rome, Italy*
[4]*IRCCS San Raffaele Pisana, Department of Human Sciences and Promotion of the Quality of Life, San Raffaele Roma Open University, Via Val Cannuta 247, 00166 Rome, Italy*
[5]*Department of Experimental Medicine, Sapienza University of Rome, Viale Regina Elena 324, 00161 Rome, Italy*
[6]*Department of Cellular and Molecular Pathology, IRCCS San Raffaele, Via Val Cannuta 247, 00166 Rome, Italy*
[7]*Department of Experimental Medicine, Sapienza University of Rome, Viale Regina Elena 324, 00161 Rome, Italy*
[8]*MEBIC Consortium, San Raffaele Rome Open University, Via Val Cannuta 247, 00166 Rome, Italy*

Correspondence should be addressed to Enza Vernucci; enza.vernucci@gmail.com, Luigi Sansone; luigi.sansone@sanraffaele.it, and Marco Tafani; marco.tafani@uniroma1.it

Received 21 February 2019; Accepted 8 April 2019; Published 9 May 2019

Guest Editor: Miguel Sanchez-Alvarez

Mitochondria are the cellular center of energy production and of several important metabolic processes. Mitochondrion health is maintained with a substantial intervention of mitophagy, a process of macroautophagy that degrades selectively dysfunctional and irreversibly damaged organelles. Because of its crucial duty, alteration in mitophagy can cause functional and structural adjustment in the mitochondria, changes in energy production, loss of cellular adaptation, and cell death. In this review, we discuss the dual role that mitophagy plays in cancer and age-related pathologies, as a consequence of oxidative stress, evidencing the triggering stimuli and mechanisms and suggesting the molecular targets for its therapeutic control. Finally, a section has been dedicated to the interplay between mitophagy and therapies using nanoparticles that are the new frontier for a direct and less invasive strategy.

1. Mitophagy

The cellular process that involves the degradation of aged and/or damaged mitochondria by autophagy is known as "mitophagy" [1]. Mitophagy is a physiological mechanism requested for mitochondrion turnover [2] and cell maintenance and for responding to novel energetic requirements [3]. In *Caenorhabditis elegans*, mitophagy is required in the oocytes for removing the mitochondria (and other organelles) of paternal origin thanks to the interaction of ALLO1 and IKKE-1 that drive organelle clearance [4]. Excessive, defective, or inappropriate mitophagy is responsible for cellular damage and death [5]. Abnormal mitophagy may be primary due to primitive mutations of genes involved in its mechanisms or secondary to an excessive mitochondrial damage, such as mitochondrial depolarizing stimuli, hypoxia, toxic agents (Table 1), radiations, and accumulation of mtDNA mutations (Figures 1 and 2).

Mitophagy is a specific form of macroautophagy which occurs as a multistep process, including (1) the selection/segregation of these organelles in a vacuole (*autophagosome*), (2) the fusion with a lysosome (*autophagolysosome*) [16], (3) the acidification of internal microenvironment [17, 18], (4) the activation of lysosomal acidic enzymes and oxidative metabolism [19], (5) the degradation of the content, and (6) the recycling and disposal of the final products (Figure 3). Only in the last few years the mechanisms and molecules involved in these different phases of mitophagy have been identified, although several questions are still unanswered.

Table 1: Agents affecting mitophagy.

Agent	Effect on mitophagy	Mechanism	Reference
Nicotinamide derivatives	Increase	NAD+ replenishment increases DCT-1- (ortholog to the mammalian BNIP3L/NIX) associated mitophagy in worms	[6]
Spermidine	Increase	Induces ATM activation that, in turn, promotes the accumulation of PINK1 and translocation of Parkin to mitochondria	[7]
Urolithin A	Increase	Upregulates of PINK1, DCT-1, and SKN-1 Mechanism not known	[8]
Rapamycin	Increase	Increases the translocation of p62 and Parkin to the damaged mitochondria	[9]
Metformin	Increase	Decreases the inhibitory interaction between Parkin and p53 and increase the degradation of mitofusins	[10]
Chloroquine	Inhibition	Inhibits phagosome/lysosome fusion	[11, 12]
Mitochondrial toxins: FCCP/CCCP, rotenone, antimycin A, valmycin, oligomycin, 1-methyl-4-phenyl-1,2,3,6-tetrahydropyridine (MPTP), and 6-hydroxydopamine	Increase	Perturb mitochondrial ATP production and cause ROS generation	[13]
Ceramides	Increase	Interact directly with LC3B-II upon Drp1-dependent mitochondrial fission, leading to inhibition of mitochondrial function and oxygen consumption	[14]
Selenite	Increase	Induces superoxide-mediated mitophagic cell death	[15]

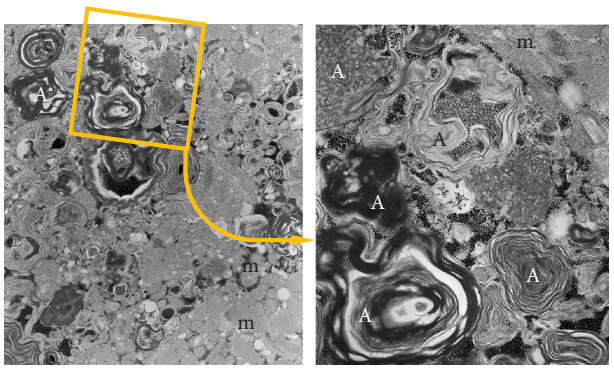

Figure 1: Autophagosomes accumulate into myocardiocytes due to the presence of chloroquine which blocks the fusion between primary lysosomes and autophagosomes. (a) Large autophagosomes (A) with different cytoplasmic components, mainly degraded lipid membranes, and glycogen. (b) Magnification of the detail indicated in the square. m: mitochondria.

When aged or irreversibly damaged mitochondria are destined to disposal, they are marked on the mitochondrial outer membrane with receptors that can interact *directly* with their *countereceptors or ligands* localized on endoplasmic reticulum membranes (Table 2) or *indirectly*, through a ubiquitin-mediated process involving Parkin (E3 ubiquitin ligase) and PINK1 (PTEN-induced kinase 1), known to interact with Beclin 1 [20] and several other proteins [21].

In both cases, a similar multistep process occurs, as outlined above:

Macroautophagocytosis is the receptor-mediated selection and encapsulation/engulfment of organelles by the endoplasmic reticulum membranes, forming a vacuole, probably with a zip interaction between the two membranes (Figure 4) [35].

The best known membrane receptors (Table 2) implicated in mitophagy are NIX/BNIP3L, BNIP3, and FUNDC1 linked to hypoxia-induced mitophagy, BCL2L13, AMBRA1, SMURF1, FKBP8, and PHB2 (prohibitin 2). Recently, NLRX1 is a Nod-like receptor family member used by *L. monocytogenes* to induce mitophagy to survive inside host organisms [34]. All of them, through their LC3-interacting regions (LIR), can recruit specific proteins and start encapsulation inside the autophagosome. FUNDC1, interestingly, interacts with OPI1, DNMIL, and LC3 according to its phosphorylation status. In fact, it has been reported that two kinases (SRC and CK2) and the phosphatase PGAM5 through phosphorylation and dephosphorylation can determine FUNDC1 "interactome" [36]. FUNDC1 interacting with HSC70 plays a pivotal role also in the translocation to the mitochondria of unfolded cytosolic proteins for degradation by LONP1 or for nonaggresomal mitochondrion-associated protein aggregate (MAPA) formation that will be eliminated by autophagy [37]. The interaction between PINK1 and Parkin, instead, is fundamental for mitochondrial quality check [38]. Parkin can be directly phosphorylated by PINK1 on serine 65 [39], or PINK1, through the ubiquitin phosphorylation on serine 65, can recruit and activate Parkin in an indirect way [40]. It has been published that a new PTEN isoform, PTEN-L (PTEN-long), can interfere with Parkin translocation and, thanks to its dephosphorylase activity, can diminish Parkin and ubiquitin phosphorylation acting as a mitophagic inhibitor [41]. When PINK1 accumulates on the mitochondrial outer membrane (MOM) following a decrease in mitochondrial membrane potential [42], it

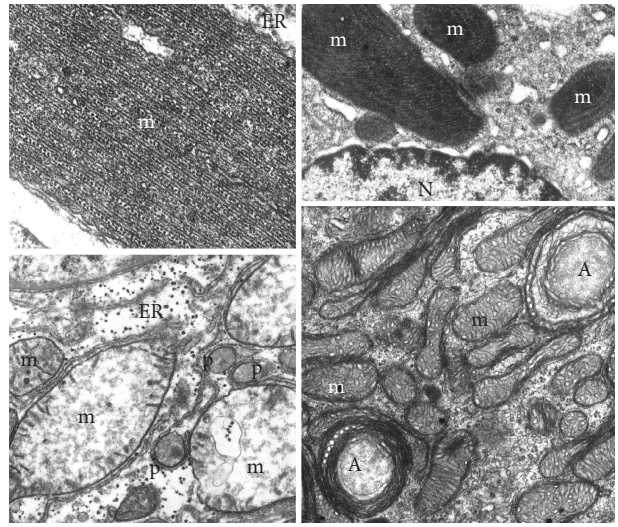

Figure 2: Mitochondria (m) have been damaged by different physiopathological conditions. (a) Mutated, misfolded, and fibrillary polymerized mitochondrial proteins may accumulate into the matrix giving rise to giant mitochondria with paracrystalline inclusions. They appear surrounded by endoplasmic reticulum (ER) membranes, indicating a process of segregation for autophagocytosis. (b) Antibiotics affecting bacterial protein synthesis may interfere with mitochondrial protein synthesis producing enlarged mitochondria (m) with paracrystalline inclusions and bizarre shape. Also, in this case, the close interaction with endoplasmic reticulum membranes suggests a process of segregation for mitophagy (N: nucleus). (c) Swollen liver mitochondria (m) after 3 hours of ischemia: they show a number of pathological changes: volume increase, dishomogeneous electron-clear and sometimes vacuolized matrix, fragmented cristae, and sometimes interrupted outer membrane. Indeed, they appear, together with apparently intact peroxisomes (p), surrounded by endoplasmic reticulum (ER) which indicates the autophagocytic process. (d) Mitochondria (m) from the glomerular zone of a suprarenal cortex which has been intensively stimulated by ACTH. The consequent hypertrophy includes also an increase of mitochondrial growth (number and volume) and an accelerated turnover as suggested by the increased mitophagy (A).

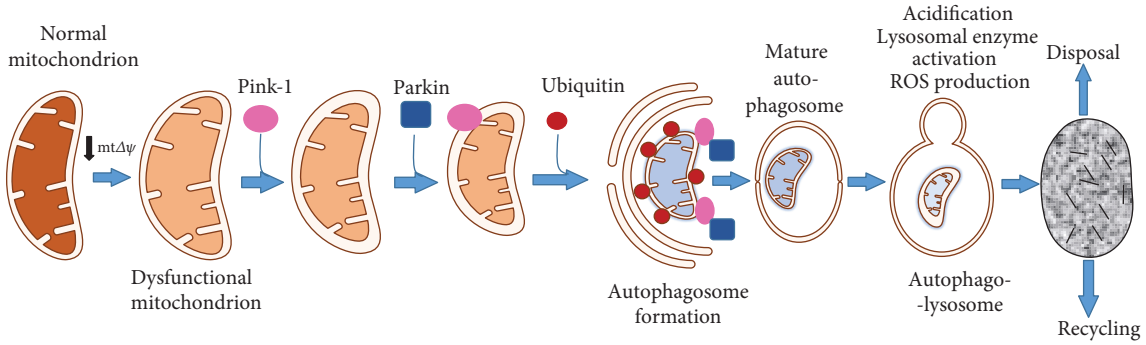

Figure 3: Sequence and molecular details of the selective mitophagy. When mitochondria undergo decrease in membrane potential (or different stress stimuli), PINK1, localized on the mitochondrial membrane, recruits Parkin that polyubiquitinates MOM protein and induces the autophagosome formation. Then, lysosome fuses with the autophagosome (autophagolysosome) and the degraded material can be recycled or disposed.

undergoes autoactivation and recruits Parkin [43] that, in turn, polyubiquitylates several proteins located on the MOM and starts the fission process [44, 45]. This polyubiquitylation process can be inhibited by USP30, a deubiquitinase found in neurons that, removing ubiquitins transferred by Parkin on damaged mitochondrial proteins, blocks Parkin-mediated mitophagy [46]. Parkin is not the only E3 ligase involved in mitophagy; recently, it has been shown that during selenite-induced mitophagy, ULK1 translocates to the mitochondria where it is ubiquitinated by MUL1 and PARK2 and FUNDC1-independent mechanism [47]. Polyubiquitylated MOM proteins mobilize many adapter proteins such as TAX1BP1, NBR1, p62, NDP52, and OPTN that are important for the PINK1/Parkin-mediated mitophagy and for the interaction between polyubiquitin chains and Atg8-like proteins [48, 49] that drive the autophagosomal-lysosomal pathway [1].

The interaction of a phagosome with a lysosome is carried out with the cooperation of many different protein complexes, including a transport system (rab/microtubules), a fusion system (SNARE proteins) responsible for the fusion of the two membranes, and a tethering system which

Table 2: Mitochondrial receptors and their ligands involved in the mitophagic process.

Receptor	Localization	Ligands (interaction)	Species	Reference
ATG32	Outer mitochondrial membrane	Atg8, Atg11	Yeast	[22]
NIX/BNIP3L	Outer mitochondrial membrane	LC3	Mammals	[23–25]
BCL2L13	Outer mitochondrial membrane	LC3	Mammals	[26]
FUNDC1	Outer mitochondrial membrane	LC3	Mammals	[27]
Cardiolipin	Mitochondrial inner membrane, any damage to mitochondria, or depolarization of its membrane results in the translocation to outer mitochondrial membrane	LC3	Mammals	[28]
PHB 2	Inner mitochondrial membrane	LC3	Mammals	[29]
Parkin	Normally in the cytosol, it is translocated to the outer mitochondrial membrane upon depolarization	AMBRA1, LC3	Mammals	[30]
BCL2L13	Outer mitochondrial membrane	LC3	Mammals	[31]
FKBP8	Outer mitochondrial membrane	LC3	Mammals	[32]
SMURF1	Cytoplasmatic, colocalized with damaged mitochondria	LC3?	Mammals	
BNIP3	Outer mitochondrial membrane	LC3	Mammals	[33]
NLRX1	Outer mitochondrial membrane	LC3	Mammals	[34]

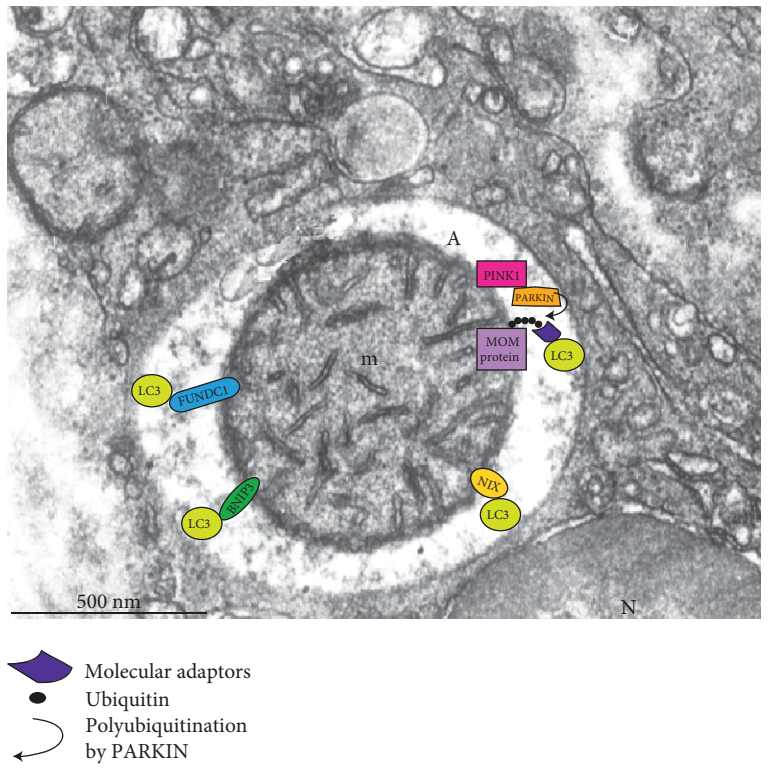

Figure 4: Electron micrograph of a mitophagic vacuole (A) containing a well-preserved mitochondrion (m). Molecules involved in selective mitophagy are indicated.

facilitate the specificity of interaction and the rapid sealing of the two opposing membranes. The detailed molecular mechanisms have been extensively reviewed by Nakamura and Yoshimori [50].

The *acidification* of the internal milieu of the phagolysosome depends on the strong activity of the "vacuolar" ATPase (V-ATPase). This protein complex acidifies the lumen of many different intracellular compartments

Table 3: Markers of mitophagy.

Marker	Localization	Species	Reference
Aup1	Mitochondrial intermembrane space	Yeast	[2]
Uth1	Cytoplasmic leaflet of the outer mitochondrial membrane	Yeast	[3]
LGG-1	Membrane of phagophore and autophagosome	Yeast	[51]
PINK1	Normally undetectable, stabilized on the outer mitochondrial membrane when mitochondria are depolarized	Mammals	[52]
Parkin	Normally in cytosol, it is translocated to the outer mitochondrial membrane when mitochondria are depolarized	Mammals	[30]
LC3-II	Cytosolic, during autophagy, recruited to form autophagosomal membranes	Mammals	[53]
p62	Parkin recruited to mitochondria	Mammals	[54]
TOM20	Outer mitochondrial membrane	Mammals	[38]
TIM23	Inner mitochondrial membrane	Mammals	[27]
CypD (cyclophilin D)	Mitochondrial matrix	Mammals	[55]
HSP60	Mitochondrial matrix	Mammals	[55]
ULK1	Recruited to fragmented mitochondria in response to hypoxia or FCCP	Mammals	[56]
SMURF1	Cytoplasmatic, colocalized with damaged mitochondria	Mammals	[57]
Mitofusins 1/2	Mitochondrial outer membrane	Mammals	[58]

(including lysosomes, phagosomes, and autophagosomes) by transporting protons against a gradient from a cytosol into the lumen of the vacuole at the expense of ATP hydrolysis. The low pH is required for lysosomal enzyme activity and for further demolition of the phagosomal content [18, 50].

The a*ctivation* of lysosomal degrading enzymes is accompanied by oxidative metabolism burst [19]. This leads to a further damage of the content, with an easier demolition, fragmentation, and digestion of the mitochondrion and other cytosolic content, and recycling or extracellular disposal of the final products.

Many autophagy-related proteins especially receptors and their interacting ligands are also known as mitophagosomal marker proteins, coded by an autophagy-specific battery of genes (Table 3).

2. Mitophagy in Cancer

Mitophagy has been linked with several physiological functions and human pathologies like neurodegenerative disease [59–61], type 2 diabetes [62], cardiac defects [63], and tumor [64]. The connection between tumor and mitophagy is complex and controversial and probably is connected to oxidative metabolism and energy homeostasis. Mitochondria are the primary site for ATP production, but they are also the place where reactive oxygen species (ROS) production and glucose metabolism occur. Generally, tumors undergo metabolic reprogramming to gain advantages with respect to surrounding cells [65, 66]. Several studies have shown that KRAS plays a pivotal role in a variety of cancers promoting readjustment of cell metabolism [67]. TBK1, a mitophagy effector, seemed to be involved in KRAS activity [68]. It is overexpressed in different kinds of malignancies such as lung, breast, and colon cancer [69], and it is requested for KRAS-driven cell transformation. TBK1 null cells infected with retrovirus encoding for KRAS were unable to proliferate and survive [70]. In KRAS-mediated lung tumors, the depletion of Atg5 or Atg7, two mitophagic effectors involved in LC3/GABARAP lipidation, has induced a reduction in tumor burden and an increase in survival compared to the counterpart even if malignancies present a faster tumor-initiation stage [71, 72]. Parkin also plays an important role in cellular metabolism balance. It has been discovered that Parkin is a p53 target gene and contributes to p53 glucose metabolism regulation and mitochondrial respiration [73]. In fact, Parkin can mediate the p53 reduction of the Warburg effect decreasing cellular glucose uptake and lactate release [74]. Parkin-mediated glycolysis reduction can also be performed through PKM2 regulation. It has been shown that Parkin can ubiquitinate this isoform of pyruvate kinase and can reduce its enzymatic activity [75]. But the role of Parkin and glycolysis regulation is contentious. In fact, Parkin can positively regulate the expression of PDHA1 reducing, in this way, mitochondrial oxidative phosphorylation and increasing the glycolytic pathway [74, 76].1Because the Warburg effect represents a hallmark of cancer cells that, using aerobic glycolysis, try to sustain the energetic demand, it is clear that mitophagy and cancer can be strongly related. Hypoxia-inducible factor 1 (HIF-1),

one of the major drivers of metabolic rewiring in cancer, is involved in mitochondrial autophagy. Through the induction of BNIP3, HIF-1 triggers mitophagy as a metabolic shift due to hypoxia and prevents ROS increase and cell death [26]. Lipid metabolism is an important biochemical step in tumorigenic cells that can either increase endogenous synthesis or promote lipid uptake to face the demand for biomass [77]. Parkin, in turn, can stabilize CD36, a fatty acid transporter, through a ubiquitin-mediated process and regulate lipid transport [78].

Genetic instability is known to be a common factor in a wide range of cancer [79]. Modification in copy number, amplifications, and mutations in genes involved in mitophagy are frequent in several tumors, and this raises the possibility that all these alterations provide an advantage for tumor growth. In colorectal cancer, for example, Parkin is deleted in 25% of cases [80] and 33% of patients revealed the heterozygous loss of the gene above [81]. A tumor suppressive role of Parkin is also detected in breast cancer where the blockage of mitophagy influences tumor progression [82, 83] and in hepatocellular carcinoma where mouse knockout for this gene showed enhanced growth of hepatic tumors [84]. Looking at the glioblastoma, the role of Parkin seems to be under debate. The TCGA database showed that a quarter of patients affected by glioblastoma exhibited a partial or total loss of *PARK2* (gene encoding for Parkin) [85] but has also demonstrated that silencing of Parkin can be related to the arrest in tumor growth through the cooperation with the Notch signaling pathway [86]. PINK1 resulted to be altered in several cancers such as ovarian cancer, glioblastoma, and neuroblastoma [87–89] and the same came from BNIP3 screening. BNIP3 appeared to be lost in invasive breast cancer [90] and in almost 60% of pancreatic cancer patients where it correlated with poor survival [91]. In fact, pancreatic cancer cells showed hypermethylation of the BNIP3 promoter that prevented HIF-1 binding and the subsequent activation of mitophagy that restrained mitochondrial mass and ROS production [92]. The correlation between BNIP3 and tumor progression/metastasis formation is investigated in triple negative breast cancer where BNIP3 null tumor cells enhanced ROS formation that, in turn, led to HIF1 alpha activation and invasive phenotype [93]. Also, FUNDC1 expression has been correlated to the initiation and progression of hepatocarcinogenesis. In a mouse model, the hepatocyte-specific knockout of FUNDC1 revealed a blockage in mitophagy characterized by an increase in mtDNA release and inflammasome activation that contributes to tumorigenesis [94]. It is an arduous task to predict the role that mitophagy has on cancer cells because it depends on different factors like cancer type, cancer stage, genetic background [95], and equilibrium between cellular demand and availability; according to the scenario, mitophagic alterations can have a dual role acting as cancer suppressors like during Atg5 or Atg7 depletion or promoters like BNIP3, FUNDC1, and PINK1 deficiency.

The connection between the immune system and cancer has been widely studied in the last decades due to the capability to be both enemies and allies [94]. In some cancers, the presence of a particular kind of immune cells in a tumor microenvironment can help to understand patient outcome. It is the case of colorectal cancer where $CD8^+$ T cells infiltrating tumor are associated with prolonged survival and a better prognosis than T helper 17 cells [95]. It has been reported that increased mitophagy, in intestinal epithelial cells, enhanced lysosomal membrane permeabilization and stimulated MHC I presentation and $CD8^+$ T cell activation showing the intrinsic antitumor function of mitophagy [95]. Also in lung cancer, autophagy/mitophagy is coupled to immunosurveillance [71]. $Kras^{G12D/+}$ $Atg5^{fl/fl}$ mice were characterized by the presence of a remarkable number of regulatory T cells (Tregs) known to suppress the immune system and responsible for the improved tumor initiation in these mice compared to the control group [71].

A plethora of genes that are not direct effectors of mitophagy resulted to be altered in malignancies. Their role has been studied, and a hypothetical correlation with mitochondrial autophagy has been developed. This is the case of YAP (yes-association protein), a downstream effector of the Hippo signaling pathway, and Bif 1 (a member of endophilin family proteins) that resulted to be altered in a variety of cancers [96–100]. Lately, the role of YAP in activating mitophagy via the SIRT1/Mfn2 axis and its contribution in migration and viability in gastric cancer have been highlighted. In fact, through the preservation of SIRT1 activity, YAP can sustain the Mfn2-mediated mitophagy, reduce ROS production, and increase ATP generation, involved in cell migration support [101]. Bif-1, conversely, is crucial for mitophagy because it regulates the maturation of autophagosome. The Bif-1 haploinsufficiency caused the accumulation of immature autophagosomes leading to damaged mitochondria and increased ROS production that has promoted MYC-driven lymphomagenesis [102].

Mitophagy seems to be also involved in cancer-induced cachexia where the analysis of the transcriptome dataset revealed the upregulation of genes involved in phagophore elongation and maturation that characterize the latest step of mitophagy [103]. An increase in the activity of lysosomal proteases has been reported in the cachectic muscle in tumor-bearing mice [104]. Furthermore, the skeletal muscles from cancer patients and mouse models have shown an increase of mitophagic parameters [105, 106]. The mitochondrial involvement in cancer-induced cachexia remains to be elucidated, but this can open the opportunity to new therapeutic strategies to reduce muscle wasting that impairs further the quality of life of cancer patients.

Because of the dual role the mitophagy has in cancer depending on different situations and cell types, a variety of studies have been developed to understand the impact the mitophagy has on chemotherapy. The efficiency of damaged mitochondrial clearance can mediate drug resistance in tumor cells [107] since the evidence indicating that chemotherapeutic drugs can induce mitochondrial dysfunction and ROS production [108]. Different agents as ceramide and ceramide analogs, causing lethal mitophagy, have been used in cancer therapy to induce cancer cell death

[14, 109] and decrease drug resistance [110]. On the other hand, mitophagy inhibitors can enhance chemotherapeutic sensitivity. Doxorubicin, salinomycin, and UNBS1450, drugs used for cancer treatment, resulted to be more effective during mitophagy inhibition [107, 111, 112]. Understanding mitophagy behavior during cancer development and growth can help to discern if mitochondrial autophagy acts as tumor promoter or suppressor. Inhibiting or activating mitophagy can be crucial for the therapy success. All these reasons highlight the relevance of this process and drive researchers to develop new drugs to regulate it.

3. Mitophagy in Aging

Mitochondria are the energy center of cells. Mitochondrial maintenance is a prerequisite for the homeostasis of cells and organisms. The equilibrium between mitochondrial biogenesis and mitochondrial removal is crucial for a healthy system. Several studies focused on the evidence the accumulation of nonfunctional mitochondria, therefore defective mitophagy, may have with aging and age-related disorders [113]. Aging is a process known to be regulated by a preserved signaling pathway. Alterations in those pathways along with perturbations in mitochondrial functions and efficiency lead to cellular and tissue degeneration [114]. AMPK is a regulator of energy metabolism [115] and has been associated with mitophagy [116]. AMPK, activated by various stress stimuli, can promote autophagy and mitochondrial autophagy through mTOR inhibition [117] or ULK1 activation [118]. Thus, AMPK stimulation could represent an option to fight age-related diseases and prolong survival. In fact, it has been reported that mTOR downregulation is involved in extended lifespan in Drosophila and mice [119]. AMPK can also interact with Sirt1, a member of the sirtuin family known to play a pivotal role in metabolism and aging [120]. SIRT1, along with other sirtuins, induced an alteration in the NAD+/NADH ratio that decreased during aging in a variety of organs [121, 122]. Sirt1 has been associated with mitophagy starting from some evidence such as excessive mitochondrial damage in Sirt1 knockout mice [123], deregulation of Pink1, and impaired mitochondrial autophagy in NAD+-Sirt1-Pgc-1 alpha axis alteration [124].

The aging process is one of the principal risks for neurodegenerative diseases like Alzheimer (AD) and Parkinson's disease (PD), and Fuchs Endothelial Corneal Dystrophy (FECD). AD is the most common neurodegenerative disorder and is characterized by neurofibrillary tangles and plaques containing amyloid-β peptide [125]. Numerous evidences linked alterations in mitochondrial quality control with AD [126]. Using a triple transgenic mouse with perturbations in APP (amyloid beta precursor protein), Tau and PS1 have shown that Parkin ubiquitinated Aβ and reduced its levels stimulating its degradation in a Beclin-dependent manner [127]. Experiments in a variety of mouse models of AD showed that the administration of NAD+ precursors could reduce Aβ plaques and the cognitive decline [128, 129]. The authors attributed the reduction of AD phenotype to the ability of NAD+ to increase Sirt1 activity as discussed above. Through the upregulation of proteins involved in autophagy/mitophagy [6] or the FOXO3-NIX axis [51] or the interaction with PGC-1α and Parkin [130], NAD +/SIRT1 can improve mitophagic activity and neuronal survival [131]. Several pieces of evidence link Parkinson to mitophagy; first of all, the mitochondria are defective (alteration in complex I of electron transport chain) [132]; second, Parkin and PINK 1 resulted mutated in PD patients [133]; and third, these mutations caused perturbations in mitochondria clearance [134]. In *Drosophila melanogaster*, knockouts of PINK 1 and Parkin have induced impaired mitophagy leading to defective dopaminergic neurons and locomotion [135]. Unfortunately, when these genes were manipulated in mice, researchers did not obtain the same phenotype [133]. Mice null for Parkin were bred with mice constituted by mutations in mtDNA polymerase; the offspring showed degeneration of dopaminergic neurons implying that the inability to repair and remove mutated mtDNA through mitophagy was linked to Parkinson-like pathologies [136]. In sporadic and familiar cases of PD, a decrease in Miro (MOM protein removed right before the beginning of mitochondrial clearance) has been reported [137]. Leucine-rich repeat kinase 2 (LRRK2), PINK 1, and Parkin were the three genes highly mutated in those patients. LRRK2 loss of function was unable to interact with Miro, and the mitophagy initiation was delayed causing neurodegeneration [137]. A recent study showed that USP30, a mitochondrial deubiquitinase, antagonized Parkin and PINK 1 activities. Thus, USP30 removed ubiquitin from damaged mitochondrial proteins and inhibited mitophagy. USP30 knockout in dopaminergic neurons can improve mitochondrial clearance and locomotion rescuing the defective mitophagy caused by mutations in Parkin and PINK 1. In this scenario, USP30 inhibitors can represent a potential target for PD [46]. FEDC is the most common degeneration of corneal endothelial cells during aging. The authors demonstrated that induction of mitophagy was involved in the reduction of mitochondrial mass and functional mitochondria. The analysis of tissues from FEDC patients revealed autophagic structures containing mitochondria that were indicative of an upregulated auto/mitophagy. To validate the role of mitophagy in FEDC, a decline in Mfn2, an important fusion protein, was detected confirming that the fusion capacity was lost and the fission-mediated mitophagy prevailed [138]. Despite the role the mitophagy plays in age-mediated diseases, as we know, mitochondria are the place where ROS are produced [139]. ROS are known to induce mutations into the nuclear DNA and mtDNA. The repair machinery in the mitochondria is less efficient compared to the one inside the nucleus, and this impairs the synthesis of enzymes involved in oxidative phosphorylation leading to an energetic failure. Thus, in this scenario, mitophagy can be seen as a mechanism to prevent the accumulation of mtDNA mutations and the development of age-associated diseases like cancer, diabetes, and neurodegenerative diseases.

The correlation between mitophagy and age-related muscle wasting and sarcopenia has been under debate

in the last decades. In a muscle, autophagy declines with aging contributing to tissue degeneration [140, 141]. Lately, it has been documented that aged skeletal muscle is characterized by an increase of autophagic/mitophagic proteins [142, 143]. A very recent study showed that, using a model of aging, the Fisher 344 Brown Norway Hybrid rat, an enhancement in mitophagy flux and increasing in mitophagy receptors was detected in an aged muscle. This observation was by the reduced presence of organelles in those muscles [144]. Also, lysosomes, involved in autophagosomal content degradation, decreased in muscle during aging [143]. Not much is known about the effect of exercise on mitophagy in an aged muscle. After chronic contractile activity (CCA), muscles were characterized by an increase in the mitochondria even if it was less evident than the younger counterpart. CCA also induced a reduction of TFEB expression, the primary regulator of lysosomal biogenesis, contributing, perhaps, to the mitochondrial asset in an aged muscle [144]. Using denervation and unilateral hind limb immobilization as a model of muscle disuse, it has been demonstrated that mitochondrial autophagy was increased [145, 146] and the silencing of Parkin was sufficient to avoid mitochondria clearance in the soleus muscle preventing the maintenance of healthy organelles [147].

Aging is also known to increase the liver sensitivity to ischemia/reperfusion (I/R) via induction of mitochondrial damage and malfunction [148]. Thinking about the increasing possibility to use elderly patients as potential liver donors, a recent study highlighted the role the defective mitophagy plays in this process. The authors demonstrated that mitophagy protected the liver from I/R injury, in fact, decreasing in Parkin and Atg5 detected in old mice's liver during hepatic I/R injury. Using salubrinal, an inhibitor of the protein phosphatase PP1 involved in EIF2α dephosphorylation has obtained an induction of Parkin and mitophagy after reperfusion enhancing the response to I/R injury [149].

4. Mitophagy and Sirtuins

Sirtuins represent a new class of proteins that, recently, has been deeply involved in controlling several pathways linked to mitophagy. In fact, sirtuins are a class of seven (SIRT1-7) NAD+-dependent deacylases with ever-growing intracellular targets: histones, transcription factors, metabolic enzymes, structural proteins, etc. [150]. Due to the NAD+ dependence, sirtuins can sense the metabolic status of the cell and increase or decrease their activity in order to maintain homeostasis [151]. In fact, sirtuin activity increases during caloric restriction or in the presence of natural activators such as resveratrol [152], curcumin [153], and piceatannol [154]. On the contrary, sirtuin activity decreases during high-fat diet [155, 156]. Moreover, sirtuin activity is fundamental for the cellular response to stresses such as hypoxia, exercise, and ROS accumulation [157–160].

Recently, sirtuin expression and activity have been linked, either directly or indirectly, to the control of mitophagy during diverse pathological conditions such as cancer, neurodegeneration, diabetes, and sepsis as well as during aging, chemotherapy toxicity, and starvation [161–166].

However, up to date, an involvement in mitophagy control has been demonstrated only for SIRT1, SIRT2, and the mitochondrial sirtuins SIRT3, SIRT4, and SIRT5.

In particular, loss of SIRT1 has been associated to decreased mitophagy and delayed PARK2 accumulation in the mitochondria in prostatic intraepithelial neoplasia. Loss of SIRT1, observed in the luminal epithelium of human prostate cancer, determined an accumulation of ROS and an inactivation of SOD2 an effect that, in turn, caused a deregulation of mitophagy, and it was at the basis of the worsening of the patient outcome [166]. Altered mitophagy due to SIRT1 decrease has also been demonstrated in Xeroderma pigmentosum group A (XPA) as well as ataxia-telangiectasia (AT) and Cockayne syndrome (CS), all associated with neurodegeneration and cancer. In this case, mitophagy deregulation is due to the activation of PARP1 that, in turn, caused the decrease of NAD+-SIRT1-PGC-1a-UCP2 axis. In fact, both PARP1 inhibitor and NAD+ precursor can rescue XPA cells and increase lifespan in xpa-1 nematodes [124]. Low levels of MKK kinase associated with high levels of Sirt1 diminished lethality of sepsis in mice through an activation of mitophagy removal of damaged mitochondria and activation of PGC-1a-induced mitochondriogenesis [167]. In cancer, SIRT1 activation by a new compound increased autophagy/mitophagy thereby reducing glioblastoma growth in vitro and in vivo [168]. However, mitophagy activation can also increase tumor survival as observed in gastric cancer where survival and migration of cancer cells were maintained by YAP-Hippo-Sirt1-MFN2 activation of mitophagy [101]. SIRT1 upregulation increased mitophagy in an infarcted heart following liraglutide treatment. Such an effect is achieved through the SIRT1-driven increase of Parkin leading to mitophagy activation [169]. Another important aspect that must be considered is that different sirtuins can interact with each other to regulate mitophagy. In fact, SIRT1 can deacetylate and activate SIRT3 that, in turn, controls mitochondrial health also by regulating mitophagy. In particular, in obese and old mice, low levels of Sirt1 are accompanied by hyperacetylated Sirt3 and dysfunctional mitochondria [170].

The involvement of SIRT2 in mitophagy control has been demonstrated in the brains of Sirt2 knockout mice that revealed a dysregulation of mitochondrial proteins and mitophagy with the appearance of small and irregular mitochondria [165]. Moreover, SIRT2 ablation following vincristine treatment activated mitophagy and apoptotic cell death in the breast cancer cell line MDA-MB-231. In this situation, SIRT2 loss determined acetylation of HSP70 that, in turn, was responsible for mitophagy activation [171].

The role of SIRT3 in mitophagy regulation has been extensively documented in several pathologies. In fact, activation of SIRT3 was associated with induction of mitophagy to control mitochondrial homeostasis and remove dysfunctional mitochondria in mammalian cells. However, in the case of tumor cells, this may result in increased survival as demonstrated in glioma and breast cancer cell lines under hypoxia. In this situation, tumor cells

increased SIRT3-driven mitophagy to counteract the damaging effects of oxygen reduction to a point that SIRT3 inhibition increased apoptotic cell death and ROS accumulation [172]. On the contrary, SIRT3-increased mitophagy was important for survival of myocardiocytes. In fact, Sirt3 KO worsened the development of diabetic cardiomyopathy (DCM) in a mouse model because of the impairment of the Foxo3A and Parkin pathway with reduction of mitophagy [173]. Similar results were obtained in aged hearts from Sirt3 KO mice that revealed a decrease in MnSOD, an increase in ROS, and an impairment of Parkin-mediated mitophagy [163]. These results suggested that a strategy is aimed at increasing SIRT3 expression and/or activity may ameliorate the outcome of cardiac pathologies linked to diabetes, aging, etc. It is worth noting that Sirt3 also activated mitophagy and cardiomyocyte survival in aged rats with stable myocardial infarction (MI). In particular, Sirt3 levels increased after short-term exercise in these rats with reduction of ROS and activation of mitophagy [174].

SIRT3 has also shown an important role in protecting hepatocytes during nonalcoholic fatty liver disease. In vivo studies have shown that Sirt3 overexpression increased Bnip3 level to activate mitophagy thereby maintaining functional mitochondria. Moreover, Bnip3 expression depends on the ERK-CREB pathway [161]. SIRT3 overexpression in amniotic fluid stem cell (AFSC) transplantation as a therapeutic strategy for diabetic nephropathy increased mitophagy and ameliorated the glucose metabolic parameters in vivo [162]. Therefore, SIRT3 overexpression or activation may be used to improve the outcome of stem cell therapy because of its prosurvival effects of these cells.

The less studied SIRT4 has been recently associated with mitophagy inhibition during aging. In fact, in aged fibroblasts, SIRT4 induction increased mitochondrial ROS production and associated with L-OPA1 to promote mitochondrial fusion. Such elongated mitochondria accumulate in aging fibroblast and are not removed by mitophagy thereby accelerating the aging process [164].

Similarly, to the other two mitochondrial sirtuins, also, SIRT5 has been linked to mitophagy. Inhibition of SIRT5 expression or activity in tumor cells or in myoblasts was accompanied by a reduction of BNIP3 and mitophagy. In these cells, SIRT5 interacted and inhibited mitochondrial glutaminase 1 impairing glutamine metabolism with reduction of ammonia levels. Ammonia reduction resulted in inhibition of autophagy and mitophagy [175]. Moreover, during starvation, SIRT5 targeted fission proteins to reduce their expression. This resulted in an elongation of mitochondria that cannot be removed by mitophagy. Therefore, SIRT5 helps to maintain mitochondria population during starvation [176].

In the case of the nuclear sirtuin SIRT6 and the nucleolar sirtuin SIRT7, no connection with mitophagy has been documented so far.

Finally, some important points arise from the scientific literature connecting sirtuins and mitophagy: (1) Mitochondrial sirtuins have crucial and opposing roles in regulating mitophagy. So far, SIRT3, the most abundant mitochondrial sirtuin, has always been linked to mitophagy activation. On the contrary, SIRT4 and SIRT5 have been linked to mitophagy inhibition. These opposing effects may be revealed important for the correct mitochondrial homeostasis. (2) There is a crosstalk between nuclear and mitochondrial sirtuins. In fact, SIRT1 can regulate SIRT3 expression by controlling the assembling of transcription factors on the SIRT3 promoter [177]. Moreover, SIRT1 can deacetylate and activate SIRT3 that can then efficiently regulate mitochondrial homeostasis through mitophagy [170]. (3) Sirtuins can control different metabolic pathways. In fact, emerging evidences indicate that mitochondrial sirtuins regulate not only glucose but also amino acid (glutamine) and fatty acid metabolism. The molecular details and importance of these global metabolic controls are still to be unraveled.

5. Mitophagy and ROS

The mitochondria are the main intracellular compartment responsible for reactive oxygen species (ROS) production. ROS generation represents a byproduct of oxidative phosphorylation, and although optimal ROS levels are essential for the regulation of physiological and biological mechanisms, ROS accumulation can alter macromolecules affecting cellular homeostasis and mitochondrial function [178]. A lot of studies suggested that damaged mitochondria can contribute to disease development and progression including NLRP3 inflammasome-related diseases. NLRP3 inflammasome enhanced innate immune defenses through proinflammatory cytokines, and its activation can be ROS-mediated [179]. A variety of stress stimuli can induce the production of ROS from the mitochondria [180]. It has been demonstrated that the blockage of complex I can increase ROS production that is positively correlated with proinflammatory cytokines like IL-1β in THP1 macrophages while the knockdown of NLRP3 did not cause the same phenomenon [181]. Dysregulated ROS-generating mitochondria are eliminated by mitophagy; therefore, inhibition of this process can increase ROS production and IL-1β secretion leading to chronic inflammatory diseases [181]. Mitophagy plays an important role also in hyperglycemia- (HG-) induced ROS overproduction; in fact, different studies showed how preventing mitochondrial dysfunction can reduce ROS concentration and endothelial damage in mice and patients affected with diabetes mellitus [182, 183]. Recently, it has emerged that mesenchymal stem cell (MSC) treatment can increase the expression of two mitophagic effectors, Parkin and Pink, reduce ROS production, and improve high-glucose-induced endothelial injury, consequently [184]. A cytoprotective role of ROS has been identified as well [185]. In fact, ROS generated during liver ischemia/reperfusion injury (IRI) in liver epithelial cells (LEC) have a regulatory role that involved the mitophagic pathway. It has been demonstrated, in *in vitro* and *in vivo* models, that ROS generation after IRI can lead to ATG7-dependent mitophagy and induce LEC survival [186]. ROS can also represent a mitophagy fuel [187, 188]. Studying the role of prooxidants, it has been observed that superoxide can drive Parkin-Pink-

mediated mitophagy and this process required the p38 signaling pathway [188].

The main consequence under ER stress is the ROS production [26, 189, 190]. It has been demonstrated that miRNA-346 is induced under ER stress, and it is involved in autophagy/mitophagy activation to facilitate cell survival [191]. In fact, an increase of ROS during ER stress can be harmful to cancer cells [192]. In this scenario, miRNA-346 promoted mitophagy activation via GSK3β and reduced ROS preserving cell viability [191].

It is known that redox and O_2 homeostasis are strictly connected. Hypoxia stimulates ROS increase leading to hypoxia-inducible factor-1α (HIF-1α) stabilization [193]. Reduced O_2 concentration and increase of ROS also induce the inhibition of the prolyl hydroxylases responsible for HIF-1α degradation [194, 195]. HIF-1α activates mitophagy in a BNIP3-dependent manner producing a metabolic adaptation that allows cell survival and ROS decrease in a hypoxic environment in MEF cells [26], and BNIP3 absence in mammary tumor cells increases the Warburg effect, followed by ROS increase and tumor progression [93]. The same correlation has been evaluated in gastric cancer cells where mitophagy played a role in cancer aggressiveness [196]. In fact, mtROS production triggered by hypoxia was under the control of mitophagy and when this process was impaired, mtROS concentration increased and stabilized HIF-1α along with an aggressive phenotype [196].

6. Mitophagy and Nanoparticles

The term nanomaterial includes particles with a size range between 10 and 100 nm [197] and a shape that is directly correlated to biodistribution efficacy as carriers and interaction with the target tissues [198]. The most common are nanospheres and nanorods, but new nanocrystals have been developed [198]. Several studies have been promoted to evaluate the effect of nanoparticles on organisms. The majority of those studies focused on the interaction of nanoparticles in blood vessels and the extracellular matrix [199, 200]. Interestingly, pharmacokinetics studies of metallic nanoparticles have shown a shorter blood half-life in rodents than in pigs or monkeys, an effect that should alert investigators on the use of small laboratory animals in the case of metallic NPs [200]. Their physicochemical characteristics (size, shape, aggregation, chemical composition, cellular uptake, etc.) constitute a big advantage in using these systems [201, 202], but nanotoxicity represents a limit in their extensive application [203, 204]. Researchers described apoptosis, oxidative stress, autophagy, and mitophagy as mechanisms of toxicity during nanoparticle-related uptake in in vitro [205–207] and in vivo systems [205].

Titanium dioxide nanoparticles (TiO_2-NPs) are the most common nanoparticles, and they can easily cross biological barriers [208]. In vivo, toxicity of TiO_2-NPs has been studied in microorganisms, algae, invertebrates, and vertebrates [203]. In particular, TiO_2-NPs exert their action by causing lipid peroxidation thereby damaging membrane structures. However, once inside the cell, TiO_2-NPs can damage organelles such as the mitochondria [203], an effect that, even if not yet proved, might promote mitophagy. Recently, the in vitro treatment of human trophoblast cells with TiO_2-NPs caused an increase in oxidative stress and mitophagy was detected. PINK 1 and Parkin accumulated in the mitochondria and LC3-II/LC3-I, p62, and Beclin1 increased as well [207].

The same effect was observed in hepatic cells and CAL 27 cells treated with SPIO-NPs (*superparamagnetic iron oxide nanoparticles*) [209] and ZnO-NPs (*zinc oxide nanoparticles*) [210], respectively. In vitro, through the increase of ROS content, these two different nanoparticles activated PINK1 that caused mitophagy through Parkin phosphorylation. Interestingly, this study also suggested that an increase in PINK1 fluorescence can be used as a tool to assess the induction of mitophagy upon nanoparticle exposure. A connection between ZnO-NPs and mitophagy has also been demonstrated, always in vitro, in murine microglia BV-2 cells. In fact, the treatment of BV-2 cells with increasing micromolar doses of ZnO-NPs increased ROS production and the association and mitochondrial translocation of the PINK 1-Parkin complex with the induction of mitophagy. Interestingly, if PINK1 was silenced, there was no PARKIN accumulation into the mitochondria an effect that increased ZnO-NP toxicity. These results confirmed the protective role of mitophagy [211].

Another interesting nanomaterial is represented by *gold nanoparticles* (AuNPs). In non-small-cell lung cancer (NSCLC) cells, AuNPs increased TRAIL toxicity by upregulating mitochondrial fission protein DRP1 and mitochondrial fragmentation followed by mitochondrial dysfunction that cannot be reversed by mitophagy [212].

Mesoporous silica nanoparticles (MSNPs) may be used in biomedical applications and drug delivery to different human body areas. In endothelial cells and neurons, MSNPs with a diameter higher than 30 nm induced mitochondrial damage followed by mitophagy to remove dysfunctional mitochondria. The authors, therefore, suggested that future in vivo experiments should use MSNPs with a diameter below of 30 nm to reduce cellular toxicity [213].

In vitro studies have also been conducted on the possible correlation between *copper oxide nanoparticle* (CuONP) toxicity and hydrogen peroxide [214, 215]. The majority of ROS production is imputed to damaged mitochondria, as discussed above, and growing evidence suggests the implication of mitochondrial dysfunction in CuONP-mediated toxicity [214, 215]. It has been demonstrated that CuONPs induced anion superoxide production that, in turn, leaded to an increase in the initial steps of mitophagic flux. These copper oxide nanoparticles are located in lysosomes inside the cell where generated lysosome dysfunction inhibits mitophagy and promotes cell death [216].

Another important aspect pertains to the possibility to modify nanoparticles (NPs) so to facilitate not only cellular uptake but also their delivery to mitochondria. To this effect, NPs have been conjugated to peptides followed by immunofluorescence. Results have demonstrated that *NP-peptide conjugates* targeted mitochondria,

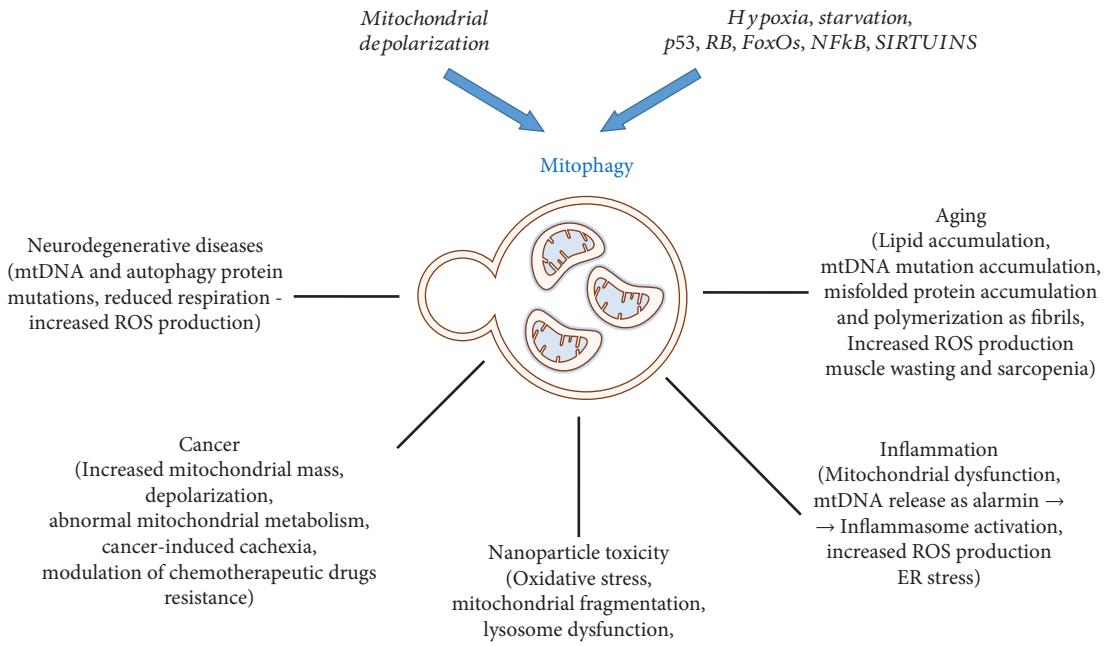

Figure 5: Schematic representation of all the aspects related to mitophagy. Two basic mechanisms have been elucidated involving a different set of molecules in relation to the prototype damage: the mitochondrial depolarization and hypoxia, starvation, and genes controlled by some master transcription factors (p53, RB/E2F, FoxOS, NFkB, sirtuins, and others).

causing membrane depolarization thereby inducing mitophagy [217]. These pilot, in vitro, experiments can help to understand the interaction between NPs and cells as well as the modifications that can increase the delivery efficacy of drugs by using NPs.

Since nanoparticles will most likely represent an important tool in future medicine, the most pressing problem concerns the little we know about their *acute* and *chronic* toxic effects on the human body [218]. This aspect has been extensively reviewed elsewhere [219, 220]. The most important aspect of NPS to consider when talking of toxicity depends on their size, composition, shape, and the large surface to mass ratio. In fact, for each type of NP, toxicity must be unraveled through in vitro and in vivo experiments. So far, a large number of in vitro experiments have been performed demonstrating how plasma membrane alteration, oxygen reactive species production, and uptake and modification of intracellular pathways cause cell damage and death. On the contrary, only a few in vivo experiments have been conducted as reviewed in [200] and [221]. On the other hand, in vivo experiments will take a considerable amount of time and high costs, and therefore, there is also a need for reliable in vitro models where to test NP toxicity [221].

Finally, in the case of mitochondria, NP effects regarding the role of autophagy and mitophagy are largely incomplete. However, a result emerging so far is that the mitophagic process observed with NPs is largely due to the NP-induced ROS accumulation that, in turn, would activate PINK 1 and/or PARKIN. A direct effect of NPs on the mitochondria to activate mitophagy might be prompted by NPs crossing the damaged plasma membrane and accumulating in the mitochondrial outer membrane or in the case of engineered NPs with mitochondria-targeted peptide.

Nonetheless, evaluating all the mechanisms that trigger nanotoxicity-mediated autophagy and mitophagy can offer a way for the toxicity assessment, for pharmacological interventions to achieve improvements for a better nanoparticle biosafety.

7. Conclusion

The mitochondria affected by oxidative damage and aging need adequate clearance carried out by the mitophagic process coupled with mitochondrial neogenesis (growth and fission). These are essential mechanisms for the cell to adapt and respond to changing energetic requirements. Therefore, as discussed in this review, abnormal mitophagy is involved in a variety of pathologic processes such as cancer, age-related diseases, and neurodegenerative and oxidative stress disorders (Figure 5). The alteration of mitophagy has an effect related to the environment, downstream and upstream effectors, cell status, etc. In addition, the fact that nanotoxicity is mediated through autophagy and mitophagy underlines the delicate role those processes have inside the cell in determining cellular health and survival. According to the context, mitophagic changes can play a promoting or inhibitory role in tumorigenic cells triggering a cascade of effects inside the cell or acting indirectly on different complexes such as the immune system. As cancer, age-related neurodegenerative diseases remain still without an effective cure. A lot of data elucidated the connection between mitophagy and age-related illnesses and how small alterations in mitochondrial autophagy can have amplified consequences on the neurons, eyes, muscles, myocardium, and liver. Alterations in ROS production as a result of defective mitophagy can act on a broad spectrum of targets like inflammatory

cytokines, hyperglycemia-related pathologies, liver ischemia/reperfusion injury, and HIF-mediated arrangements. Still a lot of work remains to do to fully know the mechanisms and the interactions behind each of them, but it seems possible that the future understanding of a variety of disease can go through the mitophagic process.

Conflicts of Interest

No conflicts of interest, financial or otherwise, are declared by the authors.

Acknowledgments

This work was supported by Ricerca Corrente 2017 and by Fondazione Roma to MAR and by Ricerca Scientifica Ateneo 2017 to MT.

References

[1] R. J. Youle and D. P. Narendra, "Mechanisms of mitophagy," *Nature Reviews Molecular Cell Biology*, vol. 12, no. 1, pp. 9–14, 2011.

[2] R. Tal, G. Winter, N. Ecker, D. J. Klionsky, and H. Abeliovich, "Aup1p, a yeast mitochondrial protein phosphatase homolog, is required for efficient stationary phase mitophagy and cell survival," *Journal of Biological Chemistry*, vol. 282, no. 8, pp. 5617–5624, 2007.

[3] I. Kissová, M. Deffieu, S. Manon, and N. Camougrand, "Uth1p is involved in the autophagic degradation of mitochondria," *Journal of Biological Chemistry*, vol. 279, no. 37, pp. 39068–39074, 2004.

[4] M. Sato, K. Sato, K. Tomura, H. Kosako, and K. Sato, "The autophagy receptor ALLO-1 and the IKKE-1 kinase control clearance of paternal mitochondria in Caenorhabditis elegans," *Nature Cell Biology*, vol. 20, no. 1, pp. 81–91, 2018.

[5] K. Tsubouchi, J. Araya, and K. Kuwano, "PINK1-PARK2-mediated mitophagy in COPD and IPF pathogeneses," *Inflammation and Regeneration*, vol. 38, no. 1, 2018.

[6] E. F. Fang, H. Kassahun, D. . L. Croteau et al., "NAD + Replenishment Improves Lifespan and Healthspan in Ataxia Telangiectasia Models via Mitophagy and DNA Repair," *Cell Metabolism*, vol. 24, no. 4, pp. 566–581, 2016.

[7] Y. Qi, Q. Qiu, X. Gu, Y. Tian, and Y. Zhang, "ATM mediates spermidine-induced mitophagy via PINK1 and Parkin regulation in human fibroblasts," *Scientific Reports*, vol. 6, no. 1, 2016.

[8] D. Ryu, L. Mouchiroud, P. A. Andreux et al., "Urolithin A induces mitophagy and prolongs lifespan in C. elegans and increases muscle function in rodents," *Nature Medicine*, vol. 22, no. 8, pp. 879–888, 2016.

[9] Q. Li, S. Gao, Z. Kang et al., "Rapamycin enhances mitophagy and attenuates apoptosis after spinal ischemia-reperfusion injury," *Frontiers in Neuroscience*, vol. 12, 2018.

[10] Y. Song, W. Lee, Y.-h. Lee, E. Kang, B.-S. Cha, and B.-W. Lee, "Metformin Restores Parkin-Mediated Mitophagy, Suppressed by Cytosolic p53," *International Journal of Molecular Sciences*, vol. 17, no. 1, p. 122, 2016.

[11] M. Redmann, G. A. Benavides, T. F. Berryhill et al., "Inhibition of autophagy with bafilomycin and chloroquine decreases mitochondrial quality and bioenergetic function in primary neurons," *Redox Biology*, vol. 11, pp. 73–81, 2017.

[12] A. Frustaci, E. Morgante, D. Antuzzi, M. A. Russo, and C. Chimenti, "Inhibition of cardiomyocyte lysosomal activity in hydroxychloroquine cardiomyopathy," *International Journal of Cardiology*, vol. 157, no. 1, pp. 117–119, 2012.

[13] Y. Zhu, G. Chen, L. Chen et al., "Monitoring mitophagy in mammalian cells," *Methods in Enzymology*, vol. 547, p. 39, 2014.

[14] R. D. Sentelle, C. E. Senkal, W. Jiang et al., "Ceramide targets autophagosomes to mitochondria and induces lethal mitophagy," *Nature Chemical Biology*, vol. 8, no. 10, pp. 831–838, 2012.

[15] E. H. Kim and K. S. Choi, "A critical role of superoxide anion in selenite-induced mitophagic cell death," *Autophagy*, vol. 4, no. 1, pp. 76–78, 2008.

[16] S. Yu and T. J. Melia, "The coordination of membrane fission and fusion at the end of autophagosome maturation," *Current Opinion in Cell Biology*, vol. 47, pp. 92–98, 2017.

[17] M. E. Maxson and S. Grinstein, "The vacuolar-type H^+-ATPase at a glance - more than a proton pump," *Journal of Cell Science*, vol. 127, no. 23, pp. 4987–4993, 2014.

[18] T. Yoshimori, A. Yamamoto, Y. Moriyama, M. Futai, and Y. Tashiro, "Bafilomycin A1, a specific inhibitor of vacuolar-type H(+)-ATPase, inhibits acidification and protein degradation in lysosomes of cultured cells," *Journal of Biological Chemistry*, vol. 266, no. 26, pp. 17707–17712, 1991.

[19] Y. Mei, M. D. Thompson, R. A. Cohen, and X. Tong, "Autophagy and oxidative stress in cardiovascular diseases," *Biochimica et Biophysica Acta (BBA) - Molecular Basis of Disease*, vol. 1852, no. 2, pp. 243–251, 2015.

[20] S. Michiorri, V. Gelmetti, E. Giarda et al., "The Parkinson-associated protein PINK1 interacts with Beclin1 and promotes autophagy," *Cell Death & Differentiation*, vol. 17, no. 6, pp. 962–974, 2010.

[21] M. Zimmermann and A. S. Reichert, "How to get rid of mitochondria: crosstalk and regulation of multiple mitophagy pathways," *Biological Chemistry*, vol. 399, no. 1, pp. 29–45, 2017.

[22] T. Kanki, K. Wang, Y. Cao, M. Baba, and D. J. Klionsky, "Atg32 is a mitochondrial protein that confers selectivity during mitophagy," *Developmental Cell*, vol. 17, no. 1, pp. 98–109, 2009.

[23] W.-X. Ding, H.-M. Ni, M. Li et al., "Nix is critical to two distinct phases of mitophagy, reactive oxygen species-mediated autophagy induction and Parkin-ubiquitin-p62-mediated mitochondrial priming," *Journal of Biological Chemistry*, vol. 285, no. 36, pp. 27879–27890, 2010.

[24] G. Bellot, R. Garcia-Medina, P. Gounon et al., "Hypoxia-induced autophagy is mediated through hypoxia-inducible factor induction of BNIP3 and BNIP3L via their BH3 domains," *Molecular and Cellular Biology*, vol. 29, no. 10, pp. 2570–2581, 2009.

[25] M. Schwarten, J. Mohrlüder, P. Ma et al., "Nix directly binds to GABARAP: a possible crosstalk between apoptosis and autophagy," *Autophagy*, vol. 5, no. 5, pp. 690–698, 2009.

[26] H. Zhang, M. Bosch-Marce, L. A. Shimoda et al., "Mitochondrial autophagy is an HIF-1-dependent adaptive metabolic response to hypoxia," *Journal of Biological Chemistry*, vol. 283, no. 16, pp. 10892–10903, 2008.

[27] L. Liu, D. Feng, G. Chen et al., "Mitochondrial outer-membrane protein FUNDC1 mediates hypoxia-induced mitophagy in mammalian cells," *Nature Cell Biology*, vol. 14, no. 2, pp. 177–185, 2012.

[28] V. E. Kagan, J. Jiang, Z. Huang et al., "NDPK-D (NM23-H4)-mediated externalization of cardiolipin enables elimination of depolarized mitochondria by mitophagy," *Cell Death & Differentiation*, vol. 23, no. 7, pp. 1140–1151, 2016.

[29] Y. Wei, W.-C. Chiang, R. Sumpter Jr, P. Mishra, and B. Levine, "Prohibitin 2 is an inner mitochondrial membrane mitophagy receptor," *Cell*, vol. 168, no. 1-2, pp. 224–238.e10, 2017.

[30] Y. Kim, J. Park, S. Kim et al., "PINK1 controls mitochondrial localization of Parkin through direct phosphorylation," *Biochemical and Biophysical Research Communications*, vol. 377, no. 3, pp. 975–980, 2008.

[31] T. Murakawa, O. Yamaguchi, A. Hashimoto et al., "Bcl-2-like protein 13 is a mammalian Atg32 homologue that mediates mitophagy and mitochondrial fragmentation," *Nature Communications*, vol. 6, no. 1, 2015.

[32] Z. Bhujabal, Å. B. Birgisdottir, E. Sjøttem et al., "FKBP8 recruits LC3A to mediate Parkin-independent mitophagy," *EMBO reports*, vol. 18, no. 6, pp. 947–961, 2017.

[33] D. Feng, L. Liu, Y. Zhu, and Q. Chen, "Molecular signaling toward mitophagy and its physiological significance," *Experimental Cell Research*, vol. 319, no. 12, pp. 1697–1705, 2013.

[34] Y. Zhang, Y. Yao, X. Qiu et al., "Listeria hijacks host mitophagy through a novel mitophagy receptor to evade killing," *Nature Immunology*, vol. 20, no. 4, pp. 433–446, 2019.

[35] V. Todde, M. Veenhuis, and I. J. van der Klei, "Autophagy: principles and significance in health and disease," *Biochimica et Biophysica Acta (BBA) - Molecular Basis of Disease*, vol. 1792, no. 1, pp. 3–13, 2009.

[36] M. Chen, Z. Chen, Y. Wang et al., "Mitophagy receptor FUNDC1 regulates mitochondrial dynamics and mitophagy," *Autophagy*, vol. 12, no. 4, pp. 689–702, 2016.

[37] Y. Li, Y. Xue, X. Xu et al., "A mitochondrial FUNDC1/HSC70 interaction organizes the proteostatic stress response at the risk of cell morbidity," *The EMBO Journal*, vol. 38, no. 3, p. e98786, 2019.

[38] N. C. Chan, A. M. Salazar, A. H. Pham et al., "Broad activation of the ubiquitin-proteasome system by Parkin is critical for mitophagy," *Human Molecular Genetics*, vol. 20, no. 9, pp. 1726–1737, 2011.

[39] C. Kondapalli, A. Kazlauskaite, N. Zhang et al., "PINK1 is activated by mitochondrial membrane potential depolarization and stimulates Parkin E3 ligase activity by phosphorylating Serine 65," *Open Biology*, vol. 2, no. 5, p. 120080, 2012.

[40] L. A. Kane, M. Lazarou, A. I. Fogel et al., "PINK1 phosphorylates ubiquitin to activate Parkin E3 ubiquitin ligase activity," *The Journal of Cell Biology*, vol. 205, no. 2, pp. 143–153, 2014.

[41] L. Wang, Y. L. Cho, Y. Tang et al., "PTEN-L is a novel protein phosphatase for ubiquitin dephosphorylation to inhibit PINK1-Parkin-mediated mitophagy," *Cell Research*, vol. 28, no. 8, pp. 787–802, 2018.

[42] M. Lazarou, S. M. Jin, L. A. Kane, and R. J. Youle, "Role of PINK1 binding to the TOM complex and alternate intracellular membranes in recruitment and activation of the E3 ligase Parkin," *Developmental Cell*, vol. 22, no. 2, pp. 320–333, 2012.

[43] K. Okatsu, T. Oka, M. Iguchi et al., "PINK1 autophosphorylation upon membrane potential dissipation is essential for Parkin recruitment to damaged mitochondria," *Nature Communications*, vol. 3, no. 1, 2012.

[44] M. E. Gegg, J. M. Cooper, K.-Y. Chau, M. Rojo, A. H. V. Schapira, and J.-W. Taanman, "Mitofusin 1 and mitofusin 2 are ubiquitinated in a PINK1/parkin-dependent manner upon induction of mitophagy," *Human Molecular Genetics*, vol. 19, no. 24, pp. 4861–4870, 2010.

[45] K. R. Pryde, H. L. Smith, K.-Y. Chau, and A. H. V. Schapira, "PINK1 disables the anti-fission machinery to segregate damaged mitochondria for mitophagy," *The Journal of Cell Biology*, vol. 213, no. 2, pp. 163–171, 2016.

[46] B. Bingol, J. S. Tea, L. Phu et al., "The mitochondrial deubiquitinase USP30 opposes parkin-mediated mitophagy," *Nature*, vol. 510, no. 7505, pp. 370–375, 2014.

[47] J. Li, W. Qi, G. Chen et al., "Mitochondrial outer-membrane E3 ligase MUL1 ubiquitinates ULK1 and regulates selenite-induced mitophagy," *Autophagy*, vol. 11, no. 8, pp. 1216–1229, 2015.

[48] M. Lazarou, D. A. Sliter, L. A. Kane et al., "The ubiquitin kinase PINK1 recruits autophagy receptors to induce mitophagy," *Nature*, vol. 524, no. 7565, pp. 309–314, 2015.

[49] A. Stolz, A. Ernst, and I. Dikic, "Cargo recognition and trafficking in selective autophagy," *Nature Cell Biology*, vol. 16, no. 6, pp. 495–501, 2014.

[50] S. Nakamura and T. Yoshimori, "New insights into autophagosome-lysosome fusion," *Journal of Cell Science*, vol. 130, no. 7, pp. 1209–1216, 2017.

[51] K. Palikaras, E. Lionaki, and N. Tavernarakis, "Coordination of mitophagy and mitochondrial biogenesis during ageing in C. elegans," *Nature*, vol. 521, no. 7553, pp. 525–528, 2015.

[52] S. M. Jin, M. Lazarou, C. Wang, L. A. Kane, D. P. Narendra, and R. J. Youle, "Mitochondrial membrane potential regulates PINK1 import and proteolytic destabilization by PARL," *The Journal of Cell Biology*, vol. 191, no. 5, pp. 933–942, 2010.

[53] G. Chen, Z. Han, D. Feng et al., "A regulatory signaling loop comprising the PGAM5 phosphatase and CK2 controls receptor-mediated mitophagy," *Molecular Cell*, vol. 54, no. 3, pp. 362–377, 2014.

[54] D. Narendra, L. A. Kane, D. N. Hauser, I. M. Fearnley, and R. J. Youle, "p62/SQSTM1 is required for Parkin-induced mitochondrial clustering but not mitophagy; VDAC1 is dispensable for both," *Autophagy*, vol. 6, no. 8, pp. 1090–1106, 2010.

[55] W. X. Ding and X. M. Yin, "Mitophagy: mechanisms, pathophysiological roles, and analysis," *Biological Chemistry*, vol. 393, no. 7, pp. 547–564, 2012.

[56] W. Wu, W. Tian, Z. Hu et al., "ULK1 translocates to mitochondria and phosphorylates FUNDC1 to regulate mitophagy," *EMBO Reports*, vol. 15, no. 5, pp. 566–575, 2014.

[57] A. Orvedahl, R. S. Jr, G. Xiao et al., "Image-based genome-wide siRNA screen identifies selective autophagy factors," *Nature*, vol. 480, no. 7375, pp. 113–117, 2011.

[58] W. X. Ding, F. Guo, H. M. Ni et al., "Parkin and mitofusins reciprocally regulate mitophagy and mitochondrial spheroid formation," *Journal of Biological Chemistry*, vol. 287, no. 50, pp. 42379–42388, 2012.

[59] J. Trinh and M. Farrer, "Advances in the genetics of Parkinson disease," *Nature Reviews Neurology*, vol. 9, no. 8, pp. 445–454, 2013.

[60] S. Lubbe and H. R. Morris, "Recent advances in Parkinson's disease genetics," *Journal of Neurology*, vol. 261, no. 2, pp. 259–266, 2014.

[61] F. Squitieri, M. Cannella, G. Sgarbi et al., "Severe ultrastructural mitochondrial changes in lymphoblasts homozygous for Huntington disease mutation," *Mechanisms of Ageing and Development*, vol. 127, no. 2, pp. 217–220, 2006.

[62] D. E. Kelley, J. He, E. V. Menshikova, and V. B. Ritov, "Dysfunction of mitochondria in human skeletal muscle in type 2 diabetes," *Diabetes*, vol. 51, no. 10, pp. 2944–2950, 2002.

[63] D. Dutta, R. Calvani, R. Bernabei, C. Leeuwenburgh, and E. Marzetti, "Contribution of impaired mitochondrial autophagy to cardiac aging: mechanisms and therapeutic opportunities," *Circulation Research*, vol. 110, no. 8, pp. 1125–1138, 2012.

[64] M. M. Alam, S. Lal, K. E. FitzGerald, and L. Zhang, "Correction to: A holistic view of cancer bioenergetics: mitochondrial function and respiration play fundamental roles in the development and progression of diverse tumors," *Clinical and Translational Medicine*, vol. 7, no. 1, p. 8, 2018.

[65] P. S. Ward and C. B. Thompson, "Metabolic reprogramming: a cancer hallmark even warburg did not anticipate," *Cancer Cell*, vol. 21, no. 3, pp. 297–308, 2012.

[66] G. Socié, M. Henry-Amar, A. Devergie et al., "Malignant diseases after allogeneic bone marrow transplantation: an updated overview," *Nouvelle revue francaise d'hematologie*, vol. 36, Suppl 1, pp. S75–SS7, 1994.

[67] J. Son, C. A. Lyssiotis, H. Ying et al., "Glutamine supports pancreatic cancer growth through a KRAS-regulated metabolic pathway," *Nature*, vol. 496, no. 7443, pp. 101–105, 2013.

[68] D. A. Barbie, P. Tamayo, J. S. Boehm et al., "Systematic RNA interference reveals that oncogenic KRAS-driven cancers require TBK1," *Nature*, vol. 462, no. 7269, pp. 108–112, 2009.

[69] C. Korherr, H. Gille, R. Schäfer et al., "Identification of proangiogenic genes and pathways by high-throughput functional genomics: TBK1 and the IRF3 pathway," *Proceedings of the National Academy of Sciences*, vol. 103, no. 11, pp. 4240–4245, 2006.

[70] Y. Chien, S. Kim, R. Bumeister et al., "RalB GTPase-mediated activation of the IkappaB family kinase TBK1 couples innate immune signaling to tumor cell survival," *Cell*, vol. 127, no. 1, pp. 157–170, 2006.

[71] S. Rao, L. Tortola, T. Perlot et al., "A dual role for autophagy in a murine model of lung cancer," *Nature Communications*, vol. 5, no. 1, 2014.

[72] J. Y. Guo, G. Karsli-Uzunbas, R. Mathew et al., "Autophagy suppresses progression of K-ras-induced lung tumors to oncocytomas and maintains lipid homeostasis," *Genes & Development*, vol. 27, no. 13, pp. 1447–1461, 2013.

[73] C. Zhang, M. Lin, R. Wu et al., "Parkin, a p53 target gene, mediates the role of p53 in glucose metabolism and the Warburg effect," *Proceedings of the National Academy of Sciences*, vol. 108, no. 39, pp. 16259–16264, 2011.

[74] K. Bensaad, A. Tsuruta, M. A. Selak et al., "TIGAR, a p53-inducible regulator of glycolysis and apoptosis," *Cell*, vol. 126, no. 1, pp. 107–120, 2006.

[75] K. Liu, F. Li, H. Han et al., "Parkin regulates the activity of pyruvate kinase M2," *Journal of Biological Chemistry*, vol. 291, no. 19, pp. 10307–10317, 2016.

[76] J. J. Palacino, D. Sagi, M. S. Goldberg et al., "Mitochondrial dysfunction and oxidative damage in parkin-deficient mice," *Journal of Biological Chemistry*, vol. 279, no. 18, pp. 18614–18622, 2004.

[77] S. Beloribi-Djefaflia, S. Vasseur, and F. Guillaumond, "Lipid metabolic reprogramming in cancer cells," *Oncogenesis*, vol. 5, no. 1, p. e189, 2016.

[78] K. Y. Kim, M. V. Stevens, M. H. Akter et al., "Parkin is a lipid-responsive regulator of fat uptake in mice and mutant human cells," *Journal of Clinical Investigation*, vol. 121, no. 9, pp. 3701–3712, 2011.

[79] P. C. Nowell, "The clonal evolution of tumor cell populations," *Science*, vol. 194, no. 4260, pp. 23–28, 1976.

[80] S. Veeriah, B. S. Taylor, S. Meng et al., "Somatic mutations of the Parkinson's disease-associated gene PARK2 in glioblastoma and other human malignancies," *Nature Genetics*, vol. 42, no. 1, pp. 77–82, 2010.

[81] G. Poulogiannis, R. E. McIntyre, M. Dimitriadi et al., "PARK2 deletions occur frequently in sporadic colorectal cancer and accelerate adenoma development in Apc mutant mice," *Proceedings of the National Academy of Sciences*, vol. 107, no. 34, pp. 15145–15150, 2010.

[82] C. Noviello, F. Courjal, and C. Theillet, "Loss of heterozygosity on the long arm of chromosome 6 in breast cancer: possibly four regions of deletion," *Clinical Cancer Research*, vol. 2, no. 9, pp. 1601–1606, 1996.

[83] V. Orphanos, G. McGown, Y. Hey, J. M. Boyle, and M. Santibanez-Koref, "Proximal 6q, a region showing allele loss in primary breast cancer," *British Journal of Cancer*, vol. 71, no. 2, pp. 290–293, 1995.

[84] M. Fujiwara, H. Marusawa, H. Q. Wang et al., "Parkin as a tumor suppressor gene for hepatocellular carcinoma," *Oncogene*, vol. 27, no. 46, pp. 6002–6011, 2008.

[85] K. S. Lee, Z. Wu, Y. Song et al., "Roles of PINK1, mTORC2, and mitochondria in preserving brain tumor-forming stem cells in a noncanonical Notch signaling pathway," *Genes & Development*, vol. 27, no. 24, pp. 2642–2647, 2013.

[86] M. Unoki and Y. Nakamura, "Growth-suppressive effects of BPOZ and EGR2, two genes involved in the PTEN signaling pathway," *Oncogene*, vol. 20, no. 33, pp. 4457–4465, 2001.

[87] S. Agnihotri, B. Golbourn, X. Huang et al., "PINK1 is a negative regulator of growth and the Warburg effect in glioblastoma," *Cancer Research*, vol. 76, no. 16, pp. 4708–4719, 2016.

[88] T. J. Pugh, O. Morozova, E. F. Attiyeh et al., "The genetic landscape of high-risk neuroblastoma," *Nature Genetics*, vol. 45, no. 3, pp. 279–284, 2013.

[89] E. A. Koop, T. van Laar, D. F. van Wichen, R. A. de Weger, E. v. d. Wall, and P. J. van Diest, "Expression of BNIP3 in invasive breast cancer: correlations with the hypoxic response and clinicopathological features," *BMC Cancer*, vol. 9, no. 1, 2009.

[90] M. Erkan, J. Kleeff, I. Esposito et al., "Loss of BNIP3 expression is a late event in pancreatic cancer contributing to chemoresistance and worsened prognosis," *Oncogene*, vol. 24, no. 27, pp. 4421–4432, 2005.

[91] Y. Li, X. Zhang, J. Yang et al., "Methylation of BNIP3 in pancreatic cancer inhibits the induction of mitochondrial-mediated tumor cell apoptosis," *Oncotarget*, vol. 8, no. 38, pp. 63208–63222, 2017.

[92] R. D. Schreiber, L. J. Old, and M. J. Smyth, "Cancer immunoediting: integrating immunity's roles in cancer suppression and promotion," *Science*, vol. 331, no. 6024, pp. 1565–1570, 2011.

[93] A. H. Chourasia, K. Tracy, C. Frankenberger et al., "Mitophagy defects arising from BNip3 loss promote mammary tumor progression to metastasis," *EMBO reports*, vol. 16, no. 9, pp. 1145–1163, 2015.

[94] W. Li, Y. Li, S. Siraj et al., "FUN14 domain-containing 1-mediated mitophagy suppresses hepatocarcinogenesis by inhibition of inflammasome activation in mice," *Hepatology*, vol. 69, no. 2, pp. 604–621, 2019.

[95] P. K. Ziegler, J. Bollrath, C. K. Pallangyo et al., "Mitophagy in intestinal epithelial cells triggers adaptive immunity during tumorigenesis," *Cell*, vol. 174, no. 1, pp. 88–101.e16, 2018.

[96] M. Maugeri-Saccà and R. De Maria, "The Hippo pathway in normal development and cancer," *Pharmacology & Therapeutics*, vol. 186, pp. 60–72, 2018.

[97] F. Zanconato, M. Cordenonsi, and S. Piccolo, "YAP/TAZ at the roots of cancer," *Cancer Cell*, vol. 29, no. 6, pp. 783–803, 2016.

[98] S. Piccolo, S. Dupont, and M. Cordenonsi, "The biology of YAP/TAZ: Hippo signaling and beyond," *Physiological Reviews*, vol. 94, no. 4, pp. 1287–1312, 2014.

[99] D. Coppola, J. Helm, M. Ghayouri, M. P. Malafa, and H. G. Wang, "Down-regulation of Bax-interacting factor 1 in human pancreatic ductal adenocarcinoma," *Pancreas*, vol. 40, no. 3, pp. 433–437, 2011.

[100] S. Y. Kim, Y. L. Oh, K. M. Kim et al., "Decreased expression of Bax-interacting factor-1 (Bif-1) in invasive urinary bladder and gallbladder cancers," *Pathology*, vol. 40, no. 6, pp. 553–557, 2008.

[101] H. Yan, C. Qiu, W. Sun et al., "Yap regulates gastric cancer survival and migration via SIRT1/Mfn2/mitophagy," *Oncology Reports*, vol. 39, no. 4, pp. 1671–1681, 2018.

[102] Y. Takahashi, T. Hori, T. K. Cooper et al., "Bif-1 haploinsufficiency promotes chromosomal instability and accelerates Myc-driven lymphomagenesis via suppression of mitophagy," *Blood*, vol. 121, no. 9, pp. 1622–1632, 2013.

[103] M. van der Ende, S. Grefte, R. Plas et al., "Mitochondrial dynamics in cancer-induced cachexia," *Biochimica et Biophysica Acta (BBA) - Reviews on Cancer*, vol. 1870, no. 2, pp. 137–150, 2018.

[104] F. Penna, D. Costamagna, F. Pin et al., "Autophagic degradation contributes to muscle wasting in cancer cachexia," *The American Journal of Pathology*, vol. 182, no. 4, pp. 1367–1378, 2013.

[105] J. P. White, M. J. Puppa, S. Sato et al., "IL-6 regulation on skeletal muscle mitochondrial remodeling during cancer cachexia in the ApcMin/+ mouse," *Skeletal Muscle*, vol. 2, no. 1, p. 14, 2012.

[106] J. M. McClung, A. R. Judge, S. K. Powers, and Z. Yan, "p38 MAPK links oxidative stress to autophagy-related gene expression in cachectic muscle wasting," *American Journal of Physiology-Cell Physiology*, vol. 298, no. 3, pp. C542–C549, 2010.

[107] C. Yan, L. Luo, C. Y. Guo et al., "Doxorubicin-induced mitophagy contributes to drug resistance in cancer stem cells from HCT8 human colorectal cancer cells," *Cancer Letters*, vol. 388, pp. 34–42, 2017.

[108] S. Fulda, L. Galluzzi, and G. Kroemer, "Targeting mitochondria for cancer therapy," *Nature Reviews Drug Discovery*, vol. 9, no. 6, pp. 447–464, 2010.

[109] J. Zhou, G. Li, Y. Zheng et al., "A novel autophagy/mitophagy inhibitor liensinine sensitizes breast cancer cells to chemotherapy through DNM1L-mediated mitochondrial fission," *Autophagy*, vol. 11, no. 8, pp. 1259–1279, 2015.

[110] M. Dany, S. Gencer, R. Nganga et al., "Targeting FLT3-ITD signaling mediates ceramide-dependent mitophagy and attenuates drug resistance in AML," *Blood*, vol. 128, no. 15, pp. 1944–1958, 2016.

[111] J. R. Jangamreddy, S. Ghavami, J. Grabarek et al., "Salinomycin induces activation of autophagy, mitophagy and affects mitochondrial polarity: differences between primary and cancer cells," *Biochimica et Biophysica Acta*, vol. 1833, no. 9, pp. 2057–2069, 2013.

[112] F. Radogna, C. Cerella, A. Gaigneaux, C. Christov, M. Dicato, and M. Diederich, "Cell type-dependent ROS and mitophagy response leads to apoptosis or necroptosis in neuroblastoma," *Oncogene*, vol. 35, no. 29, pp. 3839–3853, 2016.

[113] F. Madeo, A. Zimmermann, M. C. Maiuri, and G. Kroemer, "Essential role for autophagy in life span extension," *Journal of Clinical Investigation*, vol. 125, no. 1, pp. 85–93, 2015.

[114] K. Palikaras, E. Lionaki, and N. Tavernarakis, "Balancing mitochondrial biogenesis and mitophagy to maintain energy metabolism homeostasis," *Cell Death & Differentiation*, vol. 22, no. 9, pp. 1399–1401, 2015.

[115] M. Ritchey, D. E. Patterson, P. P. Kelalis, and J. W. Segura, "A case of pediatric ureteroscopic lasertripsy," *Journal of Urology*, vol. 139, no. 6, pp. 1272–1274, 1988.

[116] D. F. Egan, D. B. Shackelford, M. M. Mihaylova et al., "Phosphorylation of ULK1 (hATG1) by AMP-activated protein kinase connects energy sensing to mitophagy," *Science*, vol. 331, no. 6016, pp. 456–461, 2011.

[117] D. M. Gwinn, D. B. Shackelford, D. F. Egan et al., "AMPK phosphorylation of raptor mediates a metabolic checkpoint," *Molecular Cell*, vol. 30, no. 2, pp. 214–226, 2008.

[118] R. C. Laker, J. C. Drake, R. J. Wilson et al., "Ampk phosphorylation of Ulk1 is required for targeting of mitochondria to lysosomes in exercise-induced mitophagy," *Nature Communications*, vol. 8, no. 1, p. 548, 2017.

[119] S. C. Johnson, P. S. Rabinovitch, and M. Kaeberlein, "mTOR is a key modulator of ageing and age-related disease," *Nature*, vol. 493, no. 7432, pp. 338–345, 2013.

[120] L. Guarente, "Sirtuins and ageing–new findings," *EMBO reports*, vol. 14, no. 9, p. 750, 2013.

[121] X. H. Zhu, M. Lu, B. Y. Lee, K. Ugurbil, and W. Chen, "In vivo NAD assay reveals the intracellular NAD contents and redox state in healthy human brain and their age dependences," *Proceedings of the National Academy of Sciences*, vol. 112, no. 9, pp. 2876–2881, 2015.

[122] H. Zhang, D. Ryu, Y. Wu et al., "NAD^+ repletion improves mitochondrial and stem cell function and

enhances life span in mice," *Science*, vol. 352, no. 6292, pp. 1436–1443, 2016.

[123] G. Boily, E. L. Seifert, L. Bevilacqua et al., "SirT1 regulates energy metabolism and response to caloric restriction in mice," *PLoS One*, vol. 3, no. 3, article e1759, 2008.

[124] E. F. Fang, M. Scheibye-Knudsen, L. E. Brace et al., "Defective mitophagy in XPA via PARP-1 hyperactivation and NAD(+)/SIRT1 reduction," *Cell*, vol. 157, no. 4, pp. 882–896, 2014.

[125] L. M. Ittner and J. Götz, "Amyloid-β and tau–a toxic pas de deux in Alzheimer's disease," *Nature Reviews Neuroscience*, vol. 12, no. 2, pp. 65–72, 2011.

[126] Q. Cai and P. Tammineni, "Alterations in mitochondrial quality control in Alzheimer's disease," *Frontiers in Cellular Neuroscience*, vol. 10, 2016.

[127] P. J. Khandelwal, A. M. Herman, H.-S. Hoe, G. W. Rebeck, and C. E.- H. Moussa, "Parkin mediates beclin-dependent autophagic clearance of defective mitochondria and ubiquitinated A in AD models," *Human Molecular Genetics*, vol. 20, no. 11, pp. 2091–2102, 2011.

[128] B. Gong, Y. Pan, P. Vempati et al., "Nicotinamide riboside restores cognition through an upregulation of proliferator-activated receptor-γ coactivator 1α regulated β-secretase 1 degradation and mitochondrial gene expression in Alzheimer's mouse models," *Neurobiol Aging*, vol. 34, no. 6, pp. 1581–1588, 2013.

[129] A. N. Long, K. Owens, A. E. Schlappal, T. Kristian, P. S. Fishman, and R. A. Schuh, "Effect of nicotinamide mononucleotide on brain mitochondrial respiratory deficits in an Alzheimer's disease-relevant murine model," *BMC Neurology*, vol. 15, no. 1, 2015.

[130] L. Zheng, N. Bernard-Marissal, N. Moullan et al., "Parkin functionally interacts with PGC-1α to preserve mitochondria and protect dopaminergic neurons," *Human Molecular Genetics*, vol. 26, no. 3, pp. 582–598, 2017.

[131] F. M. Menzies, A. Fleming, and D. C. Rubinsztein, "Compromised autophagy and neurodegenerative diseases," *Nature Reviews Neuroscience*, vol. 16, no. 6, pp. 345–357, 2015.

[132] A. H. Schapira, J. M. Cooper, D. Dexter, P. Jenner, J. B. Clark, and C. D. Marsden, "Mitochondrial complex I deficiency in Parkinson's disease," *Lancet*, vol. 1, no. 8649, p. 1269, 1989.

[133] A. M. Pickrell and R. J. Youle, "The roles of PINK1, parkin, and mitochondrial fidelity in Parkinson's disease," *Neuron*, vol. 85, no. 2, pp. 257–273, 2015.

[134] S. Geisler, K. M. Holmström, A. Treis et al., "The PINK1/Parkin-mediated mitophagy is compromised by PD-associated mutations," *Autophagy*, vol. 6, no. 7, pp. 871–878, 2010.

[135] A. J. Whitworth and L. J. Pallanck, "PINK1/Parkin mitophagy and neurodegeneration-what do we really know in vivo?," *Current Opinion in Genetics & Development*, vol. 44, pp. 47–53, 2017.

[136] D. A. Sliter, J. Martinez, L. Hao et al., "Parkin and PINK1 mitigate STING-induced inflammation," *Nature*, vol. 561, no. 7722, pp. 258–262, 2018.

[137] C.-H. Hsieh, A. Shaltouki, A. E. Gonzalez et al., "Functional impairment in miro degradation and mitophagy is a shared feature in familial and sporadic Parkinson's disease," *Cell Stem Cell*, vol. 19, no. 6, pp. 709–724, 2016.

[138] A. S. Benischke, S. Vasanth, T. Miyai et al., "Activation of mitophagy leads to decline in Mfn2 and loss of mitochondrial mass in Fuchs endothelial corneal dystrophy," *Scientific Reports*, vol. 7, no. 1, p. 6656, 2017.

[139] A. D. N. J. De Grey, "A proposed refinement of the mitochondrial free radical theory of aging," *Bioessays*, vol. 19, no. 2, pp. 161–166, 1997.

[140] A. Terman, B. Gustafsson, and U. T. Brunk, "Mitochondrial damage and intralysosomal degradation in cellular aging," *Molecular Aspects of Medicine*, vol. 27, no. 5-6, pp. 471–482, 2006.

[141] U. T. Brunk and A. Terman, "The mitochondrial-lysosomal axis theory of aging: accumulation of damaged mitochondria as a result of imperfect autophagocytosis," *European Journal of Biochemistry*, vol. 269, no. 8, pp. 1996–2002, 2002.

[142] K. Sakuma, M. Kinoshita, Y. Ito, M. Aizawa, W. Aoi, and A. Yamaguchi, "p62/SQSTM1 but not LC3 is accumulated in sarcopenic muscle of mice," *Journal of Cachexia, Sarcopenia and Muscle*, vol. 7, no. 2, pp. 204–212, 2016.

[143] M. F. O'Leary, A. Vainshtein, S. Iqbal, O. Ostojic, and D. A. Hood, "Adaptive plasticity of autophagic proteins to denervation in aging skeletal muscle," *American Journal of Physiology-Cell Physiology*, vol. 304, no. 5, pp. C422–C430, 2013.

[144] H. N. Carter, Y. Kim, A. T. Erlich, D. Zarrin-Khat, and D. A. Hood, "Autophagy and mitophagy flux in young and aged skeletal muscle following chronic contractile activity," *The Journal of Physiology*, vol. 596, no. 16, pp. 3567–3584, 2018.

[145] A. Vainshtein, E. M. Desjardins, A. Armani, M. Sandri, and D. A. Hood, "PGC-1α modulates denervation-induced mitophagy in skeletal muscle," *Skeletal Muscle*, vol. 5, no. 1, 2015.

[146] C. Kang, D. Yeo, and L. L. Ji, "Muscle immobilization activates mitophagy and disrupts mitochondrial dynamics in mice," *Acta Physiologica*, vol. 218, no. 3, pp. 188–197, 2016.

[147] N. Furuya, S.-I. Ikeda, S. Sato et al., "PARK2/Parkin-mediated mitochondrial clearance contributes to proteasome activation during slow-twitch muscle atrophy via NFE2L1 nuclear translocation," *Autophagy*, vol. 10, no. 4, pp. 631–641, 2014.

[148] H. Schweiger, E. Lütjen-Drecoll, E. Arnold, W. Koch, R. Nitsche, and K. Brand, "Ischemia-induced alterations of mitochondrial structure and function in brain, liver, and heart muscle of young and senescent rats," *Biochemical Medicine and Metabolic Biology*, vol. 40, no. 2, pp. 162–185, 1988.

[149] Y. Li, D. Y. Ruan, C. C. Jia et al., "Aging aggravates hepatic ischemia-reperfusion injury in mice by impairing mitophagy with the involvement of the EIF2α-parkin pathway," *Aging*, vol. 10, no. 8, pp. 1902–1920, 2018.

[150] H. Dai, D. A. Sinclair, J. L. Ellis, and C. Steegborn, "Sirtuin activators and inhibitors: promises, achievements, and challenges," *Pharmacology & Therapeutics*, vol. 188, pp. 140–154, 2018.

[151] C. Cantó, K. J. Menzies, and J. Auwerx, "NAD(+) Metabolism and the control of energy homeostasis: a balancing act between mitochondria and the nucleus," *Cell Metabolism*, vol. 22, no. 1, pp. 31–53, 2015.

[152] A. Alageel, J. Tomasi, C. Tersigni et al., "Evidence supporting a mechanistic role of sirtuins in mood and metabolic disorders," *Progress in Neuro-Psychopharmacology and Biological Psychiatry*, vol. 86, pp. 95–101, 2018.

[153] T. Jayasena, A. Poljak, G. Smythe, N. Braidy, G. Münch, and P. Sachdev, "The role of polyphenols in the modulation of sirtuins and other pathways involved in

Alzheimer's disease," *Ageing Research Reviews*, vol. 12, no. 4, pp. 867–883, 2013.

[154] M. Russo, L. Sansone, L. Polletta et al., "Sirtuins and resveratrol-derived compounds: a model for understanding the beneficial effects of the Mediterranean diet," *Endocrine, Metabolic & Immune Disorders-Drug Targets*, vol. 14, no. 4, pp. 300–308, 2014.

[155] A. Chalkiadaki and L. Guarente, "High-fat diet triggers inflammation-induced cleavage of SIRT1 in adipose tissue to promote metabolic dysfunction," *Cell Metabolism*, vol. 16, no. 2, pp. 180–188, 2012.

[156] A. Biason-Lauber, M. Böni-Schnetzler, B. P. Hubbard et al., "Identification of a SIRT1 mutation in a family with type 1 diabetes," *Cell Metabolism*, vol. 17, no. 3, pp. 448–455, 2013.

[157] D. Timet, V. Mitin, M. Herak, and D. Emanović, "Absorption of monovalent and bivalent cations in various compartments of the ruminant stomach," *The Journal of Physiology*, vol. 63, no. 6, p. 145A, 1971.

[158] M. C. Haigis, R. Mostoslavsky, K. M. Haigis et al., "SIRT4 Inhibits Glutamate Dehydrogenase and Opposes the Effects of Calorie Restriction in Pancreatic β Cells," *Cell*, vol. 126, no. 5, pp. 941–954, 2006.

[159] F. Yeung, J. E. Hoberg, C. S. Ramsey et al., "Modulation of NF-κB-dependent transcription and cell survival by the SIRT1 deacetylase," *The EMBO Journal*, vol. 23, no. 12, pp. 2369–2380, 2004.

[160] R. R. Alcendor, S. Gao, P. Zhai et al., "Sirt1 regulates aging and resistance to oxidative stress in the heart," *Circulation Research*, vol. 100, no. 10, pp. 1512–1521, 2007.

[161] R. Li, T. Xin, D. Li, C. Wang, H. Zhu, and H. Zhou, "Therapeutic effect of Sirtuin 3 on ameliorating nonalcoholic fatty liver disease: the role of the ERK-CREB pathway and Bnip3-mediated mitophagy," *Redox Biology*, vol. 18, pp. 229–243, 2018.

[162] J. Feng, C. Lu, Q. Dai, J. Sheng, and M. Xu, "SIRT3 facilitates amniotic fluid stem cells to repair diabetic nephropathy through protecting mitochondrial homeostasis by modulation of mitophagy," *Cellular Physiology and Biochemistry*, vol. 46, no. 4, pp. 1508–1524, 2018.

[163] Y. Li, Y. Ma, L. Song et al., "SIRT3 deficiency exacerbates p53/Parkin-mediated mitophagy inhibition and promotes mitochondrial dysfunction: Implication for aged hearts," *International Journal of Molecular Medicine*, vol. 41, no. 6, pp. 3517–3526, 2018.

[164] A. Lang, R. Anand, S. Altinoluk-Hambüchen et al., "SIRT4 interacts with OPA1 and regulates mitochondrial quality control and mitophagy," *Aging*, vol. 9, no. 10, pp. 2163–2189, 2017.

[165] G. Liu, S. H. Park, M. Imbesi et al., "Loss of NAD-dependent protein deacetylase sirtuin-2 alters mitochondrial protein acetylation and dysregulates mitophagy," *Antioxidants & Redox Signaling*, vol. 26, no. 15, pp. 849–863, 2017.

[166] G. Di Sante, T. G. Pestell, M. C. Casimiro et al., "Loss of Sirt1 promotes prostatic intraepithelial neoplasia, reduces mitophagy, and delays PARK2 translocation to mitochondria," *The American Journal of Pathology*, vol. 185, no. 1, pp. 266–279, 2015.

[167] P. Mannam, A. S. Shinn, A. Srivastava et al., "MKK3 regulates mitochondrial biogenesis and mitophagy in sepsis-induced lung injury," *American Journal of Physiology-Lung Cellular and Molecular Physiology*, vol. 306, no. 7, pp. L604–L619, 2014.

[168] Z. Q. Yao, X. Zhang, Y. Zhen et al., "A novel small-molecule activator of sirtuin-1 induces autophagic cell death/mitophagy as a potential therapeutic strategy in glioblastoma," *Cell Death & Disease*, vol. 9, no. 7, p. 767, 2018.

[169] H. Qiao, H. Ren, H. Du, M. Zhang, X. Xiong, and R. Lv, "Liraglutide repairs the infarcted heart: the role of the SIRT1/Parkin/mitophagy pathway," *Molecular Medicine Reports*, vol. 17, no. 3, pp. 3722–3734, 2018.

[170] S. Kwon, S. Seok, P. Yau, X. Li, B. Kemper, and J. K. Kemper, "Obesity and aging diminish sirtuin 1 (SIRT1)-mediated deacetylation of SIRT3, leading to hyperacetylation and decreased activity and stability of SIRT3," *Journal of Biological Chemistry*, vol. 292, no. 42, pp. 17312–17323, 2017.

[171] F. Sun, X. Jiang, X. Wang et al., "Vincristine ablation of Sirt2 induces cell apoptosis and mitophagy via Hsp70 acetylation in MDA-MB-231 cells," *Biochemical Pharmacology*, vol. 162, pp. 142–153, 2019.

[172] A. Qiao, K. Wang, Y. Yuan et al., "Sirt3-mediated mitophagy protects tumor cells against apoptosis under hypoxia," *Oncotarget*, vol. 7, no. 28, pp. 43390–43400, 2016.

[173] W. Yu, B. Gao, N. Li et al., "Sirt3 deficiency exacerbates diabetic cardiac dysfunction: role of Foxo3A-Parkin-mediated mitophagy," *Biochimica et Biophysica Acta (BBA) - Molecular Basis of Disease*, vol. 1863, no. 8, pp. 1973–1983, 2017.

[174] D. Zhao, Y. Sun, Y. Tan et al., "Short-duration swimming exercise after myocardial infarction attenuates cardiac dysfunction and regulates mitochondrial quality control in aged mice," *Oxidative Medicine and Cellular Longevity*, vol. 2018, Article ID 4079041, 16 pages, 2018.

[175] L. Polletta, E. Vernucci, I. Carnevale et al., "SIRT5 regulation of ammonia-induced autophagy and mitophagy," *Autophagy*, vol. 11, no. 2, pp. 253–270, 2015.

[176] H. Guedouari, T. Daigle, L. Scorrano, and E. Hebert-Chatelain, "Sirtuin 5 protects mitochondria from fragmentation and degradation during starvation," *Biochimica et Biophysica Acta (BBA) - Molecular Cell Research*, vol. 1864, no. 1, pp. 169–176, 2017.

[177] I. Carnevale, L. Pellegrini, P. D'Aquila et al., "SIRT1-SIRT3 axis regulates cellular response to oxidative stress and etoposide," *Journal of Cellular Physiology*, vol. 232, no. 7, pp. 1835–1844, 2017.

[178] G. S. Shadel and T. L. Horvath, "Mitochondrial ROS signaling in organismal homeostasis," *Cell*, vol. 163, no. 3, pp. 560–569, 2015.

[179] C. Dostert, V. Pétrilli, R. Van Bruggen, C. Steele, B. T. Mossman, and J. Tschopp, "Innate immune activation through Nalp3 inflammasome sensing of asbestos and silica," *Science*, vol. 320, no. 5876, pp. 674–677, 2008.

[180] P. S. Brookes, Y. Yoon, J. L. Robotham, M. W. Anders, and S. S. Sheu, "Calcium, ATP, and ROS: a mitochondrial love-hate triangle," *American Journal of Physiology-Cell Physiology*, vol. 287, no. 4, pp. C817–C833, 2004.

[181] R. Zhou, A. S. Yazdi, P. Menu, and J. Tschopp, "A role for mitochondria in NLRP3 inflammasome activation," *Nature*, vol. 469, no. 7329, pp. 221–225, 2011.

[182] Q. Wang, M. Zhang, G. Torres et al., "Metformin Suppresses Diabetes-Accelerated Atherosclerosis via the Inhibition of Drp1-Mediated Mitochondrial Fission," *Diabetes*, vol. 66, no. 1, pp. 193–205, 2017.

[183] T. Yu, S. S. Sheu, J. L. Robotham, and Y. Yoon, "Mitochondrial fission mediates high glucose-induced cell death through elevated production of reactive oxygen species," *Cardiovascular Research*, vol. 79, no. 2, pp. 341–351, 2008.

[184] W. Zhu, Y. Yuan, G. Liao et al., "Mesenchymal stem cells ameliorate hyperglycemia-induced endothelial injury through modulation of mitophagy," *Cell Death & Disease*, vol. 9, no. 8, p. 837, 2018.

[185] R. H. Bhogal, C. J. Weston, S. M. Curbishley, D. H. Adams, and S. C. Afford, "Autophagy: a cyto-protective mechanism which prevents primary human hepatocyte apoptosis during oxidative stress," *Autophagy*, vol. 8, no. 4, pp. 545–558, 2012.

[186] R. H. Bhogal, C. J. Weston, S. Velduis et al., "The Reactive Oxygen Species-Mitophagy Signaling Pathway Regulates Liver Endothelial Cell Survival During Ischemia/Reperfusion Injury," *Liver Transplantation*, vol. 24, no. 10, pp. 1437–1452, 2018.

[187] B. Xiao, J. Y. Goh, L. Xiao, H. Xian, K. L. Lim, and Y. C. Liou, "Reactive oxygen species trigger Parkin/PINK1 pathway-dependent mitophagy by inducing mitochondrial recruitment of Parkin," *Journal of Biological Chemistry*, vol. 292, no. 40, pp. 16697–16708, 2017.

[188] B. Xiao, X. Deng, G. G. Y. Lim et al., "Superoxide drives progression of Parkin/PINK1-dependent mitophagy following translocation of Parkin to mitochondria," *Cell Death and Disease*, vol. 8, no. 10, 2017.

[189] S. S. Cao and R. J. Kaufman, "Endoplasmic reticulum stress and oxidative stress in cell fate decision and human disease," *Antioxidants & Redox Signaling*, vol. 21, no. 3, pp. 396–413, 2014.

[190] L. Poillet-Perez, G. Despouy, R. Delage-Mourroux, and M. Boyer-Guittaut, "Interplay between ROS and autophagy in cancer cells, from tumor initiation to cancer therapy," *Redox Biology*, vol. 4, pp. 184–192, 2015.

[191] J. Guo, Z. Yang, X. Yang, T. Li, M. Liu, and H. Tang, "miR-346 functions as a pro-survival factor under ER stress by activating mitophagy," *Cancer Letters*, vol. 413, pp. 69–81, 2018.

[192] A. Hanikoglu, H. Ozben, F. Hanikoglu, and T. Ozben, "Hybrid compounds & oxidative stress induced apoptosis in cancer therapy," *Current Medicinal Chemistry*, vol. 25, 2018.

[193] N. S. Chandel, D. S. McClintock, C. E. Feliciano et al., "Reactive Oxygen Species Generated at Mitochondrial Complex III Stabilize Hypoxia-inducible Factor-1α during Hypoxia," *Journal of Biological Chemistry*, vol. 275, no. 33, pp. 25130–25138, 2000.

[194] C. E. Dann III and R. K. Bruick, "Dioxygenases as O2-dependent regulators of the hypoxic response pathway," *Biochemical and Biophysical Research Communications*, vol. 338, no. 1, pp. 639–647, 2005.

[195] R. Miceli, S. Moretti, and L. Bernardi, "Our experience in the use of pneumopelvitomography in the diagnosis of gynecologic diseases," *Minerva Medica*, vol. 58, no. 59, pp. 2639–2655, 1967.

[196] M. Shida, Y. Kitajima, J. Nakamura et al., "Impaired mitophagy activates mtROS/HIF-1α interplay and increases cancer aggressiveness in gastric cancer cells under hypoxia," *International Journal of Oncology*, vol. 48, no. 4, pp. 1379–1390, 2016.

[197] S. Salatin, S. Maleki Dizaj, and A. Yari Khosroushahi, "Effect of the surface modification, size, and shape on cellular uptake of nanoparticles," *Cell Biology International*, vol. 39, no. 8, pp. 881–890, 2015.

[198] D. H. Jo, J. H. Kim, T. G. Lee, and J. H. Kim, "Size, surface charge, and shape determine therapeutic effects of nanoparticles on brain and retinal diseases," *Nanomedicine*, vol. 11, no. 7, pp. 1603–1611, 2015.

[199] C. D. Walkey, J. B. Olsen, H. Guo, A. Emili, and W. C. W. Chan, "Nanoparticle size and surface chemistry determine serum protein adsorption and macrophage uptake," *Journal of the American Chemical Society*, vol. 134, no. 4, pp. 2139–2147, 2012.

[200] Z. Lin, N. A. Monteiro-Riviere, and J. E. Riviere, "Pharmacokinetics of metallic nanoparticles," *Wiley Interdisciplinary Reviews: Nanomedicine and Nanobiotechnology*, vol. 7, no. 2, pp. 189–217, 2015.

[201] J. Li, C. Fan, H. Pei, J. Shi, and Q. Huang, "Smart drug delivery nanocarriers with self-assembled DNA nanostructures," *Advanced Materials*, vol. 25, no. 32, pp. 4386–4396, 2013.

[202] V. Linko, A. Ora, and M. A. Kostiainen, "DNA nanostructures as smart drug-delivery vehicles and molecular devices," *Trends in Biotechnology*, vol. 33, no. 10, pp. 586–594, 2015.

[203] J. Hou, L. Wang, C. Wang et al., "Toxicity and mechanisms of action of titanium dioxide nanoparticles in living organisms," *Journal of Environmental Sciences*, vol. 75, pp. 40–53, 2019.

[204] R. Gupta and H. Xie, "Nanoparticles in daily life: applications, toxicity and regulations," *Journal of Environmental Pathology, Toxicology and Oncology*, vol. 37, no. 3, pp. 209–230, 2018.

[205] Y. Liu, J. Liang, Q. Wang, Y. He, and Y. Chen, "Copper nanoclusters trigger muscle cell apoptosis and atrophy in vitro and in vivo," *Journal of Applied Toxicology*, vol. 36, no. 3, pp. 454–463, 2016.

[206] P. P. Fu, Q. Xia, H. M. Hwang, P. C. Ray, and H. Yu, "Mechanisms of nanotoxicity: generation of reactive oxygen species," *Journal of Food and Drug Analysis*, vol. 22, no. 1, pp. 64–75, 2014.

[207] Y. Zhang, B. Xu, M. Yao et al., "Titanium dioxide nanoparticles induce proteostasis disruption and autophagy in human trophoblast cells," *Chemico-Biological Interactions*, vol. 296, pp. 124–133, 2018.

[208] P. J. Borm, D. Robbins, S. Haubold et al., "The potential risks of nanomaterials: a review carried out for ECETOC," *Particle and Fibre Toxicology*, vol. 3, no. 1, p. 11, 2006.

[209] C. He, S. Jiang, H. Yao et al., "High-content analysis for mitophagy response to nanoparticles: a potential sensitive biomarker for nanosafety assessment," *Nanomedicine*, vol. 15, no. 1, pp. 59–69, 2019.

[210] J. Wang, S. Gao, S. Wang, Z. Xu, and L. Wei, "Zinc oxide nanoparticles induce toxicity in CAL 27 oral cancer cell lines by activating PINK1/Parkin-mediated mitophagy," *International Journal of Nanomedicine*, vol. 13, pp. 3441–3450, 2018.

[211] L. Wei, J. Wang, A. Chen, J. Liu, X. Feng, and L. Shao, "Involvement of PINK1/parkin-mediated mitophagy in ZnO nanoparticle-induced toxicity in BV-2 cells," *International Journal of Nanomedicine*, vol. Volume 12, pp. 1891–1903, 2017.

[212] S. Ke, T. Zhou, P. Yang et al., "Gold nanoparticles enhance TRAIL sensitivity through Drp1-mediated apoptotic and

autophagic mitochondrial fission in NSCLC cells," *International Journal of Nanomedicine*, vol. Volume 12, pp. 2531–2551, 2017.

[213] A. Orlando, E. Cazzaniga, M. Tringali et al., "Mesoporous silica nanoparticles trigger mitophagy in endothelial cells and perturb neuronal network activity in a size- and time-dependent manner," *International Journal of Nanomedicine*, vol. Volume 12, pp. 3547–3559, 2017.

[214] M. L. Kung, S. L. Hsieh, C. C. Wu et al., "Enhanced reactive oxygen species overexpression by CuO nanoparticles in poorly differentiated hepatocellular carcinoma cells," *Nanoscale*, vol. 7, no. 5, pp. 1820–1829, 2015.

[215] J. P. Piret, D. Jacques, J. N. Audinot et al., "Copper(II) oxide nanoparticles penetrate into HepG2 cells, exert cytotoxicity via oxidative stress and induce pro-inflammatory response," *Nanoscale*, vol. 4, no. 22, pp. 7168–7184, 2012.

[216] J. Zhang, B. Wang, H. Wang et al., "Disruption of the superoxide anions-mitophagy regulation axis mediates copper oxide nanoparticles-induced vascular endothelial cell death," *Free Radical Biology and Medicine*, vol. 129, pp. 268–278, 2018.

[217] Z. Zhang, L. Zhou, Y. Zhou et al., "Mitophagy induced by nanoparticle-peptide conjugates enabling an alternative intracellular trafficking route," *Biomaterials*, vol. 65, pp. 56–65, 2015.

[218] Y. Huang, C. Q. Fan, H. Dong, S. M. Wang, X. C. Yang, and S. M. Yang, "Current applications and future prospects of nanomaterials in tumor therapy," *International Journal of Nanomedicine*, vol. 12, pp. 1815–1825, 2017.

[219] Z. Moldoveanu, J. K. Staas, R. M. Gilley et al., "Immune responses to influenza virus in orally and systemically immunized mice," *Current Topics in Microbiology and Immunology*, vol. 146, pp. 91–99, 1989.

[220] M. Zoroddu, S. Medici, A. Ledda, V. Nurchi, J. Lachowicz, and M. Peana, "Toxicity of nanoparticles," *Current Medicinal Chemistry*, vol. 21, no. 33, pp. 3837–3853, 2014.

[221] S. Bakand and A. Hayes, "Toxicological considerations, toxicity assessment, and risk management of inhaled nanoparticles," *International Journal of Molecular Sciences*, vol. 17, no. 6, p. 929, 2016.

Hindawi
Oxidative Medicine and Cellular Longevity
Volume 2019, Article ID 6050123, 10 pages
https://doi.org/10.1155/2019/6050123

Review Article

Oxidative Stress-Driven Autophagy acROSs Onset and Therapeutic Outcome in Hepatocellular Carcinoma

Fabio Ciccarone,[1] Serena Castelli,[1] and Maria Rosa Ciriolo[1,2]

[1]*Department of Biology, University of Rome "Tor Vergata", Via della Ricerca Scientifica, 00133 Rome, Italy*
[2]*IRCCS San Raffaele Roma, Via di Val Cannuta 247, 00166 Rome, Italy*

Correspondence should be addressed to Maria Rosa Ciriolo; ciriolo@bio.uniroma2.it

Received 8 March 2019; Accepted 28 April 2019; Published 8 May 2019

Guest Editor: Marco Cordani

Reactive oxygen species- (ROS-) mediated autophagy physiologically contributes to management of cell homeostasis in response to mild oxidative stress. Cancer cells typically engage autophagy downstream of ROS signaling derived from hypoxia and starvation, which are harsh environmental conditions that need to be faced for cancer development and progression. Hepatocellular carcinoma (HCC) is a solid tumor for which several environmental risk factors, particularly viral infections and alcohol abuse, have been shown to promote carcinogenesis via augmentation of oxidative stress. In addition, ROS burst in HCC cells frequently takes place after administration of therapeutic compounds that promote apoptotic cell death or even autophagic cell death. The interplay between ROS and autophagy (i) in the disposal of dysfunctional mitochondria via mitophagy, as a tumor suppressor mechanism, or (ii) in the cell survival adaptive response elicited by chemotherapeutic interventions, as a tumor-promoting event, will be depicted in this review in relation to HCC development and progression.

1. Oxidative Stress

Reactive oxygen species (ROS) are the by-products of a number of oxygen-centred biochemical reactions and include free radicals, such as superoxide ($O_2^{\cdot-}$) and hydroxyl radical ($OH^{\cdot}$), as well as nonradical species, such as hydrogen peroxide (H_2O_2). Because these species are formed by sequential reduction of oxygen, they can be interconverted either spontaneously or under enzymatic catalysis [1]. Starting from the 70s, when ROS were typically considered dangerous molecules due to the fact that only damaging and irreversible effects on macromolecules were detected as proof of their ability [2], more recently, we moved to a more composite concept of the ROS role. Indeed, these molecules had a Janus-faced behaviour in cell metabolism, strictly related to their concentration. High ROS flux leads to irreversible alteration of target macromolecules contributing to biological damage inside the cells that has been associated with a number of both physiological conditions, such as aging and senescence, as well as pathological states, such as cancer, neurodegeneration, and cell death. On the contrary, low ROS flux is fundamental for cell signaling leading to cell cycle modulation and cell proliferation. Therefore, a balanced redox state is necessary for avoiding cell damage and for fine-tuning protein functions and molecular pathways [1]. The discovery of reversible redox post-translational modifications on protein cysteine residue opened the avenue for specificity of the signaling pathway, because only a small fraction of proteins becomes oxidized when cells are subjected to mild oxidative stress, due to the peculiar characteristic of surrounding amino acids of the target cysteine [3]. Nowadays, we can assert that the ROS-mediated redox signaling is central in the commitment of cell proliferation, stress response, and survival in mild/controlled ROS burst, while a persistent disequilibrium in redox homeostasis culminates in cell death.

Oxidative stress originates from the overproduction of ROS by endogenous (*e.g.*, mitochondria, peroxisomes, and oxygen-handling enzymes) and exogenous sources (*e.g.*, UV, heavy metals, and micronutrients) or by inefficient/exhausted antioxidants [4]. In particular, the endogenous ROS generation can be an inevitable consequence of the oxidative

metabolism, by means of the electron transport chain activity inside the mitochondria, or they can represent a weapon through which specialized cells counteract infections; this is the case of transmembrane enzymes belonging to the NOX family of NADPH oxidases actively producing ROS as primary function (Table 1). Cellular antioxidant equipment spans from low molecular weight nonenzymatic scavengers derived from intracellular synthesis or diet to a variety of committed enzymes. Major enzymatic antioxidants include superoxide dismutase (SOD) having the ability to dismutate the superoxide radical, and catalase and glutathione peroxidases (GPxs) able to efficiently eliminate peroxide derivatives. To these, the thioredoxin reductase enzyme should be added for its role in buffering and restoring redox modifications on proteins. The spatial distribution of antioxidant molecules permits to locally counterbalance the effects of ROS. For instance, different isoforms of SOD exist: the Mn-SOD (or SOD2) is localized in the mitochondrial matrix whereas the CuZn-SOD (or SOD1) is sited in the cytosol and in the mitochondrial intermembrane space [1]. The nonenzymatic antioxidant pattern comprises the tripeptide glutathione (GSH), the major soluble antioxidant abundantly present in all cell compartments, and several vitamins such as the lipid-soluble α-tocopherol, particularly present in the hydrophobic side of the cell membrane (Table 1). The GSH redox cycle is probably the most important cellular defense system that exists in the cell; GSH not only acts as a ROS scavenger but also functions in the regulation of the intracellular redox state. The system consists of GSH, GPx, and glutathione reductase, and the ability of the cell to regenerate GSH from its oxidized form GSSG is fundamental in buffering oxidative stress [5].

2. Regulation of Tumor Biology by Protein Oxidation

ROS levels are typically augmented in many types of cancers. In fact, diverse proliferative signals promote ROS generation as observed for those elicited by growth factor receptors coupled with NADPH oxidases [6, 7]. DNA mutations derived from oxidative DNA damage represent the typical ROS protumorigenic action. Together with 8-oxoguanine (8-oxoG), one of the most common DNA lesions caused by ROS, oxidative damages comprise DNA single-strand or double-strand breaks as well as rearrangement of DNA sequence [8]. However, ROS contribute to cell proliferation even through H_2O_2-mediated oxidation of cysteine residues present on a surface-exposed region of oncogenes/tumor suppressors. Several kinases involved in the mitogen-activated protein kinase (MAPK) pathway, which is one of the well-established cell transduction cascade contributing to cell proliferation/survival, have been demonstrated to be regulated in this way. In particular, the modulation of such pathway by oxidation can occur (i) indirectly, as demonstrated for the inhibition of the MAP kinase phosphatase 3 (MKP3) that is a Jun N-terminal kinase (JNK) antagonizing enzyme [9], or (ii) directly, as observed for the inhibition of the mitogen-activated protein kinase kinase 6 (MKK6) that specifically activates the p38 MAPK [10] (Figure 1).

Along with the regulation of cell proliferation-linked pathways that contribute to tumor initiation, ROS are also involved in tumor progression/dissemination facilitating cell motility and metastasis. In this context, a complex succession of redox reactions affects the activity of kinases—*e.g.*, protooncogene c-Src [11] and C-terminal Src kinase (CSK) [12]—and phosphatases—*e.g.*, phosphatase and tensin homolog (PTEN) [13] and Src homology 2 domain-containing phosphatase 2 (SHP-2) [14]—that coordinate the anchorage-independent cell growth downstream of integrin signaling triggered by extracellular matrix binding [15] (Figure 1).

Another process extensively connected with redox signaling in cancer cells is autophagy, which accounts for tumor development/progression in harsh conditions. In the present review, we will circumstantiate the interplay between ROS and autophagy in hepatocellular carcinoma (HCC) focusing on the carcinogenic effects of the wide range of environmental risk factors involved in and on the therapeutic sensitivity/refractoriness of this solid tumor. Before entering the main issue of this review, a brief description of the autophagic process and the ROS-mediated regulation of key players will be provided hereafter.

3. (Macro)autophagy

Autophagy typically allows cells to maintain the correct turnover of their component through the degradation of old organelles and proteins recovering energy and macromolecular precursors. Because of its intrinsic role of the recycling pathway, autophagy can regulate physiological functions in which cellular components have to be degraded, building blocks have to be formed, and the cell has to response to stress. The main biological effects inside the cell include differentiation, response to starvation, quality control mechanism through elimination of damaged proteins and organelles, and antimicrobial activity through elimination of bacteria or viruses. Consistently, a lot of different stimuli can activate the autophagic mechanism, demonstrating the complicated nature of this pathway [16].

When we talk about autophagy in this review, we consider the so-called "macroautophagy" which culminates with the fusion of mature autophagosome (the vesicle that contains the components that will be degraded) with lysosome to degrade its content by acidic hydrolases. Other mechanisms include "microautophagy," in which lysosome directly wraps around its cargo to eliminate it, and "chaperone-mediated autophagy," in which the binding between a chaperone protein and a target protein forms a complex that is recognized by LAMP2A (lysosomal-associated membrane protein 2) allowing the translocation of target protein into the lysosome [17].

The first step of (macro)autophagy is the formation of phagophore, a membrane structure that wraps parts of the cytoplasm, thanks to the interventions of a complex containing autophagy-related proteins (ATGs). During nutrient deprivation, the canonical autophagic stimulus, the target of rapamycin kinase complex I (TORC1) has a crucial role; according to the current hypothesis, TORC1 is able to sense directly the flux of extracellular amino acids from outside

Table 1: Main ROS sources/antioxidants and their localization.

Endogenous ROS sources	Main localization	Antioxidants	Main localization
NADPH oxidase	Plasma membrane	Glutathione	Ubiquitous
Respiratory complexes I and III	Mitochondrion	α-Tocopherol	Plasma membrane
CYP450	Endoplasmic reticulum	Superoxide dismutase	Mitochondrion/cytosol
Xanthine oxidase	Cytosol/peroxisome	Catalase	Peroxisome
Peroxisomal oxidases	Peroxisome	Thioredoxin	Nucleus/mitochondrion
Lipoxygenase/cyclooxygenase	Cytosol	Glutathione peroxidase	Cytosol/mitochondrion/plasma membrane

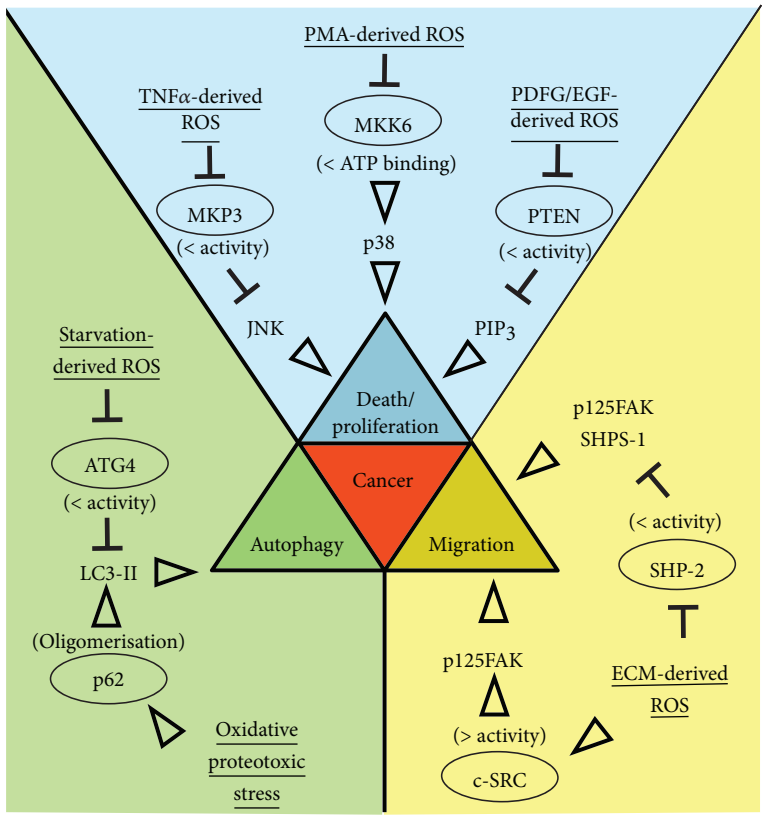

Figure 1: Scheme representing the sources of oxidative stress (underlined) that through direct oxidation affect the function (parenthesis) of key proteins (ellipse) involved in cell death/proliferation, autophagy, and migration/invasiveness, which are pathways commonly altered in cancer. PDGF: platelet-derived growth factor; EGF: epidermal growth factor; PMA: phorbol myristate acetate; TNFα: tumor necrosis factor α; PIP_3: phosphatidylinositol 3,4,5 trisphosphate; ECM: extracellular matrix.

to inside the cell [18]. In starvation condition, the inhibition of the mammalian target of rapamycin (mTOR) allows the activation of uncoordinated-51-like kinases 1 and 2 (ULK1 and ULK2), which together with ATG proteins form the complex that localizes on the phagophore to induce the autophagosome nucleation [19, 20]. Alternatively, the formation of double-membrane structure is induced via Beclin 1 forming distinct phosphatidylinositol 3-kinase complexes [20, 21]. The elongation of phagophore, principally driven by ATG9, determines the formation of a double-membrane vesicle creating the autophagosome, which then fuses with lysosome [20]. The introduction of target protein inside the autophagosome is generally mediated by binding with the light chain 3-II (LC3-II) which localizes at autophagosome surface through phosphatidylethanolamine (PE) post-translational modification [16, 22]. The process of autophagy is selective in principle as many adaptor proteins allow LC3-II to recognize specific targets; among those, p62/sequestrosome 1 (SQSTRM1) has been characterized as the selective mediator of ubiquitinated protein degradation via autophagy [16, 23].

4. ROS-Mediated Regulation of Autophagic Flux

Aberrant increase of the endogenous or exogenous source of ROS can induce macromolecule damage associated with oxidative stress that needs to be efficiently managed. In the perspective of cellular homeostasis, autophagy is a crucial response to oxidative stress, and there are many ways through which ROS can activate autophagy. A direct

regulation of autophagic machinery is exemplified by H_2O_2-mediated oxidation of (i) ATG4 that becomes inhibited and cannot delipidate LC3 promoting its association with the autophagosomes [24] and (ii) p62 that undergoes oligomerization boosting autophagosome biogenesis and autophagic flux [25] (Figure 1).

In addition, ROS are able to influence the signaling pathways involved in autophagy regulation at different levels. For instance, AMP-activated protein kinase (AMPK) is sensitive to oxidative stress both directly or indirectly with repercussion on autophagy induction [26–28]. Indeed, the activation of AMPK leads to the inhibition of TORC1 promoting autophagy. In this regard, the activation of AMPK-dependent autophagy triggered by starvation is mediated by mitochondrial ROS burst [29]. On the other side, ROS-dependent activation of the MAPK14/p38 during starvation is necessary for restraining autophagy activation in cancer cells preserving cell viability in stress conditions [30].

Along with nutrient deprivation, another stressful condition that involves autophagy as an adaptive survival mechanism in hostile environment is hypoxia. Strikingly, although in low oxygen tension conditions, increase of ROS has been extensively documented upon hypoxia [31] and consequences on autophagy induction have been shown. Hypoxia-inducible factors (HIFs), the master regulators of hypoxia response, are indeed able to promote transcription of autophagy key proteins, including BCL2 interacting protein 3 (BNIP3) and NIP-like protein X (NIX) expression [32], which positively regulate autophagy through Beclin 1 activation in oxygen-deprived condition or after mitochondrial ROS generation.

5. HCC Risk Factors and ROS

HCC accounts for about 90% of all primary liver cancers worldwide, and due to a high rate of recurrence after resection and a poor response to conservative therapy, it has a very poor prognosis. Apart from genetic predisposition, a large number of environmental and lifestyle risk factors have been documented for HCC, primarily cirrhosis and hepatitis B virus (HBV)/hepatitis C virus (HCV) infections. Among others, nonalcoholic steatohepatitis (NASH), alcohol abuse, metabolic syndrome, and aflatoxin B exposure have to be mentioned [33].

For most of these risk factors, augmentation of oxidative stress has been reported as an accepted mechanism contributing to hepatocarcinogenesis. The X protein (HBx) codified by HBV genome has been associated with increased ROS production in mitochondria where it is associated with the outer membrane affecting human voltage-dependent anion-selective channel isoform 3 (hVDAC3) with consequent mitochondrial depolarization [34–36]. In line with this, the C-terminal region of HBx was shown to be crucial for the formation of oxidative DNA damage at mitochondrial level in terms of 8-oxoG with no evidence of nuclear DNA damage [37]. Increased levels of 8-oxoG were analogously observed in human hepatoma cells infected with HCV *in vitro* [38], as well as *in vivo* in livers of transgenic mice expressing HCV core protein [39]. HCV-mediated ROS production also occurs via alteration of mitochondrial functionality including inhibition of the electron transport chain [40, 41], altered transmembrane potential [39], and endoplasmic reticulum-(ER-) mitochondrial calcium mobilization [42, 43]. Alternative mechanisms leading to augmented ROS production by HCV infection involve the upregulation of NADPH oxidases 1 and 4 subunits via the transforming growth factor β1 (TGF-β1) signaling or induction of cytochrome P450 2E1 (CYP2E1), which is a cell detoxification system producing different ROS species [44]. Imbalance in oxidative stress was also demonstrated during alcohol abuse which promotes ROS by xanthine oxidase, establishing hypoxic areas in the liver of rodents and humans [45], or by augmented activity of CYP2E1 entailed for ethanol catabolism [46, 47]. It is very interesting to note that no evidence of exacerbated ROS generation is ascribable to augmented activity of fatty acid oxidation and thus electron transport chain flux in lipid-rich condition typical of obesity- and NASH-driven HCC. In fact, analyses of the liver from patients with NASH have only revealed mutations or decreased levels of electron transport chain complexes [48, 49] and ROS generation has been hypothetically associated with CYP2E1 activity, iron accumulation, and ER stress [50]. This may imply that when ROS derive from physiological sources (e.g., lipid beta-oxidation), cells with a high level of metabolic competence like hepatocytes induce homeostatic pathways for managing ROS burst. In support of this, fatty acids liberated by the rate-limiting enzyme of triacylglycerols are able to activate the signaling of nuclear receptors, such as peroxisome proliferator-activated receptors (PPAR), affecting antioxidant response and metabolic adaptations with implications also in HCC development [51, 52].

Apart from genetic aberrations due to direct formation of 8-oxoG on DNA or to lipid peroxidation that induces the promutagenic DNA adduct cyclic γ-hydroxy-1, N2-propanodeoxyguanosine [53], oxidative stress also contributes to hepatocarcinogenesis via epigenetic mechanisms. Locus-specific epigenetic changes occurring in HCC cells include the hypermethylation of the E-cadherin promoter by H_2O_2 treatment [54] and the hypermethylation of the suppressor of cytokine signaling 3 (SOCS3) due to HBV-induced mitochondrial ROS accumulation [55]. In both these examples, the oncogene Snail is actively involved recruiting the repressive epigenetic enzymes DNA methyltransferase 1 (DNMT1) and histone deacetylase 1 (HDAC1).

6. Autophagic Response to Oxidative Stress during HCC Onset

The pivotal tumor suppressor mechanism exploited by autophagy for buffering dangerous ROS production is the removal of damaged mitochondria by mitophagy. This selective engulfment of mitochondrial cargo engages a number of adaptor proteins, such as BNIP3 and NIX, in combination with E3 ubiquitin ligases that operate when localized at mitochondria, such as Parkin and Mitochondrial E3 Ubiquitin Protein Ligase 1 (Mul1). In particular, Parkin dampens HCC development as demonstrated by the proliferative phenotype of hepatocytes and the development of macroscopic

Table 2: Molecules tested in HCC cell lines and impinging on ROS/autophagy crosstalk.

Drug	Effect	Role of ROS	Source of oxidative stress	Ref.
Sorafenib	Apoptosis and prosurvival autophagy	Dose-dependent cytostatic and cytotoxic effects; apoptotic cell death	Mitochondrial ROS and GSH depletion	[70, 71]
Oxaliplatin	Apoptosis and prosurvival autophagy	Enhanced apoptotic cell death upon autophagy inhibition	Inhibition of thioredoxin reductase	[76, 92]
Salinomycin	Apoptosis and inhibition of autophagy	Contribution to apoptosis activation	Accumulation of dysfunctional mitochondria due to impaired autophagic flux	[79]
Capsaicin	Apoptosis and induction of cytoprotective STAT3-dependent autophagy	Phosphorylation of STAT3 and activation of autophagy	Inhibition of mitochondrial complexes I and III; reduction of antioxidants (results obtained in pancreatic cancer cells)	[80, 93]
Licochalcone A	Induction of apoptosis and prosurvival ULK1/ATG13-mediated autophagy	Activation of autophagic flux	Suppression of the GSH generation and formation of superoxide	[78]
Bevacizumab	Antiangiogenic effect and induction of prosurvival autophagy	Enhancement of metabolic stress-induced oxidative damage and cytotoxicity	Indirectly obtained by metabolic stress such as starvation and hypoxia	[77]
OSU-03012	Autophagic cell death (ACD)	Activation of autophagic flux	Unknown. Mitochondrial superoxide production was demonstrated for the analogue Celecoxib	[83, 94]
DHEA	ACD	No involvement in autophagic commitment	Decrease of GSH/GSSG ratio and impaired pentose phosphate pathway	[86]
Tetrandrine	Apoptosis (high concentrations) and ACD (low concentrations)	Activation of ERK-mediated autophagic flux	Mitochondrial dysfunction	[87]
Adpa-Mn	Apoptosis and ACD	Induction of both apoptosis and autophagy	Mitochondrial dysfunction	[88]

hepatic tumors in Parkin knockout mice [56]. The activation of Parkin-dependent mitophagy was also documented in regard of ROS-mediated hepatocarcinogenic effect of ethanol. Accordingly, alcohol induced extensive mitochondrial damage and oxidative stress in Parkin knockout mouse livers, which exhibited decreased mitophagy and mitochondrial respiration [57, 58]. Moreover, relocalization of Parkin at dysfunctional mitochondria largely coincides with accumulated 8-oxoG in the liver from ethanol-treated rats [59]. A cytoprotective role of autophagy and mitochondrial disposal was also described in response to CYP2E1-dependent oxidative stress during chronic ethanol-induced liver injury [60]. The same outcome was inferred after treatment with agents able to stimulate CYP2E1-dependent toxicity, such as polyunsaturated fatty acid, arachidonic acid, and buthionine sulfoximine, in combination with autophagy modulators [61].

On the other hand, ROS-mediated autophagy has been linked with survival mechanisms of HCC to stressful conditions. Autophagic flux and ROS are both increased during ischemia/reperfusion injury, one of the major complications of liver resection, favoring proliferation and survival of HCC cells [62]. In addition, elevated ROS production was associated with the activation of AKT, which induces a survival-promoting autophagy sustaining p53 degradation and NF-κB expression in HCC [63].

Based on this complexity, a univocal functional outcome of the interplay between ROS and autophagy in HCC tumorigenesis cannot be predicted. Moreover, autophagy intersects many of the signaling pathways that are genetically altered (i.e., PI3K/Akt/mTOR, Ras/Raf/MAP kinase, and Wnt-β-catenin pathways), most of which are triggered by ROS. It is also to be noted that autophagy is directly involved in the modulation of oxidative stress response via stabilization of Nrf2, the master regulator of antioxidant pathways, by p62-mediated autophagic degradation of the Nrf2 inhibitor Keap1. However, a persistent p62-mediated stabilization of Nrf2 under stressful conditions may overcome the gatekeeper function of autophagy in the liver activating Nrf2-mediated reprogramming of metabolism, stress response, and cell cycle associated with hepatocarcinogenesis [64, 65]. Along with this, a detrimental connection between autophagy and Nrf2 has been also demonstrated in ATG5 liver-specific knockout mice, which spontaneously develop inflammation, fibrosis, and tumorigenesis, but this phenomenon is abolished in the absence of Nrf2 [66]. These examples further highlight how the complicated liaison between ROS signaling and autophagy can contribute to cancer development/progression when it is affected by genetic and chronic environmental insults.

7. Autophagic Response to Oxidative Stress during HCC Therapeutic Intervention

Due to molecular heterogeneity of HCC and resistance to common chemotherapy, the most radical curative approaches are therapeutic surgery and liver transplantation, when applicable. Systemic therapy is generally exploited when

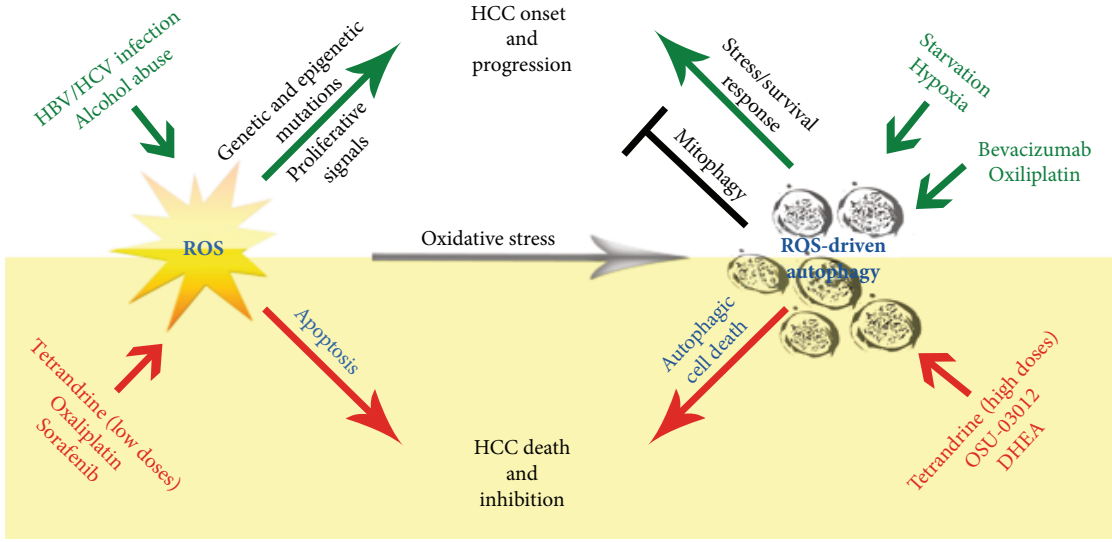

Figure 2: Interplay between ROS and autophagy in HCC as consequence of risk factors, environmental stress conditions, and therapeutic treatments.

terminal HCC occurs, and sorafenib is the only standard treatment available [33]. Sorafenib is a multikinase inhibitor impinging on MAPK/ERK-mediated cell proliferation and VEGF-driven angiogenesis thus targeting both tumor cells and endothelial cells [67]. Apoptosis has been classically considered as the major cytotoxic effect of sorafenib *in vitro* and in animal models [68], but typical signs of apoptotic cell death were not frequently observed in HCC patients treated with sorafenib, till to be considered as a weak proapoptotic molecule as a single agent [69]. This is in line with the survival of only two-three months observed for advanced HCC patients cured with sorafenib and the need of developing new effective interventions. In this regard, the research of a combinatorial therapeutic approach for enhancing sorafenib efficacy in HCC has been currently intensified based on the fact that sorafenib elicits a plethora of secondary mechanisms, including both oxidative stress and autophagy. Mitochondria-dependent ROS production accounts for cytostatic and cytotoxic effects of sorafenib in a dose-dependent manner [70, 71]. On the other hand, autophagy induction by sorafenib is largely exploited for adaptive survival response and is triggered by several cues, such as ER stress [72], mTORC1 inhibition [73], or Beclin 1 release from inhibitory factors [74]. However, autophagy seems also to improve the lethality of sorafenib against HCC cells promoting apoptosis, suggesting that individual HCC cells may activate distinct autophagy signaling pathways that allow them to respond differently to chemotherapeutic treatments [75]. Even though oxidative stress and autophagy are concomitant events linked to sorafenib, no mutual relationship has been highlighted so far. Such connection has been instead largely described for alternative chemotherapeutic agents that have been characterized in preclinical models of HCC. Oxaliplatin treatment induces proapoptotic effects via ROS generation, and hindering autophagy exacerbates that phenotype [76]. Autophagy inhibitors also foster apoptotic cell death triggered by bevacizumab in the presence of ROS derived from starvation or hypoxia [77]. The occurrence of apoptotic cell death after salinomycin, capsaicin, propyl gallate, or licochalcone A treatment was instead dependent on a direct impact of these molecules on the autophagic response to oxidative stress [78–81] (Table 2).

Notably, a number of papers have also clarified that the induction of ROS-mediated autophagic flux can culminate in HCC cytotoxicity via autophagic cell death (ACD). This mechanism was proposed during hyperthermia-dependent radiotherapy sensitization [82] and demonstrated after treatment with chemotherapeutic compounds. The administration of OSU-03012, a synthetic compound acting as a 3-phosphoinositide-dependent kinase 1 (PDK1) inhibitor, elicits ACD in HCC cells differently from other tumor types where it triggers apoptosis. Moreover, in HCC, this outcome is independent of PDK1 but connected with ROS-mediated autophagy induction [83]. Analogously, the adrenal steroid hormone dehydroepiandrosterone (DHEA) induces ACD only in some cellular contexts [84, 85], including HCC, where it acts independently of the typical inhibition of the glucose-6-phosphate dehydrogenase (G6PDH) triggering ROS burst and oxidative stress [86]. The dosage of the alkaloid tetrandrine in HCC cells was instead demonstrated to tip the balance in favor of apoptosis or ACD at high and low concentrations, respectively. In this context, ACD was triggered by ROS-mediated activation of the ERK signaling pathway and overexpression of ATG7 [87]. In many other cases, such as after treatment with the alkaloid tetramethylpyrazine or with the novel manganese (II) compound Adpa-Mn, induction of ROS-dependent autophagy and apoptosis is a concomitant event necessary for therapeutic success [88, 89] (Table 2).

The complex scenario described here can be justified by the fact that several stimuli and pathways, including ROS,

are shared by autophagy and apoptosis, and a number of mutually regulatory mechanisms exist. In this context, Beclin 1 plays a central role at the molecular level. For instance, during sustained exposure to apoptotic insults, Beclin 1 is a target of caspase proteolytic activity that generates fragments able to inhibit autophagy but to stimulate apoptosis. Moreover, Beclin 1 is inhibited by the interaction with the antiapoptotic protein Bcl-2 whereas Beclin 1-mediated autophagy prevents apoptosis by degrading the active caspase-8 [90].

8. Conclusion

Oxidative stress is a critical event linked to hepatocarcinogenesis and virtually associated with all the wide range of environmental risk factors contributing to HCC onset (Figure 2). In general, increased levels of ROS are responsible for genetic/epigenetic mutations and proliferative signals, but a failure in the counterbalance of ROS by antioxidants predisposes to cell death. Autophagy is also a double-edged sword in the context of HCC onset/progression. Autophagy acts as a tumor suppressor mechanism in the liver avoiding proteotoxicity [91] and aberrant mitochondrial ROS production via mitophagy [56] (Figure 2), but it also accounts for tumor adaptation to stressful conditions, such as starvation and hypoxia, mostly in the inner core of the tumor [62, 63]. The interplay between ROS and autophagy has a strong impact on therapeutic outcomes. Several prooxidant molecules tested in HCC were shown to induce simultaneously apoptotic cell death and autophagy. However, the latter can act as a prosurvival response typically associated with drug resistance or as an alternative/combined cytotoxic mechanism in terms of autophagic cell death (Figure 2). This definitively indicates that targeting autophagy in HCC is a complex approach that needs to be carefully evaluated for the success of a therapeutic strategy based on ROS-generating drugs.

Conflicts of Interest

The authors have no conflict of interest concerning this paper.

Acknowledgments

This work was supported by the Italian Association for Cancer Research (AIRC, n. 15403 M.R.C.) and from MIUR/-PRIN 2017 (n. 2017A5TXC3).

References

[1] M. Schieber and N. S. Chandel, "ROS function in redox signaling and oxidative stress," *Current Biology*, vol. 24, no. 10, pp. R453–R462, 2014.

[2] C. E. Cross, B. Halliwell, E. T. Borish et al., "Oxygen radicals and human disease," *Annals of Internal Medicine*, vol. 107, no. 4, pp. 526–545, 1987.

[3] L. B. Poole, "The basics of thiols and cysteines in redox biology and chemistry," *Free Radical Biology & Medicine*, vol. 80, pp. 148–157, 2015.

[4] S. Di Meo, T. T. Reed, P. Venditti, and V. M. Victor, "Role of ROS and RNS sources in physiological and pathological conditions," *Oxidative Medicine and Cellular Longevity*, vol. 2016, Article ID 1245049, 44 pages, 2016.

[5] K. Aquilano, S. Baldelli, and M. R. Ciriolo, "Glutathione: new roles in redox signaling for an old antioxidant," *Frontiers in Pharmacology*, vol. 5, p. 196, 2014.

[6] M. Sundaresan, Z. X. Yu, V. J. Ferrans, K. Irani, and T. Finkel, "Requirement for generation of H_2O_2 for platelet-derived growth factor signal transduction," *Science*, vol. 270, no. 5234, pp. 296–299, 1995.

[7] D. K. Jagadeesha, M. Takapoo, B. Banfi, R. C. Bhalla, and F. J. Miller Jr., "Nox1 transactivation of epidermal growth factor receptor promotes N-cadherin shedding and smooth muscle cell migration," *Cardiovascular Research*, vol. 93, no. 3, pp. 406–413, 2012.

[8] N. R. Jena, "DNA damage by reactive species: mechanisms, mutation and repair," *Journal of Biosciences*, vol. 37, no. 3, pp. 503–517, 2012.

[9] H. Kamata, S. Honda, S. Maeda, L. Chang, H. Hirata, and M. Karin, "Reactive oxygen species promote TNFα-induced death and sustained JNK activation by inhibiting MAP kinase phosphatases," *Cell*, vol. 120, no. 5, pp. 649–661, 2005.

[10] Y. Diao, W. Liu, C. C. L. Wong et al., "Oxidation-induced intramolecular disulfide bond inactivates mitogen-activated protein kinase kinase 6 by inhibiting ATP binding," *Proceedings of the National Academy of Sciences of the United States of America*, vol. 107, no. 49, pp. 20974–20979, 2010.

[11] E. Giannoni, F. Buricchi, G. Raugei, G. Ramponi, and P. Chiarugi, "Intracellular reactive oxygen species activate Src tyrosine kinase during cell adhesion and anchorage-dependent cell growth," *Molecular and Cellular Biology*, vol. 25, no. 15, pp. 6391–6403, 2005.

[12] J. E. Mills, P. C. Whitford, J. Shaffer, J. N. Onuchic, J. A. Adams, and P. A. Jennings, "A novel disulfide bond in the SH2 domain of the C-terminal Src kinase controls catalytic activity," *Journal of Molecular Biology*, vol. 365, no. 5, pp. 1460–1468, 2007.

[13] J. Kwon, S. R. Lee, K. S. Yang et al., "Reversible oxidation and inactivation of the tumor suppressor PTEN in cells stimulated with peptide growth factors," *Proceedings of the National Academy of Sciences of the United States of America*, vol. 101, no. 47, pp. 16419–16424, 2004.

[14] M. L. Taddei, M. Parri, T. Mello et al., "Integrin-mediated cell adhesion and spreading engage different sources of reactive oxygen species," *Antioxidants & Redox Signaling*, vol. 9, no. 4, pp. 469–481, 2007.

[15] T. R. Hurd, M. DeGennaro, and R. Lehmann, "Redox regulation of cell migration and adhesion," *Trends in Cell Biology*, vol. 22, no. 2, pp. 107–115, 2012.

[16] C. He and D. J. Klionsky, "Regulation mechanisms and signaling pathways of autophagy," *Annual Review of Genetics*, vol. 43, no. 1, pp. 67–93, 2009.

[17] S. Catarino, P. Pereira, and H. Girao, "Molecular control of chaperone-mediated autophagy," *Essays in Biochemistry*, vol. 61, no. 6, pp. 663–674, 2017.

[18] N. Hay and N. Sonenberg, "Upstream and downstream of mTOR," *Genes & Development*, vol. 18, no. 16, pp. 1926–1945, 2004.

[19] M. Zachari and I. G. Ganley, "The mammalian ULK1 complex and autophagy initiation," *Essays in Biochemistry*, vol. 61, no. 6, pp. 585–596, 2017.

[20] J. H. Hurley and L. N. Young, "Mechanisms of autophagy initiation," *Annual Review of Biochemistry*, vol. 86, no. 1, pp. 225–244, 2017.

[21] E. Itakura, C. Kishi, K. Inoue, and N. Mizushima, "Beclin 1 forms two distinct phosphatidylinositol 3-kinase complexes with mammalian Atg14 and UVRAG," *Molecular Biology of the Cell*, vol. 19, no. 12, pp. 5360–5372, 2008.

[22] Y. Kabeya, N. Mizushima, A. Yamamoto, S. Oshitani-Okamoto, Y. Ohsumi, and T. Yoshimori, "LC3, GABARAP and GATE16 localize to autophagosomal membrane depending on form-II formation," *Journal of Cell Science*, vol. 117, no. 13, pp. 2805–2812, 2004.

[23] S. Pankiv, T. H. Clausen, T. Lamark et al., "p62/SQSTM1 binds directly to Atg8/LC3 to facilitate degradation of ubiquitinated protein aggregates by autophagy," *Journal of Biological Chemistry*, vol. 282, no. 33, pp. 24131–24145, 2007.

[24] R. Scherz-Shouval, E. Shvets, E. Fass, H. Shorer, L. Gil, and Z. Elazar, "Reactive oxygen species are essential for autophagy and specifically regulate the activity of Atg4," *The EMBO Journal*, vol. 26, no. 7, pp. 1749–1760, 2007.

[25] B. Carroll, E. G. Otten, D. Manni et al., "Oxidation of SQSTM1/p62 mediates the link between redox state and protein homeostasis," *Nature Communications*, vol. 9, no. 1, p. 256, 2018.

[26] S. Cardaci, G. Filomeni, and M. R. Ciriolo, "Redox implications of AMPK-mediated signal transduction beyond energetic clues," *Journal of Cell Science*, vol. 125, no. 9, pp. 2115–2125, 2012.

[27] A. Alexander, S. L. Cai, J. Kim et al., "ATM signals to TSC2 in the cytoplasm to regulate mTORC1 in response to ROS," *Proceedings of the National Academy of Sciences of the United States of America*, vol. 107, no. 9, pp. 4153–4158, 2010.

[28] S. L. Choi, S. J. Kim, K. T. Lee et al., "The regulation of AMP-activated protein kinase by H_2O_2," *Biochemical and Biophysical Research Communications*, vol. 287, no. 1, pp. 92–97, 2001.

[29] L. Li, Y. Chen, and S. B. Gibson, "Starvation-induced autophagy is regulated by mitochondrial reactive oxygen species leading to AMPK activation," *Cellular Signalling*, vol. 25, no. 1, pp. 50–65, 2013.

[30] E. Desideri, R. Vegliante, S. Cardaci, R. Nepravishta, M. Paci, and M. R. Ciriolo, "MAPK14/p38α-dependent modulation of glucose metabolism affects ROS levels and autophagy during starvation," *Autophagy*, vol. 10, no. 9, pp. 1652–1665, 2014.

[31] R. D. Guzy and P. T. Schumacker, "Oxygen sensing by mitochondria at complex III: the paradox of increased reactive oxygen species during hypoxia," *Experimental Physiology*, vol. 91, no. 5, pp. 807–819, 2006.

[32] H. M. Sowter, P. J. Ratcliffe, P. Watson, A. H. Greenberg, and A. L. Harris, "HIF-1-dependent regulation of hypoxic induction of the cell death factors BNIP3 and NIX in human tumors," *Cancer Research*, vol. 61, no. 18, pp. 6669–6673, 2001.

[33] M. Le Grazie, M. R. Biagini, M. Tarocchi, S. Polvani, and A. Galli, "Chemotherapy for hepatocellular carcinoma: the present and the future," *World Journal of Hepatology*, vol. 9, no. 21, pp. 907–920, 2017.

[34] Z. Rahmani, K. W. Huh, R. Lasher, and A. Siddiqui, "Hepatitis B virus X protein colocalizes to mitochondria with a human voltage-dependent anion channel, HVDAC3, and alters its transmembrane potential," *Journal of Virology*, vol. 74, no. 6, pp. 2840–2846, 2000.

[35] K. W. Huh and A. Siddiqui, "Characterization of the mitochondrial association of hepatitis B virus X protein, HBx," *Mitochondrion*, vol. 1, no. 4, pp. 349–359, 2002.

[36] S. Takada, Y. Shirakata, N. Kaneniwa, and K. Koike, "Association of hepatitis B virus X protein with mitochondria causes mitochondrial aggregation at the nuclear periphery, leading to cell death," *Oncogene*, vol. 18, no. 50, pp. 6965–6973, 1999.

[37] S. Y. Jung and Y. J. Kim, "C-terminal region of HBx is crucial for mitochondrial DNA damage," *Cancer Letters*, vol. 331, no. 1, pp. 76–83, 2013.

[38] S. Pal, S. J. Polyak, N. Bano et al., "Hepatitis C virus induces oxidative stress, DNA damage and modulates the DNA repair enzyme NEIL1," *Journal of Gastroenterology and Hepatology*, vol. 25, no. 3, pp. 627–634, 2010.

[39] K. Machida, K. T. H. Cheng, C. K. Lai, K. S. Jeng, V. M. H. Sung, and M. M. C. Lai, "Hepatitis C virus triggers mitochondrial permeability transition with production of reactive oxygen species, leading to DNA damage and STAT3 activation," *Journal of Virology*, vol. 80, no. 14, pp. 7199–7207, 2006.

[40] M. Korenaga, T. Wang, Y. Li et al., "Hepatitis C virus core protein inhibits mitochondrial electron transport and increases reactive oxygen species (ROS) production," *Journal of Biological Chemistry*, vol. 280, no. 45, pp. 37481–37488, 2005.

[41] T. Tsutsumi, M. Matsuda, H. Aizaki et al., "Proteomics analysis of mitochondrial proteins reveals overexpression of a mitochondrial protein chaperon, prohibitin, in cells expressing hepatitis C virus core protein," *Hepatology*, vol. 50, no. 2, pp. 378–386, 2009.

[42] N. Dionisio, M. V. Garcia-Mediavilla, S. Sanchez-Campos et al., "Hepatitis C virus NS5A and core proteins induce oxidative stress-mediated calcium signalling alterations in hepatocytes," *Journal of Hepatology*, vol. 50, no. 5, pp. 872–882, 2009.

[43] Y. Li, D. F. Boehning, T. Qian, V. L. Popov, and S. A. Weinman, "Hepatitis C virus core protein increases mitochondrial ROS production by stimulation of Ca^{2+} uniporter activity," *The FASEB Journal*, vol. 21, no. 10, pp. 2474–2485, 2007.

[44] O. A. Smirnova, O. N. Ivanova, B. Bartosch et al., "Hepatitis C virus NS5A protein triggers oxidative stress by inducing NADPH oxidases 1 and 4 and cytochrome P450 2E1," *Oxidative Medicine and Cellular Longevity*, vol. 2016, Article ID 8341937, 10 pages, 2016.

[45] G. E. Arteel, Y. Iimuro, M. Yin, J. A. Raleigh, and R. G. Thurman, "Chronic enteral ethanol treatment causes hypoxia in rat liver tissue in vivo," *Hepatology*, vol. 25, no. 4, pp. 920–926, 1997.

[46] I. Dupont, D. Lucas, P. Clot, C. Menez, and E. Albano, "Cytochrome P4502E1 inducibility and hydroxyethyl radical formation among alcoholics," *Journal of Hepatology*, vol. 28, no. 4, pp. 564–571, 1998.

[47] T. Takahashi, J. M. Lasker, A. S. Rosman, and C. S. Lieber, "Induction of cytochrome P-4502E1 in the human liver by ethanol is caused by a corresponding increase in encoding messenger RNA," *Hepatology*, vol. 17, no. 2, pp. 236–245, 1993.

[48] M. Pérez-Carreras, P. del Hoyo, M. A. Martín et al., "Defective hepatic mitochondrial respiratory chain in patients with nonalcoholic steatohepatitis," *Hepatology*, vol. 38, no. 4, pp. 999–1007, 2003.

[49] H. Kawahara, M. Fukura, M. Tsuchishima, and S. Takase, "Mutation of mitochondrial DNA in livers from patients with alcoholic hepatitis and nonalcoholic steatohepatitis," *Alcoholism: Clinical and Experimental Research*, vol. 31, no. s1, pp. S54–S60, 2007.

[50] Z. Tariq, C. J. Green, and L. Hodson, "Are oxidative stress mechanisms the common denominator in the progression from hepatic steatosis towards non-alcoholic steatohepatitis (NASH)?," *Liver International*, vol. 34, no. 7, pp. e180–e190, 2014.

[51] L. di Leo, R. Vegliante, F. Ciccarone et al., "Forcing ATGL expression in hepatocarcinoma cells imposes glycolytic rewiring through PPAR-α/p300-mediated acetylation of p53," *Oncogene*, vol. 38, no. 11, pp. 1860–1875, 2019.

[52] R. Vegliante, L. Di Leo, F. Ciccarone, and M. R. Ciriolo, "Hints on ATGL implications in cancer: beyond bioenergetic clues," *Cell Death & Disease*, vol. 9, no. 3, p. 316, 2018.

[53] H. Coia, N. Ma, A. R. He et al., "Detection of a lipid peroxidation-induced DNA adduct across liver disease stages," *Hepatobiliary Surgery and Nutrition*, vol. 7, no. 2, pp. 85–97, 2018.

[54] S. O. Lim, J. M. Gu, M. S. Kim et al., "Epigenetic changes induced by reactive oxygen species in hepatocellular carcinoma: methylation of the E-cadherin promoter," *Gastroenterology*, vol. 135, no. 6, pp. 2128–2140.e8, 2008.

[55] K. Yuan, Y. Lei, H. N. Chen et al., "HBV-induced ROS accumulation promotes hepatocarcinogenesis through Snail-mediated epigenetic silencing of SOCS3," *Cell Death & Differentiation*, vol. 23, no. 4, pp. 616–627, 2016.

[56] M. Fujiwara, H. Marusawa, H. Q. Wang et al., "*Parkin* as a tumor suppressor gene for hepatocellular carcinoma," *Oncogene*, vol. 27, no. 46, pp. 6002–6011, 2008.

[57] H. K. Seitz and F. Stickel, "Molecular mechanisms of alcohol-mediated carcinogenesis," *Nature Reviews Cancer*, vol. 7, no. 8, pp. 599–612, 2007.

[58] J. A. Williams, H. M. Ni, Y. Ding, and W. X. Ding, "Parkin regulates mitophagy and mitochondrial function to protect against alcohol-induced liver injury and steatosis in mice," *American Journal of Physiology-Gastrointestinal and Liver Physiology*, vol. 309, no. 5, pp. G324–G340, 2015.

[59] N. Eid, Y. Ito, A. Horibe, and Y. Otsuki, "Ethanol-induced mitophagy in liver is associated with activation of the PINK1-Parkin pathway triggered by oxidative DNA damage," *Histology and Histopathology*, vol. 31, no. 10, pp. 1143–1159, 2016.

[60] Y. Lu and A. I. Cederbaum, "Autophagy protects against CYP2E1/chronic ethanol-induced hepatotoxicity," *Biomolecules*, vol. 5, no. 4, pp. 2659–2674, 2015.

[61] D. Wu and A. I. Cederbaum, "Inhibition of autophagy promotes CYP2E1-dependent toxicity in HepG2 cells via elevated oxidative stress, mitochondria dysfunction and activation of p38 and JNK MAPK," *Redox Biology*, vol. 1, no. 1, pp. 552–565, 2013.

[62] H. Du, W. Yang, L. Chen et al., "Emerging role of autophagy during ischemia-hypoxia and reperfusion in hepatocellular carcinoma," *International Journal of Oncology*, vol. 40, no. 6, pp. 2049–2057, 2012.

[63] Q. Huang, L. Zhan, H. Cao et al., "Increased mitochondrial fission promotes autophagy and hepatocellular carcinoma cell survival through the ROS-modulated coordinated regulation of the NFKB and TP53 pathways," *Autophagy*, vol. 12, no. 6, pp. 999–1014, 2016.

[64] Y. Ichimura, S. Waguri, Y. S. Sou et al., "Phosphorylation of p62 activates the Keap1-Nrf2 pathway during selective autophagy," *Molecular Cell*, vol. 51, no. 5, pp. 618–631, 2013.

[65] D. Bartolini, K. Dallaglio, P. Torquato, M. Piroddi, and F. Galli, "Nrf2-p62 autophagy pathway and its response to oxidative stress in hepatocellular carcinoma," *Translational Research*, vol. 193, pp. 54–71, 2018.

[66] H. M. Ni, B. L. Woolbright, J. Williams et al., "Nrf2 promotes the development of fibrosis and tumorigenesis in mice with defective hepatic autophagy," *Journal of Hepatology*, vol. 61, no. 3, pp. 617–625, 2014.

[67] S. M. Wilhelm, L. Adnane, P. Newell, A. Villanueva, J. M. Llovet, and M. Lynch, "Preclinical overview of sorafenib, a multikinase inhibitor that targets both Raf and VEGF and PDGF receptor tyrosine kinase signaling," *Molecular Cancer Therapeutics*, vol. 7, no. 10, pp. 3129–3140, 2008.

[68] L. Liu, Y. Cao, C. Chen et al., "Sorafenib blocks the RAF/-MEK/ERK pathway, inhibits tumor angiogenesis, and induces tumor cell apoptosis in hepatocellular carcinoma model PLC/PRF/5," *Cancer Research*, vol. 66, no. 24, pp. 11851–11858, 2006.

[69] J. M. Llovet, S. Ricci, V. Mazzaferro et al., "Sorafenib in advanced hepatocellular carcinoma," *The New England Journal of Medicine*, vol. 359, no. 4, pp. 378–390, 2008.

[70] J. F. Chiou, C. J. Tai, Y. H. Wang, T. Z. Liu, Y. M. Jen, and C. Y. Shiau, "Sorafenib induces preferential apoptotic killing of a drug- and radio-resistant Hep G2 cells through a mitochondria-dependent oxidative stress mechanism," *Cancer Biology & Therapy*, vol. 8, no. 20, pp. 1904–1913, 2009.

[71] R. Coriat, C. Nicco, C. Chereau et al., "Sorafenib-induced hepatocellular carcinoma cell death depends on reactive oxygen species production in vitro and in vivo," *Molecular Cancer Therapeutics*, vol. 11, no. 10, pp. 2284–2293, 2012.

[72] Y. H. Shi, Z. B. Ding, J. Zhou et al., "Targeting autophagy enhances sorafenib lethality for hepatocellular carcinoma via ER stress-related apoptosis," *Autophagy*, vol. 7, no. 10, pp. 1159–1172, 2011.

[73] S. Shimizu, T. Takehara, H. Hikita et al., "Inhibition of autophagy potentiates the antitumor effect of the multikinase inhibitor sorafenib in hepatocellular carcinoma," *International Journal of Cancer*, vol. 131, no. 3, pp. 548–557, 2012.

[74] W. T. Tai, C. W. Shiau, H. L. Chen et al., "Mcl-1-dependent activation of Beclin 1 mediates autophagic cell death induced by sorafenib and SC-59 in hepatocellular carcinoma cells," *Cell Death & Disease*, vol. 4, no. 2, p. e485, 2013.

[75] T. D. Fischer, J. H. Wang, A. Vlada, J. S. Kim, and K. E. Behrns, "Role of autophagy in differential sensitivity of hepatocarcinoma cells to sorafenib," *World Journal of Hepatology*, vol. 6, no. 10, pp. 752–758, 2014.

[76] Z. B. Ding, B. Hui, Y. H. Shi et al., "Autophagy activation in hepatocellular carcinoma contributes to the tolerance of oxaliplatin via reactive oxygen species modulation," *Clinical Cancer Research*, vol. 17, no. 19, pp. 6229–6238, 2011.

[77] X. L. Guo, D. Li, K. Sun et al., "Inhibition of autophagy enhances anticancer effects of bevacizumab in hepatocarcinoma," *Journal of Molecular Medicine*, vol. 91, no. 4, pp. 473–483, 2013.

[78] Q. Niu, W. Zhao, J. Wang et al., "LicA induces autophagy through ULK1/Atg13 and ROS pathway in human hepatocellular carcinoma cells," *International Journal of Molecular Medicine*, vol. 41, no. 5, pp. 2601–2608, 2018.

[79] J. Klose, M. V. Stankov, M. Kleine et al., "Inhibition of autophagic flux by salinomycin results in anti-cancer effect in hepatocellular carcinoma cells," *PLoS One*, vol. 9, no. 5, article e95970, 2014.

[80] X. Chen, M. Tan, Z. Xie et al., "Inhibiting ROS-STAT3-dependent autophagy enhanced capsaicin–induced apoptosis in human hepatocellular carcinoma cells," *Free Radical Research*, vol. 50, no. 7, pp. 744–755, 2016.

[81] P. L. Wei, C. Y. Huang, and Y. J. Chang, "Propyl gallate inhibits hepatocellular carcinoma cell growth through the induction of ROS and the activation of autophagy," *PLoS One*, vol. 14, no. 1, article e0210513, 2019.

[82] G. J. Yuan, J. J. Deng, D. D. Cao et al., "Autophagic cell death induced by reactive oxygen species is involved in hyperthermic sensitization to ionizing radiation in human hepatocellular carcinoma cells," *World Journal of Gastroenterology*, vol. 23, no. 30, pp. 5530–5537, 2017.

[83] M. Gao, P. Y. Yeh, Y. S. Lu et al., "OSU-03012, a novel celecoxib derivative, induces reactive oxygen species–related autophagy in hepatocellular carcinoma," *Cancer Research*, vol. 68, no. 22, pp. 9348–9357, 2008.

[84] R. A. Giron, L. F. Montano, M. L. Escobar, and R. Lopez-Marure, "Dehydroepiandrosterone inhibits the proliferation and induces the death of HPV-positive and HPV-negative cervical cancer cells through an androgen- and estrogen-receptor independent mechanism," *FEBS Journal*, vol. 276, no. 19, pp. 5598–5609, 2009.

[85] R. Vegliante and M. R. Ciriolo, "Autophagy and autophagic cell death: uncovering new mechanisms whereby dehydroepiandrosterone promotes beneficial effects on human health," *Vitamins and Hormones*, vol. 108, pp. 273–307, 2018.

[86] R. Vegliante, E. Desideri, L. Di Leo, and M. R. Ciriolo, "Dehydroepiandrosterone triggers autophagic cell death in human hepatoma cell line HepG2 via JNK-mediated p62/SQSTM1 expression," *Carcinogenesis*, vol. 37, no. 3, pp. 233–244, 2016.

[87] K. Gong, C. Chen, Y. Zhan, Y. Chen, Z. Huang, and W. Li, "Autophagy-related gene 7 (ATG7) and reactive oxygen species/extracellular signal-regulated kinase regulate tetrandrine-induced autophagy in human hepatocellular carcinoma," *Journal of Biological Chemistry*, vol. 287, no. 42, pp. 35576–35588, 2012.

[88] J. Liu, W. Guo, J. Li et al., "Tumor-targeting novel manganese complex induces ROS-mediated apoptotic and autophagic cancer cell death," *International Journal of Molecular Medicine*, vol. 35, no. 3, pp. 607–616, 2015.

[89] J. Cao, Q. Miao, S. Miao et al., "Tetramethylpyrazine (TMP) exerts antitumor effects by inducing apoptosis and autophagy in hepatocellular carcinoma," *International Immunopharmacology*, vol. 26, no. 1, pp. 212–220, 2015.

[90] R. Kang, H. J. Zeh, M. T. Lotze, and D. Tang, "The Beclin 1 network regulates autophagy and apoptosis," *Cell Death & Differentiation*, vol. 18, no. 4, pp. 571–580, 2011.

[91] A. Takamura, M. Komatsu, T. Hara et al., "Autophagy-deficient mice develop multiple liver tumors," *Genes & Development*, vol. 25, no. 8, pp. 795–800, 2011.

[92] A.-B. Witte, K. Anestål, E. Jerremalm, H. Ehrsson, and E. S. J. Arnér, "Inhibition of thioredoxin reductase but not of glutathione reductase by the major classes of alkylating and platinum-containing anticancer compounds," *Free Radical Biology & Medicine*, vol. 39, no. 5, pp. 696–703, 2005.

[93] K. C. Pramanik, S. R. Boreddy, and S. K. Srivastava, "Role of mitochondrial electron transport chain complexes in capsaicin mediated oxidative stress leading to apoptosis in pancreatic cancer cells," *PLoS One*, vol. 6, no. 5, article e20151, 2011.

[94] R. Pritchard, S. Rodriguez-Enriquez, S. C. Pacheco-Velazquez, V. Bortnik, R. Moreno-Sanchez, and S. Ralph, "Celecoxib inhibits mitochondrial O_2 consumption, promoting ROS dependent death of murine and human metastatic cancer cells via the apoptotic signalling pathway," *Biochemical Pharmacology*, vol. 154, pp. 318–334, 2018.

Hindawi
Oxidative Medicine and Cellular Longevity
Volume 2019, Article ID 1283075, 11 pages
https://doi.org/10.1155/2019/1283075

Review Article

Sestrins at the Interface of ROS Control and Autophagy Regulation in Health and Disease

Marco Cordani,[1] **Miguel Sánchez-Álvarez**,[2] **Raffaele Strippoli**,[3,4] **Alexandr V. Bazhin**,[5] **and Massimo Donadelli**[6]

[1]*Instituto Madrileño de Estudios Avanzados en Nanociencia (IMDEA Nanociencia), CNB-CSIC-IMDEA Nanociencia Associated Unit "Unidad de Nanobiotecnología", Madrid 28049, Spain*
[2]*Mechanoadaptation & Caveolae Biology Lab, Cell and Developmental Biology Area, Centro Nacional de Investigaciones Cardiovasculares (CNIC), Madrid 28029, Spain*
[3]*Department of Cellular Biotechnologies and Hematology, Section of Molecular Genetics, Sapienza University of Rome, Rome, Italy*
[4]*Gene Expression Laboratory, National Institute for Infectious Diseases "Lazzaro Spallanzani" I.R.C.C.S., Rome, Italy*
[5]*Department of General, Visceral and Transplantation Surgery, Ludwig Maximilian University, Munich, Germany*
[6]*Department of Neurosciences, Biomedicine and Movement Sciences, Section of Biochemistry, University of Verona, Verona, Italy*

Correspondence should be addressed to Marco Cordani; marco.cordani@imdea.org

Received 20 February 2019; Accepted 14 April 2019; Published 7 May 2019

Academic Editor: Joël R. Drevet

Reactive oxygen species (ROS) and autophagy are two highly complex and interrelated components of cell physiopathology, but our understanding of their integration and their contribution to cell homeostasis and disease is still limited. Sestrins (SESNs) belong to a family of highly conserved stress-inducible proteins that orchestrate antioxidant and autophagy-regulating functions protecting cells from various noxious stimuli, including DNA damage, oxidative stress, hypoxia, and metabolic stress. They are also relevant modulators of metabolism as positive regulators of the key energy sensor AMP-dependent protein kinase (AMPK) and inhibitors of mammalian target of rapamycin complex 1 (mTORC1). Since perturbations in these pathways are central to multiple disorders, SESNs might constitute potential novel therapeutic targets of broad interest. In this review, we discuss the current understanding of regulatory and effector networks of SESNs, highlighting their significance as potential biomarkers and therapeutic targets for different diseases, such as aging-related diseases, metabolic disorders, neurodegenerative diseases, and cancer.

1. Introduction

Reactive oxygen species (ROS) can play essential roles as intra- and extracellular messengers, encoding the functional/metabolic state of the cell for the regulation of numerous signalling pathways. However, ROS are also powerful oxidizing agents, which can induce cell injury upon modification of lipids, proteins, or DNA, disrupting cell function and increasing the risk of DNA mutation and tumorigenesis. Oxidation of specific amino acid residues in different metabolic enzyme systems (such as the 2-oxoglutarate dehydrogenase complex in the tricarboxylic acid cycle) can alter their activity by orders of magnitude, completely changing cell sensitivity to other environmental conditions, such as fuel availability or usage of nutrients [1]. Thus, aberrant ROS levels are a consequence shared by a broad list of pathologies, and ROS dysregulation substantially drives the onset and progression of a number of diseases. For example, high ROS levels found in most cancer cells can promote metabolic rewiring and growth dysregulation, as well as aberrant response of cells to different challenges by gating the activation threshold of apoptosis, necrosis, or autophagic death. Analogies can thereby be drawn for aging biology. As such, intervention of ROS levels has received substantial attention as a potential antiaging and anticancer therapeutic opportunity, including it in the renewed study of strategies, such as differential

ascorbate toxicity [2–4]. Conversely, ROS deficiency has been associated mechanistically with immune disorders, inflammation, and decreased proliferative response, partly because of the disruption of cell signalling wiring [5].

A major theme in ROS-associated disorders is their interplay with systems determining energy and nutrient homeostasis in the cell. The mechanistic target of rapamycin complex 1 (mTORC1) and 5′ AMP-activated protein kinase (AMPK) interpret multiple cues, including oxidative stress, to integrate them with the control of energy management, anabolism, and cell growth. Conversely, these signalling systems regulate metabolism and growth, which are major ROS sources themselves. These pathways, together with other stress signalling routes such as the Unfolded Protein Response (UPR), tightly regulate the autophagy flux, a key node for both the regulation of ROS levels and ROS-dependent cell regulation. This recycling function curbs ROS overproduction and, through a number of input pathways, is itself sensitive to existing ROS levels in the cell.

However, our understanding of the interplay between these two aspects of cell physiology (ROS and autophagy) is still limited. In this review, we aim to provide an overview of our current knowledge on sestrins (SESNs), a family of stress surveillance proteins which may hold a key to the integration of ROS control and autophagy regulation and may constitute an interesting source of novel therapeutic opportunities.

2. The Sestrin Protein Family

SESNs are a family of proteins induced upon various stressing conditions, such as hypoxia and metabolic imbalances [6]. Only one member is present in invertebrates (such as *Caenorhabditis elegans* (cSESN) and *Drosophila melanogaster* (dSESN), whereas three members are present in mammals, such as SESN1, SESN2, and SESN3. Vertebrate SESN1 (also known as PA26) is a transcriptional target of p53 [7]. SESN2 (also known as H195) was discovered as a gene activated by hypoxia [8]. The SESN3 gene is a largely uncharacterized open reading frame identified by homology [8]. Curiously, SESNs were named SESNs after a human genetics course held in Sestri Levante, a small town on the Ligurian coast of Italy, where researchers discovered the amino acid sequence homology between the three proteins [9]. Intriguingly, although they have close homology and likely common origin, each SESN gene maps to a different chromosome in the human genome: SESN1 to 6q21, SESN2 to 1p35.3, and SESN3 to 11q21 [8].

2.1. Structure-Function Relationships and Interactomes of SESNs. While phenotypic and pathophysiological associations for SESNs rapidly accumulated, information about their molecular underpinnings has been scarce. Inference from *in silico* studies has been limited by the fact that these proteins do not contain obvious similarity with any known structural domain or catalytic motif [6].

Recently, the determination of the human SESN2 structure by X-ray crystallography brought a novel insight into its potential function. The crystal structure revealed that hSESN2 contains two structurally similar subdomains, SESN-A and SESN-C, connected by a helix-loop-helix domain (SESN-B). Both subdomains share significant homology with proteins belonging to the alkyl hydroperoxidase family (including, for example, *M. tuberculosis* AhpD), which catalyse the reduction of peroxiredoxins [10, 11]. Alkyl hydroperoxidase activity has been confirmed for SESN2 (as reported below), while no biochemical characterization has so far been gathered for SESN1 and SESN3.

Multiple protein-protein interactions mediate activation, modulation, and function of SESNs [12]. In particular, analysis of the SESN2 structure allows the identification of three functional domains [10, 11]. An oxidoreductase active site within SESN-A, which contains the catalytic cysteine (C125) and conserved residues of the proton relay system (Y127 and H132), has been identified. These three amino acid residues were found to be critical for the antioxidant function of hSESN2. Although structural and biochemical evidence demonstrates that hSESN2 has intrinsic peroxidase activity, the physiological ROS substrate of hSESN2 remains to be identified. Secondly, a GATOR2-interacting surface at the C-terminal domain, containing a characteristic aspartate-aspartate (DD) motif, has been mapped. This DD motif appears to be required for the interaction between hSESN2 and GATOR2. The heteropentameric GATOR2 complex is a direct physical target of SESNs and mediates its mTORC1-regulating functions.

Finally, a leucine-binding site is present in the SESN-C domain. The existence of this leucine-binding site suggests that hSESN2 acts as a direct cellular sensor of leucine level, which is a relevant feature considering that leucine is a key amino acid for the lysosome-mTORC1 system to sense overall levels of amino acid nutrients [13].

Importantly, SESN2 also interacts with Kelch-like ECH-associated protein 1 (Keap1) and the autophagy regulators p62/sequestosome-1 (SQSTM1) and Unc51-like 1 (ULK1). These interactions likely underpin a substantial share of the impact of SESN2 on the suppression of oxidative damage and on autophagy regulation respectively, as detailed below (Figure 1).

2.2. Regulation of Expression and Function of SESNs. SESNs are proteins ubiquitously expressed in adults, although there exist tissue-specific variations in gene expression levels [7–9]. Interestingly, SESN1 and SESN2 are most highly expressed in skeletal muscle [7], a feature shared only by the *Drosophila* homolog, dSESN [14]. dSESN expression increases with aging [14], while expression of SESNs in humans is reduced in individuals of advanced age [15].

As a family of stress-inducible proteins, SESNs have been reported to be upregulated and activated upon exposure to DNA damage, oxidative stress, and hypoxia. Whereas SESN1 and SESN2 are mainly responsive to p53 [7, 8], SESN3 is activated by forkhead box O (FoxO) transcriptional factors [16]. Other transcription factors responsible for the expression of SESNs include nuclear factor erythroid 2-like 2 (Nrf2) [17], NH(2)-terminal kinase (JNK)/c-Jun pathway [18], and hypoxia-inducible factor-1α (HIF-1α) [19].

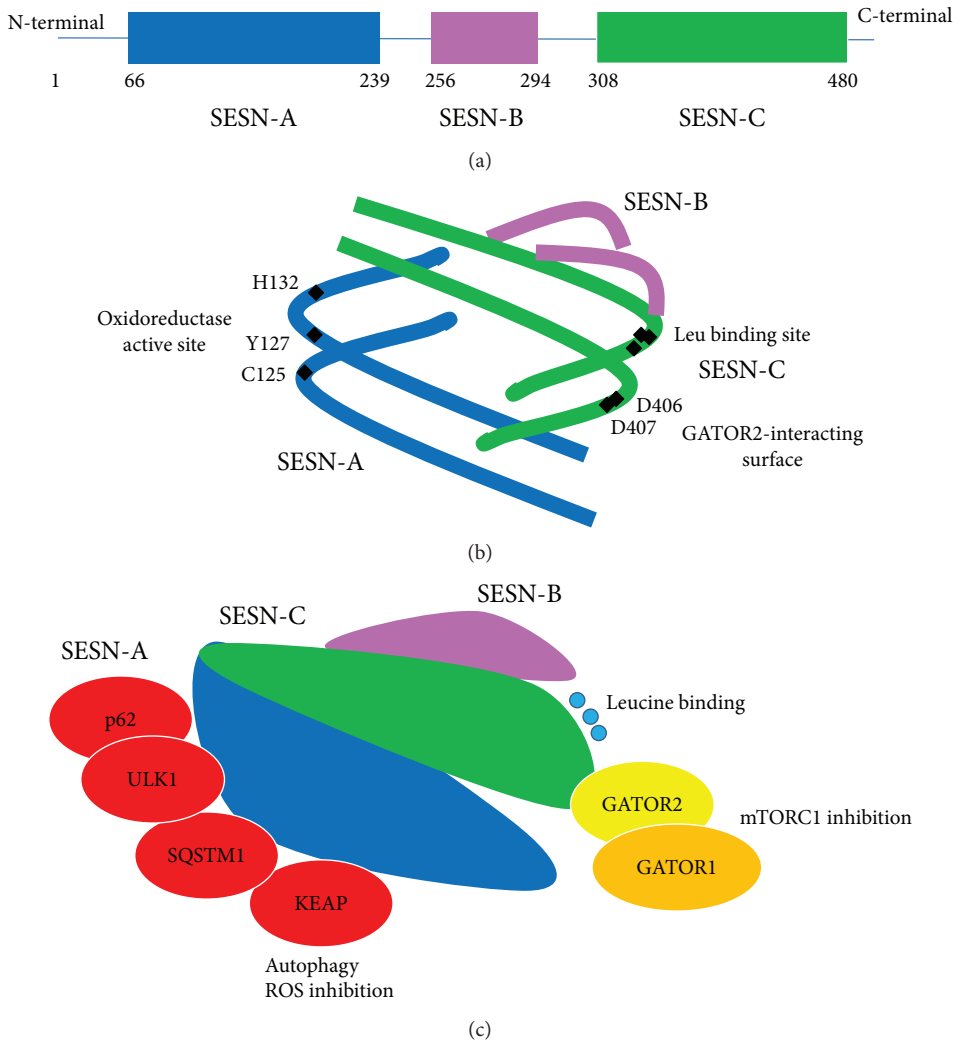

Figure 1: (a) Schematic diagram of full-length SESN2 showing the three domains SESN-A, SESN-B, and SESN-C. (b) Schematic representation of SESN2 showing the localization of the catalytic cysteine (C125) and conserved residues of the proton relay system (Y127 and H132) in the SESN-A domain, the characteristic aspartate-aspartate (DD) motif, and the Leu binding site in the SESN-C domain (based on structure analysis published by Ho et al. in reference [12], Figure 1, doi:10.1016/j.tibs.2016.04.005). (c) Schematic representation of SESN2 showing direct interactors and pathways involved.

Different stimuli modulate the SESN phosphorylation state, a key aspect of SESN regulation. Multiple phosphor-acceptor sites have been found in dSESN *in vivo* in *Drosophila* [20]. In humans, regulation by phosphorylation has been characterized mainly for the SESN2 paralog. Mass spectrometry analysis of human SESN2 revealed three highly conserved phosphorylation sites. Importantly, mutation of these sites to phosphor-mimetic amino acids in exogenously expressed SESN2 promoted its interaction with GATOR2 and dramatically repressed mTORC1 [21]. This supports a potential relevance for SESN2 phosphorylation in the negative regulation of mTOR to prevent age-related pathologies caused by chronic mTOR activation.

3. SESN2 in Antioxidant Defence

SESNs promote antioxidant adaptive responses in cells as induced upon intracellular oxidative stress by the stimulation of transcription factors, such as p53, Nrf2, AP-1, and FoxOs (Figure 2). SESN1 is induced by hydrogen peroxide in a p53-dependent manner, whereas the induction of SESN2 by oxidative stress is only partially dependent on p53 activation [22]. SESN2 can be induced in conditions of increased ROS production, in a CCAAT/enhancer binding protein-beta- (C/EBPβ-) dependent manner [23]. More recently, oxidative stress was found to induce SESN2 via activation of the transcription factor Nrf2 [17] and via the JNK/AP-1 signalling axis [18], while SESN3 is stimulated by oxidative damage via activation of FoxO transcription factors [24, 25]. Consistent with a relevant contribution of SESNs in the cellular antioxidant defence, silencing of all the three SESN isoforms blunts the antioxidant response to different oxidative stress challenges [16, 26], whereas ectopic expression of SESNs has a protective impact. However, the molecular underpinnings of this activity are still incompletely clear.

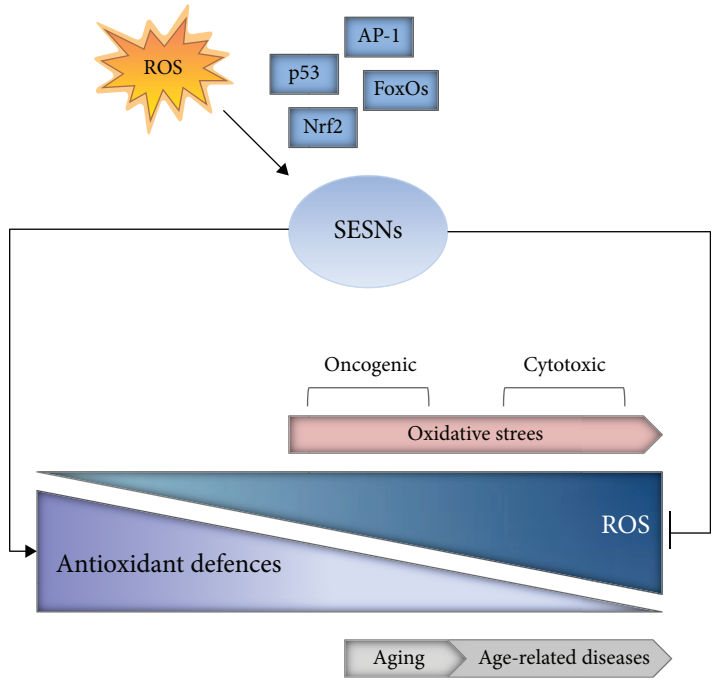

Figure 2: SESNs are master regulators of antioxidant defences. SESNs may be induced upon intracellular oxidative stress by the stimulation of transcription factors, such as p53, Nrf2, AP-1, and FoxOs. Once activated, SESNs limit ROS and oxidative stress by multiple mechanisms, thus having a functional role in age-related diseases as well as cancer.

As mentioned above, the oxidoreductase active site within SESN-A is critical for the antioxidant function of hSESN2. While structural and biochemical evidence demonstrates that hSESN2 has intrinsic peroxidase activity, the physiological ROS substrate(s) of hSESN2 is (are) currently unknown. Hydrogen peroxide, which is among the most abundant and biologically significant cellular ROS species, is not efficiently reduced by hSESN2, and the only known substrate under *in vitro* conditions for hSESN2 is cumene hydroperoxide, which is not a physiological ROS in any known cell type [10].

Since a small conserved region in SESNs shows a limited sequence homology to AhpD protein of *Mycobacterium tuberculosis* [26], this similarity was analyzed for its ability to reduce known substrates of AhpD, such as peroxiredoxin (Prx). SESNs can indeed reduce Prx, but intriguingly this does not require their catalytic activity [27]. It was hypothesized that SESNs may promote the activity of other oxidoreductases, such as sulforedoxin (Srx), that in turn can regenerate Prx. Indeed, one recent study showed that SESNs can increase Srx expression through positive feedback activation of Nrf2, a transcription factor that orchestrates antioxidant responses [28].

Independent of their Prx-regulating activity, SESNs contribute to cell redox homeostasis through the regulation of AMPK-mTORC1 signalling pathways. dSESN$^{-/-}$ Drosophila cells exhibit increased TOR activity [14]. Since mTOR activity may enhance ROS production via inhibition of autophagy or directly acting on mitochondrial function, a relevant share of the antioxidant role of SESNs may be derived from mTOR signalling inhibition.

4. SESNs as Regulators of Autophagy and Mitophagy

The term "autophagy" refers to a group of regulated mechanisms by which cells break down specific building blocks and structures, enabling their recycling, the rerouting of their energy, or their disposal when they are damaged and/or toxic [29]. While a number of pathway variants exist, the core machinery and the regulatory cascade its components map to are rather defined and evolutionarily conserved [29]. The Unc51-like kinases ULK1/2 are major phosphor-regulated initiator switches of the pathway, tightly controlled by positive growth signalling [30]. Their dephosphorylation triggers the nucleation of the phagophore, the precursory membrane structure from which the autophagic vesicle is formed, by a Vps14/Beclin1/Atg14L complex [31]. This event initiates a signalling cascade that accumulates PE-conjugated Atg8, which drives the maturation and closure of autophagosomes, enabling the docking of specific cargos and adaptor proteins, such as sequestosome-1/p62 [32]. The fusion of the autophagosome with the lysosomal compartment is mediated by multiple proteins, including SNAREs and UVRAG [33]. Autophagy is tightly linked to ROS control in the cell [34].

Mitophagy is a specialized form of autophagy by which dysfunctional or damaged mitochondria are selectively targeted by autophagosomes and delivered to lysosomes to be recycled by the cell. Hence, mitophagy represents an essential quality control mechanism to ensure the integrity and functionality of the mitochondrial network [35]. Dysregulation of mitophagy leads to unresolved damage to mitochondria, a powerful source for pathological ROS levels [36]. High

levels of mitochondrial ROS lead in turn to an inflammatory status through various mechanisms, including hyperactivation of the NLRP3 inflammasome [36]. These events have been proposed to play a role in diverse degenerative pathologies by leading to the release of mitochondrial DNA, tissue injury, and cell death [37, 38]. Several reports indicate that SESNs are positive regulators of autophagy in the face of diverse environmental stresses that entail mitochondrial dysfunction [28, 39–41]. Under energetic stress, AMPK-dependent ULK1 phosphorylation promotes autophagy by targeting several downstream crucial autophagy effectors involved in autophagy machinery [42]. p62/SQSTM1 protein is another important player in the autophagy process. Indeed, p62 can function as an adaptor protein binding to diverse autophagy substrates, such as ubiquitinated proteins, damaged mitochondria, and the Nrf2 inhibitor Keap1, and promotes their autophagic degradation, contributing to the restoration of the physiological levels of ROS [43].

SESN2 binds to p62 and promotes the autophagic degradation of p62-dependent targets, including Keap1, thereby channelling autophagy turnover flux towards functionally coherent substrate sets and upregulating the transcription of antioxidant genes [28]. In addition, SESN2 physically associates with ULK1 and p62 to form a functional complex, favouring ULK1-mediated p62 phosphorylation [44]. Furthermore, SESN2 promotes the targeting of mitochondria for recognition by the autophagic machinery, a process described as "mitochondrial priming," which is further potentiated by the intrinsic capability of SESN2 to increase ULK1 protein levels. This activity has been proposed to contribute to immunological homeostasis and the attenuation of NLRP3 hyperactivation [45]. Recently, the role of SESN2 in the protection of renal tubules during acute kidney injury (AKI) has been explored [46]. AKI is a pathophysiological condition characterized by increased mitochondrial damage that leads to oxidative stress and apoptosis in tubular renal cells [47]. Intriguingly, autophagy and mitophagy are induced in renal tubules in AKI through a p53-SESN2 axis, which may constitute a protective mechanism of the cell [46].

5. Control of the Cellular Energetic Metabolism by SESNs: Regulation of mTOR and AMPK Signalling

mTORC1 is one of the major signalling nodes coupling environmental and metabolic signals such as nutrients, growth factors, oxygen, and stress with the control of protein synthesis, lipid anabolism, and cell growth [48–50]. The recycling and scavenging of cell components prevent *de novo* a cell mass increase, and a major signal output from mTORC1 blunts autophagy [51]: mTORC1 phosphorylates ULK1 on Ser757, disrupting its interaction with AMPK, an event required to activate ULK1 to induce the canonical autophagic pathway [42].

A number of studies suggest that SESNs can serve as endogenous sensors of amino acid fluctuations in the cellular microenvironment, which are one of the central inputs regulating mTORC1 signalling. Indeed, SESN2 induction is necessary for cell survival during glutamine deprivation [52]. A SESN-dependent and AMPK-independent mechanism for mTORC1 inhibition might be mediated by the interaction of SESNs with GATOR2 [53–55]. As a result of this interaction, SESNs suppress lysosomal mTOR localization in a Rag-dependent manner. This mechanism is thus a potential integral component of mTORC1 regulation by amino acid availability, connecting stress responses with mTORC1 control [53–55]. SESNs also bind to the heterodimeric RagA/B-RagC/D GTPases, thus acting as GDIs for RagA/B [56]. Accordingly, ectopic overexpression of SESNs in HEK293T, HeLa, and MEF cell lines can inhibit amino acid-induced translocation of Rag-GEF and mTORC1 to the lysosome [56].

Intriguingly, two studies contribute biochemical and biophysical evidence suggesting that SESN2 acts as a direct sensor of leucine, which directly precludes the interaction of SESN2 with GATOR2 [11, 13, 57]. This intriguing hypothesis however has not been fully proven, and other studies question the idea that SESN2-dependent suppression of mTORC1 signalling is sensitive to leucine [14, 24, 53, 54, 56, 58–61], and the physical interaction between SESN2 and GATOR2 in cells can still be detected despite leucine-rich culture conditions [53–55]. A possible scenario to reconcile these conflicting observations might rely on the effect of leucine on SESN2 being highly context-dependent. Further studies will clarify the impact of leucine levels on the SESN2-GATOR2 interaction across conditions. Additional mechanisms have been proposed to explain the contribution of SESN2 in amino acid sensing. Ye et al. reported a signalling axis whereby the eIF2α kinase General Control Nonderepressible 2 (GCN2) is the driving sensor of amino acid scarcity and translationally upregulates the stress transcriptional regulator ATF4 to induce the expression of SESN2, which in turn may block the lysosomal recruitment and activation of mTORC1 [62]. Another report shows that in response to leucine starvation, SESN2 is phosphorylated by ULK1 thus affecting mTORC1 activation [21]. In addition to being phosphorylated by ULK1, SESN2 may sustain ULK1-dependent phosphorylation [44] and degradation of SQSTM1/p62 [28]. Because SQSTM1 is an mTORC1 regulator involved in amino acid sensing [63–65], deeper studies will be needed to clarify the functional link between SESN2, ULK1, SQSTM1, and GATOR2 in the context of amino acid sensing.

Notably, amino acid consumption (particularly that of amino acids entering anaplerotic routes as alternative intermediates for anabolism) and derived imbalances can constitute sources of redox alteration. For example, Byun et al. found that glutamine deprivation reduces GSH synthesis (possibly because of a subsequent shortage in 2-oxoglutarate), which in turn induces SESN2 expression via the ROS-p38 MAPK-C/EBP pathway. Of note, this study identified a positive feedback loop between SESN2 and mTORC2 as necessary to suppress mTORC1 activity in glutamine-depleted non-small-cell lung cancer cells (NSCLC). This divergent regulation of mTORC1 and mTORC2 by SESN2 might contribute to the maintenance of redox homeostasis in the face of

amino acid imbalance, enabling lung cancer cells to survive under glutamine-depleted conditions, and might thus constitute an attractive synergistic therapeutic target in tumours showing such metabolic "addiction" [66].

AMPK inhibits mTORC1 through the phosphorylation of TSC2 and raptor (two phosphor-dependent hallmarks of mTORC1 inactivation) in response to cellular energy cues [67–69]. Evidence indicates that SESN-dependent AMPK induction is important for mTORC1 suppression in diverse cellular contexts, and at least one SESN paralog, SESN2, has been found to coimmunoprecipitate with AMPK from tissue extracts [40, 59, 70–73]. In *Drosophila*, chronic TOR activation upregulates dSESN through accumulation of ROS. dSESN acts then as a negative feedback regulator of TOR function. In accordance, mammalian SESNs sustain the AMPK-TSC2 axis that integrates metabolic and stress inputs and prevents age-associated pathologies caused by chronic TOR activation [14]. SESN1 and SESN2 are negative regulators of mTOR signalling through the activation of AMPK and TSC2 phosphorylation in a p53-dependent manner, and this negative regulation is required for mTORC1 signalling suppression upon DNA damage [58]. In response to genotoxic stress, SESN2 expression is upregulated favouring sustained AMPK activity by orchestrating the recruitment of LKB1, as well as increasing LKB1/AMPK$\alpha\beta\gamma$ expression. In addition, both AMPK and SESN2 coordinate to suppress Akt-mTOR signalling as induced by ionizing radiation, thus acting as radiation sensitizers in MCF7 breast cancer cells [60]. The SESN2-dependent induction of AMPK activity and blunting of mTORC1 seem to bear substantial potential relevance to attenuate cell damage in conditions associated with acute ischemia, such as hypoxic-ischemic encephalopathy (HIE, caused by decreased oxygen and cerebral blood flow to the brain) or cardiomyocyte ischemia [74]. Exogenous elevation of SESN2 levels reduced the brain infarct area and brain atrophy and improved long-term neurological function in a neonatal rat model of HIE through the induction of AMPK signalling and subsequent blockade of mTOR signalling [75]. SESN2 also exerts neuroprotective effects during cerebral ischemia/reperfusion injury, a complex pathophysiological process characterized by enhanced levels of ROS and apoptosis, possibly by increasing mitochondrial biogenesis through an AMPK/PGC-1α pathway, which attenuates oxidative stress [76, 77]. SESN2 also accumulates in the heart during ischemic conditions, stabilizing an LKB1-SESN2-AMPK complex that cannot be assembled in SESN2-KO hearts, blunting AMPK during ischemic injury [70]. Somewhat expected by the prominent role that AMPK signalling has in counteracting high-glucose-induced damage and insulin resistance, SESN2 might contribute to the amelioration of disorders derived from metabolic syndrome and hyperglycaemia, such as hyperglycaemia-induced glomerular injury [73, 78], hepatosteatosis, and insulin resistance [79]. Of note, SESN2 is induced upon hypernutrition, and the genetic ablation of SESN2 exacerbates obesity-induced mTORC1-S6K activation, glucose intolerance, insulin resistance, and hepatosteatosis in the liver of obese mice, all of which are rescued by AMPK pharmacological activation [80].

SESN-driven regulation of AMPK and mTOR signalling also bears relevance for tumour biology. SESN2 and SESN3 suppress NK-92 cell-mediated cytotoxic activity on ovarian cancer cells through the induction of AMPK and inhibition of mTORC1, pointing at its potential relevance for immunotherapy in ovarian cancer [81]. SESN2 is decreased in colorectal cancer (CRC) [82], and its overexpression limits ROS production, inhibits cell growth, and stimulates apoptosis in CRC cell lines [83]. In addition, a protective role of SESN2 in gentamicin-induced stress has been reported. Genetic ablation of SESN2 enhances the sensitivity of hair cells to gentamicin suggesting that it may be involved in protecting sensory hair cells against gentamicin via modulation of the AMPK/mTOR pathway [84]. Further supporting a functional link between SESNs and AMPK signalling in cancer cells, GOF mutant p53 blocks a SESN1/AMPK/PGC-1α/UCP2 axis, increasing mitochondrial superoxide production in cancer cells [85].

In summary, SESNs might play an important role in signalling networks linking nutrient starvation to the control of major growth signalling and energy management networks (i.e., mTORC1 and AMPK) (Figure 3). While a substantial body of evidence has been gathered during the study of tumour biology, these concepts highlight the pivotal relevance of SESN-driven networks in the unfolding of processes related to aging.

6. SESNs in Aging

Dysregulation of mTORC1 and deactivation of AMPK signalling [86, 87], associated with increased ROS production or decreased ROS surveillance, are all closely related to hallmarks of aging, such as loss of metabolic homeostasis and proteostasis and reduced muscle function [88, 89]. Moreover, since SESNs are key regulators of several of these processes, they are also involved in aging. In *Caenorhabditis elegans*, SESN1 gene mutants show ROS accumulation, muscular cell abnormalities, and reduced lifespan [90]. At the same time, gain-of-function mutants induced increased lifespan with decreased muscle ROS. dSESN$^{-/-}$ flies exhibit chronic suppression of AMPK and activation of mTORC1, resulting in fat accumulation, blood sugar elevation, and skeletal and cardiac muscle degeneration [14]. In mice, however, SESN2 loss-of-function mutants have normal aging, perhaps reflecting different and multifactorial mechanisms of aging in invertebrates with respect to mammals [6]. Nonetheless, SESN level is modulated by aging. Older men show less SESN1 and SESN3 protein level in skeletal muscle and reduced amount of the phosphorylated δ-isoform of SESN2 compared to middle-aged and young men [15]. In the same experimental conditions, the mRNA expression of SESNs was highly upregulated, probably for compensatory mechanisms.

7. SESNs and Toxic Stress Tolerance

Protection from the damage exerted by xenobiotics is paramount for organismal homeostasis. SESNs may have an

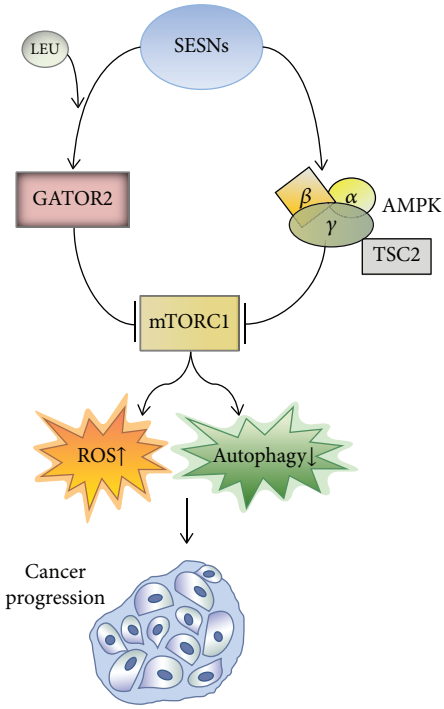

Figure 3: mTORC1 regulation by SESNs and its role in cancer progression. SESNs act as a master regulator of mTORC1 function through activation of GATOR2 (in the presence of leucine) and AMPK activation, thus playing a tumour-suppressive role.

important role in counteracting toxic chemicals through the regulation of oxidative stress and autophagy induction [14, 26]. Table 1 summarizes relevant studies reporting a role for SESNs in neuronal stress tolerance after toxic injuries. Notably, SESN2 is expressed in the central nervous system, and evidence supports that it is an important contributor to antioxidant systems in the brain [23]. For example, dysregulation of SESN expression in different conditions, such as neurodegenerative syndromes associated with advanced HIV infection, causes increased oxidative stress [91]. Moreover, SESN protein levels were found to be higher in patients suffering from Alzheimer's and Parkinson's diseases [92, 93], further highlighting their role as components of oxidative stress signatures and homeostatic surveillance in brain tissue. The heavy metal chromium (Cr) exists in different oxidation states and causes harmful effects on the organism. Reduction of Cr(VI) to Cr(III) leads to various reactive Cr intermediates and free radical generation, which results in oxidative stress [94]. Cr(VI) was reported to inhibit acetylcholinesterase activity in rats leading to oxidative damage to their brain [95]. In *Drosophila melanogaster*, Cr(VI) also causes neuronal cell death via ROS generation [96]. A recent study reported that oxidative stress, apoptosis, and neuronal cell death observed upon exposure of *D. melanogaster* larvae to Cr(VI) were reverted by ectopic SESN overexpression. Moreover, SESN overexpression enhances autophagy flux and decreases mTORC1 signalling/p-S6k levels in neuronal cells, suggesting an increased catabolic activity and cellular repair [97].

1-Methyl-4-phenylpyridinium (MPP+) is a metabolite derived from 1-methyl-4-phenyl-1,2,3,6-tetrahydropyridine (MPTP) that selectively destroys dopaminergic neurons in the substantia nigra of the brain by inducing mitochondrial dysfunction, oxidative stress, and apoptosis [98]. Because of its powerful neurotoxic activity, it is often used as a tool for studying Parkinson's disease (PD) in various animal models [99]. Of note, MMP+ induces the expression of SESN2 in SH-SY5Y human neuroblastoma cells and this induction is mediated by p53 [92]. Furthermore, knockdown of SESN2 enhances MPP+-induced neurotoxicity by triggering oxidative stress, mitochondrial dysfunction, apoptosis, and cell death [92]. Thus, the induction of SESN2 exerts a protective effect in neurons that might be effective for the therapeutical management of PD and other neurodegenerative diseases.

Sevoflurane, one of the most commonly used volatile anaesthetics in clinical treatment, can induce neuronal degeneration and cognitive impairment through ER stress-driven apoptosis in neurons of aging rats [100]. Notably, sevoflurane treatment induces SESN2 expression in a p53-dependent fashion in human neuroblastoma M17 cells, and knockdown of SESN2 blunts superoxide activity, unleashing oxidative stress and apoptosis [88].

Accumulation of amyloid β-peptide (Aβ) in senile plaques represents a pathological hallmark of Alzheimer's disease and leads to neurodegeneration by inducing cytotoxicity and oxidative stress [101]. A recent study explored a potential link between SESN2 and Aβ neurotoxicity. Chen et al. reported that SESN2 expression and the autophagy marker LC3B-II were elevated in primary rat cortical neurons upon Aβ exposure. Importantly, downregulation of SESN2 by siRNA abolished LC3B-II formation caused by Aβ and was accompanied by neuronal death. Accordingly, inhibition of autophagy by bafilomycin A1 also enhanced Aβ neurotoxicity [41]. This indicates that SESN2 induced by Aβ plays a protective role against Aβ neurotoxicity through the positive regulation of autophagy.

SESN2 also features potential beneficial activities on both vascular endothelial and liver injuries, highlighting its potential as a therapeutical target in cardiovascular and liver diseases [102, 103]. Activation of angiotensin II (AngII) signalling can trigger endothelial cell dysfunction, including proinflammatory adhesion molecules, production of ROS, and endothelial apoptosis. Again, supporting its relevant role as a component of stress adaption signatures, SESN2 expression is increased by AngII and knockdown of SESN2 enhances AngII-induced toxicity in human umbilical vein endothelial cells (HUVECs) [102].

Acetaminophen (APAP) is one of the most commonly used analgesic/antipyretic drugs, and at high doses, it can provoke acute hepatotoxicity, resulting in serious liver damage and death [104]. SESN2 exerted a protective effect against APAP-induced acute liver damage by inhibiting oxidative stress and proinflammatory signalling, possibly through the inhibition of downstream MAPK pathway activation [103]. It will be interesting in the future to explore the contribution of other pathways downstream of SESN2 that have also been closely related mechanistically to APAP toxicity, such as mitophagy [105].

Table 1: Some examples of the cytoprotective effect by SESNs.

Entry	Drugs or toxic substances	Cell lines	Tissue type/model organism	Effect on SESNs	Molecular mechanisms	Biological effect	Refs
1	Amyloid β-peptide	Primary rat cortical neurons	Transgenic mice	SESN2 ↑	LC3B-II ↑	Protective autophagy, prevention of neuronal cell death, protection against Alzheimer's disease	[41]
2	Sevoflurane	M17	Neuroblastoma	SESN2 ↑	p53-dependent mechanism	Prevention of neuroapoptosis and ROS	[88]
3	1-Methyl-4-phenylpyridinium	SH-SY5Y	Neuroblastoma	SESN2 ↑	p53-dependent mechanism	Protection against oxidative stress, mitochondrial dysfunction, apoptosis, and cell death and protection against Parkinson's disease	[92]
4	Chromium IV	Neuronal cells	Drosophila melanogaster larvae	dSESN ↑	ATG-8 ↑, p-JNK, p-Akt, p-FoxO, cleaved caspase-3 ↓, TOR/p-S6k ↓	Protection against oxidative stress, apoptosis, and neuronal cell death and protective autophagy	[97]
5	Angiotensin II	HUVECs	Endothelial	SESN2 ↑	JNK/c-Jun pathway ↑	Protection against cardiotoxicity of angiotensin II	[102]
6	Acetaminophen	Liver cell	Mice	SESN2 ↑	JNK, ERK pathway ↓, p38 ↓	Inhibition of oxidative stress, proinflammatory signalling, protection against liver toxicity	[103]

8. Conclusions

In recent years, remarkable progress has been made towards understanding the biochemical mechanisms behind the role of SESNs in physiopathology. Sestrins are integrated as components of adaptive responses against a variety of cellular stresses, including DNA damage, oxidative stress, hypoxia, and metabolic stresses. Thus, SESNs are now recognized as key regulators of cellular metabolism and indispensable contributors to cellular homeostasis in normal physiology and diseased states. As a positive regulator of AMPK and a repressor of mTORC1, SESNs elicit protective effects on various metabolic disorders such as diabetes and obesity, cancer, cardiac hypertrophy, and atherosclerosis.

Importantly, modulation of SESNs can activate an autophagic response, which in turn may lead to cancer cell death, as well as a cytoprotective effect in a manner highly dependent by the metabolic and environmental context in which tumour cells reside. Moreover, the potent antioxidant and autophagic effects orchestrated by SESNs confer neuronal stress tolerance to toxic injuries and neuroprotection in neurodegenerative disorders that are closely linked to oxidative stress, such as Parkinson's disease and Alzheimer's disease. Future studies are required to further validate such potential of SESNs as biomarkers and therapeutic targets against these disorders and to fully understand how their multiple functions are interrelated and coordinated at system level.

Conflicts of Interest

The authors declare no conflict of interest.

Acknowledgments

This work was supported by the Comunidad de Madrid (IND2017/IND-7809).

References

[1] V. I. Bunik, G. Mkrtchyan, A. Grabarska et al., "Inhibition of mitochondrial 2-oxoglutarate dehydrogenase impairs viability of cancer cells in a cell-specific metabolism-dependent manner," *Oncotarget*, vol. 7, no. 18, pp. 26400–26421, 2016.

[2] Y. Yang, S. Karakhanova, W. Hartwig et al., "Mitochondria and mitochondrial ROS in cancer: novel targets for anticancer therapy," *Journal of Cellular Physiology*, vol. 231, no. 12, pp. 2570–2581, 2016.

[3] S. Lin, Y. Li, A. A. Zamyatnin Jr., J. Werner, and A. V. Bazhin, "Reactive oxygen species and colorectal cancer," *Journal of Cellular Physiology*, vol. 233, no. 7, pp. 5119–5132, 2018.

[4] Z. Zou, H. Chang, H. Li, and S. Wang, "Induction of reactive oxygen species: an emerging approach for cancer therapy," *Apoptosis*, vol. 22, no. 11, pp. 1321–1335, 2017.

[5] Y. Yang, A. V. Bazhin, J. Werner, and S. Karakhanova, "Reactive oxygen species in the immune system," *International Reviews of Immunology*, vol. 32, no. 3, pp. 249–270, 2013.

[6] J. H. Lee, A. V. Budanov, and M. Karin, "Sestrins orchestrate cellular metabolism to attenuate aging," *Cell Metabolism*, vol. 18, no. 6, pp. 792–801, 2013.

[7] S. Velasco-Miguel, L. Buckbinder, P. Jean et al., "PA26, a novel target of the p53 tumor suppressor and member of the GADD family of DNA damage and growth arrest inducible genes," *Oncogene*, vol. 18, no. 1, pp. 127–137, 1999.

[8] A. V. Budanov, T. Shoshani, A. Faerman et al., "Identification of a novel stress-responsive gene Hi95 involved in regulation

of cell viability," *Oncogene*, vol. 21, no. 39, pp. 6017–6031, 2002.

[9] H. Peeters, P. Debeer, A. Bairoch et al., "*PA26* is a candidate gene for heterotaxia in humans: identification of a novel *PA26*-related gene family in human and mouse," *Human Genetics*, vol. 112, no. 5-6, pp. 573–580, 2003.

[10] H. Kim, S. An, S. H. Ro et al., "Janus-faced Sestrin2 controls ROS and mTOR signalling through two separate functional domains," *Nature Communications*, vol. 6, no. 1, 2015.

[11] R. A. Saxton, K. E. Knockenhauer, R. L. Wolfson et al., "Structural basis for leucine sensing by the Sestrin2-mTORC1 pathway," *Science*, vol. 351, no. 6268, pp. 53–58, 2015.

[12] A. Ho, C. S. Cho, S. Namkoong, U. S. Cho, and J. H. Lee, "Biochemical basis of sestrin physiological activities," *Trends in Biochemical Sciences*, vol. 41, no. 7, pp. 621–632, 2016.

[13] R. L. Wolfson, L. Chantranupong, R. A. Saxton et al., "Sestrin2 is a leucine sensor for the mTORC1 pathway," *Science*, vol. 351, no. 6268, pp. 43–48, 2015.

[14] J. H. Lee, A. V. Budanov, E. J. Park et al., "Sestrin as a feedback inhibitor of TOR that prevents age-related pathologies," *Science*, vol. 327, no. 5970, pp. 1223–1228, 2010.

[15] N. Zeng, R. F. D'Souza, C. J. Mitchell, and D. Cameron-Smith, "Sestrins are differentially expressed with age in the skeletal muscle of men: a cross-sectional analysis," *Experimental Gerontology*, vol. 110, pp. 23–34, 2018.

[16] V. Nogueira, Y. Park, C. C. Chen et al., "Akt determines replicative senescence and oxidative or oncogenic premature senescence and sensitizes cells to oxidative apoptosis," *Cancer Cell*, vol. 14, no. 6, pp. 458–470, 2008.

[17] B. Y. Shin, S. H. Jin, I. J. Cho, and S. H. Ki, "Nrf2-ARE pathway regulates induction of Sestrin-2 expression," *Free Radical Biology & Medicine*, vol. 53, no. 4, pp. 834–841, 2012.

[18] X. Y. Zhang, X. Q. Wu, R. Deng, T. Sun, G. K. Feng, and X. F. Zhu, "Upregulation of sestrin 2 expression via JNK pathway activation contributes to autophagy induction in cancer cells," *Cellular Signalling*, vol. 25, no. 1, pp. 150–158, 2013.

[19] X. Shi, D. M. Doycheva, L. Xu, J. Tang, M. Yan, and J. H. Zhang, "Sestrin2 induced by hypoxia inducible factor1 alpha protects the blood-brain barrier via inhibiting VEGF after severe hypoxic-ischemic injury in neonatal rats," *Neurobiology of Disease*, vol. 95, pp. 111–121, 2016.

[20] B. Zhai, J. Villén, S. A. Beausoleil, J. Mintseris, and S. P. Gygi, "Phosphoproteome analysis of *Drosophila melanogaster* embryos," *Journal of Proteome Research*, vol. 7, no. 4, pp. 1675–1682, 2008.

[21] S. R. Kimball, B. S. Gordon, J. E. Moyer, M. D. Dennis, and L. S. Jefferson, "Leucine induced dephosphorylation of Sestrin2 promotes mTORC1 activation," *Cellular Signalling*, vol. 28, no. 8, pp. 896–906, 2016.

[22] A. A. Sablina, A. V. Budanov, G. V. Ilyinskaya, L. S. Agapova, J. E. Kravchenko, and P. M. Chumakov, "The antioxidant function of the p53 tumor suppressor," *Nature Medicine*, vol. 11, no. 12, pp. 1306–1313, 2005.

[23] S. Papadia, F. X. Soriano, F. Léveillé et al., "Synaptic NMDA receptor activity boosts intrinsic antioxidant defenses," *Nature Neuroscience*, vol. 11, no. 4, pp. 476–487, 2008.

[24] C. C. Chen, S. M. Jeon, P. T. Bhaskar et al., "FoxOs inhibit mTORC1 and activate Akt by inducing the expression of Sestrin3 and Rictor," *Developmental Cell*, vol. 18, no. 4, pp. 592–604, 2010.

[25] J. Hagenbuchner, A. Kuznetsov, M. Hermann, B. Hausott, P. Obexer, and M. J. Ausserlechner, "FOXO3-induced reactive oxygen species are regulated by BCL2L11 (Bim) and SESN3," *Journal of Cell Science*, vol. 125, no. 5, pp. 1191–1203, 2012.

[26] A. V. Budanov, A. A. Sablina, E. Feinstein, E. V. Koonin, and P. M. Chumakov, "Regeneration of peroxiredoxins by p53-regulated sestrins, homologs of bacterial AhpD," *Science*, vol. 304, no. 5670, pp. 596–600, 2004.

[27] H. A. Woo, S. H. Bae, S. Park, and S. G. Rhee, "Sestrin 2 is not a reductase for cysteine sulfinic acid of peroxiredoxins," *Antioxidants & Redox Signaling*, vol. 11, no. 4, pp. 739–745, 2009.

[28] S. H. Bae, S. H. Sung, S. Y. Oh et al., "Sestrins activate Nrf2 by promoting p62-dependent autophagic degradation of keap1 and prevent oxidative liver damage," *Cell Metabolism*, vol. 17, no. 1, pp. 73–84, 2013.

[29] S. A. Tooze, L. A. Hannan, M. S. Marks, T. H. Stevens, and T. A. Schroer, "Fundamental mechanisms deliver the Nobel Prize to Ohsumi," *Traffic*, vol. 18, no. 2, pp. 93–95, 2017.

[30] E. Y. Chan, "Regulation and function of uncoordinated-51 like kinase proteins," *Antioxidants & Redox Signaling*, vol. 17, no. 5, pp. 775–785, 2012.

[31] R. Kang, H. J. Zeh, M. T. Lotze, and D. Tang, "The Beclin 1 network regulates autophagy and apoptosis," *Cell Death and Differentiation*, vol. 18, no. 4, pp. 571–580, 2011.

[32] S. Park, S. G. Choi, S. M. Yoo, J. H. Son, and Y. K. Jung, "Choline dehydrogenase interacts with SQSTM1/p62 to recruit LC3 and stimulate mitophagy," *Autophagy*, vol. 10, no. 11, pp. 1906–1920, 2014.

[33] N. Mizushima, "Autophagy: process and function," *Genes & Development*, vol. 21, no. 22, pp. 2861–2873, 2007.

[34] R. Scherz-Shouval and Z. Elazar, "Regulation of autophagy by ROS: physiology and pathology," *Trends in Biochemical Sciences*, vol. 36, no. 1, pp. 30–38, 2011.

[35] A. Eiyama and K. Okamoto, "PINK1/Parkin-mediated mitophagy in mammalian cells," *Current Opinion in Cell Biology*, vol. 33, pp. 95–101, 2015.

[36] K. Nakahira, J. A. Haspel, V. A. Rathinam et al., "Autophagy proteins regulate innate immune response by inhibiting NALP3 inflammasome-mediated mitochondrial DAN release," in *A21. Innate Immunity*, pp. A1077–A1077, Denver, CO, USA, 2011.

[37] G. Ashrafi and T. L. Schwarz, "The pathways of mitophagy for quality control and clearance of mitochondria," *Cell Death and Differentiation*, vol. 20, no. 1, pp. 31–42, 2013.

[38] M. Redmann, M. Dodson, M. Boyer-Guittaut, V. Darley-Usmar, and J. Zhang, "Mitophagy mechanisms and role in human diseases," *The International Journal of Biochemistry & Cell Biology*, vol. 53, pp. 127–133, 2014.

[39] M. C. Maiuri, S. A. Malik, E. Morselli et al., "Stimulation of autophagy by the p53 target gene Sestrin2," *Cell Cycle*, vol. 8, no. 10, pp. 1571–1576, 2009.

[40] Y.-S. Hou, J. J. Guan, H. D. Xu, F. Wu, R. Sheng, and Z. H. Qin, "Sestrin2 protects dopaminergic cells against rotenone toxicity through AMPK-dependent autophagy activation," *Molecular and Cellular Biology*, vol. 35, no. 16, pp. 2740–2751, 2015.

[41] Y. S. Chen, S. D. Chen, C. L. Wu, S. S. Huang, and D. I. Yang, "Induction of sestrin2 as an endogenous protective mechanism against amyloid beta-peptide neurotoxicity in primary

cortical culture," *Experimental Neurology*, vol. 253, pp. 63–71, 2014.

[42] J. Kim, M. Kundu, B. Viollet, and K. L. Guan, "AMPK and mTOR regulate autophagy through direct phosphorylation of Ulk1," *Nature Cell Biology*, vol. 13, no. 2, pp. 132–141, 2011.

[43] S. Pankiv, T. H. Clausen, T. Lamark et al., "p62/SQSTM1 binds directly to Atg8/LC3 to facilitate degradation of ubiquitinated protein aggregates by autophagy," *The Journal of Biological Chemistry*, vol. 282, no. 33, pp. 24131–24145, 2007.

[44] S. H. Ro, I. A. Semple, H. Park et al., "Sestrin2 promotes Unc-51-like kinase 1 mediated phosphorylation of p62/sequestosome-1," *The FEBS Journal*, vol. 281, no. 17, pp. 3816–3827, 2014.

[45] M. J. Kim, S. H. Bae, J. C. Ryu et al., "SESN2/sestrin2 suppresses sepsis by inducing mitophagy and inhibiting NLRP3 activation in macrophages," *Autophagy*, vol. 12, no. 8, pp. 1272–1291, 2016.

[46] M. Ishihara, M. Urushido, K. Hamada et al., "Sestrin-2 and BNIP3 regulate autophagy and mitophagy in renal tubular cells in acute kidney injury," *American Journal of Physiology-Renal Physiology*, vol. 305, no. 4, pp. F495–F509, 2013.

[47] P. Devarajan, "Update on mechanisms of ischemic acute kidney injury," *Journal of the American Society of Nephrology*, vol. 17, no. 6, pp. 1503–1520, 2006.

[48] M. Laplante and D. M. Sabatini, "mTOR signaling in growth control and disease," *Cell*, vol. 149, no. 2, pp. 274–293, 2012.

[49] J. L. Jewell, R. C. Russell, and K. L. Guan, "Amino acid signalling upstream of mTOR," *Nature Reviews Molecular Cell Biology*, vol. 14, no. 3, pp. 133–139, 2013.

[50] M. Shimobayashi and M. N. Hall, "Making new contacts: the mTOR network in metabolism and signalling crosstalk," *Nature Reviews Molecular Cell Biology*, vol. 15, no. 3, pp. 155–162, 2014.

[51] S. Pattingre, L. Espert, M. Biard-Piechaczyk, and P. Codogno, "Regulation of macroautophagy by mTOR and Beclin 1 complexes," *Biochimie*, vol. 90, no. 2, pp. 313–323, 2008.

[52] M. Tajan, A. K. Hock, J. Blagih et al., "A role for p53 in the adaptation to glutamine starvation through the expression of SLC1A3," *Cell Metabolism*, vol. 28, no. 5, pp. 721–736.e6, 2018.

[53] J. S. Kim, S. H. Ro, M. Kim et al., "Sestrin2 inhibits mTORC1 through modulation of GATOR complexes," *Scientific Reports*, vol. 5, no. 1, 2015.

[54] L. Chantranupong, R. L. Wolfson, J. M. Orozco et al., "The sestrins interact with GATOR2 to negatively regulate the amino-acid-sensing pathway upstream of mTORC1," *Cell Reports*, vol. 9, no. 1, pp. 1–8, 2014.

[55] A. Parmigiani, A. Nourbakhsh, B. Ding et al., "Sestrins inhibit mTORC1 kinase activation through the GATOR complex," *Cell Reports*, vol. 9, no. 4, pp. 1281–1291, 2014.

[56] M. Peng, N. Yin, and M. O. Li, "Sestrins function as guanine nucleotide dissociation inhibitors for Rag GTPases to control mTORC1 signaling," *Cell*, vol. 159, no. 1, pp. 122–133, 2014.

[57] X. Chen, J. J. Ma, M. Tan et al., "Modular pathways for editing non-cognate amino acids by human cytoplasmic leucyl-tRNA synthetase," *Nucleic Acids Research*, vol. 39, no. 1, pp. 235–247, 2011.

[58] A. V. Budanov and M. Karin, "p53 target genes Sestrin1 and Sestrin2 connect genotoxic stress and mTOR signaling," *Cell*, vol. 134, no. 3, pp. 451–460, 2008.

[59] H. W. Park, H. Park, S. H. Ro et al., "Hepatoprotective role of Sestrin2 against chronic ER stress," *Nature Communications*, vol. 5, no. 1, 2014.

[60] T. Sanli, K. Linher-Melville, T. Tsakiridis, and G. Singh, "Sestrin2 modulates AMPK subunit expression and its response to ionizing radiation in breast cancer cells," *PLoS One*, vol. 7, no. 2, article e32035, 2012.

[61] A. Brüning, M. Rahmeh, and K. Friese, "Nelfinavir and bortezomib inhibit mTOR activity via ATF4-mediated sestrin-2 regulation," *Molecular Oncology*, vol. 7, no. 6, pp. 1012–1018, 2013.

[62] J. Ye, W. Palm, M. Peng et al., "GCN2 sustains mTORC1 suppression upon amino acid deprivation by inducing Sestrin2," *Genes & Development*, vol. 29, no. 22, pp. 2331–2336, 2015.

[63] J. F. Linares, A. Duran, M. Reina-Campos et al., "Amino acid activation of mTORC1 by a PB1-domain-driven kinase complex cascade," *Cell Reports*, vol. 12, no. 8, pp. 1339–1352, 2015.

[64] J. Moscat and M. T. Diaz-Meco, "Feedback on fat: P62-mTORC1-autophagy connections," *Cell*, vol. 147, no. 4, pp. 724–727, 2011.

[65] A. Duran, R. Amanchy, J. F. Linares et al., "p62 is a key regulator of nutrient sensing in the mTORC1 pathway," *Molecular Cell*, vol. 44, no. 1, pp. 134–146, 2011.

[66] J. K. Byun, Y. K. Choi, J. H. Kim et al., "A positive feedback loop between Sestrin2 and mTORC2 is required for the survival of glutamine-depleted lung cancer cells," *Cell Reports*, vol. 20, no. 3, pp. 586–599, 2017.

[67] D. M. Gwinn, D. B. Shackelford, D. F. Egan et al., "AMPK phosphorylation of raptor mediates a metabolic checkpoint," *Molecular Cell*, vol. 30, no. 2, pp. 214–226, 2008.

[68] G. Herrero-Martín, M. Høyer-Hansen, C. García-García et al., "TAK1 activates AMPK-dependent cytoprotective autophagy in TRAIL-treated epithelial cells," *The EMBO Journal*, vol. 28, no. 6, pp. 677–685, 2009.

[69] K. Inoki, H. Ouyang, T. Zhu et al., "TSC2 integrates Wnt and energy signals via a coordinated phosphorylation by AMPK and GSK3 to regulate cell growth," *Cell*, vol. 126, no. 5, pp. 955–968, 2006.

[70] A. Morrison, L. Chen, J. Wang et al., "Sestrin2 promotes LKB1-mediated AMPK activation in the ischemic heart," *The FASEB Journal*, vol. 29, no. 2, pp. 408–417, 2015.

[71] I. Ben-Sahra, B. Dirat, K. Laurent et al., "Sestrin2 integrates Akt and mTOR signaling to protect cells against energetic stress-induced death," *Cell Death and Differentiation*, vol. 20, no. 4, pp. 611–619, 2013.

[72] L. Q. Hong-Brown, C. R. Brown, M. Navaratnarajah, and C. H. Lang, "Adamts1 mediates ethanol-induced alterations in collagen and elastin via a FoxO1-sestrin3-AMPK signaling cascade in myocytes," *Journal of Cellular Biochemistry*, vol. 116, no. 1, pp. 91–101, 2015.

[73] A. A. Eid, D.-Y. Lee, L. J. Roman, K. Khazim, and Y. Gorin, "Sestrin 2 and AMPK connect hyperglycemia to Nox4-dependent endothelial nitric oxide synthase uncoupling and matrix protein expression," *Molecular and Cellular Biology*, vol. 33, no. 17, pp. 3439–3460, 2013.

[74] J. J. Volpe, "Perinatal brain injury: from pathogenesis to neuroprotection," *Mental Retardation and Developmental Disabilities Research Reviews*, vol. 7, no. 1, pp. 56–64, 2001.

[75] X. Shi, L. Xu, D. M. Doycheva, J. Tang, M. Yan, and J. H. Zhang, "Sestrin2, as a negative feedback regulator of mTOR, provides neuroprotection by activation AMPK phosphorylation in neonatal hypoxic-ischemic encephalopathy in rat pups," *Journal of Cerebral Blood Flow and Metabolism*, vol. 37, no. 4, pp. 1447–1460, 2017.

[76] A. Tewari, V. Mahendru, A. Sinha, and F. Bilotta, "Antioxidants: the new frontier for translational research in cerebroprotection," *Journal of Anaesthesiology Clinical Pharmacology*, vol. 30, no. 2, pp. 160–171, 2014.

[77] G. Ashabi, F. Khodagholi, L. Khalaj, M. Goudarzvand, and M. Nasiri, "Activation of AMP-activated protein kinase by metformin protects against global cerebral ischemia in male rats: interference of AMPK/PGC-1α pathway," *Metabolic Brain Disease*, vol. 29, no. 1, pp. 47–58, 2014.

[78] D. K. Singh, P. Winocour, and K. Farrington, "Oxidative stress in early diabetic nephropathy: fueling the fire," *Nature Reviews Endocrinology*, vol. 7, no. 3, pp. 176–184, 2011.

[79] D. W. Haslam and W. P. T. James, "Obesity," *The Lancet*, vol. 366, no. 9492, pp. 1197–1209, 2005.

[80] J. H. Lee, A. V. Budanov, S. Talukdar et al., "Maintenance of metabolic homeostasis by Sestrin2 and Sestrin3," *Cell Metabolism*, vol. 16, no. 3, pp. 311–321, 2012.

[81] X. Wang, W. Liu, D. Zhuang, S. Hong, and J. Chen, "Sestrin2 and sestrin3 suppress NK-92 cell-mediated cytotoxic activity on ovarian cancer cells through AMPK and mTORC1 signaling," *Oncotarget*, vol. 8, no. 52, pp. 90132–90143, 2017.

[82] J. L. Wei, Z. X. Fu, M. Fang et al., "Decreased expression of sestrin 2 predicts unfavorable outcome in colorectal cancer," *Oncology Reports*, vol. 33, no. 3, pp. 1349–1357, 2015.

[83] J.-L. Wei, M. Fang, Z. X. Fu et al., "Sestrin 2 suppresses cells proliferation through AMPK/mTORC1 pathway activation in colorectal cancer," *Oncotarget*, vol. 8, no. 30, pp. 49318–49328, 2017.

[84] E. Ebnoether, A. Ramseier, M. Cortada, D. Bodmer, and S. Levano-Huaman, "Sesn2 gene ablation enhances susceptibility to gentamicin-induced hair cell death via modulation of AMPK/mTOR signaling," *Cell Death Discovery*, vol. 3, article 17024, 2017.

[85] M. Cordani, G. Butera, I. Dando et al., "Mutant p53 blocks SESN1/AMPK/PGC-1α/UCP2 axis increasing mitochondrial $O_{2}^{-\cdot}$ production in cancer cells," *British Journal of Cancer*, vol. 119, no. 8, pp. 994–1008, 2018.

[86] S. Paturi, A. K. Gutta, A. Katta et al., "Effects of aging and gender on muscle mass and regulation of Akt-mTOR-p70s6k related signaling in the F344BN rat model," *Mechanisms of Ageing and Development*, vol. 131, no. 3, pp. 202–209, 2010.

[87] R. M. Reznick, H. Zong, J. Li et al., "Aging-associated reductions in AMP-activated protein kinase activity and mitochondrial biogenesis," *Cell Metabolism*, vol. 5, no. 2, pp. 151–156, 2007.

[88] W. Yi, Y. Zhang, Y. Guo, D. Li, and X. Li, "Elevation of Sestrin-2 expression attenuates sevoflurane induced neurotoxicity," *Metabolic Brain Disease*, vol. 30, no. 5, pp. 1161–1166, 2015.

[89] B. F. Oliveira, J. A. Nogueira-Machado, and M. M. Chaves, "The role of oxidative stress in the aging process," *Scientific World Journal*, vol. 10, pp. 1121–1128, 2010.

[90] Y. L. Yang, K. S. Loh, B. Y. Liou et al., "SESN-1 is a positive regulator of lifespan in *Caenorhabditis elegans*," *Experimental Gerontology*, vol. 48, no. 3, pp. 371–379, 2013.

[91] V. Soontornniyomkij, D. J. Moore, B. Gouaux et al., "Cerebral β-amyloid deposition predicts HIV-associated neurocognitive disorders in APOE ε4 carriers," *AIDS*, vol. 26, no. 18, pp. 2327–2335, 2012.

[92] Z. Daixing, Z. Chengye, Z. Qiang, and L. Shusheng, "Upregulation of sestrin-2 expression via P53 protects against 1-methyl-4-phenylpyridinium (MPP+) neurotoxicity," *Journal of Molecular Neuroscience*, vol. 51, no. 3, pp. 967–975, 2013.

[93] N. Rai, R. Kumar, G. R. Desai et al., "Relative alterations in blood-based levels of sestrin in Alzheimer's disease and mild cognitive impairment patients," *Journal of Alzheimer's Disease*, vol. 54, no. 3, pp. 1147–1155, 2016.

[94] G. R. Borthiry, W. E. Antholine, B. Kalyanaraman, J. M. Myers, and C. R. Myers, "Reduction of hexavalent chromium by human cytochrome b5: generation of hydroxyl radical and superoxide," *Free Radical Biology & Medicine*, vol. 42, no. 6, pp. 738–755, 2007.

[95] N. Soudani, A. Troudi, I. B. Amara, H. Bouaziz, T. Boudawara, and N. Zeghal, "Ameliorating effect of selenium on chromium (VI)-induced oxidative damage in the brain of adult rats," *Journal of Physiology and Biochemistry*, vol. 68, no. 3, pp. 397–409, 2012.

[96] P. Singh and D. K. Chowdhuri, "Environmental presence of hexavalent but not trivalent chromium causes neurotoxicity in exposed *Drosophila melanogaster*," *Molecular Neurobiology*, vol. 54, no. 5, pp. 3368–3387, 2017.

[97] P. Singh and D. K. Chowdhuri, "Modulation of *sestrin* confers protection to Cr(VI) induced neuronal cell death in *Drosophila melanogaster*," *Chemosphere*, vol. 191, pp. 302–314, 2018.

[98] J. Bové and C. Perier, "Neurotoxin-based models of Parkinson's disease," *Neuroscience*, vol. 211, pp. 51–76, 2012.

[99] I. J. Kopin and S. P. Markey, "MPTP toxicity: implications for research in Parkinson's disease," *Annual Review of Neuroscience*, vol. 11, no. 1, pp. 81–96, 1988.

[100] G. Chen, M. Gong, M. Yan, and X. Zhang, "Sevoflurane induces endoplasmic reticulum stress mediated apoptosis in hippocampal neurons of aging rats," *PLoS One*, vol. 8, no. 2, article e57870, 2013.

[101] T.-C. Ju, S.-D. Chen, C.-C. Liu, and D.-I. Yang, "Protective effects of *S*-nitrosoglutathione against amyloid β-peptide neurotoxicity," *Free Radical Biology & Medicine*, vol. 38, no. 7, pp. 938–949, 2005.

[102] L. Yi, F. Li, Y. Yong et al., "Upregulation of sestrin-2 expression protects against endothelial toxicity of angiotensin II," *Cell Biology and Toxicology*, vol. 30, no. 3, pp. 147–156, 2014.

[103] S. J. Kim, K. M. Kim, J. H. Yang et al., "Sestrin2 protects against acetaminophen-induced liver injury," *Chemico-Biological Interactions*, vol. 269, pp. 50–58, 2017.

[104] A. M. Larson, "Acetaminophen hepatotoxicity," *Clinics in Liver Disease*, vol. 11, no. 3, pp. 525–548, 2007.

[105] A. Baulies, V. Ribas, S. Núñez et al., "Lysosomal cholesterol accumulation sensitizes to acetaminophen hepatotoxicity by impairing mitophagy," *Scientific Reports*, vol. 5, no. 1, 2016.

Hindawi
Oxidative Medicine and Cellular Longevity
Volume 2019, Article ID 9675450, 26 pages
https://doi.org/10.1155/2019/9675450

Research Article

Hsp90 Inhibitor SNX-2112 Enhances TRAIL-Induced Apoptosis of Human Cervical Cancer Cells via the ROS-Mediated JNK-p53-Autophagy-DR5 Pathway

Liubing Hu,[1] Yan Wang,[1] Zui Chen,[1] Liangshun Fu,[1] Sheng Wang,[1] Xinyue Zhang,[1] Pengchao Zhang,[1] Xueping Lu,[1] Huiyang Jie,[1] Manmei Li,[2] Yifei Wang,[1] and Zhong Liu[1]

[1]*Guangdong Provincial Key Laboratory of Bioengineering Medicine, Institute of Biomedicine, College of Life Science and Technology, Jinan University, Guangzhou 510632, China*
[2]*Guangdong Province Key Laboratory of Pharmacodynamic Constituents of TCM and New Drugs Research, Institute of Traditional Chinese Medicine and Natural Products, College of Pharmacy, Jinan University, Guangzhou 510632, China*

Correspondence should be addressed to Manmei Li; limanmei@hotmail.com, Yifei Wang; twang-yf@163.com, and Zhong Liu; tliuzh@jnu.edu.cn

Received 23 August 2018; Revised 8 November 2018; Accepted 19 November 2018; Published 25 March 2019

Guest Editor: Marco Cordani

Tumor necrosis factor-related apoptosis-inducing ligand (TRAIL) is a potent cancer cell apoptosis-inducing factor that can induce apoptosis in a variety of cancer cells. However, resistance to TRAIL in cancer cells is a huge obstacle in creating effective TRAIL-targeted clinical therapies. Thus, agents that can either enhance the effect of TRAIL or overcome its resistance are needed. In this study, we combined TRAIL with SNX-2112, an Hsp90 inhibitor we previously developed, to explore the effect and mechanism that SNX-2112 enhanced TRAIL-induced apoptosis in cervical cancer cells. Our results showed that SNX-2112 markedly enhanced TRAIL-induced cytotoxicity in HeLa cells, and this combination was found to be synergistic. Additionally, we found that SNX-2112 sensitized TRAIL-mediated apoptosis caspase-dependently in TRAIL-resistant HeLa cells. Mechanismly, SNX-2112 downregulated antiapoptosis proteins, including Bcl-2, Bcl-XL, and FLIP, promoted the accumulation of reactive oxygen species (ROS), and increased the expression levels of p-JNK and p53. ROS scavenger NAC rescued SNX-2112/TRAIL-induced apoptosis and suppressed SNX-2112-induced p-JNK and p53. Moreover, SNX-2112 induced the upregulation of death-receptor DR5 in HeLa cells. The silencing of DR5 by siRNA significantly decreased cell apoptosis by the combined effect of SNX-2112 and TRAIL. In addition, SNX-2112 inhibited the Akt/mTOR signaling pathway and induced autophagy in HeLa cells. The blockage of autophagy by bafilomycin A1 or Atg7 siRNA abolished SNX-2112-induced upregulation of DR5. Meanwhile, ROS scavenger NAC, JNK inhibitor SP600125, and p53 inhibitor PFTα were used to verify that autophagy-mediated upregulation of DR5 was regulated by the SNX-2112-stimulated activation of the ROS-JNK-p53 signaling pathway. Thus, the combination of SNX-2112 and TRAIL may provide a novel strategy for the treatment of human cervical cancer by overcoming cellular mechanisms of apoptosis resistance.

1. Introduction

Tumor necrosis factor-related apoptosis-inducing ligand (TRAIL), also known as apo2 ligand, is a member of the TNF family that binds to receptors to selectively target tumor cells while sparing normal cells. As a result, TRAIL and its receptor (TRAIL-R) agonist antibodies are considered attractive candidates for use as anticancer drugs in clinical studies. TRAIL leads to the formation of the death-inducing signal complex (DISC) by interacting with death receptor 4 (DR4) and death receptor 5 (DR5), followed by binding to caspase 8. Caspase 8 is recruited to DISC to activate its proteolytic

properties, which induce the activation of protease caspase 3 cascades or Bcl-2 family members, facilitating the cleavage of dead substrates, ultimately leading to apoptosis [1]. Many tumors are susceptible to TRAIL-mediated apoptosis, but the development of resistance to TRAIL is also common in many types of cancer [2, 3]. Resistance to TRAIL can result from a wide range of molecular changes: the downregulation of DR4 and DR5 expression and the upregulation of decoy receptors; the overexpression of antiapoptotic molecules, including the caspase 8 inhibitor, Fas-associated death domain-like IL-1-converting enzyme-inhibitory protein (cFLIP), inhibitors of apoptosis protein (IAP) family members, and Bcl-2 family proteins; the loss of proapoptotic proteins; and the activation of the PI3K/Akt and NF-κB signaling pathways [4–8]. Bortezomib and other protease inhibitors have been found to reverse resistance to TRAIL, but have long been considered to be highly toxic [9, 10]. Therefore, there is a great need for anticancer drugs that are able to regulate cancer cell resistance to TRAIL and thus improve the therapeutic effect of TRAIL on tumors through combined treatment.

As molecular chaperones, heat shock protein 90 (Hsp90) can help intracellular signal transduction proteins fold, stabilize, and mediate cellular homeostasis, cell survival, and transcriptional regulation. It plays an important role in both normal and stress conditions and in pathological states such as cancer [11–13]. In contrast to normal cells, Hsp90 in cancer cells is usually upregulated by exposure to different kinds of stresses, such as acidosis, low oxygen tension, and nutrient deprivation [14, 15]. It has been found that the overexpression of Hsp90 was essential in protecting therapeutic agent-induced apoptosis and could be a potential target molecule for anticancer drugs [16, 17]. One of the challenges of targeted cancer therapies is that the malignant progression of cancer cells is often related to a variety of molecular abnormalities. Hsp90 inhibitors can degrade Hsp90 client proteins (including cancerogenic proteins) by targeting a single protein (Hsp90), thereby affecting several signaling pathways. Hsp90 regulates over 100 client proteins. These client proteins include Akt, Raf-1, IKK, Her2, Cdk4, MMP2, and VEGFR2 and play an important role in tumor cell survival, growth, migration, and angiogenesis [18–20]. Besides, inhibition of Hsp90 could increase ER stress to disrupt mitochondrial homeostasis and, thereby, stimulate the production of mitochondrial ROS, leading to the selective killing of cancer cells when compared to normal cells, by elevating ER stress originating from the accumulation of unfolded protein in the ER [21–23]. Meanwhile, rational drug combination of prooxidant and antioxidant might be a potential new treatment strategy to combat drug resistance in cancer [22]. In recent years, dozens of Hsp90 have been developed for oncotherapy, including first-generation Hsp90 inhibitors (geldanamycin and its derivatives) and second-generation Hsp90 inhibitors (NVP-AUY922). Geldanamycin 17-AAG (tanespimycin) is a natural product and was the first Hsp90 inhibitor to enter clinical trials [11, 12]. Hsp90 inhibitors have therapeutic applications in melanoma, AML, castrated refractory prostate cancer, NSCLC, and other types of cancers [24]. Nevertheless, there are no FDA-approved Hsp90 inhibitors or standardized experiments that confirm the inhibitory effect of Hsp90. The most significant off-target toxicity of geldanamycin derivatives in clinical use is their hepatotoxicity caused by the benzoquinone moiety. In addition to hepatotoxicity, the ocular and cardiac toxicity of these drugs limits their further clinical development [24, 25].

Geldanamycin or 17-AAG inhibition of Hsp90 has been reported to sensitize some cells to TRAIL-induced apoptosis [26, 27]. The combination of 17-AAG and death receptors targeting agent TRAIL can synergistically increase antitumor activity and eliminate resistance to TRAIL in gliomas [28]. In TRAIL-resistant tumor cell lines, such as prostate LNCaP cells, colon cancer HT29, and RKO cells, pre- or coexposure to 17-AAG with TRAIL can induce high levels of cell apoptosis [29–31]. Studies have shown that the combination of 17-AAG with TRAIL coinduces apoptosis as a result of the deregulation of NF-κB or Akt cell survival pathways [32, 33].

We have previously proven that SNX-2112 was a novel, highly efficient, and highly selective small molecule inhibitor of Hsp90 that could competitively integrate with the N-terminal ATP-binding site of Hsp90 and exhibit anticancer activity in cancer cells, including breast cancer [34], multiple myeloma [35], melanoma [36, 37], chronic myeloid leukemia [38], esophageal cancer [39], and head and neck squamous cell carcinomas [40]. Especially in human hepatocellular carcinoma cells, SNX-2112 could induce apoptosis, elevating the role of ER stress [41]. In this study, we attempted to use SNX-2112 in combination with TRAIL to overcome the resistance of cervical cancer HeLa cells to TRAIL-induced cell apoptosis and provided a new therapeutic strategy for the clinical treatment of cervical cancer.

2. Materials and Methods

2.1. Cell Culture. Human cervical cancer cells (HeLa, SiHa, and Caski) were purchased from the Cell Bank of the Chinese Academy of Sciences (Shanghai, China), stored in liquid nitrogen, and cultured in RPMI-1640 or DMEM medium supplemented with 10% FBS and 100 U/mL penicillin/streptomycin in 5% CO_2 at 37°C.

2.2. Reagents and Antibodies. SNX-2112 was synthesized as previously described in our lab with >98.0% purity [42], dissolved in dimethyl sulfoxide (DMSO) to obtain a 100 mM stock solution, and stored at −20°C. TRAIL was purchased from Merck Millipore (Waltham, MA, USA). N-Acetyl-cysteine (NAC) and 2′,7′-dichlorofluorescein diacetate (DCFH-DA) were purchased from the Beyotime Institute of Biotechnology (Shanghai, China). Bafilomycin A1 (BFA) was purchased from Selleck Chemicals (Shanghai, China). Dimethyl sulfoxide (DMSO) and 3-(4,5-dimethylthiazol-2-yl)-2,5-diphenyltetrazolium bromide (MTT) were purchased from Sigma (St. Louis, MO, USA). Antibodies for GAPDH, Bcl-2, Bcl-xL, FLIP, pro-caspase 3, cleaved-caspase 3 (c-caspase 3), cleaved-caspase 8 (c-caspase 8), cleaved-PARP (c-PARP), Akt, p-Akt (Ser473), DR4, DR5, LC3, Beclin1, Atg7, p62, p-mTOR, p-S6, p-4EBP1, p53,

p-ERK, ERK, p-p38, p38, p-JNK, and JNK were purchased from Cell Signaling Technology (CST; Beverly, MA, USA).

2.3. Cell Viability Assay. Cell viability was evaluated using the MTT assay. Exponentially growing cells were plated in 96-well culture plates (5000/well in 100 μL medium) for 24 h and incubated with a series of concentrations of SNX-2112 (0-1 μM) or TRAIL (0-1000 ng/mL) for 48 h. A 10 μL volume of MTT working solution was added to each well for 4 h. After the medium was removed, formazan crystals solubilized in 100 μL DMSO/well, and the absorbance values were assessed at 570 nm on a microplate reader (Bio-Rad, Hercules, CA, USA). The inhibition ratio was calculated as follows: (A control − A treated)/A control × 100%, where A treated and A control are the absorbance of the treated and control groups after a 48 h incubation, respectively.

2.4. Synergy Analysis. The synergistic interaction of SNX-2112 and TRAIL was calculated by using the Chou-Talalay method [43–45]. The combination index (CI) was evaluated using CompuSyn software (ComboSyn Inc., Paramus, NJ, USA) for each combination. A fitting curve of CI value data points was plotted according to the data generated by the viability assay using CompuSyn software. When the fitting curve of the drug's CI value was near or on the additive line (CI value = 1), it represented an additive treatment effect. The fitting curve below or above the additive line represents the synergism or antagonism effect, respectively.

2.5. ROS Detection. Generation of intracellular ROS was detected using DCFH-DA, a dye that detects reactive oxygen species (ROS). After cell treatment, HeLa cells were stained with the DCFH-DA (20 μM) fluorescent dye for 20 min. Fluorescence was measured with an epifluorescence microscope (Nikon, Japan).

2.6. Western Blotting Analysis. To assess the effect of SNX-2112 on TRAIL-induced protein activation, HeLa cells were collected and lysed in sodium dodecyl sulfate (SDS) buffer for 30 min at 4°C. After centrifugation at 12000 g for 20 min, the supernatant was pipetted for analysis with a bicinchoninic acid assay. Equivalent amounts (>30 μg) of protein were separated by 10-15% SDS-PAGE and transferred onto polyvinylidene difluoride membranes. Membranes were blocked in 5% skimmed milk dissolved in Tris-buffered saline (TBS) containing 0.1% Tween 20 (TBST) at room temperature for 1 h. Membranes were then incubated with the corresponding primary antibody (1 : 1000) at 4°C overnight, then washed in TBST and probed with secondary antibody (1 : 6000-1 : 8000) in TBST for 2 h at room temperature. Protein expression was detected using an enhanced chemiluminescence kit (4 A Biotech Co. Ltd., Beijing, China). GAPDH was used as a loading control.

2.7. Flow Cytometry for Apoptosis Measurement. Cell apoptosis was quantified by flow cytometry using an Annexin V-FITC/propidium iodide (PI) staining kit (Beyotime Institute of Biotechnology). Cells were seeded at 1.0×10^5 cell/mL in 6-well plates for 24 h, then exposed to the indicated concentrations of SNX-2112 or TRAIL alone or in combination for 48 h. Cell samples were prepared according to the manufacturer's instructions. In brief, cells were washed and resuspended in 500 μL PBS, then incubated with 10 μL PI and 10 μL Annexin V-FITC at room temperature in the dark for 15 min. Data acquisition and analysis were performed using a FACSCalibur flow cytometer with CellQuest software (Becton-Dickinson, Mississauga, CA, USA).

2.8. Immunofluorescence Analysis of the Expression of Cell Surface DR5. To detect the cellular expression of DR5, HeLa cells plated in chamber slides were treated with the indicated concentrations of SNX-2112/TRAIL for 48 h at 37°C. Samples were processed as described before [46]. Briefly, after fixing, permeabilizing, and blocking, the cells were incubated for 2 h at room temperature with an antibody against DR5 (1 : 50, Cell Signaling Technology). The cells were then probed with an Alexa Fluor 594-conjugated anti-rabbit antibody (1 : 1000) for 1 h. Nuclei were stained with DAPI (1 mg/mL, Sigma-Aldrich) for 15 min. Finally, cells were washed, and fluorescence was examined by laser scanning confocal microscopy (Nikon, Japan).

2.9. Transfection of siRNA. Transfection of HeLa cells was conducted with siRNA transfection reagent of jetPRIME (Polyplus, New York, NY, USA) following the manufacturer's instructions. High-purity controls (scrambled RNA), along with DR5, DR4, and Atg7, were obtained from GenePharma. The targeting sequences of the siRNA constructs were DR5 siRNA, 5′-UUCUGGGAACACGAGCAACAG-3′; DR4 siRNA-1, 5′-AAGAACCA GCAGAGGUCACAA-3′; DR4 siRNA-2, 5′-CACCAAUGCUUCCAACAAUdTdT-3′; Atg7 siRNNA-1, 5′-CCCUGUACUCCUCAACAAG-3′; and Atg7 siRNA-2, 5′-GCCUCUCUAUGAGUUUGAA-3′.

2.10. Detection of JC-1. HeLa cells (2×10^5) were seeded in 60 mm Petri dishes for a day before the experiment. After treatment with SNX-2112 alone or in combination with TRAIL at the indicated concentrations for 48 h, cells were harvested, washed twice with ice-cold PBS, and incubated with JC-1 (10 μg/mL) in the dark for 15 min at 37°C. Cells were then washed three times with ice-cold PBS and analyzed by flow cytometry using emission wavelengths of 590 nm and 525 nm.

2.11. Statistical Analysis. All data were expressed as the mean ± SD, and three independent experiments were performed to confirm the reliability of the data. For groups of two, statistical analysis was carried out by using two-tailed unpaired Student's t test. For groups of three or more, comparison was carried out using one-way ANOVA multiple. P values <0.05 and <0.01 were considered as statistically significant.

3. Results

3.1. SNX-2112 and TRAIL Synergistically Induce Cytotoxicity in Cervical Cancer HeLa Cells. To investigate whether SNX-2112 could synergize with TRAIL to suppress human

cervical cancer cell viability, a range of cervical cancer cell lines, including HeLa, SiHa, Caski cells, were tested. Before testing the combined effect of SNX-2112 and TRAIL therapy, we first evaluated the cytotoxicity of TRAIL monotherapy in three human cervical cancer cell lines by means of a MTT assay. Our data showed that, at concentrations of 1000 ng/mL or lower, TRAIL showed no significant antitumor effect on HeLa and SiHa cells, indicating that both cervical cell lines either had low sensitivity or were resistant to TRAIL monotherapy (Figure 1(b)). Both types of cervical cells were assessed with SNX-2112 monotherapy, and similar results were found (Figure 1(c)). Meanwhile, when the cells were cotreated with 125 or 250 nM of SNX-2112 and 200 ng/mL of TRAIL for 48 h, cell viability of both cell lines was markedly inhibited (Figures 1(d) and 1(e)).

For the two cell lines, HeLa and SiHa cells, the combination of both agents within a certain concentration range was the most effective treatment for blocking cell growth rather than the use of either agent alone. To determine the effect of a combined treatment of SNX-2112 and TRAIL, a combination study was performed. We obtained the fitting curves of CI value data points, and a fitted curve analysis was performed using CompuSyn software to define the interactions between SNX-2112 and TRAIL in HeLa and SiHa cells. According to the Chou–Talalay method, CIs were always less than 1 for the combination treatments in HeLa cell lines, indicating that cotreatment of SNX-2112 and TRAIL led to synergistic inhibitory effects on cell proliferation in HeLa cell lines, but not in SiHa cell lines (Figures 1(f) and 1(g)). Based on the above observations, we concluded that SNX-2112 markedly enhanced TRAIL-induced cytotoxicity in human cervical cancer cells and that the combination was considered synergistic in HeLa cells.

3.2. SNX-2112 Sensitizes TRAIL-Mediated Apoptosis via the Activation of Caspases in TRAIL-Resistant HeLa Cells. To investigate whether SNX-2112 could sensitize HeLa cancer cells to TRAIL-mediated apoptosis, HeLa cells were initially treated with 125 nM SNX-2112 or 200 ng/mL TRAIL alone or in combination for 48 h. Their morphology was found to be significantly affected by the combined treatment compared with the control or monotherapy group (Figures 2(a) and 2(b)). Apoptosis characteristics, including cell shrinkage, apoptotic bodies, and detachment from the plate, were observed more generally in HeLa cells treated with both SNX-2112 and TRAIL (Figure 2(a)). Furthermore, the results of flow cytometry analysis for apoptosis showed that SNX-2112 or TRAIL alone induced 21.4 or 13.5% apoptosis, individually, and that the combination of treatment with SNX-2112 and TRAIL augmented apoptosis to 90.0%. Nevertheless, the synergistic effect of this treatment was abolished by pretreatment with Z-VAD-fmk, the cell-permeable pan caspase inhibitor (Figures 2(c) and 2(d)). Change in the mitochondrial membrane potential ($\Delta\psi_m$) is an early event preceding caspase activation and is regarded as a hallmark of apoptosis [47]. Therefore, we measured $\Delta\psi_m$ in TRAIL/SNX-2112-treated HeLa cells using the membrane-permeable JC-1 dye. As shown in Figures 2(e) and 2(f), treatment with TRAIL and SNX-2112 induced a marked increase in JC-1-related green fluorescence in HeLa cells.

To investigate the mechanisms behind the role of SNX-2112 in the intensification of TRAIL-induced apoptosis, we quantified multiple cell death pathway components that could be influenced by SNX-2112. The results indicated that the expression of antiapoptotic Bcl-2 and Bcl-XL was suppressed (Figure 2(g)). As single agents, SNX-2112 or TRAIL reduced the expression level of FLIP and induced low levels of caspase 3 and 8 and poly (ADP-ribose) polymerase (PARP) cleavage, whereas their combination induced profoundly higher processing of these proteins (Figure 2(h)). Furthermore, consistent with the flow cytometry analysis, the upregulation of apoptosis-associated proteins (c-caspase 3 and 8 and c-PARP) was abolished by pretreatment with Z-VAD-fmk (Figure 2(i)). At least in part, these results may help to clarify the synergistic effect. Taken together, these experimental data suggested that SNX-2112 could sensitize TRAIL-mediated apoptosis via the activation of caspases in TRAIL-resistant HeLa cells.

3.3. SNX-2112-Induced Accumulation of ROS Is Pivotal for SNX-2112-Stimulated TRAIL-Induced Apoptosis. To investigate whether ROS contributed to SNX-2112-enhanced TRAIL-induced apoptosis, we measured the level of ROS in HeLa cells. In the DCFH-DA-based fluorescent assay, HeLa cells were treated with SNX-2112, and green fluorescence was found to markedly increase in a time-dependent manner (Figures 3(a) and 3(b)), suggesting the production of ROS in HeLa cells. However, we found that treatment with TRAIL alone could not increase the level of ROS in HeLa cells (Figures 3(c) and 3(d)).

Notably, flow cytometry analysis showed that pretreatment with NAC, a ROS scavenger, significantly rescued SNX-2112/TRAIL-induced apoptosis in HeLa cells (Figures 3(e) and 3(f)). Sensitization to apoptosis was completely abolished by NAC. These results suggest that SNX-2112-induced ROS plays a key role in apoptosis induced by treatment with a combination of SNX-2112 and TRAIL.

3.4. DR5 Upregulation Mediates SNX-2112-Stimulated TRAIL-Induced Apoptosis. Two TRAIL receptors, DR4 and DR5, are known to trigger apoptotic signals upon TRAIL binding via the functional death domain. In certain cancer cell lines, reduced expression of TRAIL receptors DR4 and DR5 and/or upregulation of the decoy receptors DcR1 and DcR2 have been defined as the main causes of TRAIL resistance [48]. To further explore the molecular mechanisms underlying ROS-mediated TRAIL sensitization in HeLa cells, we investigated whether SNX-2112-induced TRAIL receptor upregulation and its subsequent increased expression contributed to synergistic apoptosis caused by the combination of SNX-2112 and TRAIL. As expected, our Western blotting results showed that SNX-2112 alone or in combination with TRAIL obviously upregulated DR5 in HeLa cells. Although the expression of DR4 was also significantly increased (Figures 4(a) and 4(b)), the upregulation of DR5 was predominant compared to DR4. As a result, in subsequent experiments, we focused on DR5. Consistent with

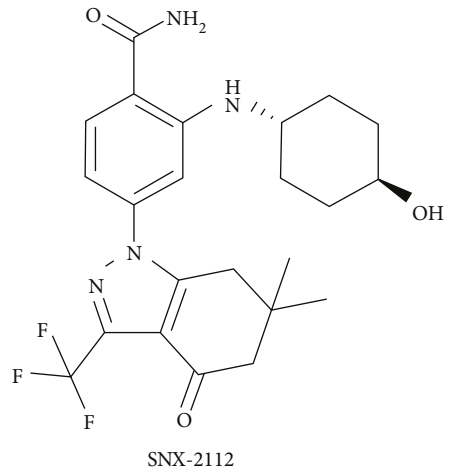

SNX-2112

(a)

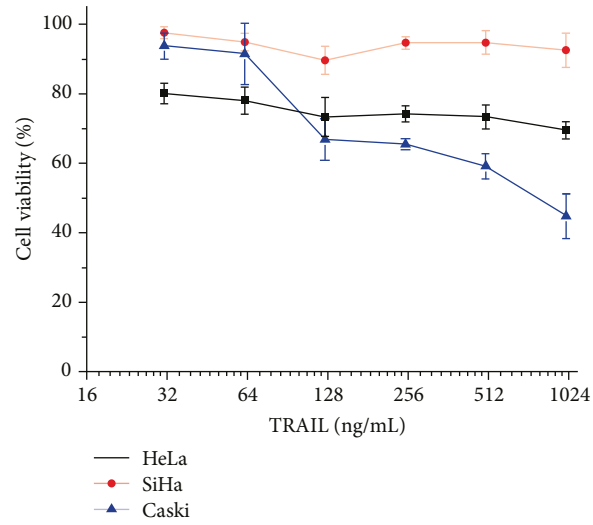

(b)

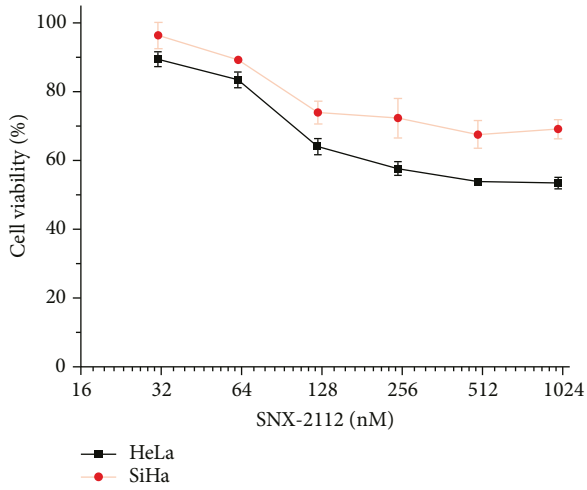

(c)

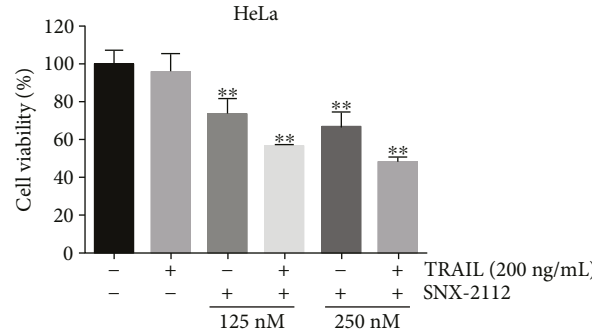

(d)

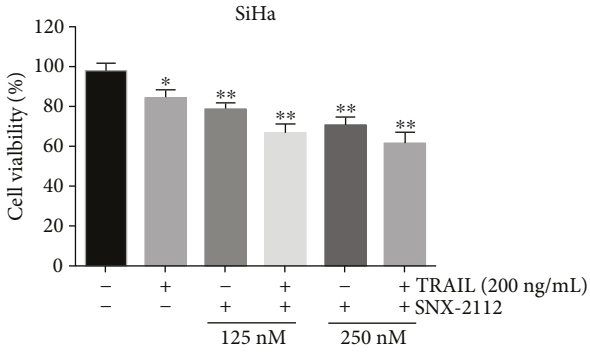

(e)

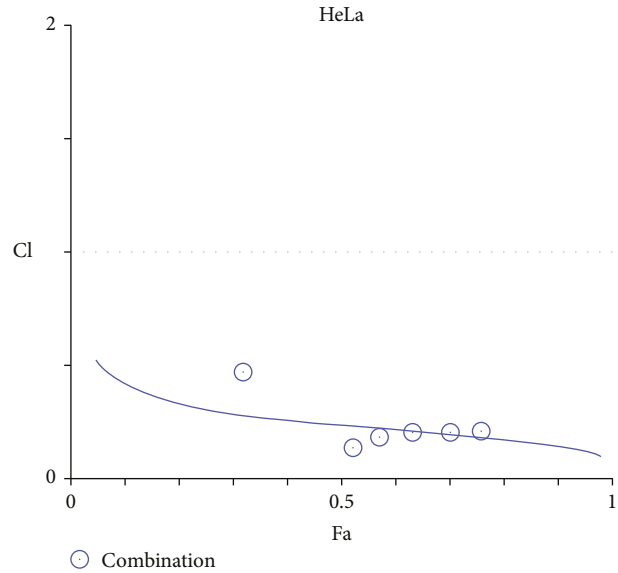

(f)

Figure 1: Continued.

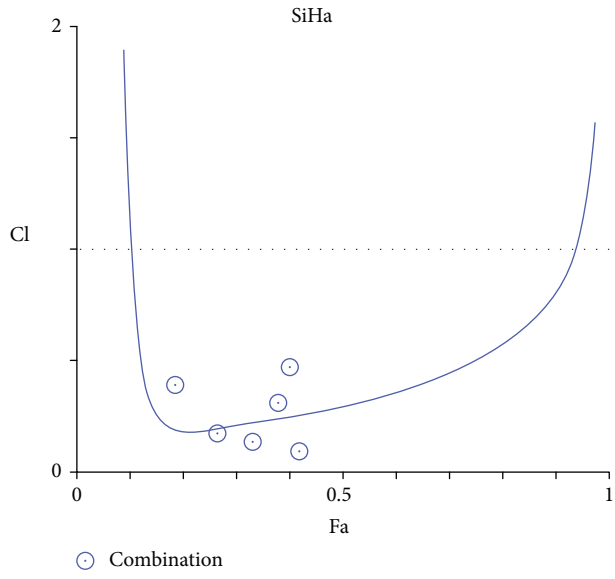

(g)

Figure 1: SNX-2112 enhances TRAIL-induced cytotoxicity in human cervical cancer cells. (a) Chemical structure of SNX-2112. (b) Cervical cancer cell lines, HeLa, SiHa, and Caski, were treated with TRAIL at different concentrations (0, 31.25, 62.5, 125, 250, 500, and 1000 ng/mL) for 48 h. Cell viability was assessed by MTT assay. (c) Cervical cancer cell lines, HeLa and SiHa, were treated with SNX-2112 at different concentrations (0, 31.25, 62.5, 125, 250, 500, and 1000 nM) for 48 h. Cell viability was assessed by MTT assay. (d) HeLa or (e) SiHa cells were treated with either TRAIL (200 ng/mL) or SNX-2112 (125, 250 nM) or in combination for 48 h. Cell viability was assessed by MTT assay. (f-g) Fitting curves of CIs for TRAIL and SNX-2112 combination in SiHa and HeLa cell lines plotted and calculated using CompuSyn software. Data are represented as mean ± SD. Error bars represent SD from three separate experiments. $^{*}P < 0.05$ and $^{**}P < 0.01$ compared with the control group.

the changes observed in the protein, immunofluorescence analysis showed that SNX-2112 treatment increased DR5 cell surface expression (Figure 4(c)). Subsequently, we found that the treatment of HeLa cells with SNX-2112 could significantly induce increased protein levels of DR5 in both concentration-dependent and time-dependent manners (Figures 4(d)-4(g)).

To determine the role of DR5 and DR4, we applied a specific siRNA to silence DR5 and DR4 expression. Western blotting revealed that SNX-2112-induced upregulation of DR5 was abolished by DR5 siRNA (Figures 4(h) and 4(i)). Flow cytometry analysis showed that the silencing of DR5 significantly decreased the apoptosis induced by TRAIL/SNX-2112 (Figures 4(j) and 4(k)). However, cleaved-PARP induced by SNX-2112 was not affected by DR5 siRNA (Figure 4(h)). On the other hand, Western blotting also showed that SNX-2112-induced upregulation of DR4 was abolished by DR4 siRNAs (Figures 4(l) and 4(m)). However, flow cytometry analysis showed that the silencing of DR4 did not affect the apoptosis induced by TRAIL/SNX-2112 (Figures 4(n) and 4(o)). These results suggest that DR5 upregulation significantly enhanced apoptosis induced by treatment with a combination of SNX-2112 and TRAIL.

3.5. SNX-2112 Can Significantly Induce Autophagy to Enhance Apoptosis by Inhibiting the Akt/mTOR Signaling Pathway in HeLa Cells. By the downregulation of DR4 and DR5 surface expression, the accumulation of autophagosomes in TRAIL-resistant breast cancer cells induces TRAIL resistance [49]. We studied whether autophagy was related to the mechanism that accounted for the upregulation of SNX-2112-induced DR5. The turnover of LC3 protein, a characteristic autophagosomal marker, from the cytosolic form LC3-I to the lipidated form LC3-II is associated with the formation of autophagosomes [50]. Beclin1 is a pivotal protein in autophagy, whose upregulation can lead to autophagy [51].

We determined the expression levels of LC3 and Beclin1 treated with SNX-2112 alone or in combination with TRAIL for 48 h in HeLa cells. First, the combination of TRAIL and SNX-2112 was found to markedly upregulate LC3-II and Beclin1 (Figures 5(a) and 5(b)). Additionally, the autophagy markers were dramatically upregulated by SNX-2112 alone in other treated groups (Figures 5(c)-5(f)). This indicates that SNX-2112 can markedly induce autophagy in HeLa cells in a concentration- and time-dependent manner. Moreover, as shown in Figures 5(g) and 5(h), SNX-2112 was found to inhibit the expression of Akt, a client protein of Hsp90. Subsequent testing showed that Akt/mTOR signaling protein, p-Akt, p-mTOR, p-4EBP1, and p-S6 were inhibited by SNX-2112 alone or in combination with TRAIL in HeLa (Figures 5(g)-5(j)). These results suggest that the autophagy effect of SNX-2112 is a result of the inhibition of the Akt/mTOR signaling pathway in HeLa cells.

Subsequently, an autophagy inhibitor, bafilomycin A1 (BFA), was used to determine the correlation between autophagy and DR5 expression. BFA is an inhibitor of vacuolar ATPase that prevents fusion between lysosomes and autophagosomes [52]. The accumulation of LC3-II induced by SNX-2112 was found to increase in HeLa cells that had

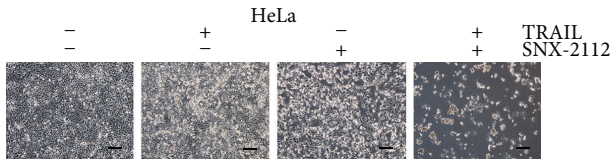

(a)

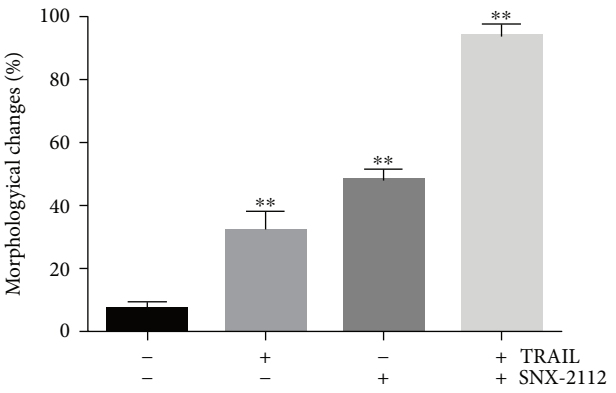

(b)

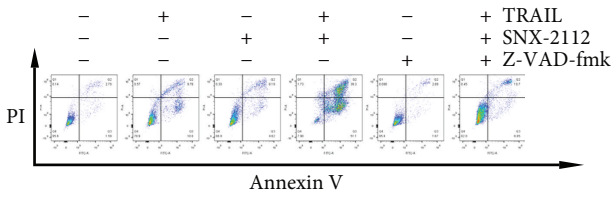

(c)

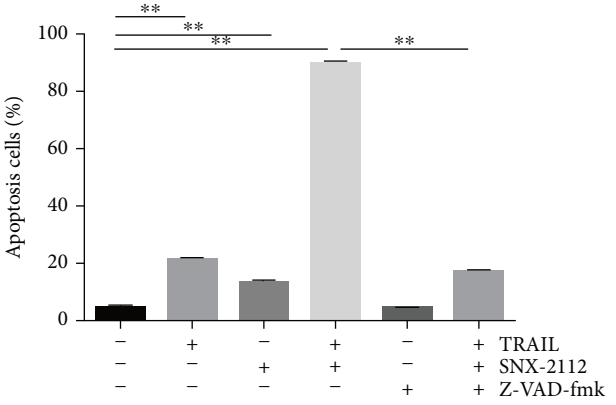

(d)

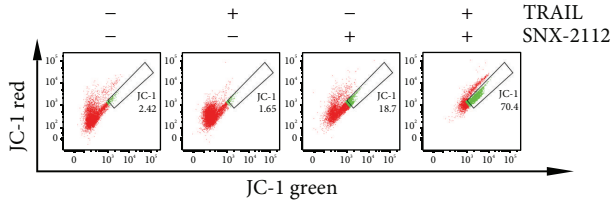

(e)

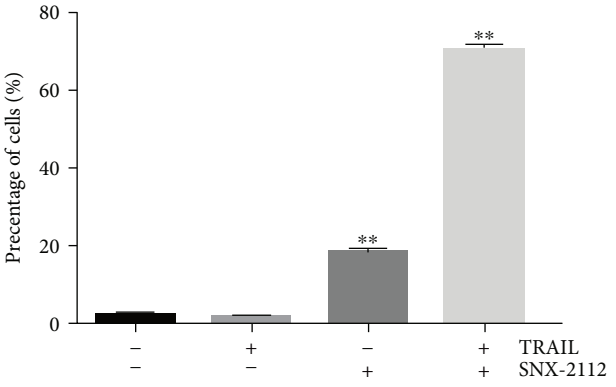

(f)

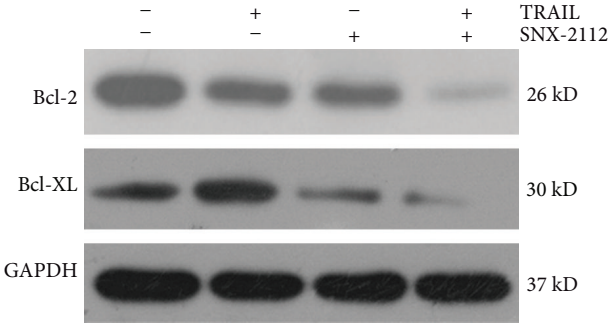

(g)

Figure 2: Continued.

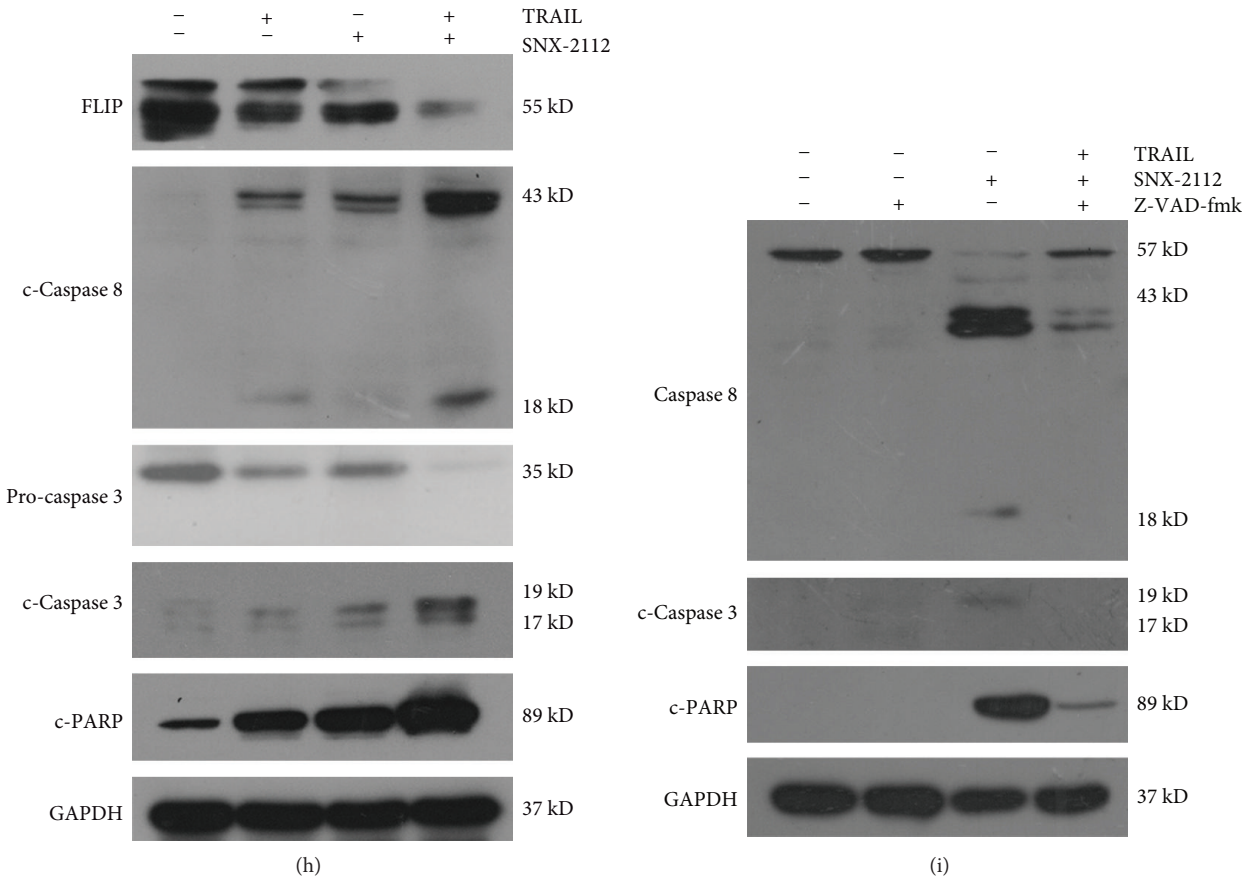

Figure 2: SNX-2112 is synergistic to TRAIL and coinduces HeLa cell apoptosis. (a-i) Cells were treated with either TRAIL (200 ng/mL) or SNX-2112 (125 nM) alone or in combination for 48 h. Using FACS analysis assays, the cells were pretreated with or without 20 μM Z-VAD-fmk for 1 h. (a, b) Microscopic cell morphologies. Scale bar: 250 μm. Morphologically altered cells were counted and analyzed. (c, d) The cells were stained with Annexin V and propidium iodide (PI), followed by FACS analysis. (e, f) FACS analysis of $\Delta\psi_m$ by JC-1 staining. After treatment with drugs, cells were stained with JC-1 for 20 min. (g h) The Bcl-2, Bcl-XL, FLIP, pro-caspase 3, c-caspase 3 and 8, and c-PARP proteins were analyzed by Western blotting. (i) Apoptosis-associated proteins (c-caspase 3 and 8 and c-PARP) were detected in the presence of Z-VAD-fmk by Western blotting. GAPDH was used as a protein loading control. Data are represented as mean ± SD. Error bars represent SD from three separate experiments. $^*P < 0.05$ and $^{**}P < 0.01$ compared with the control group.

been pretreated with BFA at a concentration of 50 nM for 2 h (Figures 5(k) and 5(l)). These results indicate that BFA inhibits the degradation of LC3-II, thus blocking the autophagy. As expected, subsequently, this resulted in the downregulation of SNX-2112-induced DR5 and cleaved PARP (Figures 5(k) and 5(l)). Furthermore, we applied two specific siRNAs to silence Atg7 expression, a protein marker for autophagy. Western blotting demonstrated that SNX-2112-induced upregulation of Atg7, LC-II, DR5, and c-PARP was abolished by Atg7 siRNAs (Figures 5(m) and 5(n)). Flow cytometry analysis showed that the silencing of Atg7 significantly decreased the apoptosis induced by TRAIL/SNX-2112 (Figures 5(o) and 5(p)). These results suggest that autophagy induced by SNX-2112 is dependent on Akt/mTOR signaling and plays an important role in improving the expression of DR5 but also affects SNX-2112-induced apoptosis in HeLa cells.

3.6. SNX-2112 Increases p53 Expression to Enhance TRAIL-Induced Apoptosis. DR5 is a p53-regulated DNA damage-inducible cell death receptor. p53 is an important protein for the regulation of DR4 and DR5 expression at the transcriptional level. Some agents have been found to induce p53-dependent transcription of DR5 to synergize with TRAIL [53, 54].

To investigate whether p53 contributed to SNX-2112-induced DR5 upregulation, we treated HeLa cells with SNX-2112 and examined p53 levels by Western blotting. As shown in Figures 6(a)-6(d), the expression of p53 was increased in a time-dependent and concentration-dependent manner by SNX-2112. Furthermore, we found that SNX-2112-induced p53 was inhibited by PFTα, a p53-specific inhibitor. Moreover, DR5 expression induced by SNX-2112 was abolished in these p53-inhibited HeLa cells (Figures 6(e) and 6(f)), indicating a p53-dependent mechanism. Here, we were particularly interested in the relationship between autophagy and p53. Interestingly, p53 inhibition was correlated with the downregulated expression of LC3-II (Figures 6(e) and 6(f)). Furthermore, the results of the flow cytometry assay showed that PFTα significantly reduced apoptosis induced by TRAIL and

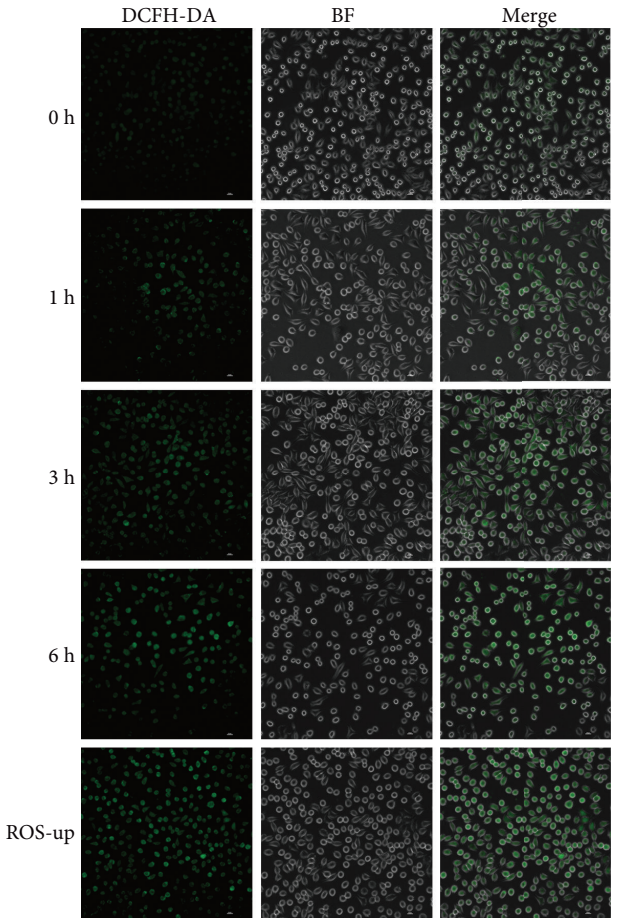

(a)

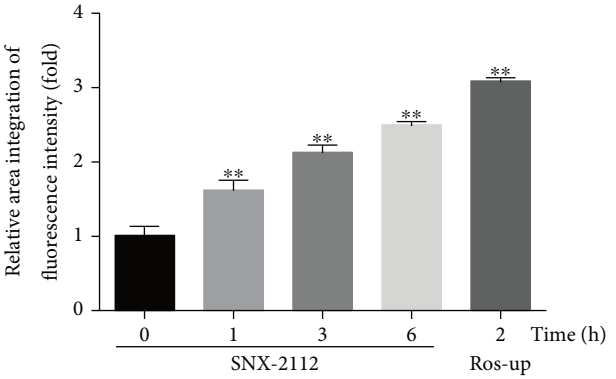

(b)

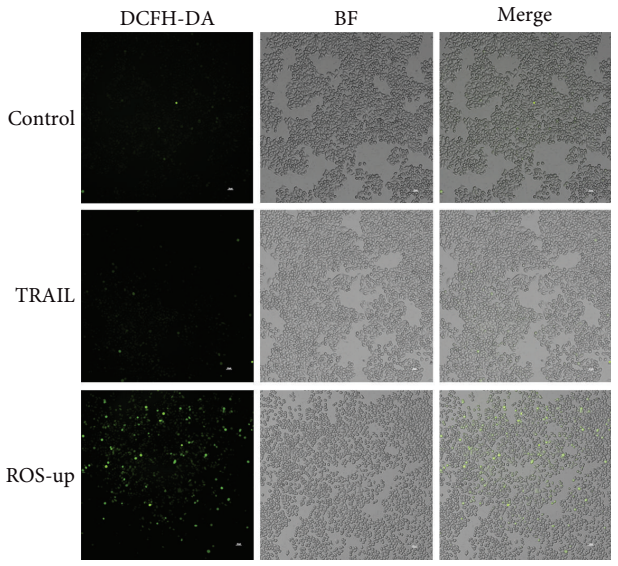

(c)

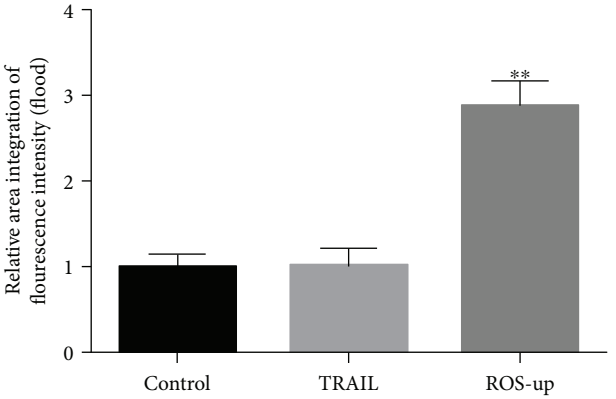

(d)

Figure 3: Continued.

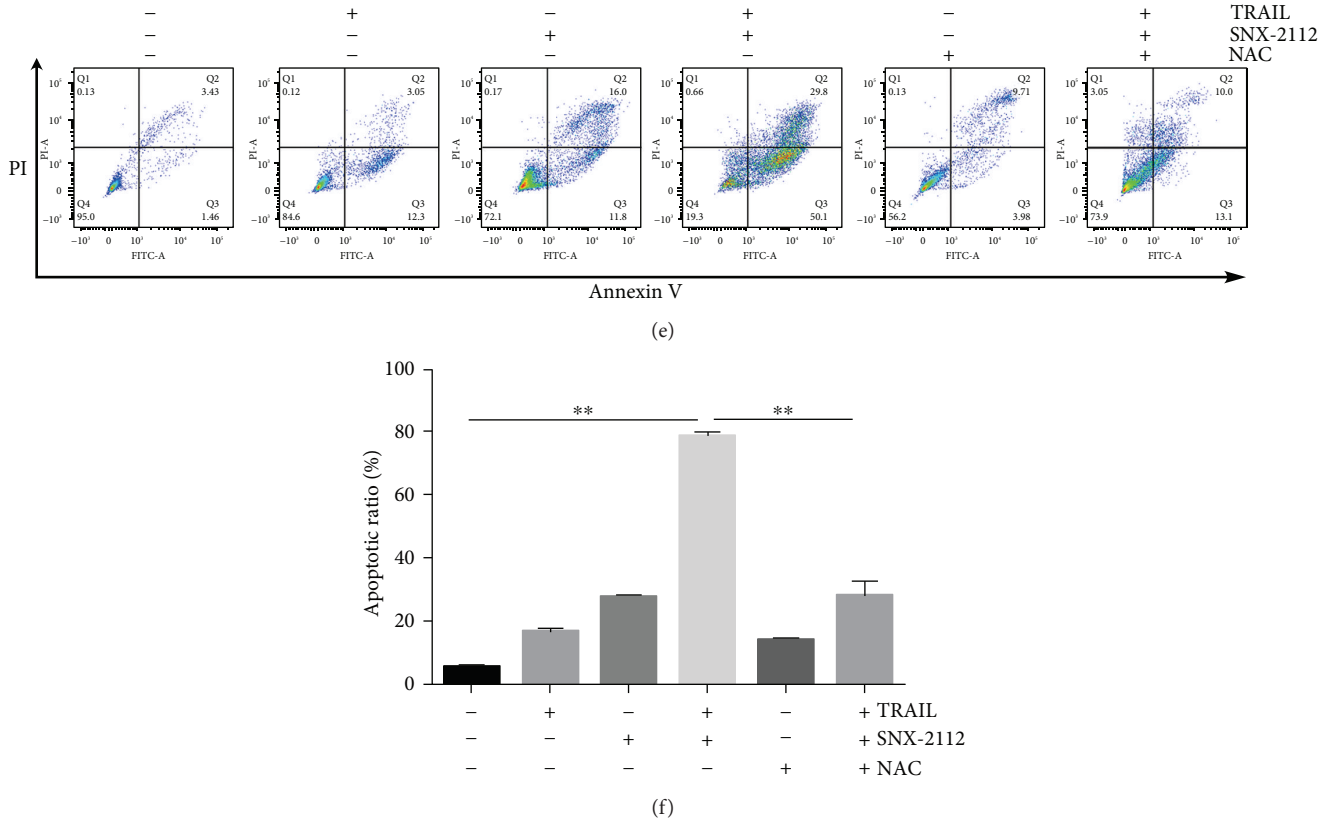

Figure 3: SNX-2112-induced accumulation of ROS significantly enhances apoptosis induced by TRAIL. HeLa cells were treated with (a, b) SNX-2112 (125 nM) for the indicated time (0, 1, 3, and 6 h) or (c, d) TRAIL (200 ng/mL) for 6 h. ROS-up was used to be the positive control. ROS levels were measured with an epifluorescence microscope by DCFH-DA staining. (e, f) HeLa cells were pretreated with or without 20 mM NAC for 2 h and then treated with or without TRAIL/SNX-2112 for 48 h. The cells were stained with Annexin V/PI and TRAIL/SNX-2112-induced apoptosis was analyzed by flow cytometry. Data are represented as mean ± SD. Error bars represent SD from three separate experiments. $^{*}P < 0.05$ and $^{**}P < 0.01$ compared with the control group.

SNX-2112 (Figures 6(g) and 6(h)). These results suggest that SNX-2112-induced DR5 is p53-dependent and regulated through the p53-autophagy pathway. Additionally, we found that SNX-2112-induced c-PARP was abolished by PFTα (Figures 6(e) and 6(f)), suggesting that p53 also regulates the apoptosis induced by SNX-2112 alone. In summary, the apoptotic effect induced by the combination of SNX-2112 with TRAIL is involved in the activation of the p53-autophagy-DR5 signaling pathway in HeLa cells.

3.7. JNK Activation Is Involved in TRAIL/SNX-2112-Induced Apoptosis. It has been previously reported that by upregulating the level of ROS, drugs can activate the MAPK signaling pathway to overcome TRAIL resistance, sensitizing TRAIL-induced cancer cells to apoptosis. Here, we investigated whether SNX-2112 could induce MAPK in TRAIL/SNX-2112-induced apoptosis.

Western blotting was used to detect the expression of MAPKs, including extracellular signal-regulated kinases (ERKs), JNKs, and p38-MAPKs. The results showed that SNX-2112 markedly increased JNK and p38 phosphorylation, but slightly downregulated ERK phosphorylation, in a dose-dependent manner (Figures 7(a) and 7(b)). Downregulation of ERK by SNX-2112 may account, at least in part, for the synergistic effect.

HeLa cells were pretreated with the JNK inhibitor SP600125, p38 inhibitor SB203580, and ERK inhibitor PD98059. The results of the flow cytometry assay showed that SP600125 significantly reduced the apoptosis induced by a combination of SNX-2112 with TRAIL (Figures 7(c) and 7(d)). However, SB203580 and PD98059 did not abolish apoptosis induced by TRAIL and SNX-2112 (Figures 7(e)-7(h)). These results suggest that SNX-2112 can induce the activation of JNK to potentiate TRAIL-induced apoptosis in HeLa cells.

We further analyzed the relationship of JNK between the p53-autophagy-DR5 signaling pathways. As shown in Figures 7(i) and 7(j), JNK inhibitor SP600125 was applied to determine the role of JNK in the p53-autophagy-DR5 pathway. We detected the expression levels of p53, LC3, and DR5 in the presence of SP600125 by Western blotting in HeLa cells. The data showed that the upregulation of SNX-2112-induced DR5 was abolished, as with p53 and LC3-II. Thus, our results suggested that the apoptotic effect induced by the combination of SNX-2112 with TRAIL is induced by the activation of the JNK-p53-autophagy-DR5 signaling pathway in HeLa cells.

3.8. SNX-2112-Induced Accumulation of ROS Activates the JNK-p53-Autophagy Pathway to Mediate DR5 Expression. Many studies have confirmed that DR5 expression was

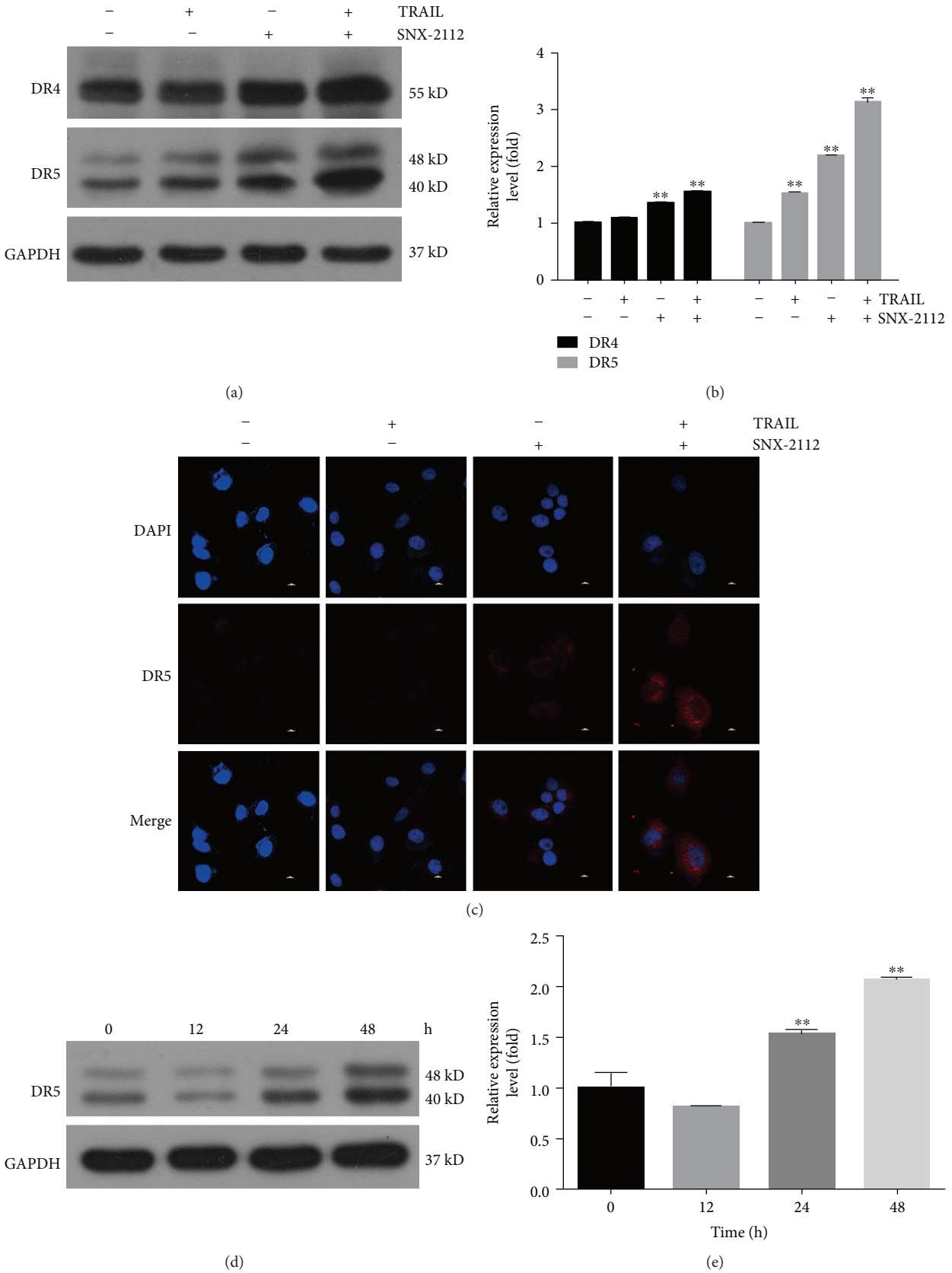

Figure 4: Continued.

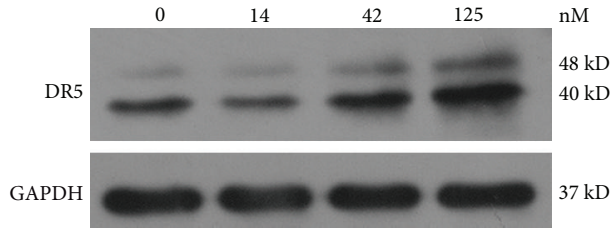

(f)

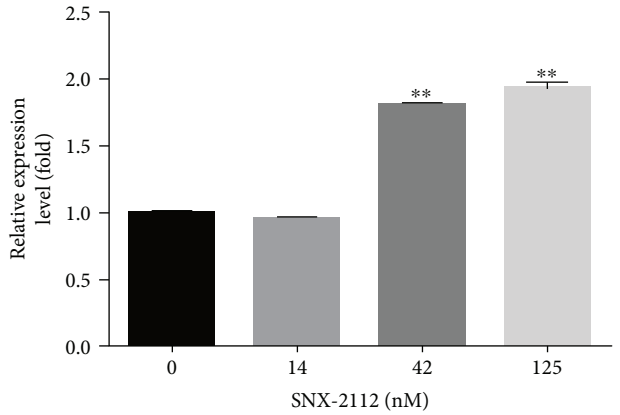

(g)

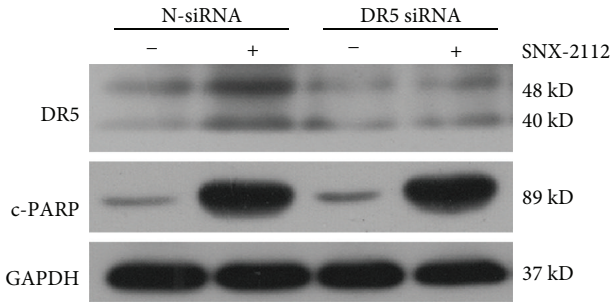

(h)

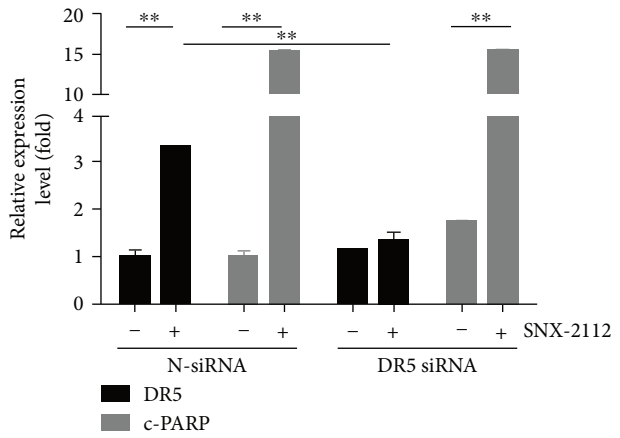

(i)

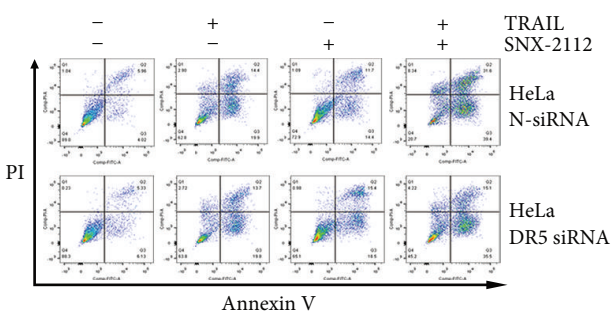

(j)

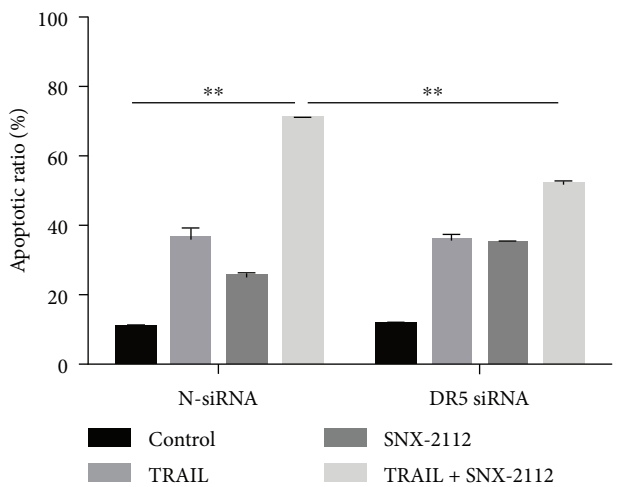

(k)

Figure 4: Continued.

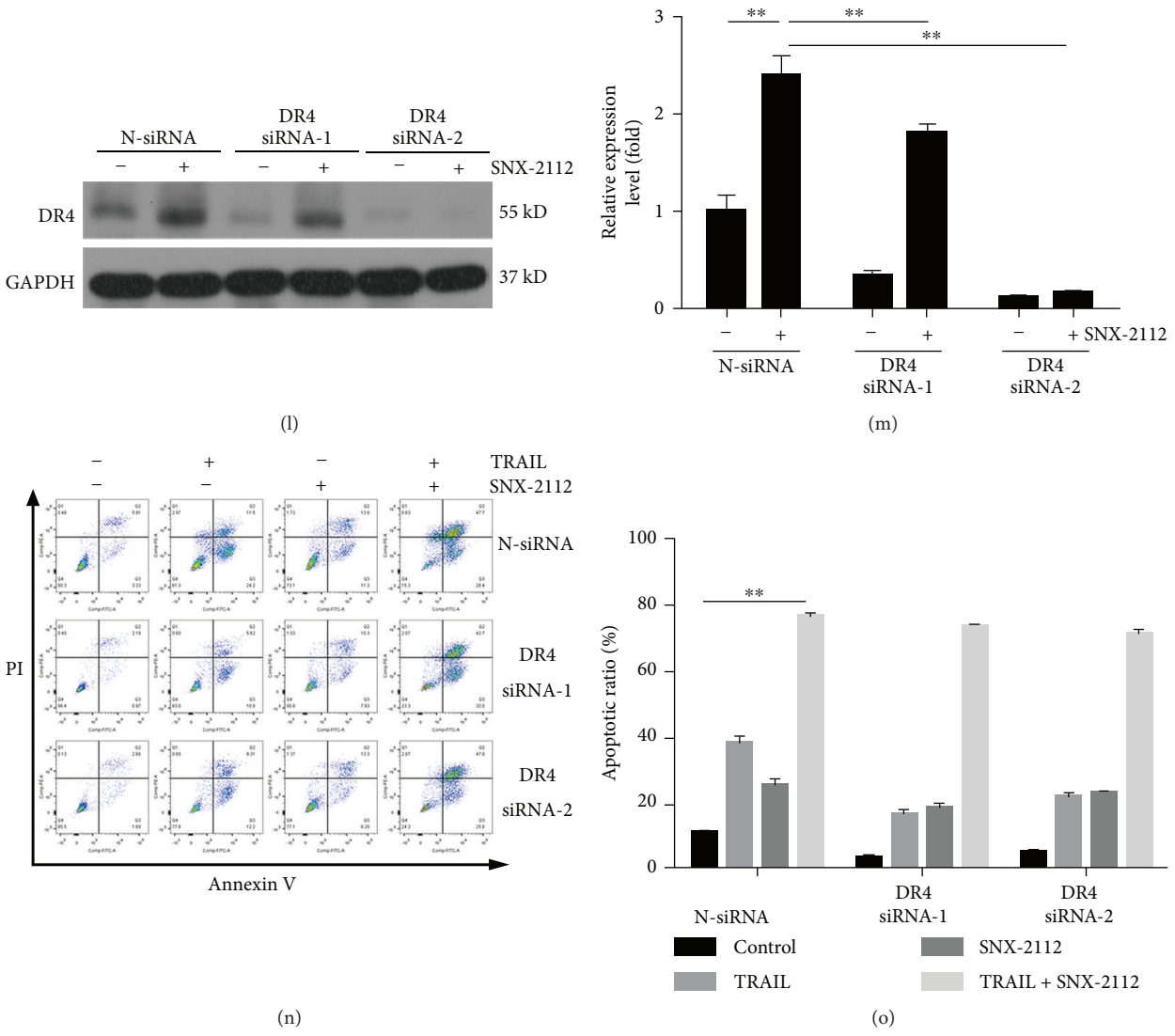

Figure 4: SNX-2112-induced DR5 mediates the combined effect of TRAIL and SNX-2112. HeLa cells were treated with SNX-2112 (125 nM) in either the absence or the presence of TRAIL (200 ng/mL) for 48 h. (a, b) Western blotting was performed to detect the levels of DR4 and DR5. Densitometry analyses of the bands for each protein were performed. (c) Immunofluorescence analyses were carried out using the indicated antibody (DR5) to detect the cellular expression of DR5. Scale bar: 10 μm. (d, e) HeLa cells were treated with SNX-2112 (125 nM) for the indicated time (12, 24, and 48 h). The protein levels of DR5 in whole cell lysates were determined using the specific antibody. Densitometry analyses of the bands for the protein were performed. (f, g) HeLa cells were treated with SNX-2112 at different concentrations (0, 14, 42, and 125 nM) for 48 h. The protein levels of DR5 in whole cell lysates were determined using the specific antibody. Densitometry analyses of the bands for the protein were performed. (h, i) HeLa cells were transfected with control siRNA (N-siRNA) or DR5 siRNAs. After treatment with SNX-2112 (125 nM) for 48 h, Western blotting was used to analyze whole-cell extracts. The protein levels of DR5 and c-PARP were determined using the specific antibody. Densitometry analyses of the bands for each protein were performed. (j, k) The resultant cells were exposed to SNX-2112 (125 nM) in either the absence or the presence of TRAIL (200 ng/mL) for 48 h. Cells were stained with Annexin V/PI, and cell death was measured by FACS. (l, m) HeLa cells were transfected with control siRNA (N-siRNA) or DR4 siRNAs. After treatment with SNX-2112 (125 nM) for 48 h, Western blotting was used to analyze whole-cell extracts. The protein levels of DR4 were determined using the specific antibody. Densitometry analyses of the bands for each protein were performed. (n, o) The resultant cells were exposed to SNX-2112 (125 nM) in either the absence or the presence of TRAIL (200 ng/mL) for 48 h. Cells were stained with Annexin V/PI, and cell death was measured by FACS. Data are represented as mean ± SD. Error bars represent SD from three separate experiments. $^{*}P < 0.05$ and $^{**}P < 0.01$ compared with the control group.

induced by ROS generation [55, 56] and that autophagy-mediated cell death was mediated by ROS [57]. The effect of ROS on the potentiation of TRAIL-induced apoptosis by SNX-2112 was also investigated here.

To determine the role of ROS to JNK-p53-autophagy-mediated DR5 signaling, NAC, a reactive oxygen scavenger, was applied. In HeLa cells pretreated with NAC, we found that the upregulation of SNX-2112-induced DR5 was

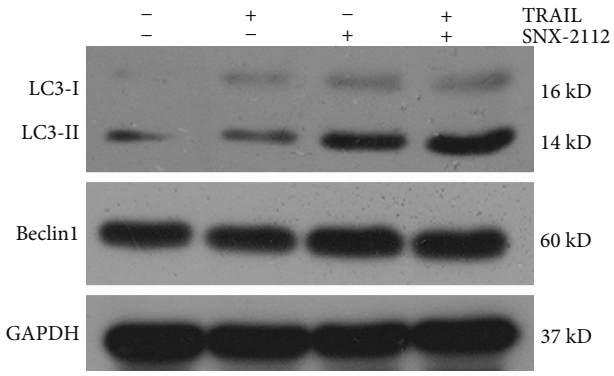

(a)

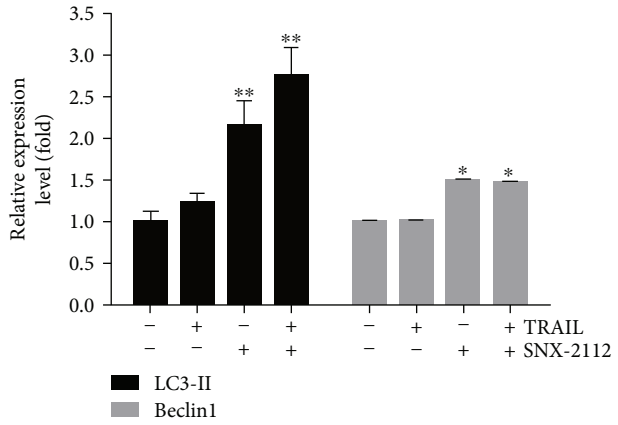

(b)

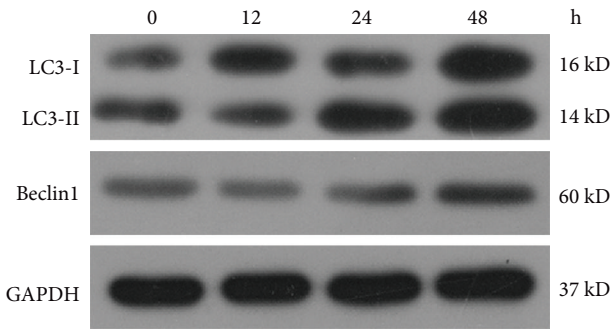

(c)

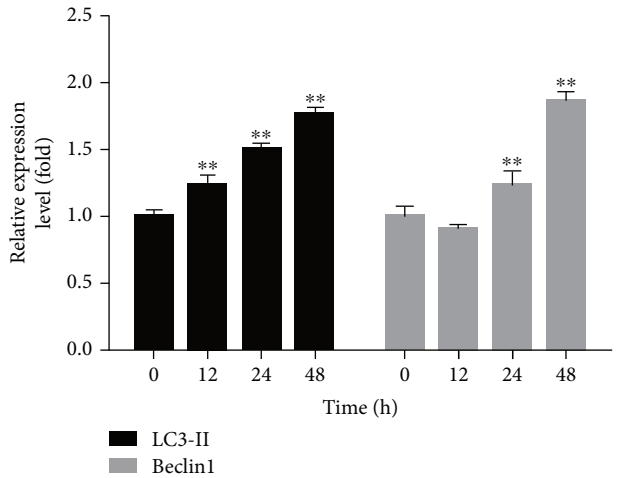

(d)

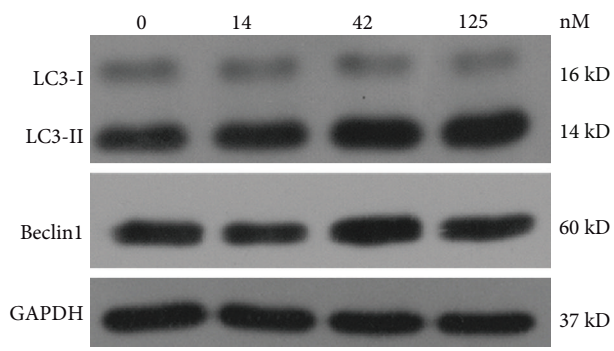

(e)

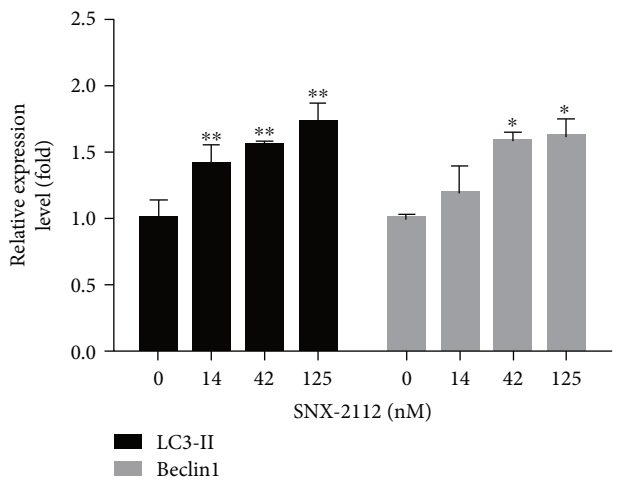

(f)

Figure 5: Continued.

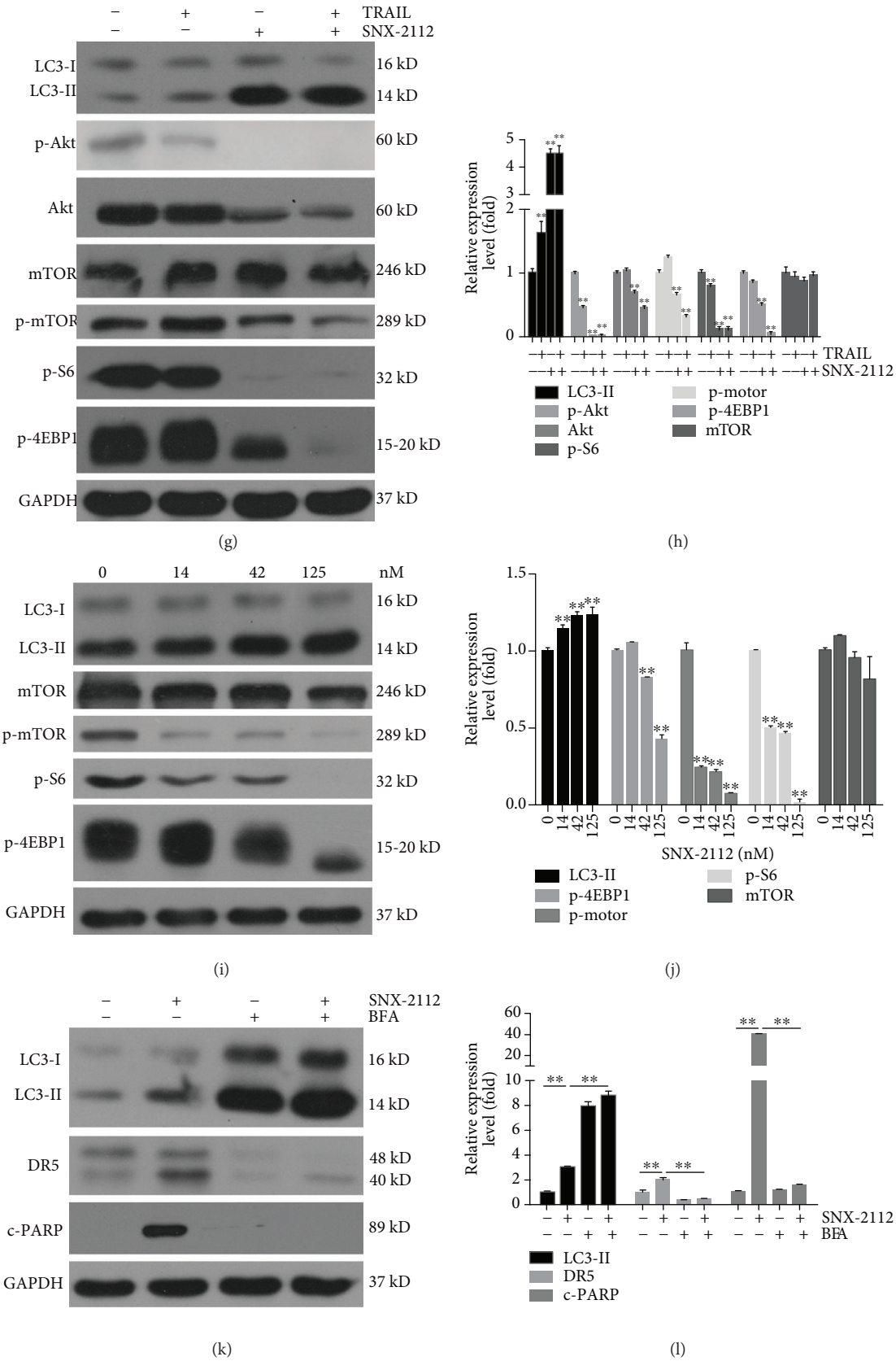

Figure 5: Continued.

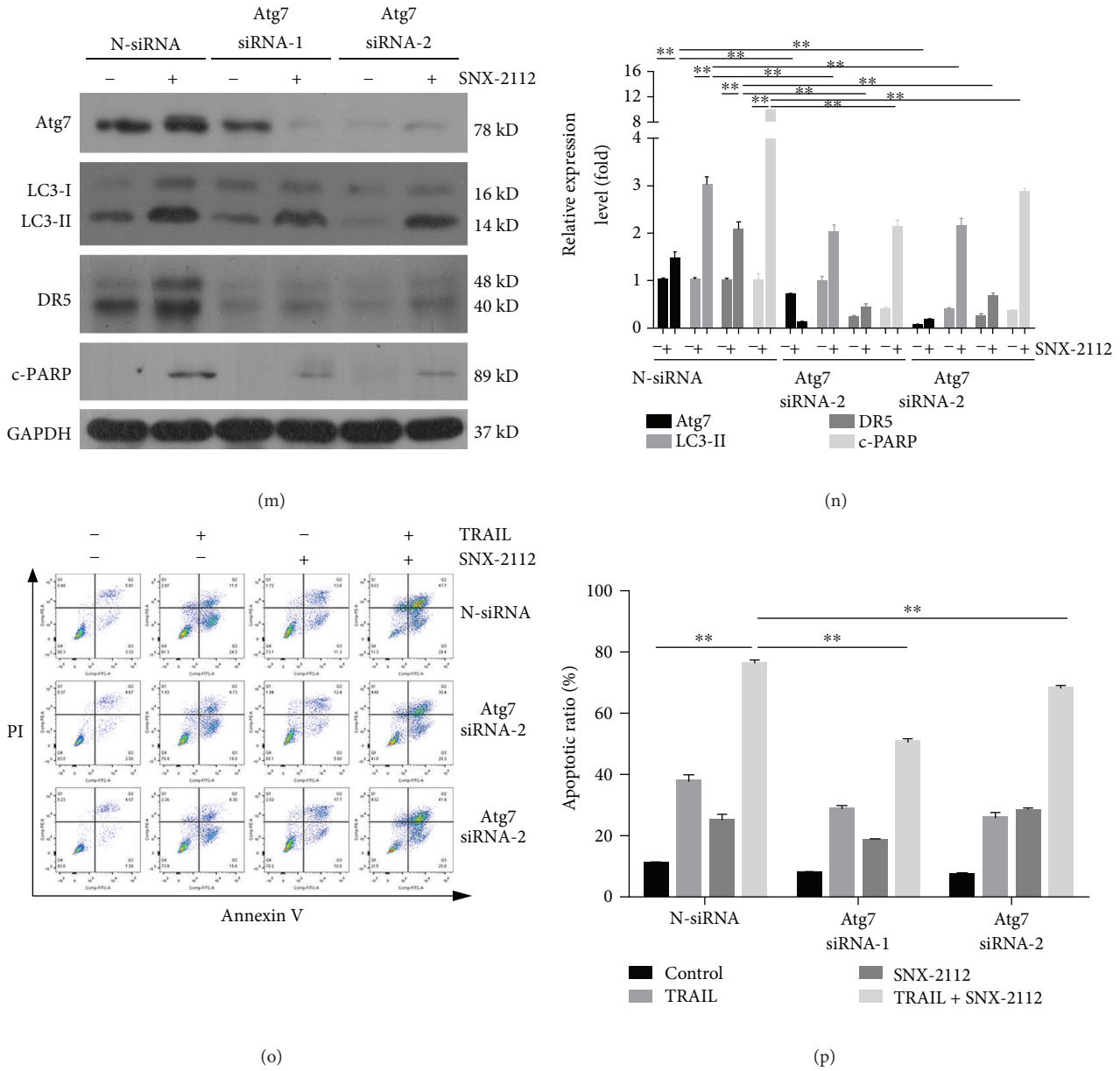

Figure 5: DR5 expression is regulated by SNX-2112-induced autophagy. (a, b) HeLa cells were treated with either TRAIL (200 ng/mL) or SNX-2112 (125 nM) alone or in combination for 48 h. Western blotting was performed to detect the levels of LC3 and Beclin1. Densitometry analyses of the bands for each protein were performed. (c-f) HeLa cells were treated with SNX-2112 for the indicated time (12, 24, and 48 h) or concentration (0, 14, 42, and 125 nM). Western blotting was performed to detect the levels of LC3 and Beclin1. Densitometry analyses of the bands for each protein were performed. (g, h) HeLa cells were treated with SNX-2112 (125 nM) alone or in combination with TRAIL (200 ng/mL) for 48 h. Western blotting was performed to detect the levels of LC3, p-Akt, Akt, p-mTOR, mTOR, p-S6, and p-4EBP1. Densitometry analyses of the bands for each protein were performed. (i, j) HeLa cells were treated with SNX-2112 for the indicated concentration (0, 14, 42, and 125 nM). Western blotting was performed to detect the levels of LC3, p-mTOR, mTOR, p-S6, and p-4EBP1. Densitometry analyses of the bands for each protein were performed. (k, l) HeLa cells were pretreated with BFA (50 nM) for 2 h and then treated with SNX-2112 for 48 h. LC3, DR5, and c-PARP were detected by Western blotting. Densitometry analyses of the bands for each protein were performed. (m, n) HeLa cells were transfected with control siRNA (N-siRNA) or Atg7 siRNAs. After treatment with SNX-2112 (125 nM) for 48 h, Western blotting was used to analyze whole-cell extracts. The protein levels of Atg7, LC3, DR5, and c-PARP were determined using the specific antibody. Densitometry analyses of the bands for each protein were performed. (o, p) The resultant cells were exposed to SNX-2112 (125 nM) in either the absence or the presence of TRAIL (200 ng/mL) for 48 h. Cells were stained with Annexin V/PI, and cell death was measured by FACS. Data are represented as mean ± SD. Error bars represent SD from three separate experiments. $^{*}P < 0.05$ and $^{**}P < 0.01$ compared with the control group.

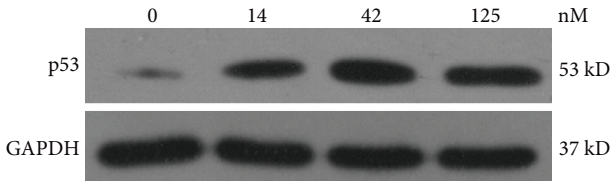

(a)

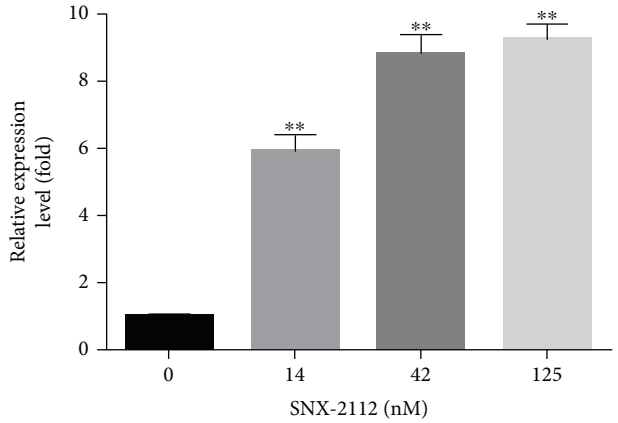

(b)

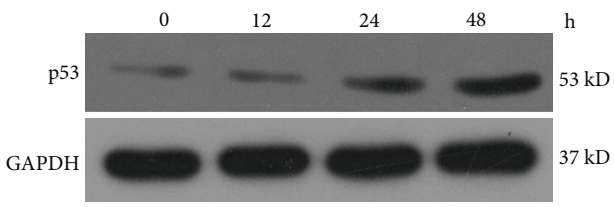

(c)

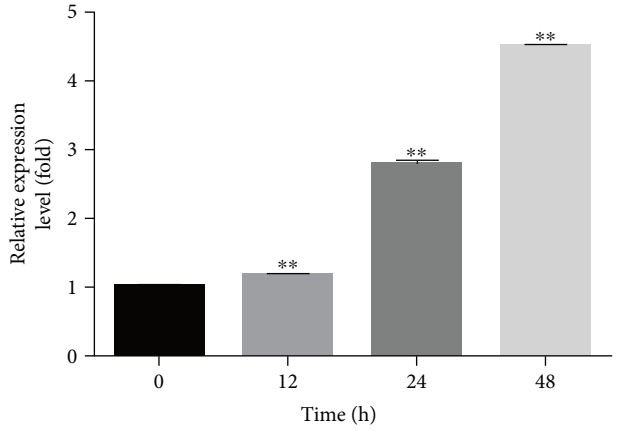

(d)

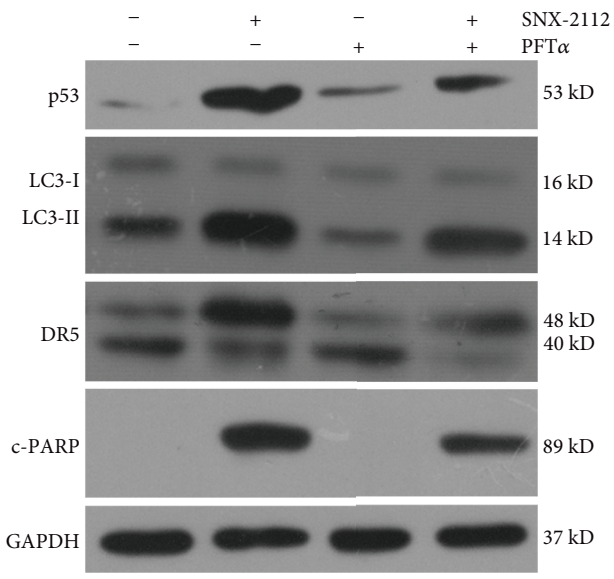

(e)

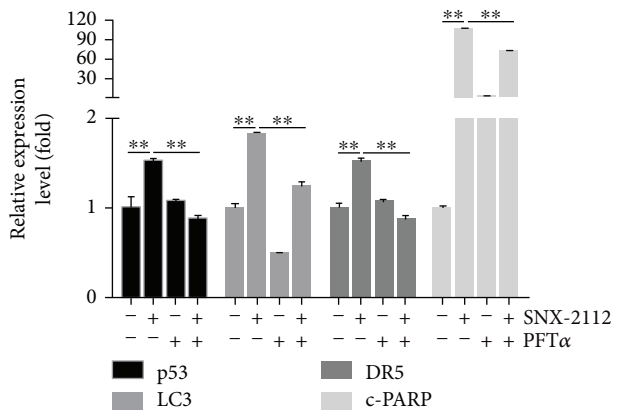

(f)

Figure 6: Continued.

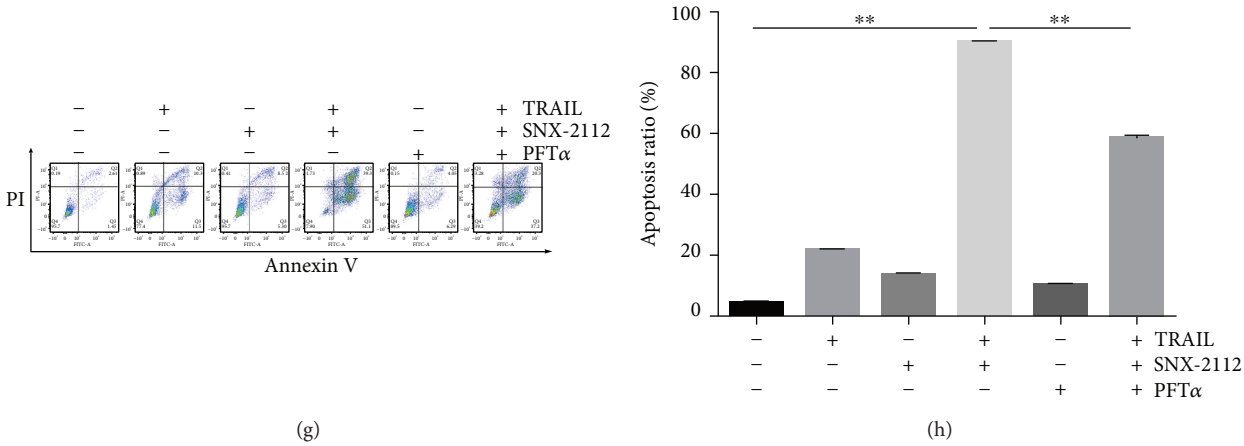

(g) (h)

Figure 6: SNX-2112-induced p53 expression enhances apoptosis induced by TRAIL. (a, b) HeLa cells were exposed to SNX-2112 at the indicated dose for 48 h. Western blotting was performed to detect the levels of p53. Densitometry analyses of the bands for the protein were performed. (c, d) HeLa cells were exposed to SNX-2112 (125 nM) at the indicated time intervals. Western blotting was performed to detect the levels of p53. Densitometry analyses of the bands for the protein were performed. (e, f) HeLa cells were pretreated with the p53 inhibitor PFTα (20 μM) and then exposed to SNX-2112 at the indicated doses. Western blotting was performed to detect the levels of p53, LC3, DR5, and c-PARP. Densitometry analyses of the bands for each protein were performed. (g, h) HeLa cells were pretreated with the p53 inhibitor PFTα (20 μM) and then treated with either TRAIL (200 ng/mL) or SNX-2112 (125 nM) alone or in combination for 48 h. Apoptosis induced by TRAIL and SNX-2112 was measured by FACS. Data are represented as mean ± SD. Error bars represent SD from three separate experiments. $^{*}P < 0.05$ and $^{**}P < 0.01$ compared with the control group.

abolished, as with p-JNK, p53, LC3-II, and c-PARP (Figures 8(a) and 8(b)). SNX-2112-induced ROS activated the expression of p-JNK, p53, autophagy protein LC3-II, and death receptor DR5. Overall, it suggested that by increasing the level of ROS, SNX-2112 enhanced TRAIL-induced apoptosis via the JNK-p53-autophagy-mediated DR5 pathway in HeLa cells.

4. Discussion

TRAIL is a promising anticancer drug, but the resistance of cancer cells to this agent presents a huge obstacle for effective TRAIL-targeted therapy. As a result, agents that can either enhance the effect of TRAIL or overcome its resistance are needed. Many reports have shown that combination therapies produced a higher rate of apoptosis than did monotherapies in many cancers, including renal carcinoma [58] and human colon cancer [59]. In our study, we found that the Hsp90 inhibitor SNX-2112 enhanced TRAIL-induced apoptosis in human cervical cancer cells.

The Hsp90 complex mediates the maturation and stability of a variety of client proteins, many of which are crucial in oncogenesis, including Akt and mutant p53 [60]. Inhibition of Hsp90 function disrupts the complex and leads to degradation of client proteins in a proteasome-dependent manner. This results in simultaneous interruption of many signal transduction pathways pivotal to tumor progression and survival. It has been reported that the trial of silencing Hsp90 expression through transfection of Hsp90 siRNAs into HeLa cells could prevent the proliferation, the same as treating with the Hsp90 inhibitor 17-AAG [61]. Also, in lung cancer Calu-1 and H157 cells, inhibiting the Hsp90 expression by special siRNAs could reduce the expression of c-FLIPL [62, 63].

Although SNX-2112 has been previously found to be an anticancer agent against various cancer cells, its effect was generally limited. Our study first provided that the combination of SNX-2112 with TRAIL could enhance cancer cell death by downregulating antiapoptosis proteins, including Bcl-2, Bcl-XL, and FLIP, and elucidate the mechanism by which SNX-2112 sensitizes TRAIL to apoptosis in cervical cancer cells. At a mechanistic level, our results showed that SNX-2112 inhibited Akt/mTOR signaling to induce autophagy by the downregulation of Hsp90 client protein Akt (Figure 5) and upregulated the TRAIL-receptor DR5 (Figure 4) through the ROS-activated JNK-p53-autophagy singling pathway (Figures 3-8). We concluded that low concentrations of SNX-2112 allowed TRAIL to activate the death-receptor pathways.

It has been shown that when inhibiting the Hsp90 expression by special siRNAs, the expression of c-FLIPL was reduced in the cells, suggesting that c-FLIPL is a client protein of Hsp90, consistent with the downregulation induced by SNX-2112 (Figure 2(h)). 17-AAG, one of the Hsp90 inhibitors, could downregulate the expression of FLIP and, due to the inhibition of Hsp90, could recruit the CHIP to degrade the FLIP [62, 63].

In clinical studies, the downregulation of death-receptor expression has been one of the crucial causes of cancer cell resistance to TRAIL, and competitive antibodies targeting death-receptors are increasingly gaining attention. Understanding the role of DR5 in synergistic effect and the mechanisms of DR5 upregulation would be very informative. In colorectal cancer cells, tunicamycin was found to effectively enhance TRAIL-induced apoptosis through JNK-CHOP-mediated DR5 upregulation [59], and gefitinib enhanced TRAIL-induced apoptosis by autophagy- and JNK-mediated death-receptor upregulation

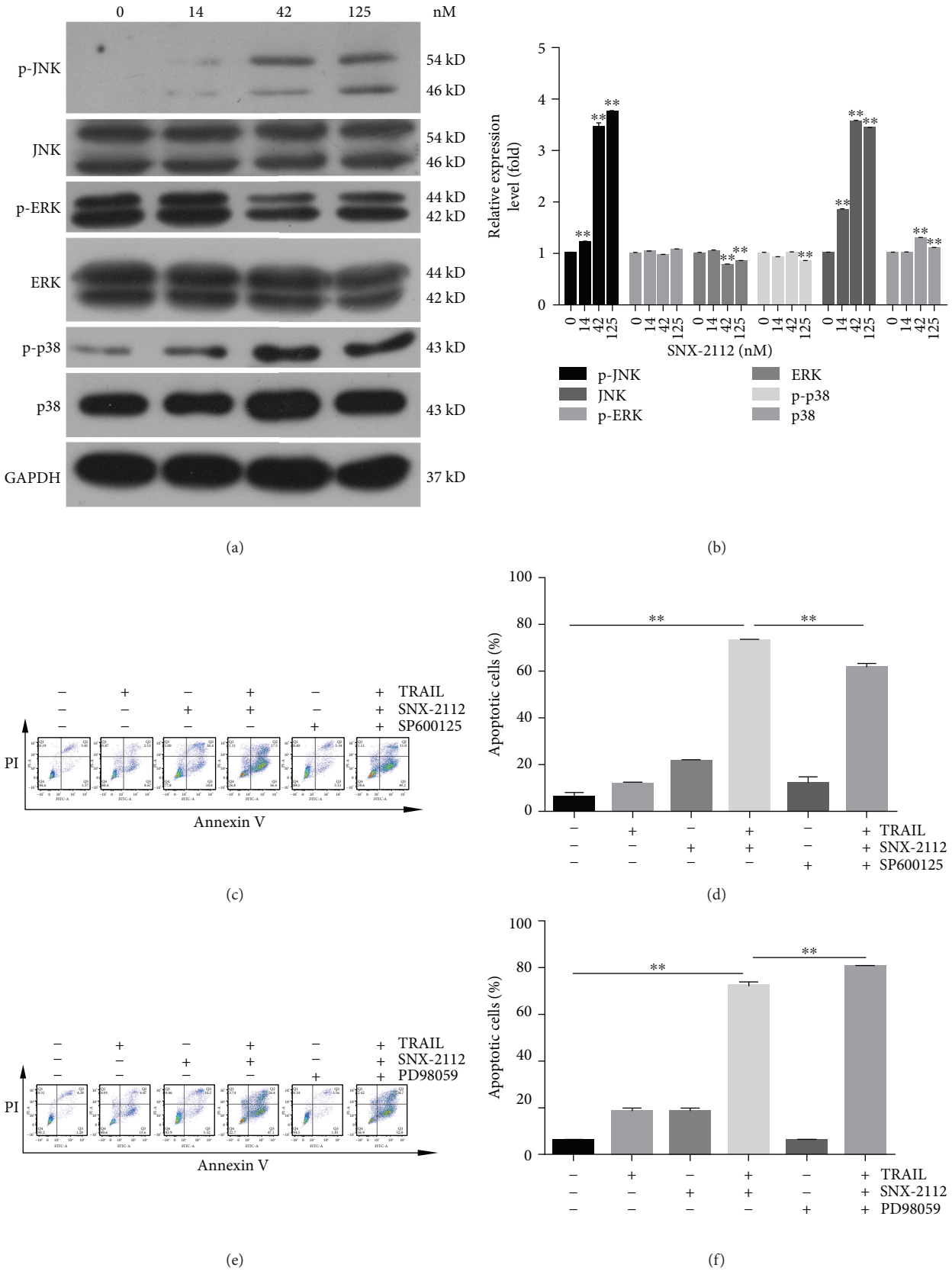

Figure 7: Continued.

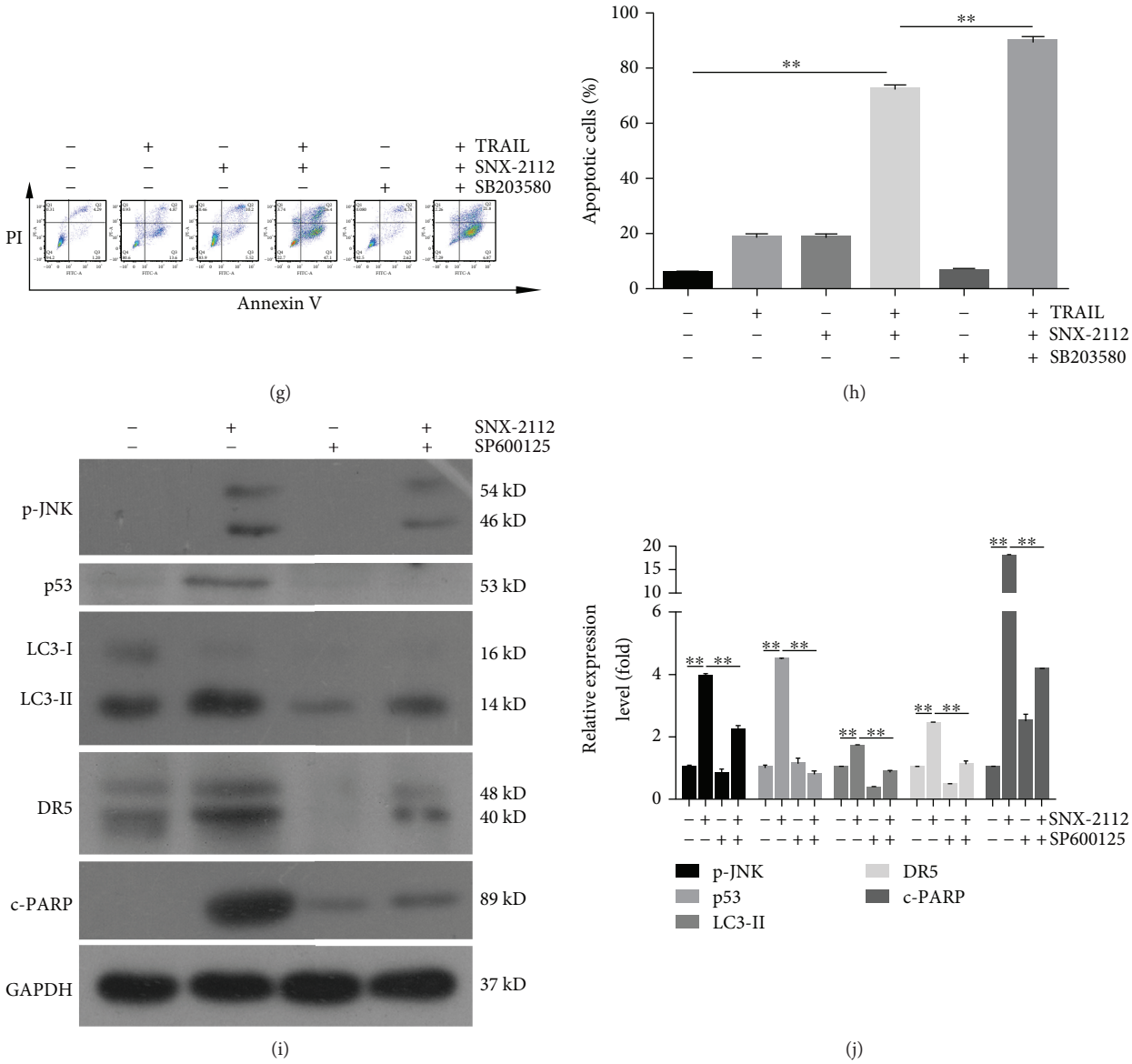

Figure 7: SNX-2112-induced JNK activation is involved in apoptosis induced by TRAIL/SNX-2112. (a, b) HeLa cells were treated with SNX-2112 at indicated doses for 6 h. Western blotting was performed to detect the levels of p-ERK, ERK, p-JNK, JNK, p-p38, and p38. Densitometry analyses of the bands for each protein were performed. HeLa cells were pretreated with (c, d) 10 μM SP600125, (e, f) 25 μM PD98059, and (g, h) 10 μM SB203580 for 2 h and then treated with either TRAIL (200 ng/mL) or SNX-2112 (125 nM) alone or in combination for 48 h. TRAIL/SNX-2112-induced apoptosis was analyzed by flow cytometry. (i, j) HeLa cells were pretreated with or without 10 mM SP600125 for 2 h and then treated with or without SNX-2112 for 48 h. Western blotting were used to analyze whole-cell extracts and detect the levels of p53, LC3, and DR5. Densitometry analyses of the bands for each protein were performed. Data are represented as mean ± SD. Error bars represent SD from three separate experiments. $^{*}P < 0.05$ and $^{**}P < 0.01$ compared with the control group.

[64]. Isoobtusilactone A sensitizes human hepatoma Hep G2 cells to TRAIL-induced apoptosis via ROS and CHOP-mediated DR5 upregulation [56]. Apigenin potentiates TRAIL therapy of non-small cell lung cancer via upregulation of DR4/DR5 expression in a p53-dependent manner [48]. These reports indicated that the drug-induced upregulation of death-receptor DR5 played a key role in the sensitization of TRAIL to cancer cells and demonstrated the great potential of DR5 in the development of antitumor drugs. Our results showed that SNX-2112 upregulated DR5 expression in HeLa cells in a concentration-dependent and time-dependent manner (Figures 4(d)-4(g)). Silencing of DR5 by DR5 siRNA significantly decreased cell apoptosis induced by SNX-2112 and TRAIL (Figures 4(j)-4(h)). This result was consistent with previous reports and indicated that death-receptor DR5 played a key role in TRAIL/SNX-2112-induced apoptosis. Our study showed for the first time that the upregulation of DR5 induced by SNX-2112 was the result of the activation of the ROS-p53-autophagy pathway. These results provide a novel strategy for

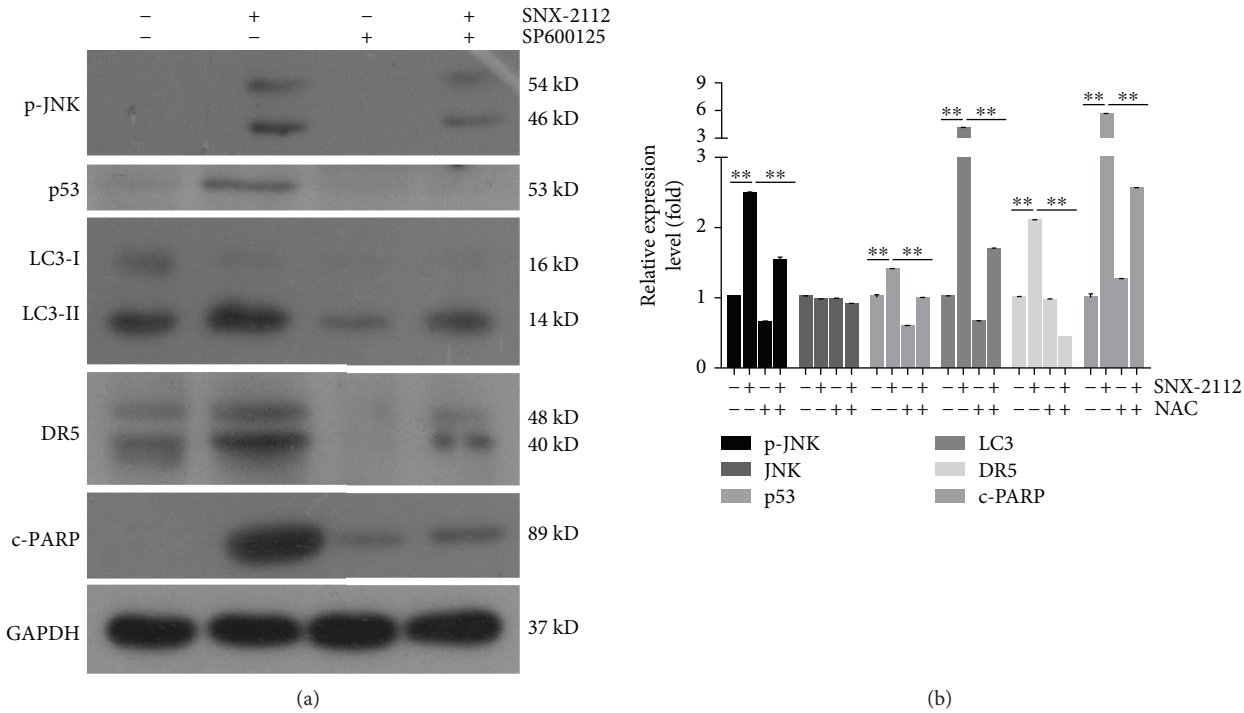

(a) (b)

Figure 8: SNX-2112-induced ROS activates the JNK-p53-autophagy pathway to induce DR5 expression. HeLa cells were pretreated with or without 20 mM NAC for 2 h and then treated with or without SNX-2112 for 48 h. (a, b) Western blotting were used to analyze whole-cell extracts and detect the levels of p-JNK, JNK, p53, LC3, DR5, and c-PARP. Densitometry analyses of the bands for each protein were performed. Data are represented as mean ± SD. Error bars represent SD from three separate experiments. $^{*}P<0.05$ and $^{**}P<0.01$ compared with the control group.

oncological treatment, which is the combination of TRAIL with SNX-2112.

Both apoptosis and autophagy are essential cellular pathways related to degradation. They are induced by similar stimuli and regulated by similar pathways. Their crosstalk affects anticancer drug sensitivity and cell death [65]. However, the underlying mechanism remains unclear. It has been previously reported that autophagy and apoptosis cooperated to affect the fate of cells [66, 67]. Our previous study indicated that SNX-2112 could promote tumor cell death by inducing apoptosis and autophagy in human melanoma A-375 cells [36]. It was this same SNX-2112 that was found to induce autophagy by affecting the Akt/mTOR signaling pathway in HeLa cells in this study (Figures 5(a)-5(j)). The autophagy inhibitor BFA was found to effectively inhibit SNX-2112-induced cleavage of PARP, indicating that autophagy synergistically promoted apoptosis in HeLa cells (Figures 5(k) and 5(l)).

It has also been previously reported that TRAIL resistance was regulated by autophagy in some cells. However, the molecular mechanism of autophagy-mediated TRAIL resistance was not yet known [68]. The Guidelines by Klionsky et al. 2016 reported that lysosomal degradation can be prevented by protease inhibitors bafilomycin A1 and chloroquine, which could block the fusion of autophagosomes and increase the level of LC3-II [69]. It was recently found that, in the selected TRAIL-resistant cells (HepG2-TR), the inhibition of autophagy partially restored TRAIL-induced apoptosis and cytotoxicity [70]. However, in a study with colorectal cancer cell lines, the inhibition of autophagy by 3MA was found to significantly decrease DR4 and DR5 upregulation and reduce apoptosis [64]. These results indicated that autophagy might affect TRAIL resistance by regulating the expression of DR5, and our own results are consistent with these findings. We found that autophagy was induced by low concentrations of SNX-2112, and the inhibition of autophagy by BFA or Atg7 siRNAs significantly decreased upregulation of DR5 and the synergistic effect of TRAIL and SNX-2112 (Figure 5). Our findings provide an insight into the mechanism of action between SNX-2112-induced autophagy and TRAIL-mediated apoptosis.

The role of autophagy in DR5 regulation has been previously explored in human breast cancer cells. The data showed that high basal levels of autophagosomes sequestered DR4 and DR5 and effected cellular localization of death receptors, thought to contribute to their deficiency on the cell surface [49]. Also, the researchers speculated that bafilomycin A1 hinders the fusion of autophagosomes after apoptotic proteins are enclosed in lysosomes, in which the proteins were degraded. Hence, we considered the possibility that many apoptotic proteins are already trapped in the autophagosomes without being degraded during SNX-2112/TRAIL-induced apoptosis, which could not be stimulated to induce apoptosis. Same as our results, when the HeLa cells incubated with bafilomycin A1, DR5, a cell membrane receptor, was downregulated as shown in Figure 5(k).

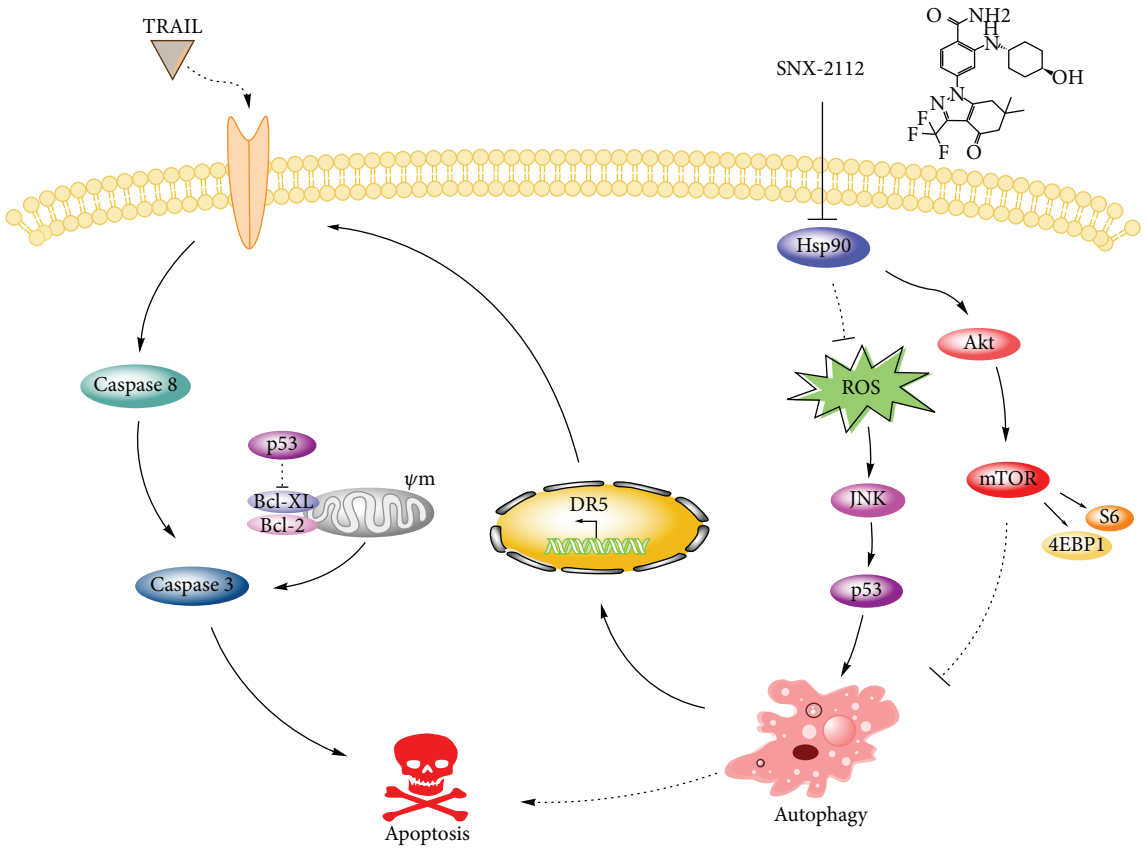

Figure 9: Illustration of the synergistic effect of SNX-2112 and TRAIL in HeLa cells.

From this, we hypothesized that drug-induced autophagy may play a different role than basal autophagy and that its function may be to act as an effective vector for death receptors or to protect and stabilize the structure of the death receptor. Further studies would be needed to determine the precise role of autophagy on death receptors.

As we all know, TRAIL has two receptors DR4 and DR5, and both can induce cell death in cancer cells. It has been reported that the two genes were transcriptional targets of p53 [71]. However, some cancer cells are not equally sensitive to TRAIL through the two receptors [72]. In accordance with these findings, our data showed that SNX-2112 could induce the expression of both DR4 and DR5, but only DR5 affects the apoptosis induced by a combination of TRAIL with SNX-2112 (Figure 4).

TRAIL receptors are differentially regulated. TRAIL differentially binds to TRAIL-R as illustrated by the phosphorothioate-modified CpG nucleotides, which block the binding of TRAIL to DR5 but not to DR4 [73]. TRAIL mutants with selective binding to DR4 or DR5 also showed that binding of TRAIL to DR4 and DR5 involved different amino acids [74].

SNX-2112 has been previously found to significantly decrease the expression of p53 and inhibit the proliferation of esophageal cancer cells [39]. As a target gene of p53, the gene transcription of DR5 is directly regulated by p53. Triptolide increased the level of DR5 in OCI-AML3, whereas increased DR5 was found to decrease in p53-knockdown OCI-AML3 and p53-mutated U937 cells, confirming the role of p53 in regulating DR5 expression [53]. The same phenomena were observed in myeloma cells [72], human hepatocellular carcinoma cells [75], prostate cancer cells [76], and human renal carcinoma cells [54]. Our results confirmed that SNX-2112-induced p53 could upregulate DR5 expression in cervical cancer HeLa cells. Interestingly, our results were the first to find that SNX-2112-induced p53 also conduced to the autophagy, contributing to a synergistic effect between SNX-2112 and TRAIL (Figure 6). This is a novel idea to explain the mechanism of action between p53 and DR5. Above all, our results suggest that the combination of TRAIL and SNX-2112 is more effective in cervical cancer cells with wild-type p53.

The detection of the MAPK signaling pathway proved that SNX-2112 activated TRAIL-induced apoptosis by activating JNK signaling in HeLa cells (Figure 7). The generation of drug-induced ROS has previously been found to activate JNK signaling in cancer cells, subsequently perturb the function of mitochondria, and result in mitochondria-related apoptosis in HeLa and other cancer cells [77–81]. Consistently, our results confirmed that SNX-2112-induced ROS upregulated p-JNK, following activation of the p53-autophagy-DR5 pathway.

One of the hallmarks of cancer is the deregulation of cellular energetics, causing a production of higher levels of ROS concomitant with alterations in antioxidant pathways [22]. Suffering from oxidative stress in the long term has made

cancer cells acquire the adaptivity allowing them to survive in hypoxia and to become drug-resistant [82], so that, for different treatment strategies aiming at enhancing ROS production in cancer cells, it indicated a grand prospect leading to the selective killing of these cells when compared to normal cells [22]. There is much evidence that drug-induced ROS acting as an upstream signal can induce the upregulation of DR5 [77, 78]. Our results showed that ROS generation contributed to SNX-2112-induced upregulation of JNK-p53-autophagy-mediated DR5 (Figure 8), consistent with the induction of ROS production by other Hsp90 inhibitors [83]. The accumulation of ROS in HeLa cells is a striking feature of SNX-2112-induced apoptosis. Moreover, excessive ROS accumulation might play crucial roles in inducing both cell apoptosis and autophagy [57, 84]. Besides destabilizing Hsp90 client oncoproteins, SNX-2112 exerts cytotoxicity by generating ROS. There may be two explanations for this mechanism. Firstly, it has been reported that some Hsp90 inhibitors could induce mitochondrial ROS production by elevating endoplasmic reticulum (ER) stress originating from the accumulation of unfolded protein in the ER [21]. As a consequence of increased ER stress, mitochondrial homeostasis was disrupted and, thereby, the production of mitochondrial ROS was increased [21, 23]. Meanwhile, we have previously proven that SNX-2112 could elevate the role of ER stress to induce apoptosis [41]. Hsp90, a chaperone protein, regulates a variety of cellular processes by assisting in the folding of client proteins. Secondly, the α,β-unsaturated ketone moiety of SNX-2112 may interact with some oxidoreductases, such as thioredoxin reductase, and consequently cause the accumulation of ROS in cells [85–87].

In summary, our study is the first to demonstrate that SNX-2112 enhances TRAIL-induced apoptosis in HeLa cells through the ROS-mediated activation of JNK-p53-autophagy-DR5 (Figure 9). Our work contributes to further understanding the antitumor mechanism of SNX-2112. Most importantly, our results detailed the mechanisms of SNX-2112 in combination with TRAIL in cervical cancer cells, providing a reliable theoretical basis for the combination of TRAIL with Hsp90 inhibitor as a novel strategy for the treatment of human cervical cancer.

Abbreviations

TRAIL:	Tumor necrosis factor-related apoptosis-inducing ligand
Hsp90:	Heat shock protein 90
DISC:	The death-inducing signal complex
VEGFR2:	Vascular endothelial growth factor receptor 2
ROS:	Reactive oxygen species
Z-VAD-fmk:	The cell-permeable pan caspase inhibitor
NAC:	N-Acetyl-L-cysteine
BFA:	Bafilomycin A1.

Data Availability

The data used to support the findings of this study are available from the corresponding author upon request.

Conflicts of Interest

The authors declare that they have no conflict of interest.

Authors' Contributions

Liubing Hu and Yan Wang carried out most of the experiments; Liubing Hu, Yan Wang, and Zhong Liu wrote the manuscript; Liubing Hu, Zhong Liu, and Manmei Li analyzed the data and results. Zhong Liu, Yifei Wang, and Manmei Li designed this study and revised the entire manuscript. Manmei Li, Zui Chen, Liangshun Fu, and Sheng Wang participated in some of the experiments and revised the paper. Pengchao Zhang, Xinyue Zhang, Xueping Lu, and Huiyang Jie participated in the study design and some of the experiments. Zui Chen was added as one of the co-authors after acceptance of the manuscript since he performed some of the experiments while revising the manuscript according to the reviewers' comments. All authors have read and approved the final manuscript.

Acknowledgments

This work was supported by the National Natural Science Foundation of China (81673670), Guangdong Natural Science Foundation (2017A030306008, 2017A030313732, and 2015A030313724), Guangdong Special Support Plan for High-level Talents (2016TQ03R849), the Science and Technology Program of Guangzhou (201610010108, 201707010399), and Jinan Double Hundred Talents Plan.

Supplementary Materials

Supplemental Figure 1: the effect of SNX-2112 on the expression level of p62. HeLa cells were treated with SNX-2112 for the indicated (a-b) time (12, 24, and 48 h) or (c-d) concentration (0, 14, 42, and 125 nM). Western blotting was performed to detect the levels of p62. Densitometry analyses of the bands for each protein were performed. Data are represented as mean ± SD. Error bars represent SD from three separate experiments. *(Supplementary Materials)*

References

[1] Z. Chen, V. Sangwan, S. Banerjee et al., "Triptolide sensitizes pancreatic cancer cells to TRAIL-induced activation of the death receptor pathway," *Cancer Letters*, vol. 348, no. 1-2, pp. 156–166, 2014.

[2] K. Azijli, B. Weyhenmeyer, G. J. Peters, S. de Jong, and F. A. E. Kruyt, "Non-canonical kinase signaling by the death ligand TRAIL in cancer cells: discord in the death receptor family," *Cell Death and Differentiation*, vol. 20, no. 7, pp. 858–868, 2013.

[3] L. Y. Dimberg, C. K. Anderson, R. Camidge, K. Behbakht, A. Thorburn, and H. L. Ford, "On the TRAIL to successful cancer therapy? Predicting and counteracting resistance against TRAIL-based therapeutics," *Oncogene*, vol. 32, no. 11, pp. 1341–1350, 2013.

[4] J. G. Clohessy, J. Zhuang, J. de Boer, G. Gil-Gómez, and H. J. M. Brady, "Mcl-1 interacts with truncated Bid and inhibits its induction of cytochrome c release and its role in

receptor-mediated apoptosis," *Journal of Biological Chemistry*, vol. 281, no. 9, pp. 5750–5759, 2006.

[5] M. Chawla-Sarkar, S. I. Bae, F. J. Reu, B. S. Jacobs, D. J. Lindner, and E. C. Borden, "Downregulation of Bcl-2, FLIP or IAPs (XIAP and survivin) by siRNAs sensitizes resistant melanoma cells to Apo2L/TRAIL-induced apoptosis," *Cell Death and Differentiation*, vol. 11, no. 8, pp. 915–923, 2004.

[6] A. V. Franco, X. D. Zhang, E. van Berkel et al., "The role of NF-κB in TNF-related apoptosis-inducing ligand (TRAIL)-induced apoptosis of melanoma cells," *Journal of Immunology*, vol. 166, no. 9, pp. 5337–5345, 2001.

[7] D. Mahalingam, E. Szegezdi, M. Keane, S. . Jong, and A. Samali, "TRAIL receptor signalling and modulation: are we on the right TRAIL?," *Cancer Treatment Reviews*, vol. 35, no. 3, pp. 280–288, 2009.

[8] J. J. Song, J. Y. An, Y. T. Kwon, and Y. J. Lee, "Evidence for two modes of development of acquired tumor necrosis factor-related apoptosis-inducing ligand resistance. Involvement of Bcl-xL," *Journal of Biological Chemistry*, vol. 282, no. 1, pp. 319–328, 2007.

[9] L. H. A. M. de Wilt, J. Kroon, G. Jansen, S. de Jong, G. J. Peters, and F. A. E. Kruyt, "Bortezomib and TRAIL: a perfect match for apoptotic elimination of tumour cells?," *Critical Reviews in Oncology/Hematology*, vol. 85, no. 3, pp. 363–372, 2013.

[10] J. Lemke, S. von Karstedt, J. Zinngrebe, and H. Walczak, "Getting TRAIL back on track for cancer therapy," *Cell Death and Differentiation*, vol. 21, no. 9, pp. 1350–1364, 2014.

[11] L. Neckers and P. Workman, "Hsp90 molecular chaperone inhibitors: are we there yet?," *Clinical Cancer Research*, vol. 18, no. 1, pp. 64–76, 2012.

[12] Y. Miyata, H. Nakamoto, and L. Neckers, "The therapeutic target Hsp90 and cancer hallmarks," *Current Pharmaceutical Design*, vol. 19, no. 3, pp. 347–365, 2013.

[13] O. M. Grbovic, A. D. Basso, A. Sawai et al., "V600E B-Raf requires the Hsp90 chaperone for stability and is degraded in response to Hsp90 inhibitors," *Proceedings of the National Academy of Sciences of the United States of America*, vol. 103, no. 1, pp. 57–62, 2006.

[14] M. D. Siegelin, "Inhibition of the mitochondrial Hsp90 chaperone network: a novel, efficient treatment strategy for cancer?," *Cancer Letters*, vol. 333, no. 2, pp. 133–146, 2013.

[15] A. Kamal, L. Thao, J. Sensintaffar et al., "A high-affinity conformation of Hsp90 confers tumour selectivity on Hsp90 inhibitors," *Nature*, vol. 425, no. 6956, pp. 407–410, 2003.

[16] M. J. van de Vijver, Y. D. He, L. J. van 't Veer et al., "A gene-expression signature as a predictor of survival in breast cancer," *The New England Journal of Medicine*, vol. 347, no. 25, pp. 1999–2009, 2002.

[17] L. J. Van't Veer, H. Dai, M. J. Van De Vijver et al., "Gene expression profiling predicts clinical outcome of breast cancer," *Nature*, vol. 415, no. 6871, pp. 530–536, 2002.

[18] S. Modi, A. Stopeck, H. Linden et al., "HSP90 inhibition is effective in breast cancer: a phase II trial of tanespimycin (17-AAG) plus trastuzumab in patients with HER2-positive metastatic breast cancer progressing on trastuzumab," *Clinical Cancer Research*, vol. 17, no. 15, pp. 5132–5139, 2011.

[19] A. Taiyab and C. M. Rao, "HSP90 modulates actin dynamics: inhibition of HSP90 leads to decreased cell motility and impairs invasion," *Biochimica et Biophysica Acta (BBA) - Molecular Cell Research*, vol. 1813, no. 1, pp. 213–221, 2011.

[20] J. Travers, S. Sharp, and P. Workman, "HSP90 inhibition: two-pronged exploitation of cancer dependencies," *Drug Discovery Today*, vol. 17, no. 5-6, pp. 242–252, 2012.

[21] J. G. Kim, S. C. Lee, O. H. Kim et al., "HSP90 inhibitor 17-DMAG exerts anticancer effects against gastric cancer cells principally by altering oxidant-antioxidant balance," *Oncotarget*, vol. 8, no. 34, pp. 56473–56489, 2017.

[22] L. Postovit, C. Widmann, P. Huang, and S. B. Gibson, "Harnessing oxidative stress as an innovative target for cancer therapy," *Oxidative Medicine and Cellular Longevity*, vol. 2018, Article ID 6135739, 2 pages, 2018.

[23] A. Taiyab, A. S. Sreedhar, and C. M. Rao, "Hsp90 inhibitors, GA and 17AAG, lead to ER stress-induced apoptosis in rat histiocytoma," *Biochemical Pharmacology*, vol. 78, no. 2, pp. 142–152, 2009.

[24] K. Jhaveri, T. Taldone, S. Modi, and G. Chiosis, "Advances in the clinical development of heat shock protein 90 (Hsp90) inhibitors in cancers," *Biochimica et Biophysica Acta (BBA) - Molecular Cell Research*, vol. 1823, no. 3, pp. 742–755, 2012.

[25] E. M. Gartner, P. Silverman, M. Simon et al., "A phase II study of 17-allylamino-17-demethoxygeldanamycin in metastatic or locally advanced, unresectable breast cancer," *Breast Cancer Research and Treatment*, vol. 131, no. 3, pp. 933–937, 2012.

[26] C. Stolfi, F. Pallone, and G. Monteleone, "Molecular targets of TRAIL-sensitizing agents in colorectal cancer," *International Journal of Molecular Sciences*, vol. 13, no. 7, pp. 7886–7901, 2012.

[27] I. A. Vasilevskaya and P. J. O'Dwyer, "17-Allylamino-17-demethoxygeldanamycin overcomes TRAIL resistance in colon cancer cell lines," *Biochemical Pharmacology*, vol. 70, no. 4, pp. 580–589, 2005.

[28] M. D. Siegelin, A. Habel, and T. Gaiser, "17-AAG sensitized malignant glioma cells to death-receptor mediated apoptosis," *Neurobiology of Disease*, vol. 33, no. 2, pp. 243–249, 2009.

[29] C. R. Williams, R. Tabios, W. M. Linehan, and L. Neckers, "Intratumor injection of the Hsp90 inhibitor 17AAG decreases tumor growth and induces apoptosis in a prostate cancer xenograft model," *The Journal of Urology*, vol. 178, no. 4, pp. 1528–1532, 2007.

[30] S. Pacey, M. Gore, D. Chao et al., "A phase II trial of 17-allylamino, 17-demethoxygeldanamycin (17-AAG, tanespimycin) in patients with metastatic melanoma," *Investigational New Drugs*, vol. 30, no. 1, pp. 341–349, 2012.

[31] J. E. H. Day, S. Y. Sharp, M. G. Rowlands et al., "Inhibition of Hsp90 with resorcylic acid macrolactones: synthesis and binding studies," *Chemistry - A European Journal*, vol. 16, no. 34, pp. 10366–10372, 2010.

[32] G. V. Georgakis, Y. Li, G. Z. Rassidakis, H. Martinez-Valdez, L. J. Medeiros, and A. Younes, "Inhibition of heat shock protein 90 function by 17-allylamino-17-demethoxy-geldanamycin in Hodgkin's lymphoma cells down-regulates Akt kinase, dephosphorylates extracellular signal-regulated kinase, and induces cell cycle arrest and cell death," *Clinical Cancer Research*, vol. 12, no. 2, pp. 584–590, 2006.

[33] X. Wang, W. Ju, J. Renouard, J. Aden, S. A. Belinsky, and Y. Lin, "17-Allylamino-17-demethoxygeldanamycin synergistically potentiates tumor necrosis factor-induced lung cancer cell death by blocking the nuclear factor-κB pathway," *Cancer Research*, vol. 66, no. 2, pp. 1089–1095, 2006.

[34] S.-X. Wang, H.-Q. Ju, K.-S. Liu et al., "SNX-2112, a novel Hsp90 inhibitor, induces G2/M cell cycle arrest and apoptosis

in MCF-7 cells," *Bioscience, Biotechnology, and Biochemistry*, vol. 75, no. 8, pp. 1540–1545, 2014.

[35] Y. Okawa, T. Hideshima, P. Steed et al., "SNX-2112, a selective Hsp90 inhibitor, potently inhibits tumor cell growth, angiogenesis, and osteoclastogenesis in multiple myeloma and other hematologic tumors by abrogating signaling via Akt and ERK," *Blood*, vol. 113, no. 4, pp. 846–855, 2009.

[36] K. S. Liu, H. Liu, J. H. Qi et al., "SNX-2112, an Hsp90 inhibitor, induces apoptosis and autophagy via degradation of Hsp90 client proteins in human melanoma A-375 cells," *Cancer Letters*, vol. 318, no. 2, pp. 180–188, 2012.

[37] K. S. Liu, W. C. Ding, S. X. Wang et al., "The heat shock protein 90 inhibitor SNX-2112 inhibits B16 melanoma cell growth in vitro and in vivo," *Oncology Reports*, vol. 27, no. 6, pp. 1904–1910, 2012.

[38] R. Wang, F. Shao, Z. Liu et al., "The Hsp90 inhibitor SNX-2112, induces apoptosis in multidrug resistant K562/ADR cells through suppression of Akt/NF-κB and disruption of mitochondria-dependent pathways," *Chemico-Biological Interactions*, vol. 205, no. 1, pp. 1–10, 2013.

[39] C. Y. Li, Y. J. Ren, and Y. D. Li, "Effect of SNX-2112 on proliferation of esophageal cancer cells via regulation of excision repair cross-complementing 1, epidermal growth factor receptor, and p53 expression," *Genetics and Molecular Research*, vol. 15, no. 2, 2016.

[40] J. A. Friedman, S. C. Wise, M. Hu et al., "HSP90 inhibitor SNX5422/2112 targets the dysregulated signal and transcription factor network and malignant phenotype of head and neck squamous cell carcinoma," *Translational Oncology*, vol. 6, no. 4, pp. 429–IN5, 2013.

[41] X. Wang, S. Wang, Y. Liu et al., "The Hsp90 inhibitor SNX-2112 induces apoptosis of human hepatocellular carcinoma cells: the role of ER stress," *Biochemical and Biophysical Research Communications*, vol. 446, no. 1, pp. 160–166, 2014.

[42] J. H. Qin, K. Wang, X. L. Fu et al., "Hsp90 inhibitor induces KG-1a cell differentiation and apoptosis via Akt/NF-κB signaling," *Oncology Reports*, vol. 38, no. 3, pp. 1517–1524, 2017.

[43] T. C. Chou, "Drug combination studies and their synergy quantification using the Chou-Talalay method," *Cancer Research*, vol. 70, no. 2, pp. 440–446, 2010.

[44] T. C. Chou, "Theoretical basis, experimental design, and computerized simulation of synergism and antagonism in drug combination studies," *Pharmacological Reviews*, vol. 58, no. 3, pp. 621–681, 2006.

[45] T. Chou and N. Martin, *CompuSyn for Drug Combinations: PC Software and User's Guide: a Computer Program for Quantitation of Synergism and Antagonism in Drug Combinations, and the Determination of IC50 and ED50 and LD50 Values*, ComboSyn, Paramus, NJ, USA, 2005.

[46] Q. Liu, X. H. Xiao, L. B. Hu et al., "Anhuienoside C ameliorates collagen-induced arthritis through inhibition of MAPK and NF-κB signaling pathways," *Frontiers in Pharmacology*, vol. 8, p. 299, 2017.

[47] F. Y. Shao, Z. Y. du, D. L. Ma et al., "B5, a thioredoxin reductase inhibitor, induces apoptosis in human cervical cancer cells by suppressing the thioredoxin system, disrupting mitochondrion-dependent pathways and triggering autophagy," *Oncotarget*, vol. 6, no. 31, pp. 30939–30956, 2015.

[48] M. Chen, X. Wang, D. Zha et al., "Apigenin potentiates TRAIL therapy of non-small cell lung cancer via upregulating DR4/DR5 expression in a p53-dependent manner," *Scientific Reports*, vol. 6, no. 1, article 35468, 2016.

[49] X. Di, G. Zhang, Y. Zhang, K. Takeda, L. A. Rivera Rosado, and B. Zhang, "Accumulation of autophagosomes in breast cancer cells induces TRAIL resistance through downregulation of surface expression of death receptors 4 and 5," *Oncotarget*, vol. 4, no. 9, pp. 1349–1364, 2013.

[50] L. Zhao, S. Liu, J. Xu et al., "A new molecular mechanism underlying the EGCG-mediated autophagic modulation of AFP in HepG2 cells," *Cell Death & Disease*, vol. 8, no. 11, article e3160, 2017.

[51] J. Zhu, W. Yu, B. Liu et al., "Escin induces caspase-dependent apoptosis and autophagy through the ROS/p38 MAPK signalling pathway in human osteosarcoma cells in vitro and in vivo," *Cell Death & Disease*, vol. 8, no. 10, article e3113, 2017.

[52] M. J. Hsieh, T. L. Tsai, Y. S. Hsieh, C. J. Wang, and H. L. Chiou, "Dioscin-induced autophagy mitigates cell apoptosis through modulation of PI3K/Akt and ERK and JNK signaling pathways in human lung cancer cell lines," *Archives of Toxicology*, vol. 87, no. 11, pp. 1927–1937, 2013.

[53] B. Z. Carter, D. H. Mak, W. D. Schober et al., "Triptolide sensitizes AML cells to TRAIL-induced apoptosis via decrease of XIAP and p53-mediated increase of DR5," *Blood*, vol. 111, no. 7, pp. 3742–3750, 2008.

[54] K.-j. Min, J.-O. Nam, and T. Kwon, "Fisetin induces apoptosis through p53-mediated up-regulation of DR5 expression in human renal carcinoma Caki cells," *Molecules*, vol. 22, no. 8, 2017.

[55] M. T. Do, M. K. Na, H. G. Kim et al., "Ilimaquinone induces death receptor expression and sensitizes human colon cancer cells to TRAIL-induced apoptosis through activation of ROS-ERK/p38 MAPK-CHOP signaling pathways," *Food and Chemical Toxicology*, vol. 71, pp. 51–59, 2014.

[56] C. Y. Chen, S. J. Yiin, J. L. Hsu, W. C. Wang, S. C. Lin, and C. L. Chern, "Isoobtusilactone a sensitizes human hepatoma Hep G2 cells to TRAIL-induced apoptosis via ROS and CHOP-mediated up-regulation of DR5," *Journal of Agricultural and Food Chemistry*, vol. 60, no. 13, pp. 3533–3539, 2012.

[57] L.-U. Ling, K. B. Tan, H. Lin, and G. N. C. Chiu, "The role of reactive oxygen species and autophagy in safingol-induced cell death," *Cell Death & Disease*, vol. 2, no. 3, article e129, 2011.

[58] K. J. Min, J. H. Jang, J. T. Lee, K. S. Choi, and T. K. Kwon, "Glucocorticoid receptor antagonist sensitizes TRAIL-induced apoptosis in renal carcinoma cells through up-regulation of DR5 and down-regulation of c-FLIP(L) and Bcl-2," *Journal of Molecular Medicine*, vol. 90, no. 3, pp. 309–319, 2012.

[59] X. Guo, Y. Meng, X. Sheng et al., "Tunicamycin enhances human colon cancer cells to TRAIL-induced apoptosis by JNK-CHOP-mediated DR5 upregulation and the inhibition of the EGFR pathway," *Anti-Cancer Drugs*, vol. 28, no. 1, pp. 66–74, 2017.

[60] H. Zhang and F. Burrows, "Targeting multiple signal transduction pathways through inhibition of Hsp90," *Journal of Molecular Medicine*, vol. 82, no. 8, pp. 488–499, 2004.

[61] Y. Niikura, S. Ohta, K. J. Vandenbeldt, R. Abdulle, B. F. McEwen, and K. Kitagawa, "17-AAG, an Hsp90 inhibitor, causes kinetochore defects: a novel mechanism by which 17-AAG inhibits cell proliferation," *Oncogene*, vol. 25, no. 30, pp. 4133–4146, 2006.

[62] Q. Wang, W. Sun, X. Hao, T. Li, L. Su, and X. Liu, "Down-regulation of cellular FLICE-inhibitory protein (Long Form) contributes to apoptosis induced by Hsp90 inhibition in human lung cancer cells," *Cancer Cell International*, vol. 12, no. 1, p. 54, 2012.

[63] A. Panner, J. C. Murray, M. S. Berger, and R. O. Pieper, "Heat shock protein 90alpha recruits FLIPS to the death-inducing signaling complex and contributes to TRAIL resistance in human glioma," *Cancer Research*, vol. 67, no. 19, pp. 9482–9489, 2007.

[64] L. Chen, Y. Meng, X. Guo et al., "Gefitinib enhances human colon cancer cells to TRAIL-induced apoptosis of via autophagy- and JNK-mediated death receptors upregulation," *Apoptosis*, vol. 21, no. 11, pp. 1291–1301, 2016.

[65] M. Yang, L. Liu, M. Xie et al., "Poly-ADP-ribosylation of HMGB1 regulates TNFSF10/TRAIL resistance through autophagy," *Autophagy*, vol. 11, no. 2, pp. 214–224, 2015.

[66] S. Mukhopadhyay, P. K. Panda, N. Sinha, D. N. Das, and S. K. Bhutia, "Autophagy and apoptosis: where do they meet?," *Apoptosis*, vol. 19, no. 4, pp. 555–566, 2014.

[67] Y. Liu, B. Yang, L. Zhang et al., "Ginkgolic acid induces interplay between apoptosis and autophagy regulated by ROS generation in colon cancer," *Biochemical and Biophysical Research Communications*, vol. 498, no. 1, pp. 246–253, 2018.

[68] B. Z. Yuan, J. Chapman, M. Ding et al., "TRAIL and proteasome inhibitors combination induces a robust apoptosis in human malignant pleural mesothelioma cells through Mcl-1 and Akt protein cleavages," *BMC Cancer*, vol. 13, no. 1, p. 140, 2013.

[69] D. J. Klionsky, K. Abdelmohsen, A. Abe et al., "Guidelines for the use and interpretation of assays for monitoring autophagy (3rd edition)," *Autophagy*, vol. 12, no. 1, pp. 1–222, 2016.

[70] S. C. Lim, H. J. Jeon, K. H. Kee, M. J. Lee, R. Hong, and S. I. Han, "Involvement of DR4/JNK pathway-mediated autophagy in acquired TRAIL resistance in HepG2 cells," *International Journal of Oncology*, vol. 49, no. 5, pp. 1983–1990, 2016.

[71] X. Liu, P. Yue, F. R. Khuri, and S. Y. Sun, "p53 upregulates death receptor 4 expression through an intronic p53 binding site," *Cancer Research*, vol. 64, no. 15, pp. 5078–5083, 2004.

[72] S. Surget, D. Chiron, P. Gomez-Bougie et al., "Cell death via DR5, but not DR4, is regulated by p53 in myeloma cells," *Cancer Research*, vol. 72, no. 17, pp. 4562–4573, 2012.

[73] D. Chiron, C. Pellat-Deceunynck, M. Maillasson, R. Bataille, and G. Jego, "Phosphorothioate-modified TLR9 ligands protect cancer cells against TRAIL-induced apoptosis," *Journal of Immunology*, vol. 183, no. 7, pp. 4371–4377, 2009.

[74] A. M. van der Sloot, V. Tur, E. Szegezdi et al., "Designed tumor necrosis factor-related apoptosis-inducing ligand variants initiating apoptosis exclusively via the DR5 receptor," *Proceedings of the National Academy of Sciences of the United States of America*, vol. 103, no. 23, pp. 8634–8639, 2006.

[75] C. Wang, R. Qi, N. Li et al., "Notch1 signaling sensitizes tumor necrosis factor-related apoptosis-inducing ligand-induced apoptosis in human hepatocellular carcinoma cells by inhibiting Akt/Hdm2-mediated p53 degradation and up-regulating p53-dependent DR5 expression," *Journal of Biological Chemistry*, vol. 284, no. 24, pp. 16183–16190, 2009.

[76] H. Xiaowen and S. Yi, "Triptolide sensitizes TRAIL-induced apoptosis in prostate cancer cells via p53-mediated DR5 up-regulation," *Molecular Biology Reports*, vol. 39, no. 9, pp. 8763–8770, 2012.

[77] R. Trivedi, R. Maurya, and D. P. Mishra, "Medicarpin, a legume phytoalexin sensitizes myeloid leukemia cells to TRAIL-induced apoptosis through the induction of DR5 and activation of the ROS-JNK-CHOP pathway," *Cell Death & Disease*, vol. 5, no. 10, article e1465, 2014.

[78] C. C. Chang, C. P. Kuan, J. Y. Lin, J. S. Lai, and T. F. Ho, "Tanshinone IIA facilitates TRAIL sensitization by up-regulating DR5 through the ROS-JNK-CHOP signaling axis in human ovarian carcinoma cell lines," *Chemical Research in Toxicology*, vol. 28, no. 8, pp. 1574–1583, 2015.

[79] T. Sophonnithiprasert, W. Mahabusarakam, Y. Nakamura, and R. Watanapokasin, "Goniothalamin induces mitochondria-mediated apoptosis associated with endoplasmic reticulum stress-induced activation of JNK in HeLa cells," *Oncology Letters*, vol. 13, no. 1, pp. 119–128, 2017.

[80] C. C. Su, K. I. Lee, M. K. Chen, C. Y. Kuo, C. H. Tang, and S. H. Liu, "Cantharidin induced oral squamous cell carcinoma cell apoptosis via the JNK-regulated mitochondria and endoplasmic reticulum stress-related signaling pathways," *PLoS One*, vol. 11, no. 12, article e0168095, 2016.

[81] K. I. Lee, C. C. Su, C. Y. Yang et al., "Etoposide induces pancreatic β-cells cytotoxicity via the JNK/ERK/GSK-3 signaling-mediated mitochondria-dependent apoptosis pathway," *Toxicology in Vitro*, vol. 36, pp. 142–152, 2016.

[82] H. Xie and M. C. Simon, "Oxygen availability and metabolic reprogramming in cancer," *Journal of Biological Chemistry*, vol. 292, no. 41, pp. 16825–16832, 2017.

[83] M. H. Chen, K. C. Chiang, C. T. Cheng et al., "Antitumor activity of the combination of an HSP90 inhibitor and a PI3K/mTOR dual inhibitor against cholangiocarcinoma," *Oncotarget*, vol. 5, no. 9, pp. 2372–2389, 2014.

[84] C. Zhang, L. Yang, X. B. Wang et al., "Calyxin Y induces hydrogen peroxide-dependent autophagy and apoptosis via JNK activation in human non-small cell lung cancer NCI-H460 cells," *Cancer Letters*, vol. 340, no. 1, pp. 51–62, 2013.

[85] S. Carlson, L. Marler, S. J. Nam, B. Santarsiero, J. Pezzuto, and B. Murphy, "Potential chemopreventive activity of a new macrolide antibiotic from a marine-derived Micromonospora sp," *Marine Drugs*, vol. 11, no. 12, pp. 1152–1161, 2013.

[86] D. Duan, J. Zhang, J. Yao, Y. Liu, and J. Fang, "Targeting thioredoxin reductase by parthenolide contributes to inducing apoptosis of HeLa cells," *Journal of Biological Chemistry*, vol. 291, no. 19, pp. 10021–10031, 2016.

[87] E. Davioud-Charvet, M. J. McLeish, D. M. Veine et al., "Mechanism-based inactivation of thioredoxin reductase from Plasmodium falciparum by Mannich bases. Implication for cytotoxicity," *Biochemistry*, vol. 42, no. 45, pp. 13319–13330, 2003.

Hindawi
Oxidative Medicine and Cellular Longevity
Volume 2019, Article ID 7187128, 12 pages
https://doi.org/10.1155/2019/7187128

Research Article

Melatonin Enhances Cisplatin and Radiation Cytotoxicity in Head and Neck Squamous Cell Carcinoma by Stimulating Mitochondrial ROS Generation, Apoptosis, and Autophagy

Beatriz I. Fernandez-Gil,[1] Ana Guerra-Librero,[1] Ying-Qiang Shen,[1] Javier Florido,[1] Laura Martínez-Ruiz,[1] Sergio García-López,[1] Christian Adan,[1] César Rodríguez-Santana,[1] Darío Acuña-Castroviejo,[1,2,3] Alfredo Quiñones-Hinojosa,[4] José Fernández-Martínez,[1] Ahmed E. Abdel Moneim,[5] Luis C. López,[1,2,3] José M. Rodríguez Ferrer,[2] and Germaine Escames[1,2,3]

[1]*Instituto de Biotecnología, Centro de Investigación Biomédica, Universidad de Granada, Granada, Spain*
[2]*Departamento de Fisiología, Facultad de Medicina, Universidad de Granada, Granada, Spain*
[3]*CIBERFES, Ibs.Granada, Hospital Campus de la Salud, 18016 Granada, Spain*
[4]*Department of Neurosurgery, Mayo Clinic, School of Medicine, Jacksonville, Florida, USA*
[5]*Department of Zoology and Entomology, Faculty of Science, Helwan University, Cairo, Egypt*

Correspondence should be addressed to Germaine Escames; gescames@ugr.es

Received 29 October 2018; Revised 18 December 2018; Accepted 31 December 2018; Published 28 February 2019

Guest Editor: Marco Cordani

Head and neck cancer is the sixth leading cancer by incidence worldwide. Unfortunately, drug resistance and relapse are the principal limitations of clinical oncology for many patients, and the failure of conventional treatments is an extremely demoralizing experience. It is therefore crucial to find new therapeutic targets and drugs to enhance the cytotoxic effects of conventional treatments without potentiating or offsetting the adverse effects. Melatonin has oncostatic effects, although the mechanisms involved and doses required remain unclear. The purpose of this study is to determine the precise underlying mitochondrial mechanisms of melatonin, which increase the cytotoxicity of oncological treatments, and also to propose new melatonin treatments in order to alleviate and reverse radio- and chemoresistant processes. We analyzed the effects of melatonin on head and neck squamous cell carcinoma (HNSCC) cell lines (Cal-27 and SCC-9), which were treated with 0.1, 0.5, 1, and 1.5 mM melatonin combined with 8 Gy irradiation or 10 μM cisplatin. Clonogenic and MTT assays, as well as autophagy and apoptosis, involving flow cytometry and western blot, were performed in order to determine the cytotoxic effects of the treatments. Mitochondrial function was evaluated by measuring mitochondrial respiration, mtDNA content (RT-PCR), and mitochondrial mass (NAO). ROS production, antioxidant enzyme activity, and GSH/GSSG levels were analyzed using a fluorometric method. We show that high concentrations of melatonin potentiate the cytotoxic effects of radiotherapy and CDDP in HNSCC, which are associated with increased mitochondrial function in these cells. In HNSCC, melatonin induces intracellular ROS, whose accumulation plays an upstream role in mitochondria-mediated apoptosis and autophagy. Our findings indicate that melatonin, at high concentrations, combined with cisplatin and radiotherapy to improve its effectiveness, is a potential adjuvant agent.

1. Introduction

Head and neck cancer, which is the sixth leading cancer by incidence worldwide, with more than 300,000 mortalities annually [1], has become a major health burden, especially as cell resistance to radio and chemotherapy develops.

Radiotherapy (RT), which is one of the most commonly used tumor treatments [2], damages biomolecules, such as

proteins and lipoids, particularly DNA, resulting in the termination of cell division and proliferation and even in cell necrosis or apoptosis. However, many unwanted effects, such as radioresistance, can complicate the prognosis [2]. One way to overcome these problems is to increase RT effectiveness by using radiosensitizers to enhance tumor cell radiosensitivity [3].

On the other hand, cisplatin (CDDP), one of the most commonly used chemotherapeutic agents, is the treatment of choice for most head and neck squamous cell carcinoma (HNSCC) patients. CDDP is a highly reactive molecule that binds to RNA, DNA, and proteins to form different types of adducts. CDDP also induces mitochondria-dependent reactive oxygen species (ROS) formation which contributes to cell-killing processes by enhancing the damaging effect of drugs on nuclear DNA (nDNA) [4]. However, the high incidence of chemoresistance and its many side effects limit the clinical usefulness of CDDP as an anticancer treatment [5, 6]. Therefore, new anticancer therapeutic strategies to attenuate cytotoxicity in normal tissues and to prevent or reverse the development of radio and chemoresistance are required.

Mitochondria have a major impact on cancer cells due to the source of ATP, their capacity to produce ROS, and their central position in the apoptosis signaling pathway [7, 8]. Although very low supraphysiological levels of mitochondrial ROS can promote tumor diversification by favoring mutagenesis [9], ROS overproduction, leading to severe mitochondrial dysfunction, is generally incompatible with tumor progression, which promotes cell death and cellular senescence [10]. Thus, given the impact of mitochondrial metabolism on the treatment response, a considerable effort has been devoted to developing a chemo/radiosensitization strategy involving the development of molecules to target mitochondria [9, 11]. However, one of the main drawbacks of this strategy of targeting mitochondria to kill malignant cells or to increase their sensitivity to treatment is that multiple immune effector cells bear a remarkable metabolic similarity to cancer cells [9, 12].

Although the indoleamine melatonin (N-acetyl-5-methoxytryptamine) is synthetized in the pineal gland, it is produced by many other organs at even higher concentrations [13]. Melatonin has a variety of biological features including anti-inflammatory and antioxidant activity, as well as immune system regulation mechanisms. It also has oncostatic effects, although the mechanisms involved remain unclear [14–17]. Our previous studies show that melatonin enhances the cytotoxic effects of rapamycin in HNSCC cells [18]. However, little data exist on the mechanisms of melatonin involved in increasing chemo- and radiotherapy-induced cancer cell injury or cell death and in simultaneously decreasing its adverse effects.

In this study, we first explore the potential capacity of melatonin to enhance the antitumor effects of irradiation and CDDP on HNSCC. We then investigate the precise underlying mitochondrial mechanisms which enhance the cytotoxic effects of these treatments on HNSCC.

2. Materials and Methods

2.1. Cell Culture. Human tongue squamous carcinoma cell lines Cal-27 and SCC-9, obtained from the American Type Culture Collection (ATCC® CRL2095™ and CRL1629™, respectively) in the Cell Bank of the Centre for Scientific Instrumentation at the University of Granada, were cultured in a humidified atmosphere (5% CO_2 and 95% air at 37°C). The cells were cultured in high-glucose Dulbecco's modified Eagle's medium (DMEM), GlutaMAX supplemented with 10% fetal bovine serum, and 2% antibiotic-antimycotic (Fisher Scientific, Madrid, Spain) for Cal-27 and were grown in DMEM-F12 Nutrient Mixture Ham medium (1 : 1) containing 2 mM L-glutamine (Fisher Scientific, Madrid, Spain) and 0.5 mM sodium pyruvate supplemented with 10% FBS, 0.4 μg/mL hydrocortisone (Sigma-Aldrich, Madrid, Spain), and 2% antibiotic-antimycotic for SCC-9.

Melatonin stock solution (Fagron Ibérica S.A.U., Terrasa, Spain) was prepared in 15% propylene glycol (PG) (VWR, Radnor, PA, USA). Cells were grown to 60%-70% confluence and serum starved for 24 hours. Then, cells were treated with and without melatonin (100, 500, 1000, and 1500 μM). After 48 hours, cells were exposed to 8 Gy irradiation using a cesium-137 gamma radiation source (8 Gy/min) or treated with 10 μM CDDP for 5 hours (Sigma-Aldrich, Madrid, Spain). Cells of the control group were treated with a vehicle (PG 15%). Assays were performed 48 hours after irradiation and CDDP treatment.

2.2. Colony Formation Assay. Cells were plated into 6-well plates and allowed to attach overnight. They were treated with melatonin and, after 48 hours, were irradiated or treated with CDDP. Colonies were allowed to grow for 2 weeks to form colonies of at least 50 cells. Finally, the medium was removed, the cells were fixed, and the colonies were then stained with 2.3% crystal violet and counted [18].

2.3. Cell Proliferation Assay. Cell viability was determined using an MTT assay (Life Technologies, Madrid, Spain) based on the reduction of yellow 3-(4,5-dimethylthiazol-2-yl)-2,5-diphenyltetrazolium bromide to purple formazan by mitochondrial dehydrogenases. Cells were plated into 96-well plates, and the assay was performed according to the manufacturer's instruction.

2.4. Apoptosis. Apoptosis was measured by flow cytometry using FITC Annexin V staining (Immunostep, Salamanca, Spain). Cells were treated as described above. Finally, cells were collected, washed with cold PBS, and then simultaneously stained with FITC-labeled annexin V and PI and analyzed by flow cytometry in a Becton Dickinson FACSCanto II cytometer (Madrid, Spain).

2.5. Western Blot Analysis. Protein extraction and western blot analyses were performed as described previously [19]. Bax (sc-526), Bcl-2 (sc-492), ATG12 C6 (sc-271688), and GAPDH (sc-32233) antibodies and a mouse anti-goat IgG-HRP secondary antibody (sc-2354) were purchased from Santa Cruz Biotechnology (Santa Cruz, CA, USA), NIX from Sigma-Aldrich (Madrid, Spain), and HRP goat anti-mouse IgG from BD Pharmingen™ (San Jose, CA, USA). The proteins were visualized using a Western Lightning Plus-ECL chemiluminescence kit (PerkinElmer, Billerica, MA, USA) according to the manufacturer's

protocol. Images were analyzed using the Kodak Image Station 2000R (Eastman Kodak Company, Rochester, NY, USA). Protein band intensity was normalized to GAPDH, and data were expressed in percentage terms relative to controls.

2.6. Mitochondrial Respiration. The oxygen consumption rate (OCR), an indicator of mitochondrial respiration under typical *in vitro* cell culture conditions [18], was determined using the Seahorse Extracellular Flux (XFe24) analyzer (Seahorse Bioscience, MA, USA). The day before the experiment, live treated cells (exclusion by trypan blue) were seeded in DMEM in 24-well culture plates at a density of $8 \cdot 10^4$ cells/well and were allowed to adhere overnight in a cell culture incubator in order to minimize division or death. Cell growth and health were monitored using a microscope following the manufacturer's instructions, and the assay was only performed if the cells under all conditions formed a consistent monolayer. Subsequently, the assays were initiated by replacing the media with assay medium (Seahorse Bioscience), and the cells were equilibrated for 1 h at 37°C without CO_2. The microplate was then placed into the XFe24 instrument to measure the OCR and free protons in the medium. Basal OCR was measured three times and plotted as a function of cells under the basal condition, followed by the sequential addition of oligomycin 1 mM. Subsequently, carbonyl cyanide 4-(trifluoromethoxy)phenylhydrazone (FCCP) 0.5 mM was added in two injections (1 mM in total). Finally, rotenone/antimycin A (1 mM) was injected. OCR was measured throughout the different injections of the test compounds. The progress curve was annotated to show the relative contribution of basal, ATP-linked, and maximal oxygen consumption after the addition of FCCP, and the reserve capacity of the cells. OCR values were normalized to cell number.

2.7. Determination of Mitochondrial Mass. We measured mitochondrial mass using acridine orange 10-nonyl bromide (NAO; Invitrogen Life Technologies, Madrid, Spain), which specifically binds to cardiolipin at the inner mitochondrial membrane, according to the protocol described by Shen et al. [18]. Fluorescence was read by an FLx800 microplate fluorescence reader (BioTek Instruments Inc., Winooski, VT, USA) at excitation 485 nm and emission 530 nm.

2.8. Mitochondrial DNA Quantification. Human mitochondrial DNA (mtDNA) was quantified by real-time PCR using the Stratagene Mx3005P Real-Time PCR System (Agilent Technologies Inc., CA, USA). We used primers and probes for the human 12S gene (mtDNA) and 18S. The mtDNA values were normalized to nDNA data (mtDNA/nDNA ratio).

2.9. Measurement of ROS Production. ROS production was measured using the 2′-7′-dichlorofluorescin diacetate (DCFH-DA) probe (Sigma-Aldrich, Madrid, Spain). Cells were seeded in 96-well culture plates. Then, the cells were incubated with 100 μM DCFH-DA in culture medium without phenol red for 30 min at 37°C and then rinsed with PBS and filled with Krebs-Ringer bicarbonate buffer. ROS levels were measured in a multiwell plate reader spectrofluorometer (BioTek Instruments Inc., Winooski, VT, USA) for 45 minutes each 5 minutes at 485 nm to excitation and 530 nm to emission [18].

2.10. Measurement of GSH and GSSG Levels and GPx Activity. To measure glutathione (GSH) and glutathione disulfide (GSSG), we used an established fluorometric method using a microplate fluorescence reader (PowerWaveX FLx800; BioTek Instruments Inc., Winooski, VT) [20]. We spectrophotometrically measured glutathione peroxidase (GPx) activity in a UV spectrophotometer (model UV-1603; Shimadzu Deutschland GmBH, Duisburg, Germany) [21].

2.11. Statistical Analysis. Statistical analyses were performed using GraphPad Prism 6 scientific software (GraphPad Software Inc., La Jolla, CA) and one-way analysis of variance (ANOVA) followed by Tukey's multiple comparison tests. Data were expressed as the mean ± SEM of a minimum of three independent experiments. A P value of $<.05$ was considered statistically significant.

3. Results

3.1. Melatonin Enhances the Cytotoxic Effects of Irradiation and CDDP in HNSCC. To evaluate the biological effect of melatonin on HNSCC sensitivity to irradiation and CDDP treatments, the clonogenic capacity and viability of both Cal-27 and SCC-9 were analyzed. As shown in Figures 1(a)–1(c), treatment with melatonin alone and in combination with irradiation significantly inhibited colony formation and resulted in a notable decrease in the colony ratio in a dose-dependent manner as compared to control or to irradiation alone. In fact, melatonin alone totally blocked colony growth. However, CDDP displayed a greater capacity than irradiation to decrease clonogenic formation (Figures 1(f)–1(h)).

MTT assays of both cell lines were also performed. In line with the inhibition of clonogenic capacity, melatonin markedly decreased cell viability in the irradiated cells in a dose-dependent manner, especially at doses 500 and 1500 μM, as compared to control and irradiation alone (Figures 1(d)–1(e)), although SCC-9 cells were found to be more resistant than Cal-27 cells to the treatments. Surprisingly, 100 μM melatonin did not significantly reduce viability, particularly in SCC-9 (Figures 1(d)–1(e)). On the other hand, melatonin significantly decreased cell viability in the CDDP-treated cells in a dose-dependent manner as compared to the control and CDDP alone (Figures 1(i)–1(j)). SCC-9 cells were also more resistant to melatonin exposure than Cal-27 cells. The results were more significant for Cal-27 cells, which were therefore used in subsequent experiments.

3.2. Melatonin Enhances the Apoptotic Effects of Irradiation and CDDP in HNSCC. Since the MTT assay is a quantitative measure of cell proliferation and a decrease in proliferating cells can be caused by either cell death or halted/slow proliferation, apoptotic cell death was therefore evaluated.

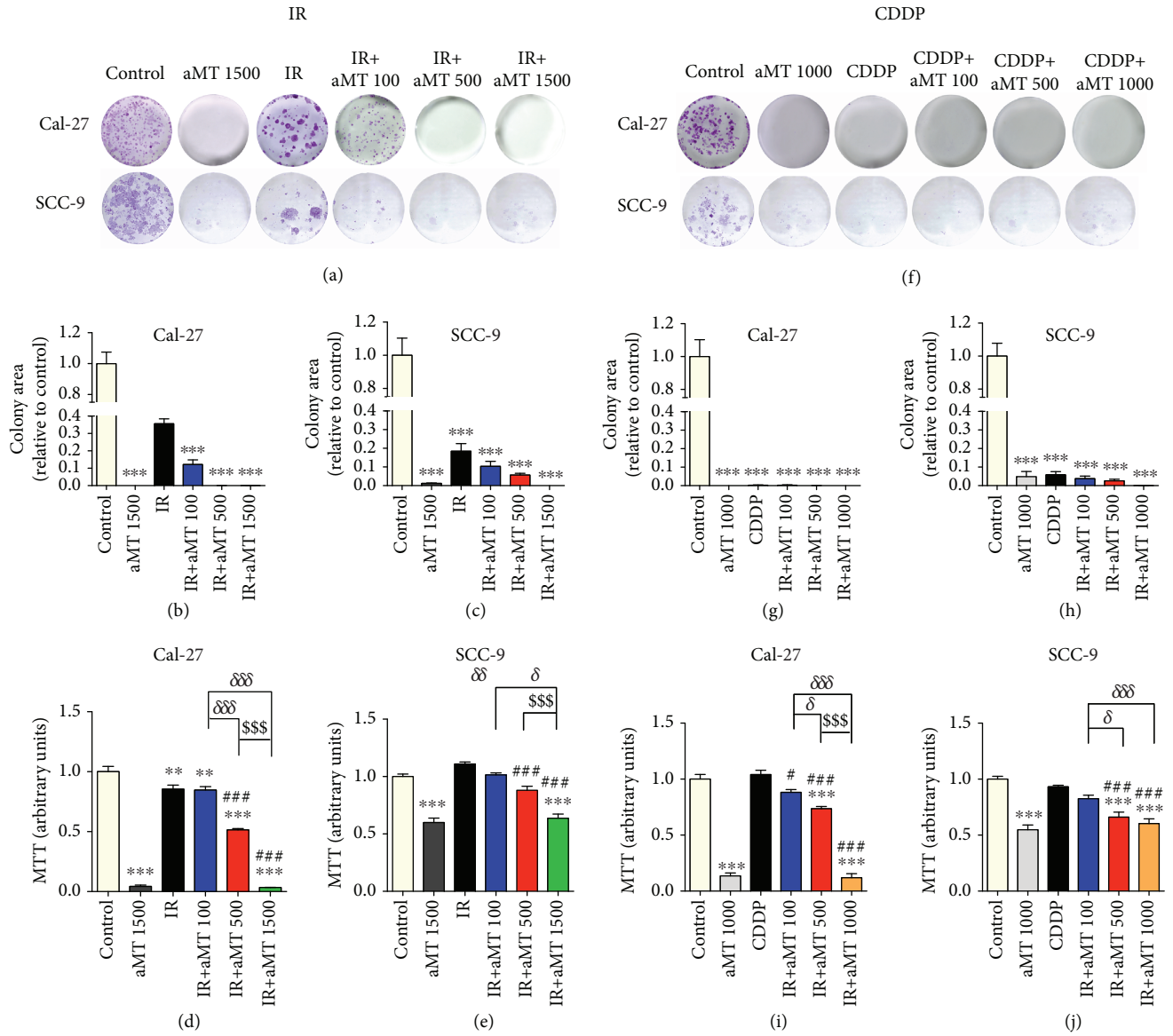

FIGURE 1: Melatonin increases the cytotoxic effects of irradiation (IR) and CDDP in HNSCC cell lines Cal-27 and SCC-9. Clonogenic assay of cells exposed to IR (a–c) or CDDP (f–h) and viability of cells exposed to IR (d, e) or CDDP (i, j). Treatment groups include the control (vehicle), IR (8 Gy), CDDP 10 μM, melatonin (aMT) 1000 or 1500 μM, and CDDP or IR plus aMT 100, 500, 1000, or 1500 μM. $n = 6$ per group. Data are presented as mean ± SEM. $^{**}P < .01$ and $^{***}P < .001$ vs. the control, $^{\#}P < .05$ and $^{\#\#\#}P < .001$ vs. the IR- or CDDP-treated group, $^{\delta}P < .05$ and $^{\delta\delta\delta}P < .001$ vs. IR+aMT 100, and $^{\$}P < .05$ and $^{\$\$\$}P < .001$ vs. IR+aMT 500.

Early apoptotic cells showed an annexin V-FITC+/PI- staining pattern, while late apoptotic cells exhibited an annexin V-FITC+/PI+ pattern (Figure 2) due to plasma membrane integrity loss [22]. In the combined melatonin/irradiation treatment, melatonin increased early apoptosis, which reached a maximum level at 1500 μM as compared to that of the control (Figures 2(a)–2(b)). However, irradiation alone enhanced late apoptosis but did not affect early apoptosis (Figures 2(a)–2(b)). This indicates that melatonin increases the acute cytotoxicity of irradiation. By contrast, treatment with CDDP alone did not increase apoptosis pathway activation (Figures 2(g)–2(h)), while the combined treatment increased late apoptosis at a melatonin dose of 500 μM (Figure 2(h)).

Apoptosis initiation is associated with the translocation of the inactive form of Bax from the cytoplasm to the mitochondria and suppression of the prosurvival protein Bcl-2. Bax and Bcl-2 protein expression was explored using western blot analysis. In line with the results above, Bcl-2 levels were clearly attenuated by 500 and 1500 μM melatonin doses combined with irradiation, which increased the Bax/Bcl-2 ratio, with a maximum effect being observed at 1500 μM (Figures 2(c)–2(f)). Moreover, melatonin combined with CDDP increased the Bax/Bcl-2 ratio more than when combined with irradiation despite using a lower concentration of melatonin (1000 μM vs. 1500 μM) (Figures 2(i)–2(l)). These data indicate that melatonin combined with CDDP increases cytotoxicity more than irradiation.

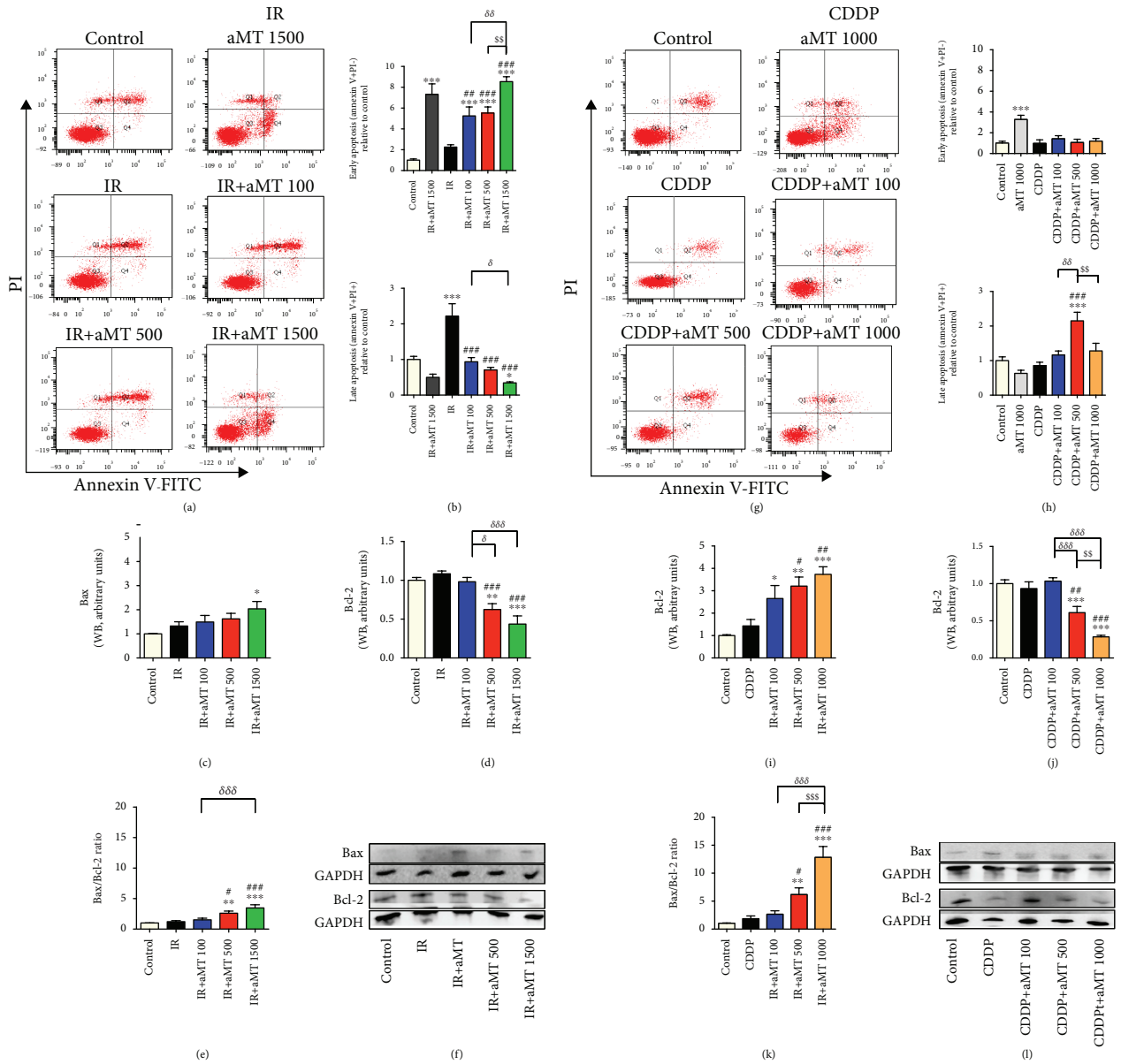

FIGURE 2: Combined treatment with melatonin and IR or CDDP increases apoptotic cell death in the HNSCC cell line Cal-27. Apoptosis was analyzed by flow cytometry. (a–g) Representative plots showing the redistribution of phosphatidylserine (annexin V staining) in the presence of propidium iodide (PI). The bottom right quadrant represents the percentage of early apoptotic cells (annexin V+/PI-), whereas the top right quadrant represents the percentage of late apoptotic cells (annexin V+/PI+). Statistical analysis of early and late apoptosis of cells exposed to IR (b) and CDDP (h), respectively. Western blot analysis (f–l) and densitometric quantification of Bax (c–i) and Bcl-2 (d–j) and the Bax/Bcl-2 ratio (e–k) in cells exposed to IR or CDDP, respectively. Treatment groups include the control (vehicle), IR (8 Gy), CDDP 10 μM, melatonin (aMT) 1000 or 1500 μM, and CDDP or IR plus aMT 100, 500, 1000, or 1500 μM. $n = 6$ per group. Data are presented as mean ± SEM. $^{*}P<.05$, $^{**}P<.01$, and $^{***}P<.001$ vs. the control; $^{\#}P<.05$, $^{\#\#}P<.01$, and $^{\#\#\#}P<.001$ vs. the IR- or CDDP-treated group; $^{\delta}P<.05$, $^{\delta\delta}P<.01$, and $^{\delta\delta\delta}P<.001$ vs. IR+aMT 100; and $^{\$}P<.05$, $^{\$\$}P<.01$, and $^{\$\$\$}P<.001$ vs. IR+aMT 500.

3.3. Enhancement of Mitochondrial Changes by Melatonin. Mitochondria are critically involved in controlling regulated cell death triggered by different cancer treatments [9], and several metabolic aspects of the mitochondrial biology also influence therapeutic responses [23]. As melatonin regulates mitochondrial homeostasis [24, 25], we hypothesized that melatonin potentiates the cytotoxicity of irradiation and CDDP treatments modifying mitochondrial function. We first determined the oxygen consumption rate (OCR), which is an indicator of mitochondrial oxidative phosphorylation activity and ATP production. While measuring oxygen consumption rates, we sequentially added oligomycin, FCCP, and a combination of rotenone and antimycin to the cells to assess electron transport chain integrity (Figures 3(a)–3(k)). Irradiated Cal-27 cells exhibited a significant increase in basal respiration (Figure 3(b)) and in the maximal respiratory capacity of the electron transport system (ETS) (Figure 3(c)) at melatonin 500 μM, which correlated with

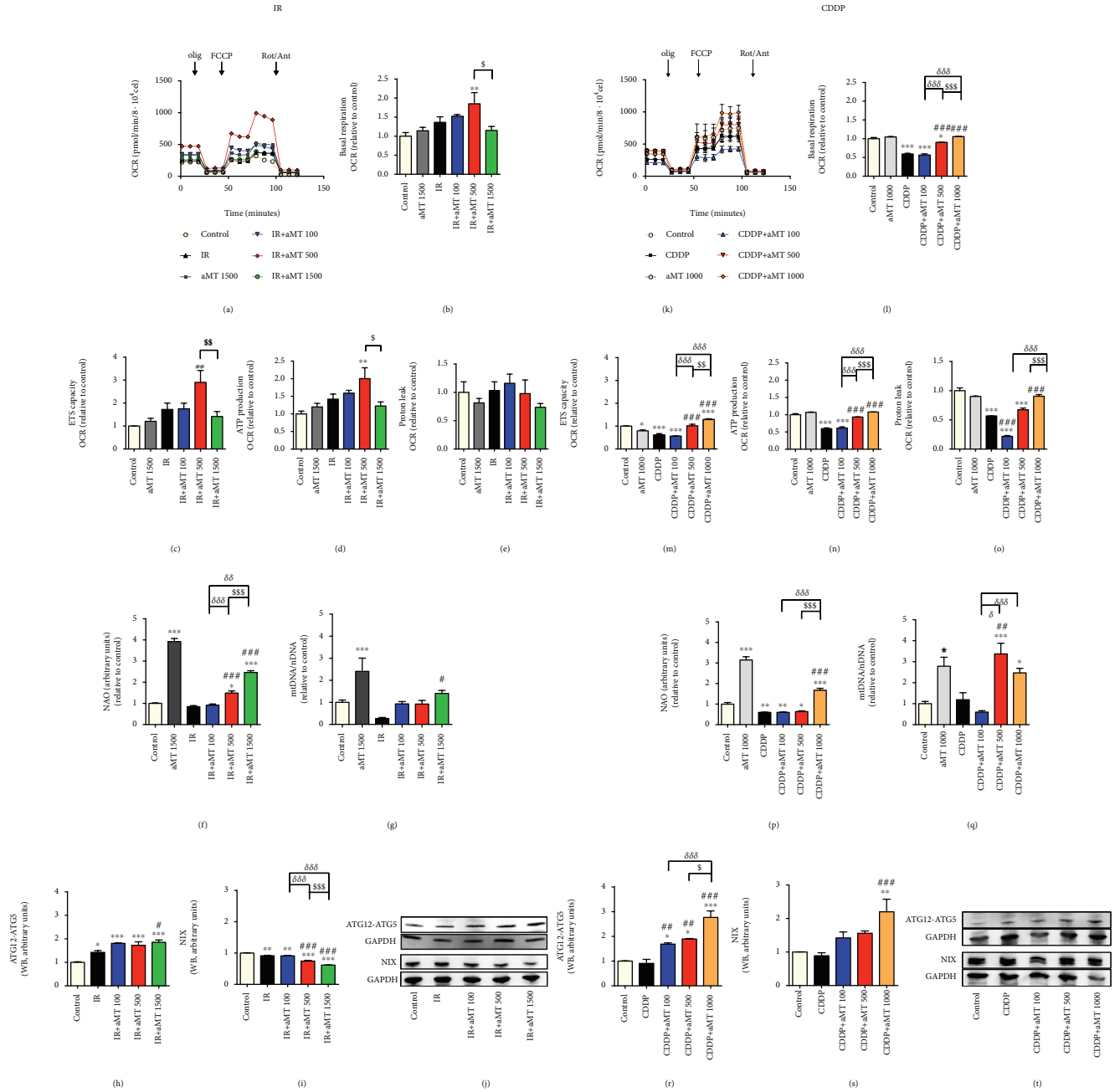

FIGURE 3: Effects of combined treatment with melatonin and IR or CDDP on Cal-27 HNSCC mitochondria. Oxygen consumption rate (OCR) (a, k), basal respiration (b, l), maximal respiratory capacity (ETS) (c, m), ATP production (d, n), and proton leak (e, o) in cells exposed to IR or CDDP, respectively. Mitochondrial mass (NAO) (f, p), mtDNA (g, q), western blot analysis, and densitometric quantification of ATG12-ATG5 (h, j, r, t) and NIX (i, j, s, t) in cells exposed to IR or CDDP, respectively. Treatment groups include the control (vehicle), IR (8 Gy), CDDP 10 μM, melatonin (aMT) 1000 or 1500 μM, and CDDP or IR plus aMT 100, 500, 1000, or 1500 μM. $n = 6$ per group. Data are presented as mean ± SEM. $^{*}P<.05$, $^{**}P<.01$, and $^{***}P<.001$ vs. the control; $^{\#}P<.05$, $^{\#\#}P<.01$, and $^{\#\#\#}P<.001$ vs. the IR- or CDDP-treated group, $^{\delta}P<.05$, $^{\delta\delta}P<.01$, and $^{\delta\delta\delta}P<.001$ vs. IR+aMT 100; $^{\$}P<.05$, $^{\$\$}P<.01$, and $^{\$\$\$}P<.001$ vs. IR+aMT 500.

an increase of ATP (Figure 3(d)) with no change in proton leak (Figure 3(e)). Surprisingly, melatonin 1500 μM caused a decrease in the OCR as compared to melatonin 500 μM (Figures 3(b)–3(d)), suggesting defective mitochondrial function at higher concentrations of melatonin. By contrast, cells treated with CDDP alone or melatonin 100 μM showed a decrease in the OCR (Figures 3(l)–3(n)), while melatonin doses of 500 and 1000 μM rescued the OCR as compared to the control. These results are in line with the direct effect of CDDP on mitochondria which interferes with mtDNA transcription, resulting in reduced mitochondrial function [26].

To further determine changes in mitochondria in the presence of melatonin, we next analyzed mitochondrial mass and mtDNA (Figures 3(f), 3(g), 3(p), and 3(q)). To examine mitochondrial mass, we used acridine orange.

Fluorescence data revealed that high concentrations of melatonin significantly augmented mitochondrial mass compared to the control, especially at 1500 and 1000 μM, in cells exposed to irradiation or CDDP (Figures 3(f)–3(p)). Moreover, similar doses of melatonin increased the mtDNA/nDNA ratio (Figures 3(g) and 3(q)), indicating that melatonin significantly increases mtDNA.

In a previous study, we demonstrated that melatonin may induce both apoptosis and autophagy in HNSCC [18]. We determined the levels of autophagy-related proteins ATG12-ATG5, as autophagy requires the covalent attachment of protein Atg12 to protein ATG5 through an ubiquitin-like conjugation system and the mitophagic marker NIX. The combined melatonin and irradiation treatment increased ATG12-ATG5 levels at all doses (Figures 3(h) and 3(j)) but decreased NIX levels (Figures 3(i) and 3(j)). However, the combination of melatonin and CDDP increased both ATG12-ATG5 and NIX (Figures 3(r)–3(t)). These data indicate that the combined melatonin and CDDP treatment, with its higher toxicity, results in autophagy and mitophagy.

These results could denote a correlation between an increase of mitochondrial activity induced by melatonin and ROS production.

3.4. Enhancement of Oxidative Stress in the Presence of Melatonin. To determine whether mitochondrial changes correlate with an increase in ROS, we measured ROS generation intensity using the DCFH-DA probe (Figure 4(a)). We observed a significant increase in intracellular ROS levels at melatonin 1500 μM in irradiated cells and, consequently, an increase in the GSSG/GSH ratio (Figures 4(c)–4(e)). Moreover, melatonin 500 and 1000 μM resulted in a sharper increase in ROS production in cells exposed to CDDP as compared to irradiation (Figure 4(g)). However, the increase in the GSSG/GSH ratio was only observed at 1000 μM (Figures 4(i)–4(k)), indicating that high doses of melatonin increased glutathione synthesis (Figures 4(f) and 4(l)). A parallel decrease in GPx activity was observed at the highest concentration of melatonin, especially in cells treated with CDDP (Figure 4(h)). However, at melatonin 100 μM combined with irradiation, we observed an increase in GPx activity (Figure 4(b)). These results are consistent with the lower levels of ROS observed at melatonin 100 μM as compared to 1500 μM. These data suggest that mitochondria cause a melatonin-induced ROS response in cancer cells which enhances the cytotoxic effects of irradiation and CDDP. Furthermore, despite being known to be a strong antioxidant, previous studies have shown that melatonin increases ROS production in tumor cells [18]. Thus, melatonin induces apoptosis in HNSCC by generating intracellular ROS and activating the mitochondrial pathway, thus increasing the effect of irradiation and CDDP.

4. Discussion

Radio- and chemotherapeutic resistance remains the major obstacle to successful cytotoxic therapy for human cancers. After the failure of the usual treatments, following chemo- or radiotherapy, even more distressing situations occur. Therefore, finding a coadjuvant treatment to suppress or reduce this resistance would represent a major advance for both patients and the health system as a whole. On the other hand, the treatments currently used usually present a high degree of toxicity in healthy cells. In this study, we demonstrate that melatonin significantly affects sensitivity to irradiation and CDDP in HNSCC, as reflected by reduced cell proliferation and clonogenicity, as well as apoptosis induction. Although the antitumor activity of melatonin has been reported elsewhere [27–29], the potential mechanisms involved remain unclear. Despite all the studies carried out, there are a disconcertingly large number of possible mechanisms which could explain the oncostatic effects of melatonin, involving almost as many mechanisms as tumor types. This suggests that only epiphenomena of an as yet unknown underlying mechanism of melatonin have been observed [29, 30].

In this study, we not only demonstrate the role of melatonin in improving the effects of irradiation and CDDP antitumor treatment but also, more importantly, describe the possible mechanisms involved in combined treatments which enhance their anticancer properties.

Cancer cells display increased resistance to regulated cell death, often due to alterations in the mitochondrial control of this process [31]. It has been suggested that the ability of most cancer cells to flexibly rewire their mitochondrial metabolism underlies multiple instances of chemoresistance [9]. Moreover, as melatonin has recently been shown to increase neural stem cell differentiation due to increased mitochondrial function [32], a similar mechanism could, in our view, occur in tumor cells. We therefore hypothesize that melatonin raises ROS production levels by increasing mitochondrial function in tumor cells. Consequently, cellular differentiation is expected to be caused by a change in cell metabolism, thereby increasing tumor sensitivity to other drugs. In this study, we provide, for the first time, evidence that the increase in irradiation and CDDP cytotoxicity caused by melatonin is partly due to enhanced mitochondrial function.

Our results show that melatonin-induced apoptosis coincides with a significant upregulation of the proapoptotic protein Bax and a downregulation of the antiapoptotic protein Bcl-2 on HNSCC. Bcl-2 overexpression is often associated with considerable cancer cell resistance to apoptosis [33]. When the Bax/Bcl-2 ratio increases, the mitochondrial permeability transition pore opens which, in turn, releases apoptogenic mitochondrial proteins to activate caspases which induce cell apoptosis [34]. Interestingly, the combined melatonin and cisplatin treatment had higher cytotoxicity than the combined treatment with irradiation. The main bulk of irradiated cells may take longer to enter apoptosis than those treated with CDDP. Other authors, such as Mirzayans et al. [35], have made a similar observation that different cancer cell lines such as HCT116, MCF7, and AT12 are markedly refractory to apoptosis in response to ionizing radiation. In this regard, it is possible to broadly classify cell death mechanisms into two classes: those occurring relatively soon after irradiation and before cell division leading to early cell death and those occurring comparatively late or after division leading to late cell death. The vast majority

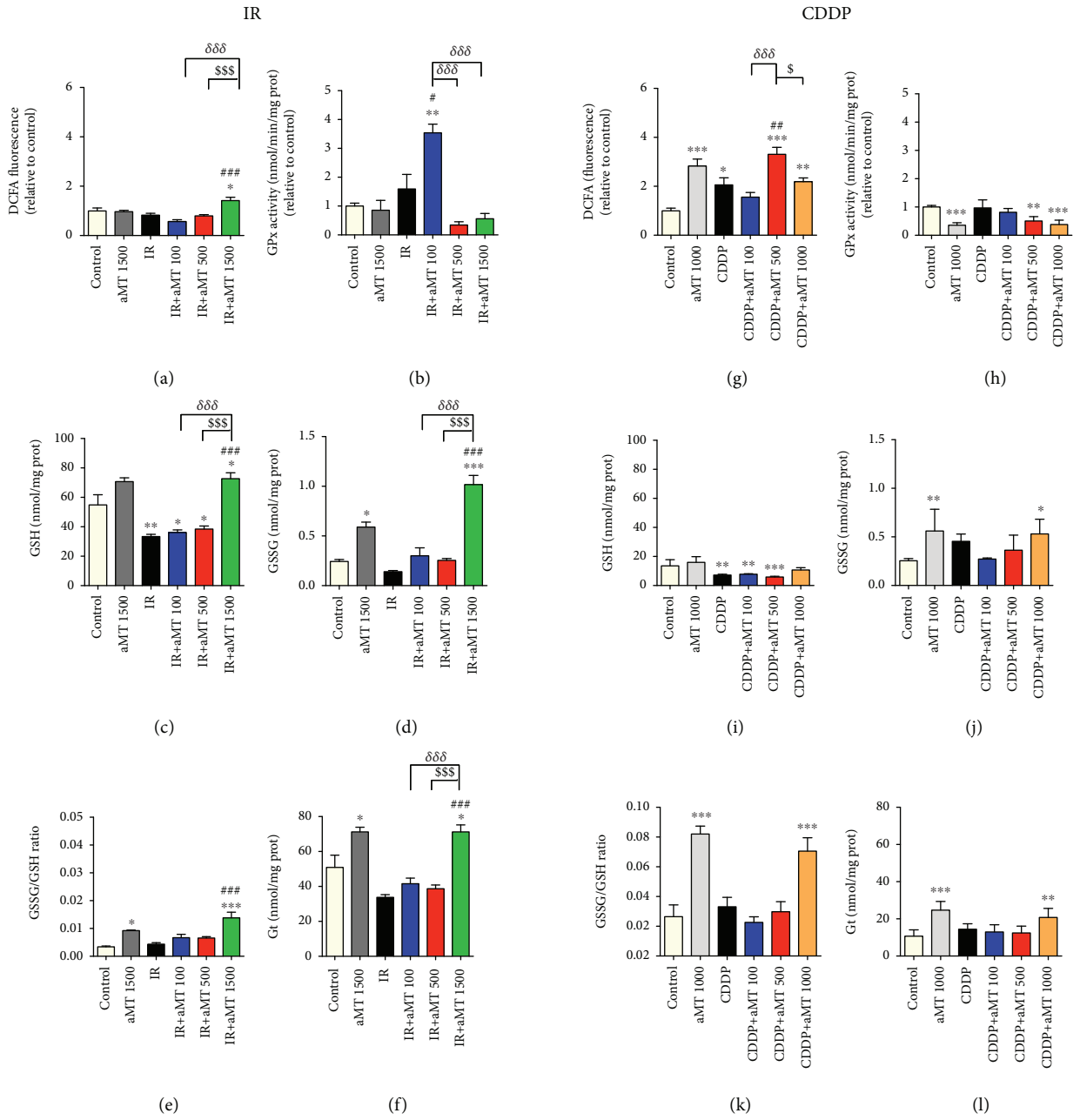

Figure 4: Combined treatment with melatonin and IR or CDDP increases oxidative stress in the HNSCC cell line Cal-27. Measurements of intracellular ROS levels by fluorometry after staining with the DCF fluorescent probe (a, g), GPx activity (b, h), content of GSH (c, i) and GSSG (d, j), GSSG/GSH ratio (e, k), and total glutathione (Gt) (f, l) in cells exposed to IR or CDDP, respectively. Treatment groups include the control (vehicle), IR (8 Gy), CDDP 10 μM, melatonin (aMT) 1000 or 1500 μM, and CDDP or IR plus aMT 100, 500, 1000, or 1500 μM. $n = 6$ per group. Data are presented as mean ± SEM. $^{*}P<.05$, $^{**}P<.01$, and $^{***}P<.001$ vs. the control; $^{\#}P<.05$, $^{\#\#}P<.01$, and $^{\#\#\#}P<.001$ vs. the IR- or CDDP-treated group; $^{\delta}P<.05$, $^{\delta\delta}P<.01$, and $^{\delta\delta\delta}P<.001$ vs. IR+aMT 100; $^{\$}P<.05$, $^{\$\$}P<.01$, and $^{\$\$\$}P<.001$ vs. IR +aMT 500.

of proliferating normal and tumor cells die after a relatively long period following irradiation, usually after attempting mitosis one or more times [36]. As a result, alterations in a particular gene may dramatically alter the levels of radiation-induced apoptosis, without changing the overall ability of the cell to survive [36]. In this case, cells die regardless of whether apoptosis is subsequently induced. On the other hand, the cytotoxic effect is dependent on drug concentrations, time of exposure, and time after exposure [37]. Generally, CDDP induces cell cycle arrest or apoptosis when administered at lower concentrations and induces necrosis at higher concentrations, although the effect differs between cell lines. Since CDDP exposure induces mitochondrial impairment and subsequently promotes cell death [38], high levels of mitochondrial metabolic activity are expected to enhance cisplatin cytotoxicity in cancer cells.

In order to mechanistically explain our findings, we investigated the effect of the combined treatments on mitochondrial respiration. We found that melatonin combined with irradiation or CDDP increased ETS capacity and ATP production. During late-stage apoptosis, ATP levels declined, mainly due to mitochondrial function loss and reduced consumption by ATP-dependent proteases [39]. In line with this finding, we observed a decrease in ATP levels following the combined treatment with irradiation and melatonin 1500 μM as compared to the combined treatment with melatonin 500 μM. These results are consistent with the increase in apoptosis at melatonin 1500 μM alone or combined with irradiation. However, the combined treatment with melatonin and CDDP was more toxic than that with irradiation. The occurrence of ATP deprivation in all types of cell death suggests that energy metabolism may play a critical role in cancer cell survival under stress conditions. Thus, we demonstrate that the strong antitumor effect of irradiation or CDDP combined with melatonin is partly due to enhanced mitochondrial function.

Mitochondria also contain other molecules such as mtDNA that can act as extracellular danger signals. In fact, head and neck tumor cells lacking mtDNA become cisplatin resistant [40]. Our results show that melatonin increases mitochondrial mass and mtDNA copy number in a dose-dependent manner and raises sensitivity to irradiation and CDDP.

The release of mtDNA promotes the secretion of type I interferon by malignant cells, which is necessary for the activation of optimal anticancer immune responses following chemo- and radiation therapy [41]. Thus, mtDNA also acts as a danger signal [42] linking intracellular stress responses to the preservation of extracellular homeostasis [43].

In addition, autophagy is one of the principal mechanisms involved in controlling cellular homeostasis [44, 45]. Although there is evidence to suggest that autophagy has a prosurvival function, excessive autophagy may lead to cell death, a process morphologically distinct from apoptosis [46]. Moreover, autophagy-deficient malignant cells, which succumb to *in vivo* chemotherapy and radiation therapy, lose their ability to drive anticancer immunity [9]. We detected increased expression of ATG12-ATG5, which plays a critical role in the biogenesis and elongation of the autophagosomal membrane following treatment with high concentrations of melatonin combined with irradiation or CDDP. However, NIX, which is required for the selective mitophagy-dependent elimination of mitochondria [47], only increased with high concentrations of melatonin combined with CDDP. The role of mitophagy in cancers is controversial. Mitophagy can facilitate survival through adaptation to stress, and mitophagic defects also promote metastatic dissemination [48], most likely due to moderate overproduction of ROS [49], which activate several signal transduction cascades associated with metastatic dissemination [49]. Conversely, under severe oxidative stress conditions, ROS de facto inhibit metastatic dissemination, most likely as a direct consequence of increased apoptosis [50, 51].

Therefore, given that mitochondria are the main source of cellular ROS, we hypothesize that melatonin enhances the cytotoxic effects of irradiation and CDDP caused by increased ROS production. Our study shows that melatonin significantly increases intracellular ROS in cells exposed to irradiation or CDDP. However, ROS production levels increased following the combined treatment with CDDP as compared to treatment with irradiation. Other research, which reinforces our conclusions, has found that the ROS-scavenging enzyme expression increases in CDDP-resistant cancer cells as compared to normal cells and that mitochondrial dysfunction may bestow resistance on CDDP due to the absence of or reduction in mitochondrial ROS responses [26].

The accumulation of intracellular ROS, which damages organelle proteins, enzymes, and membranes, eventually activates apoptosis signaling pathways [52]. ROS can also cause cell death either directly or through activation of intracellular proapoptotic pathways [52]. Besides triggering apoptosis, oxidative stress can promote permanent proliferative arrest known as cellular senescence [53].

Increasing oxidative stress-targeting mitochondria is therefore a novel therapeutic strategy for selectively killing cancer cells. Our results clearly indicate that the potentiation of the cytotoxic and proapoptotic effects of irradiation and CDDP by melatonin is mediated, at least partially, by the activation of mitochondrial function and subsequent overproduction of ROS *in vitro* in a dose-dependent manner. Our data suggest that there is a correlation between the cell content of melatonin and its apoptotic effects, thus supporting the notion that high concentrations of melatonin in cancer cells are required to enhance the cytotoxic effect of irradiation or CDDP.

A major limitation in the use of irradiation for therapeutic purposes is the development of side effects. Previous studies have shown that melatonin not only enhances the oncostatic effects of radio- and/or chemotherapy on tumor cells but also protects normal cells against the adverse effects of these treatments [18, 54–56]. We have patented a melatonin gel to prevent mucositis, which has completed a phase II clinical trial (EudraCT number: 2015-001534-13) in 80 patients with head and neck cancer, and have demonstrated that melatonin protects oral mucosa against the side effects of radiotherapy. All these data show that melatonin constitutes an innovative adjuvant strategy in the treatment of cancer.

5. Conclusions

Our study suggests that high doses of melatonin sensitize cancer cells to CDDP and irradiation by enhancing their mitochondrial function. Melatonin is a ROS inducer in HNSCC, and the accumulation of intracellular ROS plays an upstream role in mitochondria-mediated apoptosis. Our findings indicate that melatonin has great potential not only in augmenting radio- and chemosensitivity to cisplatin and other treatments but also in reducing toxicity caused by radio- and chemotherapeutic agents in cancer patients. Our study could provide a basis and guidelines for the

application of treatment with melatonin combined with radiotherapy or CDDP or other chemotherapeutic agents to improve therapeutic efficiency for cancers, especially for head and neck squamous cell carcinoma.

Data Availability

The datasets generated during and/or analyzed during the current study are available from the corresponding author on reasonable request.

Conflicts of Interest

The authors declared that they have no conflicts of interest to this work.

Authors' Contributions

Beatriz I. Fernandez-Gil and Ana Guerra-Librero contributed equally to this work.

Acknowledgments

This study was partially supported by grants from the Ministerio de Economía y Competitividad, Spain, and the FEDER Regional Development Fund (nos. SAF2013-49019 and SAF2017-85903), from the Instituto de Salud Carlos III (no. CB/10/00238), and from the Consejería de Economía, Innovación, Ciencia y Empleo, Junta de Andalucía (CTS-101). JF was supported by a grant from the University of Granada (ACG122/12a) and is a "FPU fellow" from the Ministerio de Educación Cultura y Deporte, Spain. AQH was supported by the Mayo Clinic Professorship and a Clinician Investigator award as well as the NIH (R43CA221490, R01CA200399, R01CA183827, R01CA195503, and R01CA216855). We wish to thank Michael O'Shea for proofreading the paper and Dr. Jesús López Peñalver (University of Granada) for providing technical support.

References

[1] World Health Organisation, *Locally Advanced Squamous Carcinoma of the Head and Neck*, Union Int. Cancer Control Rev. Cancer Med. WHO List Essent. Med, 2014.

[2] P. Maier, L. Hartmann, F. Wenz, and C. Herskind, "Cellular pathways in response to ionizing radiation and their targetability for tumor radiosensitization," *International Journal of Molecular Sciences*, vol. 17, no. 1, p. 102, 2016.

[3] H. Wang, X. Mu, H. He, and X.-D. Zhang, "Cancer radiosensitizers," *Trends in Pharmacological Sciences*, vol. 39, no. 1, pp. 24–48, 2018.

[4] J. M. Pascoe and J. J. Roberts, "Interactions between mammalian cell DNA and inorganic platinum compounds. I. DNA interstrand cross-linking and cytotoxic properties of platinum(II) compounds," *Biochemical Pharmacology*, vol. 23, no. 9, pp. 1359–1365, 1974.

[5] Y. Yamano, K. Uzawa, K. Saito et al., "Identification of cisplatin-resistance related genes in head and neck squamous cell carcinoma," *International Journal of Cancer*, vol. 126, no. 2, pp. 437–449, 2010.

[6] Y. Benhamou, V. Picco, and G. Pagès, "The telomere proteins in tumorigenesis and clinical outcomes of oral squamous cell carcinoma," *Oral Oncology*, vol. 57, pp. 46–53, 2016.

[7] G. Kroemer, L. Senovilla, L. Galluzzi, F. André, and L. Zitvogel, "Natural and therapy-induced immunosurveillance in breast cancer," *Nature Medicine*, vol. 21, no. 10, pp. 1128–1138, 2015.

[8] A. Erez and R. J. DeBerardinis, "Metabolic dysregulation in monogenic disorders and cancer — finding method in madness," *Nature Reviews. Cancer*, vol. 15, no. 7, pp. 440–448, 2015.

[9] P. E. Porporato, N. Filigheddu, J. M. B. S. Pedro, G. Kroemer, and L. Galluzzi, "Mitochondrial metabolism and cancer," *Cell Research*, vol. 28, no. 3, pp. 265–280, 2018.

[10] D. J. Hausenloy and D. M. Yellon, "Ischaemic conditioning and reperfusion injury," *Nature Reviews. Cardiology*, vol. 13, no. 4, pp. 193–209, 2016.

[11] S. Fulda, L. Galluzzi, and G. Kroemer, "Targeting mitochondria for cancer therapy," *Nature Reviews. Drug Discovery*, vol. 9, no. 6, pp. 447–464, 2010.

[12] L. Galluzzi, O. Kepp, M. G. V. Heiden, and G. Kroemer, "Metabolic targets for cancer therapy," *Nature Reviews Drug Discovery*, vol. 12, no. 11, pp. 829–846, 2013.

[13] D. Acuña-Castroviejo, G. Escames, C. Venegas et al., "Extrapineal melatonin: sources, regulation, and potential functions," *Cellular and Molecular Life Sciences*, vol. 71, no. 16, pp. 2997–3025, 2014.

[14] C. Alonso-González, A. González, C. Martínez-Campa, J. Gómez-Arozamena, and S. Cos, "Melatonin sensitizes human breast cancer cells to ionizing radiation by downregulating proteins involved in double-strand DNA break repair," *Journal of Pineal Research*, vol. 58, no. 2, pp. 189–197, 2015.

[15] P. Plaimee, N. Weerapreeyakul, S. Barusrux, and N. P. Johns, "Melatonin potentiates cisplatin-induced apoptosis and cell cycle arrest in human lung adenocarcinoma cells," *Cell Proliferation*, vol. 48, no. 1, pp. 67–77, 2015.

[16] Z. Ma, Y. Yang, C. Fan et al., "Melatonin as a potential anticarcinogen for non-small-cell lung cancer," *Oncotarget*, vol. 7, no. 29, pp. 46768–46784, 2016.

[17] Y.-X. Lu, D.-L. Chen, D.-S. Wang et al., "Melatonin enhances sensitivity to fluorouracil in oesophageal squamous cell carcinoma through inhibition of Erk and Akt pathway," *Cell Death & Disease*, vol. 7, no. 10, article e2432, 2016.

[18] Y.-Q. Shen, A. Guerra-Librero, B. I. Fernandez-Gil et al., "Combination of melatonin and rapamycin for head and neck cancer therapy: suppression of AKT/mTOR pathway activation, and activation of mitophagy and apoptosis via mitochondrial function regulation," *Journal of Pineal Research*, vol. 64, no. 3, article e12461, 2018.

[19] C. Venegas, J. A. García, G. Escames et al., "Extrapineal melatonin: analysis of its subcellular distribution and daily fluctuations," *Journal of Pineal Research*, vol. 52, no. 2, pp. 217–227, 2012.

[20] P. J. Hissin and R. Hilf, "A fluorometric method for determination of oxidized and reduced glutathione in tissues," *Analytical Biochemistry*, vol. 74, no. 1, pp. 214–226, 1976.

[21] R. H. Jaskot, E. G. Charlet, E. C. Grose, M. A. Grady, and J. H. Roycroft, "An automated analysis of glutathione peroxidase, S-transferase, and reductase activity in animal tissue," *Journal of Analytical Toxicology*, vol. 7, no. 2, pp. 86–88, 1983.

[22] E. Brauchle, S. Thude, S. Y. Brucker, and K. Schenke-Layland, "Cell death stages in single apoptotic and necrotic cells monitored by Raman microspectroscopy," *Scientific Reports*, vol. 4, no. 1, article 4698, 2015.

[23] D. R. Green, L. Galluzzi, and G. Kroemer, "Metabolic control of cell death," *Science*, vol. 345, no. 6203, article 1250256, 2014.

[24] C. Doerrier, J. A. García, H. Volt et al., "Permeabilized myocardial fibers as model to detect mitochondrial dysfunction during sepsis and melatonin effects without disruption of mitochondrial network," *Mitochondrion*, vol. 27, pp. 56–63, 2016.

[25] D. Acuña-Castroviejo, I. Rahim, C. Acuña-Fernández et al., "Melatonin, clock genes and mitochondria in sepsis," *Cellular and Molecular Life Sciences*, vol. 74, no. 21, pp. 3965–3987, 2017.

[26] R. Marullo, E. Werner, N. Degtyareva et al., "Cisplatin induces a mitochondrial-ROS response that contributes to cytotoxicity depending on mitochondrial redox status and bioenergetic functions," *PLoS One*, vol. 8, no. 11, article e81162, 2013.

[27] R. Reiter, S. Rosales-Corral, D.-X. Tan et al., "Melatonin, a full service anti-cancer agent: inhibition of initiation, progression and metastasis," *International Journal of Molecular Sciences*, vol. 18, no. 4, p. 843, 2017.

[28] S. Casado-Zapico, J. Rodriguez-Blanco, G. GarcÃ-a-Santos et al., "Synergistic antitumor effect of melatonin with several chemotherapeutic drugs on human Ewing sarcoma cancer cells: potentiation of the extrinsic apoptotic pathway," *Journal of Pineal Research*, vol. 48, no. 1, pp. 72–80, 2010.

[29] R. J. Reiter, J. C. Mayo, D.-X. Tan, R. M. Sainz, M. Alatorre-Jimenez, and L. Qin, "Melatonin as an antioxidant: under promises but over delivers," *Journal of Pineal Research*, vol. 61, no. 3, pp. 253–278, 2016.

[30] R. J. Reiter, D. X. Tan, and A. Galano, "Melatonin: exceeding expectations," *Physiology*, vol. 29, no. 5, pp. 325–333, 2014.

[31] D. Hanahan and R. A. Weinberg, "The hallmarks of cancer," *Cell*, vol. 100, no. 1, pp. 57–70, 2000.

[32] M. Mendivil-Perez, V. Soto-Mercado, A. Guerra-Librero et al., "Melatonin enhances neural stem cell differentiation and engraftment by increasing mitochondrial function," *Journal of Pineal Research*, vol. 63, no. 2, 2017.

[33] R. M. Perciavalle, D. P. Stewart, B. Koss et al., "Anti-apoptotic MCL-1 localizes to the mitochondrial matrix and couples mitochondrial fusion to respiration," *Nature Cell Biology*, vol. 14, no. 6, pp. 575–583, 2012.

[34] M. H. Kang and C. P. Reynolds, "Bcl-2 inhibitors: targeting mitochondrial apoptotic pathways in cancer therapy," *Clinical Cancer Research*, vol. 15, no. 4, pp. 1126–1132, 2009.

[35] R. Mirzayans, B. Andrais, and D. Murray, "Impact of premature senescence on radiosensitivity measured by high throughput cell-based assays," *International Journal of Molecular Sciences*, vol. 18, no. 7, article 1460, 2017.

[36] B. G. Wouters, "Cell death after irradiation: how, when and why cells die," in *Basic Clinical Radiobiology Fourth Edition*, CRC Press, London, 2009.

[37] V. Janson, P. Behnam-Motlagh, R. Henriksson, P. Hörstedt, K. G. Engström, and K. Grankvist, "Phase-contrast microscopy studies of early cisplatin-induced morphological changes of malignant mesothelioma cells and the correspondence to induced apoptosis," *Experimental Lung Research*, vol. 34, no. 2, pp. 49–67, 2008.

[38] F. M. Santandreu, P. Roca, and J. Oliver, "Uncoupling protein-2 knockdown mediates the cytotoxic effects of cisplatin," *Free Radical Biology & Medicine*, vol. 49, no. 4, pp. 658–666, 2010.

[39] Y. Zhou, F. Tozzi, J. Chen et al., "Intracellular ATP levels are a pivotal determinant of chemoresistance in colon cancer cells," *Cancer Research*, vol. 72, no. 1, pp. 304–314, 2012.

[40] Z. Yang, L. M. Schumaker, M. J. Egorin, E. G. Zuhowski, Z. Guo, and K. J. Cullen, "Cisplatin preferentially binds mitochondrial DNA and voltage-dependent anion channel protein in the mitochondrial membrane of head and neck squamous cell carcinoma: possible role in apoptosis," *Clinical Cancer Research*, vol. 12, no. 19, pp. 5817–5825, 2006.

[41] C. Vanpouille-Box, A. Alard, M. J. Aryankalayil et al., "DNA exonuclease Trex1 regulates radiotherapy-induced tumour immunogenicity," *Nature Communications*, vol. 8, article 15618, 2017.

[42] L. Galluzzi, O. Kepp, and G. Kroemer, "Mitochondria: master regulators of danger signalling," *Nature Reviews. Molecular Cell Biology*, vol. 13, no. 12, pp. 780–788, 2012.

[43] L. Galluzzi, A. López-Soto, S. Kumar, and G. Kroemer, "Caspases connect cell-death signaling to organismal homeostasis," *Immunity*, vol. 44, no. 2, pp. 221–231, 2016.

[44] M. Marinković, M. Šprung, M. Buljubašić, and I. Novak, "Autophagy modulation in cancer: current knowledge on action and therapy," *Oxidative Medicine and Cellular Longevity*, vol. 2018, Article ID 8023821, 18 pages, 2018.

[45] L. Galluzzi, E. H. Baehrecke, A. Ballabio et al., "Molecular definitions of autophagy and related processes," *The EMBO Journal*, vol. 36, no. 13, pp. 1811–1836, 2017.

[46] A. V. Kulikov, E. A. Luchkina, V. Gogvadze, and B. Zhivotovsky, "Mitophagy: link to cancer development and therapy," *Biochemical and Biophysical Research Communications*, vol. 482, no. 3, pp. 432–439, 2017.

[47] R. L. Schweers, J. Zhang, M. S. Randall et al., "NIX is required for programmed mitochondrial clearance during reticulocyte maturation," *Proceedings of the National Academy of Sciences*, vol. 104, no. 49, pp. 19500–19505, 2007.

[48] A. H. Chourasia, K. Tracy, C. Frankenberger et al., "Mitophagy defects arising from BNip3 loss promote mammary tumor progression to metastasis," *EMBO Reports*, vol. 16, no. 9, pp. 1145–1163, 2015.

[49] P. E. Porporato, V. L. Payen, J. Pérez-Escuredo et al., "A mitochondrial switch promotes tumor metastasis," *Cell Reports*, vol. 8, no. 3, pp. 754–766, 2014.

[50] E. Piskounova, M. Agathocleous, M. M. Murphy et al., "Oxidative stress inhibits distant metastasis by human melanoma cells," *Nature*, vol. 527, no. 7577, pp. 186–191, 2015.

[51] V. I. Sayin, M. X. Ibrahim, E. Larsson, J. A. Nilsson, P. Lindahl, and M. O. Bergo, "Antioxidants accelerate lung cancer progression in mice," *Science Translational Medicine*, vol. 6, no. 221, article 221ra15, 2014.

[52] M. Redza-Dutordoir and D. A. Averill-Bates, "Activation of apoptosis signalling pathways by reactive oxygen species," *Biochimica et Biophysica Acta (BBA) - Molecular Cell Research*, vol. 1863, no. 12, pp. 2977–2992, 2016.

[53] B. G. Childs, M. Gluscevic, D. J. Baker et al., "Senescent cells: an emerging target for diseases of ageing," *Nature Reviews. Drug Discovery*, vol. 16, no. 10, pp. 718–735, 2017.

[54] F. Ortiz, D. Acuña-Castroviejo, C. Doerrier et al., "Melatonin blunts the mitochondrial/NLRP3 connection and protects against radiation-induced oral mucositis," *Journal of Pineal Research*, vol. 58, no. 1, pp. 34–49, 2015.

[55] B. Fernández-Gil, A. E. A. Moneim, F. Ortiz et al., "Melatonin protects rats from radiotherapy-induced small intestine toxicity," *PLoS One*, vol. 12, no. 4, article e0174474, 2017.

[56] A. E. Abdel Moneim, A. Guerra-Librero, J. Florido et al., "Oral mucositis: melatonin gel an effective new treatment," *International Journal of Molecular Sciences*, vol. 18, no. 5, article 1003, 2017.

Hindawi
Oxidative Medicine and Cellular Longevity
Volume 2018, Article ID 1471682, 12 pages
https://doi.org/10.1155/2018/1471682

Research Article

WIPI1, BAG1, and PEX3 Autophagy-Related Genes Are Relevant Melanoma Markers

Daniela D'Arcangelo,[1] **Claudia Giampietri**,[2] **Mario Muscio**,[1] **Francesca Scatozza**,[1] **Francesco Facchiano**,[3] **and Antonio Facchiano**[1]

[1]*Istituto Dermopatico dell'Immacolata, IDI-IRCCS, via Monti di Creta 104, 00167 Rome, Italy*
[2]*Department of Anatomical, Histological, Forensic Medicine and Orthopedic Sciences, Sapienza University, Rome, Italy*
[3]*Department of Oncology and Molecular Medicine, Istituto Superiore di Sanità, ISS, viale Regina Elena 299, 00161 Rome, Italy*

Correspondence should be addressed to Francesco Facchiano; francesco.facchiano@iss.it
and Antonio Facchiano; a.facchiano@idi.it

Received 3 August 2018; Accepted 9 October 2018; Published 2 December 2018

Guest Editor: Miguel Sanchez-Alvarez

ROS and oxidative stress may promote autophagy; on the other hand, autophagy may help reduce oxidative damages. According to the known interplay of ROS, autophagy, and melanoma onset, we hypothesized that autophagy-related genes (ARGs) may represent useful melanoma biomarkers. We therefore analyzed the gene and protein expression of 222 ARGs in human melanoma samples, from 5 independent expression databases (overall 572 patients). Gene expression was first evaluated in the GEO database. Forty-two genes showed extremely high ability to discriminate melanoma from nevi (63 samples) according to ROC (AUC $\geq$ 0.85) and Mann-Whitney ($p < 0.0001$) analyses. The 9 genes never related to melanoma before were then in silico validated in the IST online database. BAG1, CHMP2B, PEX3, and WIPI1 confirmed a strong differential gene expression, in 355 samples. A second-round validation performed on the Human Protein Atlas database showed strong differential protein expression for BAG1, PEX3, and WIPI1 in melanoma *vs* control samples, according to the image analysis of 80 human histological sections. WIPI1 gene expression also showed a significant prognostic value ($p < 0.0001$) according to 102 melanoma patients' survival data. We finally addressed in Oncomine database whether WIPI1 overexpression is melanoma-specific. Within more than 20 cancer types, the most relevant WIPI1 expression change ($p = 0.00002$; fold change = 3.1) was observed in melanoma. Molecular/functional relationships of the investigated molecules with melanoma and their molecular/functional network were analyzed via Chilibot software, STRING analysis, and gene ontology enrichment analysis. We conclude that WIPI1 (AUC = 0.99), BAG1 (AUC = 1), and PEX3 (AUC = 0.93) are relevant novel melanoma markers at both gene and protein levels.

1. Introduction

Cutaneous melanoma is the most aggressive skin cancer; it accounts for less than 5% of all skin cancers but causes about 80% of skin cancer-related mortality. Effective diagnostic markers are therefore needed to reduce melanoma-related mortality. Melanoma pathogenesis is usually related to the skin phototype, and risk factors include environmental factors, lifestyles such as intermittent excessive UV exposure and sunburns, and genetic predisposition. Excessive UV exposure results in DNA damage and gene mutations, mostly on BRAF, in almost half of melanoma cases, leaving the remaining half without a specific genetic marker. Despite that melanoma genetics is under extensive investigation [1–4], a melanoma-specific genetic profile has not been identified yet, and early markers of melanoma onset are still unknown. While S100B and LDH are recognized as clinically reliable prognostic markers in late stages, LDH is the only marker accepted by NCCN and AJCC current melanoma guidelines for TNM scoring and clinical staging. Therefore, clinically relevant diagnostic early biomarkers are still to be identified. We [5, 6] and others identified

mechanisms affecting melanoma onset, including immune surveillance control [7], IL8/bcl-XL axis [8], aberrant expression of kallikrein-related peptidase 7 [9], fatty acid oxidation [10], lipid droplet accumulation [6], and PDGF-Rα expression in [11, 12].

The role autophagy plays in physio-pathological conditions is under intense investigation. It has both protective and detrimental effects, depending on the conditions [13], including pro- or antitumor effects [14–17]. As an example, chaperone-mediated autophagy degrades different substrates, with both cancer-suppressor and cancer-promoting activity [18]. Autophagy is considered as tumor-suppressive in melanoma early stages and tumor-promoting in melanoma later stages [19]. SQSTM1 and AMBRA1 are emerging as prognostic markers for early-stage melanoma [18, 20]. Further, endoplasmic reticulum stress-induced unfolded proteins [21, 22] appear to mediate the resistance to antimelanoma therapies, and removal dysfunctional/aged mitochondria, known as "mitophagy," may play a role in melanoma setup and progression [23].

All such studies support a key role of autophagy-related genes (here referred to as ARGs) in melanoma setup. We therefore hypothesized that ARGs may represent suitable melanoma markers and investigated for the first time the expression levels of 222 ARGs in several melanoma samples. Several hundred human melanoma samples from 4 different and independent public databases in 4 consecutive validation stages were analyzed.

2. Materials and Methods

ARGs were from HADb, Human Autophagy Database, at http://www.autophagy.lu/clustering/, from the Luxemburg Institute of Health, including 222 genes at the date of March 2017 (Supplementary Table 1). Expression in a total of 572 human samples was investigated from 5 different public datasets, via 1 screening phase + 3 consecutive validations phases.

2.1. ARG Expression from the GEO Database: Melanoma vs Nevi Samples. Expression of 222 ARGs was evaluated in the melanoma GDS1375 dataset, from the GEO database (https://www.ncbi.nlm.nih.gov/gds/). This human dataset reports expression data from the most numerous collections of melanoma and nevi samples, available within GEO. It reports the actual expression values; calculations such as mean, Mann-Whitney test, and ROC analysis were then carried out on 63 samples (45 melanoma patients *vs* 18 nevi patients). ROC analysis, the most accepted method in binary tests, was used to measure how effective the expression level of any given gene to discriminate healthy from melanoma biopsies is. The computed area under the curve (AUC) value ranges from 0.5 to 1, indicating 50% to 100% discrimination ability. Sensitivity and specificity were selected from the expression levels showing the best sensitivity-specificity combination.

2.2. Selection of Genes Not Known to Have a Relation with Melanoma. Genes selected from the GEO analysis, having AUC $\geq$ 0.85, were then searched in Pubmed for any co-occurrence with melanoma, at the date of April 19, 2018. Search in "ALL fields" was carried out to minimize false-negative results. Genes showing no co-occurrence with melanoma were considered novel in the melanoma field and were selected for the following validation steps.

2.3. First-Round Validation of Gene Expression Data in the IST Online Database. The first-round validation step was carried out by analyzing expression levels of the selected genes in the independent IST Online database (http://ist.medisapiens.com/), having 208 melanoma samples and 147 healthy skin samples. Differently from the GEO database, IST Online does not show actual numbers; rather, it expresses data as scatter plots. Therefore, scatter plots were obtained according to a previously reported procedure [11]. Genes showing expression levels in melanoma strongly different to controls were then selected for the following validation steps.

2.4. Second-Round Validation: Protein Expression in the Human Protein Atlas Database. The 4 genes identified and validated within the previous phases were then analyzed at the protein expression level in Human Protein Atlas (https://www.proteinatlas.org/). Eighty histological sections (47 cutaneous melanoma and 33 healthy skin controls) were retrieved and transformed in grayscale by using the GIMP image editor (version 2.8) (GNU Image Manipulation Program; https://www.gimp.org) according to the following steps:

(1) Image selection

(2) Background removal by converting the white background to transparent

(3) RGB image color conversion to grayscale

(4) Histograms, mean, pixel numbers, median, and standard deviation obtained from the image menu: Colors → Information → Histogram

2.5. Chilibot Analysis. Chilibot analysis was then performed (http://www.chilibot.net) [24]. Chilibot identifies known relationships within the user-defined terms, by looking at their coexistence in the same sentence within Pubmed abstracts, identifying much closer relations as compared to a plain Pubmed search. Chilibot then associates same-sentence co-occurrence to stimulatory or inhibitory or noninteractive relationships. A "two-list analysis" was carried out, the first list containing the term "melanoma" and the second list containing the 42 ARG gene list of Table 1; the "advanced options" button was turned on, to account for all known synonyms of the given terms and minimize false-negative findings.

2.6. Third-Round Validation: Investigating the Specificity of WIPI1 Overexpression. Cancer types showing the most relevant WIPI1 upregulation were identified on Oncomine database (http://www.oncomine.com). WIPI1 expression in a "cancer *vs* normal" analysis was investigated in 170 independent human datasets from more than 20 different cancer types, onto 31,931 human biopsy samples; a list was obtained

Table 1: ROC analysis of ARGs, according to the GDS1375 dataset from GEO database. Only genes showing AUC ≥ 0.85 are reported; genes highlighted in white font on black background have still unknown relationships with melanoma diagnosis or prognosis. CTSB shows the highest fold increase (10-fold increase in melanoma *vs* nevi); WIPI1 shows the second highest fold increase (8.1-fold increase). EGFR shows the highest fold decrease (−10.7 fold), PTK6 the second highest fold decrease (−8.8 fold).

	Symbol	Mean expression in melanoma	Mean expression in nevi	Fold change melanoma vs nevi	AUC	*p* value of the computed AUC	Number of Pubmed abstracts with the gene symbol and "melanoma" in ALL field (up to April 19 2018)
1	ATF4	5611	7598	+1.3	0.87	<0.0001	≥1
2	ATG4B	1016	739	+1.4	0.88	<0.0001	≥1
3	**ATG9A**	**1014**	**735**	**+1.4**	**0.89**	**<0.0001**	**0**
4	**BAG1**	**727**	**1891**	**−2.6**	**1**	**<0.0001**	**0**
5	BAG3	1098	1831	−1.7	0.87	<0.0001	≥1
6	BAX	498	186	+2.7	0.93	<0.0001	≥1
7	BCL2	1409	180	+7.8	0.99	<0.0001	≥1
8	BCL2L1	1244	375	+3.3	0.99	<0.0001	≥1
9	BIRC5	590	230	+2.6	0.92	<0.0001	>1
10	**CAPN2**	**9236**	**5096**	**+1.8**	**0.96**	**<0.0001**	**0**
11	CAPNS1	8826	4392	+2.0	0.93	<0.0001	≥1
12	CDKN1A	2790	1397	+2.0	0.90	<0.0001	≥1
13	CDKN2A	650	335	+1.9	0.86	<0.0001	≥1
14	CFLAR	472	796	−1.7	0.85	<0.0001	≥1
15	**CHMP2B**	**282**	**561**	**−2.0**	**0.87**	**<0.0001**	**0**
16	CTSB	16,713	1655	+10.0	0.99	<0.0001	≥1
17	CTSD	2115	1029	+2.0	0.89	<0.0001	≥1
18	CX3CL1	266	627	−2.3	0.91	<0.0001	≥1
19	EGFR	184	1976	−10.7	0.98	<0.0001	≥1
20	EIF2AK3	566	282	+2.0	0.93	<0.0001	≥1
21	EIF2S1	16,903	9247	+1.8	0.90	<0.0001	0
22	ERBB2	2107	1695	+1.2	0.90	<0.0001	≥1
23	FAS	338	681	−2.0	0.89	<0.0001	≥1
24	FOXO1	482	1055	−2.2	0.96	<0.0001	≥1
25	**GNAI3**	**193**	**362**	**−1.9**	**0.94**	**<0.0001**	**0**
26	HDAC1	1614	1146	+1.4	0.86	<0.0001	≥1
27	HSPA5	3830	2390	+1.6	0.86	<0.0001	≥1
28	HSPB8	200	947	−4.7	0.94	<0.0001	≥1
29	ITGA3	2436	497	+4.9	0.95	<0.0001	≥1
30	**ITGB4**	**206**	**944**	**−4.6**	**0.87**	**<0.0001**	**0**
31	**KIAA0226**	**186**	**104**	**+1.8**	**0.85**	**<0.0001**	**0**
32	MAPK1	730	1339	−1.8	0.86	<0.0001	≥1
33	MLST8	833	453	+1.8	0.90	<0.0001	≥1
34	NFE2L2	1410	2622	−1.8	0.91	<0.0001	≥1
35	PARP1	2212	975	+2.3	0.99	<0.0001	≥1
36	PEA15	5307	3477	+1.5	0.94	<0.0001	≥1
37	**PEX3**	**343**	**670**	**−1.9**	**0.93**	**<0.0001**	**0**
38	PTK6	63	556	−8.8	0.96	<0.0001	≥1
39	SQSTM1	4197	2636	+1.6	0.95	<0.0001	≥1
40	TP63	131	1067	−8.1	0.93	<0.0001	≥1
41	TP73	578	785	−1.3	0.89	<0.0001	≥1
42	**WIPI1**	**3043**	**374**	**+8.1**	**0.99**	**<0.0001**	**0**

of cancer types and relevant datasets where WIPI1 is significantly over- or underexpressed.

A "cancer *vs* cancer analysis" was also carried out, with filter "Dataset type: Cell line panel datasets," to address expression in all cancer lines available. In this case, 26 different datasets with 7410 samples from 18 different cancer types were analyzed.

The Oncomine search engine applies a combination of threshold values, namely, p value, fold change *vs* controls, and gene rank (rank of that gene in that dataset, based on its p value, indicating how many other genes in the analysis are more or less significant). Very strict thresholds were imposed, namely, $p \leq 0.0001$, fold change ≥ 3, and gene rank top 5%. An additional validation of normal vs melanoma expression data was achieved by analyzing an additional dataset in the GEO database (namely, GSE 15605 containing 74 samples: 16 normal, 46 primary, and 12 metastatic-melanoma) and by accessing the Expression Atlas database at EMBL-EBI available at (https://www.ebi.ac.uk/gxa/home).

2.7. Network Analysis and Functional Grouping Analysis. Additional analyses were carried out to investigate the functional grouping and the structural/functional network of the identified genes. To this aim, the enrichment analysis was performed onto the 42 genes reported in Table 1, at the link http://www.geneontology.org/page/go-enrichment-analysis. It is a Gene Ontology tool that identifies GO terms over- or underrepresented within the GO annotations of the given gene list. In addition, the STRING analysis at https://string-db.org/ was performed to identify a functional network of the three main hits identified in the present study, namely, WIPI1, BAG1, and PEX3. The STRING database is from the STRING consortium (Swiss Institute for Bioinformatics, CPR NNF Center for Protein Research, EMBL-European Molecular Biology Laboratory).

2.8. Statistics. Analysis was performed on 498 human samples, including the selection phase and the first- and second-round validation phases, namely, 45 melanoma and 18 nevi from GEO, 208 melanoma and 147 healthy skin from IST Online, and 47 melanoma and 33 healthy skin from HPA. Within the third-round validation in Oncomine, 31,931 human samples were analyzed from 170 datasets with 22 different cancer types and on 3392 samples from 11 different cancer cell lines. Mean, two-tailed t test, Mann-Whitney test, and ROC analysis were carried out, with a threshold p value set at ≤ 0.05. Gaussian distribution was investigated with D'Agostino and Pearson normality test. GraphPad Prism version 5.01 was used (GraphPad Software Inc.).

3. Results

3.1. ARG Gene Expression Analysis in the GEO Database. Expression data of 222 ARGs (list reported in Supplementary Table 1) were collected from the GDS1375 dataset in GEO. ROC analysis and Mann-Whitney analyses were carried out to measure the ability to discriminate melanoma biopsies from nevi controls. Expression of 42 genes was found to discriminate melanoma biopsies from nevi in a very effective way, i.e., with an $AUC \geq 0.85$ and $p < 0.0001$ (Table 1). Most of such 42 genes are known to be involved in melanoma. A Pubmed search carried out on April 19, 2018, identified 9 genes never directly related to melanoma diagnosis. Such 9 genes (namely, ATG9A, BAG1, CAPN2, CHMP2B, GNAI3, ITGB4, KIAA0226, PEX3, and WIPI1) are highlighted in white font on black background in Table 1 and are here considered as novel candidate melanoma markers. Figure 1 reports the corresponding ROC curve for the expression values; BAG1, PEX3, and WIPI1, selected in the following validation steps, show AUC 1, 0.93, and 0.99, respectively, with extremely high sensitivity and specificity values. Namely, the BAG1 expression level of 1037 shows 100% sensitivity and 100% specificity; the PEX3 expression level of 387.8 shows 77.8% sensitivity and 94.4 specificity; and the WIPI1 expression level of 913.3 shows 95.6% sensitivity and 100% specificity.

3.2. First-Round Validation: Gene Expression Analysis in the IST Online Database. The 9 genes reported in Figure 1 were then validated in an independent public database, namely, IST Online, having 208 melanoma patients and 147 healthy skin controls. BAG1, CHMP2B, PEX3, and WIPI1 confirm strongly different expression levels in melanoma *vs* healthy skin in IST Online (Figure 2). Dashed ovals in Figure 2 select 90% of samples from the remaining 10%. We conclude that BAG1, CHMP2B, PEX3, and WIPI1 show a strongly different expression in melanoma *vs* control biopsies, according to data from 418 patients, and have never been related to melanoma according to Pubmed.

3.3. Second-Round Validation: Protein Expression Analysis in the Human Protein Atlas Database. BAG1, CHMP2B, PEX3, and WIPI1 protein expression levels were then analyzed on Human Protein Atlas (HPA) (https://www.proteinatlas.org/). Eighty histological section images from melanoma patients and healthy skin were analyzed. Grayscale conversion and pixel distribution quantification were obtained as reported in Materials and Methods. Figure 3 shows the distribution plot of the pixels of any given density; the right-end site indicates distribution of darker pixels, i.e., higher expression. Darker pixels are more frequent in melanoma as compared to normal tissues for BAG1, PEX3, and WIPI1, while CHMP2B expression is unchanged. The median pixel-darkness, reported in each panel, indicates the shift toward higher expression of BAG1, PEX3, and WIPI1 in melanoma *vs* healthy skin. Noteworthy, WIPI1 increases in melanoma at both gene (Figure 2) and protein expression levels (Figure 3).

3.4. Mechanisms Underlying Functional Interaction of ARGs with Melanoma

3.4.1. Chilibot Analysis. The molecular mechanisms underlying the functional interaction of BAG1, PEX3, and WIPI1 with melanoma were investigated with Chilibot analysis. According to this analysis, no direct and strong relationship is reported so far, of such genes with melanoma, while their interaction to melanoma may be mediated via

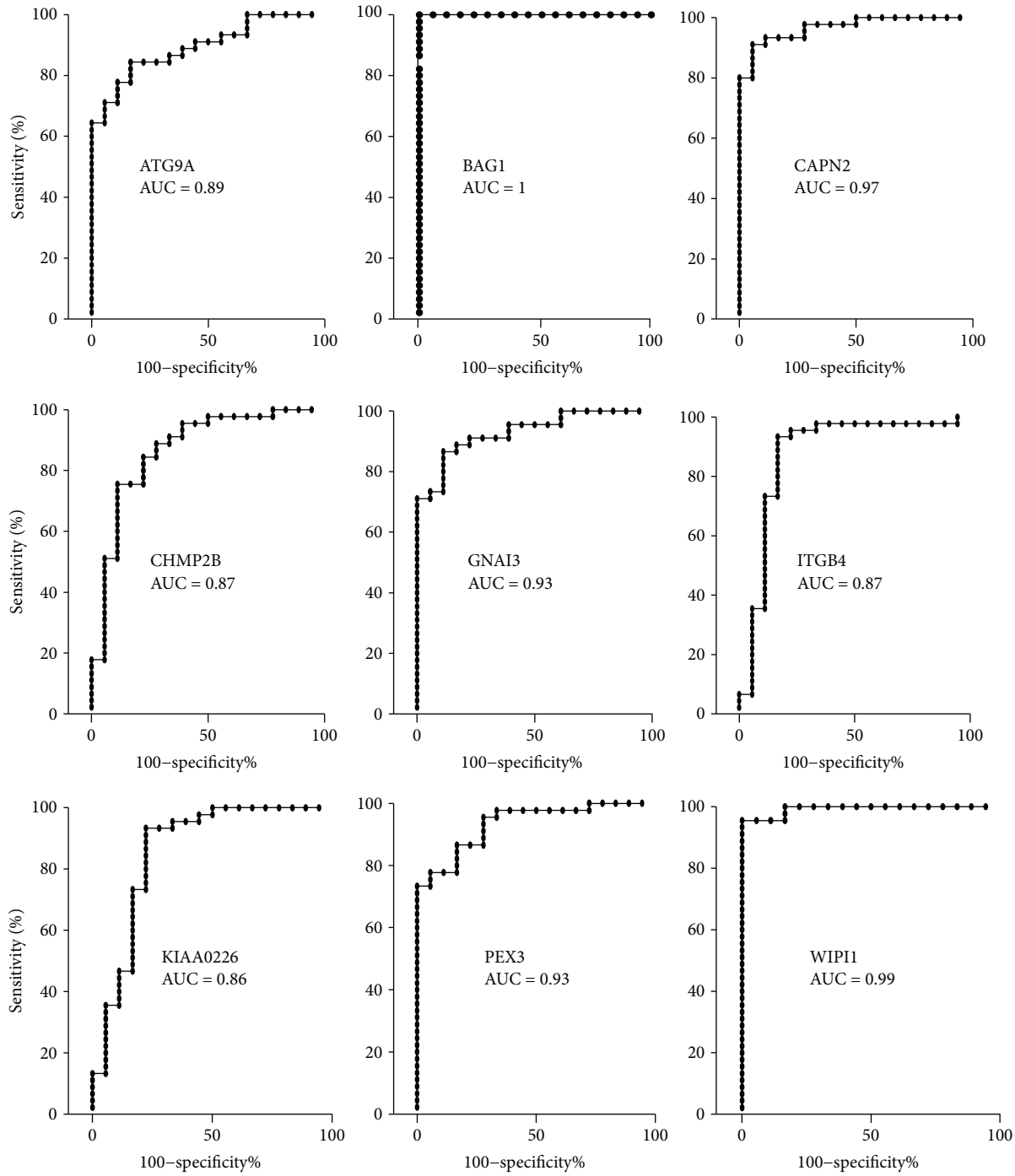

Figure 1: ROC analysis on the expression data of 9 genes never related to melanoma diagnosis or prognosis. The area under the curve (AUC) is plotted as sensitivity% *vs* 100-specificity%. The calculated AUC is reported in each case. The p value is <0.0001 in all cases.

autophagy (Figure 4(a)) or via several intracellular vesicles (Figure 4(b)) or via several molecules selected from the ARG list (Figure 4(c)). We concluded that the role of BAG1, PEX3, and WIPI1 as potential melanoma markers is novel and their action on melanoma may occur at the intracellular vesicle level via molecular pathways involving other ARGs. Interestingly, ARSA (arylsulfatase A) is the only ARG mediating BAG1, PEX3, and WIPI1 relation with melanoma.

3.4.2. GO Enrichment Analysis. As an additional way to investigate mechanisms underlying the functional interactions of the identified ARGs, the GO enrichment analysis was carried on the 42 genes reported in Table 1. The analysis, available as one of the Gene Ontology tools at http://www.geneontology.org/page/go-enrichment-analysis, identifies GO terms (cellular components, molecular functions, or biological processes) overrepresented or underrepresented in the annotations of the given gene list. A sort of molecular/

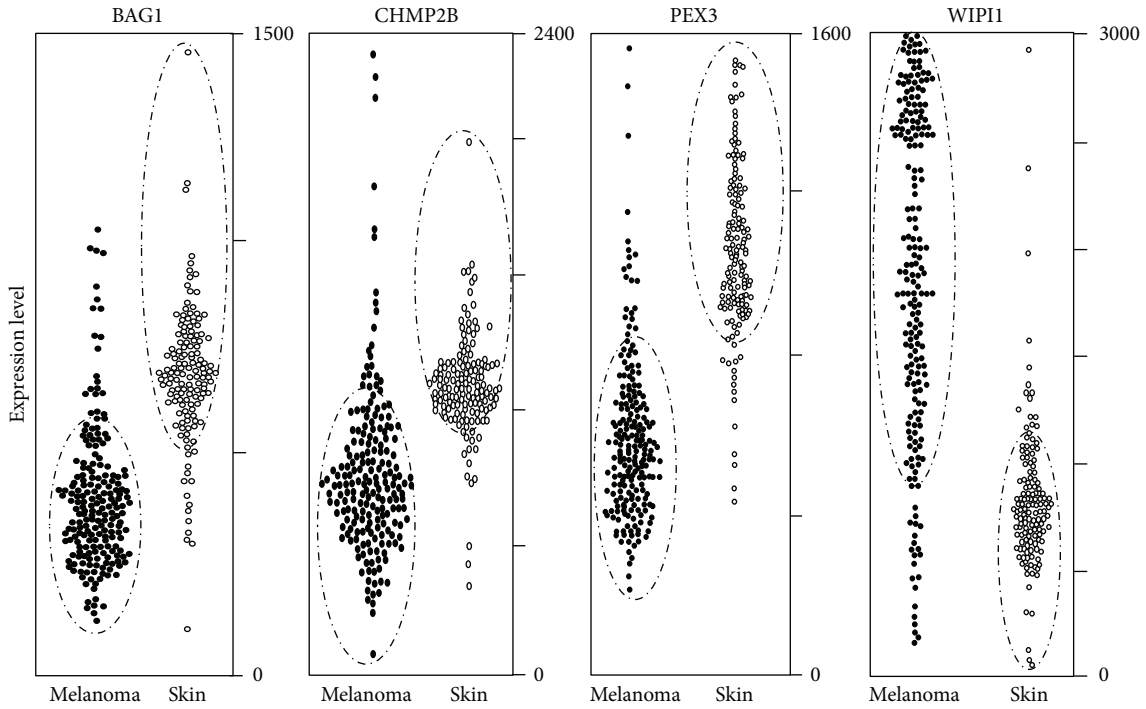

Figure 2: Gene expression according to the IST online database. The four reported genes show different expression levels in melanoma *vs* healthy skin. The expression level of each gene is reported in 208 melanoma biopsies and 147 healthy skin biopsies, according to the IST Online database. Gating indicated with dashed lines include 90% of melanoma and 90% of ctrl skin samples. PEX3, BAG1, and CHMP2B expression in melanoma is clearly lower than healthy skin. WIPI1 expression in melanoma is clearly higher than healthy controls.

functional fingerprint of the given gene list is then obtained. The cellular component terms overrepresented in the GO annotations of the given 42-gene list include cytosol, membrane raft, and whole membrane as the most significantly enriched cellular components within the 42-gene list, fully confirming the above reported Chilibot analysis which highlights the role of such genes in intracellular organelle regulation. The same analysis carried out on the molecular function terms indicates protein binding and enzyme binding as the most significantly enriched functions. Finally, the GO enrichment analysis carried out on the biological processes indicates negative regulation of cell death, cellular response to external stimulus, negative regulation of apoptosis, and regulation of cellular response to stress, as the most significantly enriched biological processes.

3.5. Prognostic Value. The prognostic value of ARG expression was investigated according to 3-year survival data in 102 melanoma patients reported in Human Protein Atlas, stratified as "high"- or "low"-expressing patients. The prognostic value is calculated by the Human Protein Atlas by classifying patients in two groups on the basis of the FPKM gene expression value. The prognosis of each group is examined by Kaplan-Meier analysis, and the survival outcomes of the two groups are compared by log-rank tests. According to such analysis, BAG1 expression shows a slightly significant prognostic value, i.e., higher survival in low-expressing patients ($p = 0.04$). BAG1 also shows a favorable prognostic value in renal cancer ($p < 0.0001$). PEX3 expression shows no significant prognostic value in melanoma patients while it is a favorable prognostic marker in renal cancer patients ($p < 0.0001$). WIPI1 expression shows a favorable prognostic value in melanoma, with very high statistical significance ($p = 0.0003$).

An additional way to evaluate the potential prognostic values of BAG1, PEX3, and WIPI1 was carried out by assessing their expression in primary *vs* metastatic melanoma samples. The GSE15605 dataset in the GEO database was investigated, which reports expression data from 16 normal skin samples, 46 primary melanoma samples, and 12 metastatic melanoma samples. Expression of all three genes BAG1, PEX3, and WIPI1 was found to be significantly different in normal *vs* primary melanoma samples ($p < 0.01$ in all cases) and normal vs primary + metastatic samples ($p < 0.001$ in all cases), fully confirming the differences observed in the GDS1375 dataset reported in Table 1. BAG1 and PEX3 expression was also found significantly reduced in metastatic *vs* primary melanoma ($p = 0.00004$ and $p = 0.002$, respectively), indicating their possible role in the metastatic dissemination phase.

3.6. Third-Round Validation on WIPI1 Overexpression in Melanoma. We then addressed the question of what cancer types show the most significant and relevant WIPI1 upregulation. More than 20 cancer types, several hundred datasets, and several thousand human biopsies and cell line samples were investigated in Oncomine. Table 2 shows that the WIPI top 5% most relevant overexpression is found in two melanoma datasets, 3 lymphoma, 1 esophagus, and 1 oropharyngeal datasets. When such analysis was carried out on cancer

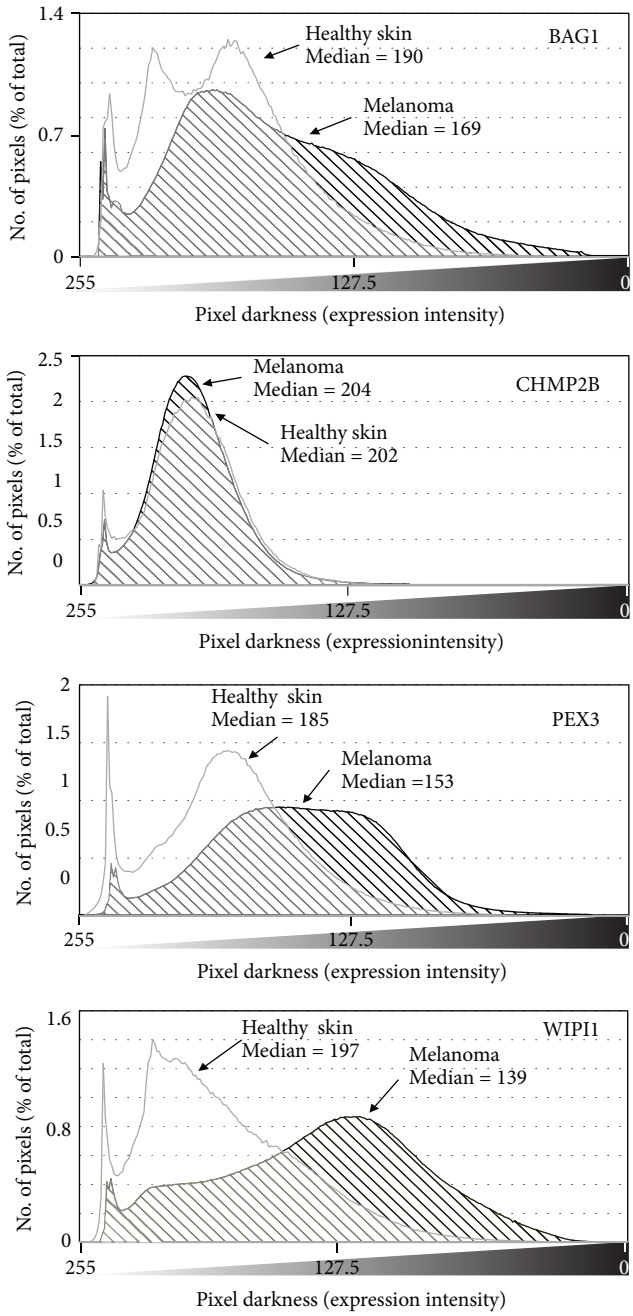

Figure 3: Protein expression according to the Human Protein Atlas. The plot reports the distribution of pixel as function of the expression level. Positions at the right end of the graph indicate higher protein expression. Median level in melanoma samples (dashed curve) shows a clear right shift as compared to healthy skin (gray curve), for BAG1, PEX3, and WIPI1 proteins.

cell lines, mostly melanoma cell lines show a significant and relevant change of WIPI1 (6 melanoma cell lines and 1 myeloma cell line). This data indicate that a strongly significant and relevant WIPI1 overexpression is mostly observed in melanoma and not observed in most other cancer types.

One additional validation was achieved by accessing the Expression Atlas database at EMBL-EBI available at (https://www.ebi.ac.uk/gxa/home). At the homepage of such database, by typing "WIPI1," "*Homo sapiens*," and "melanoma" in the search dialog windows, the Pan Cancer Analysis of Whole Genomes Project reports a clear increase of WIPI1 expression in melanoma *vs* normal skin (35 TPM *vs* "below cutoff," respectively). In addition, according to the Human Protein Atlas, WIPI1 shows in melanoma the highest protein expression, as compared to any other cancer investigated (12 of 12 patients show medium/high WIPI1 protein expression in melanoma, while 9 of 10 in breast cancer and 8 of 10 in prostate cancer and then all others) by HPA007493 antibody staining.

3.7. Analysis of the Physical/Functional Features of the Gene Network. STRING analysis allows integrating data regarding protein-protein physical and functional interactions, either predicted or experimentally demonstrated. STRING analysis was carried out to identify intermediate players within the ARGS listed in Supplemental Table 1, able to functionally connect WIPI1 to BAG1 to PEX3. According to this analysis, the tripolar network depicted in Figure 5 was identified, indicating that WIPI1 is physically/functionally related to BAG1 and PEX3 via ATG9A, BCL2, and PEX14, with HDAC1 at the three-arm interconnection. The functional enrichment analysis of this network highlights the following biological processes significantly enriched: "protein targeting to peroxisome," "cellular response to starvation," "protein localization to pre-autophagosomal structure" and "nucleophagy." The enriched "cellular components" are "pre-autophagosomal structure," "autophagosome membrane," "peroxisomal membrane," "whole membrane," and "autophagosome."

4. Discussion

The current study represents the first extensive analysis of the expression levels of several ARGs in melanoma human biopsies and histological sections. ARG expression was analyzed in 498 human samples from both transcriptomic and proteomic independent databases, according to a multistep validation procedure. BAG1, PEX3, and WIPI1 were identified as the best three novel candidates as validated markers in both DNA and protein melanoma samples, while CHMP2B has validated differential expression at the DNA level, not observed at the protein level. Such genes are known autophagy-related molecules, and their role has been studied in different cancers. BAG1 is a survival promoter in different cancers [25, 26]; WIPI aberrant expression in melanoma cell lines has been reported [27], and its specific mutations are known in melanoma cell lines [28]. Nevertheless, an extensive analysis of their gene and protein expression levels in human samples has not been reported in full manuscripts, yet.

A mechanism underlying the role of these genes as melanoma markers may relate to their physical/functional interactions with intracellular vesicles. Noteworthily, BAG1, PEX3, and WIPI1 are all membrane-associated molecules and intracellular vesicles play a key role in melanoma biology. BAG1 localizes in the nucleus and cytosol; PEX3 in peroxisomes, nucleus, and endoplasmic reticulum; and WIPI1 in cytoskeleton, cytosol, Golgi apparatus, and endosomes.

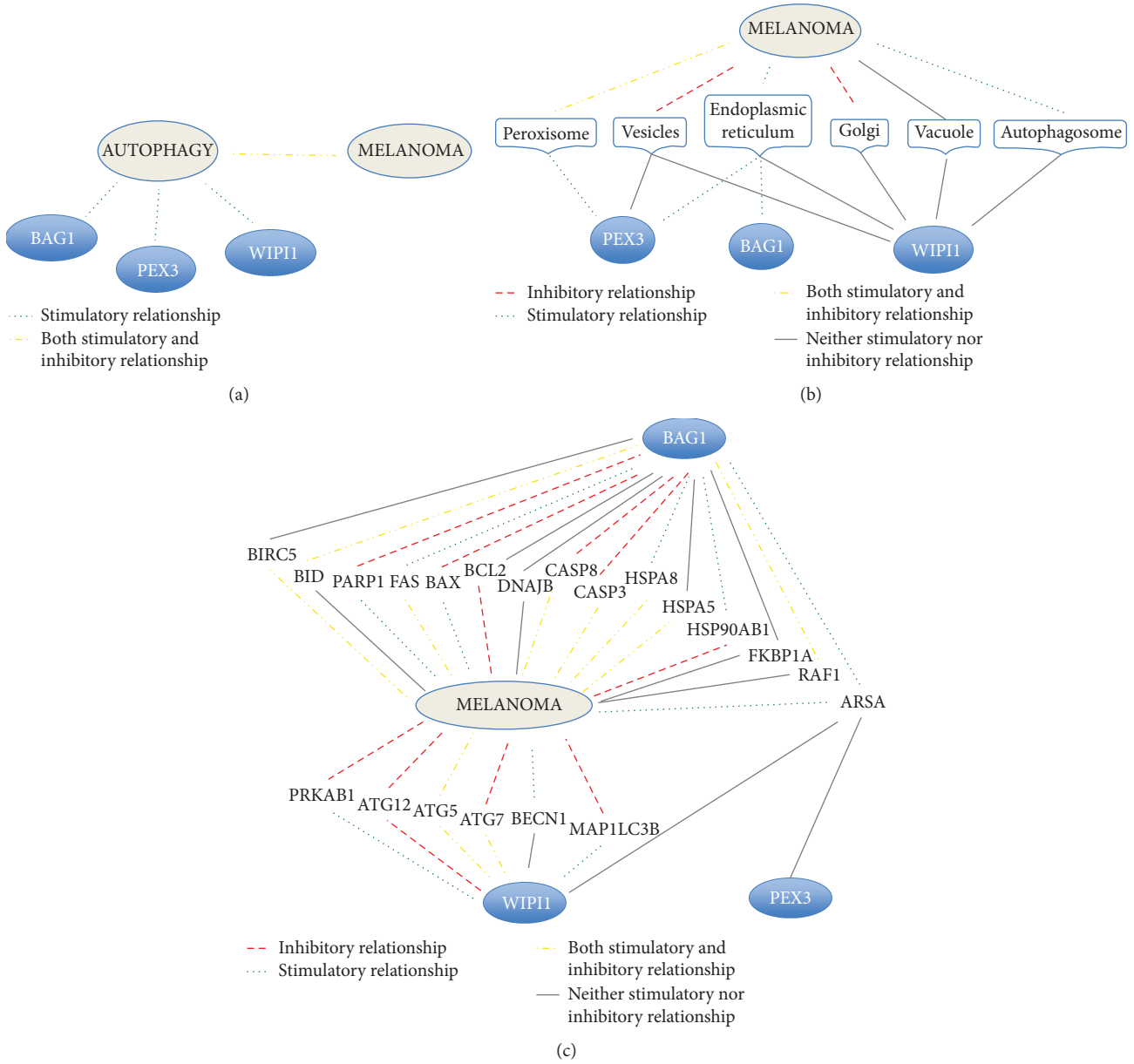

Figure 4: Functional relations reported in Pubmed abstracts, according to Chilibot analysis. Only strong interactive relationships are reported (i.e., interactive relationships reported by at least 5 Pubmed abstracts). Green dotted lines indicate stimulatory relationships; yellow dashed/dotted lines indicate both stimulatory and inhibitory relationships; red dashed lines indicate inhibitory relationships; and continuous gray lines indicate neither stimulatory nor inhibitory relationship, according to Chilibot categories. (a) None of the 3 selected autophagy-related genes has any direct known interactive relationship with melanoma; rather, the relationships are all mediated by autophagy. This indicates that the proposed role of BAG1, PEX3, and WIPI1 in melanoma is novel. (b) Strong interactive relationships of the 3 genes occur with intracellular vesicles, and, through these, they may relate to melanoma. (c) Strong interactive relationships of all 222 ARGs taken from Supplementary Table 1 with melanoma were investigated. Neither BAG1, nor PEX3 nor WIPI1, has a direct strong interactive relationship with melanoma. BAG1 may have indirect strong interactive relationships with melanoma, mediated by BIRC5, BID, PARP1, FAS, BAX, DNAJB, and many others. WIPI1 interaction with melanoma is mediated by PRKAB1, ATG12, ATG5, ATG7, BECN1, and MAP1LC36. Interestingly, ARSA is the only autophagy-related gene having known strong interactive relationships with both BAG1, PEX3, and WIPI1 and with melanoma.

Therefore, proteins coded by these 3 genes interact with such vesicles, as highlighted in Figure 4(b). Intracellular vesicles are emerging as relevant mediators of tumorigenesis. The altered expression of genes/proteins controlling biogenesis and stability of intracellular vesicles may control the melanoma setup. In fact, melanoma-derived exosomes act onto the bone marrow toward melanoma progression and metastasis, carrying the proteome repertoire derived from the primary melanoma [29]. Thus, intracellular vesicles may carry genetic and nongenetic material to "educate"

Table 2: Cancer types showing significant overexpression of WIPI1. In human biopsy cancers (left column), 2 melanoma datasets are within the top 5% ranked datasets with relevant WIPI1 overexpression. In human cell lines (right column), 6 melanoma and 1 myeloma cell lines are present in the top 5% ranked datasets of cell lines with relevant WIPI1 overexpression. Left column: WIPI1 expression in 31,931 human biopsy samples from more than 20 different cancer types was analyzed, namely, biopsies from bladder; brain and central nervous systems; and breast, colorectal, cervical, esophageal, gastric, head and neck, kidney, leukemia, liver, lung, lymphoma, melanoma, myeloma, ovarian, pancreatic, prostate, sarcoma, mesothelioma, and seminoma cancers. Right column: 26 different datasets with 7410 samples from 18 different cancer types were analyzed (melanoma, lymphoma, leukemia, testicular germ cell neoplasm, breast, brain, liver, gastrointestinal, sarcoma, lung, prostate, colorectal, kidney, ovarian, bladder, pancreatic, and esophageal tumors). The following stringent thresholds were selected: $p \leq 0.0001$; fold change $(\mathrm{FC}) \geq 3$; gene rank top 5% (data from Oncomine, http://www.oncomine.com).

Top 5% human biopsies of different cancer types, with WIPI1 overexpression	Top 5% human cancer cell lines, with WIPI1 overexpression
Riker melanoma dataset: Cutaneous melanoma: $p = 0.00002$; FC 3.1; rank 79	Shankavaram melanoma cell line: $p = 0.00001$; FC 6.8; rank 207
Compagno lymphoma dataset: Diffuse large B-cell lymphoma: $p = 4.5E-27$; FC 4.9; rank 111	Compendia melanoma cell line: $p = 0.00001$; FC 6.7; rank 218
Compagno lymphoma dataset: Activated B-cell like diffuse large B-cell lymphoma: $p = 1.6E-10$; FC 4.2; rank 544	Garnett melanoma cell line: $p = 2.2E-13$; FC 5.4; rank 232
Hao esophagus dataset: esophageal adenocarcinoma: $p = 1.6E-10$; FC 4.2; rank 544	Adai melanoma cell line: $p = 3.4E-8$; FC 7.4; rank 285
Piccaluga lymphoma: Anaplastic large cell lymphoma $p = 2.2E-6$; FC 4.9; rank 193	Barretina melanoma cell line: $p = 1.5E-19$; FC 4.77; rank 301
Pyeon multicancer dataset: oropharyngeal carcinoma $p = 2.3E-5$, FC 3.5; rank 323	Barretina myeloma cell line: $p = 1.2E-8$; FC 3.3; rank 551
Talantov melanoma dataset: cutaneous melanoma: $p = 7.3E-7$; FC 8.4; rank 467	Wagner melanoma cell line: $p = 4.8E-8$; FC 5.2; rank 533

target cells toward a more or less aggressive behavior. Autophagosomes are an additional example of how intracellular vesicle trafficking may control the cellular phenotype. Other intracellular compartments such as melanosomes are connected to the epitope presentation and immune recognition of melanoma-related epitopes [30]. Intracellular vesicle formation in melanoma cells is under GSK3 and Wnt signaling control and directly relates to the melanoma proliferation potential [31, 32]. Formation and maturation of melanosomes and other vesicles are therefore strongly related to autophagy. Melanin synthesis has been shown by us [33] and others [34–37] as one of the key steps in the melanoma setup and progression. Indeed, inhibition of melanogenesis relates to autophagy activation [38], pigmentation enhancement is related to autophagy inhibition

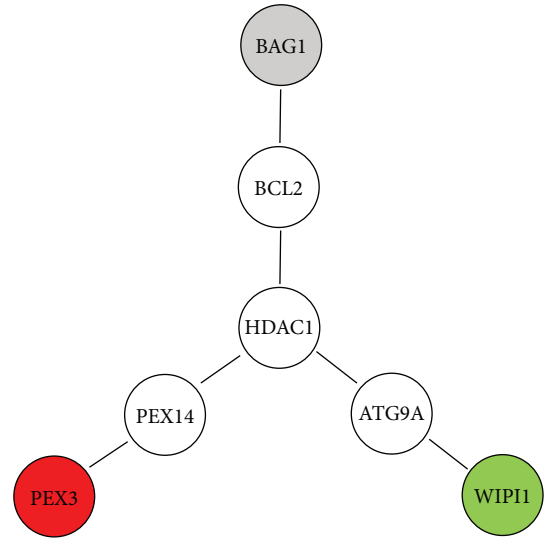

Figure 5: STRING analysis of WIPI1, BAG1, and PEX3 network. BCL2, PEX14, and ATG9A physically/functionally connect BAG1, PEX3, and WIPI1 (respectively) via HDAC1.

[39, 40], and the entire autophagy machinery directly controls melanosome movements and translocations [41]. Further, melanocytes having reduced autophagy undergo senescence and lipid oxidation [6, 42].

BAG1 is a BCL2-associated athanogene; it enhances BCL2 antiapoptotic effects, therefore the reduced expression in melanoma reported in Figure 2 and Table 1 may promote melanoma onset. The HPA database reports higher survival in BAG1 low-expressing melanoma patients ($p = 0.04$) and a favorable prognostic value in renal cancer.

CHMP2B interacts with endosomal originated vesicles, being part of the ESCRT-III complex, which degrades/recycles membrane receptors. This gene is associated with a familial frontotemporal lobar degeneration and with amyotrophic lateral sclerosis. Melanoma association with neurological cancers is known [43], and correlation with other neurological disorders is an emerging field of investigation [44]. Further, CHMP2B has a key role in melanin synthesis or accumulation; in fact, a mutated form of CHMP2B induces melanization in fly eye [45].

PEX3 is involved in biosynthesis and integrity of peroxisome and membrane vesicle assembly. It is reduced in melanoma (Figure 2 and Table 1); within the cancers reported in HPA, the lowest expression is observed in melanoma. As CHMP2B, PEX3 has been related to neurological diseases. Namely, PEX3 mutations are related to Zellweger syndrome (ZWS), a neurologic dysfunction with craniofacial abnormalities and liver dysfunction. According to the "Orphan disease connections" portal (http://csbg.cnb.csic.es/odcs/disease_showresults.php?dis0=Melanoma%20and%20neural%20system%20tumor%20syndrome) [46], melanoma and Zellweger syndrome are considered connected diseases and PEX3 falls in the CDKN2A interactome, one of the most frequently mutated genes in melanoma.

Finally, WIPI1 controls autophagosome assembly and binds phosphoinositides, essential components of any

membrane. It is known to have a relevant role in starvation- and calcium-mediated autophagy and in mitophagy. Its expression is strongly increased in melanoma at both DNA and protein levels (Figure 2, Table 1, Figure 3), and it has one of the highest AUC values (Figure 1) and according to HPA shows a favorable prognostic value in melanoma with a very high statistical significance ($p < 0.0001$). WIPI1 is an ATG18 homolog; it colocalizes with the LC3 autophagy marker in melanoma cells [27] and localizes within autophagosomes and endosomes. Via mTOR pathway inhibition, it induces melanogenic enzyme transcription and melanosome formation [47], revealing a specific role of WIPI1 in melanosome maturation. Therefore, WIPI1 and CHMP2B are both involved in melanin metabolism.

MAPK phosphorylation is reduced by WIPI1 knockdown [48], underlying the WIPI1-MAPK axis indicated in Figure 4(c), indicating the possible molecular pathway relating WIPI1 to melanoma setup and progression via MAPK and PD-L1 [49].

Figure 4(c) shows that BAG1, PEX3, and WIPI1 have no known direct relation with melanoma and at least 20 ARGs may mediate their interaction with melanoma. According to Pubmed searches, ARSA, the arylsulfatase A gene, appears to mediate BAG1, PEX3, and WIPI1 interaction with melanoma (Figure 4(c)). Namely, arylsulfatase may control melanoma progression [50]. Its deficiency leads to metachromatic leukodystrophy, a rare genetic lysosomal storage disease with metabolism deficit at the sphingolipid level, affecting membrane structure and function, pointing again toward membrane metabolism. The STRING analysis carried out on ARSA indicates the most significant biological process enrichment in the ARSA network as the "glycosphingolipid metabolic process" (false discovery rate $1.25E-21$), the most significant molecular function enrichment as the "sulfuric ester hydrolase activity" (false discovery rate $8.8E-17$), and the most significant cellular component enrichment as the "endoplasmic reticulum lumen" (false discovery rate $3.9E-14$), highlighting again a biochemical modification at the lipid level within intracellular vesicles. Finally, regarding the tripolar connection reported in Figure 5, it should be noticed that HDAC1, predicted by the STRING analysis as the central player physically/functionally connecting WIPI1 to BAG1 to PEX3, has been shown to be involved in melanoma drug resistance and melanoma progression [51–53]. STRING analysis carried out on other secondary hits reported in Table 1 indicates functional enrichment of axon guidance and phagocytosis (for CAPN2), cell separation and viral budding (for CHMP2B), response to glucagon and regulation of G-protein-coupled receptors (for GNAI3), hemidesmosome assembly (for ITGB4), endosomal transport (for KIAA0226), and unfolded protein response (for EIF2AK3). In all such cases, cellular component enrichment analysis identifies cellular membrane components.

In conclusion, the present study highlights 3 genes (BAG1, PEX3, and WIPI1), known to play a key role in autophagy, as novel relevant melanoma markers. WIPI1 is significantly upregulated at both gene and protein levels in melanoma samples, showing the highest expression fold change, the highest ability to discriminate healthy individuals from patients, and the strongest prognostic value, and it has never been related to melanoma. Therefore, such molecules may represent valuable novel markers of melanoma setup and progression.

Data Availability

The data used to support the findings of this study are available from the corresponding author upon request.

Ethical Approval

All data reported in the present study were derived from publically available databases.

Conflicts of Interest

All authors have read the journal's policy on disclosure of potential conflicts of interest and declare non conflict of interest.

Acknowledgments

This study has been supported in part by a grant from the Italian Ministry of Health, RC3.4-2017 to AF.

Supplementary Materials

Supplementary Table 1: autophagy-related genes (ARGs) investigated in the present study. *(Supplementary Materials)*

References

[1] M. Kunz and M. Hölzel, "The impact of melanoma genetics on treatment response and resistance in clinical and experimental studies," *Cancer Metastasis Reviews*, vol. 36, no. 1, pp. 53–75, 2017.

[2] X.-Y. Zhang and P.-Y. Zhang, "Genetics and epigenetics of melanoma," *Oncology Letters*, vol. 12, no. 5, pp. 3041–3044, 2016.

[3] S. Ribero, C. Longo, D. Glass, P. Nathan, and V. Bataille, "What is new in melanoma genetics and treatment?," *Dermatology*, vol. 232, no. 3, pp. 259–264, 2016.

[4] M. C. Sini, V. Doneddu, P. Paliogiannis et al., "Genetic alterations in main candidate genes during melanoma progression," *Oncotarget*, vol. 9, no. 9, pp. 8531–8541, 2018.

[5] C. Tabolacci, M. Cordella, L. Turcano et al., "Aloe-emodin exerts a potent anticancer and immunomodulatory activity on BRAF-mutated human melanoma cells," *European Journal of Pharmacology*, vol. 762, pp. 283–292, 2015.

[6] C. Giampietri, S. Petrungaro, M. Cordella et al., "Lipid storage and autophagy in melanoma cancer cells," *International Journal of Molecular Sciences*, vol. 18, no. 6, 2017.

[7] S. P. Fortis, L. G. Mahaira, E. A. Anastasopoulou, I. F. Voutsas, S. A. Perez, and C. N. Baxevanis, "Immune profiling of melanoma tumors reflecting aggressiveness in a preclinical model," *Cancer Immunology, Immunotherapy*, vol. 66, no. 12, pp. 1631–1642, 2017.

[8] C. Gabellini, E. Gómez-Abenza, S. Ibáñez-Molero et al., "Interleukin 8 mediates bcl-xL-induced enhancement of human melanoma cell dissemination and angiogenesis in a zebrafish

xenograft model," *International Journal of Cancer*, vol. 142, no. 3, pp. 584–596, 2018.

[9] T. Delaunay, L. Deschamps, M. Haddada et al., "Aberrant expression of kallikrein-related peptidase 7 is correlated with human melanoma aggressiveness by stimulating cell migration and invasion," *Molecular Oncology*, vol. 11, no. 10, pp. 1330–1347, 2017.

[10] I. Lazar, E. Clement, S. Dauvillier et al., "Adipocyte exosomes promote melanoma aggressiveness through fatty acid oxidation: a novel mechanism linking obesity and cancer," *Cancer Research*, vol. 76, no. 14, pp. 4051–4057, 2016.

[11] D. D'Arcangelo, F. Facchiano, G. Nassa et al., "PDGFR-alpha inhibits melanoma growth via CXCL10/IP-10: a multi-*omics* approach," *Oncotarget*, vol. 7, no. 47, pp. 77257–77275, 2016.

[12] D. Faraone, M. S. Aguzzi, G. Toietta et al., "Platelet-derived growth factor-receptor α strongly inhibits melanoma growth *in vitro* and *in vivo*," *Neoplasia*, vol. 11, no. 8, pp. 732–7W7, 2009.

[13] D. J. Klionsky, K. Abdelmohsen, A. Abe et al., "Guidelines for the use and interpretation of assays for monitoring autophagy (3rd edition)," *Autophagy*, vol. 12, no. 1, pp. 1–222, 2016.

[14] L. Mainz and M. T. Rosenfeldt, "Autophagy and cancer - insights from mouse models," *The FEBS Journal*, vol. 285, no. 5, pp. 792–808, 2018.

[15] S. Byun, E. Lee, and K. W. Lee, "Therapeutic implications of autophagy inducers in immunological disorders, infection, and cancer," *International Journal of Molecular Sciences*, vol. 18, no. 9, p. 1959, 2017.

[16] Y. Jin, Y. Hong, C. Park, and Y. Hong, "Molecular interactions of autophagy with the immune system and cancer," *International Journal of Molecular Sciences*, vol. 18, no. 8, 2017.

[17] J. M. M. Levy, C. G. Towers, and A. Thorburn, "Targeting autophagy in cancer," *Nature Reviews. Cancer*, vol. 17, no. 9, pp. 528–542, 2017.

[18] D. Y. L. Tang, R. A. Ellis, and P. E. Lovat, "Prognostic impact of autophagy biomarkers for cutaneous melanoma," *Frontiers in Oncology*, vol. 6, p. 236, 2016.

[19] A. Ndoye and A. T. Weeraratna, "Autophagy-an emerging target for melanoma therapy," *F1000Research*, vol. 5, 2016.

[20] S. G. Mathiassen, D. De Zio, and F. Cecconi, "Autophagy and the cell cycle: a complex landscape," *Frontiers in Oncology*, vol. 7, p. 51, 2017.

[21] X.-X. Meng, H.-X. Xu, M. Yao, Q. Dong, and X. Dong Zhang, "Implication of unfolded protein response and autophagy in the treatment of BRAF inhibitor resistant melanoma," *Anti-Cancer Agents in Medicinal Chemistry*, vol. 16, no. 3, pp. 291–298, 2016.

[22] M. Hassan, D. Selimovic, M. Hannig, Y. Haikel, R. T. Brodell, and M. Megahed, "Endoplasmic reticulum stress-mediated pathways to both apoptosis and autophagy: significance for melanoma treatment," *World Journal of Experimental Medicine*, vol. 5, no. 4, pp. 206–217, 2015.

[23] H. Maes and P. Agostinis, "Autophagy and mitophagy interplay in melanoma progression," *Mitochondrion*, vol. 19, Part A, pp. 58–68, 2014.

[24] H. Chen and B. M. Sharp, "Content-rich biological network constructed by mining PubMed abstracts," *BMC Bioinformatics*, vol. 5, no. 1, p. 147, 2004.

[25] R. I. Cutress, P. A. Townsend, M. Brimmell, A. C. Bateman, A. Hague, and G. Packham, "BAG-1 expression and function in human cancer," *British Journal of Cancer*, vol. 87, no. 8, pp. 834–839, 2002.

[26] J. Song, M. Takeda, and R. I. Morimoto, "Bag1-Hsp70 mediates a physiological stress signalling pathway that regulates Raf-1/ERK and cell growth," *Nature Cell Biology*, vol. 3, no. 3, pp. 276–282, 2001.

[27] T. Proikas-Cezanne, S. Waddell, A. Gaugel, T. Frickey, A. Lupas, and A. Nordheim, "WIPI-1α (WIPI49), a member of the novel 7-bladed WIPI protein family, is aberrantly expressed in human cancer and is linked to starvation-induced autophagy," *Oncogene*, vol. 23, no. 58, pp. 9314–9325, 2004.

[28] T. Proikas-Cezanne, Z. Takacs, P. Donnes, and O. Kohlbacher, "WIPI proteins: essential PtdIns3P effectors at the nascent autophagosome," *Journal of Cell Science*, vol. 128, no. 2, pp. 207–217, 2015.

[29] H. Peinado, M. Alečković, S. Lavotshkin et al., "Melanoma exosomes educate bone marrow progenitor cells toward a pro-metastatic phenotype through MET," *Nature Medicine*, vol. 18, no. 6, pp. 883–891, 2012.

[30] V. Robila, M. Ostankovitch, M. L. Altrich-VanLith et al., "MHC class II presentation of gp100 epitopes in melanoma cells requires the function of conventional endosomes and is influenced by melanosomes," *Journal of Immunology*, vol. 181, no. 11, pp. 7843–7852, 2008.

[31] D. Ploper, V. F. Taelman, L. Robert et al., "MITF drives endolysosomal biogenesis and potentiates Wnt signaling in melanoma cells," *Proceedings of the National Academy of Sciences of the United States of America*, vol. 112, no. 5, pp. E420–E429, 2015.

[32] R. Mancinelli, G. Carpino, S. Petrungaro et al., "Multifaceted roles of GSK-3 in cancer and autophagy-related diseases," *Oxidative Medicine and Cellular Longevity*, vol. 2017, Article ID 4629495, 14 pages, 2017.

[33] E. Cesareo, L. Korkina, G. D'Errico et al., "An endogenous electron spin resonance (ESR) signal discriminates nevi from melanomas in human specimens: a step forward in its diagnostic application," *PLoS One*, vol. 7, no. 11, article e48849, 2012.

[34] E. Buitrago, R. Hardré, R. Haudecoeur et al., "Are human tyrosinase and related proteins suitable targets for melanoma therapy?," *Current Topics in Medicinal Chemistry*, vol. 16, no. 27, pp. 3033–3047, 2016.

[35] J. Vachtenheim and J. Borovanský, ""Transcription physiology" of pigment formation in melanocytes: central role of MITF," *Experimental Dermatology*, vol. 19, no. 7, pp. 617–627, 2010.

[36] J. Leclerc, R. Ballotti, and C. Bertolotto, "Pathways from senescence to melanoma: focus on MITF sumoylation," *Oncogene*, vol. 36, no. 48, pp. 6659–6667, 2017.

[37] H. E. Seberg, E. van Otterloo, and R. A. Cornell, "Beyond MITF: multiple transcription factors directly regulate the cellular phenotype in melanocytes and melanoma," *Pigment Cell & Melanoma Research*, vol. 30, no. 5, pp. 454–466, 2017.

[38] Y. H. Cho, J. E. Park, D. S. Lim, and J. S. Lee, "Tranexamic acid inhibits melanogenesis by activating the autophagy system in cultured melanoma cells," *Journal of Dermatological Science*, vol. 88, no. 1, pp. 96–102, 2017.

[39] N.-H. Kim, S.-H. Choi, N. Yi, T. R. Lee, and A. Y. Lee, "Arginase-2, a miR-1299 target, enhances pigmentation in melasma by reducing melanosome degradation via senescence-induced

autophagy inhibition," *Pigment Cell & Melanoma Research*, vol. 30, no. 6, pp. 521–530, 2017.

[40] K. W. Lee, H. W. Ryu, S.-s. Oh et al., "Depigmentation of α-melanocyte-stimulating hormone-treated melanoma cells by β-mangostin is mediated by selective autophagy," *Experimental Dermatology*, vol. 26, no. 7, pp. 585–591, 2017.

[41] A. Ramkumar, D. Murthy, D. A. Raja et al., "Classical autophagy proteins LC3B and ATG4B facilitate melanosome movement on cytoskeletal tracks," *Autophagy*, vol. 13, no. 8, pp. 1331–1347, 2017.

[42] C. Ni, M. S. Narzt, I. M. Nagelreiter et al., "Autophagy deficient melanocytes display a senescence associated secretory phenotype that includes oxidized lipid mediators," *The International Journal of Biochemistry & Cell Biology*, vol. 81, Part B, pp. 375–382, 2016.

[43] E. Azizi, J. Friedman, F. Pavlotsky et al., "Familial cutaneous malignant melanoma and tumors of the nervous system. A hereditary cancer syndrome," *Cancer*, vol. 76, no. 9, pp. 1571–1578, 1995.

[44] D. M. Freedman, R. E. Curtis, S. E. Daugherty, J. J. Goedert, R. W. Kuncl, and M. A. Tucker, "The association between cancer and amyotrophic lateral sclerosis," *Cancer Causes & Control*, vol. 24, no. 1, pp. 55–60, 2013.

[45] S. T. Ahmad, S. T. Sweeney, J.-A. Lee, N. T. Sweeney, and F. B. Gao, "Genetic screen identifies serpin5 as a regulator of the toll pathway and CHMP2B toxicity associated with frontotemporal dementia," *Proceedings of the National Academy of Sciences of the United States of America*, vol. 106, no. 29, pp. 12168–12173, 2009.

[46] S. Fernandez-Novo, F. Pazos, and M. Chagoyen, "Rare disease relations through common genes and protein interactions," *Molecular and Cellular Probes*, vol. 30, no. 3, pp. 178–181, 2016.

[47] H. Ho, R. Kapadia, S. al-Tahan, S. Ahmad, and A. K. Ganesan, "WIPI1 coordinates melanogenic gene transcription and melanosome formation via TORC1 inhibition," *The Journal of Biological Chemistry*, vol. 286, no. 14, pp. 12509–12523, 2011.

[48] C.-C. Liao, M. Y. Ho, S. M. Liang, and C. M. Liang, "Recombinant protein rVP1 upregulates BECN1-independent autophagy, MAPK1/3 phosphorylation and MMP9 activity via WIPI1/WIPI2 to promote macrophage migration," *Autophagy*, vol. 9, no. 1, pp. 5–19, 2013.

[49] Q. Luan, L. Jin, C. C. Jiang et al., "RIPK1 regulates survival of human melanoma cells upon endoplasmic reticulum stress through autophagy," *Autophagy*, vol. 11, no. 7, pp. 975–994, 2015.

[50] S. Bhattacharyya, L. Feferman, K. Terai, A. Z. Dudek, and J. K. Tobacman, "Decline in arylsulfatase B leads to increased invasiveness of melanoma cells," *Oncotarget*, vol. 8, no. 3, pp. 4169–4180, 2017.

[51] A. Krumm, C. Barckhausen, P. Kucuk et al., "Enhanced histone deacetylase activity in malignant melanoma provokes RAD51 and FANCD2-triggered drug resistance," *Cancer Research*, vol. 76, no. 10, pp. 3067–3077, 2016.

[52] H. Schipper, V. Alla, C. Meier, D. M. Nettelbeck, O. Herchenröder, and B. M. Pützer, "Eradication of metastatic melanoma through cooperative expression of RNA-based HDAC1 inhibitor and p73 by oncolytic adenovirus," *Oncotarget*, vol. 5, no. 15, pp. 5893–5907, 2014.

[53] C. R. Goding, "Melanoma senescence. HDAC1 in focus," *Pigment Cell Research*, vol. 20, no. 5, pp. 336–338, 2007.